Forschungszentrum Jülich

Institut für Festkörperforschung

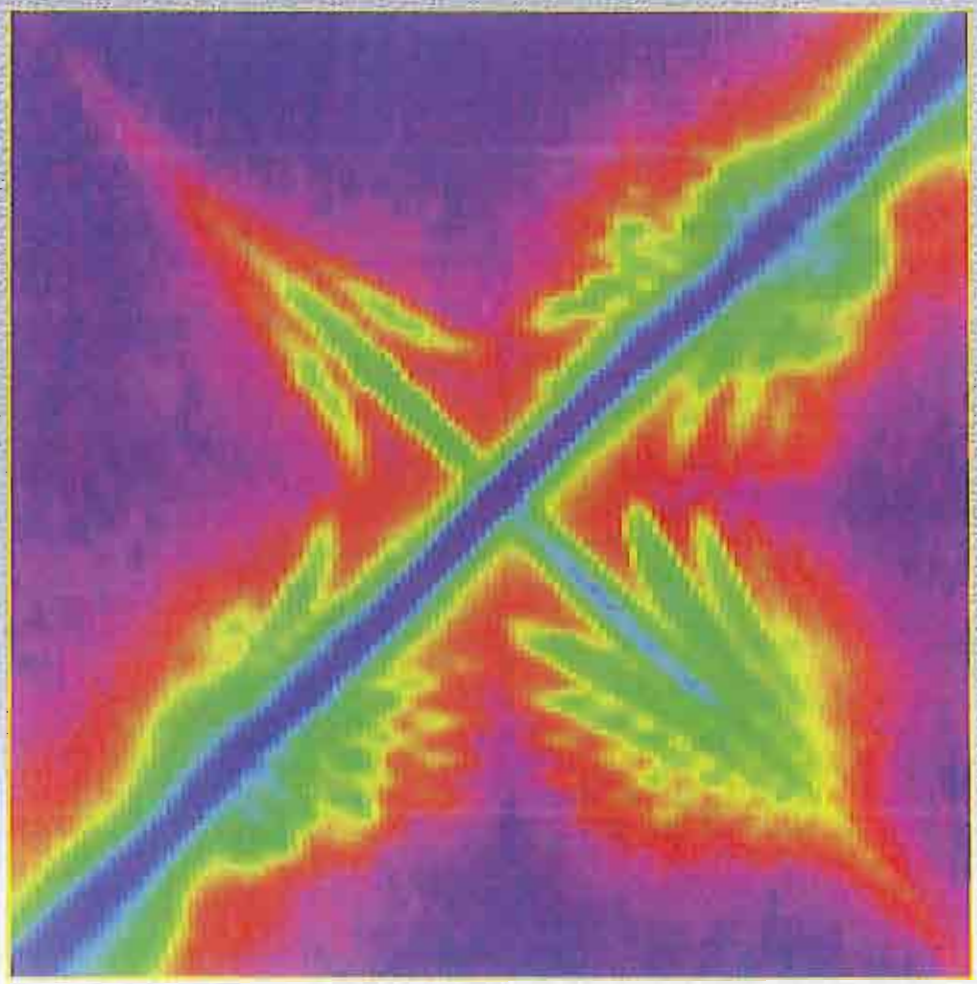

Scientific Report 2001/2002

Institut für Festkörperforschung

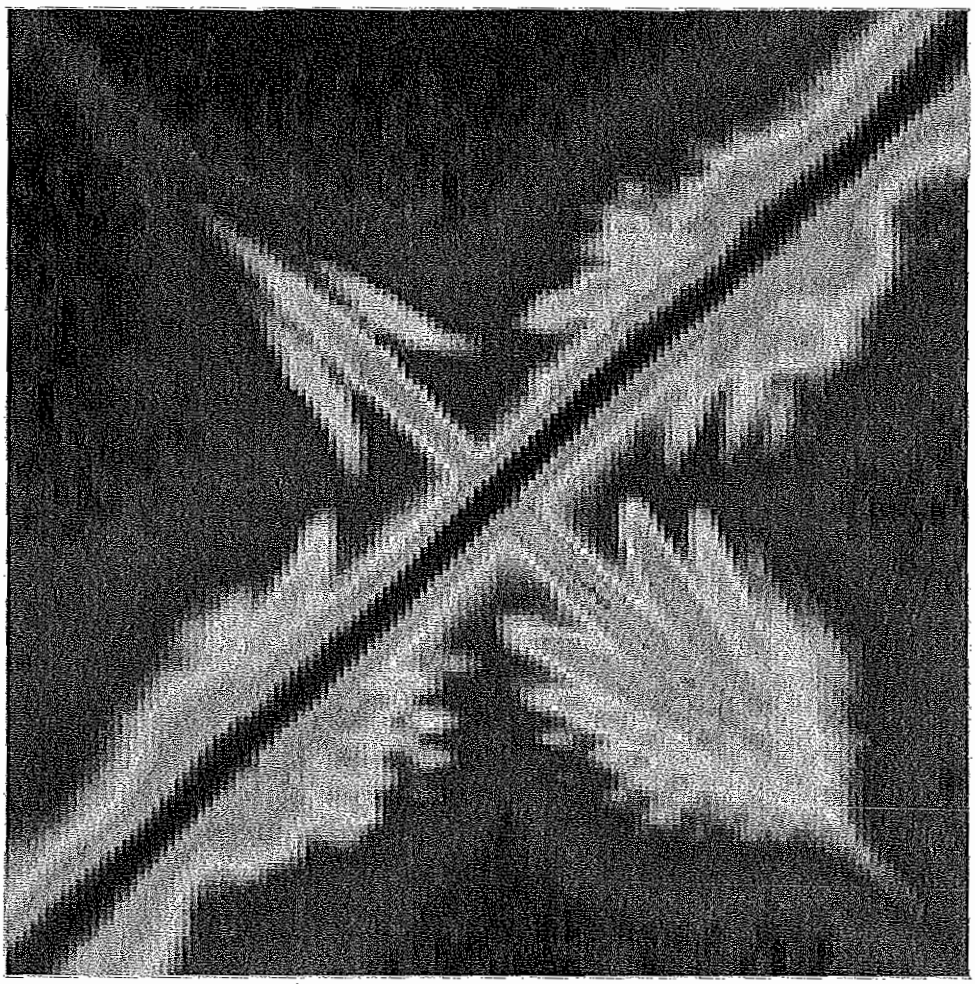

Scientific Report 2001/2002

Published by Forschungszentrum Jülich GmbH
D-52425 Jülich
Telephone: +49 2461 61-0 – Telex: 833556-0 kfa d
Responsible for content: the Managing Director of the IFF
tel: +49 2461 614465, fax: +49 2461 612410, e-mail: h.geisler@fz-juelich.de
Wholly set-up by BD-SG, Grafische Betriebe, Forschungszentrum Jülich GmbH
Time of going to press: 22.02.2002

Introduction

The "Institut für Festkörperforschung" (IFF) is devoted to condensed matter research. Topics range from the physics and chemistry of liquids, via membranes, clusters, surfaces and thin films to homogeneous and inhomogeneous bulk solids. The IFF has a department structure consisting of 9 institutes and service groups. Its wide spectrum of experimental facilities and individual expertise enables the IFF to successfully tackle complex problems in close collaboration between preparative, experimental and theoretical groups. Specialized laboratories and facilities exist for preparation of polymers, colloids and ceramics or the growth of thin films and bulk single crystals. Besides standard methods for characterization, highly sophisticated techniques are available and constantly further developed such as ultra high resolution electron microscopy, neutron- and synchrotron x-ray scattering, and femtosecond laser spectroscopy. Characteristic for an institute of the HGF (Hermann von Helmholtz Association of National Research Centers) is the fact that the IFF builds, operates and makes available to external users the neutron scattering instruments at the research reactor FRJ-2. Last but not least, the IFF has a long tradition in teaching and training of young researchers, not only through the approximately 25 IFF scientists teaching at universities, but in particular through the Spring Schools of the IFF and the annual Neutron Laboratory Course.

This annual report is intended to inform the international scientific community, including our scientific advisory board, about the scientific activities at the IFF during the past year. We have attempted to present a typical cross section through the research done at IFF, including scientific highlights as well as results of long term developments, for example the construction of new large-scale instruments. The scientific activities of the IFF have lead this year to 349 publications,of which 267 articles were published in refereed journals, and a total of 340 external talks of which 230 were invited. I hope you will enjoy learning about our activities.

As in previous years before, IFF researchers have received or accepted offers for faculty positions at universities and research institutes:In the spring of 2001, Prof. Dr. W. Eberhardt has accepted an offer for a faculty position at the Technical University of Berlin and as scientific director of the BESSY GmbH. Prof. Dr. S. Blügel has received an offer for a C4-professorship at the Universität Kaiserslautern. Dr. D. E. Bürgler was offered a faculty position for experimental physics at the Martin-Luther-Universität Halle-Wittenberg.We are proud of the scientific recognition of the IFF, which is reflected in these offers. On the other hand, we are of course sorry that these excellent scientist have left - or might leave - the IFF. In particular, with Prof. Dr. W. Eberhardt having taken up his new job in Berlin, we are again in the position that we are looking for new directors for two of our nine institutes. The institutes "Theory I" and "Electronic Properties" are currently lead by Dr. A. Liebsch and by Prof. Th. Brückel, respectively, as acting directors.

After his important role in the organization of the "Jahr der Physik" in 2000, Prof. Dr. H. Müller-Krumbhaar has become even more active in German and European science organization this year. In April 2001, he has become Editor-in-Chief of the Journal "Europhysics Letters". Furthermore, he has been elected into the board of directors of the "Deutsche Physikalische Gesellschaft" at the end of the year.

Prof. Dr. D. Richter has become scientific director of the European Spallation Source (ESS); he is also chairman of the scientific advisory committee (SAC) of the ESS. This demonstrates the strong commitment of the IFF to building a world-class neutron facility in Europe, of course preferentially in Jülich.

With the entry of the "Forschungszentrum Jülich" into the "Hermann von Helmholtz-Gemeinschaft Deutscher Forschungszentren", we have entered a new era of funding of the large research centers in Germany. Clearly, as happens in all large-scale reorganizations, this opens new possibilities but also implies new dangers. There is a lot of work ahead before we will see clearly how the new funding structures will affect our way of doing research. The IFF has always thrived on the freedom of research, the stimulating environment within the IFF – with its combination of basic and applied, experimental and theoretical, solid state and soft matter research -, and the interdisciplinary environment of the "Forschungszentrum Jülich". These strengths also put us in a very good starting position for the future.

Gerhard Gompper
IFF Managing Director 2002

Contents

Institute for Solid State Research (IFF)

1. Management and Structure

Prof. Dr. G. Gompper
Institute 'Theory II'
IFF-Managing Director for 2002

H. Geisler (Permanent Deputy of the Managing Director)

Institutes:

Institute 'Theory I'
Acting Director: Dr. A. Liebsch

Institute 'Theory II'
Prof. Dr. G. Gompper

Institute 'Theory III'
Prof. Dr. H. Müller-Krumbhaar

Institute 'Scattering Methods'
Prof. Dr. Th. Brückel

Institute 'Neutron Scattering'
Prof. Dr. D. Richter

Institute 'Electroceramic Materials'
Prof. Dr. R. Waser

Institute 'Soft Matter'
Prof. Dr. J. Dhont

Institute 'Microstructural Research'
Prof. Dr. K. Urban

Institute 'Electronic Properties'
Acting Director: Prof. Dr. Th. Brückel

Central Facilities:
'Networks and Numerical Methods'
H. Geisler

'Accelerator'
DI R. Hölzle

'Construction'
H. Feilbach

'Mechanical Workshop'
K. Hirtz

'Administration'
H. Geisler

The Institute of Solid State Research (IFF) pursues research on condensed materials in the solid or liquid state. Based on its studies of bulk properties of condensed phases, the IFF is concerned with inhomogeneous systems and with the consequences of reduced dimensionality. This refers in particular to

the physics of clusters, phase boundaries, thin films and membranes. With regard to both theory and experiment, the institute's research can be understood in terms of three strategically distinct categories:

- **Phenomena oriented research:** The search for, the discovery and explanation of general phenomena and behaviour in condensed matter systems, including the mathematical and physical concepts and structures underlying this behaviour.

- **Materials oriented research:** The investigation of specific materials or classes of materials with a view of gaining an understanding of their special properties and, where appropriate, exploring their potential for practical application. Production of novel materials, and preparation as well as characterisation of well-defined samples.

- **Method oriented research:** Development of new methods and the improvement of existing methods, both in the experimental and the theoretical/numerical sectors.

The general physical basis for these research areas is provided by statistical physics and quantum mechanics. Together they describe on a microscopic scale the behaviour and the reaction to external influences of electrons, atoms and molecules, the building blocks whose aggregation and cooperation is responsible for the formation of condensed phases. The issues to which these connections give rise in the context of current research form the basis of the work of *theoretical* and *experimental* groups within the institute.

Based on new techniques of preparation and characterization on a microscopic atomic scale, the *experimental* groups have increased their efforts to develop devices and taylor systems with new properties. This, in turn, has triggered the *theoretical* groups, employing modern techniques, to describe and come to an understanding of the extremely complex behaviour of these new systems.

The following specific foci of work in the IFF are symptomatic of the nature and purpose of a Helmholtz-Research Centre:

- Contributions to the construction and operation of new experimental equipment and instruments for international sources of neutron and synchrotron radiation. In addition to the Jülich Research Reactor "DIDO", the neutron sources at Argonne, Berlin, Gaithersburg, Grenoble, München, Oak Ridge, Saclay and Appleton are used. Experiments with synchrotron radiation are carried out at BESSY, DELTA and HASYLAB in Germany, and internationally at Argonne (APS), Berkeley (ALS), Brookhaven (NSLS), Grenoble (ESRF) and Trieste (ELETTRA).

- Use of the Jülich Computer Centre, mainly for theoretical investigations and large-scale numerical simulations.

- Projects that require high levels of investment and/or the continuity of a highly qualified team of staff (in most cases in the context of national and international cooperative projects and services). Examples are the Centre for High-resolution Microscopy, the operation of accelerators, the Electro-ceramics laboratory, superconductor technology and the development of sophisticated numerical algorithms and programs.

Over the long term, the research results of the IFF have led to a broad and internationally recognized status. Special technical and scientific excellence was achieved in the following areas: application of synchrotron-radiation and neutron scattering, electron-microscopy, electron-spectroscopy, high-temperature superconductivity, magneto-electronics, the physics of clusters, electron theory, dynamical features of phase-transitions, quasi-crystals, colloids, membranes and polymers.

A prerequisite for the focal areas of research in the IFF mentioned above and its position in the international community as a valued partner for cooperation is its strong position in basic research. The IFF carries out basic research in areas with potential for the future of condensed matter science, also as a hotbed for applied research projects.

Genuine innovation (as distinct from continuous development) occurs typically as a by-product of curiosity-driven research. This is exemplified particularly well by the discovery of the "giant-

magnetoresistance" effect, which over the past years has become a very active area in solid state research. The effect has attractive applications for magnetic sensors e.g. as read heads for data storage and for control of moving parts. The license revenue from the patents on this effect represents the largest contribution to the total patent revenue of the Jülich Research Centre devolving from a single application! With this activity the IFF is also participating in the BMBF (Bundesministerium für Bildung und Forschung, i.e. Ministry of Education and Research) project "Magnetoelectronics" and also carries out accompanying basic investigations within the Strategy-Fund Project "Magnetoelectronics".

The Jülich Research Centre contributes to the RD Program for the European Spallation Source *(ESS)*, a common project of 11 European countries. The IFF is strongly involved in the ESS project on several levels: by providing the scientific director and the chairman of the scientific advisory committee, via research into shock-wave effects in the liquid mercury target, the optimisation of the target and the moderators, and by the development of instrumentation.

In 2001, the scientific work of the IFF generated 349 publications (267 in refereed journals and 82 others), 8 patents and 9 patent applications. 340 scientific talks were presented. Among these were 230 invited talks. 134 posters were presented at conferences. In addition IFF staff members gave 52 educational seminars at universities. 25 staff members are lecturers at universities.

The traditional IFF-Spring School was held in 2001 with the topic "Neue Materialien für die Informationstechnik" (New Materials for Information Technology) and attracted 211 participants. In addition the IFF organises an annual two week lecture and practical laboratory course on "Neutron Scattering" in October. In the year 2001, we had 39 participants, 14 of which were from other european countries.

In 2001, 10 diploma students and 19 doctoral students completed their thesis; 17 diploma students and 63 doctoral students worked at IFF.

2. Scientific and Technical Infrastructure

In the context of a general reduction in the number of personell at the research center Jülich, the IFF was forced to tighten its technical infrastructure. Through organisational and strategic measures, the IFF tried to maintain the optimal efficiency of the central services despite the decrease in the number of staff. As a consequence the central facilities *Electronics Laboratory* and *Numerical Methods and Data Processing* were merged into a group *Networks and Numerics*. These measures have now reached a critical limit.

Research "at the cutting-edge" requires the capability to build and maintain experimental facilities in high-tech areas. This holds as well for the basic research performed by the IFF at national and international sources as for its applied research. Equipment must meet high international standards, and especially so when the work performed is to be "relevant for industry". A basic requirement for the work of the Department is an infrastructure, within the IFF and the Research Centre itself, which supplies the necessary expertise, effectiveness and facilities.

The group *Networks and Numerics* maintains the workstation cluster and computer networks, and supports scientific staff in the design and performance of experiments. It supplies expert assistance in hard- and software, maintains the system-software of the IFF-Workstation-Cluster and trains mathematical-technical assistants.

The *Accelerator Group* is responsible for the operation of the Compact-Cyclotron and the Tandetron.

Construction and *Workshop* develop and build equipment for the IFF, from simple mechanical components to sophisticated modern technology. The facility works closely together with the scientists and engineers of the Institute to achieve the ambitious quality and tolerance goals set by the experimentalists.

Staff members in the central facilities:

K. v. Ameln, S. Berger, H.P. Esser, A. Bremen, H. Cremer, P. Eickenberg, M. Emmerich, H. Feilbach, U. Funk-Kath, R. Gehlhaar, E. Gundt, R. Heckmann, J. Heinen, D. Henkel, K. Hirtz, R. Hölzle, K.H. Johnen, K. Kaulen., S. Krahe, J. Lingenbach, T. Matulewski, W. Noack, T. Nguyen-Vu, P. Pickartz, M. Pohl, B. Radermacher, H. Sachsenhausen, L. Schätzler, H. Schnitzler, J. Schramm, P. Stefelmanns, W. Stellmacher, H. Terberger, R. Thomas, E. Westphal, K. Wingerath.

J. Hengesbach (INC), L. Kasterke (IME), H. Schwalbach (ISG)

3. Other Scientific Activities: Collaborations with Universities, Institutions and Industry

The productivity of a Research Institute depends strongly on its capacity for scientific exchange and for scientific and technical cooperation. In this regard, the Jülich Research Center offers excellent possibilities. The Centre's top class infrastructure offers efficient assistance, also for visiting scientists. Modern neutron scattering instrumentation appropriate for cutting-edge studies are available to many IFF guest scientists in the DIDO reactor hall and in the neutron guide hall ELLA. The wide variety of collaborations in which the institutes for Neutron Scattering and Scattering Methods of the IFF are involved leads to optimal usage of these large scale instruments. On the other hand, the availability of complementary facilities at other institutions is essential for the IFF. With the construction of instruments the IFF contributed to the development and improved usage of external large scale facilities such as ILL and CEN (Grenoble), APS (Argonne, USA), DELTA (Dortmund), HASYLAB (Hamburg), BESSY (Berlin), NSLS (Brookhaven), and NIST (Washington).

Bilateral agreements have been concluded with the Paul-Drude Institute, Berlin, RWTH Aachen, IBM Rüshlikon, and the Universities Bonn, Göttingen and Kiel for the use of the Jülich centre for high-resolution microscopy for specialized studies in the area of quantitative and high-resolution microscopy, and the use of the Jülich microscope with correction of spherical abberation.

In the past years, the IFF has expanded its activities as a *sub-contractor* to large companies (e.g. Bosch, Siemens, Daimler-Benz, Thompson, Philips) and contract work has become the main focus of the scientific work of several groups, especially in the context of large national (German) and international projects. Of special importance is the IFF's participation in the BMBF-Project "Magnetoelectronics". Under the auspices of the Technology Transfer Bureau of the Jülich Research Centre, the IFF leases equipment to companies that have established themselves in the Jülich Technology Centre. In addition, the IFF has designed and built pilot equipment for industrial companies.

One of the most important duties of a Research Centre is to make its large scale instruments available to universities and other research organisations for research projects that need not necessarily have a direct connection with active research programs of the Centre. In this context it is of paramount importance for the IFF to keep the 16 neutron scattering instruments at the research reactor DIDO operating and to improve them further. In the year 2000, neutrons were available for users at 177 days altogether. During this time 87 experiments were performed by IFF scientists and 114 experiments by external groups (19 groups from each national and international universities, 4 groups from national and 11 from international research institutes and 5 groups from industry).

Many staff members of the IFF serve in scientific committees (e.g. advisory boards for institutes and scientific societies, program committees for international meetings, editors of proceedings, journals and databases, members or presidents of the boards of directors of scientific societies as well as referees, e.g. for the German Research Community, special research areas and prize committees).

Personal Honours, Awards and Distinctions

Dr. D.E. Bürgler has received an offer for a C4 professorship at the Martin-Luther-University, Halle-Wittenberg, Experimental Physics

Prof. Dr. J. Dhont has been nominated guest member of the "Netherlands Foundation for Fundamental Research on Matter (FOM)", Division: "Vloeinstoffen en Grensvlakken"

Prof. Dr. W. Eberhardt and Dr. J. Morenzin have been awarded the first prize of the "Mitteldeutscher Rundfunk", MDR, of the series "Einfach genial" for the invention of counterfeit-prove magnetic stripes

Dr. P. Ebert completed successfully his "Habilitation" at the RWTH Aachen, Department of Physics

Dr. B. Jahnen received a prize for the best poster at the conference of the Royal Microscopical Society in Oxford

Dr. H.H. Kohlstedt completed successfully his "Habilitation" at the University of Cologne, Experimental Physics

Prof. Dr. H. Müller-Krumbhaar has been appointed editor-in-chief for the Journal "Europhysics Letters" by the European Physical Society

Prof. Dr. H. Müller-Krumbhaar represents the European Physical Society in the Scientific Advisory Committee of the Journals "European Physical Journal B,D, and E"

Prof. Dr. H. Müller-Krumbhaar has been elected member of the board of management of the "Deutsche Physikalische Gesellschaft"

Prof. Dr. H. Müller-Krumbhaar has been elected chairman of the Scientific Advisory Committee "Minerva Center for Nonlinear Physics" at the Weizmann Institute, Rehovot and at the Technion, Haifa, Israel

Dr. G. Nägele has been appointed extraordinary professor at the University of Konstanz

Prof. Dr. D. Richter has been appointed Scientific Director of the European Spallation Source (ESS) Project

Dr. R. Rzehak received the "Dr. Eduard Martin Preis" of the University of Saarland for his PhD

Prof. Dr. R. Waser received the prize for "Outstanding Achievement" for his work in the area of characterization and physical interpretation of ferroelectric thin films for applications in memory devices on occasion of the "International Symposium on Integrated Ferroelectrics 2001" in Colorado Springs

Prof. Dr. R. Waser was awarded together with Dr. K. Prume, Dr. K. Franken, and Prof. H. Meier (IKKM, RWTH Aachen) the "Edward C. Henry Award" – Electronics Division Best Paper Award 2000 – for the paper "Finite-Element Analysis of Ceramic Multilayer Capacitors: Modeling an Electrical Impedance Spectroscopy for a Nondestructive Failure Test" on the occasion of the Annual Meetings 2001 of the American Ceramic Society

Dr. R. Winkler has been appointed extraordinary professor at the University of Ulm

Alexander von Humboldt Research Prize

Prof. F. Spaepen, Harvard University, Cambridge, USA
Prof. N. Smith, Law. Berkeley Nat. Lab., Berkeley, USA, Institute "Electronic Properties"

Alexander von Humboldt Scholars

Dr. Z. Dogic, Brandeis University, USA
Prof. H. Ishida, Nihon University, Tokyo, Japan

Institute Reports with Selected Research Results 2001

Institute Theory I

General Overview

Introduction:

The research activities of the Institute encompass several key areas of condensed matter theory: (i) electronic and structural properties of complex systems ranging from large organic molecules and mesoscopic contacts to complex solids; (ii) electronic excitations and dynamical properties of molecular clusters, solids and solid surfaces, as well as the quasiparticle behavior of transition metals and oxides resulting from electronic correlations; (iii) nano-scale tribology, friction, plastic deformation, adhesion and brittle fracture.

The principal goal of these studies is to achieve a microscopic understanding of complex phenomena on an electronic and atomic scale. Although most of these topics involve fundamental issues associated with many-body interactions, they are nevertheless relevant to a wide host of practical applications in modern materials science. In fact, the majority of research topics is directly motivated by the aim of providing a quantitative or qualitative physical basis for possible future technologies.

In line with the range of topics investigated a wide variety of conceptual and computational methods is currently employed: density functional theory, molecular dynamics calculations, genetic algorithms, data mining techniques, time-dependent generalization of density functional theory, diagrammatic perturbation approaches, classical and Quantum Monte Carlo methods, exact diagonalization schemes, as well as analytical methods. Needless to say that the state-of-the-art use of these methods benefits greatly from the excellent computational facilities available at the research center. The unique combination of basic physics questions and possible practical applications, investigated with these theoretical tools, is the hallmark of modern condensed matter and computational materials science research.

Research Topics:

1. *Ballistic electron transport through mesoscopic contacts:*
Narrow contacts between electron reservoirs are the heart of modern storage devices. Modern technology allows one to make nanoscale connections which the electrons can pass phase-coherently. A method has been developed to determine the conductivity of such quantum-contacts from a Schroedinger equation, and was applied to devices studied experimentally. As a next step, this method will be extended to cover the case of connections via single molecules. (A. Bringer; in collaboration with J. Appenzeller)

2. *Femtosecond spectroscopy of molecular clusters:*
Via time-delayed short laser pulses it is possible to determine lifetimes of excited quantum states in the femtosecond range and to identify the decay mechanisms. This "pump-probe" technique is applied in the experimental Institute for Electronic Properties (IFF-IEE) to study the dynamics of molecular clusters. Previous theoretical interpretations of the spectra are still largely phenomenological and efforts to improve existing models for relaxation processes in quantum systems are necessary. In connection to recent experiments on Au_2CO clusters in the IEE the process of photon excitation and subsequent electronic

and vibrational relaxation will be simulated by a suitable time dependent Schroedinger equation. (A. Bringer; in collaboration with P. Bechthold, M. Neeb)

3. *Mathematical modelling using a genetic algorithm:*
Many quantities of considerable interest (such as the electrical conductivity of a real material) cannot be predicted by first principles theory. However, by mining existing data for hidden correlations (using e.g. the genetic algorithm) it may be possible to generate mathematical models for such quantities that use readily computed descriptors and which are able to predict these quantities with a certain degree of reliability. (J. Harris; A. Bringer)

4. *Computation of thermal and mechanical properties using density functional methods:*
A body of recent work has shown that the DFT method with well-established exchange-correlation energy functionals describes the small changes necessary to compute quantities such as the stiffness matrix (elastic moduli) of even quite complicated crystals. Furthermore, application of full Grueneisen theory gives a good description of thermo-mechanical properties like the coefficient of thermal expansion. These are currently supercomputer applications, however, requiring a very careful treatment of phonon spectra. A lower level of theory (Debye-Grueneisen) is available but so far has been tested only for some elemental metals. The current status of the programme is to establish procedures for implementing Debye-Grueneisen theory in general and testing its area of applicability. (J. Harris; in collaboration with J. Rodgers, Y. LePage, P. Schmidt)

5. *Energy surfaces, structures and reactions of polymers:*
The electronic and structural properties of organic molecules are evaluated using density functional theory and molecular dynamics methods with the aim of understanding in detail the mechanism of reactions between polymer chains, and the catalysts and additives used in their production. The density functional programs run on the T3E supercomputers and are very demanding of computer resources for systems of the complexity studied here. An example is provided by the reaction between the nucleophilic molecule lithium phenoxide (LiOPh) and a segment of a polycarbonate chain, which involves calculations for a total of 145 atoms. The resulting energy surfaces, however, provide a consistent and extendible data base for developing simplified models that allow calculations on much larger systems. Of particular interest are: (i) the refinement of classical force fields for use in molecular dynamics and Monte Carlo simulations, (ii) the development of a model of 'living polymers' that allows one to study the polymerization process in polycarbonate over a wide range of temperatures and densities. This has lead to the identification of the nature of the polymerization transition. (R.O. Jones; in collaboration with J. Akola, P. Ballone, Bayer AG)

6. *Dynamical Response at metal surfaces:*
Quantum well behavior in adsorbed thin films is usually observed for electrons confined by the band gap of the underlying substrate. Recent photoemission spectra for Na films on Al(111), however, reveal such behavior also for the resonances induced by the large negative potential step between adlayer and substrate. Using time-dependent density functional theory it was shown that this observation is made feasible via the local screened photonfield which is enhanced and confined to the overlayer if the photon frequency is tuned to the Na collective modes. (A. Liebsch; in collaboration with S. Barman, K. Horn)

7. *Magneto-optical Kerr effect for non-equilibrium electron distributions:*
There is currently great interest in understanding the dynamical response of magnetic surfaces to excitations via ultrafast lasers (e.g., recent experiments in this area in the institute

IFF-IEE). In order to investigate to what extent the Kerr signal provides information on the time-varying magnetization of the sample, the optical conductivity tensor is evaluated for non-equilibrium electron distributions generated by the initial pump laser. Of particular interest is the so-called bleaching effect (closing of certain excitation channels) at high laser intensities. (A. Liebsch; in collaboration with P. Oppeneer)

8. *Trajectories and their discrete counterparts:*
It is generally believed that trajectories can well be represented by their discrete counterparts, the so called Poincaré maps (PM) which quite often are much easier to handle (e.g. numerically). It is shown, that in repelling systems (transient chaos) the PM gives misleading results. Even the sign of drifts can be erroneous. Modifying the PM by including the return time (time between two intersections) leads to correct results. At present correlation funtions and diffusion are computed and compared by using PM and the modified PM. (H. Lustfeld; in collaboration with Z. Kaufmann)

9. *Characterization of tracer gas concentrations in the atmosphere:*
In the atmosphere small scale fluctuations of tracer gas, in particular pollutant, concentrations occur signalizing that the concentrations are singular functions. It is shown that these singularities have to be characterized not by just one Hölder exponent but by an ensemble classifying the strength of these singularities. The situation is quite analogous to that of trajectories: These have to be classified by an ensemble of Lyapunov exponents as well. Just one exponent is not sufficient. (H. Lustfeld; in collaboration with Z. Neufeld)

10. *Friction, nano-scale tribology:*
A research activity related to many practical applications concerns the area of tribology, in particular, friction and related topics such as plastic deformation, adhesion and brittle fracture. The influence of surface roughness on adhesion between elastic bodies is also investigated. Furthermore, Molecular Dynamics calculations are performed to understand the transition between boundary lubrication and hydrodynamic lubrication. An important result was obtained within a recently developed theory of contact mechanics between randomly rough surfaces, where the solids are assumed to deform elastically when the stress is below the yield stress, and plastically when the stress reaches the yield stress. Of key interest is the dependence of the (apparent) area of contact on the magnification. In most cases the area of real contact is proportional to the load. If the rough surface, however, is self-affine fractal (Hurst exponent H) up to the lateral size L of the nominal contact area, and assuming no plastic deformation, then the real contact area is proportional to L^H. (B.N.J. Persson; in collaboration with A. Volokitin, V. Samoilov, S. Zilbermann).

11. *Rubber Friction*
When rubber slides on a hard, rough substrate, the surface asperities of the substrate exert oscillating forces on the rubber surface leading to energy "dissipation" via the internal friction of the rubber. A recently developed theory shows how the resulting friction force depends on the nature of the substrate surface roughness and on the sliding velocity both for stationary and non-stationary sliding. Numerical results were obtained for the case when the substrate surface has a self affine fractal structure and are in good agreement with experimental observations. The theory is now used by tire companies in developing new rubber compounds for tires. At present the theory is extended to take into account the flash temperature in the rubber-substrate contact areas. (B.N.J. Persson)

12. *Dynamical correlations in the electron gas:*
To understand dynamical correlations in the electron gas beyond the RPA, lowest order

corrections in the dynamically screened Coulomb interaction are evaluated numerically. The corresponding irreducible polarization diagrams have been known for 40 years but have resisted computation because of their complexity. By analytical means the resulting 7-dimensional integrals were now reduced to 3-dimensional integrals. For (k, ω) outside the particle-hole continuum, dynamical correlations consist of two-particle-hole-pair, two-plasmon and coupled particle-hole-pair-plasmon excitations. The results in this range compare well with experiments. Presently the calculations are extended to (k, ω) inside the particle-hole continuum with the aim of analyzing additional available data. (K. Sturm; in collaboration with A. Gussarov, H. Lustfeld)

External Funding:

1. R.O. Jones receives support within the framework of the Kompetenzzentrum "Werkstoffmodellierung: Wege zum computergestützen Materialsdesign", 01.01.2000 – 31.12.2004, funded by the BMBF (50 %), Bayer AG, FZJ. Total grant: 1.929.240 DM, BMBF: 997.240 DM (Personell: 780.000 DM, travel: 52.000 DM, equipment 100.000 DM).

2. A. Liebsch receives support within the European Community Network on Ultrafast Magnetization Dynamics (total grant 1.500.000 Euro).

3. Between 1994 and 2002 Bo Persson obtained research grants from the DFG (about 100.000 DM) for several 3-months visits of Prof. A. Volokitin (Samara, Russia).

4. As a participant in a 5-year BMBF supported German-Israeli Cooperative Project on "Novel Tribological Strategies: from the Nano-to Meso-Scales" Bo Persson receives annual funding of 50 000 DM.

5. Bo Persson also receives a European Community grant (about 350.000 DM) within the network: SMART QUASICRYSTALS, 2001 (total grant 20.000.000 Euro).

Ansgar Liebsch
Acting Head since 01.08.2001

Personnel 2001/2002 and areas of activity:

Staff Members

Dr. A. Bringer	Genetic algorithms for materials research Problems of electron correlation	23.20.0
Dr. J. Harris	Practical applications of computational and informational methods to materials research	23.20.0
Dr. R.O. Jones	Structure and dynamics of clusters, molecules, and disordered systems; Project: "Chemistry Laboratory Computer"	23.20.0
Dr. A. Liebsch	Electronic response at surfaces; correlated systems; ultrafast demagnetization	23.20.0
Dr. H. Lustfeld	Theory of nonlinear systems; atmospheric chemistry; dynamical electron correlations in metals	23.20.0
Dr. B.N.J. Persson	Electronic response at surfaces, adsorbate modes, atomic friction, crack propagation	23.20.0

Guests

Prof. P. Ballone	(University of Messina) Development and applications of the MD/DF method, Monte Carlo calculations	23.20.0
Prof. G. Eilenberger	(FZ Jülich, retired since 1.8.2001)	23.20.0
Prof. K. Fischer	(FZ Jülich, retired) Vortices in high Tc superconductors	23.20.0
Prof. H. Ishida	(Nihon University, Tokyo) Electronic properties of surfaces, transport through interfaces	23.20.0
Prof. A. Samoilov	(Moskau State University) Theory of friction	23.20.0
Prof. K. Sturm	(FZ Jülich, retired since 1.4.2001) Dynamical correlations	23.20.0
Prof. A. Volokitin	(Samara University, Russia) Theory of friction	23.20.0

Postdocs

Dr. J. Akola	(Jyväskylä, Finland) Structure and dynamics of organic molecules	23.20.0
Dr. C. Lopez	(Cuernavaca, Mexico) Electron dynamics at surfaces	23.20.0
Dr. C. Maytorena	(Cuernavaca, Mexico) Electron dynamics at surfaces	23.20.0
Dr. S. Zilbermann	(Tel Aviv University, Israel) Theory of friction	23.20.0

Graduate Students

D. Boukhvalov	(Ekaterinburg, Russia) Molecular magnets	23.20.0

Application of the density functional method to thermo-mechanical Properties.

John Harris
Institute Theory I, IFF.

It is now well established that the DFT method can track the small changes in the energy with unit cell size that are needed to compute the stiffness matrix, from which one can obtain all the elastic moduli of the crystal and other information such as the velocity of sound. The method has also recently been applied to thermo-mechanical properties such as the coefficient of thermal expansion. Such calculations are computationally intensive because they involve the determination of derivatives of the phonon frequencies with respect to the volume. It is therefore useful to consider simpler methods that may give results of lower, but yet useful accuracy. One such method is assumes a Debye spectrum for the phonons and involves an averaged Grüneisen parameter. Such a method was proposed many years ago, but its consequences have not been explored to any great extent. The two essential elements that are missing are a a) a reliable, efficient computational scheme for the relevant parameters and b) a large number of computations over a wide variety of materials to establish when the method is reliable and when it is not.

F&E-Nr: 23.20.0

The density functional scheme of Kohn and Sham [1] has long been an established method for calculating the energies and equilibrium geometries of aggregates of atoms, whether in molecules, clusters or periodic structures. Application of the methodology to mechanical and thermal properties of materials has lagged somewhat behind chemistry applications. However, the past decade has seen important advances. Calculation of the elasticity moduli of materials is now a standard application of the theory, with results having similar quality to those obtained in chemistry. This indicates that the DFT method is able to track the energy of crystalline structures sufficiently well to allow the small energy changes associated with shear deformations to be determined with sufficient accuracy to allow computation of the full stiffness matrix. Standard methods compute the $C_{i,j}$ from the energy differences of deformed and unperturbed lattices [see, for example, 2 - 6]. Specifically, the energy associated with strain field e_i is

$$\Delta E(e) = \frac{1}{2}\sum_{i,j} C_{i,j} e_i e_j, \qquad (1)$$

In using this relationship to compute the C-coefficients, a very precise determination of the optimal lattice constants is necessary. A way of circumventing this requirement and allowing explicitly for a residual strain was published by LePage and Saxe [7].

More recently, these authors have proposed and implemented a method based on direct computation of the stress [8]. This method allows for an initial strain of any magnitude. For internal strain E and the corresponding stress $S(E)$, a set of C-coefficients can be defined for each E and computed by determining the stress in deformed samples for a range of strains $E+e$, with e small. Under these conditions, the stress-strain relation can be linearized in the small quantities additional stress, s, and strain, e, about S and E,

$$S(E+e) = S(E) + s = S(E) + C(E) \qquad (2)$$

and 'elastic coefficients' $C(E)$ of the material under strain E determined. A stress-based method of this kind requires accurate calculation of the stress, but it has been found that the commercially available VASP module developed at the University of Vienna [9] incorporates stress computation with the required degree of accuracy.

The computation of thermo-mechancial properties like the thermal expansion coefficient is one stage more difficult than the determination of the stiffness matrix, and accordingly the literature is relatively more sparse. The framework for computing properties such as the thermal expansion coefficient was laid out in the original very elegant work of Grüneisen [10] and involves a computation of the volume derivative of the material's phonon frequencies and a sum over normal modes. This scheme can be carried out in practice and is found to be highly accurate, but is quite CPU intensive (see, for example, [11] and references therein).

A simpler level of theory, the so-called "Grüneisen-Debye" approximation, combines Grüneisen's theory with a Debye model for the phonons. The result is a set of simple formulae for the thermal expansion coefficient that contains two essential material parameters, the "Debye Temperature" and an averaged "Grüneisen constant". This approach, however, is not entirely straightforward because there is no unique way of determining these parameters. A review of the approach and some of its pitfalls was given by Segletes and Walters [12]. Within a Debye model for the phonons, the averaged Grüneisen parameter, γ, reduces to the derivative of the Debye temperature with respect to volume. The issue then is how the Debye temperature should be determined. This can be done most directly by using the relation between the Debye temperature and the averaged velocity of sound in the material, in which case a value for γ can be obtained

directly from the stiffness matrix, which determines the sound velocities in the crystal.

Alternatively,γ can be related to the pressure-volume equation of state, reflecting its connection with the anharmonicity of the inter-atomic interactions within the material. However, the extraction of the Grüneisen parameter requires fitting a computed pressure-volume curve to an assumed functional form that can be analytically differentiated and is far from straight forward. In the light of the new methods referred to above for computing the stiffness matrix as a function of strain, it is worth revisiting the issue of finding a clear-cut procedure for determining the Grüneisen parameter that is at once computationally efficient and delivers reasonable accuracy. Clearly, the averaged theory can be applied only to a limited range of materials where the k-dependence of the Grüneisen parameter is relatively unimportant. This k-dependence has been determined for several test cases. For Ag, the k-dependence seems rather unimportant [13], whereas for SiN, there is a strong difference between acoustic and optical branches which, presumably, must be accounted for [14]. Two main foci are therefore identified:

1. Establishing a reliable and efficient way to compute the averaged Grüneisen parameter.
2. Determining the class of materials for which the averaged theory gives reasonable results.

Acknowledgement:
Work on thermo-mechanical properties is part of an ongoing collaboration with Peter Schmidt of the Technical University of Darmstadt, Jürgen Sticht and Paul Saxe of Materials Design and John Rodgers and Yvon Le Page of NRC, Canada

References

1. W. Kohn and L. J. Sham, Phys. Rev. 140, A1133 (1965)
2. M. J. Mehl, J. E. Osburn, D. A. Papaconstantopoulos and B. M. Klein, M. J. Mehl and D A. Papaconstantopoulos, Phys. Rev. B 54, 4519-4530 (1996)
3. R. Stadler, W. Wolf, R. Podloucky, G. Kresse, J. Furthmüller and J. Hafner, Phys. Rev. B 54, 1729-1734 (1996)
4. S.Hong, C.L.Fu and M.H.Yoo, Intermetallics 7 (1999), 1169-1172
5. P. Ravindran, L. Fast, P. A. Korzhavyi, B. Johansson, J. Wills and O. Eriksson, Journal of Applied Physics 84, 4891-904 (1998)
6. B. Mayer, H. Anton, E. Bott, M. Methfessel, J.Sticht, J.Harris and P.C. Schmidt, (Intermetallics, to be published)
7. Y. Le Page and P. W. Saxe, Phys. Rev. B63 174103 (2001)
8. Y. LePage and P. W. Saxe (to be published)
9. G. Kresse and J. Furthmüller, Phys. Rev. B 54, 11169 (1996); Computat. Mat. Sci. 6, 15 (1996)
10. E. Grüneisen, Handbuch der Physik, Bd.X, p.1, Springer Verlag Berlin (1928)
11. A. I. Lichtenstein, R. O. Jones, S de Gironcoli and S. Baroni, Phys Rev. B 62 11487 (2000)
12. S. L. Segletes and W. P. Walters, J. Phys.Chem Solids 59, 425 (1998)
13. J. Xie, S de Gironcoli, S. Baroni, M.Sheffler Phys. Rev. B 59 965 (1999)
14. K. Karch, P. Pavone, W. Windl, O. Schütt and D. Strauch, Phys. Rev. B 50 17054 (1994)

Equilibrium polymerization of polycarbonate – polymerization transitions in 2D and 3D

R. O. Jones and P. Ballone†
Institute Theory I

Density functional (DF) calculations have provided a detailed picture of the basic catalytic reaction in the ring-opening polymerization of bisphenol-A polycarbonate (BPA-PC). Simple nucleophilic molecules such as lithium phenoxide (LiOPh) react with the carbonate group of the cyclic ring oligomer, leading with low barriers and almost no change in total energy to a chain with a phenyl carbonate at one end and a phenoxide at the other. The alkali atom at the end of the chain can repeat this process, producing a "living polymer". In our report last year we showed that a classical simulation of a model suggested by the DF calculations showed that polymerization in this case is entropy driven. We have now extended these calculations to multiple active sites (the Li ions in this case) and learned more about the polymerization transition.

F&E-Nr: 23.20.0

Bisphenol-A polycarbonate (BPA-PC) is one of the most important polymers in industrial production, and its structural unit contains 33 atoms. Of its many cyclic oligomers the strain-free tetramer, which shows the *cis-trans* isomerization found in polycarbonate chains, provides an ideal model for PC. The reaction of the nucleophilic molecule Li phenoxide LiOPh with the carbonate group leads to the rupture of ring systems (ring-opening polymerization) [1]. The reactants and products of this reaction are shown in Fig. 1, and the method used in the DF calculations is described in detail in Ref. [2]. The chain shown in 1(b) has an "active" -C-O-Li termination, so that a series of catalytic reactions can result, resulting in the breaking of rings and the formation of long chains. The energy barrier to the reaction and the change of energy between reactants and products are both small, and the number of bonds and their nature is the same in 1(a) and 1(b). We have used these facts to develop a simple model of the ring-opening mechanism and perform extensive numerical simulations with it.

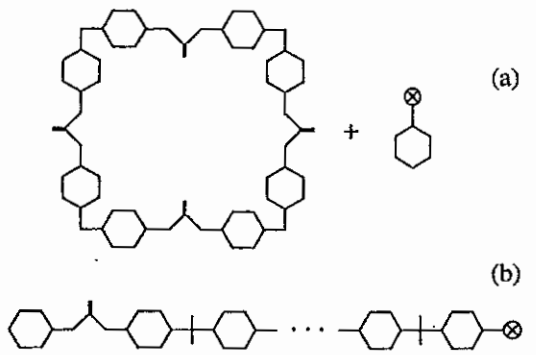

FIG. 1. Reaction of LiOPh with cyclic tetramer of BPA-PC. The product (b) is a Li-terminated chain.

In our model, diphenyl carbonate (DPC) units are represented by Lennard-Jones particles, with harmonic springs describing the covalent bonds in the polymer backbone. Each particle forms at most two harmonic bonds, so that the system comprises open chains or rings without branching. If we have $(N/4)$ cyclic tetramers, the potential energy is then:

$$V(\mathbf{r}_1,...,\mathbf{r}_N) = 4\epsilon\sum_{i>j}^{N'}\left\{\left(\frac{\sigma}{|\mathbf{r}_i-\mathbf{r}_j|}\right)^{12}-\left(\frac{\sigma}{|\mathbf{r}_i-\mathbf{r}_j|}\right)^{6}\right\}+ +\frac{1}{2}k\sum_{\alpha=1}^{(N/4)}\left\{(\mathbf{r}_{4\alpha-3}-\mathbf{r}_{4\alpha})^2+(\mathbf{r}_{4\alpha-3}-\mathbf{r}_{4\alpha-2})^2+ +(\mathbf{r}_{4\alpha-2}-\mathbf{r}_{4\alpha-1})^2+(\mathbf{r}_{4\alpha-1}-\mathbf{r}_{4\alpha})^2\right\} \quad (1)$$

where the prime on the first sum indicates that the Lennard-Jones interaction is turned off when i and j are connected by the harmonic potential. The units of length and energy are σ and ϵ, respectively, and the density is measured in terms of the packing fraction η ($\eta = \pi\rho\sigma^2/4$ in 2D, $\eta = \pi\rho\sigma^3/6$ in 3D). We perform simulations for systems with fixed bonding patterns and for which a fixed number N_a of "active" particles can interchange bonds with another particle. Details of the calculations with $N_a = 1$ are given in Ref. [3], and more information on the cases to $N_a = 36$ can be found in Ref. [4]

The simulation samples both different bonding configurations and the particle positions. At regular intervals we link the active particles and their nearest neighbors (excluding the particle connected to it by an intramolecular bond), as well as two of their covalently bonded neighbors (Fig. 2). The interchange always conserves the total number of bonds, and is accepted or rejected using the Metropolis algorithm according to the change of the potential energy and temperature. The bonding configurations are sampled using the (constant volume) Monte Carlo (MC) method in 2D and 3D, with periodic

boundary conditions. The simulations were started from a system of 2500 tetramers and N_a dimers, each carrying one active particle. For $N_a = 36$ this corresponds to a catalyst concentration similar to those used in industrial practice. The simplicity of the model allows us to perform very long simulations with up to several million steps *per particle*.

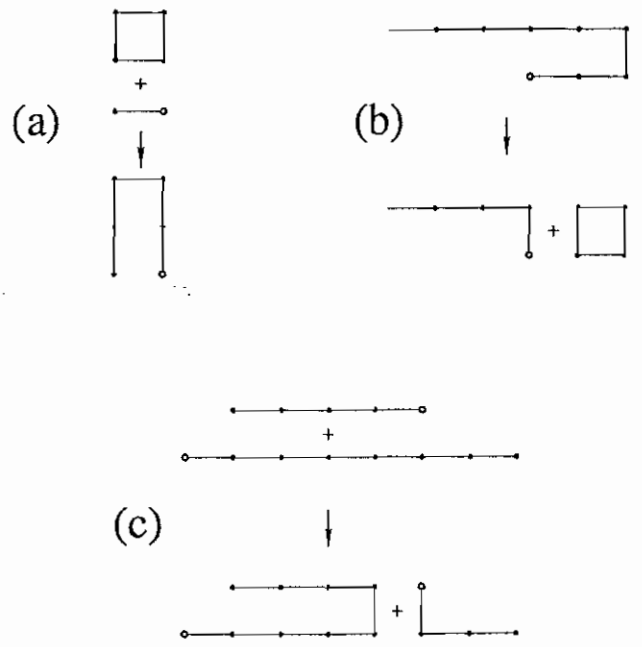

FIG. 2.

In the present report we focus on the polymerization transition in 2D. The addition of dimers with active heads gives rise to continuing bond interchanges in all 2D samples. The chains grow slowly at low density ($\eta < 0.15$), evolving almost independently and with an average length $\langle L_l \rangle$ that depends on the concentration of active particles c_a. In Fig. 3 we show the dependence of $\langle L_l \rangle$ on η for different values of c_a.

The $\langle L_l \rangle(\eta)$ curves show a steep rise at $\eta \sim 0.15$, which can be viewed as a rounded transition to the polymeric state. To quantify this observation, we fit each S-shaped curve of Fig. 3 with a Padé ratio, so that the value $\bar{\eta}$ at which the curvature of the interpolated function changes sign is our estimate of the transition point, while the slope of $\langle L_l \rangle$ at $\bar{\eta}$ is a measure of its steepness. Fig. 4 shows that the steepness increases rapidly and without apparent upper bound as c_a decreases, suggesting that the transition becomes discontinuous in the limit that c_a vanishes.

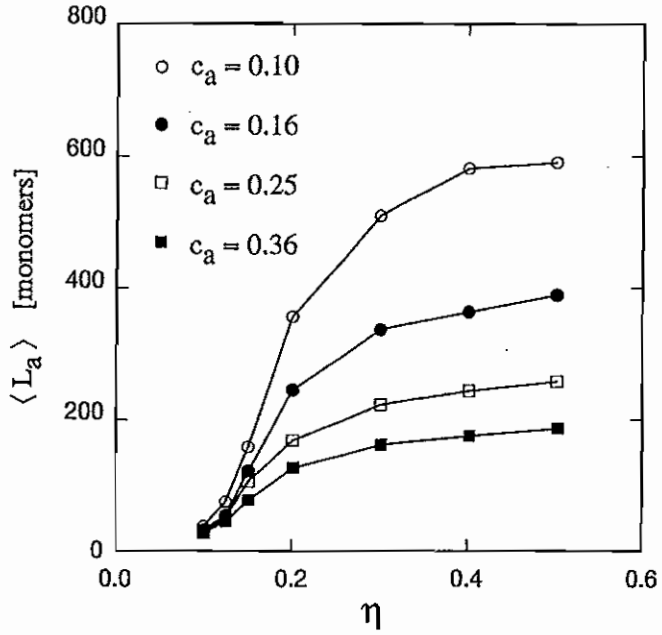

FIG. 3. Average length of open chains as a function of packing fraction η for different concentrations (in %) of active particles. Simulations in 2D.

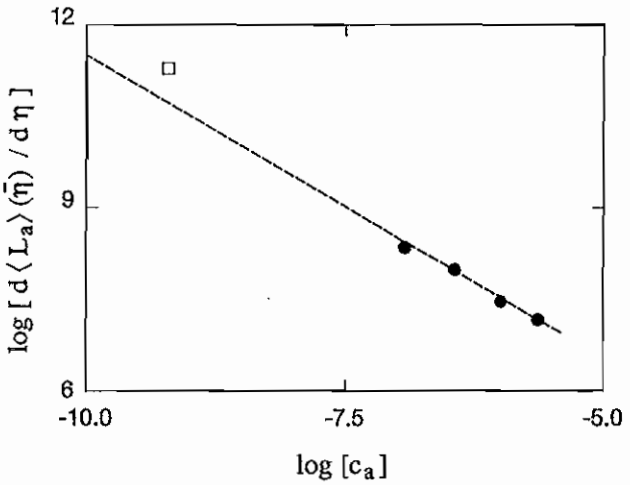

FIG. 4. Logarithmic plot of $\frac{d}{d\eta}\langle L_l \rangle(\bar{\eta})$ computed at the inflection point $\bar{\eta}$ of $\langle L_l \rangle(\eta)$ as a function of the concentration c_a of active particles. The empty square is the result for $N_a = 1$.

The equilibrium size distributions of rings and chains are characterized by the mass-fraction distributions $P_r(M)$ and $P_l(M)$, defined as the percentage of monomers belonging to a ring or a chain, respectively, of mass M. The dependences of $P_l(M)$ and $P_r(M)$ on η is shown in Fig. 5. The distributions for chains are relatively broad, and the Zimm-Schulz form:

$$P_l(M) \propto M^{\beta} \exp\left[-\beta M / \langle L_l \rangle\right] \qquad (2)$$

provides a fair fit to all curves, with an exponent ($1.1 < \beta < 1.4$) close to the value predicted by analytic theories $\beta = 43/32$. [5]

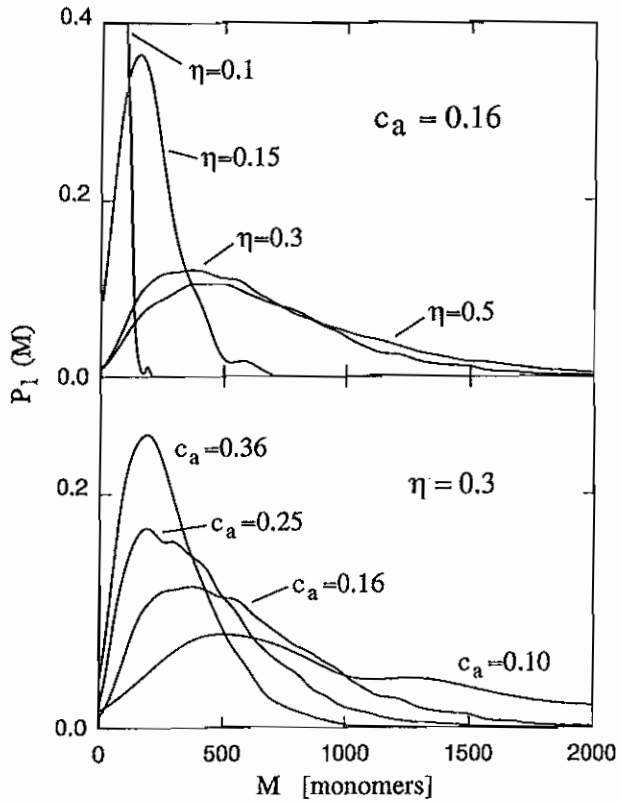

FIG. 5. Mass-fraction distribution functions for open chains in 2D systems. Upper panel: results for different densities at fixed concentration of active particles ($c_a = 0.16\%$). Lower panel: results for different values of c_a at fixed packing fraction ($\eta = 0.3$).

Simulations for systems in 3D yield analogous results to those for $N_a = 1$ [3], where we showed that the tendency to polymerization is much greater in 3D than in 2D. In Fig. 6 we compare the fraction of the total mass represented by open chains in 2D and 3D over a wide density range (for $T = 3$ and $c_a = 0.16\%$). The polymerized fraction is systematically higher in 3D, reaching 90% of the total mass already at densities of the order of $\eta \sim 0.25$.

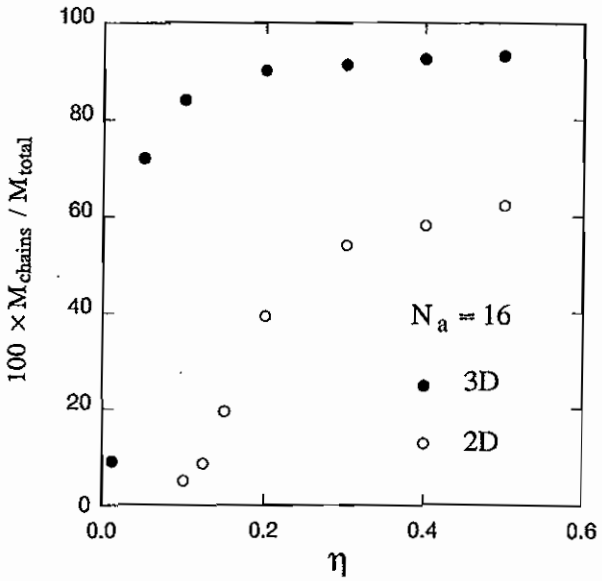

FIG. 6. Fraction of the total system mass in open chains in 2D and 3D as a function of packing fraction η.

The degree of polymerization in 3D decreases slightly but monotonically with decreasing T, as found in 2D. At $\eta = 0.3$ and $c_a = 0.16\%$, for example, open chains account for 91.3% of the total mass for $T = 3$, decreasing to 84.8% at $T = 0.6$. We did not observe any clear polymerization transition on changing T alone, so that the polymerization line in the $\eta - T$ plane is a very steep function of η. Full details of the results in 2D and 3D are given in Ref. [4].

The present series of simulations has identified configurational entropy as the driving force behind polymerization in this model, and we have been able to identify the polymerization transition in both 2D and 3D. We emphasize, however, that this model does not describe *all* types of "living polymer", particularly those that polymerize by condensation and evaporation of monomers. However, there is a strong analogy to other systems, such as the polymerization of sulphur, and we are studying this case in more detail.

† Permanent address: Università degli Studi di Messina, Dipartimento di Fisica, I-98166 Messina, Italy.

[1] D. J. Brunelle, In *Ring-Opening Polymerization: Mechanisms, Catalysis, Structure, Utility*; Edited by D. J. Brunelle, (Hanser, München, 1993), p. 1, p. 309.
[2] P. Ballone, B. Montanari, and R. O. Jones, J. Phys. Chem. **104**, 2793 (2000); P. Ballone and R. O. Jones, J. Phys. Chem. A **105**, 3008 (2001).
[3] P. Ballone and R. O. Jones, J. Chem. Phys. **115**, 3895 (2001).
[4] P. Ballone and R. O. Jones, J. Chem. Phys. (submitted).
[5] L. Schäfer, Phys. Rev. B **46**, 6061 (1992); P. D. Gujrati, Phys. Rev. B **40**, 5140 (1989).

Quantum Well Behavior without Confining Barrier Observed via Dynamically Screened Photon Field

A. Liebsch
Institute Theory I

Angle resolved photoemission spectra from Na adlayers on Al(111) reveal features which behave like quantum well resonances although the substrate provides no confining barrier. The quantum well behavior is shown to be due to surface resonances of the Na/Al system. The resonances are observable using photoemission because of spatial confinement and dynamical enhancement of the local electric field within the Na films.

F& E-Nr. 23.20.0

Quantum well states are a striking manifestation of elementary quantum mechanics.[1] An electron confined in a one-dimensional potential well may occupy discrete energy levels whose quantum number n specifies the number of half-wavelengths spanning the well. Quantum well states have been observed experimentally in a variety of layered semiconductor and metallic films where potential barriers restrict the electron's motion in the direction normal to the film. Here we discuss a different mechanism, namely, quantum well behavior in the absence of a confining wall between adsorbed metal film and underlying substrate.[2] The resonances are observable since the screened photon field is dynamically enhanced and spatially confined to the overlayer. We demonstrate that angle resolved photoemission for Na on Al(111) reveals quantum well like spectral features associated with virtual states induced by the large *negative potential step* between overlayer and substrate. To observe these resonances it is crucial to suppress emission from substrate bands in the same energy region. This is achieved by tuning the photon energy to the collective modes of the overlayer. The local electric field is then enhanced and confined to the overlayer so that the Na resonances can be observed in a wide range of coverages. Thus, while in usual quantum well systems the photon field plays no special role, here it serves as a novel mechanism ensuring the confinement of the excitation region.

For simplicity, we represent overlayer and substrate in terms of the jellium model which, combined with the time dependent local density approximation, provides an excellent description of excitation spectra of adsorbed alkali metal films.[3] Fig. 1 illustrates the ground state potential and the dynamical local potential, which includes the response of the electron density to the incident photon field. The potential step between Na and Al corresponds the difference between their Fermi energies. Since the Al substrate does not provide a suitable band gap which can act as a reflecting potential barrier, the electronic states within the overlayer are continuous functions of energy and film thickness. In the region of constant Na potential the ground state wave functions may be written as $\psi_{k_\perp}(z) = A_{k_\perp}\sin(k_\perp z - \gamma_{k_\perp})$, where the normal momentum $k_\perp$ is measured with respect to the bottom of the Na potential and $\gamma_{k_\perp}$ is a boundary phase shift. z is the coordinate normal to the surface. The quasi-discrete nature of the Na valence band induced by the potential step at the Na/Al interface manifests itself in the oscillatory behavior of $A_{k_\perp}$. Since $\gamma_{k_\perp}$ is slowly varying, the maxima of $A_{k_\perp}$ are approximately given by the condition $k_\perp a = n\pi$, where a is the overlayer thickness. Thus, below k_F there are about $n = k_F a/\pi$ peaks whose width results from single-particle hybridization with substrate states and depends on the thickness a and the potential difference between overlayer and substrate. With increasing thickness the peaks become sharper and move to lower $k_\perp$ corresponding to higher binding energies. Apart from the broadening, therefore, the potential drop between Na and Al ensures that the overlayer resonances obey the same variation with binding energy and overlayer thickness as true quantum well states.

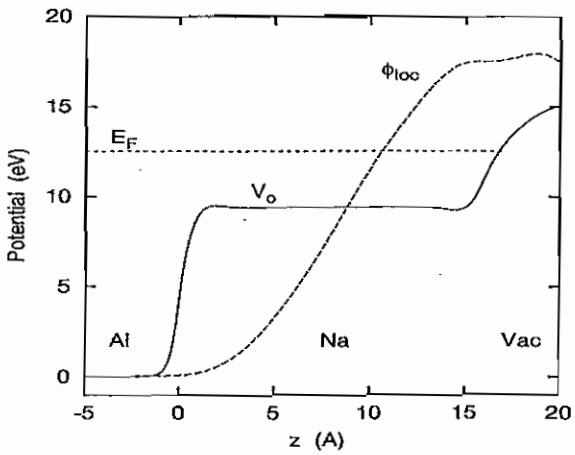

FIG. 1. Ground state one-electron potential $V_0(z)$ (solid curve) and real part of dynamical local potential $\phi_{\rm loc}(z, 5.5\,{\rm eV})$ (arbitr. units; dashed curve) for 5 ML Na on Al ($a = 16$ Å). E_F denotes the Fermi level.

We now discuss the effect of the photon field which has a unique influence on the observed quantum well behavior. The screening response of the Na valence electrons to the incident photons generates an induced field normal to the surface which together with the bare photon field forms the effective local field governing the photoexcitation cross section. Our microscopic dynamical calcula-

tions show that this response becomes resonant near the overlayer collective excitations: the bulk like mode at $\hbar\omega_p$, whose fluctuating charge is a standing wave extending across the Na film, and the multipole surface mode at $\hbar\omega_m$, whose charge is concentrated near the Na/vacuum interface. Since the frequencies of these excitations are far below the Al bulk plasma frequency, the effective local field is spatially confined to the overlayer so that emission from substrate states is suppressed. This is illustrated in Fig. 1, which also depicts the dynamical potential $\phi_{\rm loc}$. Near $\hbar\omega_p$ the normal component of the local electric field in the overlayer, i.e., the gradient of $\phi_{\rm loc}$, is about two orders of magnitude larger than in the substrate.

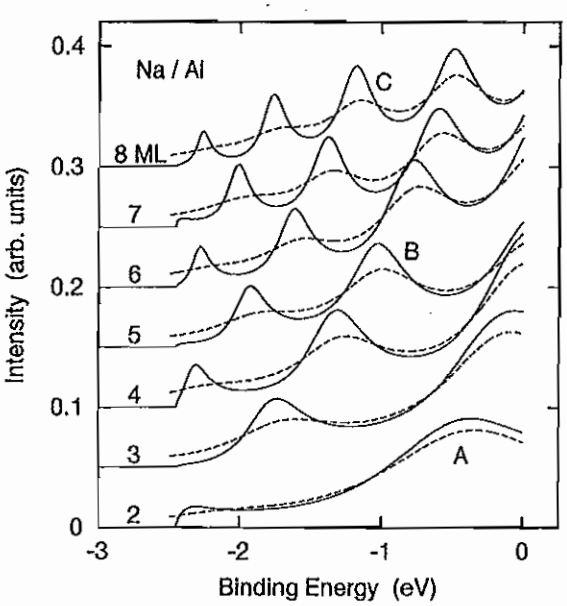

FIG. 2. Calculated energy distributions for Na on Al for various coverages at 5.5 eV photon energy. The lower cut off is due to the work function. Letters refer to analogous spectral features observed in Fig. 1. Dashed curves indicate the broadening due to hole life time and experimental resolution.

As shown in Fig. 2, the quasi-discrete nature of the Na overlayer states leads to characteristic features in the photoemission spectra. Since the local potential limits emission to the overlayer, the matrix element for normal emission is in fact proportional to the amplitude $A_{k_\perp}$ of the ground state wave function within the overlayer. Accordingly, the theoretical spectra exhibit a series of peaks which appear to move upwards as the overlayer thickness increases. At larger coverages, this pattern continues to evolve in a regular manner, with spectral peaks becoming more densely spaced, in close analogy to the experimental features. In practice, the oscillatory behavior of $A_{k_\perp}$ can be seen most clearly near E_F since various broadening mechanisms affect the deeper lying spectral features. To account for the hole life time we have included an imaginary self-energy of the form $0.1\,E_i^2$ eV, corresponding to the quasi-particle broadening of a homogeneous electron gas with electron density of Na. In addition, we have accounted for the experimental resolution of 0.15 eV. At the coverages shown, the finite life time of the outgoing electron plays only a minor role since the mean free path is long compared to the overlayer thickness. Deviations from layer-by-layer growth, however, should give rise to peak averaging, in particular, at high binding energies. For these reasons, only quasi-discrete Na states within about 1 eV of E_F can be identified in the measured spectra.

The bulk like interband transition within the Na film can be qualitatively included via a one-dimensional pseudo-potential. Since this potential is weak, the oscillatory behavior of the amplitude $A_{k_\perp}$ is preserved. The main effect of this potential is to add Fourier components to the final state related to the interplanar spacing. Remarkably, the energy of this direct transition (-1.5 eV binding energy at 5.5 eV photon energy) agrees with the data if the reciprocal lattice vector corresponds to (111) planes of an equivalent fcc lattice rather than to (110) planes of bulk Na. Since the overlayers exhibit a hexagonal electron diffraction pattern, these results support the epitaxial fcc like growth up to rather large coverages. The variation of the fcc like interband peak with photon energy was also found to be in agreement with the data. The theoretical spectra indicate that the interband transition peak shows a Fano profile resulting from the interference of the discrete direct transition with the continuum of non-direct transitions from Na valence states. With decreasing overlayer thickness, this interference becomes stronger, giving rise to a broader, less symmetric line shape and a slight shift which is also seen in the experimental spectra.

In summary, quantum well behavior was observed in photoemission from thin alkali metal films in the absence of a reflecting barrier in the band structure of the underlying substrate. Instead, the large negative potential step between overlayer and substrate gives rise to quasi-discrete levels within the overlayer that exhibit similar characteristics as traditional quantum well states. By tuning the photon frequency to the collective overlayer modes, emission from these levels is resonantly enhanced while emission from substrate bands is suppressed. Similar effects should be observable on other systems with large one-electron potential steps and well separated collective excitations.

[1] J. J. Paggel, T. Miller, and T.-C. Chiang, Science **283**, 1709 (1999); R. K. Kawakami *et al.*, Nature **398**, 132 (1999).

[2] S. R. Barman, P. Häberle, K. Horn, J. A. Maytorena, and A. Liebsch, Phys. Rev. Lett. **86**, 5108 (2001).

[3] H. Ishida and A. Liebsch, Phys. Rev. B **45**, 6171 (1992).

Contact Mechanics and Adhesion between Elastic Bodies with Rough Surfaces

B.N.J. Persson
Institute Theory I

I study the contact between elastic solids with randomly rough surfaces, and discuss the role of surface roughness on the adhesion of elastic solids.

F&E-Nr: 23.20.0

Even a highly polished surface has surface roughness on many different length scales. When two solid bodies with nominally flat surfaces are brought into contact, the area of real contact will usually only be a small fraction of the nominal contact area. We can visualize the contact regions as small areas where asperities from one solid are squeezed against asperities of the other solid. The area of real contact depends not only on the pressure by which the solids are squeezed together, but also on the adhesional interaction between the surfaces.

We have developed a theory of contact mechanics [1,2], valid for randomly rough surfaces, but neglecting adhesion. We have also studied the role of adhesion, but focusing mainly on the case where the contact between the two solids is complete [3], or partial contact between surfaces with roughness on a single lengthscale [4]. Adhesion is particular important for elastically soft solids, e.g., rubber or gelatine, where it may pull the two solids in direct contact over the whole nominal contact area.

The new theory of contact mechanics [1,2] consider the (apparent) area of contact $A(\lambda)$ on the length scale λ, defined to be the area of real contact when the surface roughness on shorter length scales than λ has been removed i.e., the surfaces has been "smoothened" on length scales shorter than λ. The theory predict that as long as the $A(\lambda)$ is small compared to the nominal contact area A_0, $A(\lambda)$ is proportional to the normal load F_N. In the last few years several (exact) numerical studies of contacts between randomly rough surfaces have been presented which clearly show that $A \sim F_N$ holds accurately (see below). Furthermore, the nearly universally observed linear relation between the sliding friction force F and the normal load is most naturally explained by assuming that $A \sim F_N$. Deviations from this "law" have been observed for soft elastic solids (e.g., rubber), where adhesion is important [3], and also in friction force microscopy studies, where a very sharp tip is slid on a substrate; however, in this latter case the contact area is too small (the diameter is usually below 100 Å) for the statistical contact theory to be valid.

It is possible to generate surface roughness profiles which are very similar to experimentally observed surfaces profiles, as follows: The surface height profile $h(\mathbf{x})$ is written as [5]:

$$h(\mathbf{x}) = \sum_{\mathbf{q}} B(\mathbf{q})\, e^{i[\mathbf{q}\cdot\mathbf{x}+\phi(\mathbf{q})]}, \qquad (1)$$

where, since $h(\mathbf{x})$ is real, $B(-\mathbf{q}) = B^*(\mathbf{q})$ and $\phi(-\mathbf{q}) = -\phi(\mathbf{q})$. In (1) $\phi(\mathbf{q})$ are independent random variables, uniformly distributed in the interval $[0, 2\pi]$. $B(\mathbf{q})$ is determined so as to reproduce the measured surface roughness power spectrum

$$C(q) = \frac{1}{(2\pi)^2}\int d^2x\ \langle h(\mathbf{x})h(\mathbf{0})\rangle e^{-i\mathbf{q}\cdot\mathbf{x}}.$$

Using (1) gives

$$C(q) = \frac{A_0}{(2\pi)^2} B(\mathbf{q})B^*(\mathbf{q}),$$

where $A_0 = L^2$ is the nominal contact area. This equation is satisfied with $B(\mathbf{q}) = (2\pi/L)\ C^{1/2}(q)$. If $C(q)$ is chosen as $\sim 1/q^{2(H+1)}$ then surfaces generated from (1) will be self affine fractal with the fractal dimension $D_f = 3 - H$. Greenwood [5] has shown that surfaces generated as described above are virtually indistinguishable from rough surfaces produced by e.g., cleaving or sand blasting. Eq. (1) shows that the amplitude of the different surface roughness wave vector components are uncorrelated, so that averaging over different $h(\mathbf{q})$ are independent processes, as assumed in Ref. [1,2]. As an example of contact between surfaces with roughness of the form (1), consider the results of Brunetto et al. [6].

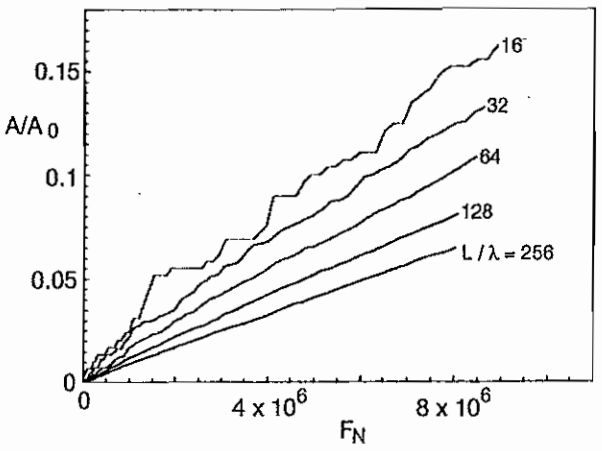

FIG. 1. The area of contact, A, as a function of the applied load F_N. Results are presented for 5 different magnifications L/λ. The fractal dimension $D_f = 2.3$. From Ref. [6].

Fig. 1 shows the area of contact, A, as a function of the applied load F_N (from Ref. [6]). Results are presented for 5 different magnifications L/λ. Note that within the accuracy of the calculations, $A \sim F_N$. Note also that the slope of the curves decreases with increasing magnification; if we (arbitrarily) denote the slope for the magnification $L/\lambda = 256$ with unity, then the slopes for $L/\lambda = 128$, 64, 32 and 16 will be 1.24, 1.57, 1.93 and 2.32. This is in accordance with the theory presented in Ref. [1] where it was shown that the area of contact on the length scale λ is proportional to $A(\lambda) \sim (\lambda/L)^{1-H}$. Since $D_f = 2.3$ we have $1 - H = D_f - 2 = 0.3$ so that the theoretical slopes are 1.23, 1.52, 1.87 and 2.30, in excellent agreement with the numerical results.

The discussion above has neglected the adhesion. For smooth surfaces adhesion is important at short enough length scales. In a classic paper Fuller and Tabor [7] have shown that already a relative small surface roughness can completely remove the adhesion. They assumed that the rough surface can be represented as a distribution of spherical bumps of *identical* radius R, but with a Gaussian height distribution. However, self affine fractal surfaces have roughness on many different length scales, and when this is taken into account a qualitatively new picture emerges (see below), where, e.g., the adhesion force may even vanish (or at least be strongly reduced), if the fractal dimension $D_f > 2.5$. Thus the theory of Fuller and Tabor overlooks the perhaps most important aspects of real surfaces–the existence of a wide distribution of length scales. Here I would like to present some simple arguments which illustrate the profound importance of not excluding any surface roughness length scale in the analysis [2].

Fuller and Tabor have shown that for elastic solids with surface roughness on a *single length scale* λ, the competition between adhesion and elastic deformation is characterized by the parameter $\theta = Eh^2/\lambda\Delta\gamma$, where h is the amplitude of the surface roughness. The parameter θ is the ratio between the elastic energy and the surface energy stored at the interface, assuming that complete contact occur. When $\theta >> 1$ only partial contact occur, where the elastic solids make contact only close to the top of the highest asperities, while complete contact occur when $\theta << 1$.

Surfaces or real solids have roughness on a wide distribution of length scales. Assume, for example, a self affine fractal surface. In this case the statistical properties of the surface are invariant under the transformation

$$\mathbf{x} \to \mathbf{x}\,\zeta, \qquad z \to z\,\zeta^H$$

where $\mathbf{x} = (x, y)$ is the 2D position vector in the surface plane, and where $0 < H < 1$. This implies that if h_a is the amplitude of the surface roughness on the length scale λ_a, then the amplitude h of the surface roughness on the length scale λ will be of order

$$h \approx h_a\,(\lambda/\lambda_a)^H$$

Thus we get

$$\theta_a = \theta(\lambda_a/\lambda)^{2H-1}$$

where $\theta_a = Eh_a^2/\lambda_a\Delta\gamma$. Hence, when we study the system on shorter and shorter length scale $\lambda_a < \lambda$, θ_a will decrease or increase depending on if $H > 1/2$ and $H < 1/2$, respectively. In the former case, if $\theta < 1$ the adhesion will be important on any length scale $\lambda_a < \lambda$. In particular, if λ is the long-distance cut-off length λ_0 in the self affine fractal distribution, then *complete contact will occur at the interface.* In the latter case, even if $\theta < 1$ so that the adhesion may seem important on the length scale λ, at short enough length scale $\theta_a > 1$. Thus, without a short-distance cut off, *adhesion and the area of real contact will vanish.* In reality, a finite short-distance cut off will always occur, but this case requires a more detailed study (see Ref. [2]). I suggest that the present problem may be studied by a renormalization group type of approach, where during the process of eliminating short-wavelength roughness components, the effective interfacial energy $\Delta\gamma_{\rm eff}(\lambda)$ depends on the wavelength λ of observation. At present, no accurate theory exists for contact mechanics with adhesion when the surfaces have roughness on many length scales – we are investing a considerable effort in developing such a theory which would be of tremendous practical importance.

[1] B.N.J. Persson, Phys. Rev. Lett. **87**, 1161 (2001).

[2] B.N.J. Persson, J. Chem. Phys. **115**, 3840 (2001); B.N.J. Persson, F. Bucher and B. Chiaia, Phys. Rev. B (in press).

[3] B.N.J. Persson and E. Tosatti, J. Chem. Phys. **115**, 5597 (2001).

[4] S. Zilberman and B.N.J. Persson, Phys. Rev. Lett. (submitted).

[5] J.A. Greenwood, in *Fundamentals of Friction, Macroscopic, and Microscopic Processes*, edited by I.L. Singer and H.M. Pollack (Kluwer, Dordrecht, 1992).

[6] M. Borri-Brunetto, B. Chiaia and M. Ciavarella, Comput. Methods Appl. Mech. Engrg. **190**, 6053 (2001).

[7] K.N.G. Fuller and D. Tabor, Proc. R. Soc. London A**345**, 327 (1975).

Publications in refereed journals

Akola J.; M. Manninen1
1 Dept. of Physics, University of Jyväskylä, Finland
Heating of Al13 and Al14 clusters
Phys. Rev. B 63, 193410 (2001)
23.20.0

Akola J.; Rytkönen K.1; Manninen M.1
1 Dept. of Physics, University of Jyväskylä, Finland
Metallic evolution of small magnesium clusters
Eur. Phys. J. D 16, 21 (2001)
23.20.0

Ballone P.1; Jones R.O.
1 University of Messina, Italy
Equilibrium polymerization of cyclic carbonate oligomers
J. Chem. Phys. 115, 3895-3905 (2001)
23.20.0

Barman S.R.1; Häberle P.2; Horn K.3; Maytorena J.; Liebsch A.
1 Inter University Consortium, Indore, India
2 Universidad Técnica, Valparaíso, Chile
3 Fritz Haber Institut Berlin
Quantum well behavior without confining barrier observed via dynamically screened photon field
Phys. Rev. Lett. 86, 5108 (2001)
23.20.0

Jones R.O.; Ballone P.1
1 University of Messina, Italy
A combined density functional and Monte Carlo study of polycarbonate
Mat. Res. Soc. Symp. 677, AA3.1.1-12 (2001)
23.20.0

Jones R.O.; Ballone P.1
1 University of Messina, Italy
Density functional calculations for polymers and clusters - progress and limitations
Comput. Materials Science 22, 1-6 (2001)
23.20.0

Jones R.O.; Clare B.W.1; Jennings P.J.1
1 Murdoch University, Perth, Australia
Si-H clusters, defects, and hydrogenated silicon
Phys. Rev. B 64, 125203-1-9 (2001)
23.20.0

Kaufmann Z.1; Lustfeld H.
1 Dept. of Physics of Complex Systems, Eötvös University, Budapest
Comparison of averages of flows and maps
Phys. Rev. E RC. 64, 1 (2001)
23.20.0

Liebsch A.; Kim B.-O.1; Plummer E.W.1
1 Depart. of Physics, University of Tennessee, Knoxville, Tennessee, USA
Collective excitations in adsorbed alkali-metal films: Critical analysis of photoyield and electron-energy-loss spectra for K on Al(111)
Phys. Rev. B 63, 125416-1-10 (2001)
23.20.0

Liebsch A.
Comment on: ``Fermi Surface, Surface States and Surface Reconstruction in Sr2RuO4"
Phys. Rev. Lett. 87, 239701 (2001)
23.20.0

Lustfeld H.; Pohlmeier A.1
1 FZ-ICG IV
Electric potential and reaction rates at charged surfaces in asymmetric electrolytes - an analytic approach
J. Colloid Interface Science 181, 45 (2001)
23.20.0

López Bastidas C.; Liebsch A.; Mochán W.L.1
1 Centro de Ciencias Físicas, UNAM, Cuernavaca, Mexico
Influence of d electrons on the dispersion relation of Ag surface plasmons for different single-crystal faces
Phys. Rev. B 63, 165407-1-12 (2001)
23.20.0

Maassen R.1; Eisenriegler E.1; Bringer A.
1 Theory II, IFF
Density depletion profile and solvation free energy of a colloidal particle in a polymer solution
J. Chem. Phys. 115, 5292 (2001)
23.20.0

Persson B.N.J.; Tosatti E.1
1 ICTP Trieste, Italy
The effect of surface roughness on the adhesion of elastic solids
J. Chem. Phys. 115, 5597 (2001)
23.20.0

Persson B.N.J.
Elastic instabilities at a sliding interface
Phys. Rev. B 63, 104101 (2001)
23.20.0

Persson B.N.J.
Elastoplastic contact between randomly rough surfaces
Phys. Rev. Lett. 87, 116101 (2001)
23.20.0

Persson B.N.J.
Theory of Rubber Friction and Contact Mechanics
J. Chem. Phys. 115, 3840 (2001)
23.20.0

Scharte M.1; Porath R.1; Ohms T.1; Aeschlimann M.1; Krenn J.R.2; Ditlbacher H.2; Aussenegg F.R.2; Liebsch A.
1 Dept. of Physics, University of Kaiserslautern
2 Inst. for Experimental Physics, University of Graz, Austria
Do Mie Plasmons have a longer lifetime on resonance than off-resonance?
Appl. Phys. Lett. B73, 305-310 (2001)
23.20.0

Valadares A.A.1; Alvarez F.1; Liu Z.2; Sticht J.3; Harris J.
1 Instituto de Investigaciones en Materiales, UNAM, Mexico
2 Molecular Simulations Inc., San Diego, USA
3 Materials Design Inc., Oceanside, USA
Ab-initio studies of the atomic and electronic structure of pure and hydrogonated -Silicon
Eur. Phys. J. B 22, 443 (2001)
23.20.0

Volokitin A.I.1; Persson B.N.J.
1 Samara University, Russia
Frictional drag between quantum wells mediated by fluctuating electromagnetic field
J. Phys. C 13, 859 (2001)
23.20.0

Volokitin A.I.1; Persson B.N.J.
1 Samara University, Russia
Radiative heat transfer between nanostructures
Phys. Rev. B63, 205404 (2001)
23.20.0

Zilberman S.1; Persson B.N.J.; Nitzan A.1, Mugele F.2; Salmeron M.2
1 School of Chemistry, Tel Aviv University, Israel
2 Materials Science Division, University of California, Berkeley, USA
Boundary lubrication: dynamics of squeeze-out
Phys. Rev. B 63, 55103-1 (2001)
23.20.0

Zilberman S.1; Persson B.N.J.; Nitzan A.1
1 School of Chemistry, Tel Aviv University, Israel
Theory and simulations of squeeze-out dynamics in boundry lubrication
J. Chem. Phys. 115, 11268 (2001)
23.20.0

Invited talks

Akola J.; Ballone P.1; Jones R.O.
1 University of Messina, Italy
Improved Classical Force Fields for Hydrogen Bonds
Leverkusen (Bayer): BMBF project meeting
3.5.2001
23.20.0

Akola J.; Ballone P.1; Jones R.O.
1 University of Messina, Italy
Polymer Modelling based on Density Functional Calculations
SISSA, Trieste
21.9.2001
23.20.0

Bene J.1; Lustfeld H.
1 Institute for Theoretical Physics, Eötvös University, Budapest
Simulating viscuous 2D Flows using wavelet dynamics
General Assembly der European Geophysical Society, Nizza
26.3.2001
23.20.0

Harris J.
Calculation of Elastic Constants of Materials using Density Functional Theory
University of Dortmund: Gemeinsames Kolloquim Physik/Chemie
17.7.2001
23.20.0

Harris J.
Computation and Information in Materials Science
University of Kyoto, Japan
24.10.2001
23.20.0

Harris J.
Computational Methods in Materials Science
Ecole Polytechnique de Montreal, Canada
6.6.2001
23.20.0

Harris J.
Computational Methods in Materials Science
General Motors Research Center, Warren, Michigan
21.2.2001
23.20.0

Jones R.O.
A combined density functional and Monte Carlo study of polycarbonate
Spring Meeting, Materials Research Society, San Francisco, USA
19.4.2001
23.20.0

Jones R.O.
Density functional calculations for some real materials - thermal expansion in glass ceramics, and reactions in polycarbonate (the stuff of CD's)
Department of Physics, University of California, Berkeley, USA
16.4.2001
23.20.0

Jones R.O.
Density functional calculations on supercomputers
Supercomputing Global Workshop (Denver, Jülich)
15.11.2001
23.20.0

Jones R.O.
Density functional/Monte Carlo study of ring-opening polymerization
Conference on Computational Physics, Aachen
6.9.2001
23.20.0

Jones R.O.
Ring-opening polymerization and ``living polymers" - density functional calculations and beyond
NIC-Symposium 2001, Jülich
6.12.2001
23.20.0

Liebsch A.
Do Mie Plasmons have a longer lifetime on resonance than off-resonance?
San Sebastian, Spanien
12.7.2001
23.20.0

Liebsch A.
Dynamischer Response an Metalloberflächen
Universität Konstanz
11.5.2001
23.20.0

Liebsch A.
Hot electron lifetimes at noble metal surfaces
Fritz Haber Institut Berlin
28.5.2001
23.20.0

Liebsch A.
Hot electron lifetimes at noble metal surfaces
LEPES-CNRS, Grenoble, France
23.3.2001
23.20.0

Liebsch A.
Hot electron lifetimes at noble metal surfaces
San Sebastian, Spanien
5.7.2001
23.20.0

Liebsch A.
Modern Materials Research in Jülich
DAAD Promotion Tour; Delhi, Pune, Chennai, Colcatta, India
29.10.-9.11.2001
23.20.0

Lustfeld H.; D. Poppe1
1 FZ-ICG II
Fast/slow behavior in realistic pollutant reaction equations of the troposphere
Hamburg, Frühjahrstagung der Arbeitsgemeinschaft Exterrestrische Forschung der DPG
22.3.2001
23.20.0

Lustfeld H.
Relevanter Informationsverlust bei Poincaré Abbildungen?
Universität Duisburg
10.7.2001
23.20.0

Lustfeld H.
Ursache und Beschreibung kleinskaliger Konzentrationsschwankungen von Spurengasen in der Atmosphaere
Universität Duisburg
3.7.2001
23.20.0

Persson B.N.J.
Rubber Friction
ACS Rubber Division meeting on Rubber Friction, Ohio, USA
October 16-19, 2001
23.20.0

Persson B.N.J.
Rubber Friction
Colmar-Berg, Luxembourg
05.12.2001
23.20.0

Persson B.N.J.
Rubber Friction
Deutsches Institut für Kautschuktechnologie e.V., Hannover, Germany
09.10.2001
23.20.0

Persson B.N.J.
Rubber Friction
Pirelli Reifenwerke, Höchts/Odenwald
11.01.2001
23.20.0

Persson B.N.J.
Rubber Friction
Pirelli, Milano, Italy
12.10.2001
23.20.0

Persson B.N.J.
Sliding Friction
ACS Symposium on MOLECULAR TRIBOLOGY, San Diego, USA
1.4.2001
23.20.0

Persson B.N.J.
Sliding Friction
CECAM-SIMU Workshop on ``Simulation and theory of solid friction", Lyon, France
August 27-30, 2001
23.20.0

Persson B.N.J.
Sliding Friction
DIP meeting, Mainz
4.5.2001
23.20.0

Persson B.N.J.
Sliding Friction
Nonlinear Phenomena in Materials Science, Dresden, Germany
September 10-15, 2001
23.20.0

Persson B.N.J.
Sliding Friction
Ohio State University, Columbus, OH, USA
15.10.2001
23.20.0

Persson B.N.J.
Sliding Friction
SISSA, Trieste, Italy
26.01.2001
23.20.0

Persson B.N.J.
Sliding Friction
Sensing and Manipulating in the Nanoworld, Mauterndorf, Austria
18.2.2001
23.20.0

Persson B.N.J.
Sliding Friction
The second Stig Lundqvist research conference on Advancing Frontiers in Condensed Matter Physics: ``Non-Conventional Systems and New Directions", Trieste, Italy
July,2-6, 2001
23.20.0

Persson B.N.J.
Sliding Friction
University of Delf, The Netherlands
24.01.2001
23.20.0

Persson B.N.J.
Sliding Friction
University of Düsseldorf, Germany
20.12.2001
23.20.0

Persson B.N.J.
Sliding Friction
University of Erlangen, Germany
18.01.2001
23.20.0

Persson B.N.J.
Sliding Friction
University of Essen, Germany
07.06.2001
23.20.0

Persson B.N.J.
Sliding Friction
University of Ilmenau, Germany
12.12.2001
23.20.0

Persson B.N.J.
Sliding Friction
University of Ulm, Germany
23.01.2001
23.20.0

Persson B.N.J.
Sliding Friction
Workshop on ``Computational Materials Science", Sardinia, Italy
September 17-23, 2001
23.20.0

Persson B.N.J.
Surface Vibrations
Vibrations at Surfaces 10, Saint Malo, France
17.6.2001
23.20.0

Persson B.N.J.
Vibrational Dynamics at Surfaces
University of Heidelberg, Germany
28.11.2001
23.20.0

Lecture courses

Lustfeld H.
Methoden der Theoretischen Physik I, Beispiele in C++
Universität Duisburg
WS 2001/2002
23.20.0

Lustfeld H.
Moderne Probleme der Geophysik
Universität Duisburg
WS 2001/2002

23.20.0

Lustfeld H.
Wavelets in der Physik I mit Beispielen in C++
Universität Duisburg
WS 2000/2001
23.20.0

Lustfeld H.
Wavelets in der Physik II mit Beispielen in C++
Universität Duisburg
SS 2001
23.20.0

Institute Theory II

General Overview

Introduction: Soft Matter Research

The main research topic of the Institute is the theory of "complex fluids" and "soft matter" systems. Soft matter physics is an interdisciplinary research area encompasing statistical physics, material science, chemistry, and biology. The systems are characterized by

- Supramolecular structure and self-assembly
- Typical length scales ranging from nano- to micro-meters
- Typical energy scales comparable to the thermal energy k_BT.

Classical examples of complex fluids are

- Polymer solutions, mixtures, and melts
- Mixtures of block copolymers and homopolymers
- Lyotropic liquid crystals
- Amphiphilic systems, i.e. mixtures of oil, water and amphiphiles
- Colloidal suspensions.

While these areas remain active fields of research, the focus has recently shifted to more complex systems which are obtained by combining two or more of the components listed above. A few examples are

- Colloidal particles in polymer solutions
- Mixtures of surfactants and amphiphilic block-copolymers
- Mixtures of several surfactants or lipids
- Colloids in liquid crystals

This brings the systems which are studied in physics closer to applications in material science or biology.

Since the structures in soft matter systems often contain a large numer of molecules, *mesoscale modelling* is typically required to bridge the length- and time-scale gap between the microscopic domain — of atoms and their interactions — and the emerging properties of supramolecular assemblies on meso- or macroscopic scales. Microscopic models are employed to study properties of complex systems on the molecular scale, and to provide a link of mesoscale models to molecular architecture.

A large variety of methods is used to study soft matter systems. In fact, a combination of analytical and numerical methods is often needed to successfully characterize these complex systems. In particular, simulation methods (Monte Carlo, molecular dynamics), computational hydrodynamics, field theory, perturbation theory, and exact solutions are employed in our institute.

A characteristic feature of soft-matter research is the fruitful interaction between theory and experiment. With a third of the IFF institutes [Neutron Scattering (Richter), Theory II and Soft Matter (Dhont)] now focusing on soft matter research, many of the essential aspects of these systems are investigated here.

Research projects and results:
(in alphabetic order)

1. *Cell Locomotion:*
   The locomotion of biological cells is based on signal-mediated polymerization of their cytoskeletons. It has been shown that the persistency of the random motion or the chemotaxis of a cell is basically due to the autocatalytic polymerization kinetics of the cytoskeletal actin network. We are currently investigating models including more complex signaling pathways of actin-regulating proteins. (A. Baumgärtner, R. Sambeth)

2. *Proton transfer in bacteriorhodopsin and in ion channels:*
   Proton transfer reactions represent a unique class of processes of paramount importance in many different fields in physics and biology. Important examples are the proton transport in biological pumps as bacteriorhodopsin and the proton-induced gating of some ion channels. We are currently developing classical models and methods to include these proton reactions in standard molecular dynamics simulations. First results seem to indicate that in the case of ion channels the protonation and deprotonation of charged amino acids in the cytoplasmic region of an ion channel may lead to a charge redistribution which triggers the opening and closing of the channel. In the case of bacteriorhodopsin the amount of water seems to be crucial for the stability of certain protonation patterns and hence for the controled contruction of proton pathways. (A. Baumgärtner, E. Markous, S. Grudinin, J. F. Gwan)

3. *Center of mass distribution of a polymer near a repulsive wall:*
   An exact analytic expression is obtained for the center of mass density profile of free ideal polymer chains in a half space bounded by a hard planar wall. The profile is found by a mapping to a polymer chain in a gravitational field. While the monomer density profile and the density profiles of chain ends or midpoints tend to zero with power laws on approaching the hard wall, the center of mass profile tends to zero *exponentially*. The first moments of these qualitatively different profiles are identical and determine the polymer-induced surface tension of the hard wall. (E. Eisenriegler, R. Maassen)

4. *Shape Transformations of Two-Component Membranes under Weak Tension:*
   Domain formation and phase transitions are investigated for two-component membranes of planar topology in the strong segregation limit. The composition of a membrane is coupled to the spontaneous curvature. The stability of various spatially periodic phases, formed by domains of one component, is examined systematically as a function of composition, the ratio of spontaneous curvatures of both components, and the surface tension. We find new stable phases composed of one- and two-bead buds and new phase transition between these phases. (W. T. Gozdz, G. Gompper)

5. *Semiflexible polymer in a uniform force field in two dimensions:*
   The influence of external forces on the conformational properties of polymers has been studied extensively in recent years. In particular, fluorescently labelled DNA molecules have been pulled at their ends or stretched in uniform flow flields. We have studied a simple, two-dimensional model for a semiflexible polymer chain, anchored at one end in a uniform force field. Recursion relations are derived for the partition function and then iterated numerically. We calculate the angular fluctuations of the polymer about the direction of the force field and the average polymer configuration as functions of the bending rigidity, chain length, chain orientation at the anchoring point, and field strength. (A. Lamura, T. Burkhardt, G. Gompper)

6. *Multi-particle-collision dynamics: Flow around a circular and a square cylinder:*
   Mesoscale simulation techniques have attracted considerable attention in recent years in order to overcome the length- and time-scale gap in simulations of the hydrodynamic behavior of complex fluids. We have used a new particle-based model for mesoscopic fluid dynamics to investigate steady and unsteady flows around a circular and a square cylinder in a two-dimensional channel for a range of Reynolds number between 10 and 130. Numerical results for the recirculation length, the drag coefficient, and the Strouhal number are reported and compared with previous experimental measurements and computational fluid dynamics data. The good agreement demonstrates the potential of this method for the investigation of complex flows. (A. Lamura, G. Gompper, T. Ihle, D. M. Kroll)

7. *Density profile and solvation free energy of a colloidal particle in a polymer solution:*
The solvation free energy and polymer density profile of a single colloidal particle in a solution of free nonadsorbing polymer chains are investigated for *arbitrary* particle to polymer size ratio and degree of inter-chain overlap within the dilute and semidilute regime. While most of our results are obtained within a mean-field approach, we also use a 'renormalized tree approximation' to estimate the surface tension for large size ratio. This turns out to be in good agreement with results from simulations. There is a weak maximum in the density profile for arbitrary size ratio. For small size ratio the maximum can be explained in terms of a minimum in the bulk polymer density correlation function. (R. Maassen, E. Eisenriegler, A. Bringer)

8. *Disorder and finite-size effects in entangled polymers:*
It is shown rigorously in the framework of an extended Rubinstein-Duke model for entangled polymers that kinematic disorder (which does not change the equilibrium state) leaves asymptotic reptation results for the diffusion coefficient of a polymer unchanged, except for a disorder-dependent amplitude that we calculate analytically. The asymptotic viscosity of a polymer melt depends on the strength of the entropic tensile force acting at the ends of a single chain, but not on the microscopic details of this force. A partially self-consistent density matrix renormalization group (DMRG) treatment of constraint release (using input from Rouse theory) does not reveal a substantial change in the length dependence of the viscosity of chains of finite length. (M. Paeßens, R. Willmann, G.M. Schütz)

9. *Integrable stochastic many-body systems:*
Two-component driven diffusive systems play an important role in the description of tracer diffusion, gel electrophoresis, charged particles and other areas of nonequilibrium physics. Using the so-called dynamical matrix product ansatz we have found a constructive method which allows for the identification of integrable stochastic processes, a subclass of multicomponent driven diffusive systems. Thus the explicit calculation of relaxation times and other quantities becomes possible for those models. (G.M. Schütz, E. Fouladvand, V. Popkov)

10. *Exact time-dependent correlation functions:*
We investigate the nonequilibrium tube-length fluctuations during the relaxation of an initially stretched, entangled polymer chain. The time-dependent variance of the tube length follows in the early-time regime a simple universal square root power law originating in the diffusive motion of the polymer segments. The amplitude is calculated analytically both from standard reptation theory and from an exactly solvable lattice gas model for reptation and its dependence on the initial and equilibrium tube length respectively is discussed. The non-universality suggests the measurement of the fluctuations (e.g. using flourescence microscopy) as a test for reptation models. (G.M. Schütz, J.E. Santos)

11. *Structure of polyelectrolyte solutions:*
The structure of polyelectrolyte solutions is investigated using the Polymer Reference Interaction Site Model (PRISM). Taking counterions into account explicitly, the pair correlation functions among the various components of the solution are calculated as a function of Bjerrum length and density applying the Laria Wu Chandler Closure. An effective potential is extracted from these quantities between the monomers and counterions, respectively. Our results indicate the appearance of counterion condensation and a counterion mediated attraction among the equally charged polyelectrolyte chains. (R. G. Winkler, T. Hofmann, P. Reineker)

12. *Conformational properties of a single polyelectrolyte chain:*
The conformational properties of a single polyelectrolyte chain are obtained in a perturbative manner by introducing a semiflexible reference chain which is adjusted to yield the same mean-square end-to-end distance (Edwards-Singh) as the charged chain. The extracted effective persistence length allows us to calculate a variety of characteristic quantities of a polyelectrolyte chain. We find excellent agreement between Monte Carlo simulations and the results of our reference chain for the density dependence of the mean-square end-to-end distance. For a sufficiently strong Coulomb interaction we find a transition in the scaling behavior of the mean-square end-to-end distance with respect to chain length from a rodlike behavior to a short range type dependence with increasing chain length. (R. G. Winkler, T. Hofmann, P. Reineker)

13. *Computer simulations of the adsorption of molecular brushes:*
Molecular brushes consist of a backbone polymer and crafted side chains. Depending on the crafting density and the length of side chains, the conformations of a macromolecule are modified, particular for two-dimensional systems. By molecular dynamics simulations, we investigate the adsorption behavior on a planer surface and the conformational properties of adsorbed molecular brushes as a function of the length of the side chains. Calculating the correlation function of the bond vectors we find a power law decay instead of an exponential decay. This indicates strong correlations along the chain backbone induced by steric obstructions. (R. G. Winkler, D. Shirvanyants)

Some Remarks:

- An international one-day symposium on *New Trends in DMRG (density matrix renormalization group)* was organized by G. Schütz (Theory II), P. Grassberger (Neumann Institute for Computing, FZJ) and A. Schadschneider (Theoretical Physics, University of Cologne) on July 23, 2001. Seven invited speakers gave introductory lectures as well as more specialized talks about their current research. Some of the 40 participants also contributed posters.
- An international workshop, the *Jülich Soft Matter Days 2001*, was organized by J. Dhont (IFF Soft Matter), G. Gompper (Theory II), D. Richter and M. Monkenbusch (IFF Neutron Scattering) at the Congresscentrum Rolduc in Kerkrade (NL) on Nov. 13-16, 2001. The program consisted of 5 plenary talks, 18 invited talks, 16 contributed talks, and 49 posters. The workshop was attended by 130 participants.
- The paper of Sambeth und Baumgärtner about the motion of biological cells, which has been published in *Physical Review Letters*, has been reviewed in *Nature Science Update* (13. September 2001).

Awards etc.:

- Dr. Wojciech Góźdź has received a DAAD Fellowship to visit the Institute Theory II for two months.
- Dr. Roland Winkler, who joined the Institute Theory II at the beginning of 2001, has been appointed "außerplanmäßiger Professor" at the University of Ulm on November 29, 2001.

Gerhard Gompper

Personnel 2001/2002 and areas of activity

Scientific Staff

Dr. A. Baumgärtner	Statistical mechanics of proteins and membranes;	23.30.0
Prof. E. Eisenriegler	Polymers near surfaces, colloid-polymer mixtures	23.30.0
Prof. G. Gompper Institute Director	Statistical mechanics of amphiphilic systems	23.30.0
Dr. G. Schütz	Non-equilibrium Statistical Mechanics; Polymer dynamics	23.30.0
Dr. R. G. Winkler	Charged and uncharged macromolecular systems	23.30.0

Technical Staff

H. Paffen	Secretary

Postdocs

Dr. E. Allakhiarov	Charged Colloids	23.30.0
Dr. A. Lamura	Hydrodynamics of Simple and Complex Fluids	23.30.0
Dr. V. Popkov	Driven Diffusive Systems	23.15.0

Diploma and Graduate Students

T. Auth	Polymers at membranes	23.30.0
R. Maassen	Polymer depletion interaction	23.30.0
M. Paeßens	Finite-size effects in entangled polymers	23.30.0
T. Schilling	Wetting in amphiphilic systems	23.30.0
R. Willmann	Polymer dynamics in disordered media	23.30.0

Guests

Dr. V. Popkov	(Institute for Low Temperature Physics, Kharkov, Ukraine) Driven diffusive systems (Feb. - Apr. 2001)	23.15.0
S. Grosskinsky	(Technische Universität München) Boundary-induced phase transitions (May 2001)	23.15.0
T. Hoffmann	(Universität Ulm) Polyelectrolyte solutions (July & Nov. 2001)	23.30.0
Dr. G. Papadopoulos	(University of Thessaloniki, Griechenland) Molecular dynamics of ribosomal proteins (Aug. 2001)	23.30.0
Dr. J.-H. Lin	(University of California, San Diego, USA) Molecular dynamics of ion channels (Sep. 2001)	23.30.0
Dr. W. Goźdź	(Polish Academy of Sciences, Warsaw, Poland) Membrane shapes (Sep. - Nov. 2001)	23.30.0
Dr. M. Müller	(Universität Mainz) Polymer interfaces (Oct. - Nov. 2001)	23.30.0

Discrete charge patterns, Coulomb correlations and interactions in protein solutions

E. Allahyarov[1], H. Löwen[1], A.A. Louis[2], J.P. Hansen[2]
[1]*Institute Theory II*
[2]*Institut für Theoretische Physik II, Heinrich-Heine-Universität Düsseldorf, D-40225 Düsseldorf, Germany*
[3]*Department of Chemistry, Lensfield Rd, Cambridge CB2 1EW, UK*

The effective Coulomb interaction between globular proteins is calculated as a function of monovalent salt concentration c_s, by explicit Molecular Dynamics simulations of pairs of model proteins in the presence of microscopic co and counterions. For discrete charge patterns of monovalent sites on the surface, the resulting osmotic virial coefficient B_2 is found to be a strikingly non-monotonic function of c_s. The non-monotonicity follows from a subtle Coulomb correlation effect which is completely missed by conventional non-linear Poisson-Boltzmann theory and explains various experimental findings.

F&E-Nr. 23.30.0

A more fundamental understanding of the interactions between nano-sized biomolecules is critical to the long-term advance of modern biomedical research. A particular issue is the aggregation and crystallization of globular proteins in solution, driven by their mutual interactions, including steric repulsion, van der Waals attraction, Coulombic interactions, hydration forces, hydrophobic attraction and depletion forces. Most of these are effective interactions which depend sensitively on solution conditions. One possible indirect determination of the total force between two proteins may be achieved via measurements of the osmotic equation of state by static light scattering, which in the low protein concentration regime yields the value of the second osmotic virial coefficient B_2. The variation of B_2 with solution conditions yields valuable information on the underlying effective protein pair interactions. Moreover, it has been shown empirically that there is a strong correlation between the measured values of B_2 and the range of solution conditions under which protein crystallization is achieved.

This report focuses on the effective interactions between globular proteins mediated by the microscopic co and counterions, and on the resulting B_2. The conventional Derjaguin-Landau-Verwey-Overbeek approach [1], borrowed from colloid science, leads one to expect that B_2 will monotonically decrease as the concentration of salt increases. We show that the discrete nature of the protein surface charge distribution, together with the Coulomb correlations between all charges involved, lead to a striking non-monotonic variation of B_2 with salt concentration c_s. The occurrence of a minimum of B_2 as a function of c_s has recently been reported in lysozyme solutions for $c_s = 0.3$ M [2] and in Apoferritin solutions for $c_s = 0.15$ M [3]. Related experimental findings are non-monotonic variations of other quantities which strongly correlate with B_2 [2] such as the interaction parameter [4],the cloud point temperature [5], and the solubility [6]. All these trends can be qualitatively understood by our calculation.

We consider two spherical proteins of diameter σ_p, each carrying a total charge Ze (where Z depends on pH), surrounded by monovalent co and counterions, assumed to have identical diameters σ_c.

In the case of highly charged colloidal particles, the total charge Ze is usually assumed to be uniformly distributed on the surface, a situation which will be referred to as the "smeared charge model" (SCM). This simplification is much less justified for the smaller, weakly charged proteins (where $Z \simeq 10$). We have hence adopted a second, discrete charge model (DCM) where Z monovalent discrete point charges are distributed over the surface of a sphere of diameter $\sigma_p - 2\Delta = 0.96\sigma_p$ (i.e. slightly inside, a distnace $\Delta = 0.02\sigma_p$ beneath the surface of the protein), in such a way as to minimize the electrostatic energy of the distribution; the resulting pattern does not correspond to the real charge distribution

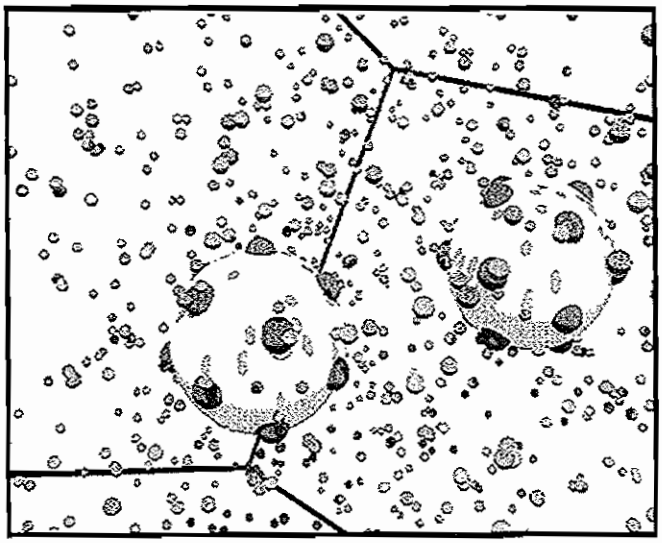

FIG. 1. Snapshot of a typical MD-generated microion configuration around two proteins, separated by $r = 1.7\sigma_p$. The proteins carry 15 discrete charges e; monovalent salt molarity is $c_s = 0.206 Mol/l$. The globular protein molecules are shown as two large yellow spheres. The embedded small red spheres on their surface mimic the discrete protein charges in the DCM model. The small blue spheres are counterions, while the green spheres are coions.

on any specific protein, but does provide a well-defined discrete model for comparison with the SCM, and between different values of Z. At this stage the two models (SCM and DCM) involve only excluded volume and bare Coulombic interactions (reduced by a factor $1/\epsilon$ to account for the solvent) between all particles (proteins and microions). However, in view of the large size asymmetry, the effective force between the proteins, which ultimately determines the second virial coefficient, involves a statistical average over microion configurations in the field of two fixed proteins. For our model to be a rough representation of lysozyme, we chose $\sigma_p = 4nm$, and $Z = 6, 10$ and 15, corresponding to three different values of the solution pH. The microion diameter is $\sigma_c = 0.267nm$. Note that the SCM always implies vanishing multipole moments, whereas within the present DCM, the only charge pattern with a non-vanishing dipole moment is that for $Z = 15$. A snapshot of a typical equilibrium microion configuration around two proteins is shown in Fig.1, for the case $Z = 15$. The total force $\vec{F}_1 = -\vec{F}_2$ depends only on the centre-to-centre distance r for the SCM, but is also a function of the orientations of the two charge patterns of the DCM, embodied by two unit vectors $\vec{\omega}_1$ and $\vec{\omega}_2$; $\vec{F}_1 = \vec{F}_1(r, \vec{\omega}_1, \vec{\omega}_2)$. The effective radial pair interactions between proteins, $V(r)$ reads,

$$V(r) = \int_r^\infty dr' \langle \frac{\vec{r}}{|\vec{r}|} \cdot \vec{F}(r', \vec{\omega}_1, \vec{\omega}_2) \rangle_{\omega_1 \omega_2}. \qquad (1)$$

Here $\langle \ldots \rangle_{\omega_1,\omega_2}$ refers to a statistical average over mutual orientations of the two proteins. The second virial coefficient in units of its value $2\pi\sigma_p^3/3$ for hard spheres of diameter σ_p, $B_2^* = B_2/B_2^{(HS)}$, can then be proven to be given by:

$$B_2^* = 1 + \frac{3}{\sigma_p^3} \int_{\sigma_p}^\infty dr r^2 \left[1 - \exp\left\{-V(r)/k_B T\right\}\right], \qquad (2)$$

a result formally identical to that valid for spherically symmetric forces. Results for B_2^* as a function of salt concentration are shown in Fig.2 for the SCM and DCM models, with three values of the total protein charge. In order to obtain values of B_2 comparable to measured virial coefficients, we have taken short-range attractions between proteins into account, by adding to the effective Coulomb potential in Eq. (2) a "sticky" hard-sphere potential of the Baxter form [9], with potential parameters $\delta = 0.02\sigma_p$ and $\tau = 0.12$, which are known to yield reasonable osmotic data for lysozyme solutions in the high salt concentration regime, where Coulombic interactions are essentially screened out.

The key result, illustrated in Fig.2, lies in the considerable *qualitative* difference between the predictions of the SCM and the DCM models for the variation of B_2^* with monovalent salt concentration c_s, irrespective of the total protein charge Ze. While the SCM (dashed curves) predicts a monotonic decay of B_2^* with c_s, the DCM leads to a markedly non-monotonic variation, involving an initial decay towards a minimum followed by a subsequent increase to a maximum and a final decrease towards a high c_s value similar to that predicted by the SCM. The location of the minimum and of the maximum shift to higher values of c_s for larger protein charges Z.

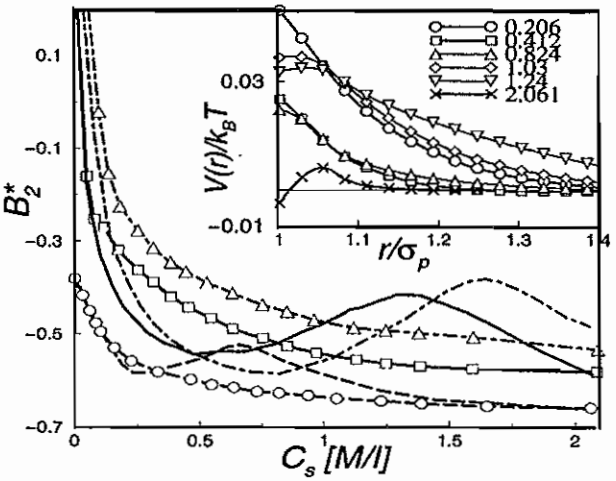

FIG. 2. Normalized second virial coefficient $B_2^* = B_2/B_2^{HS}$ of a protein solution versus added salt molarity. Results are shown for protein charges $Z = 6$ (dashed lines), $Z = 10$ (solid lines) and $Z = 15$ (dot-dashed lines). The lines with (without) symbols correspond to the SCM (DCM) model. The inset shows the effective protein-protein interaction $V(r)$ in the DCM model versus separation distance r for $Z = 10$. Various symbols in the inset relate to the different added salt molarities, indicated in the legend.

We chose our simple models to help highlight and separate the effects of discrete charge patterns and Coulomb correlations. Extending our MD calculations to the more complex (pH dependent) charge patterns of realistic proteins is technically straightforward. We expect that the physical mechanism leading to enhanced protein repulsion at intermediate salt concentration will carry over. Since the second osmotic virial coefficient determines much of the excess (non-ideal) part of the chemical potential of semi-dilute protein solutions, it is anticipated that the non-monotonicity of B_2 may have a significant influence on protein crystallization from such solutions in the course of a "salting-out" process. The non-monotonic behavior also suggests the possibility of an inverse, "salting-in" effect, whereby a reduction of salt concentration may bring B_2 into the "crystallization slot".

[1] E.J.W. Verwey, J.T.G. Overbeek *Theory of the Stability of Lyophobic Colloids* (Elsevier, Amsterdam, 1948).
[2] B.Guo *et al*, J.Cryst.Growth **196**, 424 (1999).
[3] D.N. Petsev *et al*, Biophys. J. **78**, 2060 (2000).
[4] J.J.Grigsby *et al*, J.Phys.Chem.B **104**, 3645 (2000).
[5] J.Z.Wu *et al*, J.Chem.Phys. **111**, 7084 (1999).
[6] T.Arakawa *et al*, Biochemistry **29**, 1914 (1990)
[7] P. Attard, J. Chem. Phys. **91**, 3083 (1989).
[8] J. Piasecki *et al*, Physica A **218**, 125 (1995).
[9] R.J. Baxter, J. Chem. Phys. **49**, 2770 (1968).

Center of Mass Density Profile of Polymers near a Hard Wall

E. Eisenriegler and R. Maassen
Institute Theory II

An exact analytic expression is obtained for the center of mass density profile of free ideal polymer chains in a half space bounded by a hard planar wall. The result differs qualitatively from the monomer density profile and the density profiles of chain ends or midpoints.

F&E-Nr: 23.30.0

Polymer chains interacting with a hard wall is one of the paradigms on the way to understand colloid-polymer mixtures [1, 2]. A hard wall changes the fractal structure of the polymers in a profound way which is reflected in the forms of the various polymer density profiles. Besides the density of all the chain segments and the densities of particular segments such as the endpoints or the midpoint, the density of the center of mass of a polymer chain is of most interest. While simulations [2] have confirmed the expectation that finding the center of mass close to the wall is a much rarer event than to find mid- or endpoints it is surprising that even for *ideal*, random walk like, polymers no analytic expression was available for the center of mass density profile.

Recently we filled this gap and derived an exact analytic expression for the bulk-normalized center of mass density profile $\rho(z)/\rho_{\text{bulk}}$ of free ideal polymer chains in a half space bounded by a hard planar wall [3]. With R_g^2 the mean square radius of gyration in free space and z the distance from the wall the profile only depends on the scaled distance $\zeta = z/R_g$.

Of particular interest is the case $z \ll R_g$ in which we find

$$\frac{\rho(z)}{\rho_{\text{bulk}}} \;\to\; 2.85\,\frac{1}{\zeta}\exp\!\left(-1.89\,/\,\zeta^2\right) \quad . \tag{1}$$

For $\zeta \to 0$ the center of mass density profile (1) drops to zero much more rapidly than profiles for the monomer density or the density of the chain midpoint or endpoints. These display power laws [2, 4] proportional to ζ^2 or ζ rather than the exponential behavior in (1). As a consequence the corresponding repulsive free energy of interaction $\delta F_{\text{cm}}(z) = -k_B T \ln[\rho(z)/\rho_{\text{bulk}}]$ between the polymer center of mass and the wall is of the power law type $\propto \zeta^{-2}$ while the interaction between a fixed end δF_{end} or a fixed midpoint δF_{mid} of the polymer and the wall is of the much softer logarithmic type $\propto \ln(1/\zeta)$. The qualitative difference in entropy loss is obvious since fixing the center of mass close to the wall restricts the polymer configurations much more than fixing an end or the midpoint. For example a vanishing center of mass distance from the wall is realized only for conformations in which *all* the monomers are located right at the wall. Note the close similarity of (1) with [1] the ratio $8\pi^{-2}\exp\!\left(-\pi^2 R_g^2/D^2\right)$ of the partition function of a chain between *two* walls a small distance D apart and averaged over the position of its fixed end to the partition function with fixed end in the bulk.

To derive the form of $\rho(z)/\rho_{\text{bulk}}$ for arbitrary ζ consider a single chain of N monomers in the space between two parallel walls at $z = 0$ and $z = \mathcal{D}$. Then

$$\frac{\rho(z)}{\rho_{\text{bulk}}} = \lim_{\mathcal{D}\to\infty} \mathcal{D}\,\langle \delta(z_{\text{cm}} - z)\rangle \tag{2}$$

where the angular brackets denote an average over all chain configurations. Here $z_{\text{cm}} = \sum_{j=1}^{N} z_j/N$ is the component perpendicular to the wall of the center of mass of the chain with z_j the distance from the wall of monomer j. A Laplace transform

$$\tau \equiv \int_0^\infty d\zeta\, \mathrm{e}^{-q\,R_g^2\,z}\,\frac{\rho(z)}{\rho_{\text{bulk}}} = \lim_{\mathcal{D}\to\infty} \mathcal{D}\,\langle \mathrm{e}^{-q\,R_g^2\,z_{\text{cm}}}\rangle / R_g \tag{3}$$

with respect to the distance z maps the problem onto a polymer chain which is trapped by the hard wall and a gravitational field with a strength proportional to the Laplace conjugate q. For an ideal polymer chain one can make use of the strong similarity between the partition function of the chain in an external potential field and the propagator of a quantum mechanical particle in an external potential [5] and finds [3]

$$\tau \equiv \int_0^\infty d\zeta\, \mathrm{e}^{-Q\zeta}\,\frac{\rho(z)}{\rho_{\text{bulk}}} = Q^{-1/3}\sum_n \mathrm{e}^{-Q^{2/3}\,|a_n|}\,B_n\,|a_n| \tag{4}$$

with $Q = qR_g^3$ and

$$B_n = \left[\int_{a_n}^\infty dY\,\mathrm{Ai}(Y)\right]^2 \Big/ \left\{|a_n|\,\left[\mathrm{Ai}'(a_n)\right]^2\right\} . \tag{5}$$

Here a_n is the n'th zero [6] of the Airy function Ai and the prime in Ai$'$ denotes a derivative. The reason is that the eigenfunctions ψ_n for the linear gravitational potential which vanish at the hard wall can be expressed in terms of the Airy function. Inverting the Laplace transform [7] in Eq. (4) finally leads to the result

$$\frac{\rho(z)}{\rho_{\text{bulk}}} = \frac{3\sqrt{3}}{2\pi}\sum_{n=1,2,..}^{\infty} B_n\,X_n\,\mathrm{e}^{-X_n}\left[K_{1/3}(X_n)+K_{2/3}(X_n)\right] \tag{6}$$

with K modified Bessel functions and the distance z from the wall is contained in

$$X_n = \frac{2}{27}\,|a_n|^3\,/\,\zeta^2 . \tag{7}$$

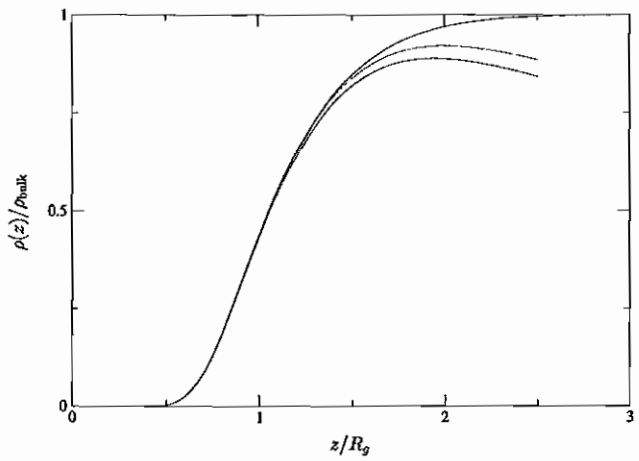

FIG. 1: Normalized center of mass density profile for ideal polymer chains near a hard wall as given by Eq. (6) (solid line). The dotted line shows the contribution from the 'ground state' $n = 1$ in (6) and the line of dashes shows the asymptotic expression given in Eq. (1).

While for $z/R_g \gg 1$ the sum in (6) is dominated by the terms with $n \gg 1$, for $z/R_g \ll 1$ the first term in the sum dominates and leads to the result (1). The behavior of the center of mass density profile (6) for arbitrary z/R_g is shown as the solid line in Fig. 1.

We have checked that the integral

$$\int_0^\infty d\zeta \, [1 - \rho(z)/\rho_{\rm bulk}] \qquad (8)$$

with the center of mass density profile $\rho/\rho_{\rm bulk}$ for ideal chains from Eq. (6) has the known value $2/\sqrt{\pi}$. This integral has the *same* value for the different profiles of the monomer density, the density of chain ends or midpoints, and the center of mass density and it determines the polymer induced surface tension of the wall to be $(2/\sqrt{\pi})\, p\, R_g$. Here p is the bulk osmotic pressure $k_B T n$ with n the chain density in the bulk.

It would be interesting to generalize the center of mass density profile to the case of a *spherical particle* in which the chain center of mass can be outside as well as inside the particle.

[1] S. Asakura and F. Oosawa, J. Chem. Phys. **22**, 155 (1954)).

[2] P. G. Bolhuis, A. A. Louis, J. P. Hansen, E. J. Meijer, J. Chem. Phys. **114**, 4296 (2001).

[3] E. Eisenriegler and R. Maassen, J. Chem. Phys. **116**, 1 January 2002

[4] E. Eisenriegler, *Polymers near Surfaces* (World Scientific, Singapore, 1993).

[5] P.G. de Gennes, *Scaling Concepts in Polymer Physics* (Cornell University, Ithaca, 1979).

[6] M. Abramowitz and I. Stegun, *Handbook of Mathematical Functions* (Dover Publications, New York 1965).

[7] A. Prudnikov, Yu. Brychkov, and O. Marichev, *Integrals and Series* (Gordon and Breach, London 1992).

Multi-particle-collision dynamics: Flow around a circular and a square cylinder

A. Lamura[1], G. Gompper[1], T. Ihle[2], and D. M. Kroll[2]

[1] Institute Theory II
[2] Supercomputing Institute, University of Minnesota,
1200 Washington Ave. S., Minneapolis, MN 55415, USA

A particle-based model for mesoscopic fluid dynamics is used to simulate steady and unsteady flows around a circular and a square cylinder in a two-dimensional channel for a range of Reynolds number between 10 and 130. Numerical results for the recirculation length, the drag coefficient, and the Strouhal number are reported and compared with previous experimental measurements and computational fluid dynamics data. The good agreement demonstrates the potential of this method for the investigation of complex flows.

F&E-Nr: 23.30.0

The main problem in simulations of the hydrodynamic behavior of complex fluids is the large length- and time-scale gap between the microscopic scale of the solvent, the mesoscopic scale of the embedded colloidal particles, and the macroscopic scale of the flow geometry. Therefore, mesoscale simulation techniques have attracted considerable attention in recent years. The main idea behind all these methods is to simplify the solvent dynamics in order to speed up the elementary particle motions as much as possible, but at the same time satisfy all important conservation laws to guarantee the correct hydrodynamic behavior on larger scales. Several computational fluid dynamics approaches, such as lattice gas automata, lattice-Boltzmann methods, and dissipative-particle dynamics, have been proposed and developed in order to describe the dynamical behavior of these systems on mesoscopic length scales. The first two methods, despite of their conceptual simplicity, suffer mainly from the lack of Galilean invariance. Moreover, since these are lattice based methods, practical applications involving irregular geometries often require the use of adapted computational meshes. Dissipative particle dynamics is an off-lattice, particle-based method which does not have these problems; however, it is often complex and difficult to analyze analytically.

We have investigated in some detail [1] another particle-based simulation method which is a modification of Bird's Direct Simulation Monte Carlo algorithm [2]. The fluid is modeled by N "particles", whose positions $\mathbf{r}_i(t)$ and velocities $\mathbf{v}_i(t)$ are continuous variables, while time is discretized. The evolution of the system occurs in two steps: propagation and collision (compare Fig. 1). Each particle is first streamed by its displacement during the time interval $\Delta t = 1$,

$$\mathbf{r}_i(t+1) = \mathbf{r}_i(t) + \mathbf{v}_i(t) \qquad (1)$$

For the collision step, the system is divided into the cells of a regular lattice of mesh size a_0, with $a_0 = 1$. A novel algorithm for the collision step was introduced recently by Malevanets and Kapral [3]. The cells are taken to be the collision volumes for many-particle collisions — which is why we refer to this method as multi-particle collision dynamics (MPCD) —, which conserve mass, momentum and energy. These multi-particle collision are defined by

$$\mathbf{v}_i(t+1) = \mathbf{u}(t) + \Omega\,[\mathbf{v}_i(t) - \mathbf{u}(t)], \qquad (2)$$

where $\mathbf{u}$ is the macroscopic velocity, defined as the average velocity of the colliding particles, which we assume to have coordinates of the center of the cell. In the case of two spatial dimensions, which we consider here, Ω denotes a stochastic rotation matrix which rotates by an angle of either $+\pi/2$ or $-\pi/2$ with probability $1/2$. The collisions are simultaneously performed on all the particles in a cell with the same rotation Ω, but Ω may differ from cell to cell. The local momentum and kinetic energy do not change under this dynamics.

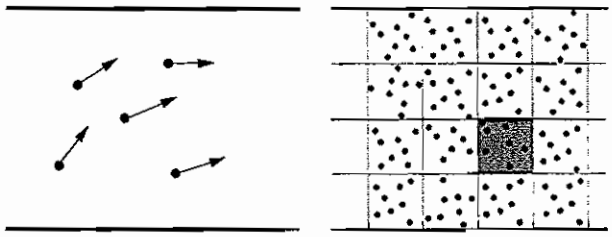

FIG. 1. Streaming (left) and collision (right) step of the MPCD algorithm. During the collision step, the velocities relative to the average velocity of all particles within one cell (green) are rotated by a fixed angle.

When the mean-free path is small compared to the cell size a_0, particles remain within the same cell for many collisions, and become correlated. These correlations depend on the presence of flow, and Galilean invariance is broken. It was shown in Ref. [4] that this problem can be cured by performing the collision operation in a cell grid which is shifted each time step by a random vector with components in the interval $[-a_0/2, a_0/2]$. The collision environment is then independent of the macroscopic velocity, and Galilean invariance is *exactly* restored.

We present the results of a quantitative analysis of the MPCD method in order to determine whether it can provide a convenient alternative to other computational fluid dynamics approaches [1]. In particular, we study the

problem of two-dimensional incompressible flow around a circular and a square cylinder with diameter D inside a plane channel of height H and length L was investigated. The blockage ratio $B = D/H$ is fixed at 0.125 for both the cylinders. In order to reduce the influence of inflow and outflow boundary conditions, the length L is set to $L/D = 50$. The cylinder is centered inside the channel at a distance $L/4$ from the inflow region. The average number of particles per cell is $n_{av} = 10$ and the temperature is fixed at $k_BT = 0.4$. The flow is driven by assigning Maxwell-Boltzmann-distributed velocities with parabolic profile $v_x(y) = 4v_{max}(H-y)y/H^2$ to particles in the region $0 < x \leq 10$. Periodic boundary conditions are imposed in the x-direction, no-slip boundary conditions on the channel and cylinder walls.

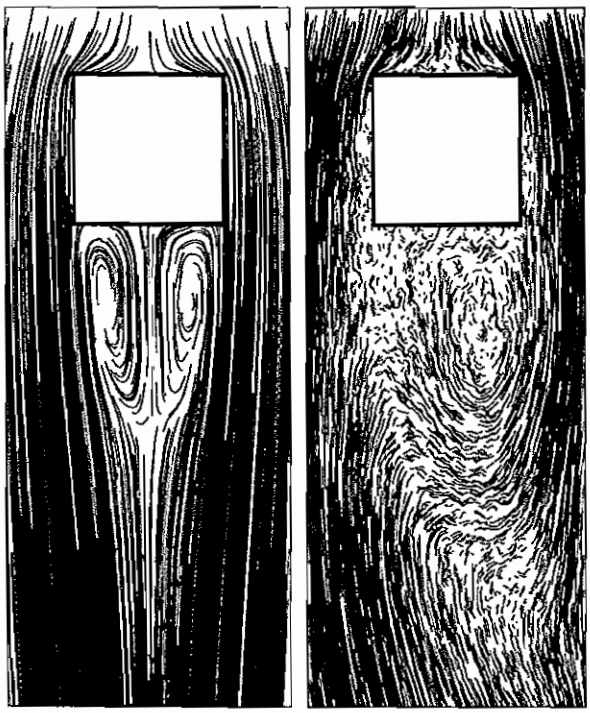

FIG. 2. Velocity field for the square cylinder at Reynolds number $Re = 30$ (left) and $Re = 100$ (right). Only a fraction of the simulation box is shown in each case.

Reynolds numbers, $Re \equiv v_{max}D/\nu$, in the range $10 \leq Re \leq 130$ were investigated. Both steady flows, with a closed steady recirculation region consisting of two symmetric vortices behind the body, and unsteady flows, with the well-known von Karman vortex street with periodic vortex shedding from the cylinder, are observed to occur for this range of Reynolds numbers. The critical Reynolds number above which flow becomes unsteady, is approximately 49 for the circular cylinder and 60 for the square cylinder [5]. Figure 2 shows the macroscopic velocity field of the final steady-state for $Re = 30$, and of the periodic vortex shedding for $Re = 100$ — consistent with experiments.

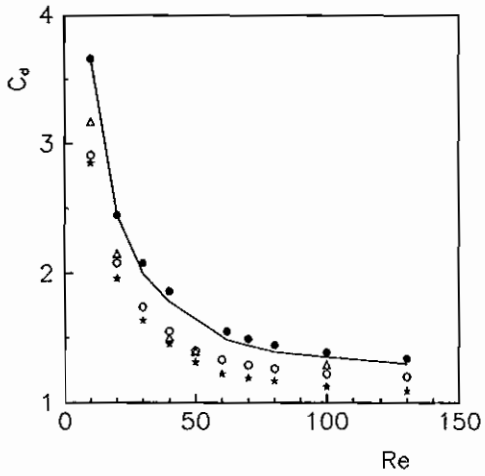

FIG. 3. The drag coefficient $C_d = 2F_{\|}/(n_{av}v_{max}^2 D)$ — where $F_{\|}$ is the force exerted on the cylinder in the direction parallel to the flow — as a function of the Reynolds number. Square cylinder: (•) this study, (——) Breuer *et al.* [5]; Circular cylinder: (⋆) this study, (○) Tritton [6], (△) He and Doolen [7].

As an example for the quantitative analysis of the simulation data, Figure 3 shows the drag coefficient C_d as a function of the Reynolds number. For the square cylinder, agreement between our data and the previous numerical measurements is satisfactory, with a small but systematic deviation to larger values compared to Ref. [5] for $Re > 20$. In the case of the circular cylinder, our results are compared with the experiments and with numerical simulations with the lattice-Boltzmann method. In contrast to the current simulations, Refs. [6] and [7] both used a constant incoming velocity profile and a very small blockage ratio. This is the reason why our results fall below (about 5%) the literature data in this case; a detailed discussion of this point can be found in Ref. [1].

The present model provides a simple alternative scheme that can be used to treat a wide class of physical and chemical problems. Many directions are accessible to exploration. The algorithm can be used, for example, for a mesoscopic model of the solvent dynamics which can be coupled to a microscopic treatment of solute particles.

[1] A. Lamura, G. Gompper, T. Ihle, and D. M. Kroll, Europhys. Lett. **56**, 319 (2001).

[2] G. A. Bird, *Molecular Gas Dynamics*(Clarendon Press, Oxford, 1976).

[3] A. Malevanets and R. Kapral, J. Chem. Phys. **110**, 8505 (1999); ibid.**112**, 7269 (2000).

[4] T. Ihle and D. M. Kroll, Phys. Rev. E **63**, 020201(R) (2001).

[5] M. Breuer, J. Bernsdorf, T. Zeiser and F. Durst, Int. J. Heat Fluid Flow**21**, 186 (2000).

[6] D. J. Tritton, J. Fluid Mech.**6**, 547 (1959).

[7] H. He and G. Doolen, J. Comput. Phys. **134**, 306 (1997); Phys. Rev. E**56**, 434 (1997).

Influence of disorder and constraint release on reptation dynamics

M. Paeßens, R. Willmann, and G.M. Schütz

Institute Theory II

We study how properties of the entanglement experienced by a single polymer chain in a polymer melt or a gel affect two key macroscopic properties of the polymer dynamics. Using a lattice gas model we prove rigorously that kinematic disorder leaves the scaling relation for the diffusion constant of the original reptation model unchanged and we also calculate the exact scaling amplitude as a function of the disorder distribution. From a numerical DMRG investigation we conclude that shape fluctuations of the tube caused by constraint release are not a likely candidate for improving Doi's crossover theory for the scaling of the polymer viscosity. The closely related tube renewal time depends on the entropic tensile force acting at the boundary segments of the polymer, but not on the details of the boundary dynamics by which this force is generated.

F&E-Nr: 23.30.0

Among the basic problems of polymer science is the derivation of large scale properties of entangled polymers from microscopic properties, such as the molecular weight, which is proportional to the chain length L. A polymer chain moving in a gel or melt experiences severe constraints in its motion due to the entanglements with gel fibers or other polymers. De Gennes named the resulting wormlike motion 'reptation' [1] and presented scaling arguments which predict for the diffusion constant D of a reptating polymer chain that to leading order $D \propto L^{-z_D}$, $z_D = 2$, and for the viscosity $\eta \propto L^{z_\eta}$, $z_\eta = 3$. In constrast to that experiments show $z_D \approx 2.3$ and $z_\eta \approx 3.3$. More refined reptation theories accounting for contour length fluctuations (CLF) and constraint release (CR) offer an explanation of this behaviour and predict for increasing chain length a crossover to $z_D = 2$ and $z_\eta = 3$. So far, however, this region is not experimentally accessible. In terms of the Rubinstein-Duke (RD) model [2,3] the proportionality constants of the scaling relations as well as finite–size–corrections are known. The RD model is a discrete model which maps the reptation dynamics of a three dimensional polymer onto a one dimensional lattice–gas. This model takes into account tube length fluctuations as well as the effect of a possible external electric field F which acts on a charged polymer.

In the RD model the entanglement network is represented as a cubic lattice, the lattice constant being equal to the mean entanglement length. A string of $L+1$ 'reptons', i.e., sections with a length of the lattice constant, represents the polymer. The repton dynamics is defined as follows:

a) Each cell occupied by the chain must contain at least one repton to ensure connectivity of the chain.

b) End reptons can move to adjacent cells provided rule a) is not violated.

c) Interior reptons can move to cells occupied by the neighbouring reptons if allowed by a).

The field F points in the (111)-direction of the cubic lattice and serves as a projection axis for the dynamics which is isotropic on the long time scales investigated here. Even in the absence of the field the configuration of the chain can then be rephrased as a one-dimensional lattice gas model with L sites by considering the links between reptons with respect to F. Links between reptons in the same cell are represented as '0' (vacancy), those which are oriented along (against) the field and across a cell boundary as particles of type 'A' ('B'). As for each site three states are possible this model can be identified with a "quantum" spin–one chain. [4,5]

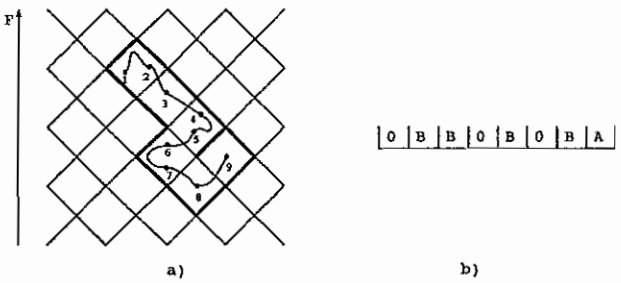

FIG. 1. a) The repton model in two dimensions: the circles represent the reptons; the primitive path is marked by the bold lines. b) Projection onto one dimension.

In contrast to this idealized network real entanglements have a random structure whose effects on the motion of the polymer have to be taken into account [6]. One may have spatial variations of the mobility of the 'defects' of stored length, locally fluctuating potential energies due to interactions between chain and environment, relaxation of the environment (CR) and other phenomena. As many effects are at interplay, it is experimentally impossible to isolate the influence of a single one. However, with theoretical considerations and computer simulations one can investigate each effect separately.

We develop a modified RD model incorporating kinematic disorder, i.e. disorder affecting the mobility of the reptons while leaving the equilibrium configurations of

the chain unaffected. In contrast to existing Monte Carlo simulations [6] we focus on very large chains to clarify if the scaling behavior of D is robust against the introduction of this kind of disorder.

In the presence of kinematic disorder each boundary between cells has assigned to it an individual hopping rate for a repton crossing in any direction. We assume $\sigma \in \mathbb{N}$ possible rates W_α, each occurring with probability $f(W_\alpha)$ throughout the network. We require for the distribution $f(W_\alpha)$ that the disorder averages $\langle 1/W \rangle$ and $\langle 1/W^2 \rangle$ be finite. This model is mapped to a one dimensional lattice gas model with $2\sigma + 1$ states at each site. For the lattice gas model with periodic boundary conditions an exact analytical calculation yields a rigorous lower bound on $D_L L^2$ in the limit of infinite chain length, while a variational treatment as in [7] gives a rigorous upper bound

$$\frac{1}{(2d+1)} \frac{1}{< 1/W >} \leq D_L L^2 \leq \frac{< W >}{(2d+1)}. \qquad (1)$$

Here, d is the dimension of the network and $\langle 1/W \rangle$ the disorder average over the inverse hopping rates. As both upper and lower bound scale with the inverse length squared, it is proved that de Gennes' scaling relation prevails in presence of kinematic disorder. Monte Carlo simulations lead to the conclusion that in the limit of infinite chain length the lower bound describes the behavior of the chain correctly. Remarkably, the factor $\langle 1/W \rangle$ also occurs when studying single particle diffusion in a random barrier model.

In order to study how entanglement properties determine the viscosity of of a polymer melt we investigate numerically with the density renormalization group technique the longest relaxation time of the lattice gas model which is proportional to the viscosity [8]. The DMRG algorithm is a numerical method to diagonalize huge matrizes by reducing the Hilbert space to the most important states. We incorporate constraint release caused by fluctuations in the location of the surrounding polymer chains by allowing for permutation of AB–pairs. This is motivated by assuming that a constraining polymer moves so far that the constraint for the investigated polymer is released so that it can move freely in this region. After a short time the constraining polymer returns so that the free movement in this region is again prevented. The lattice has regained its originally structure but chain conformation may have changed in the bulk. Using input from Rouse theory the rates for the CR are determined in a self-consistent way. Our results show that the crossover to the asymptotic reptation result is slow, but not as slow as suggested by visual inspection of experimental viscosity curves. We conclude that the shape fluctuations of the tube caused by constraint release are not a likely condidate for improving Doi's crossover theory [8] for the scaling of the polymer viscosity.

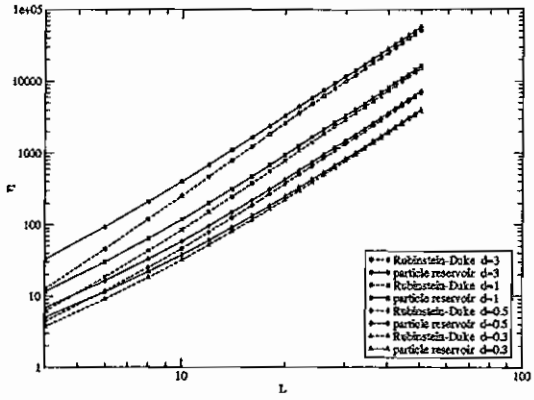

FIG. 2. Viscosity in dependence of the chain length – comparison of the different boundary dynamics.

The asymptotic amplitude of the viscosity increases with increasing dimension of the lattice [2]. The lattice dimension determines the rates for adding and removing new segments to the tube (rule b) and thus fixes the equilibrium particle density in the lattice gas picture. The same density, however, could be achieved by other boundary rates [9] which – given the sensity of the bulk behavior on the boundary dynamics – leads naturally to the question how the viscosity depends on the microscopic boundary parameters. We compared DMRG results for the asymptotic relaxation times using different boundary mechanisms. We found that the asymptotic viscosity depends not on microscopic details of the dynamics at the end segments, but only on the entropic tensile force which acts on the end segments of the chain and which determines the particle density. In the RD model a repton has more possibilities ($2d - 1$ in a d-dimensional hypercube) of moving out of the tube than moving back into it (only 1 by construction) and therefore leads to a purely entropic dependence of the viscosity on the dimensionality within this particular model.

[1] P. G. de Gennes, *Scaling concepts in polymer physics* (Cornell University Press, Ithaca, 1979).

[2] M. Rubinstein, Phys. Rev. Lett **59**, 1946 (1987).

[3] T.A.J. Duke, Phys. Rev. Lett. **62**, 2877 (1989).

[4] G.M. Schütz, in *Phase Transitions and Critical Phenomena*, edited by C. Domb and J. Lebowitz (Academic, London, 2000), Vol. 19.

[5] G.T. Barkema and G.M. Schütz, Europhys. Lett. **35**, 139 (1996).

[6] L. Schäfer, A. Baumgärtner, and U. Ebert, Eur. Phys. J. B **10**, 105 (1999).

[7] M. Prähofer and H. Spohn, Physica A **233**, 191 (1996).

[8] M. Doi and S.F. Edwards, *The Theory of Polymer Dynamics* (Clarendon Press, Oxford, 1986).

[9] G.M. Schütz, Europhys. Lett **48**, 623 (1999).

Motility of Biological Cells

R. Sambeth[1] and A. Baumgaertner[1,2]
[1] *Forum Modellierung, FZJ, and* [2] *Theorie II, IFF, FZJ*

The autocatalytic polymerization kinetics of the cytoskeletal actin network provides the basic mechanism for a persistent random walk of a crawling cell. It is shown that network remodeling by branching processes near the cell membrane is essential for the bimodal spatial stability of the network which induces a spontaneous breaking of isotropic cell motion. Details of the phenomena are analyzed using a simple polymerization model studied by analytical and simulation methods.

F&E-Nr. 23.30.0

The amoeboid crawling of animal cells like fibroblasts and keratocytes or the advancing neural growth cone has been the subject of intensive experimental [1] (and references therein) and theoretical [2–7] studies. It is now commonly accepted that the continuous remodeling of the actin cytoskeleton of a cell provides the main contribution [3,4] to the driving force which leads to cell motility. In particular, it has been suggested that the polymerization of monomeric G-actin to filamentous F-actin oriented essentially perpendicular to the cell membrane provides the necessary motor for membrane protrusion and hence motility. However, the phenomena of cell locomotion cannot be explained solely based on the G- to F-actin transition. In particular, the reasons for the observed characteristic traces of cell migration exhibiting a pattern similar to a random walk with a certain persistency [9] has remain obscure. Recently it has been shown [8] that random walk characteristics and persistency can be the results of the special bifurcated structure of the actin cytoskeleton [10] and of its inherent autocatalytic polymerization kinetics. In particular, it has been shown that the autocatalytic properties of network polymerization near the cell membrane represent the predominant mechanism which spontaneously breaks the symmetry of motion and induces a persistent random walk. A typical snapshot of the simulatiuon model is depicted in Fig. 1. The model represents a horizontal section cut from a large two-dimensional cell model where the cell membrane is represented by a large flexible polymer ring. The cut has been performed along the upper and lower broken line as shown in Fig. 1. Henceforth the broken lines are called the upper and lower walls because they are impenetrable for molecules. The cell section contains a certain number of actin molecules which are depicted in Fig. 1 by open circles. Some of the actin molecules are connected to filamentous networks. The actin networks are assumed to be tightly coupled to an underlying substrate by external harmonic forces in order to break momentum conservation of the entire cell [7]. Hence, the networks are at rest on the average with respect to an external coordinate system in the xy-plane. Each network (as depicted in Fig. 1) can grow by addition polymerization of actin monomers at the ends. The growth rate is purely diffusion-limited.

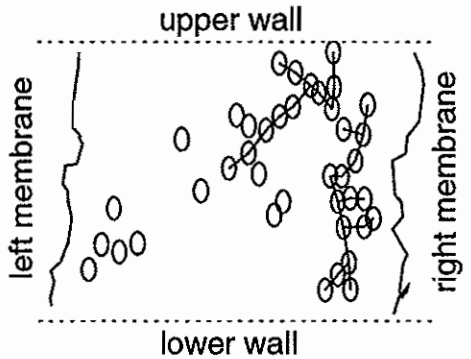

FIG. 1. Snapshot of the computer model, explained in the text.

A branching mechanism is introduced in accordance with experimental observations which indicate that association of cytosolic Arp2/3 proteins with actin molecules induces branching of actin filaments [10]. Arp2/3 proteins are not explicitly simulated but are assumed to be continuously generated by some biochemical processes near the intracellular cell membrane [10]. Networks can shrink by depolymerization processes. The dissociation of actin molecules from filaments *in vitro* is asymmetric in the sense that the two ends of a filament behave differently [9]. The "polarity" of actin molecules leads to a fast-growing (plus) end with a low dissociation rate and a slower-growing (minus) end with a high dissociation rate. Branching points are dissociated with rate k_b. The trajectory of a typical simulation is given in Fig. 2: the large solid curve represents the x-displacements $x_M(t)$ of the center of the cell, i.e. the center-of-mass of the two membranes, as a function of time t/τ. Displacements $x_M(t)$ and distribution $p_F(x,t)$ clearly exhibit a correlation: motion in one of the two x-directions is in concomitance with a strongly asymmetric distribution of F-actin towards the same direction. Obviously, the interpretation is that asymmetric growth and distribution of F-actin push the membrane in one direction as long as the diffusion-limited supply of new G-actin monomers near one cell membrane is possible.

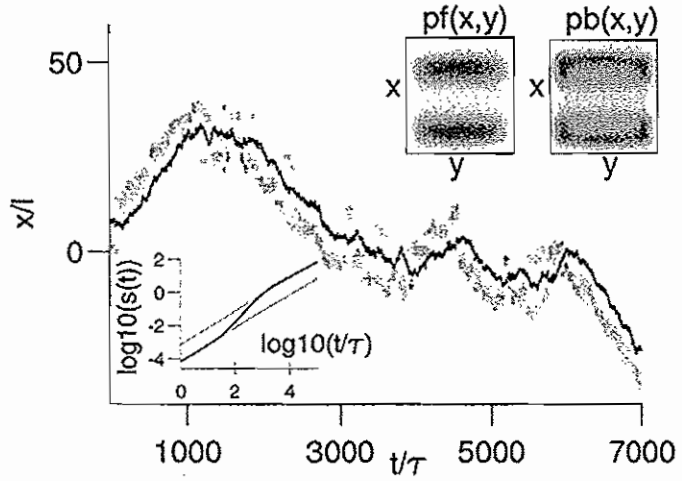

FIG. 2. Trajectory, F-actin distribution (upper right insets) and mean square displacement (lower left inset) of a simulation. The shaded areas above and below the trajectory represent the number distribution $p_F(x,t)$ of actin molecules bound into networks (F-actin). Black, grey and white shading correspond to high, intermediate and low probability, respectively. Averaging in y-direction has been performed.

The stochasticity of the polymerization process may lead sometimes to an amplified growth near the opposite membrane which may change then the direction of migration. Therefore, on the average, the distribution of F-actin is bimodal. This is shown by the two-dimensional distribution $pf(x,y)$ in the upper right inset of Fig. 2. The important point is that this bimodal distribution is strongly correlated to the distribution of the plus ends of the networks which is shown by the probability $pb(x,y)$ in the the upper right inset of Fig. 2. The distribution indicates that the plus ends are found with higher probability at the boundary of the cell than anywhere else. Since the number of plus ends are closely related to the number of branching points, this indicates that the stability of a certain asymmetric distribution of F-actin within the cell must be related to the statistical properties of the branching processes, and not to chemical processes. This is an important point and explains experimental observations [1] similar to the distribution $pb(x,y)$.

Long runs of simulations provide the complete picture of a persistent random walk which can be characterized by the mean square displacements of the center-of-mass X of the entire cell $s(t)$ This is shown in the lower left inset of Fig. 2. At short times, $\log 10(t) < 2$, the center-of-mass exhibits Brownian motion according to $s(t) = D_1 t$. At intermediate times, $2 < \log 10(t) < 3$, a rectified motion is observed, $s(t) = (vt)^2$, where v is the average velocity. And finally for $\log 10(t) > 3$ the cell performs a persistent random walk, $s(t) = D_2 t$, where $D_2 \approx 6.5 D_1$.

The simulation results as described above can be understood and described by a mathematical model which provides an explanation for the stability and amplification of network inhomogenity. The polymerization process can be described as a one-step process [11] by the fmaster equation for the probability $p(n)$ to find n particles polymerized,

$$\frac{dp(n)}{dt} = (1-\delta_{n1})j(n) - (1-\delta_{nN})j(n+1) \qquad (0.1)$$

where $j(n) = g(n-1)p(n-1) - r(n)p(n)$ is the current, $g(n) = k^+ n^\alpha (N-n)/N$ is the polymerization rate, and $r(n) = k^- n^\beta$ is the depolymerization rate. For $\alpha > 0$ the number of sites increases with the number of polymerized units which corresponds to a branching network. Similarly, the depolymerization rate $r(n)$ corresponds to a fixed number of depolymerization site for $\beta = 0$ whereas for $\beta > 0$ the number of such sites increases leading to the disintegration of a given network into separate networks.

At values $\theta = k^-/k^+ < 1$ and $\gamma = \alpha - \beta > 0$ the stationary probability distribution $p^s(n)$ [11] is peaked around a value $n_p \gg 0$ which can be found approximately by solving the deterministic equation corresponding to Eq. 0.1. $dn_p/dt = (N-n_p)n_p^\gamma - N\theta = 0$, It can be shown numerically that for $\gamma > 0$ the magnitude increases by several orders resulting in two metastable states. The transition between those states is induced by fluctuations. The values of α and β in the computer simulation described above are not set externally but can be estimated from the simulation results. For the parameters of fig. 1 the values are $\alpha = 0.97$ and $\beta = 0.72$, so that indeed $\gamma = \alpha - \beta > 0.2$ which provides a bimodal distribution of F-actin: networks are found either at the left or at the right of the model cell.

[1] A. B. Verkhovsky, T. M. Svitkina, and G. G. Borisy, Curr. Biol. **9**, 11 (1999).
(1993).
[2] H. Gruler, Blood Cells **19**, 91 (1993).
[3] C. S. Peskin, G. M. Odell, and G. F. Oster, Biophys. J. **65**, 316 (1993).
[4] A. Mogilner and G. F. Oster, Biophys. J. **71**, 3030 (1996).
[5] D. C. Bottino and L. J. Fauci, Eur. Biophys. J. **27**, 532 (1998).
[6] W. Alt and M. Dembo, Math. Biosc. **156**, 207 (1999).
[7] R. Sambeth and A. Baumgaertner, J.Biol.Systems **9**, 201 (2001).
[8] R. Sambeth and A. Baumgaertner, Phys. Rev. Lett. **86**, 5196 (2001).
[9] D. Bray, *Cell movements* (Garland, New York, 1992).
[10] R. D. Mullins, J. A. Heuser, and T. D. Pollard, Proc. Nat. Acad. Sci. USA **95**, 6181 (1998).
[11] N. G. van Kampen, *Stochastic processes in physics and chemistry* (North-Holland, Amsterdam, 1992).

Counterion mediated attraction between equally charged polyelectrolyte molecules

R. G. Winkler†, T. Hofmann‡, and P. Reineker‡
†*Institute Theory II;* ‡*Abteilung Theoretische Physik, Univeristät Ulm, 89069 Ulm*

The structure of rodlike polyelectrolyte molecules in solution has been studied using the Ornstein-Zernike integral equation for molecular systems. The polymer reference interaction site model together with the reference Laria-Wu-Chandler closure is solved numerically taking counterions into account explicitly. The counterions and the polymer chains interact through an unscreened Coulomb potential. The pair correlation functions among the different entities are calculated for various Bjerrum lengths and densities. Based upon these quantities, the effective potential between the monomers and the counterions, respectively, is extracted. Our calculations yield a minimum at short separations of the effective counterion-counterion and monomer-monomer potentials, respectively, corresponding to an attractive interaction between the equally charged units.

F&E Nr. 23.30.0

Polyelectrolytes are macromolecules build of monomers with ionizable groups. When the molecules are dissolved in a polar solvent such as water, the ion pairs dissociate. The electrostatic charges of one sign remain localized on the chain whereas the large number of oppositely charged counterions are scattered in the solution. The long range Coulomb interaction among the various charges is the origin of a rich variety of properties of such solutions which are not found for neutral polymers. Hence, polyelectrolyte systems are of considerable interest from a basic scientific point of view. On the other hand, polyelectrolytes play a fundamental role in our everyday live. Most biopolymers, including DNA and many proteins, are polyelectrolytes. Technologically they are used in a wide-range of applications such as dewatering agents, drug reduction agents, as additives in detergents and cosmetics, in gels, in superabsorbants etc. Despite more than 50 years of continuing interest, the unique properties of charged polymers are poorly understood compared to those of their neutral counterparts [1, 2]. Experiments on polyelectrolyte solutions using different methods often lead to controversial results. Furthermore, experimental results on single polyelectrolyte chains are still lacking due to the immense problems caused by trace impurities and very low scattering intensities when measuring dilute solutions. Thus, scattering experiments and measurements of the radius of gyration are almost always performed in the semidilute regime. From a theoretical point of view the problem is the long range Coulomb interaction. Renormalization group theories and scaling ideas, which have proved to be very successful for neutral polymer solutions, are now difficult to apply. The long range Coulomb interaction, together with screening effects caused by counterions, introduces more than one new length scale in the problem, which means that short and medium to long range interactions are simultaneously present. This coupling of different length scales leads to a severe influence of local chain properties on the properties of the whole system.

Valuable insight into the properties of polyelectrolyte solutions is obtained by computer simulations and liquid state theory. The later is based upon the Ornstein-Zernike integral equation and, in the case of polymeres, uses the *Polymer Reference Interaction Site Model* (PRISM) [3].

To characterize the structure of a solution of rodlike polyelectrolytes, we adopted the PRISM approach [3–5]. The PRISM theory as well as the Ornstein-Zernike equation relates the total correlation function $h(\mathbf{r})$, which is related to the pair correlation function $g(\mathbf{r})$ via $h = g-1$, with the direct correlation function $c(\mathbf{r})$ and, in the case of polymers, with the intramolecular structure factor ω. For the considered primitive model three different correlation functions are relevant: the monomer-monomer (g_{mm}), the counterion-counterion (g_{cc}), and the monomer-counterion (g_{mc}) correlation function (no salt is present). Neglecting chain end effects and hence considering all monomers on a chain as equivalent, a set of three coupled equations for the correlation functions is obtained. Using the reference Laria-Wu-Chandler (RLWC) closure the set of equations can be solved iteratively.

The chains are modelled as a sequence of N touching charged hard spheres of diameter σ. The counterions, which are taken into account explicitly, are also modelled as charged hard spheres of diameter σ. The overall system is neutral. Since we consider rodlike chains, the structure factor of a molecule is known. The influence of the solvent is treated in a mean field manner. It is described as a homogeneous dielectric continuum with the dielectric constant ϵ. The pair interaction potential for all ionic species is given by the hard core potential $v_{ij}^{HC}(r)$ and the Coulomb potential:

$$\beta v_{ij}(r) = \beta v_{ij}^{HC}(r) - \frac{l_B}{r}\,; \qquad i,j \in \{m,c\}\,, \qquad (1)$$

where $l_B = e^2/(k_B T \epsilon)$ is the Bjerrum length.

Based on this model, we calculated the various correlation functions. An interesting result is the appearance of a peak in the counterion-counterion correlation function for Bjerrum lengths $l_B/\sigma \gtrsim 1$. This peak increases with increasing interaction strength and can only be explained by counterion condensation.

The behavior of g_{cc} indicates the appearance of an attractive interaction between the counterions above a certain Bjerrum length. This attractive interaction is reflected in an effective potential between two counterions.

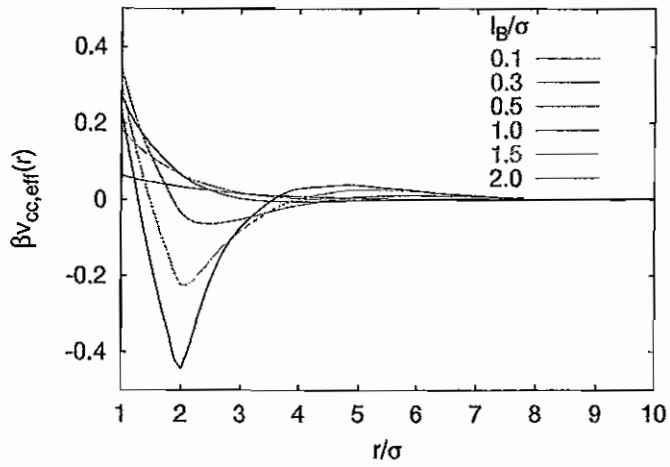

FIG. 1: Effective potential between two counterions for various Bjerrum lengths l_B. The density is $\eta = 10^{-2}$ and the chain length $N = 80$.

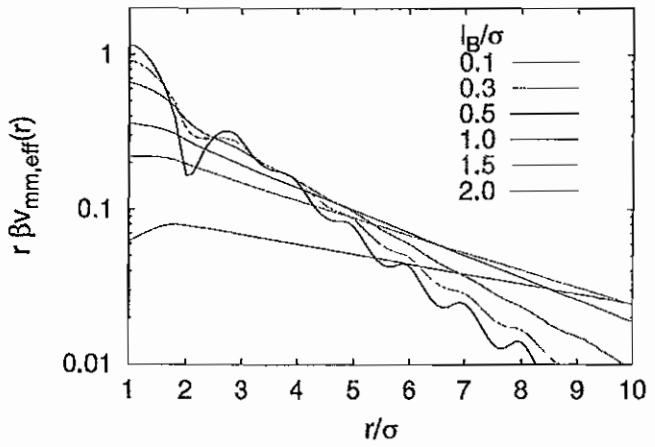

FIG. 2: Effective potential between two monomers for various Bjerrum lengths l_B at the density $\eta = 10^{-2}$. The chain length is $N = 80$.

An effective potential between two counterions or two monomers, respectively, can be calculated if the multicomponent model with polymers and counterions is reduced to a simpler model consisting only of counterions or chains. We define the simplified model in such a way that the effective potential between the counterions or monomers, respectively, of the new system yields exactly the same correlation function (g_{cc}, g_{mm}) as found in the multicomponent case at the same density. Starting from the correlation function g_{cc} – respectively g_{mm} – of the multicomponent model we calculate an effective direct correlation function c_{eff} via the one component Ornstein-Zernike equation. An effective potential is then obtained from the RLWC closures of the one- and multicomponent models [4]. For low and moderate densities the effective potential is well approximated by

$$\beta v_{\alpha\alpha,\text{eff}}(r) = \beta v_{\alpha\alpha}(r) + (c_{\alpha\alpha}(r) - c_{\alpha\alpha,\text{eff}}(r)) \ , \qquad (2)$$

where $\alpha \in \{m, c\}$. Hence, the effective potential is equal to the bare potential plus a modification given by the correlation functions of the multicomponent and one-component model.

Figure 1 exhibits the effective counterion-counterion potential for different Bjerrum lengths. As is obvious from this figure, the effective potential is purely repulsive for low values of l_B and can very well be approximated by the bare Coulomb potential between the counterions. With increasing Bjerrum length the potential becomes negative for distances larger than a certain critical distance leading to an attractive force between two counterions. For even larger values of l_B, the effective potential exhibits a distinct minimum at a distance of about $r = 2\sigma$ in agreement with the position of the peak in g_{cc}. Figure 2 shows the effective monomer-monomer potential. Similar to the counterion-counterion potential, we observe a minimum at $r \approx 2\sigma$ for Bjerrum lengths $l_B \gtrsim 1.5\sigma$ Hence, the monomers attract each other at large interaction strengths and small distances. The distance of $r \approx 2\sigma$ indicates that the attraction is counterion mediated and that precisely one counterion is located between two monomers. Moreover, the effective potential is a monotonous decreasing function for $r > 2\sigma$ in agreement with the Debye-Hückel approximation. For $r < 2\sigma$ we find deviations from the Debye-Hückel potential due to the depletion interaction. At high Bjerrum lengths ($l_B > \sigma$) the effective potential still decays in the average as predicted by the Debye-Hückel model. The quantitative comparison between our calculations and the Debye-Hückel potential exhibits excellent agreement for the screening length as well as the dependence of that potential on the interaction strength. The deviations from the Debye-Hückel representation of the interaction among the monomers is not surprising. The condensation of the counterions leads to a screening of the Coulomb interaction which is not captured by the Debye-Hückel potential.

In conclusion, the PRISM approach provides valuable insight into the structure of polyelectrolyte solutions. For sufficiently large interaction strengths counterions condense on a polymer chain and lead to a counterion mediated attraction among the equally charged molecules. As found by our calculations, the Debye-Hückel potential describes the effective potential among the monomers excellently for appropriate parameters.

[1] S. Förster and M. Schmid, Adv. Polym. Sci. **120**, 51 (1995)
[2] J.-L. Barrat, J.-F. Joanny, Adv. Chem. Phys. **XCIV**, 1 (1996)
[3] K. S. Schweizer and J. G. Curro, J. Chem. Phys. **87**, 1842 (1987)
[4] T. Hofmann, R. G. Winkler, and P. Reineker, J. Chem. Phys. **114**, 10181 (2001)
[5] C. Y. Shew and A. Yethiraj, J. Chem. Phys. **110**, 11599 (1999)

Publications in refereed journals

Belitsky V.1; Krug J.2; Jordao Neves I.1; Schütz G.M.
1 Univ. Sao Paolo, Brazil
2 Univ. Essen, Germany
A Cellular Automaton for Two-Lane Traffic
J. Stat. Phys. 103, 945-971 (2001)
23.15.0

Endo H.; Mihailescu M.; Monkenbusch M.; Allgaier J.; Gompper G.; Richter D.; Jakobs B.1; Sottmann T.1; Strey R.1; Grillo I.1
1 Univ. Köln, Germany
Effect of amphiphilic block copolymers on the structure and phase behavior of oil-water-surfactant mixtures
J. Chem. Phys. 115, 580-600 (2001)
23.30.0

Gallos L.K.1; Argyrakis P.1; Kehr K.W.
1 Univ. Thessaloniki
Trapping and survival probability in two dimensions
Phys. Rev. E63, 021104 (2001)
23.15.0

Gompper G.; Endo H.; Mihailescu M.; Allgaier J.; Monkenbusch M.; Richter D.; Jakobs B.1; Sottmann T.1; Strey R.1
1 Univ. Köln, Germany
Measuring Bending Rigidity and Spatial Renormalization in Bicontinuous Microemulsions
Europhys. Lett. 56, 683-689 (2001)
23.30.0

Gompper G.; Richter D.; Strey R.1
1 Univ. Köln, Germany
Amphiphilic block copolymers in oil-water-surfactant mixtures: efficiency boosting, structure, phase behaviour and mechanism
J. Phys.: Condens. Matter 13, 9055-9074 (2001)
23.30.0

Gozdz W.1,3; Gompper G.
1 Academy of Sciences, Warsaw, Poland
3 MPI Golm
Shape Transformations of Two-Component Membranes under Weak Tension
Europhys. Lett. 55, 587-593 (2001)
23.30.0

Hofmann T.1; Winkler R.G.; Reineker P.1
1 Univ. Ulm, Germany
Integral equation theory approach to rodlike polyelectrolytes: Counterion condensation
J. Chem. Phys., 114, 10181 (2001)
23.30.0

Lamura A.; Burkhardt T.W.1; Gompper G.
1 Univ. Philadelphia, USA
Semi-Flexible Polymer in a Uniform Force Field in Two Dimensions
Phys. Rev. E 64, 061801 [1-8] (2001)
23.30.0

Lamura A.; Gompper G.; Ihle T.1; Kroll D.M.1
1 Univ. Minnesota, USA
Multi-particle-collision dynamics: Flow around a circular and a square cylinder
Europhys. Lett. 56, 319-325 (2001)
23.30.0

Lamura A.; Gonnella G.1
1 Univ. Bari, Italy
Lattice Boltzmann simulations of segregating binary fluid mixtures in shear flow
Physica A, 294, 295 (2001)
23.30.0

Maassen R.; Eisenriegler E.; Bringer A.
Density depletion profile and solvation free energy of a colloidal particle in a polymer solution
Journal of Chem. Phys. 115, 5292-5309 (2001)
23.30.0

Mihailescu M.; Monkenbusch M.; Endo H.; Allgaier J.; Gompper G.; Stellbrink J.; Richter D.; Jakobs B.1; Sottmann T.1; Farago B.1
1 Univ. Köln, Germany
Dynamics of bicontinuous microemulsion phases with and without amphiphilic block-copolymers
J. Chem. Phys. 115, 9563-9577 (2001)
23.30.0

Popkov V.; Hager J.1; Krug J.2; Schütz G.M.
1 RWTH Aachen, Germany
2 Univ. Essen, Germany
Minimal current phase and boundary layers in driven diffusive systems
Phys. Rev. E 63 (2001), 056110
23.15.0

Popkov V.; Peschel I.1
1 FU Berlin, Germany
Symmetry breaking and phase coexistence in a driven diffusive two-channel system
Phys. Rev. E, 64 (2001)026126
23.15.0

Popkov V.; Santen L.1; Schadschneider A.2; Schütz G.M.
1 Univ. Nancy, France
2 Univ. Köln, Germany
Boundary-induced phase transition in traffic flow
J. Phys. A 34,L1 - L8 (2001)
23.15.0

Sambeth R.; Baumgaertner A.
Autocatalytic Polymerization Generates Persistent Random Walk of Crawling Cells
Phys. Rev. Lett. 86,(2001)
23.30.0

Sambeth R.; Baumgaertner A.
Locomotion of a two dimensional keratocyte model
J. Biol. Systems 9, 201-219 (2001)
23.30.0

Santos J.E.1; Schütz G.M.
1 TU München, Germany
Exact time-dependent correlation functions for the symmetric exclusion process with open boundary
Phys. Rev. E. 64, 036107 (2001)
23.15.0

Schilling T.; Theissen O.; Gompper G.
Dynamics of the swollen lamellar phase
Eur. Phys. J E4, 103-114 (2001)
23.30.0

Schwarz U.S.1; Gompper G.
1 Weizmann Inst.,Rehovot, Israel
Bending Frustration of Lipid-Water Mesophases Based on Cubic Minimal Surfaces
Langmuir 17, 2084-2096 (2001)
23.30.0

Schütz G.M.; Ispolatov I.1; Barkema G.2; Widom B.1
1 Cornell Univ. USA
2 Univ. Utrecht, Netherlands
Symmetries and Equivalences in a lattice model for hydrophobic
interaction.
Physica A 291, 24 - 38 (2001)
23.30.0

Schütz G.M.; Santos J.1

1 TU München, Germany
Nonequilibrium tube-length fluctuations of entangled polymers
J. Chem. Phys. (Comm.) 114, 8733- 8736 (2001)
23.30.0

Sunil Kumar P.B.1; Gompper G.; Lipowsky R.2
1 IIT, Chennai, India
2 MPI Potsdam, Germany
Budding dynamics of multicomponent membranes
Phys. Rev. Lett. 86, 3911 (2001)
23.30.0

Invited talks

Baumgaertner A.
Advancements in Molecular Dynamics Simulations
Meeting of EC network "Protein-Lipid Interactions"
Bruessel, Belgien
1.6.2001
23.30.0

Baumgaertner A.
Molecular dynamics simulations of membrane proteins
Biophysics School on Lipid-Protein Interactions and the Organization of Membranes.
Szeged, Ungarn
29.6.2001
23.30.0

Baumgaertner A.
Molekulardynamik eines Ionenkanals
Universitaet Duisburg
22.5.2001
23.30.0

Baumgaertner A.
Simulations of gating properties of the KcsA ion channel
University of Ljubljana, Slowenien
2.11.2001
23.30.0

Baumgaertner A.
The protein-lipid interface
Conference on "Protein-Lipid Interaction".
Zagreb, Croatia
31.8.2001
23.30.0

Baumgaertner A.
Why cells are persistent
Int.Center of Theoret.Phys., Trieste
20.9.2001
23.30.0

Eisenriegler E.
Polymer depletion potentials: Center of mass distribution of a polymer
Chain near a repulsive wall
Jülich Soft Matter Days, Roiduc, Kerkrade, Niederlande
14. 11. 2001
23.30.0

Gompper G.; Theissen O.
Lattice-Boltzmann Study of Spontaneous Emulsification
Dynamic Days 2001, Dresden
05.-08. Juni 2001
23.30.0

Gompper G.
Dynamics of the Swollen Lamellar Phase in Ternary Amphiphilic
Systems
4th International Discussion Meeting on Relaxation in Complex Systems, Kreta, Greece
17.-23. Juni 2001
23.30.0

Gompper G.
Effect of amphiphilic block copolymers on membrane elasticity and
phase behavior
Adriatico Research Conference on "Interaction and Assembly of Biomolecules", International Center for Theoretical Physics, Trieste
27.-31. August 2001
23.30.0

Gompper G.
Lebendige Membranen
Antrittsvorlesung, Mathematisch-Naturwissenschaftliche Fakultät,
Universität zu Köln
29.05.2001
23.30.0

Gompper G.
Struktur und Phasenverhalten von Mikroemulsionen und Schwammphasen
Seminarvortrag, Physikalische Chemie, Universität zu Köln
20.04.2001
23.30.0

Popkov V.
A sufficient criterion of integrability for nonequilibrium statistical models
International Conference "Theory of Functions and Mathematical Physics", Kharkov, Ukraine
10.-17. August, 2001
23.15.0

Schütz G.
Aging in quantum spin chains
Universität Nancy
25.5.2001
23.15.0

Schütz G.
Boundary-induced phase transitions in driven diffusive systems
Max-Planck-Institut für Kolloid- und Grenzflächenforschung, Golm
19.2.2001
23.15.0

Schütz G.
Diffusion and interaction of shocks in exactly solvable many-body systems
Summer School on Fundamental Problems in Statistical Mechanics, Altenberg
30.8.2001
23.15.0

Schütz G.
Diffusion und Wechselwirkung von Schocks in exakt lösbaren Vielteilchensystemen
Hauptvortrag der DPG-Tagung, Bonn
26.3.2001
23.15.0

Schütz G.
From Many Interacting Particles to Collective Few-Body Modes: Motion of Shocks in Driven Diffusive Systems
Universität Utrecht
28.3.2001
23.15.0

Schütz G.
From many individual particles to single collective modes: Diffusion and
interaction of shocks in nonequilibrium systems
German-American Frontiers of Science Symposium, Bad Homburg
9.6.2001

23.15.0

Schütz G.
Getriebene diffusive Systeme fern vom Gleichgewicht
Physikalisches Kolloquium, Universität Leipzig
15.5.2001
23.15.0

Schütz G.
Getriebene diffusive Systeme fern vom Gleichgewicht,
Physikalisches Kolloquium, Universitaet Ulm
22.1.2001
23.15.0

Schütz G.
Nonequilibrium relaxation law for entangled polymers
Dynamics Days, Dresden
5.6.2001
23.30.0

Schütz G.
Nonequilibrium relaxation law for entangled polymers
University of Leeds
5.10.2001
23.30.0

Schütz G.
Von diffundierenden Teilchen zu nichtlinearen Wellen:
Phasendiagramm von
Vielteilchensystemen fern vom Gleichgewicht
Universität GH Wuppertal
29.5.2001
23.15.0

Schütz G.
q-deformed symmetries and multiple shocks in the asymmetric
simple
exclusion process
Nankai Symposium, Tianjin
9.10.2001
23.15.0

Winkler R.G.; Hofmann T.1; Reineker P.1
1 Univ. Ulm, Germany
Influence of Counterions and Salt on the Structure of
Polyelectrolyte Solutions
Schwerpunkt "Polyelektrolyte", Berlin
13.09.01 -- 14.09.01
23.30.0

Winkler R.G.
Structure of Polyelectrolyte Solutions
Fachbereich Physik
Bergische Universität Wuppertal
10.12.01
23.30.0

Other talks

Gompper G.
Structure and Phase Behavior of Membrane Ensembles
Vortrag auf der "2nd Conference on Spatial Statistics and
Statistical Physics", Wuppertal
05.-09. März 2001
23.30.0

Posters

Döbereiner H.G.1, Haluska C.K.1, Godzd W.2 and Gompper
G.
1 MPI Golm
2 Academy of Sciences, Warsaw, Poland
Micro-structured Diblock-Copolymer Membranes
Poster auf der Konferenz über "Assembly and Self-Assembly
at the
Interface of Biology, Chemistry and Physics", Gioccoi, Italien
20.-25. August 2001
23.30.0

Hofmann T.1; Winkler R. G.; Reineker P.1
1 Univ. Ulm, Germany
Structure of Polyelectrolyte Solutions: An Integral Equation
Theory
Approach
DPG Frühjahrstagung, Berlin
2.4. - 4.4.2001
23.30.0

Schilling T., Gompper G.
Twist Grain Boundaries in Lamellar Phases of Ternary
Amphiphilic Systems,
Kurzvortrag und Poster beim 249. WE-Heraeus-Seminar
"Wetting of Structured Materials", Bad Honnef
12.-14. Februar 2001
23.30.0

Winkler R.G.; Hofmann T.1 ; Reineker P.1
1 Univ. Ulm, Germany
Structure of Rodlike Polyelectrolytes in Solution
Jülich Soft Matter Days 2001, Kerkrade
13.11. - 16.11.2001
23.30.0

Winkler R.G.; Hofmann T.1; Reineker P.1
1 Univ. Ulm, Germany
Integral Equation Theory Approach to Polyelectrolyte
Solutions
Bridging the Time-Scale Gap, Konstanz
13.11. - 16.11.2001
23.30.0

Lecture courses

Baumgaertner A.
Einführung in die Bioinformatik
Universität Duisburg, V2
WS 2001/2002
23.30.0

Baumgaertner A.
Einführung in die theoretische Biophysik II
Universität Duisburg, V2
WS 2000/2001
23.30.0

Baumgaertner A.
Einführung in die theoretische Biophysik
Universität Duisburg, V2
SS 2001
23.30.0

Gompper G.
Statistische Mechanik von Grenzflächen und Membranen
Universität Köln
SS 2001
23.30.0

Schütz G.
Physik der Finanzmärkte
Universität Bonn
SS 2001
23.15.0

Winkler R.G.
Einführung in die Theorie der Soft-Matter Systeme
Universität Ulm
SS 2001
23.30.0

Internal reports

Paessens M.
Reptationsdynamik von kurzen verschlauften Polymeren
DMRG Studien für Rubinstein-Duke-Modelle
Diplomarbeit, RWTH Aachen
23.30.0

Willmann R.
Lattice gas model for reptation with Disorder
Diplomarbeit, Universität Bonn
23.30.0

Internal seminars

Allakhiarov E.
Multicollisional mesoscopic solvent model and its application to
solvent flow over spherical obstacle
Klausurtagung Theorie der Weichen Materie, Monschau
30.9.-2.10.2001
23.30.0

Auth T.
Effect of anchored polymers on the elasticity of membranes
Klausurtagung Theorie der Weichen Materie, Monschau
30.9.-2.10.2001
23.30.0

Baumgaertner A.
Motility of Cells
Klausurtagung Theorie der Weichen Materie, Monschau
30.9.-2.10.2001
23.30.0

Eisenriegler E.
Colloids in polymer solutions: the depletion interaction
Joint Soft Matter Seminar, IFF, FZJ
3. 5. 2001
23.30.0

Eisenriegler E.
Polymer depletion interaction for anisotropic particles
Klausurtagung Theorie der Weichen Materie, Monschau
30.9.-2.10.2001
23.30.0

Gompper G.
Forschungsarbeiten auf dem Gebiet der Weichen Materie
Vortrag auf der Informationstagung aus Anlaß der 16. Sitzung des Wissenschaftlichen Beirats des IFF, Forschungszentrum Jülich
26.4.2001
23.30.0

Gompper G.
Structure and Phase Behavior of Microemulsions
Klausurtagung Theorie der Weichen Materie, Monschau
30.9.-2.10.2001
23.30.0

Paessens M.
Reptation dynamics of short entangled polymers
Klausurtagung Theorie der Weichen Materie, Monschau
30.9.-2.10.2001
23.30.0

Popkov V.
Spontaneous symmetry breaking in 2-component diffusive systems
Klausurtagung Theorie der Weichen Materie, Monschau
30.9.-2.10.2001
23.30.0

Schütz G.
Nonequilibrium relaxation law for entangled polymers,
Klausurtagung Theorie der Weichen Materie, Monschau
30.9.-2.10.2001
23.30.0

Schütz G.
Vom Mikrokosmos zum Makrokosmos - Strukturbildung und Phasenuebergaenge
in Zufallsprozessen fern vom Gleichgewicht
FZJ-Kolloquium
9.3.2001
23.15.0

Willmann R.
Diffusion coefficient of polymers with kinematic disorder
Klausurtagung Theorie der Weichen Materie, Monschau
30.9.-2.10.2001
23.30.0

Winkler R.G.
Integral Equation Theory Applied to Polyelectrolyte Systems
Klausurtagung Theorie der Weichen Materie, Monschau
30.9.-2.10.2001
23.30.0

Institute Theory III

General Overview

The institute Theory III investigates the mechanisms of the formation of structures and their consequences in condensed matter. The research starts from electronic properties which define the shortest length and time scales, but it also encompasses the macroscopic consequences. The analytical and numerical investigations are in many ways closely connected with experimental studies performed in other groups of the IFF, but also with activities in other institutes of the Research Center Juelich.

Central points of interest for the research in Theory III are in the field of electronic structure of solids. Materials classes under consideration are metals and semiconductors, specifically with respect to their importance for information technology. A second mainstream is formed by cooperative phenomena in condensed matter. Questions here aim at the dynamics of structure and pattern formation and the statistical mechanics of order and disorder processes. Specific activities in the field of complex fluids are concerned with structure and dynamics of soft matter.

The research of Theory III employs all analytical and numerical techniques applicable to many-body problems in condensed matter. In addition the development of new methodological concepts and numerical procedures is part of our research interest. The development of parallel program codes adapted to massively parallel computers has received special attention in recent years.

The explanation of the microstructure and dynamics of real solids requires the understanding of the electronic properties. One of the most important methods for the calculation of the electronic structure of real solids is the density functional theory in connection with appropriate numerical procedures. While in recent years bulk properties of metals and semiconductors have been at the center of our research a main concern now is directed towards the understanding of surface and interface properties, with particular emphasis on magnetism.

Many properties of metals in practical use depend on the structure and properties of their surfaces. From first-principles calculations it was found that the rearrangement of the electronic charge for noble metals and FCC-transition-metals does not lead to a significant change of the remaining bonds, when a bond is broken. This novel finding can lead to the development of simple models to describe the energetics of a surface like step and kink formation, crystal growth, alloy formation, equilibrium shape of mesoscopic crystallites and surface facetting.

The simulation of scanning-tunneling-microscope(STM)-images by density-functional methods with pseudo-potentials help to clarify the detailed structure of inhomogeneities on Si(111)-surfaces covered by As, which are relevant for epitaxial growth. Steps on Si(111):As always have the height of a double layer. For both typical step orientations the exposed second layer Si-atoms at the step-edge are replaced by As-atoms, which means As-passivated steps. The structures are much more prominently exhibited for negative bias-voltage of the STM as compared to positive bias.

For the formation of epitaxial layers on crystalline substrates a model which is capable to incorporate elastic strain was formulated and studied by Monte Carlo Methods. The description based on rate-equations leads to scaling predictions for cluster-statistics and diffusion rates. A particular result is that elastic repulsion between the adsorbed particles shifts the formation of islands to higher values of the coverage.

The pressure-dependence of the chemical diffusion constant of a glass was calculated by molecular dynamics simulations of a binary Lennard-Jones model. Four temperature-regimes were observed. The apparent activation drops from high values in the hot liquid to a plateau-value. Near the critical temperature of the mode-coupling-theory it rises steeply, but in the glassy state values similar to the liquid state are observed.

A system of parallel cracks in a uniaxially strained solid allows for stress-relaxation under coarsening of the cracks. A conventional mean-field theory breaks down and several independent lengths have to be taken into account. Scaling laws for this coarsening behavior have been derived which differ markedly form the conventional coarsening theories.

The drag-coefficient for a polymer-chain in a flowing medium depends in a nonlinear way on the velocity of the flow, in contrast to the linear Stokes-law for simple bodies. This effect is due to both an intra-chain and an inter-chain interaction mediated by hydrodynamics. Computer-simulations supported by analytical calculations have given an explanation of this effect and of its dependence upon fluctuations.

A phase-field method for the treatment of hydrodynamic flow with free interfaces was developed and applied to the phase-transition between partial wetting and dewetting on a substrate. At low Reynolds numbers the calculation agrees with the creep-flow approximation, at higher Reynolds numbers hydrodynamic vorticity leads to significant deviations like surface ripples.

Finally we are pleased that Dr. Roland Rzehak received the Dr.-Eduard-Martin-award for his doctoral thesis at university Saarbrücken during this year.

H. Müller-Krumbhaar

Personnel 2000/2001 and areas of activity

Scientific Staff

Dr. E. Brener	Kinetics of phase transformations	23.15.0
Prof. P.H. Dederichs	Electronic structure and magnetism	23.20.0
Dr. K. Mika	Structure maps for binary systems	23.15.0
Prof. H. Müller-Krumbhaar - Institute Director -	Non-linear dynamics of dissipative systems	23.15.0
Dr. R. Rzehak	Polymer dynamics and hydrodynamic flow	23.15.0
Dr. H. Schober	Statics and dynamics of glasses, defects and phonons	23.30.0
Prof. K. Schroeder	Electronic and atomic structure of defects in semiconductors	23.42.0
Dr. R. Zeller	Electronic structure and magnetic properties of metals	23.20.0
L. Snyders	Secretary	

Visitors

Dr. V. Caciuc (RO)	Atomic force microscopy	23.20.0
Dr. J. Dobnikar (SLO)	Poisson-Boltzmann molecular dynamics	23.15.0
Dr. M. Freyss (F)	Spin-dependent transport	23.20.0
Dr. I. Galanakis (GR)	Half-metallic ferromagnets	23.20.0
Prof. V. Gurevich (GUS)	Low energy modes in glasses	23.30.0
Dr. Ph. Mavropoulos (GR)	Complex bandstructure and transport	23.20.0
Dr. D.A. Parshin (GUS)	Low energy modes in glasses	23.30.0
Dr. Z. Szotek (GB)	Correlated oxyde-systems	23.20.0
Dr. D. Temkin (GUS)	Pattern formation at interfaces	23.15.0
Dr. W. Temmerman (GB)	SIC-calculations	23.20.0

PhD and Diploma Students (University = RWTH Aachen)

MSc. N. Atodiresei	Dispersion of localized electronic states of semiconductor surfaces	23.42.0
Dipl.-Phys. A. Antons	Ab-initio calculations on surface reconstruction	23.42.0
Dipl.-Phys. Y. Cao	Structural stability of surfactant-covered semiconductor surfaces	23.42.0
Dipl.-Phys. F. Gutheim	Cluster growth on surfaces	23.15.0
Dipl.-Phys. M. Hartmann	Collective effects of cracks and dislocations	23.15.0
Dipl.-Phys. H. Höhler	Defects in semiconductors	23.42.0
Dipl.-Phys. D. Kienle	Transport coefficients in polymer solutions	23.15.0
Dipl.-Phys. M. Kluge	Binary metallic glasses	23.30.0
Dipl.-Phys. Wi. Kromen	Point defects and interfaces in Nitride-semiconductors	23.42.0
Dipl.-Phys. R. Spatschek	Collective effects of cracks in solids	23.15.0
Dipl.-Phys. O. Wunnicke	Tunneling Magneto Resistance (TMR)	23.20.0

Broken-Bond Rule for the Surface Energies of FCC Metals

I. Galanakis, G. Bihlmayer, N. Papanikolaou, R. Zeller, S. Blügel, and P. H. Dederichs
Institute IFF-Theory III

Using two different full-potential *ab initio* techniques we introduce a very simple rule based on the number of broken first-neighbor bonds to determine the surface energies of the noble metals and fcc transition metals . When a bond is broken, the rearrangement of the electronic charge for these metals does not lead to a significant change of the remaining bonds. Thus the energy needed to break a bond is independent of the surface orientation. This novel finding can lead to the development of simple models to describe the energetics of a surface like step and kink formation, crystal growth, alloy formation, equilibrium shape of mesoscopic crystallites and surface faceting.

The surface energy represents a fundamental material property. It is given by half the energy needed to cut a given crystal into two half crystals. As such the surface energy naturally depends on the strength of the bonding and on the orientation of the surface plane. A variety of experimental techniques have been developed to measure the surface energy [1], but all measurements are performed at high temperatures where surfaces are badly defined. The most comprehensive data stem from surface tension measurements in the liquid phase and by extrapolating the resulting orientation-averaged surface free energies to zero temperature [2]. The knowledge of the orientation-dependence of the surface energies is necessary to predict the equilibrium shape of a mesoscopic crystal and to study a series of important phenomena in materials science like crystal growth, creation of steps and kinks on surfaces, growth, stability and alloy formation of thin films or surface-melting faceting.

The lack of experimental data can be replaced by *ab initio* calculations. Due to the development of the density functional theory during the last two decades, *ab initio* methods are able to calculate many physical properties with unprecedented accuracy. In two recent publications [3] we have shown that irrespective of the orientation the surface energies of the noble metals Cu, Ag, and Au and the fcc transition metals Rh, Ir, Pd and Pt are simply proportional to the number of broken bonds between a surface atom and its nearest neighbors (for all surface orientations, except the (111) and (100), one has to take into account also the nearest-neighbor bonds lost by the subsurface atoms). We demonstrate this in calculations for the low-index surfaces (111), (100), and (110) as well as for three vicinal surfaces (311), (331) and (210). The resulting anisotropy ratios, *i.e.* the ratio of the surface energy for a given surface orientation with respect to the (111) surface energy, practically always agree with the "ideal" broken bond ratios, *i.e.* the number of broken bonds between nearest neighbors for this surface with respect to the (111) surface. Therefore, the energy needed to break a bond does not depend on the orientation, so that for each metal the surface energy for only one orientation is needed. To perform the calculations, we have used both the full-potential screened Korringa-Kohn-Rostoker (FKKR) method [4], and the full-potential linearized augmented plane wave (FLAPW) method [5] as implemented in the FLEUR code.

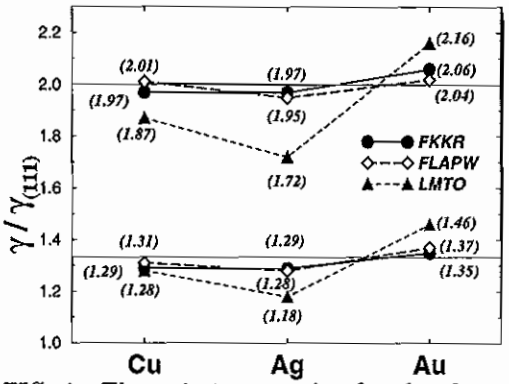

FIG. 1. The anisotropy ratios for the three noble metals, $\gamma_{(100)}/\gamma_{(111)}$ and $\gamma_{(110)}/\gamma_{(111)}$, using both FKKR and FLAPW. The LMTO results are from Ref. [6]. Surface energies are calculated in eV/(surface atom). The two straight solid lines represent the ideal first neighbor broken-bond ratios; 4/3 for (100) and 6/3=2 for (110).

In Fig. 1 we present the anisotropy ratios for the low-index surfaces of noble metals. We remark that both FKKR and FLAPW calculations produce practically the same anisotropy ratios for all the noble metals, while previous calculations employing the linear muffin-tin orbitals (LMTO) method [6] gave anisotropy ratios that deviate considerably from the present results, especially for Ag. Notably, both FKKR and FLAPW give results that are very close to 4/3 for the $\gamma_{(100)}/\gamma_{(111)}$ ratio and close to 6/3 for the $\gamma_{(110)}/\gamma_{(111)}$ ratio. These are exactly the ratios between the number of first-neighbor broken bonds for these surfaces. This finding can lead to two independent conclusions. Firstly, the broken bonds between a surface or a subsurface atom and its second and further neighbors have a negligible contribution to the surface energy. Secondly, the energy needed to break a bond is the same for any surface orientation. This is surprising, since one expects that breaking a bond in a surface leads to a rearrangement of the electronic charge resulting in a strengthening of the remaining bonds, so that one needs more energy to break them. But it seems that this bond strengthening, due to the reduction of

the number of nearest neighbors, is negligible for the noble metals. During our tests we also identified the most probable reason for the failure of the previous LMTO calculations. The (111) surface energy of noble metals is very sensitive to the number of $k_{||}$-points due to a surface state centered at the $\bar{\Gamma}$ point, which all three noble metals possess and which requires a very dense $k_{||}$-grid to account for it, which has not been used in the LMTO calculations.

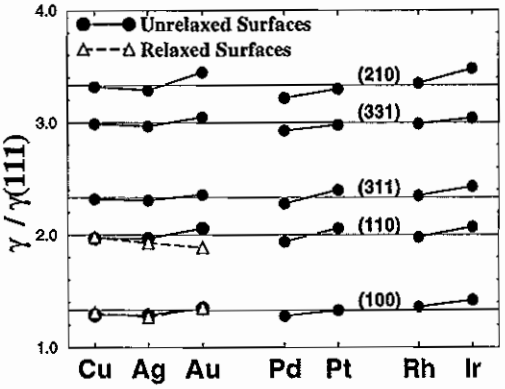

FIG. 2. Anisotropy ratios with respect to the (111) surface energy calculated using the FKKR for the low-index and vicinal surfaces of the noble and transition metals. The open triangles denote the anisotropy ratios as calculated by the FLAPW method by including relaxations of the first three layers.

To examine whether this finding also holds for the vicinal surfaces we used the FKKR method and calculated the surface energies and the anisotropy ratios for the next three more close-packed surfaces. In Fig. 2 we have plotted the anisotropy ratios with respect to the (111) surface for the noble and transition metals for both the low-index surfaces and the three most close-packed vicinal surfaces together with the ideal broken bonds ratios. The ideal broken bond ratios with respect to the (111) surface, for which we break 3 nearest-neighbors bonds, are 4/3, 2, 7/3, 3 and 10/3, for the (100), (110), (311), (331) and (210) surface orientations, respectively. The calculated surface energy anisotropy ratios deviate only slightly from these ideal numbers. Au shows slightly larger deviations from these ideal ratios compared to the two other noble metals, Ag and Cu. For Pd the calculated ratios are smaller than the ideal ones by ~3-4% for all the surface orientations, while the Ir ratios are larger from the ideals ones by ~4-7% for all the surface orientations except the (331) where the calculated Ir ratio is by 1.3% larger than the ideal ratio. Pt and Rh show a mixed behavior but in general the ratios differ less than 3% from the ideal nearest-neighbors broken bonds ratios for any surface. So the free energy $\gamma_{(hkl)}$ in eV/(surface atom) needed to create any surface with a Miller index (hkl) reduces just to the product of $\gamma_{(111)}$ and the ratio of the first-neighbor broken bonds, $N_{(hkl)}$, and $N_{(111)} = 3$:

$$\gamma_{(hkl)} = \frac{N_{(hkl)}}{3}\gamma_{(111)}. \qquad (1)$$

$N_{(hkl)}$ can be easily obtained for any fcc surface [7]:

$$N_{(hkl)} = \begin{cases} 2h+k & h,k,l \text{ odd} \\ 4h+2k & \text{otherwise} \end{cases} \qquad h \geq k \geq l. \qquad (2)$$

All previous results have been obtained by neglecting the lattice relaxations of the atoms at the surface. We have calculated the relaxation effect on the anisotropy ratios for the low-index surfaces of the noble metals and the resulting anisotropy ratios are also presented in Fig. 2 by the triangles. We allowed the first three surface layers to relax. Although the calculated surface energies change, the effect on the anisotropy ratios is much smaller. For Cu and Ag, relaxations leave the anisotropy ratios practically unchanged. The Au(110) surface shows a large relaxation; the distance between the first and the second layer (Δd_{12}) is reduced by 13.8%, the Δd_{23} is expanded by 6.9% and finally the Δd_{34} is also reduced by 3.2%. The surface energy is reduced by 6.5% and the anisotropy ratio is now 1.89 compared to the 2.04 for the unrelaxed structure, but remains close to the broken-bond rule value of 2. So even large relaxations have a rather small impact on the calculated anisotropy ratios which are reasonably described by the broken-bond rule.

In short we have found a very simple rule for the surface energies of the noble and fcc transition metals which has been overlooked up to now: for each of these metals the surface energies scale for different surface orientations accurately with the number of broken nearest-neighbor bonds, so that the calculated anisotropy ratios of the surface energies for different orientations always agree well with the ideal broken-bond ratios. We have demonstrated this in FKKR and FLAPW calculations for six low-index and vicinal surfaces. The surprising simplicity of these results is of great interest for a variety of problems in materials science like step, kink, and alloy formation, crystal growth, surface-melting faceting or the shape of small crystallites on a catalyst.

[1] V. K. Kumikov and Kh. B. Khokonov, J. Appl. Phys. **54**, 1346 (1983).
[2] W. R. Tyson and W. A. Miller, Surf. Sci. **62**, 267 (1977).
[3] I. Galanakis *et al.*, arXiv:cond-mat/0105207; I. Galanakis, N. Papanikolaou and P. H. Dederichs, arXiv:cond-mat/0110236.
[4] R. Zeller *et al.*, Phys. Rev. B **52**, 8807 (1995).
[5] M. Weinert *et al.*, Phys. Rev. B **26**, 4571 (1982).
[6] L. Vitos *et al.*, Surf. Sci. **411**, 186 (1998).
[7] J. Mackenzie *et al.*, J. Phys. Chem. Solids **23**, 185 (1962).

Simulation of STM images of steps on As-covered Si(111) using *ab initio* calculations

A. Antons, R. Berger, S. Blügel[1] and K. Schroeder
Institute Theory III

We have simulated STM images for the most stable structures of $(11\bar{2})$ and $(\bar{1}\bar{1}2)$ oriented steps on As terminated Si(111) using the Tersoff-Hamann-aproximation. The structures are determined using first-principles molecular statics calculations based on total energy and force minimization. All calculations are carried out with our EStCoMPP-code within the density functional formalism in the local-density approximation, using norm-conserving separable pseudopotentials and a plane-wave basis-set. On Si(111):As the steps always have the height of a double layer. For both step orientations the exposed second layer Si-atoms at the step edge are replaced by As atoms (As passivated steps). At the $(\bar{1}\bar{1}2)$ step edge this leads to the formation of As dimers. The different structures show up prominently for negative bias voltage when the occupied states are imaged. For positive bias voltage, i. e. in the unoccupied states, differences are washed out to a large extent.

Reducing the size of electronic devices requires new materials combinations and improved perfection in crystal growth techniques. A technologically interesting example is the Si/Ge-system. One would like to grow flat-layer-heterostructures for use in lasers, light-emitting diodes or fast transistors. Other applications require the growth of ordered arrays of mono-sized islands of Si on Ge or vice versa. Unfortunately, due to the lattice mismatch of 4% Ge naturally grows on clean Si in large 3-dimensional islands. However, if the Si-surface is covered with a "surfactant"-layer, i.e. a mono-atomic layer of group-V atoms (As, Sb, Bi), flat-layer growth can be achieved for Ge. Due to the extra electron the group-V layer passivates the (111) surface. It modifies the surface reconstruction, has a lower surface free energy, and floats on top of the growing crystal.

In previous investigations on the kinetics of single group-IV adatoms (Si, Ge) on the unreconstructed (1×1) As terminated Si(111) surface we found that the competition between diffusion on top of the As layer and incorporation into the layer by exchange with an As atom is decisive for the growth mode. Si and Ge adatoms behave differently: Si has about the same activation energy for exchange as for diffusion ($E_{EX} \approx 0.27$ eV) and is readily incorporated to a substitutional site in the As layer. It gains an energy of $E_B \approx 0.8$ eV upon exchange [2]. Thus, Si adatoms make only very few diffusion jumps before they are incorporated substitutionally. This results in a large nucleation rate for Si islands on terraces as is observed experimentally for homoepitaxy on Si(111):As [3]. On the other hand, Ge has to overcome a much larger exchange barrier ($E_{EX} \approx 0.7$ eV) and gains only $E_B \approx 0.2$ eV [4]. Ge atoms thus perform many diffusion jumps on Si(111):As before they are incorporated (at T = 580 K the average number of jumps is $\approx 10^4$). Thus, most Ge atoms can reach the pre-existing terrace steps. If they are readily incorporated there, growth would proceed by step flow which is not observed experimentally. Thus, an idea put forward by Kaxiras *et al.* [5] has to be checked, that the step edges are very effectively passivated by surfactant atoms and the Ge atoms are repelled from the steps. Then, in spite of the large diffusion length, one would expect Ge island nucleation on the terraces, as is observed. In addition, if islands grow large their edges resemble the structure of terrace steps. The structure of steps on As-covered Si(111) determines the reaction path and activation energy for incorporation of adatoms.

STM images always show double-layer steps and irregularly shaped islands for Si homoepitaxy on As passivated Si(111) with mainly two kinds of steps: $(11\bar{2})$ and $(\bar{1}\bar{1}2)$ orientation [3]. Detailed atomic resolution STM-imaging of the steps is underway [6]. In the Tersoff-Hamann-approximation [7] STM images can be understood as a mapping of the local electronic density of states (LDOS) of the surface at the site of the STM-tip. To enable the interpretation of the experimental images, especially the extraction of the atomic structure, theoretical simulations of STM-images have to be made which relate the LDOS to the underlying atomic structure.

Using our parallelized *ab initio* EStCoMPP-code [8] we have investigated a number of possible step structures for both step orientations. The EStCoMPP-code employs the density functional formalism in the local-density approximation and norm-conserving separable pseudo-potentials with a plane wave basis set. For the STM-simulations we used an inversion-symmetric supercell laterally extending over 2×4 unit cells and vertically containing a slab of 22 Si(111)-layers and a vacuum equivalent to 10 layers. For the structure optimization a slab of 10 layers was used. The lateral translation vectors of the supercell are chosen to connect an atom on the upper terrace to an equivalent atom a double layer below. In this way one can generate a supercell which contains only one type of step. The large vertical extension is necessary in the STM-simulation in order to separate the electronic structure at the opposing surfaces both across the vacuum and across the Si bulk. The calculations were performed with six k-points in the irreducible wedge of the Brillouin zone. A plane-wave basis set with an energy cutoff of 13.7 Ry was used. The structure optimization was done by minimizing the total energy of the system and the forces on the atom. The relaxations were terminated when the forces on all ions

were smaller than 0.1 mRy/au.

The lowest energy structures for both step orientations are the **As passivated steps** as shown in Fig.1. The exposed second layer Si atoms at the step edges are replaced by As atoms. At the $(11\bar{2})$ step this leads to a stable configuration since the As atoms are in a naturally threefold coordinated position, i.e. the As atoms at the step edge are in equivalent positions as on the (111) oriented terraces. At the $(\bar{1}\bar{1}2)$ step the As atoms are only twofold coordinated in the unrelaxed positions. They form dimers to saturate their bonds. The energy difference between these step edges is only ≈ 0.1 eV per unit length. At both step edges the replacement of Si with As atoms requires an additional As atom per unit step length compared to the monolayer coverage.

We have calculated [9] the constant-LDOS STM-images for bias voltages varying between -2 V and +2 V. These calculated images closely relate to the measured constant-current STM-images. Results are shown if Fig. 1. – For **negative bias voltage**, when the occupied states of the surface contribute to the tunneling current, the lone-pair occupied states of the exposed As atoms make a major contribution. At the $(11\bar{2})$ step the second layer As atom gives a current maximum exactly in the middle between two As atoms terminating the upper terrace. At the $(\bar{1}\bar{1}2)$ step the As-dimers lead to a distinctly different image, exhibiting the superstructure along the direction of the step. The side views clearly show that the surface projected positions of the atoms are not identical with the maxima of the tunneling current at the step edges. – For **positive bias voltage**, when the unoccupied states contribute, the differences are nearly completely washed out. At both step directions there seems to be an upward relaxation of the upper terrace As edge atom. Our calculations show that there is no real change of position, but that the increase of the tunnel current can be understood from the increased density of states found in the lower part of the conduction band at this As edge atom compared to As atoms on the terrace.

[1] present address: Fachbereich Physik, Universität Osnabrück

[2] K. Schroeder *et al.*, Phys. Rev. Lett. **80**, 2873 (1998)

[3] B. Voigtländer *et al.*, Phys. Rev. **B 51**, 7583 (1995)

[4] K. Schroeder, A. Antons, R. Berger, S. Blügel, Phys. Rev. Lett. accepted

[5] D. Kandel and E. Kaxiras, Phys. Rev. Lett. **75**, 175 (1996)

[6] B. Voigtländer *et al.*, to be published

[7] T.Tersoff and D.R.Hamann, Phys. Rev. **B31**, 805 (1985)

[8] **EStCoMPP**, Electronic Structure Code for Materials Properties and Processes, Forschungszentrum Jülich, 1999. R. Berger *et al.*, Proceedings of the NIC-Workshop "Molecular Dynamics on parallel Computers", held at Jülich, 08.-10. Februar 1999 (World Scientific 2000), p.185

[9] A. Antons, Ph.D.-Thesis, RWTH Aachen, July 2001

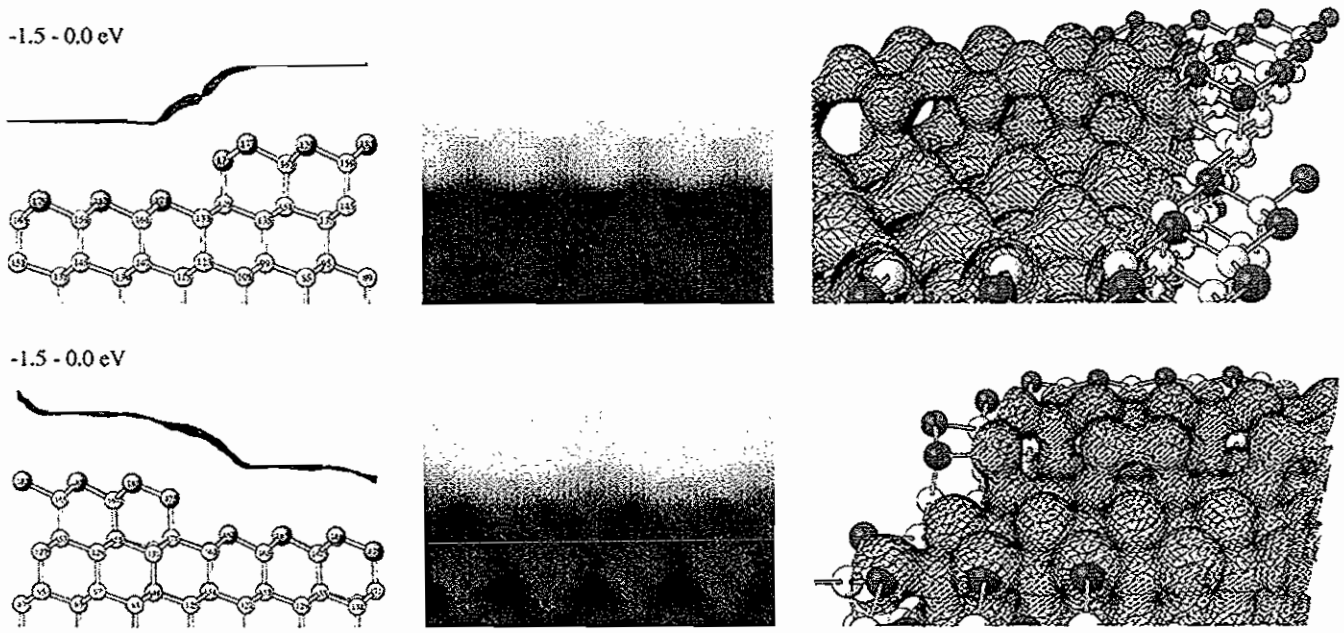

FIG. 1. Structure of the As-passivated $(11\bar{2})$ step (upper panels) and $(\bar{1}\bar{1}2)$ step (lower panels) on Si(111):As. For both orientations (a) the side view with a contour of the LDOS, (b) the simulated STM-image for a bias voltage of -1.5 V (occupied states image), and (c) the electron density contour which characterizes the bonding character at each atom, are shown. Si atoms are gray, As atoms red (dark) circles. On the terraces the As atoms replace the Si atoms of the upper half of a double layer. At the terrace edge the exposed second layer Si atoms are replaced by As. In the STM-image the As atoms are represented by the vacuum coil of the lone-pair electron wavefunctions. Notice, that the maxima in the tunneling current do not coincide with the surface projected positions of the As atoms at the step edges. At the $(11\bar{2})$ step the exposed 2nd layer As atom are clearly placed symmetrically in the middle between the As atoms in the upper layer. At the $(\bar{1}\bar{1}2)$ step the As dimers show up as broad maxima resembling the superstructure along the step edge.

Epitaxial Growth with Elastic Interaction: Submonolayer Island Formation

F. Gutheim, H. Müller-Krumbhaar, and E. Brener
Institute IFF-Theory III

A model for island formation in the submonolayer epitaxy has been studied in presence of elastic strain by means of Monte Carlo simulation. The description based on rate equations leads to scaling predictions for cluster-statistics and diffusion rates. We generalize these predictions to include the effects of the repulsive $1/r^3$ elastic interaction, which is caused by the deformation of the underlying substrate. One particular result is, that elastic repulsion between the adsorbed particles hampers the formation of islands and island nucleation is deferred to higher coverage values.

Heteroepitaxial growth is a process of great interest in crystal-growth and for the manufacturing of semiconductor-devices. One has to assume that in the majority of cases elastic strain influences the properties of growth and gives rise to a variety of growth morphologies. The lattice mismatch between the adsorbed layers and a substrate of different material leads to deformation of both adsorbate and substrate. Up to some critical size, the adsorbate will adopt the lattice structure of the substrate, apart from a local change in the lattice parameter. This "coherent" lattice deformation typically leads to a repulsive long-range interaction potential between any two adsorbed atoms, which depends on their distance r like $1/r^3$ [1] at long distances and is mediated by the substrate. Here we will be concerned with the early stage of island nucleation in a system with fixed deposition flux.

The system is realized on a two dimensional $L \times L$ sized simple square lattice with lattice parameter Δx. As we mean to model molecular beam epitaxy, we assume the deposition process to be ballistic in the sense that deposition onto the surface is not biased by the local chemical potential. The rate of deposition F (measured in number of particles per cm^2 and second) is equal for all lattice sites. Single adatoms, here referred to as monomers, diffuse on the surface, interacting by a repulsive potential U_0/r^3. We assume that the temperature T is low enough to neglect desorption and to satisfy a critical island size of 2, i. e. once two monomers have met, they form a stable dimer which grows by incorporation of further monomers.

In order to efficiently evaluate the energy difference ΔU needed for our Monte Carlo implementation of monomer diffusion, we employ a multigrid scheme based on [2], which avoids introducing a potential cutoff by treating the interaction with distant adsorbate atoms on a coarse grained level in the manner of a multipole expansion. Starting with zero coverage, the number of monomers increases almost linear with the flux until it reaches its maximum. Afterwards the number of monomers decreases, while the number of islands finally supersedes the number of monomers and increases until the coverage is almost one monolayer, where island coalescence leads to a rapid decrease of the number of islands. With increasing ratio D/F the maximum number of the monomers decreases and is shifted to lower coverages. This refers to the simulation both with and without interaction. If one compares the data for different interaction strength U_0/T, as plotted in Fig. 1 for identical D/F, one notices that interaction shifts the maximum of the monomer density towards higher coverage values because repulsion will drive monomers apart, hampering the formation of dimers.

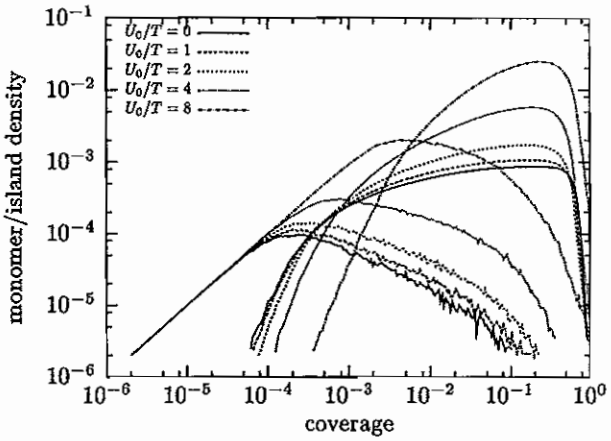

FIG. 1. Monomer ρ_1 and island densities ρ vs. coverage θ with $4D/F = 10^8$, U_0/T ranging from 0 to 8.

A newly deposited monomer will diffuse during a characteristic time τ_c until it reaches an island or another monomer. The capture time τ_c can be related to the flux F and the surface-density of monomers ρ_1 by $\rho_1 \sim F\tau_c$. If the length of a timestep Δt is given, the macroscopic diffusion constant D is $D \sim \Delta x^2/(4\Delta t)$. For the description of a random walker it is more convenient to use the number of steps n rather than time t. The mean number of distinct sites $S(n)$ visited by a random walker on a simple two-dimensional square lattice after n steps will be an important quantity because it can be related to the probability for a diffusing monomer to meet another adatom. We see that for small $n \sim$ 10–1000 the number of sites visited behaves like $S(n) \sim \pi n/\ln 8n$. An even better approximation is available by using the expansion derived by F. S. Henyey and V. Seshadri [3]. For the sake of simplicity we will write $S(n)$ as $S(n) \sim nf_c(n)$, where f_c includes all deviations from linear behavior.

Knowing the number of distinct lattice sites visited, we can interpret $\Delta x^2 S(\tau_c/\Delta t)$ as the effective area covered by a monomer. The probability for a diffusing monomer of lifetime τ_c to collide with an island or another monomer is thus proportional to $\Delta x^2 S(\tau_c/\Delta t)/\tau_c$ and the corresponding densities.

At this point we introduce a set of rate equations connecting the density of diffusing monomers ρ_1 to the density of islands ρ. Defining the characteristic length scale

$$l_c(\rho_1) = \left(\alpha f_c\left(\alpha \frac{\rho_1}{\Delta x^2}\right)\right)^{1/4}, \qquad \alpha = \frac{4D}{F} \tag{1}$$

the rate equations can be represented in the form

$$\frac{d\rho}{d\theta} = l_c^4(\rho_1)\rho_1^2, \tag{2}$$

$$\frac{d\rho_1}{d\theta} = 1 - 2l_c^4(\rho_1)\rho_1^2 - l_c^4(\rho_1)\rho\rho_1. \tag{3}$$

The number of monomers ρ_1 (2) gains by deposition and loses by dimer formation as well as by the growth of existing islands, whereas the number of islands ρ (3) increases by dimer formation only, because the growth of islands does not change their number.

Because the characteristic length scale l_c shows a rather weak dependence on the coverage θ, this dependence on θ can be ignored on the left hand side of (2) and (3). Scaled variables are now introduced as $\tilde{\theta} = \theta l_c^2(\rho_1)$, $\tilde{\rho} = \rho l_c^2(\rho_1)$ and $\tilde{\rho}_1 = \rho_1 l_c^2(\rho_1)$.

By this approximate scaling procedure the equations become dimensionless, and we obtain

$$\frac{d\tilde{\rho}}{d\tilde{\theta}} = \tilde{\rho}_1^2, \qquad \frac{d\tilde{\rho}_1}{d\tilde{\theta}} = 1 - 2\tilde{\rho}_1^2 - \tilde{\rho}\tilde{\rho}_1, \tag{4}$$

which allows for leading correction terms due to f_c by the definition of the tilded variables.

But how can we incorporate the effects of elastic repulsion into the scheme of rate equations? We first note that the ratio D/F is entirely the ratio of two time-scales $D/F \sim \tau_F/\tau_D$. τ_F is the time it takes to deposit one monolayer, and τ_D is determined by the diffusion barrier E_D. The case of elastic repulsion gives rise to another time-scale τ_e, which is governed by the height of the elastic interaction potential U_0/r^3. Thus we have $\tau_D \sim \exp(E_D/T)$ and $\tau_e \sim \exp(U_0/T)$ governing the motion of the monomers. It is quite obvious that if $U_0 \ll E_D$, $\tau_D \gg \tau_e$ or $U_0 \gg E_D$, $\tau_D \ll \tau_e$ the aggregation is triggered by the slower of the two processes. We argue that in order to account for elastic repulsion τ_D has to be replaced by $\tau_D + \tau_e$, which is equivalent to the replacement

$$\alpha = \frac{4D}{F}\left(1 + \exp\left(\frac{U_0 - E_D}{T}\right)\right)^{-1}. \tag{5}$$

As long as the interaction strength is lower than the diffusion barrier, elastic repulsion will only have small effect in the nucleation regime, whereas with strong interaction the correction term to D/F on the right hand side of (5) is of the order of $\exp(-U_0/T)$.

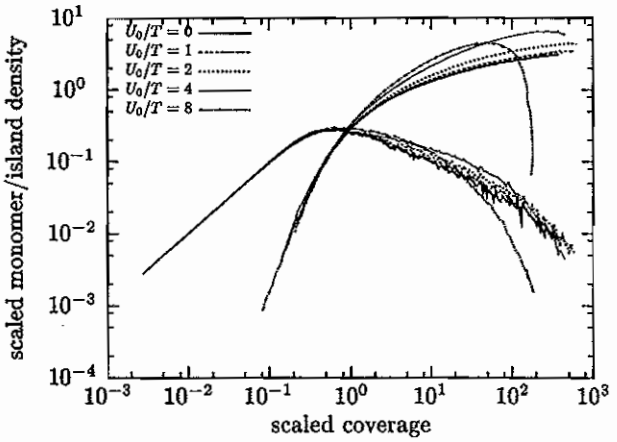

FIG. 2. Scaled monomer $\tilde{\rho}_1$ and island densities $\tilde{\rho}$ vs. scaled coverage $\tilde{\theta}$ with $4D/F = 10^8$ fixed, $U_0/T = 0$, 1, 2, 4 and 8.

The plot in Fig. 2 shows data from Fig. 1 scaled by the l_c according to (5). The plotted data scales as predicted.

As the scaling transformation only depends on α, it has the form

$$\tilde{\rho}_1 = \rho_1 g_\alpha(\rho_1), \quad \tilde{\rho} = \rho g_\alpha(\rho_1), \quad \tilde{\theta} = \theta g_\alpha(\rho_1) \tag{6}$$

with g_α depending on α. Because the data collapses under the same mapping, the unscaled data has to be identical. All systems obeying the relation (5) for fixed α, show identical low temperature, low coverage nucleation properties. An example for the interpretation of this data is, that the estimation of the diffusion constant D from the usual scaling arguments (1) might fail in presence of elastic effects, the estimate will turn out too small.

In summary, we have shown the effect of elastic interaction on low temperature submonolayer island formation in the low coverage regime by Monte Carlo simulation, and analyzed the results with scaling arguments. A particular result is, that with increasing elastic interaction strength U_0/T, the formation of islands is hampered and island nucleation is deferred to higher values of coverage. A new scaling relation (1) together with (5) was found [4], connecting the strength of elastic interaction U_0, diffusion constant D and the flux F. This scaling regime holds as long as the average size of the clusters is much smaller than the distance between them.

[1] V.I. Marchenko and A.Y. Parshin, Sov. Phys. JETP **52**, 129 (1980)

[2] J. Steinbrecher, H. Müller-Krumbhaar, E. Brener, C. Misbah and P. Peyla, Phys. Rev. E **59**, 5600 (1999)

[3] F. S. Henyey and V. Seshadri, J. Chem. Phys. **76**, 5530-5534 (1982)

[4] F. Gutheim, H. Müller-Krumbhaar, and E. Brener, Phys. Rev. E **63**, 041603 (2001)

Pressure dependence of diffusion in simple glasses and supercooled liquids

H. R. Schober
Institute IFF-Theory III

Using molecular dynamics simulation, we have calculated the pressure dependence of the diffusion constant in a binary Lennard-Jones Glass. We observe four temperature regimes. The apparent activation volume drops from high values in the hot liquid to a plateau value. Near the critical temperature of the mode coupling theory it rises steeply, but in the glassy state we find again small values, similar to the ones in the liquid. The peak of the activation volume at the critical temperature is in agreement with the prediction of mode coupling theory.

Diffusion in glasses and their melts has been studied intensively for many years. Despite this effort there is still no agreement on the nature of diffusion on an atomic level or on its change at temperatures near the glass transition. This even holds for simple densely packed glasses, such as binary metallic ones [1].

In a hot liquid, diffusion is by flow, whereas, in the glass well below the transition temperature, it will be mediated by hopping processes. One key question is the transition between the two regimes. For fragile glasses, such as most polymers and amorphous metallic glasses, mode coupling theory (MCT) predicts an arrest of the homogeneous viscous flow in the undercooled melt at a temperature T_c, well above the glass transition temperature T_g. [2] Hopping processes will suppress the predicted singularities and will become the dominant diffusion process near T_c. The nature of the hopping process is another issue of controversy. Is it by a vacancy mechanism, similar to diffusion in the crystalline state, or is it via a collective process inherent to the disordered structure ?

In crystalline materials the pressure dependence of the diffusion constant can often be used to identify the diffusion mechanism. For thermally activated diffusion the diffusion constant can be described by an Arrhenius law

$$D(T) = D_0 \exp\left(-H/kT\right) \tag{1}$$

where D_0 is a pre-exponential factor and H is the activation enthalpy.

Using $V = \partial G/\partial p$ with $G = H - TS$ one obtains the activation volume for a diffusion by a single jump process

$$V_{\rm act} = -kT\left[\frac{\partial \ln D}{\partial p}\right]_T + kT\left[\frac{\partial \ln D_0}{\partial p}\right]_T . \tag{2}$$

In crystals one finds that the second term is only a minor correction which can be neglected. For diffusion via thermal vacancies the formation volume dominates and $V_{\rm act}$ varies between 0.6Ω and 1Ω, where Ω is the average atomic volume. For the migration part one estimates $V^m \sim 0.1\Omega$. Concomitantly in crystals high values of $V_{\rm act}$ are taken as a signature of a thermally activated diffusion mechanism.

Assuming that also in the glass the first term in Eq. 2 dominates, one usually describes, also in amorphous materials, the pressure dependence of diffusion by an apparent activation volume given by the first term in Eq. 1. Experiments on a number of metallic glasses give a large spread of values in the range of 0.05 to 1 Ω. [1] Low values were, e. g., observed in $Co_{81}Zr_{19}$ [3] where no significant isotope effect is observed [4]. This result can be interpreted in terms of a collective diffusion mechanism inherent to the glassy structure. The situation is not so clear for the case of large activation volumes $V_{\rm act}$. Values of around 0.5Ω have been observed in several materials. Such values are also found in materials where the vanishing isotope points to diffusion by collective jumps. [5] Whether collectivity can induce migrational activation volumes of the order 0.5 to 1 Ω is still open.

From MCT one derives for the diffusion in the liquid state

$$D^{\rm MCT}(T) = D_0^{\rm MCT}\left(T - T_c^{\rm MCT}\right)^{\gamma} \tag{3}$$

$$V_{\rm act}^{\rm MCT} = -kT\left[\frac{\partial \ln D_0^{\rm MCT}}{\partial p} - \gamma\frac{1}{(T - T_c^{\rm MCT})}\frac{\partial T_c^{\rm MCT}}{\partial p} + \ln\left(T - T_c^{\rm MCT}\right)\frac{\partial \gamma}{\partial p}\right]_T . \tag{4}$$

The diffusion constant extrapolates to zero at $T_c^{\rm MCT}$, well above T_g, and the pressure dependence shows a singularity.

The aim of the present work is to present a systematic study of the pressure dependence of diffusion as function of temperature. In order to relate closely to other work the simulations were done for the well studied binary Lennard-Jones system (LJ) of Kob and Anderson [6]. In the following, we will give all results in the reduced units of energy, ϵ_{AA}, length, σ_{AA}, and atomic mass m_A.

The calculations were done at each temperature with constant volume, corresponding to zero pressure, and periodic boundary conditions. At each temperature we had 8 independent samples, each of 5488 atoms in a ratio 4 : 1 of A- and B-atoms. The diffusion constants were calculated from the asymptotic slope of the atomic mean square displacements.

Fig. 1 shows the densities and diffusion constants for the zero pressure configurations. From the change in slope of the volume expansion we estimate the glass transition temperature as $T_g \approx 0.35\epsilon/k$. The diffusion constant can be fitted very well by the MCT expression with

$T_c = 0.36\epsilon/k$ for both species and $\gamma = 1.87$ and $\gamma = 2.02$ for A and B, respectively.

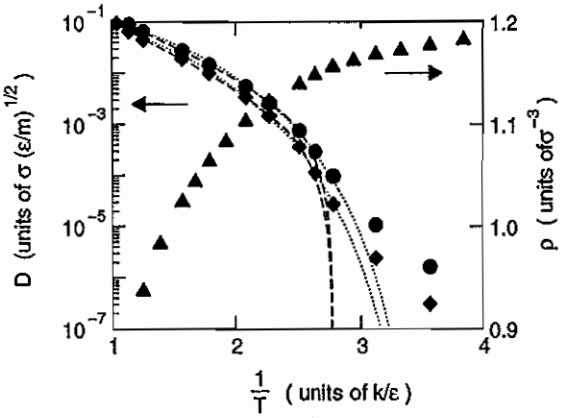

FIG. 1. Diffusion constants (majority A-atoms, diamonds, and minority B-atoms, circles) and density (triangles) at zero pressure against inverse temperature (all in reduced units). The dashed and dotted lines show the fits with the MCT and Vogel-Fulcher expressions, respectively

To calculate the pressure dependence we did additional runs with higher and lower densities, respectively. At each temperature the zero pressure samples were taken as starting configurations which were then compressed (expanded) and subsequently aged. The change of density was 2% at the highest and 0.5% at the lowest temperature. Fig. 2 shows the resulting values together with the fit with the MCT-expression. One can clearly distinguish four temperature regions. At the highest temperature $V_{\rm act} \approx 0.6\ \Omega$, nearly identical for both components. Upon cooling the activation volume drops to a plateau value $V_{\rm act} \approx 0.3\ \Omega$. The larger component has, as one would expect, a slightly higher activation volume. Below $T = 0.5$ the activation volume rises sharply for both components and reaches a maximum of order Ω around $T = 0.4$, near T_g and $T_c^{\rm MCT}$. In the glassy state it drops again to a value below 0.3Ω.

The drop of the activation volume in the liquid correlates nicely with the drop of the isotope effect parameter reported for the same system. [7]

The onset of the increase to the maximum near T_g coincides with the onset of a pronounced curvature in the Arrhenius plot of $D(T)$, Fig. 1. At this temperature and below the isotope effect parameter indicates collective motion. [7] From previous work we expect a predominance of chain motion with increasing chain length upon cooling.

Our values for the activation energy in the glass are of similar magnitude as the estimate of Teichler [8] for the NiZr system. We find higher activation volumes for less well aged samples. In previous simulations of metallic glasses collective jumps of chains of atoms have been observed, an indication of an inherent collective diffusion mechanism.

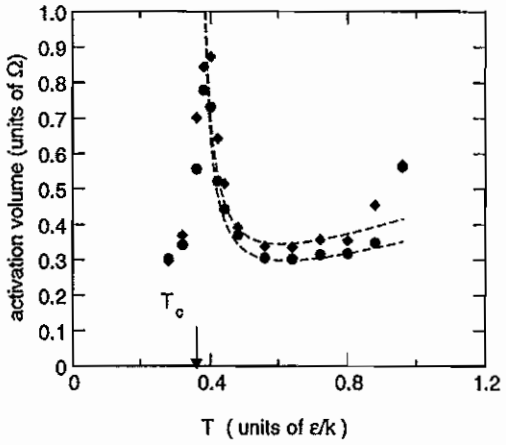

FIG. 2. Calculated activation volume (majority A-atoms, diamonds, and minority B-atoms, circles) versus temperature. The dashed line is a fit with the MCT expression using a common critical temperature for both components.

The fit with the MCT-expression, is shown by the dashed line in Fig. 2. We get an excellent fit with $\partial T_c^{\rm MCT}/\partial p = 0.028$ for both components and $\partial \ln D_0^{\rm MCT}/\partial p = -0.338$ and -0.278 for A and B atoms, respectively. We take this as an indication that the divergence of the activation volume would in deed be at $T_c^{\rm MCT}$. Of course the glass transition intervenes before the divergence is reached.

In conclusion, we find, both in the liquid and the glass, activation volumes of around 0.3 atomic volumes. This correlates with a high collectivity seen in the isotope effect. In the hot liquid, where diffusion is no longer by collective motion, the activation volume rises to about 0.6 atomic volumes. Cooling towards the critical temperature mode coupling theory predicts a $1/(T - T_c)$ singularity, cut off by the glass transition. This is clearly observed in the simulation.

[1] F. Faupel *et al.*, Rev. Mod. Phys. **74**, in press (2002).
[2] W. Götze and A. Sjölander, Rep. Prog. Phys **55**, 241 (1992).
[3] P. Klugkist *et al.*, Phys. Rev. Lett. **80**, 3288 (1998).
[4] A. Heesemann *et al.*, Europhys. Lett. **29**, 221 (1995).
[5] A. Heesemann, K. R. V. Zöllmer, and F. Faupel, Z. Metallkd. **91**, 909 (2000).
[6] W. Kob and H. Andersen, Phys. Rev. E **51**, 4626 (1995).
[7] H. R. Schober, Solid State Commun. **119**, 73 (2001).
[8] H. Teichler, J. Non-Cryst. Solids in press (2001).

Coarsening of cracks in a uniaxially strained solid

Efim A. Brener, H. Müller-Krumbhaar, and R. Spatschek
Institute IFF-Theory III

We discuss the stress relaxation in a uniaxially strained solid due to the coarsening of a system of parallel cracks. We emphasize similarities and differences of this process in comparison to Ostwald ripening in a first order phase transition. A conventional mean-field approximation breaks down and several independent length scales have to be taken into account. Strong elastic interactions between the cracks determine the growth behavior. We derive scaling laws for the coarsening of the different length scales involved and the time evolution of stress relaxation which finally leads to the equilibrium state of a fractured body.

In the early theory of fracture, Griffith [1] developed a criterion which predicts the irreversible growth of a crack, provided a critical length is exceeded. The critical length depends on the external tension P in the sense that a higher tension leads to a lower critical length for the instability to occur. The origin of this instability is based on a competition between a release of elastic energy, caused by the opening of the crack, and an increase of surface energy. The critical Griffith crack is analogous to the critical nucleus in a first order phase transition. In a sense, a solid under stretching is similar to a supercooled gas: the point of zero external stress plays the role of the liquid-gas condensation point [2].

The late stage of phase separation is characterized by Ostwald ripening when a new phase coarsens in order to lower the interfacial free energy. Larger droplets are energetically more favorable because of their smaller interface curvature. Thus they grow at the expense of smaller inclusions which dissolve again and finally disappear. This collective behavior leads to a growth of the average droplet size and simultaneously to a decrease of their number. Finally the system reaches the full thermodynamic equilibrium. The same coarsening process should take place in a system of cracks according to the analogy mentioned above.

The coarsening of a new phase is generally well understood for vanishingly small initial supersaturations (characterized by a dimensionless parameter $\Delta_0 \ll 1$ defining the deviation from equilibrium) as long as only one length scale, the size of the particles R, is relevant in the system. In this case the distance between the different precipitates is large and a mean field theory in the sense of Lifshitz, Slyozov and Wagner is applicable.

The aim of this Letter [3] is to analyze the coarsening of cracks in uniaxially strained solids. Since the length of the cracks is growing with time, they come close to each other during the coarsening process and therefore a mean-field description breaks down. This limit has so far been practically inaccessible to analytic and numerical calculations.

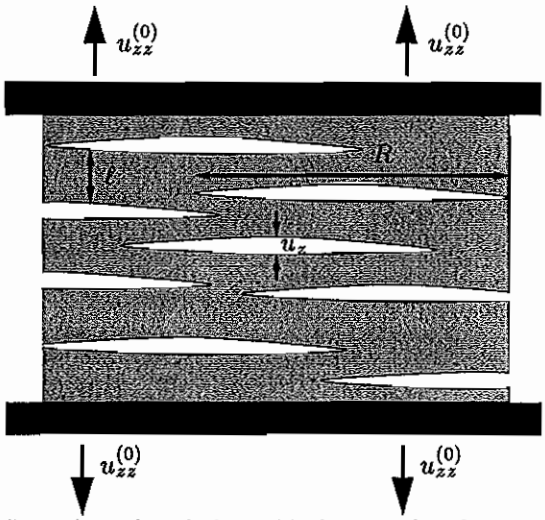

FIG. 1. An infinitely large block of solid is fixed between two pistons (black). Initially no cracks exist in the system and a homogeneous strain $u_{zz}^{(0)}$ is present everywhere.

We stretch a block of a perfect solid in only one direction (z-direction, to be explicit) and then fix it in this position such that a uniform strain $u_{zz}^{(0)}$ is maintained in the solid (see fig. 1). Obviously the initial uncracked configuration is far from equilibrium: a high elastic energy density $w_{el}^{(0)} \sim E{u_{zz}^{(0)}}^2$ could be dramatically reduced through the appearance of cracks in the system (E is the Young modulus). Finally, if only one long crack traverses the whole block, the system is completely unstretched and only a small amount of surface energy remains due to the two new crack surfaces. We assume now that a statistical ensemble of cracks appears in the solid with a growing mean size similar to the coarsening during a phase transition. These cracks are mainly aligned perpendicular to the z axis because this maximizes the release of elastic energy. Apart from the average size of the nuclei R we introduce another lengthscale ℓ, which is the characteristic distance in z-direction between cracks. One can easily understand that a single (macroscopic) lengthscale L is not sufficient, because the average stress would remain almost constant $P \sim Eu_{zz}^{(0)}$. Under these circumstances the system can never reach its equilibrium configuration with $P = 0$ and therefore the assumption

of only one relevant lengthscale cannot be correct. In the following we will restrict our calculations to some simple order-of-magnitude estimates, assuming that the lengthscales of the system obey the self-consistent order relation $R \gg \ell \gg u_z$.

In the late stage of the coarsening process the main displacement comes from opening of the cracks and not from stretching. Thus $u_{zz}^{(0)} \sim u_z/\ell$, where by u_z we denote the average opening of the cracks. This equation corresponds to the global conservation law of conventional Ostwald ripening when almost all excess heat of the initially overheated system is converted to latent heat in order to perform the phase transition.

The solid between two neighboring cracks in vertical direction can be understood as a thin circular disk of lateral extent R and height ℓ. Its top and bottom are free surfaces with boundary conditions $\sigma_{zz} = \sigma_{rz} = 0$. At the tips of the cracks three (or more) of those plates come together and exert forces and torques on each other. These forces produce an average stress $P \sim \sigma_{zz}$ in the plates, which causes a bending of them. Bending of thin plates subject to a stress P is described by

$$u_z \sim P \frac{1-\nu^2}{E\ell^3} R^4, \tag{1}$$

where ν and E are the Poisson and Young coefficients respectively. The related release of the elastic energy per plate is

$$W_{el} \sim -P^2 \frac{1-\nu^2}{E\ell^3} R^6. \tag{2}$$

On the other hand the growth of the cracks is accompanied by an increase of surface energy $W_s \sim \alpha R^2$ with the surface tension α.

Near the crack tips the theory of thin plates breaks down and stresses exhibit the typical $\sigma \sim r^{-1/2}$-behavior at a distance $r \ll \ell$ from the tip. Local equilibrium requires an additional variation of the total energy $W = W_s + W_{el}$ with respect to R. This results in a relation between the length scales and the stress in the system

$$R \sim \frac{E\alpha}{1-\nu^2} \frac{1}{P^2} \left(\frac{\ell}{R}\right)^3. \tag{3}$$

It is a generalization of the Griffith condition for a single crack which can be retained by setting $\ell \sim R$ on the right hand side. Eq. (3) gives the critical size: bigger cracks grow and smaller ones shrink.

The global conservation of the total displacement implies

$$P \sim u_{zz}^{(0)} \frac{E}{1-\nu^2} \frac{\ell^4}{R^4}. \tag{4}$$

One of the most important differences to usual Ostwald ripening is the lack of a conserved order parameter. In the case of crack propagation dissipation predominantly takes place in the close vicinity of the tips. Therefore kinetics of this mechanism is relatively fast and is commonly described by the phenomenological equation

$$R\dot{R} = -\kappa \frac{dW}{dR} \sim \kappa \left(P^2 \frac{1-\nu^2}{E\ell^3} R^5 - \alpha R \right). \tag{5}$$

κ is the kinetic coefficient that relates the energy release rate to the tip velocity. It contains information about small scale physics in the vicinity of the tip of the propagating crack.

In (5) both energy contributions are of the same order because of the Griffith condition and one immediately obtains

$$R \sim \alpha\kappa t \tag{6}$$

and also

$$\ell \sim \left(\frac{E}{1-\nu^2}\right)^{-1/5} \alpha\, u_{zz}^{(0)\,-2/5} (\kappa t)^{4/5}. \tag{7}$$

Thus the average stress indeed decreases to zero like

$$P \sim \left(\frac{E}{1-\nu^2}\right)^{1/5} u_{zz}^{(0)\,-3/5} (\kappa t)^{-4/5}. \tag{8}$$

The preceding three formulas are the main results [3]. They show the transition to equilibrium, i.e. the decrease of stress and the growth of length scales. The scaling $R \sim t$ is probably the fastest growth law which is possible in dissipative systems. We mention that the velocity v is completely determined by material parameters and does not contain the "supersaturation parameter" $u_{zz}^{(0)}$. If the material tends to be robust against fracture, characterized by a small κ, this velocity can be smaller than the speed of sound and below the branching threshold. In this case, it is conceivable that the process described here can be observerd in small-scale laboratory experiments, provided that a statistical ensemble of cracks is present. The system otherwise can break into pieces by the very fast growth of one single or only a very few cracks. With higher velocities it should even be possible to observe such a behavior in geological systems extending over kilometers.

[1] A. A. Griffith, Philos. Trans. R. Soc. London A **221**, 163 (1920).

[2] A. Buchel and J. P. Sethna, Phys. Rev. Lett. **77**, 1520 (1996); A. Buchel and J. P. Sethna, Phys. Rev. E **55**, 7669 (1997).

[3] E. A. Brener, H. Müller-Krumbhaar, and R. Spatschek, Phys. Rev. Lett. **86**, 1291 (2001).

Nonlinear Stokes law and strong fluctuations of polymers in flow

D. Kienle[1], R. Rzehak[1], and W. Zimmermann[2]
Institut für Festkörperforschung, Forschungszentrum Jülich, D-52425 Jülich[1]
Theoretische Physik, Universität des Saarlandes,D-66041 Saarbrücken[2]

The drag coefficient for polymers depends *nonlinearly* on the velocity as shown by numerical simulations of a single tethered polymer, of two tethered polymers, and of a polymer anchored at a large sphere, all exposed to a uniform flow. This nonlinear behavior may be considered as a generalization of the famous Stokes law, which is a *linear* relation $\mathbf{F} = \zeta \mathbf{u}$ between the velocity of the sphere and the drag force $\mathbf{F}$ acting on it, where the drag coefficient ζ is *independent* of the velocity . The intra–chain as well as the inter–chain hydrodynamic interaction lead to a nonlinear velocity dependence of the drag coefficient which is especially pronounced for a polymer anchored at a large sphere. Since drag forces deform polymers in streaming fluids, this nonlinear behavior causes interesting rheological effects in polymer solutions and therefore has to be considered in rheological modeling. In calculations of hydrodynamic interaction effects it is quite common to use a preaveraged mobility matrix, but as shown in this work preaveraging suppresses fluctuations of the flow–induced polymer deformation.

The rheological properties of diluted polymeric liquids are determined by the interplay of polymer deformation and the hydrodynamic backflow, where the so-called tubulent drag reduction might be the most spectacular effect based on this complex polymer-flow interaction [1].

Recent advances in single molecule microscopy, especially on DNA molecules, combined with micromanipulation by laser tweezers have made possible a direct measurement of the polymer deformation in simple flows [2]. Closely related to the deformation is the total drag force $\mathbf{F}$ experienced by polymers in a uniform flow field. For a rigid sphere this force has been known for 150 years and is condensed in the famous Stokes law $\mathbf{F} = \zeta \mathbf{u}$, where ζ is the constant friction coefficient.

Does this linear relation hold for a deformable object like polymers, too? For a free draining polymer in a uniform flow field, which is completely penetrated by the flow, a linear Stokes law is expected with a velocity independent drag coefficient, although the polymer deformation, of course, depends on the flow velocity. However, the flow field within real polymers is partially screened, because of the hydrodynamic interactions between different parts of the polymer [3], so that both the polymer deformation *and* the drag coefficient ζ depend on the flow velocity. Therefore, for the case of uniform flow the velocity dependence of ζ is a clear signature of the relevance of hydrodynamic effects in polymers as shown by recent computer simulations [3].

For polymers, attached on the surface of a large sphere as illustrated in Figure 1 (left), one cannot expect that a linear dependency between the drag and u_{ext} still holds even for the free-draining limit, because the flow around the sphere is from the first non-uniform and inhomogeneous. As can be seen in Fig. 1 (right) for the chain without HI (upper curve) the dragcoefficient shows an initial decrease within an intermediate velocity range of $0 < u_{ext} < 0.1$, and becomes constant for larger velocities.

The reason for this non-linear behavior is, that at rather low flow velocities the chain is deformed and stretched along the spherical surface, thus reducing the mean distance between the segments and the sphere.

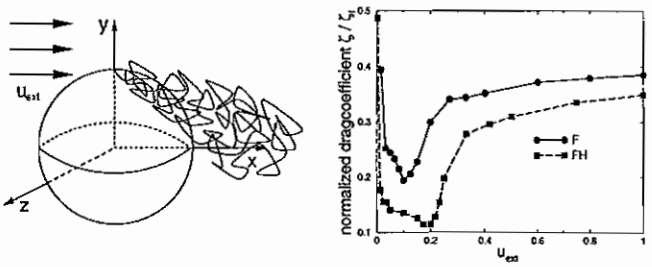

FIG. 1. Sketch of a polymer fixed at one end to a sphere (left) which is exposed to a Stokes flow with a flow velocity u_{ext} far from the sphere. The contribution of a polymer to drag coefficient ζ as function of u_{ext} for different models (more details are described in the text).

Due to the boundary condition that the flow must vanish on the surface of the sphere, the mean flow near the surface is rather low, so that the drag is reduced. For stronger flows $u_{ext} \geq 0.1$ the mean distance of the chain from the surface is gradually increased and parts of the chain are pulled into regions of larger flow. The dragcoefficient becomes constant, if the chain is nearly fully stretched at rather strong flow velocity. This dependency is not changed in principle, if hydrodynamic interaction is included (lower curve), i.e. the non-linear relation is only due to the non-uniformity of the flow field, which is controlled by the size of the sphere R_s. The effect of hydrodynamic screening is just to shift the onset of the initial decrease to larger u_{ext} and to broaden the dip range where the dragcoefficient is low. Note, that the curve for the FENE chain with HI (lower curve) has been rescaled, in order to emphasize the qualitative

agreement between the models with and without HI. The velocity u_{ext} has been reduced by a factor of 4 and the drag coefficient ζ has been enlarged by the same factor ($u_{ext} \to u_{ext}/4$, $\zeta \to 4\zeta$).

Besides the hydrodynamic interaction within one chain, the so-called inter-chain screening becomes important for many-chain systems, so that the effective drag on a single chain is additionally changed. Of course, the hydrodynamic interaction between the chains depends both on their mutual distance of the tether points and on their extension.

The hydrodynamic interaction between two tethered polymers as indicated by the sketch in Fig. 2 is twofold. First, the drag per chain increases continuously with larger flow u_{ext} due to the uncoiling of the polymer, so that the screening is reduced, cf. Fig. 2. However, this increase is always lower than for the single chain ($D_{sep} = \infty$: upper curve) because of the hydrodynamic interaction between the chains. The inter-chain screening is more pronounced for smaller distance D_{sep} of the tether points as shown by the inset of Fig. 2.

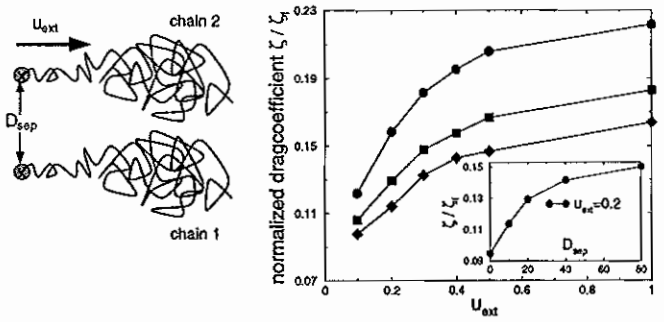

FIG. 2. Two polymers in uniform flow with their tethered ends at a distance D_{sep}. The contribution to the drag coefficient ζ per chain is calculated as function of the external flow and for $D_{sep} = 10.0$ (squares) and for $D_{sep} = 20.0$ (diamonds). The upper curve (circles) is the drag-coefficient for a single polymer (corresponding to $D_{sep} = \infty$). The inset shows ζ as function of D_{sep} and for $u_{ext} = 0.2$.

The polymer conformation does not only change in response to an external force or flow, but also due to thermal fluctuations, which are correlated by hydrodynamic interaction. A rather common approximation in calculations of hydrodynamic effects in polymer dynamics is to use a pre-averaged mobility matrix, which corresponds to a mean-field desription. How the neglect of fluctuations in the hydrodynamic interactions affects average values and fluctuations of the total drag force and the overall polymer deformation is not known. As long as stationary properties of polymers are of interest, the mean values of the chain tension or end-to-end vector are not changed remarkably within the errors. However, this is no longer the case for the corresponding standard deviations as measure of the fluctuations.

In Fig. 3 we compare the standard deviations of the x-component of the end-to-end vector with and without pre-averaged hydrodynamics (HI). The lower curve belongs to the free-draining case, where HI is omitted. As expected, the strenght of the fluctuations decrease as with larger flow the external forces dominate the thermal forces. Due to the averaging of the mobility matrix the fluctuations of the fluid are smoothed, so that the standard deviation $\sigma(R^x_{ee})$ is lowered, especially at intermediate flow velocities. In contrast, the fluctuations in the free-draining limit (lower curve) is reduced by nearly a factor of 2. Hence, the total fluctuations are amplified by HI according to the hydrodynamic fluctuations of the velocity field caused by the random moving polymer segments.

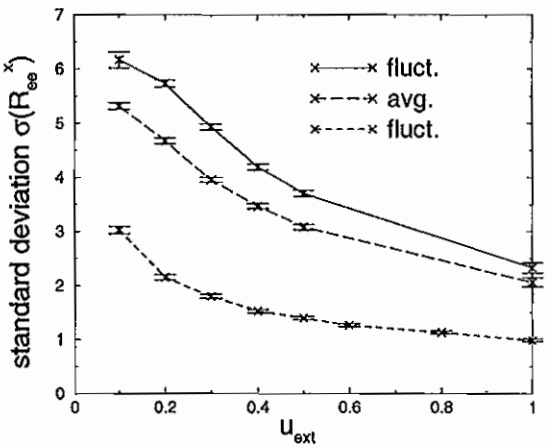

FIG. 3. Comparison of the standard-deviations of the x-component of the end-to-end vector for a FENE-chain with and without pre-averaged hydrodynamics, where the fluctuations for the free-draining limit (lower curve) is included as reference.

[1] A. Gyr and H.-W. Bewersdorff, "Drag Reduction of Turbulent Flows by Additives", *Kluwer*, London (1995)

[2] T. T. Perkins, D. E. Smith, R. Larson, and S. Chu, *Science*, **268**, 83 (1995)

[3] R. Rzehak, D. Kienle, T. Kawakatsu, and W. Zimmermann, Europhys. Lett. **46**, 821 (1999)

Dewetting Hydrodynamics in 1+1-Dimensions

H. Müller-Krumbhaar, E. Brener and M. Hartmann
Institut IFF-Theory III

A phase-field method for the treatment of hydrodynamic flow with free interfaces is presented and applied to the phase transition between partial wetting and dewetting on a substrate. We demonstrate that our model works well in the viscosity range of creeping flow and give first qualitative results for higher Reynolds numbers.

Wetting and dewetting of a substrate by a film of fluid is a particularly interesting process of pattern formation with obvious significance in many technical applications of surface coating. Various ingredients of equilibrium thermodynamics, diffusion and convection transport on different time scales together with nonlocal effects and external fields have to be considered simultaneously.

In the phenomenon of *partial wetting* [1–3] considered here a thin film of well-defined thickness is formed on the surface of a substrate, coexisting with a dry part of the substrate and a gas phase above the substrate. Under nonequilibrium "dewetting" conditions the front between the dry and the wet part of the surface moves towards the wet part inducing hydrodynamic flow inside the wet layer. The forces responsible for this film are in addition to the cohesive forces between water molecules Van-der-Waals forces and polar forces [2–4] from the substrate. Recently beautiful experiments have been performed by Lipson et al. [5], Herminghaus et al.[6], continuing and extending earlier work by Reiter [7] and Brochard-Wyart et al. [4].

Our numerical approach is based on a Phasefield-algorithm coupled to the incompressible Navier-Stokes equations. This approach allows to treat the moving interface directly even in the case where it has to be considered reactive. The phasefield enters the incompressible Navier-Stokes equations through the surface force

$$\vec{f}_{s0} = \gamma K \vec{n}\, \delta(\vec{x} - \vec{x}_s) = \gamma K \frac{1}{2} \nabla \phi, \qquad (1)$$

where K is the local curvature of the phasefield ϕ, γ the surface tension and the delta function taking into account the position of the interface. The Navier-Stokes equation couples back into the equation of motion for the phase field via an advection equation:

$$\frac{\partial \phi}{\partial t} = -\vec{u} \cdot \nabla \phi + F\{\phi\}, \qquad (2)$$

with the nonlinear phasefield operator

$$F\{\phi\} = \frac{1}{\tau}\{\xi^2 \vec{n} \cdot \nabla(\vec{n} \cdot \nabla \phi) + V_0 (\phi - \phi^3)\} \qquad (3)$$

according to previous experience [8, 9]. To include the external Van-der-Waals and polarizing forces which cause the phenomenon of partial wetting we add an additional surface force

$$\vec{f}_{s1} = \delta(\vec{x} - \vec{x}_s)\, \vec{n} \cdot (\vec{n} \cdot \nabla \Psi(z)), \qquad (4)$$

resulting from a double minimum potential $\Psi(z)$ and acting on the interface [9]. Therefore the total force on the interface coupling into the Navier-Stokes equation is :

$$\vec{f}_s = \vec{f}_{s0} + \vec{f}_{s1}. \qquad (5)$$

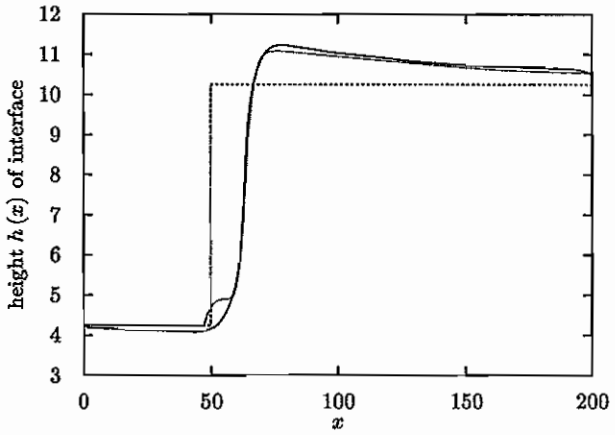

FIG. 1: Dewetting process in 1+1 dimensions (full line) and diffusion-model eq. (6) (dotted line) at time t=1000. The agreement is quite satisfactory, since there were no adjustable parameters. Effective Reynolds-numbers are of order 0.05.

Naturally, a first application of the resulting algorithm was to simulate the limit of creeping flow of a 1+1 dimensional system, corresponding to low Reynolds-numbers or a high viscosity. In this limit the hydrodynamic flow equation for dewetting degenerates to a diffusion equation of Cahn-Hilliard type [10] with an effective diffusion constant inversely proportional to the viscosity:

$$\frac{\partial u}{\partial t} = D_{eff} \Delta u - \lambda_{eff} u. \qquad (6)$$

D_{eff} and λ_{eff} are derived from a linearisation of the hydrodynamic equations [11].

In Fig.1 we compare our simulation results with the diffusional Cahn-Hilliard model for a dewetting scenario. The x coordinate represents the direction parallel to the surface of the substrate, which is located at $z = 0$. The

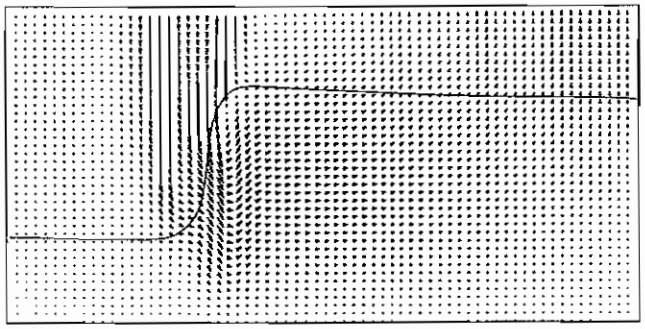

FIG. 2: Velocity-field for flow corresponding to Fig.1 (arbitrary units).

z coordinate of the interface represents the normal direction away from the substrate into the gas-phase and therefore the local height of the liquid film. The original front between the dry and the wet part of the substrate was given as a step function (dashed line). During the dewetting process the front moves towards the wet part (Fig.2), forming a distinct bump on the wet side right of the moving front. In the full three dimensional scenario this redistribution ultimately leads to the patterns observed in the dewetting experiments.

Our interest is now to understand what happens, if the conditions for replacing the Navier-Stokes-equations by an effective diffusion equation are no more valid.

For higher Reynolds-numbers significant changes due to increasing vorticity in the inertial range of wavelengths should be expected. Fig.3 shows the same scenario as Fig.1 for a somewhat smaller viscosity. Deviating from the diffusional behavior in the high viscosity

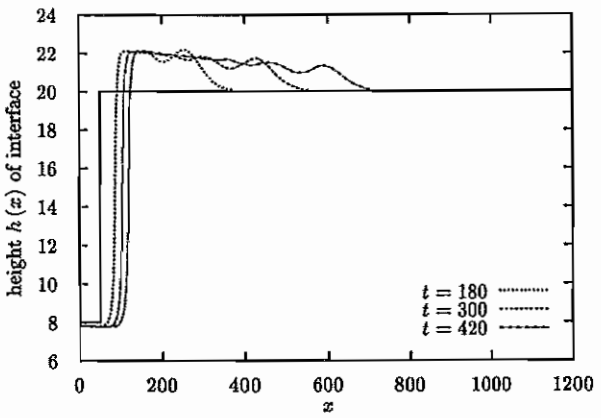

FIG. 3: Dewetting process for a somewhat smaller viscosity $\nu = 0.5$ at times t = 180,300,420 respectively. Note the increase in length scale of the x direction. Effective Reynolds-numbers are of order 3.

limit, the interface "overshoots" towards the equilibrium height and gives rise to spatial oscillations at least as a transient phenomenon. Nevertheless the average shape of the slope is still determined by the limited amount of fluid which is transported to the right due to viscous friction.

In summary we have constructed a model together with a numerical scheme which allows us to examine the structure formation at interfaces (possibly reactive) when diffusion as well as convection acting on different time scales and further external fields are involved, as in the case of thin film growth. The model shows reasonable quantitative agreement with an effective diffusion-model (Cahn-Hilliard-type) in the range of Reynolds-numbers below the order of unity.

For higher Reynolds-numbers corresponding to smaller viscosities the appearance of characteristic surface oscillations modifies the shape of the interface and creates a pronounced deviation from the viscous-creeping limit. These oscillations are to be expected in the fully three-dimensional case and could change the pattern-formation process significantly.

We are currently working on further calculations in the higher Reynolds-numbers regime. Additionally the model was extended to the fully three-dimensional situation confirming the Mullins-Sekerka instability of the dewetting front, including capillar damping in the stable regime.

[1] K.Binder, *Thin Films and Phase Transitions on Surfaces*, ed. M.Michailov and I.Gutzow, (1994)

[2] G. Forgacs, R. Lipowsky, T.M. Nieuwenhuizen, *Phase Transitions and Critical Phenomena*, eds. C. Domb and J. Lebowitz, (Academic Press, London, 1991), Vol. **14**.

[3] P.G. de Gennes, *Rev. Mod. Phys*, **57**, 827 (1985).

[4] C. Redon, F. Brochard-Wyart, F. Rondelez, Phys. Rev. Lett. 66, 715 (1991).

[5] N. Samid-Merzel, S.G. Lipson, D.S. Thannhauser, *Physica A*, **257**, 413 (1998)

[6] K. Jacobs and S. Herminghaus, K.R. Mecke: ,Langmuir **14** ,965 (1998); S. Herminghaus, K. Jacobs, K. Mecke, J. Bischof, A. Fery, M. Ibn-Elhaj and S. Schlagowski, Science, **282** (1998) 916.

[7] G. Reiter, *Phys. Rev. Lett.* **68**, 75 (1992); G. Reiter, A. Sharma, A. Casoli, M.-O. David, R. Khanna, P. Auroy,, *Langmuir*, **15** , 2551 (1999)

[8] A. Boesch, O. Shochet, H. Müller-Krumbhaar, *Z. Physik*, **B97**, 367 (1995).

[9] H. Müller-Krumbhaar, H. Emmerich, E. Brener, M. Hartmann, Phys. Rev. E 63, 026304 [1-9] (2001)

[10] J. W. Cahn, J. E. Hilliard,*J. Chem. Phys.*, **31**, 688 (1959).

[11] E. A. Brener, H. Müller-Krumbhaar and D.Temkin, Solid State Ionics, **131**, 23 (2000).

[12] H. Müller-Krumbhaar, T. Abel, E. Brener, M. Hartmann, N. Eissfeldt, D. Temkin, JSME **B**, (Feb 2002).

Publications in refereed journals

Barashev A.V. 1; Golubov S.I. 2; Trinkaus H.
1 Materials Science and Engineering, University of Liverpool, UK
2 Scientific Center of Russian Federation, Obninsk, Russian Federation
Reaction kinetics of glissile interstitial clusters in a crystal containing voids and dislocations
Phil. Mag. A 81, 2515-2532 (2001)
23.15.0

Bellini V.; Papanikolaou N.; Zeller R; Dederichs P. H.
Magnetic 4d monoatomic rows on Ag vicinal surfaces
Phys. Rev. B 64, 094403 (2001)
23.20.0

Bellini V.; Zeller R.; Dederichs P. H.
Cd hyperfine fields at the bcc Fe/Co interface
Phys. Rev. B 64, 144427 (2001)
23.20.0

Brener E. A.; Müller-Krumbhaar H.; Spatschek R.
Coarsening of cracks in a uniaxially strained solid
Phys. Rev. Lett. 86, 1291 (2001)
23.15.0

Caprion D.; Schober H. R.
Is diffusion in selenium heterogeneous or homogeneous?
Defect and Diffusion Forum 194-199, 841-848 (2001)
23.30.0

Caprion D.; Schober H. R.
Vibrational density of states of selenium through the glass transition
J. Chem. Phys. 114, 3236 (2001)
23.30.0

Galanakis I.; Alouani M.1; Oppeneer P.M.2; Dreysse H.1; Eriksson O.3
1 Institut de Physique et Chimie des Materiaux de Strasbourg, Strasbourg, France
2 Institute of Solid State and Materials Research, Dresden
3 Department of Physics, Uppsala University, Uppsala, Sweden
Tuning the orbital moment in transition metal compounds using ligand states
J. Phys.: Condens. Matter 13, 4553-4566 (2001)
23.20.0

Golubov S.I. 1; Singh B.N. 1; Trinkaus H.
1 Department of Materials Research, Riso National Laboratory, Roskilde, Denmark
Defect accumulation in fcc and bcc metals and alloys under cascade damage conditions - Towards a generalisation of the production bias model
J. Nucl. Mat. 276, 78-89 (2000)
23.15.0

Gutheim F.; Müller-Krumbhaar H.; Brener E. A.
Epitaxial growth with elastic interaction: Submonolayer island formation
Phys. Rev. E 63, 041603 (2001)
23.15.0

Kluge M.; Schober H. R.
Simulation of diffusion in amorphous solids and liquids
Defect and Diffusion Forum 194-199, 849-854 (2001)
23.30.0

Korhonen T.1; Settels A.; Papanikolaou N.; Zeller R.; Dederichs P. H.
1 Lab. of Physics, Helsinki University of Technology, Finland
Effect of lattice relaxations on the hyperfine fields of heavy impurities in Fe
J. Mag. Mag. Mat. 226-230, 1024-1026 (2001)
23.20.0

Müller-Krumbhaar H.; Gutheim F.; Spatschek R.; Brener E. A.
Elastic effect on growth processes
Appl. Surface Science 182, 265 (2001)
23.15.0

Nonas B.; Cabria I.; Zeller R.; Dederichs P.H.; Huhne T.1; Ebert H.1
1 Institut für Phys. Chemie, Universität München
Strongly enhanced orbital moments and anisotropies of adatoms on the Ag(001) surface
Phys. Rev. Lett. 86, 2146 (2001)
23.20.0

Schober H. R.
Isotope effect in the diffusion of binary liquids
Solid State Commun. 119, 73-77 (2001)
23.30.0

Spatschek R.; Brener E. A.
Grinfeld instability on crack surfaces
Phys. Rev. E 64, 046120 (2001)
23.15.0

Trinkaus H.; Singh B.N. 1; Golubov S.I. 2
1 Department of Materials Research, Riso National Laboratory, Roskilde, Denmark
2 Scientific Center of Russian Federation, Obninsk, Russian Federation
Progress in modelling the microstructural evolution in metals under cascade damage conditions
J. Nucl. Mat. 283-287, 89-98 (2000)
23.15.0

Trinkaus H.; Ullmaier H.
Does pulsing in spallation neutron sources affect radiation damage?
J. Nucl. Mat. 296, 101-111 (2001)
23.15.0

Other publications

Antons A.
First-principles investigation of initial stages of surfactant Me diated growth on the Si(111) substrate
Dissertation, RWTH Aachen, Juli 2001
23.42.0

Bellini V.
Electronic structure of low-dimensional magnetic systems
Berichte des Forschungszentrums Jülich, Jül-3856 (2001)
23.20.0

Kienle D.
Forschungszentrum Jülich: "Fließt wie geschmiert" - Computersimulationen helfen Verhalten einzelner Polymermoleküle zu verstehen
IHK Aachen, Wirtschaftliche Nachrichten WN 4/2001
23.30.0

Kienle D.
Verankerte Polymere in einfache Strömungen
Dissertation, Universität des Saarlandes, Saarbrücken (2001)
23.30.0

Kluge M.
Molekulardynamik-Simulation der Diffusion in binären unterkühlten metallischen Schmelzen und Gläsern aus Cu33Zr67
Jül-Bericht 3913, Forschungszentrum Jülich (2001)
23.30.0

Kromen Wi.
Die Projector Augmented Wave-Methode: Ein schnelles Allelektronenverfahren für die ab-initio-Molekulardynamik
Jül-Bericht 3887, Forschungszentrum Jülich (2001)

23.42.0

Invited Talks

Dederichs P.H.
Ballistic spininjection
Seminar Universität Kyoto, 12.12.2001
23.20.0

Dederichs P.H.
Ballistic spininjection from Fe into ZnSe and GaAs
Center of Excellence Symposium, Osaka, Japan, 13.12.2001
23.20.0

Dederichs P.H.
Ballistic spininjection from Fe into ZnSe and GaAs
Symposium "Selforganizing Nanostructures and Magnetic Heterostructures", Universität Duisburg, 29.11.2001
23.20.0

Dederichs P.H.
Ballistic spininjection from Fe into ZnSe and GaAs
Symposium on Magnetoelectronics, Regensburg, 25.07.2001
23.20.0

Dederichs P.H.
Complex band structure and resonant states in the barrier problem
APS March Meeting, Seattle, USA, 15.03.2001
23.20.0

Dederichs P.H.
Importance of complex band structure and resonant states for tunneling
Symposium on Metallic Multilayers, Aachen, 26.06.2001
23.20.0

Dederichs P.H.
Surface magnetism
The European Graduate School on Condensed Matter: Physics of Magnetic Multilayers, Prag, 09.06.2001
23.20.0

Gutheim F.; Müller-Krumbhaar H.
Epitaktisches Wachstum unter elastischer Wechselwirkung: Inselbildung im Submonolagenbereich
DGKK, Arbeitskreis Kinetik, 22.02.2001, Erlangen
23.15.0

Hartmann M.
Strukturbildung an fest-flüssig Phasengrenzen unter hydrodynamischer Wechselwirkung
Universität Magdeburg, 15.01.2001
23.15.0

Müller-Krumbhaar H.
Elastic effects on pattern formation
Calcutta, Indien, 07.03.2001
23.15.0

Müller-Krumbhaar H.
Elastische Effekte beim Cluster-Wachstum
Erlangen, 22.02.2001
23.15.0

Müller-Krumbhaar H.
Growth-morphologies in solidification and hydrodynamics
AFI-Conference, Sendai, Japan, 05.10.2001
23.15.0

Müller-Krumbhaar H.
Phase-field models for crystal growth
ICCG-13, Kyoto, Japan, 31.07.2001
23.15.0

Müller-Krumbhaar H.
Physik, das ungeliebte Schulfach
Institut für Lehrerbildung, Soest, 04.05.2001
23.15.0

Müller-Krumbhaar H.
Propagation fraktaler Fronten
Heraeus-Seminar, Bad Honnef, 23.03.2001
23.15.0

Müller-Krumbhaar H.
Propagation fraktaler Fronten
Universität Leipzig, 09.10.2001
23.15.0

Müller-Krumbhaar H.
Schulphysik - Kooperation zwischen Schule und Universität
GDNÄ-Tagung Schulphysik, Frankfurt, 05.11.2001
23.15.0

Schober H. R.; Caprion D.; Kluge M.
Collectivity of motion in undercooled liquids and amorphous solids
4th International Discussion Meeting on Relaxations in Complex Systems, Heraklion, Kreta, Griechenland, 21.06.2001
23.30.0

Schober H. R.; Caprion D.; Kluge M.
Collectivity of motion in undercooled liquids and amorphous solids
8th International workshop on disordered solids, Andalo, Trento, Italien, 12.03.2001
23.30.0

Schober H. R.
Atomic motion in amorphous solids
ISS PMS '2001, Jasowiec, Polen 28.-29.09.2001
23.30.0

Schober H. R.
Dynamik in Gläsern
Universität Heidelberg, 05.11.2001
23.30.0

Schober H. R.
Niederenergetische Anregungen in Gläsern
Universität Freiburg, 16.05.2001
23.30.0

Zeller R.
Recent developments in the full-potential KKR-method
International Conference on Applied Density Functional Theory, 14.-17.01.2001, Wien, Österreich
23.20.0

Other talks

Antons A.; Berger R.; Blügel S.; Schroeder K.
Ab-initio Untersuchung des Wachstums kleiner Si Cluster auf As und Sb bedecktem Si(111)
DPG-Frühjahrstagung, Hamburg, 29.03.2001
23.42.0

Blügel S.; Kromen Wi.; Schroeder K.
Implementierung und Anwendung einer Projektor-Augmentierten Wellen (PAW) Methode für die ab-initio Molekulardynamik
DPG-Frühjahrstagung, Hamburg, 29.03.2001
23.42.0

Cao Y.; Antons A.; Berger R.; Kromen Wi.; Schroeder K.; Blügel S.
Stability and adatom dynamics on surfactant covered growing Ge(111) films
DPG-Frühjahrstagung, Hamburg, 29.03.2001

23.42.0

Dederichs P.H.; Cabria I.; Nonas B.; Zeller R.
Spin- und Bahnmagnetismus von Übergangsmetall-Adatomen und -Clustern auf Ag und Au-Oberflächen
DPG-Frühjahrstagung, Hamburg, 28.03.2001
23.20.0

Dederichs P.H.; Cabria I.; Nonas B.; Zeller R.
Strongly enhanced orbital moments and anisotropies of single adatoms and small clusters on Ag(001) and Pt(111)
APS March Meeting, Seattle, USA, 12.03.2001
23.20.0

Dederichs P.H.
Ballistic spininjection from Fe into ZnSe and GaAs
Midterm-Meeting-Strategiefonds Magnetoelektronik, 22.11.2001, Jülich
23.20.0

Galanakis I.; Papanikolaou N.*; Dederichs P.H.
*Martin-Luther-Universität Halle-Wittenberg, FB Physik, Halle
Half-metallic Heusler alloys: bulk and surface properties
1st Annual Meeting of the Research Training Network "Computational Magnetoelectronics", 27.-30.09.2001, Budapest, Ungarn
23.20.0

Gutheim F.; Brener E. A.; Müller-Krumbhaar H.
Epitaktisches Wachstum unter elastischer Wechselwirkung: Lagen und Cluster-Wachstum
DPG-Frühjahrstagung, Hamburg, 26.-30.03.01
23.15.0

Mavropoulos Ph.; Wunnicke O.; Papanikolaou N.*; Zeller R.; Dederichs P.H.
*Martin-Luther-Universität Halle-Wittenberg, FB Physik, Halle
Ballistic spininjection through Fe/ScFe junctions
1st Annual Meeting of the Research Training Network "Computational Magnetoelectronics", 27.-30.09.2001, Budapest, Ungarn
23.20.0

Schober H. R.; Kluge M.
Atomare Hüpfprozesse in Cu33Zr67: Bestimmung von Sprungweiten und Wartezeiten
DPG-Frühjahrstagung, Hamburg, 26.03.2001
23.30.0

Spatschek R.; Brener E. A.; Müller-Krumbhaar H.
Theorie der Rißbildung
Arbeitstreffen RWTH Aachen, Altenberg, 26.09.2001
23.15.0

Spatschek R.; Brener E. A.; Müller-Krumbhaar H.
Vergröberung von Rissen
DPG-Frühjahrstagung, Hamburg, 29.03.2001
23.15.0

Wunnicke O.
Ballistic spininjection from Fe(001) into ZnSe and GaAs
1st Annual Meeting of the Research Training Network: Computational Magnetoelectronics, Budapest, Ungarn, 27.-30.09.2001
23.20.0

Wunnicke O.
Effects of interface states on tunneling
DPG-Frühjahrstagung, Hamburg, 26.-30.03.01
23.20.0

Posters

Antons A.; Berger R.; Blügel S.; Schroeder K.
Structure of steps and small islnads on Si(111): As
Conference on Computational Physics 2001, Aachen, 05.-08. September 2001
23.42.0

Hartmann M.
Dewetting Hydrodynamics in 1+1 Dimension
Vorbereitungstreffen zum Gutachterkolloquium des Schwerpunktprogramms
Reisensburg, 18.07.-20.07.2001
23.15.0

Hartmann M.
Dewetting Hydrodynamics in 2+1 Dimension
Gutachterkolloquium des Schwerpunktprogramms
Bad Honnef, 07.11.-09.11.2001
23.15.0

Kienle D.
Grafted polymers in simple flows
Minerva-Workshop "Frontiers in the physics o complex systems"
Israel, 25.03.-28.03.2001
23.30.0

Rzehak R.; Müller-Krumbhaar H.; Marquardt W. 1
1 Lehrstuhl für Prozesstechnik, RWTH Aachen
Liquid-liquid phase change in systems with flow
253. WE-Heraeus Seminar, Bad Honnef, 22.-24.03.2001
23.15.0

Wunnicke O.
Effects of Interface States on Tunneling Magnetoresistance
4th International Symposium on Metallic Multilayers
Aachen, 24.06.-29.06.2001
23.20.0

Wunnicke O.
Effects of Interface States on Tunneling Magnetoresistance
European Graduate School on Condensed Matter: Physics of Magnetic
Multilayers-Theory and Experiment
Prague, Tschechien, 09.06.-16.06.2001
23.20.0

Wunnicke O.
Effects of Interface States on Tunneling Magnetoresistance
Summerschool on Density Functional Theory
Caramulo, Portugal, 28.08.-01.09.2001
23.20.0

Lecture

Blügel S.; Dederichs P.H.; Müller-Krumbhaar H.; .Schroeder K.
Computeranwendungen in der Festkörperphysik
Physikalisches Seminar (6h), WS 2000/2001, RWTH Aachen
23.20.0

Dederichs P.H.; Schroeder K.
Theoretische Festkörperphysik I
Vorlesung (4h) und Übung (2h), SS 2001, RWTH Aachen
23.20.0

Dederichs P.H.; Schroeder K.
Theoretische Festkörperphysik II
Vorlesung (4h) und Übung (2h), WS 2001/02, RWTH Aachen
23.20.0

Institute for Scattering Methods

General Overview

Modern solid state physics goes far beyond a phenomenological description and bases the understanding of solid state properties and phenomena on atomic theories. To obtain information about the atomic structure of solids, probes with sub-nanometer spatial resolution are needed. To study the excitation spectra, an appropriate energy resolution is necessary in addition. All these requirements can be met by scattering methods. In this sense, scattering methods provide the basis of our present understanding of the structure, excitations and phase transitions of condensed matter on a microscopic level.

At the Institute for Scattering Methods (ISM), synchrotron x-ray scattering and neutron scattering are employed for the investigation of condensed matter on an atomic microscopic level. The emphasis lies on exploiting fully the complementarity of the two probes. Besides the application of scattering methods to solid state problems, major activities are concentrated on the methodology. This includes the further development of experimental techniques by improving instrument components and data treatment algorithms, the development of new experimental methods and the corresponding instruments and the development, construction and operation of scattering instruments at large-scale facilities. At present, ISM operates five instruments at the research reactor DIDO of the Research Center Jülich and two instruments at the Hamburger Synchrotronstrahlungslabor HASYLAB. In addition, we participate in the operation of a sector at the Advanced Photon Source APS in Argonne, USA. These instruments are open for the use by external groups from universities, research centers and industry. The instrument responsibles from ISM provide scientific and technical support during the experiment and the data processing. ISM is open for all research areas in condensed matter science, where scattering methods can be applied. At present, the research activities are concentrated in the fields: "solid state magnetism", "structural disorder", "novel materials" and "ultra thin liquid films". For the purpose of this research, ISM is also engaged in sample preparation (e.g. by molecular beam epitaxy and single crystal growth) and characterisation (e.g. AC and DC susceptibility and magnetisation measurements).

Magnetic nanostructures
Within the framework of the so-called „HGF Strategiefond Magnetoelektronik", a larger collaboration within the research center has been established. Magnetic nanostructures in the form of magnetic thin films and laterally structured thin films are the subject of investigation. Research topics extend from basic research on quantum phenomena of nanostructured magnetic systems up to application oriented questions. In the Institute for Scattering Methods, we are aiming at a full structural and magnetic characterisation of magnetic nanostructures on a microscopic atomic up to mesoscopic level. For the structure characterisation, we have developed techniques of grazing incidence x-ray reflection employing anomalous scattering for contrast variation. The combination of reflectivity and diffuse scattering data allows us to perform a full statistical description of the interface morphology in layered systems. Polarised neutron scattering under grazing incidence allows us to determine the magnetic coupling, domain structure and magnetic roughness at the interfaces. In collaboration with other groups (e. g. from the Institute for Electronic Properties), we are working on a correlation of the obtained microscopic structure and magnetic parameters with macroscopic properties such as interlayer coupling or magneto-resistance-effects. Many of the systems we study are produced in our own MBE chamber. But we also characterise epitaxial or sputtered layer-systems from other groups within the research centre. A program-package has been developed which allows us to simulate and refine x-ray data as well as polarised neutron data from grazing incidence scattering experiments. In 2001 we have studied transition metal multi-layers such as the FeCo/Mn/FeCo, Fe/Cr/Fe, Co/Cu/Co-systems, rare-earth multilayers of Er/Tb as well as TMR and GMR-systems produced by other groups. For all these systems a systematic study of the interface-morphology as function of preparation condition was performed and the preparation conditions could be optimised. To give an example for a systematic structural study of these multilayers, we mentioned the system Co/Cu/Co where a square root dependence of the roughness on layer thickness was found. Another important result was achieved in collaboration with the IEE: Two samples of Fe/Cr/Fe with the same layer-structure but different interface roughness have been prepared and fully characterised. It was found that the magneto- resistance effect was significantly enhanced for the sample with rougher interfaces. These experiments will be continued to identify the influence of the buffer roughness. In addition to thin films, we are now studying laterally structured magnetic layers. In a first experiment on an optical grating covered with a Ni layer, the magnetic shape anisotropy could be observed in a

polarised neutron scattering experiment. Fe/Cr/Fe multi-layer stripes with a period of 400 nanometers could be produced by electrolithography and are now being studied with grazing incidence neutron scattering. The application of resonance exchange scattering of synchrotron x-rays from rare-earth multilayers allows us to obtain new inside into the mechanism of interlayer coupling. This has been shown by studies of the Er/Tb multilayer system. For a certain interface morphology and layer thickness, a coherent cone structure develops in the Er throughout the entire stack of Er-layers. How the coupling is mediated through the Tb layers could be observed with element specific magnetic x-ray scattering tuning the x-ray energy to the Tb L_{II} and L_{III} edges. In this way we could prove that a spin density wave corresponding to the magnetic order of the Er layers develops in the 5d-conduction band of the ferromagnetic Tb layers.

Magnetic bulk materials

Due to their often simple Hamiltonian, magnetic systems are ideally suited to study quantum phenomena in many body systems. We employ advanced methods of neutron or magnetic x-ray scattering to study fundamental questions such as the nature of elementary excitations, magnetic phase-transitions or spin and orbital ordering phenomena. By applying neutron polarisation analysis we could for the first time determine the spectrum of longitudinal excitations in a Heisenberg antiferro-magnet with a small spin-wave gap, the model system MnF_2. An excitation-gap appears close to the position of the transverse (spin-wave) excitation separating a quasielastic from a truely inelastic part of the spectrum. Our results are in good agreement with recent theories on multi-magnon-processes. The behaviour of the spin-dynamics and magnetisation in the low- and intermediate temperature range has been studied on a wide range of materials. Deviations from the low temperature Bloch-law have been found and a classification into simple power laws is proposed. A major research effort is concentrated on the investigation of the electronically highly correlated manganites. These are not only interesting from a fundamental point of view but also for possible applications as magnetoelectronics devices. Resonant x-ray scattering experiments reveal the orbital ordering in $La_{1-x}Sr_xMnO_3$ single crystals. The interplay between spin ordering, orbital ordering, lattice distortions and charge ordering is being investigated by neutron diffraction and diffuse neutron scattering, resonant and non-resonant (high-energy) x-ray scattering and magnetisation and resistivity measurements.

Research on advanced materials

While many research efforts within the Institute for Scattering Methods are dealing with magnetic systems we apply scattering methods for the microscopic investigation of a wide range of novel or interesting materials. With small angle x-ray scattering such varied systems have been investigated as amorphous silicon-germanium alloys relevant for solarcell-technology, CdTe quantum-dots, proton conducting polymer-films or three-dimensional networks of platin nanoparticles separated by organic spacer on molecules. First studies have been made for a structure determination of biological macromolecules in solution from x-ray small angle scattering data. Another research focus is the research on thin liquid or polymeric films, where the film thickness is in the range of only a few molecular diameters. These two-dimensional systems usually have completely different behaviour compared to the bulk and also are of importance for applications as lubricants, coatings or insulating layers. A report on recent results obtained with synchrotron radiation is attached. The research on structural disorder in alloys has shifted away from bulk materials towards the investigation of order-disorder phenomena near surfaces, see the report on a synchrotron radiation study of CuAu.

Research and development for the European Spallation Source Project ESS

The Forschungszentrum Jülich has taken a leading role in the research and development for a future new generation neutron source, the European Spallation Source ESS. The Institute for Scattering Method is engaged in this research, wherever the expertise of the neutron scatterers and the material experts are concerned. The research group for „Materials under heavy irradiation loads" has been incorporated in the institute and performs research mainly for the ESS project. Besides the development of ideas for innovative neutron instrumentation, most activities concentrate on the target-moderator- and reflector-module of a future high intensity spallation source. This comprises the investigation of changes of the mechanical and microstructure properties of candidate materials for the spallation target. Studies are made on spend targets from existing spallation sources. Microstructure changes of candidate structure-materials by helium-implantation are being investigated at the cyclotron. The effect of shock-waves within the Hg target are being studied both experimentally and with finite element calculations. For the first time a rather good agreement could be achieved. On the full-size target-moderator-reflector test-stand JESSICA at the COSY-synchrotron the time-structure of neutron-pulses could be measured and gave the expected resolution.

Development of methods for neutron and x-ray scatting

A qualified use of the large facilities for neutron- and synchrotron-radiation research requires the continuous development of the instrument park, largely triggered by the requirements for the scientific problems and by the available state-of the art mechanical, optical and electronical devices.

Neutron instrumentation: A continuous program of instrument development and instrument up-grade is being pursued for the neutron scattering instruments at the DIDO reactor in Jülich. The new high resolution small angle scattering machine KWS-3, based on a technique employing focusing mirrors, is completely erected in the neutron guide-hall ELLA of the research reactor DIDO. A first test of the imaging properties with neutrons did not show any influence of gravity on the focus. A momentum space resolution of up to $2x10^{-4}Å^{-1}$ can be reached with an entrance aperture of 1 x 1 mm^2. The neutron-reflectometer HADAS has been commissioned and permits the measurement of diffuse scattering with polarisation analysis from 1 cm^2 big magnetic layer systems. The new diffractometer/spectrometer for thermal neutrons with full polarisation analysis SV30 is close to completion. The beam-tube insert has been installed during the long reactor shut-down in summer. Major development for this machine include research on neutron spin-filter cells with polarised ^3He and on a large solid angle area-detector based on a neutron image-plate. Highly polarised ^3He at mbar pressure could be produced with a degree of polarisation exceeding 60 %. Important progress has been achieved with the development of the neutron image-plate with low sensitivity for γ-radiation by employing the szintillators KBr and KCl in connection with LiF as neutron converter. While the neutron sensitivity is comparable with commercial image plates, the γ-sensitivity could be reduced by at least one order of magnitude.

Synchrotron instrumentation: Forefront experiments with synchrotron radiation can only be performed if a continuous method development program is being pursued. Examples are the monochromator development for the high-energy undulator station at the Advanced Photon Source APS. At this station an image plate detector for the measurement of diffuse scattering of high-energy synchrotron radiation in transmission geometry has been successfully commissioned. For the study of confined liquids with synchrotron radiation a sample cell has been developed with which a pressure of up to 300 kN can be applied perpendicular to the film-surface. The cell has been successfully commissioned in a first experiment on tetrachlormethan which could be confined to 160 Å gap-distance between two flat Al_2O_3-substrates. A new method to measure resonant exchange scattering from ferromagnetic layer-systems has been developed and tested on the model-systems EuS, Tb and Er/Tb multilayers. The method is based on the polarisation properties of synchrotron radiation.

Sample preparation and scientific infrastructure

Besides the MBE-techniques for the growth of metallic films, the institute operates a small chemistry lab for sample preparation and facilities for single crystal growth. The existing facilities for the growth of metallic single crystals by the Czochralski and Bridgman-techniques will in the future be complemented by a mirror furnace employing the floating zone technique which is currently under construction at the institute. Manganite single crystals have been grown successfully in the existing mirror furnace of the RWTH Aachen (collaboration with the institute for crystallography, Prof. Heger). Besides the manganites, single crystals of metallic alloys such as CuPd, rare-earth-sulfides ($Eu_{1-x}Gd_xS$) and carbonites have been prepared. A new x-ray laboratory with a high intensity low temperature four circle diffractometer, a small-angle-scattering machine and reflectometer is currently being set up.

I would like to close this report by thanking all members of the institute for their dedicated work during the past year.

Thomas Brückel

Personnel 2001/2002 and areas of activity

Scientific Staff

Prof. Dr. Th. Brückel	Institute director; neutron and synchrotron x-ray scattering; magnetism.	23.89.1
Dr. J. Chen *- since 17.10.2001 -*	Mechanical tests and TEM on irradiated spallation materials	23.60.0
Dr. H. Conrad	European Spallation Source project ESS: target and moderators.	23.89.1
Dr. G. Goerigk *- HASYLAB, Hamburg -*	Material research with anomalous small angle x-ray scattering (ASAXS); instrument responsible for Jülich's user-dedicated small-angle scattering facility JUSIFA.	23.89.1
Dr. H.-G. Haubold	Anomalous small angle x-ray scattering ASAXS and x-ray absorption spectroscopy XAS from highly dispersive systems; in-situ studies of electro-chemical processes.	23.89.1
Dr. A. Ioffe	Development of neutron scattering methods and instrumentation for polarization analysis. Instrument responsible for the triple axis spectrometer SV-30; construction and development of the new polarized thermal neutron scattering instrument.	23.89.1
Dr. P. Jung *since 17.10.2001 -*	Radiation damage and hydrogen effects in metals and ceramics, thermal desorption spectroscopy.	23.60.0
Dr. E. Kentzinger	Neutron and synchrotron x-ray scattering from magnetic thin film materials.	23.89.1
Dr. U. Köbler	Magnetisation and neutron diffraction studies of materials with fourth-order exchange interactions.	23.89.1
Dr. R. Mueller	Development of the ^{3}He filter for neutron polarisation analysis.	23.89.1
Dr. U. Rücker	Instrument responsible for the neutron reflectometer HADAS; preparation and characterisation of magnetic thin film systems.	23.89.1
Dr. W. Schweika	Diffuse neutron scattering for the investigation of short-range order in alloys, oxides, perovskites and quasi-crystals; instrument responsible for the diffuse neutron scattering instrument DNS.	23.89.1

Technical Staff

A. Broch	Diffuse neutron scattering instrument DNS.	23.89.1
Dipl.-Ing. K. Bussmann *- since 01.05.2001 -*	Electronic engineer; responsible for spectrometer control hard- and software.	23.89.1
L. Dohmen	Project engineer for the small angle scattering instrument KWS III.	23.89.1
M. Abdel Fattah *- since 01.04.2001 -*	Single crystal growth.	23.89.1
P. Foucart *- since 01.08.2001 -*	Sample preparation, single crystal growth.	23.89.1
Dipl.-Ing. D. Hamann *- HASYLAB, Hamburg since 01.05.2001 -*	Project engineer JUSIFA beamline.	23.89.1
Dipl.-Ing. P. Hiller	Project engineer for μCAT-collaboration at the Advanced Photon Source APS; x-ray scattering laboratory.	23.89.1
Ms. C. Horriar-Esser	Ultra low-temperature magnetometry and ^{3}He filter project.	23.89.1
H. Jungbluth	Software development for x-ray small angle scattering.	23.89.1
H. Klein *- since 17.10.2001 -*	Instrumentation and data processing, TEM, irradiation experiments.	23.60.0
Ms. B. Köppchen	Secretary.	23.89.1
Dipl.-Ing. E. Küssel	Project engineer for the new polarised thermal neutron scattering instrument.	23.89.1
B. Olefs	Magnetometry, electronics and PC responsible.	23.89.1
B. Schmitz	Triple axis spectrometer SV-30 and cryotechniques.	23.89.1
W. Schmitz *- since 17.10.2001 -*	SEM, irradiation experiments, specimen preparation.	23.60.0
T. Sorkalla	Laboratory assistant.	23.89.1
J. Thelen *- since 19.01.2001 -*	Reflectometer HADAS. Small angle scattering KWS-3 and molecular beam epitaxy MBE.	23.89.1

Scientists

Dr. D. Hupfeld *- APS, Argonne, USA, until 30.06.2001; HASYLAB, Hamburg, since 01.07.2001-*	Magnetic x-ray scattering; instrument responsible at the μ-CAT sector of the APS.	23.89.1
Dr. O. Seeck *- HASYLAB, Hamburg -*	X-ray scattering from ultrathin liquid films in confined geometries; instrument responsible of the Wiggler beamline W1.	23.89.1
Dr. Y. Su *- since 01.07.2001 -*	X-ray and neutron scattering from strongly correlated systems.	23.89.1
Dr. Th. Vad	Further development of the instrument control and data treatment programs for Jülich's user-dedicated small-angle scattering facility (JUSIFA); ASAXS measurements.	23.89.1

Thesis Students

Dipl.-Phys. W. Babik	(RWTH Aachen) Interface morphology of GMR and TMR layer structures.	23.89.1
M. Sc. K. Istomin	(RWTH Aachen) Interplay of charge, orbital and magnetic ordering in manganites.	23.89.1
Ms. M. Sc. M. Mihaylova *- HASYLAB, Hamburg -*	(RWTH Aachen) Liquids in confined geometry investigated by scattering methods.	23.89.1
Dipl.-Ing. M. Schlapp *- TU Darmstadt -*	(TU Darmstadt) Development of highly efficient materials and image plates for neutron detection.	23.89.1
Dipl.-Phys. J. Voigt	(RWTH Aachen) Influence of proximity and reduced dimensionality on structure and phase transition in rare earth superlattices.	23.89.1
Ms. cand. phys. N. Ziegenhagen *- since 01.08.2001 -*	(RWTH Aachen) Laterally structural multilayers.	23.89.1

Guests

Dr. B. Alefeld	Development of neutron scattering methods; instrument responsible for the lattice parameter instrument LAP; construction and development of the small angle scattering machine KWS-3.	23.89.1
Ms. Dr. J. Bos	(RWTH Aachen) Preparation of powder and single crystal samples; magnetic structures and phase transitions by neutron- and x-ray scattering.	23.89.1
Dr. S. Massalovitch	(Kurchatov Institute, Moscow, Russia) Development of a large-area image plate detector of thermal neutrons.	23.89.1
Dr. S. Romanzetti *- since 17.10.2001 -*	(Universita degli Studi di Ancona, Italy) ESS-project: target materials.	23.60.0
Dr. B. Toperverg	(Petersburg Nuclear Physics Institute, Russia) Theory for grazing incidence diffraction.	23.89.1
Z. Yao *- since 17.10.2001 -*	(China Institute of Atomic Energy (CIAE), Beijing, China) ESS-project: target materials.	23.60.0

Trainees

Ms. S. Bluhm
- until 25.01.2001; since 05.06.2001 -
A. Christ
- until 31.10.2001 -
Ms. I. Schulte
- since 12.11.2001 -

Structural characterization of multilayers for magnetoelectronis

W. Babik, E. Kentzinger, U. Rücker, G. Goerigk, O. H. Seek, T. Brückel
FZJ, Institute for Scattering Methods

X-ray scattering from multilayer structures opens the possibility to determine structural properties such as layer thickness and interface roughness as well as material properties i.e. scattering length densities.
X-ray reflectivity and diffuse scattering was used to characterize monocrystalline, MBE grown Co/Cu/Co multilayers based on a Si(001) waver and a thick Cu(001) buffer.

F&E-Nr:23.89.1

X-ray reflectivity [1, 2] and diffuse scattering [3–5] from multilayer interface structures are powerfull and nondestructive measurement techniques which allow to describe structural properties of layers and interfaces on nm to μm lengthscales averaged over the illuminated sample area.
For small scattering vectors $\vec{q}$, the atomic structure of matter can be neglected and a continuously varying x-ray refractive index $n(\vec{r})$ is used to describe the relevant material property. The interface morphology is described using fractal concepts, a basic assumption for the height-height correlation function and a Gaussian height distribution with rms parameter σ. Figure 1 depicts schematically an interface between two media. Thin film multilayers which consist of sandwiched mag-

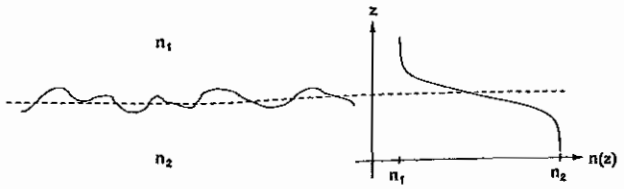

FIG. 1: Schematic picture of an interface between two materials with refrective indices n_1 and n_2. At the interface there is a continous crossing of the laterally averaged index of refration which in the case of Gaussian height distribution has a Gaussian error function dependence.

netic materials are fundamental to magnetoelectronics. Their interface morphology is of basic interest since it influences magnetic as well as electronic properties.
Among those systems which exhibit interlayer exchange coupling, Co/Cu/Co multilayers are, besides Fe/Cr/Fe, the earliest discovered and possess a strong GMR effect. The work described below is a model study of (001)-oriented Co/Cu/Co sandwich structures based on a Si(001) substrate and a thick Cu(001) buffer as well as a methodic development contributing new concepts like 2-dimensional diffuse scattering and enhanced modelling technique.

The Si(001) substrate preparation follows an often used recipe [6, 7] for growing copper on silicon : the silicon waver is etched in flourine acid to remove the overlaying oxide, cleaned in deionized water and pull dried. After loading the sample inside a UHV chamber epitaxial layers were prepared by MBE deposition at a base pressure of about 10^{-10} mbar. Different kinds of samples concerning the number of layers were prepared , a simple Si(001) waver, several buffer systems Cu(001)/Si(001) with different thicknesses of the copper buffer (250 Å, 500 Å, 2000 Å) and various Co(70 Å)/Cu(d_{Cu})/Co(70 Å) trilayer systems with different copper spacer layer thicknesses d_{Cu} (9 Å, 22 Å, 35 Å, 60 Å). All multilayers were covered with amorphous SiO which is a well suited protection coating [8].

TABLE I: Roughness parameters σ for several copper buffer thicknesses. The errors represent statistical uncertaincies from best fits.

d[Å]	σ[Å]	$\sqrt{d}/\sigma$
250	5.10(5)	3.1
500	6.8(2)	3.3
2000	17.4(2)	2.6

Due to a lattice mismatch of 6% the crystal quality of grown copper on silicon depends on its thickness, since the lattice mismatch relaxes with coverage. X-ray reflectivity measurements show a steady increase of Cu buffer surface roughness with thickness and a massive interdiffusion zone of Cu into bulk Si. Table I shows the numeric results from best fits. This trend is in rough agreement with results on the evolution of mound morphology in homoepitaxy on Cu(001) [9] where a squareroot dependance ($\sigma \propto \sqrt{d}$) of the roughness on coverage is reported. Since the surface crystal quality still improves beyond a thickness of 1000 Å, the buffer thickness for Co/Cu/Co trilayers was chosen to be 2000 Å.
Diffuse scattering experiments show for a Cu buffer of that thickness a lateral correlation length ξ_{Cu} of 600 Å, while a correlation length of 20000 Å is present on the top interface of the SiO coating. Thus the roughness structure is composed of 3-dimensional islands on grains. There is no evidence of appreciable interdiffusion between Co and Cu since the σ parameters determined by a fit to the specular reflectivity data suit well to diffuse scattering simulations. For trilayer systems a vertical roughness correlation length ξ_v of about 1000 Å is in good agreement with the data. This means that there

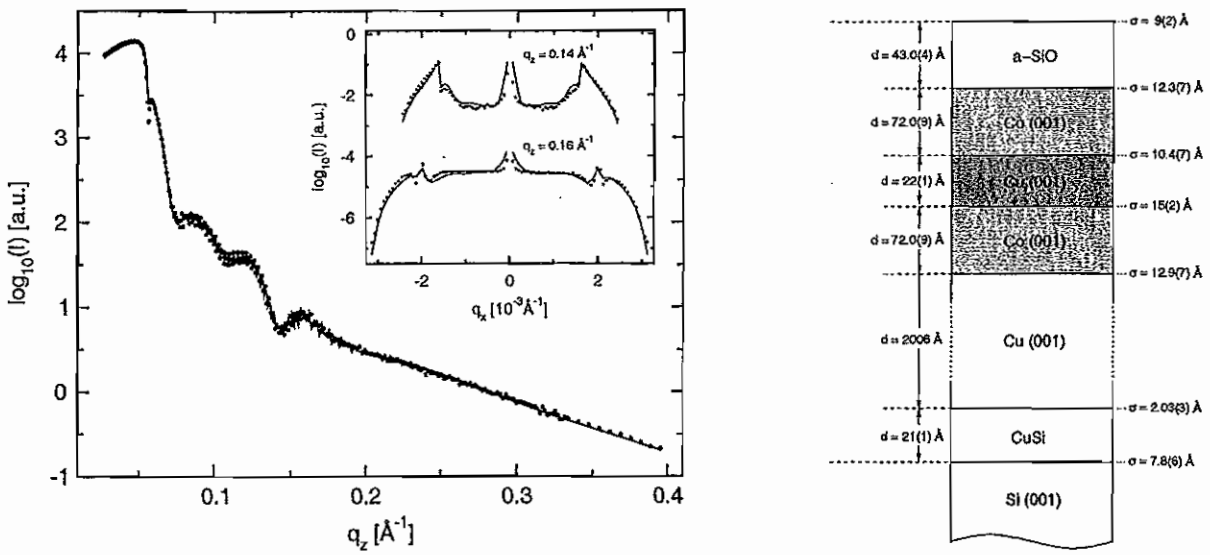

FIG. 2: Reflectivity an diffuse scattering data with fitcurves and schematic layout of a Co(70 Å)/Cu(22 Å)/Co(70 Å) multilayer. The insert on the left shows ω-scans measured at an x-ray energy of 7705 eV keeping the total scattering angle constant at values of 2.1° and 2.3° which corresponds to nearly constant q_z values of 0.14 $Å^{-1}$ and 0.16 $Å^{-1}$ respectively. As can be seen in the layout the results for the layer thicknesses are very close to the preparation demands as controlled by a quartz crystal ballance.

is strong roughness replication across all interfaces between Co and Cu. This property is most likely due to good epitaxy between Co and Cu which, in fcc structure like here, have a lattice mismatch of only ~2%. Consequently the Cu spacer layer interfaces which are most important with respect to magnetoelectronics exhibit a nearly similar mound morphology as the Cu buffer surface. Figure 2 shows the specular reflectivity and diffuse scattering as well as the whole layer architecture with annotated thickness and roughness parameters as determined from a fit for a sample with 22 Å spacer layer thickness. Rather large σ parameters compared to the spacer layer thickness are no contradiction since, as mentioned above, the interfaces are strongly correlated in vertical direction. Moreover it seems that the Co/Cu growth increases the roughness whereas Cu/Co growth reduces it.

Magneto Optical Kerr Effect (MOKE) measurements which were done on a sample with a wedge-like copper spacer layer, did not show oscillatory antiferromagnetic interlayer exchange coupling. The shape of the magnetic hysteresis loops looks the same for copper spacer thicknesses in the range 0-36 Å and indicates a ferromagnetic alignment of the magnetic layers. The reason is most probably a dipole field interaction across the copper spacer which is typical for large correlated roughness at magnetic material interfaces, the so called *orange peel coupling* [10].

In conclusion the preceded discussion shows that the morphology of Co/Cu/Co trilayer systems, which are based on a thick copper buffer, depends basically on its surface quality. A high degree of vertical correlation leads to replicated interface roughness. Since the roughness increases with buffer thickness but surface crystal quality improves, a compromise has to be met. This may apply to many copper buffered trilayer systems in (001)-orientation as far as mound morphology develops in heteroepitaxy like here.

Magnetic thin film properties are closely connected to the rather large interface roughness which results in a ferromagnetic coupling by means of dipolar interaction.

[1] L. G. Parrat, Phys. Rev. **95**, 359 (1954).

[2] L. Névot and P. Croce, Revue de Physique appliquée **15**, 761 (1980).

[3] S. K. Sinha, E. B. Sirota, S. Garoff, and H. B. Stanley, Phys. Rev. B **38**, 2297 (1988).

[4] V. Holý, J. Kuběna, I. Ohlídal, K. Lischka, and W. Plotz, Phys. Rev. B **47**, 15896 (1993).

[5] V. Holý and T. Baumbach, Phys. Rev. B **49**, 10668 (1994).

[6] C.-A. Chang, J. Liu, and J. Angilello, Appl. Phys. Lett. **57**, 2239 (1990).

[7] C.-A. Chang, J. Appl. Phys. **67**, 566 (1990).

[8] N. Chand et al., J. Crys. Growth. **148**, 336 (1995).

[9] J.-K. Zuo and J. Wendelken, Phys. Rev. Lett. **78**, 2791 (1997).

[10] P. Grünberg, Zwischenschichtaustauschkopplung : Phänomenologische Beschreibung, Materialabhängigkeit, 30. Ferienkurs des Instituts für Festkörperforschung 1999.

Single-Crystal Growth and Synchrotron X-ray Scattering Studies of Highly Correlated $La_{1-x}Sr_xMnO_3$ ($0.1<x<0.17$)

Y. Su, K. Istomin, A. Fattah, P. Foucart, D. Hupfeld, O. Seeck, B. Schmitz, Th. Brückel
Institute for Scattering Methods

R. Fischer, E. Würtz
Institute for Microstructural Research

S. Stein
Institute for Electronic Ceramics

A series of high-quality single crystals of highly correlated $La_{1-x}Sr_xMnO_3$ ($0.1<x<0.17$) were grown successfully by the floating-zone method, and characterized by comprehensive chemical, electric, magnetic and structural methods. Synchrotron X-ray resonant scattering and high-energy X-ray diffraction on a single crystal (x~0.125) were undertaken. Experiments revealed a strong interplay between orbital ordering, lattice distortions and metal-to-insulator transition.

The study of highly correlated electron systems is among the most fascinating areas of condensed matter physics. Electronic correlation plays a decisive role in many transitional-metal oxides from simple binary compounds like MnO to Colossal Magnetoresistance (CMR) perovskite manganites [1] or high-T_C superconductors [2]. Due to the presence of these correlations macroscopic quantum phenomena appear such as charge/orbital ordering, metal-to-insulator transition [3] (MIT) and superconductivity. The basic mechanisms are far from being understood. Besides of modern theoretical approaches, e.g. density-function theory with local correlations described by the Hubbard U parameter (LDA + U-method) [4], experimental investigations with a microscopic probe coupling to the relevant degrees of freedom (lattice, charge, orbital and spin) are a prerequisite for a fundamental understanding of correlation effects. Among all possible techniques, synchrotron X-ray scattering methods are particularly suitable since charge, orbital, magnetic and lattice correlations can be investigated in one experiment simultaneously.

Lightly doped $La_{1-x}Sr_xMnO_3$ (LSMO) ($0.1<x<0.17$) is such a material where electronic correlation effects dominate. A small change in some parameters, such as chemical doping, can have a dramatic effect on the ground state of this compound. The origin of this sensitivity is believed to lie in the fact that no single degree of freedom dominates the response, but rather all degrees of freedom mentioned above may be active. The interplay between charge, orbital, spin and lattice degrees of freedom is extremely complicated and remains a central issue of the physics of manganites. Upon cooling, lightly doped LSMO transforms from a paramagnetic insulating (PMI) state to a ferromagnetic metallic (FMM) state at the Cure temperature (T_C). An intriguing ferromagnetic insulating phase (FMI) appears further below T_C. To explain this insulating behavior, a charge/orbital-ordering scenario in PMI was proposed for the interpretation of a resonant X-ray scattering (RXS) experiment on LSMO (x=0.12) [5]. There are also reports [6,7] claiming that the RXS is not a direct probe for orbital ordering, but much more sensitive to cooperative Jahn-Teller distortions and strongly coupled to fine details of the band structure. A number of subsequent detailed structural characterizations [8-9] revealed a complicated phase diagram and identified a few novel structural phases with lower symmetry which might be associated to RXS.

To clarify the controversial behaviors reported so far, and to quantitatively evaluate the complex interplay between resonant scattering, orbital ordering and structure effects, a range of lightly doped LSMO single crystals with finely tuned Sr- concentration (x = 0.105, 0.115, 0.125, 0.135) were successfully grown. The best method to grow high quality single crystals of complex oxides with high purity is the floating-zone technique (FZT) with a mirror furnace, like the one we used at Institut für Kristallographie in RWTH, Aachen. In the

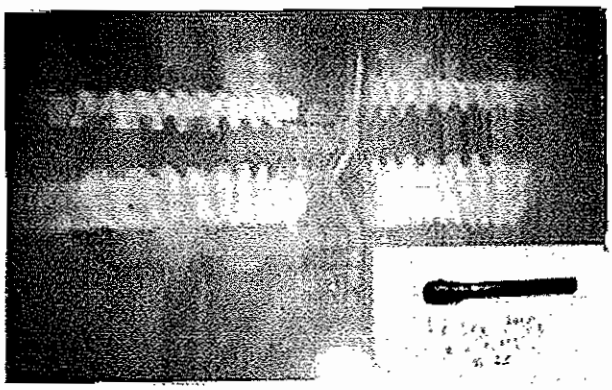

FIG. 1 A photo showing a molten section in a FZT furnace (The inset shows a grown LSMO single crystal)

FZT two polycrystalline rods are mounted coaxially and brought close together. The ends of the rods are heated up until melting, as shown in Fig. 1. Then the rods are reduced to a single one with a molten section. The molten zone is slowly moved along the rod by vertical movement of the mirrors and the crystal growth takes place in the region behind the molten zone while cooling down. The speed of the crystal growth varied between 5-8 mm/h. The homogeneous powder rods

were prepared by standard solid-state-synthesis process and examined to show a single phase by powder X-ray diffraction.

All crystals were then extensively characterized by various chemical, electric and magnetic measurements. The quality and orientation of crystals were checked by the Laue method. A Scanning Electron Microscopy with chemical analysis was employed to determine the chemical composition and homogeneity along a crystal.

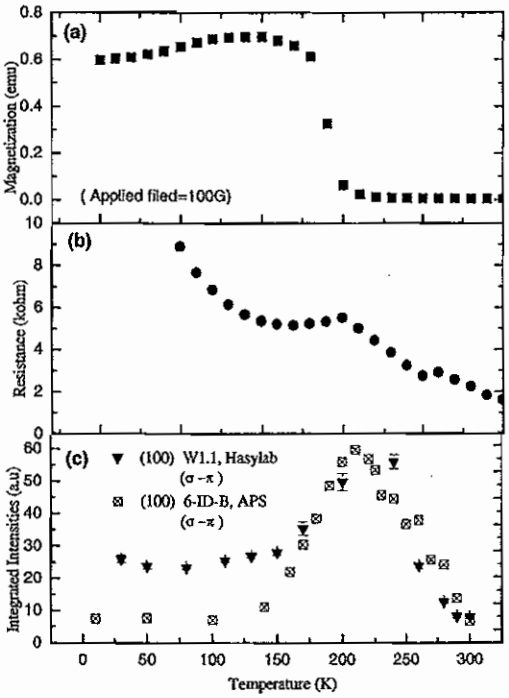

FIG. 2 Temperature behaviors of (a) magnetization; (b) resistance; (c) integrated intensities of the (100) resonant reflection (the black triangle: W1.1 data; the red square: 6-ID-B data)

A low temperature 4-contact-probe facility and a SQUID were used for the measurements of resistance and magnetization, respectively. The electric and magnetic characterizations of the x~0.125 sample is shown in Fig. 2 (a) and (b). It has a very sharp FM transition at T_C ~ 200 K, the resistance shows a small down turn below T_C, which is an indication of metallic behavior. A typical insulating feature appears again below T_{OO} ~ 170 K.

The RXS of the Mn K-absorption edge appears to be an ideal probe for the interplay between charge, orbital and lattice degrees of freedom. RXS measurements were undertaken using a standard four-circle vertical scattering geometry, both at the W1.1 beamline, HASYLAB and the 6-ID-B undulator beamline, the Advanced Photon Source (APS) near Chicago. The (100) plane of the sample was aligned within the scattering plane. A huge resonant enhancement of the forbidden reflections (100) and (300) was observed at a photon energy close to the Mn K-edge. The energy dependence of (100) reflection measured at 6-ID-B is shown in Fig. 3. This reflection shows similar energy dependence at all three temperatures. This observation is consistent with the one obtained at the W1.1 beamline, but with much improved quality due to much

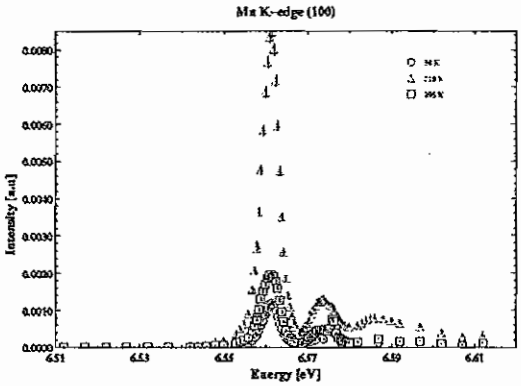

FIG. 3 Energy dependence of integrated intensities of the (100) resonant reflection at three temperature (the blue square: 295K; the green triangle: 210K; the red circle: 50K)

higher photon flux and also better energy resolution achieved at 6-ID-B. With polarization analysis, it is confirmed that the scattered beam of the (100) reflection is $\sigma \rightarrow \pi$ dominated. This is an indication of a dipolar transition (1s→4p). The temperature dependence of the (100) resonant scattering is displayed in Fig. 2 (c). The measurements at two different beamlines show similar behavior. The (100) resonance can even be observed at room temperature. A peak splitting was observed for the (100)/(300) resonance and the (200) Bragg reflection in the intermediate temperature region (150 - 260K). This is an indication of the presence of cooperative Jahn-Teller distortions. Therefore, our data clearly demonstrates a strong interplay between lattice distortion, orbital ordering and RXS. Furthermore, a high-energy X-ray diffraction measurement was undertaken to determine the complex structural feature in the same sample at the 6-ID-D side station of Mu-CAT, APS. High-energy X-ray photons have a very large penetration, making it very suitable for the studies of true bulk properties of materials. In addition, a shorter wavelength means a much larger reciprocal space that can be accessed. During measurements, X-rays of an energy of 88 keV were used and a MAR345 image plate detection system was employed. The data analysis is still in progress.

We acknowledge the invaluable technical and scientific supports from RWTH (Aachen, Dr. Kaiser), HASYLAB (Hamburg), and APS (Argonne, D. Robinson).

1] *Colossal magnetoresistance oxides*, edited by Y. Tokura (Gordon and Breach Science Publishers, London, 2000)
[2] J. Orenstein and A.J. Millis, Science **288**, 468 (2000)
[3] M. Imada, *et. al.*, Rev. Mod. Phys. **70**, 1039 (1998)
[4] V.I. Anisimov *et. al.*, Adv. in Cond. Matt. Sci. **1**, 97(2000)
[5] Y. Endoh *et. al.*, Phys. Rev. Lett. **82**, 4328 (1999)
[6] M. Benfatto, *et. al.*, Phys. Rev. Lett. **83**, 636 (1999)
[7] P. Benedetti *et. al.*, Phys. Rev. B **63**, 060408(R) (2001)
[8] D.E. Cox *et. al.*, Phys. Rev. B **64**, 024431 (2001)
[9] K. Tsuda *et. al.*, J. Phys. Soc. Jpn. **70**, 1010 (2001)

Near surface order at CuAu (001)-surfaces

W. Schweika*,W. Babik*,H. Reichert+, O. Klein+, S. Engemann+, A. Fattah*, W. Caliebe*
*Institut für Streumethoden, IFF
+Max-Planck-Institut für Metallforschung, 70569 Stuttgart

By in-situ x-ray reflectivity measurements we observed an ordered layer near the (001) surface of a CuAu single crystal well above the bulk transition temperature. An Au-rich uppermost layer induces a temperature dependent oscillating order profile perpendicular to the surface, which is accompanied by strong lattice relaxations consistent with the tetragonal near surface structure and the cubic disordered bulk. The Parrat recursion formalism was used to model the Fresnel reflectivities resolving the electron density distributions on an atomic scale.

F&E-Nr.: 23.55.0

Phase transitions in real crystals are affected by the presence of free surfaces and internal interfaces [1]. Missing bonds may reduce the order near a surface, which could lead to surface induced disorder, a wetting phenomenon that, for example, describes the melting of ice [2]. Intuitively, one might not expect the opposite, surface induced order. However, experiments and Monte Carlo simulations demonstrated the possibilities of stable near surface order in equilibrium with an disordered bulk [3]. Lateral surface ordering may occur in systems with frustrated bulk order and furthermore, a wide-spread phenomenon of surface enrichment of an alloy component may induce order perpendicular to the surface [4]. Both ordering mechanisms are competing at CuAu(001) surfaces, although surface enrichment of Au is expected from other experiments. Any possible surface induced layering of AuCu will be accompanied by lattice strain arising at the interface between the phases of different symmetries and lattice parameter, the cubic disordered bulk phase and surface layer of ordered tetragonal CuAu.

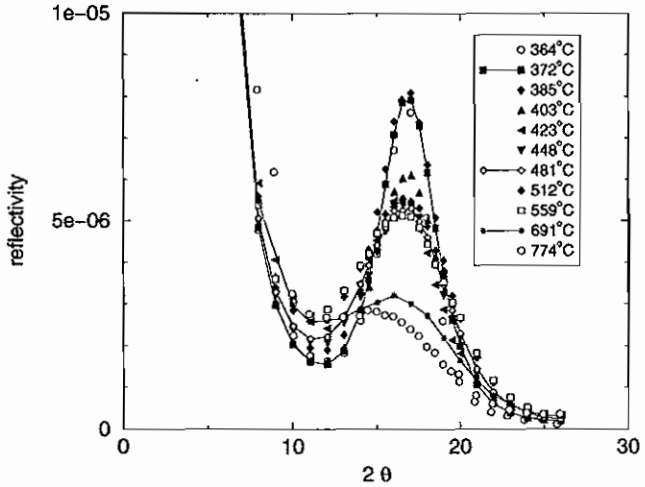

FIG. 1. Temperature dependence of the near surface order measured by reflectivity of the (001) surface.

We have performed in-situ x-ray scattering experiments at the HASYLAB beamline W1.1 on a single crystal of CuAu with a (001)-surface cut. A modulation of the specular intensity, as shown in Fig. 1, is observed near the (001) ordering wave vector, which gives direct information about the excess order perpendicular and near to the (001) surface. The temperature dependence indicates a marked increase of the ordered layer thickness and a growth of the ordered surface layer upon the disordered bulk.

In order to model these intensities the usual approaches within the Distorted Wave Born Approximation (DWBA) based on the continuum description are quantitatively not adequate, since at high Q the increase due to the truncation rod around the (002) Bragg peak is significant. Corrections within a kinematic approach do not account for interference terms. Therefore, we have devised a new approach using the realistic electron density distribution on an atomistic scale, and based on a recursion algorithm (Parrat [5]), calculating numerically the coefficients of reflexion and transmission of the wave in slices, which are sufficiently small compared to interatomic spacings. [6]

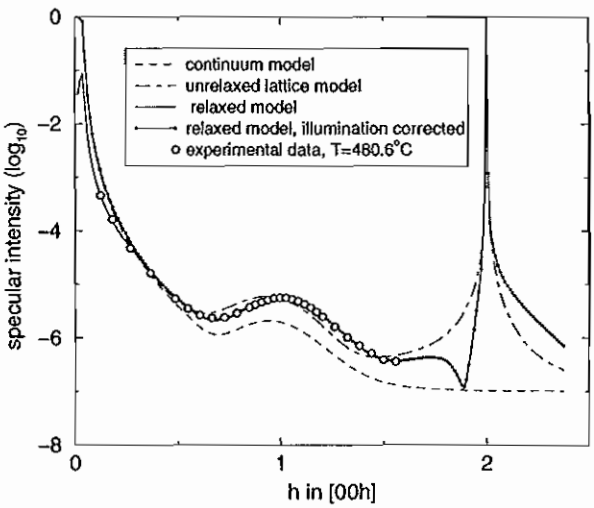

FIG. 2. Intensity modeling (within the DWBA) due to near surface order and induced lattice relaxation at the (001)-surface; $T = T_{c,bulk} + 70°C = 480.6°C$.

Within our approach the measured intensities can be successfully modeled as shown in Fig. 2. In detail, a tanh-profile is used to describe the oscillating near surface order of Au- and Cu-rich planes, determining in particular, the interfacial width and position, and simultaneously the lattice relaxation across the interface. The surface roughness is modeled by another independent tanh-profile. The surface roughness is small, typically 0.5 Å for all temperatures. The comparison with the unrelaxed model reveals an asymmetry around the (001) that is related to lattice relaxations, of typically -7% at the surface. This asymmetry is even more evident at the truncation rod near the (002) Bragg.

Figure 3 displays the concentration and relaxation profile of the ordered state near the surface. This example is related to the intensity modeling shown in Fig. 2. The ordered state near the surface still exists at temperatures well above the bulk order-disorder transition temperature. The uppermost layer is essentially occupied by pure Au even at high temperatures near to 800°C, and subsequent deeper atomic layers display an oscillating concentration profile and lattice relaxations consistent with the expected tetragonal lattice parameter of ordered CuAu-I domains.

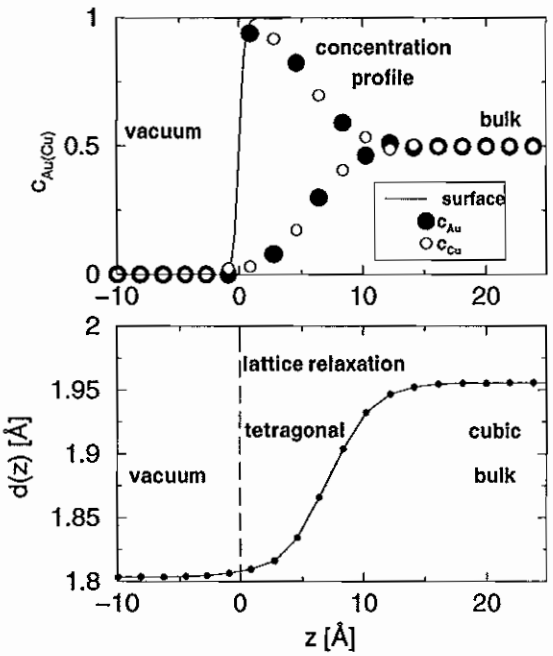

FIG. 3. Near surface order and induced lattice relaxation at the (001)-surface ($T = 480.6°C$), related to the data and fit shown in Fig. 2.

With decreasing temperatures there is an increase of both, position and width of the interface between the ordered surface layer and the disordered bulk. The wetting theory [1] predicts a logarithmic growth of the surface layer thickness, as the temperature approaches the bulk transition. However, even in the undercooled state and close to the bulk transition, the thickness of the near surface ordered layer does not exceed more than a very few atomic layers, see Fig. 4.

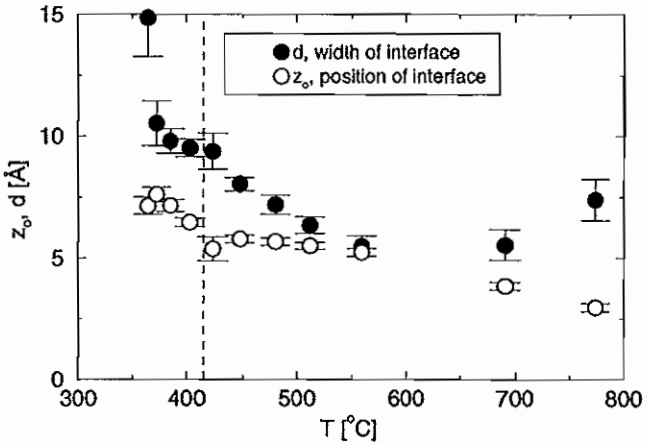

FIG. 4. The temperature dependence of the interface position and width.

In a previous study of (001)-surfaces of Cu_3Au it was also found that the ordering perpendicular to the surface does not diverge at the transition temperature but at an extrapolated spinodal temperature below. However, in the Cu_3Au case only the perpendicular component of the order parameter and but not the lateral component is induced by the surface [7]. In analogy to the melting of ice [2], which cannot be overheated due the presence of a disordered surface layer acting as a nuclei, here, the ordered surface layer, which indeed is a complete nucleus of the CuAu-I bulk phase, should wet the bulk at the transition near $410°C$. Therefore, we conclude that the observed incomplete wetting and undercooling is a consequence of lattice relaxations near the surface.

[1] R. Lipowsky, Ferroelectrics 73, 69 (1987)

[2] H. Dosch, L. Mailänder, A. Lied, J. Peisl, F. Grey, R.L. Johnson, Phys. Rev. Lett. 60, 2382 (1988).

[3] W. Schweika, K. Binder, D.P. Landau, Phys. Rev. Lett. 65, 3321 (1990);

[4] W. Schweika, D.P. Landau, K. Binder, Phys. Rev. B 53, 8937 (1996); W. Schweika, D.P. Landau, K. Binder, in *Stability in Materials*, Edited by A. Gonis and P.E.A. Turchi, Plenum Press, New York (1996) p.165.

[5] L. G. Parrat, Phys. Rev. **95**, 359 (1954).

[6] W. Babik, Ph.D. thesis, to be published.

[7] H. Reichert, P.J. Eng, H. Dosch, I.K. Robinson, Phys. Rev. Lett. 74, 2006 (1995).

Investigation of confined soft matter thin films using scattering methods

O.H. Seeck, M. Mihaylova, and E. Küssel
Institute for Scattering Methods

Block copolymer thin films on silicon substrates and liquid films confined between two sapphire crystals have been studied with x-ray scattering methods in order to determine their microscopic and mesoscopic structure. The block copolymers were investigated depending on the chemical composition, the film thickness and the temperature. Very interesting results could be obtained concerning an ordering of the molecules and a forming of micrometer sized holes at the surface. First experiments on confined liquids using a specially built setup have been performed. A short description of the cell, the diffractometer and the first results is given.

F&E-Nr: 23.89.1

The investigation of soft matter thin films is of enormous interest not only for fundamental physics (e.g. [1, 2]). It is also important for industrial applications. E.g., ultra thin polymer films can serve as coatings or membranes with unique properties. Specially designed polymer films are since short time used in micro electronics or for flexible display screens. Also of great interest is the behavior of extremely confined liquids, e.g. in micro hydraulics or as lubricants in micro machines.

To determine the exact properties of soft matter thin films, depending on parameters such as temperature, chemical composition or externally applied fields, the proper probe has to be chosen. Scattering experiments are usually superior if a complete picture of the film structure is desired [3]. A sketch of a typical scattering experiment to study the lubrication properties of a confined organic liquid with polar end groups is shown in Fig. 1.

I. BLOCK COPOLYMER THIN FILMS

Block copolymers are made from different homopolymer subchains which are chemically connected at their ends. Especially, if the homopolymers are immissible the block copolymer can self–assemble into periodic structures or form microscopic domains where the size and the shape is determined by a balance of entropic and enthalpic terms. For thin films the interaction with the substrate has to be taken into account. It can change the wetting behavior [4] and may cause an orientation of the molecules with respect to the substrate surface.

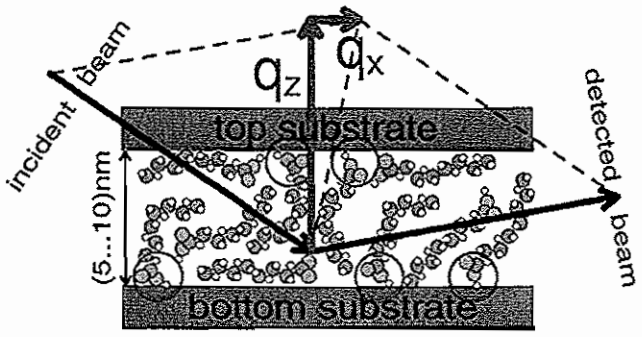

FIG. 1: Sketch of an x–ray scattering experiment at a confined lubricant. Some polar groups are attached to the substrates (circles) whereby lubrication is prevented. The vector sum of the incident and the scattered beam defines the components q_x and q_z of the wave vector transfer which are the scan parameters for the scattering experiments shown in this article.

The structure of polystyrene (PS) polyvinylpyridine (PVP) block copolymer films have been investigated with x-ray reflectivity and diffuse scattering synchrotron Hasylab/Desy (beamline W1) using a photon energy of 10.5keV. The samples were prepared on silicon substrates by Y. Séréro (AMOLF, Amsterdam) using a spin coating process. Symmetric diblock films were used with a molecular mass of the homopolymers of M_W = 28.2k each. Also, symmetric PS–PVP–PS triblocks (M_W of PVP is 60k) were prepared.

Figure 2 displays some reflectivities (q_z–scans at q_x=0), the respective Patterson functions, longitudinal diffuse scans (q_z–scans at a fixed offset q_x) and q_x–scans at fixed q_z. The films have a rather complex structure: The triblock film is not homogeneous but layered in z–direction with characteristic lengths of 75Å and 265Å, respectively. The surface is unstructured with hints to capillary wave roughness [3]. At the diblock films additionally to the layering an island/hole–structure forms on the surface which changes in temperature. Atomic force microscopy (AFM) pictures confirm the surface structure (Fig. 2) but they are not sensitive to the film bulk structure. Also, in situ temperature series can hardly be done with AFM. Detailed analysis of the scattering data will yield the information which the AFM cannot give.

II. THE CONFINED LIQUID SETUP

Confined liquids are thin films of only some molecular diameter thickness which are trapped between two flat substrates. They are strongly influenced by the substrate potential and show completely different behavior compared to the bulk [5]. For investigation scattering methods which can penetrate the substrates are most suitable but an extremely complex environment is required. We built up a diffractometer at the beamline Petra 1 (Hasylab/Desy) and a sample cell to apply high pressure perpendicular to the substrate surfaces (Figure 3).

The setup can be used for reflectivity and grazing incidence diffraction measurements to determine the in–plane and perpendicular structure of the confined films while tuning the temperature between 0°C and 100°C

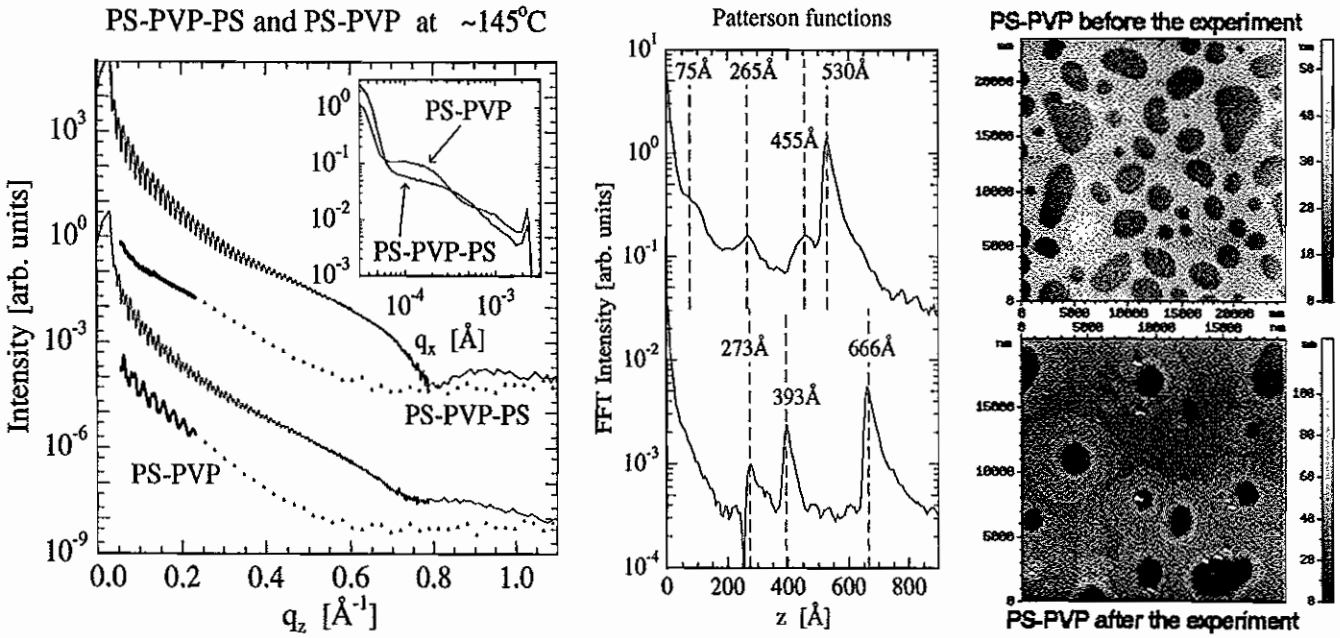

FIG. 2: Left: Reflectivities (lines) and longitudinal diffuse scans (symbols) of a PS–PVP–PS sample and a PS–PVP film. The diblock data is shifted by 4 orders of magnitude. Inset: diffuse q_x–scans where the PS–PVP sample has a rather complex structure. Center: Patterson functions of the reflectivities. The diblock data is shifted by two orders of magnitude. Right: AFM–pictures of the diblock before and after the experiment. The heating process causes halos around the holes.

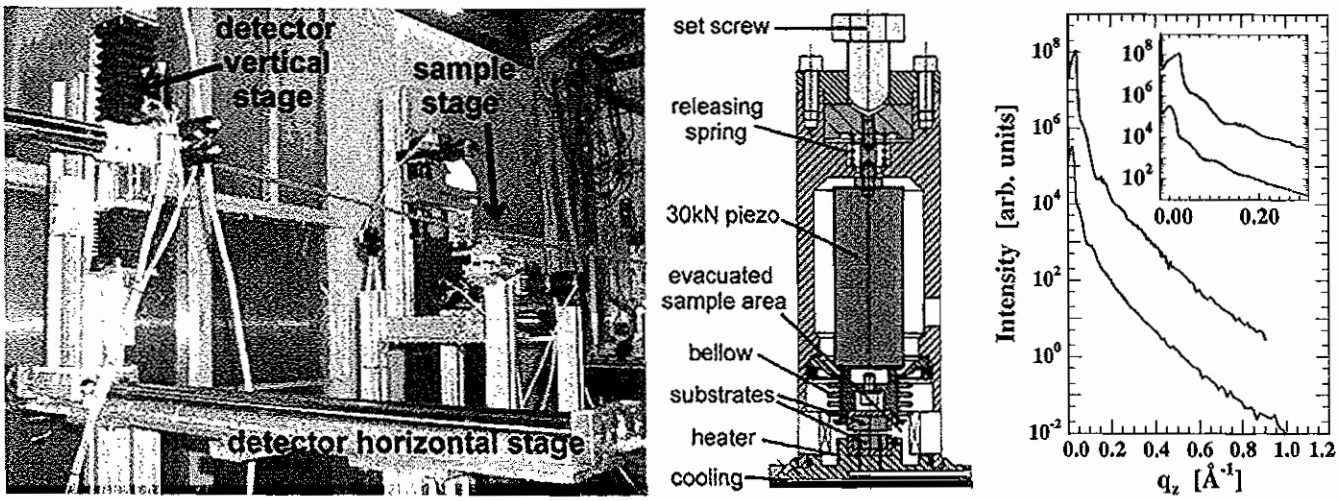

FIG. 3: Left: Overview of the diffractometer at Petra 1. The incident beam from the right is marked magenta, the outgoing beam is green. Center: Sketch of the confined liquid sample cell which can be put on the sample stage. Right: Top reflectivity (red) taken from a single substrate with 80Å CCl_4–layer. Bottom reflectivity (green, shifted in intensity) taken from a confined CCl_4–film (about 160Å gap size). The inset shows the small q_z–range.

and the perpendicular pressure up to 30kN. First test experiments have successfully been performed with Tetrachloromethane (CCl_4) which could be confined to 160Å gap distance (Fig. 3). After improving the cell further experiments will be done to reach to even smaller gap distances.

[1] M. Tolan, et al., Phys. Rev. Lett. **81**, 2731 (1998).
[2] J. Wang, et al., Phys. Rev. Lett. **83**, 564 (1999).
[3] M. Tolan, *X-ray Scattering from Soft Matter Thin Films*, Springer Tracts in Modern Physics, Vol. 148 (Springer, Berlin, 1999).
[4] G. Wong, et al., Phys. Rev. Lett. **77**, 5221 (1996).
[5] J.N. Israelachvili, et al., Science **240**, 189 (1988).

Development of low γ-sensitive neutron image plate detector

S. Masalovich, M. Schlapp, A. Ioffe, E. Küssel, H. von Seggern*, Th. Brückel
Institute for Scattering Methods
** Darmstadt University of Technology*

Different storage phosphors and neutron converters have been tested to find an appropriate mixture for the neutron image plate with low γ-sensitivity. It is shown that the mixture KCl:Eu^{2+} (storage phosphor) and ^{6}LiF (neutron converter) is a very attractive detector material to be used in a high γ-background environment.

F&E-Nr: 23.89.1

A large area position-sensitive neutron detector is under construction at the Forschungszentrum Jülich. The design specifications for the detector aimed to measure both high intensity Bragg reflection peaks and low intensity neutron diffuse scattering of thermal neutrons are the following:

- wide dynamic range with a linear response;
- high efficiency for thermal neutrons ($\lambda_t \geq 0.8$ Å);
- large area (~600 x 600 mm^2);
- spatial resolution of about 1 mm.

In addition, the ability for the detector to operate in a relatively high γ-background environment becomes extremely important since it will be installed directly in the reactor hall.

Neutron image plates (IP) based on a photostimulable storage phosphor correspond closely to these requirements and are presently commercially available. Unfortunately, they feature a relatively high γ-sensitivity. We found experimentally [1] that the γ-ray dose rate of 1μS/h is equivalent to a neutron flux of about 1.2 n/cm^2sec, which is comparable to magnitudes of weak diffraction peaks and diffuse scattering at thermal neutron scattering experiments. The high γ-sensitivity of a neutron IP results from the fact that originally image plate was developed as a detector for X-ray radiography [2]. Thereafter, different methods have been proposed to develop a neutron sensitive IP. These methods are mainly based on the addition of a neutron absorbing material (converter) to the same storage phosphor [3]. After absorbing a neutron, the converter emits ionising radiation, which can create a latent image in the phosphor. At present commercially available neutron IP's are composed of a fine mixture of storage phosphor (BaFBr:Eu^{2+}) and neutron converter (Gd_2O_3) powders in an organic binder coated onto a plastic support.

We present here the experimental results obtained with the use of alternative materials with reduced γ-sensitivity aimed at a development of a neutron image plate detector for low neutron flux measurements and capable to operate in a relatively high γ-background.

An apparent way to suppress the γ-ray sensitivity is the use of materials with a smaller effective atomic number. Thus, the compound ^{6}LiF with a low atomic number on the one hand and with large neutron absorption cross section on the other is well suited to be used as a neutron converter instead of Gd_2O_3 [4]. The use of ^{6}LiF results in some problems due to a low neutron capture cross section compared to Gd_2O_3. However one could expect this disadvantage is compensated by a much higher energy released in the neutron capture reaction (Table 1).

	^{6}LiF	Gd_2O_3
Neutron absorption length (μm), λ = 1.8Å	170	8.5
Released energy, MeV (usable)	4.8	0.07

Table 1. A comparison of ^{6}LiF and Gd_2O_3 as a neutron converter material for an image plate.

As for a new storage phosphor for a neutron IP, two promising candidates are known: KCl:Eu^{2+} and KBr:Eu^{2+}, which have already be shown to be applicable as x-ray, electron beam and UV storage phosphors [5].

Fig.1 shows the calculated photon energy stopping power (γ-ray sensitivity) for different materials under investigation.

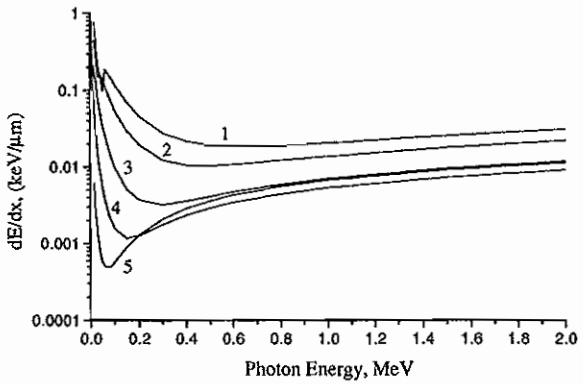

Fig.1. Photon energy stopping power:
1 – Gd_2O_3, 2 – BaFBr, 3 – KBr, 4 – KCl, 5 – LiF

One can see that the energy transferred to the particular material by photons during their passage through this material depends on the photon energy.

We found experimentally the γ-rays energy spectrum in a reactor hall (FRJ-2) is rather soft with an effective average energy of about 0.3 MeV. Therefore, a considerable advantage of new materials with respect to the sensitivity to such γ-rays is evident.

Experimental investigations of different storage phosphors and neutron converters were performed at the reactor FRJ-2, FZ Jülich. Three different storage phosphors are used in the experiments: (1) BaFBr:0.1% Eu^{2+} (average grain size: 40 μm), (2) KCl:0.05% Eu^{2+} (grain size: 50 μm) and (3) KBr:0.05% Eu^{2+} (grain size: 50 and 100 μm). Each phosphor was mixed with various amounts of ^{nat}LiF (30, 50, 70 and 90 mol%, grain size: 3 μm) or GdF_3 (20, 35

and 50 mol%, grain size: 2 μm) and placed in 1 mm thick quartz cells. Neutron exposure was done at the nonmonochromatic neutron beam with maximum of spectra at $\lambda \approx 5$ Å. In the case of γ-exposure the 0.6 mm thick Cd shield was used to block all neutrons and to increase the γ-rays dose. After exposure, the photo-stimulated luminescence (PSL) from each sample was determined with a set-up developed in Darmstadt University of Technology. The intensity of this luminescence is proportional to the energy deposited in the storage phosphor and thus determines the sensitivity of an image plate. The measured PSL intensities for different phosphors and for different neutron converters mixed with each phosphor are shown in Fig.2 [6]. The intensities induced by neutrons and γ-rays are further denoted as PSL(n) and PSL(γ) respectively. While the PSL(n) was measured for all samples, the determination of γ-sensitivity was done only on selected samples.

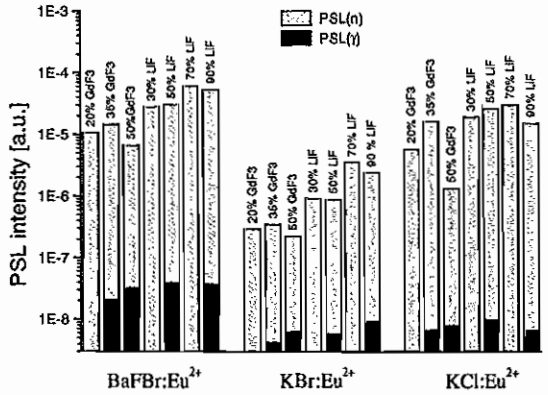

Fig.2. Comparison of PSL after neutron and γ irradiation. For samples displaying only PSL(n) the PSL(γ) was not determined; PSL(γ) superimposed on the PSL(n) intensity. PSL(n) intensities are normalized to the same neutron absorption.

It can be seen that the PSL(γ) measured for the (KCl + ^{nat}LiF) mixture is about 10 times less against the (BaFBr + GdF_3) with about the same PSL(n). Thus, it is observed for the first time that the system KCl-LiF is very attractive material for neutron image plates to be used in environments with a high γ-background. In spite of a relatively small PSL(n), the system (KBr + ^{nat}LiF) has to be considered as well. An advantage of this system is that the stimulation spectrum in case of KBr:Eu matches well a He-Ne laser wavelength, thus expediting a readout processing.

To maximize the neutron signal (PSL(n)) for a desired neutron energy the appropriate molar ratio for the storage phosphor – neutron converter mixture has to be found. Figure 3 displays the calculated and the measured dependence of the PSL(n) on the relative part (molar ratio) of the storage phosphor in a mixture. The calculation is based on the following formula:

$$PSL(n) \propto \{1 - \exp(-N^{*}\sigma(\lambda)d\}\frac{(1-k)}{kA+(1-k)} \qquad (1)$$

Here N* - averaged atomic density of the neutron converter material in a sample; $\sigma(\lambda)$ – absorption cross section for neutrons with wavelength λ; d – sample thickness; $k = N^*/(N \cdot d \cdot f)$; N – bulk atomic density of neutron converter; f – packing ratio for powdered sample; $A = [dE/dx]_c/[dE/dx]_p$ – converter/phosphor energy deposition ratio; dE/dx – stopping power for charged particle (alpha, triton) in a neutron converter or in a storage phosphor.

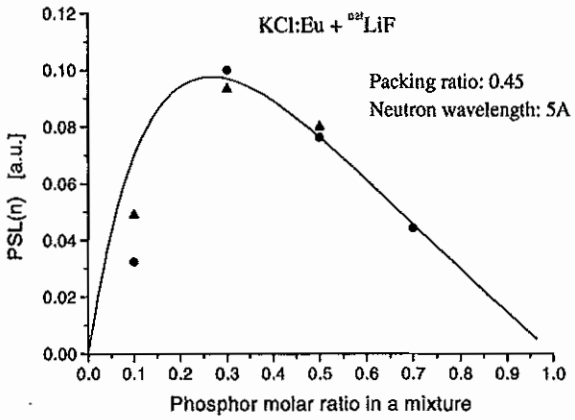

Fig.3. Photostimulated luminescence (PSL) of the samples with different molar ratio of the storage phosphor.
Solid line corresponds to the equation (1); • - experimental data (normalized) measured in June, 2001; ▲ - experimental data (normalized) measured in October, 2001 with a different geometry of the experimental setup.

One can see that the calculated curve in Fig.3 matches well the experimental data. Thus the equation (1) can be used for an estimation of an appropriate molar ratio for the storage phosphor – neutron converter mixture and for a study of an influence of other parameters (neutron wavelength, isotope content, packing ratio) as well.

The use of ^{6}LiF as a neutron converter and the first realization of a position sensitive neutron detector based upon new materials are in progress.

1. S.Masalovich, A.Ioffe et al, Appl. Phys. A, in press
2. J.Miyahara, K.Takahashi et al, Nucl. Instr. and Meth. **A246**, 572 (1986)
3. Y.T.Cheng, D.F.R Mildner, Nucl. Instr. and Meth. **A454**, 452 (2000)
4. M.Thoms, Nucl. Instr. and Meth. **A424**, 34 (1999)
5. H.Nanto, M.Miyazaki et al, IEEE Trans. Nucl. Sci., **47**(4), 1620 (2000)
6. M.Schlapp, H. von Seggern et al, Appl. Phys. A, in press

Stress Wave Experiments with the ASTE Mercury Spallation Target

H. Conrad[1], C. Byloos[1], M. Cates[2], B. Riemer[2], J. Hastings[3], H. Spitzer[4]
[1] *Institute "Scattering Methods"*
[2] *Oak Ridge National Laboratory, USA*
[3] *Brookhaven National Laboratory, USA*
[4] *Paul-Scherrer-Institut, Schweiz*

Single and multi-bunch pulses from the Brookhaven AG synchrotron have been employed to measure stress waves on the surface of the ASTE mercury target container. A systematic study of both axial and hoop stresses has been made using 30 fiber-optical Fabry-Perot strain gauges distributed over the container surface. Simultaneous power deposition measurements with 31 thermocouples placed within the mercury have been done in order to serve as input for computer simulations. Selected results from these experiments are presented and compared to finite elements calculations. A reasonably good quantitative agreement of experiment and simulation seems to be obtained. Tentative conclusions concerning the integrity of a liquid metal target container exposed to high-energetic short proton bursts are presented.

F 23 600

The European spallation source (ESS) is a project for a proton accelerator driven pulsed neutron source of the next generation (www.kfa-juelich.de/ess/). It is planned to comprise both a long and a short pulse target station of 5 MW time average proton beam power each. The former will be operated at a pulse repetition rate of 16 2/3 s^{-1} and a proton pulse duration of 2 ms, whereas the latter will be operated at a pulse repetition rate of 50 s^{-1} and a proton pulse duration of 1.4 μs. A proton energy of 1.33 GeV has been selected, which will be generated by a linear accelerator. Whereas the long pulse station will be fed directly by the linac, the short pulses are obtained by accumulating additional linac pulses in two compressor rings. For both stations liquid mercury has been chosen as the target material. The energy content of each pulse on the short pulse target is 100 kJ, of which about 60% are deposited within the mercury.

A particular problem of a liquid metal target subject to extremely short proton pulses are the pressure and stress waves due to the shock-like energy deposition into the target and its container within only 1.4 μs. Thereby, stress waves within the container walls are generated by direct heating of the beam window as well as by pressure waves due to the rapid heating of the mercury proper. Numerical calculations had indicated [1] that stresses in the container wall may be close or even beyond permissible limits for typical austenitic or martensitic steels.

Checking these predictions is of utmost importance for a service life assessment of liquid metal targets, in particular with respect to spallation sources in the MW regime like SNS, JSNS or ESS. Therefore it had been decided to perform experiments under realistic energy deposition conditions. An international collaboration (ASTE, AGS Spallation Target Experiment) had been established employing the Alternating Gradient Synchrotron (AGS) at Brookhaven for these studies. The mercury target used by the ASTE collaboration is of cylindrical shape with a length of 1.3 m and a semi-spherical beam window. The vessel diameter is 0.2 m with a wall thickness of 0.25 cm (see Fig. 1). The target is equipped with thermocouples in 31 relevant locations within the mercury in order to measure the distribution of energy deposition during the pulse. Stress waves are measured with 30 ultra-fast fiber-optical Fabry-Perot strain gauges attached to appropriate positions on the container surface.

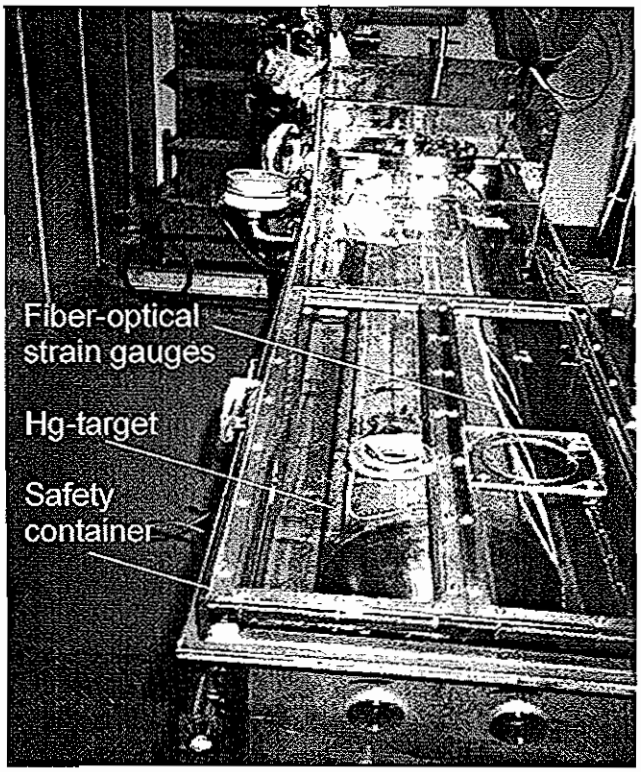

FIG. 1. The ASTE mercury target system with 30 ultra fast fiber-optical Fabry-Perot strain gauges distributed over the target surface.

According to the operating mode of the AGS, multiple bunches of 24 GeV protons with up to 3×10^{12} particles per bunch could be delivered to the target at a rate of approximately 30 Hz. Due to only 8 available data acquisition units

for the strain gauges, some 50 single bunch shots had been taken using varying combinations of gauges. Several 6 and 12 bunch shots were recorded in addition in order to check the absence of unwanted disastrous stress build-up with multiple bunches.

An example of energy deposition in mercury with a 12 bunch shot is shown in Figure 2. The plotted temperature rise measured with thermocouples located along the target axis corresponds roughly to that expected in a single ESS pulse of 1 μs duration. A typical result of axial stress wave propagation along the target surface is shown in Figure 3. For the sake of clarity, the response of only two strain sensors are shown in this plot.

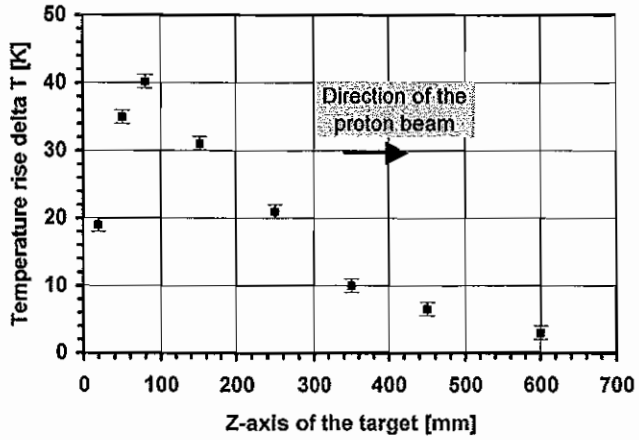

FIG. 2 Temperature distribution along the Z-axis of the ASTE mercury target with 12 proton bunches of 85 kJ total energy deposited within 330 ms.

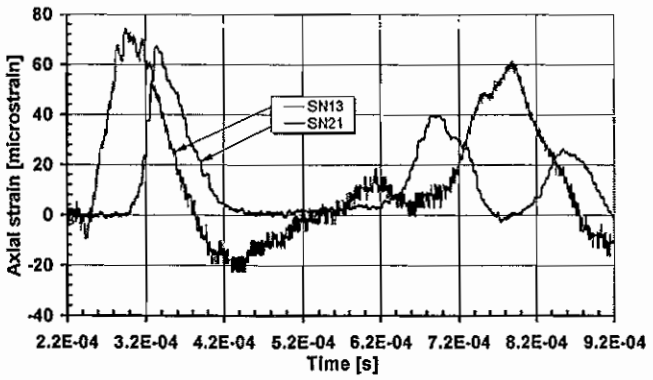

FIG. 3. Response of two selected strain sensors on the ASTE mercury target as a function of time after the impact of a single pulse with 2.54×10^{12} protons of 24 GeV. Deposited energy is 6kJ corresponding to about 10% of an ESS pulse. The sensors are mounted aligned along the target surface at 11 cm (SN13) and 40 cm (SN21) from the beam window. They quantitatively exhibit the different propagation times of axial stress waves in steel (pulse impact is at $t = 2.2\times10^{-4}$ s). Even the striking feature of stress wave reflections from a massive flange at the target end is seen by observing a reversal of the time sequence of strain maxima.

The absolute strain numbers and the time dependence are in good agreement with finite elements calculation using the commercial code ABAQUS. An example is shown in Figure 4. It should be pointed out that in order to speed up the computations, the length of the model target used had been 0.7 m only. Therefore stress wave reflections occur at correspondingly shorter times in the numerical calculations as compared to the experimental observation. Remarkably, the calculations exhibit more details than the experimental data. In particular, the double peak structure of the calculated strains (viz. Fig. 4) fit extremely well the superposition of stress waves caused by direct heating of the steel container and stresses due to the impact of the pressure wave generated in the mercury proper.

From the results of the present experiment we can conclude that reliable and reproducible strain data are available now. Numerical calculations with a parabolic beam profile ($r = 2$ cm, $E_{dep} = 2.5$ kJ) yield axial strains between 56 and 70×10^{-6} at selected locations, whereas the experimental data at corresponding locations with a Gaussian profile ($\sigma = 1.3$ cm, $E_{dep} = 5.8$ kJ) range from 64 to 74×10^{-6}. Despite the different energy density distributions with their maxima differing by about 40%, the agreement is surprisingly good. With a measured maximum strain of 100×10^{-6} (not shown here), the corresponding maximum stress is estimated to be 30 MPa at about 12 % of ESS energy deposited. With a wider beam cross section, extrapolation to full energy would at least not harm a cylindrically shaped target container. From multi-bunch runs it is deduced that no constructive stress interference is to be feared. Applicability of the present stress related conclusion to the much more sophisticated target shapes envisaged for SNS or ESS is not considered obvious. Experiments with corresponding target container shapes are proposed.

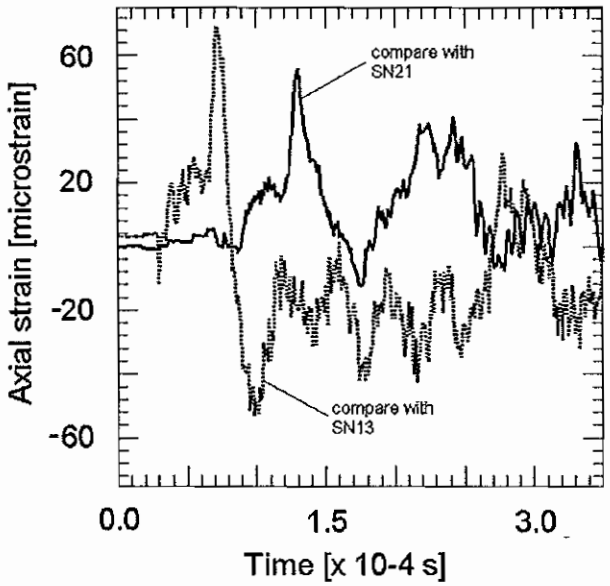

FIG. 4. Results from numerical simulations of stress waves in an ASTE-type target. The strains are plotted for the same positions on the target container surface as those selected for Fig. 3. Due to the shorter model target used in the calculations, the stress wave reflections occur at correspondingly shorter times.

REFERENCES

[1] L. Ni, G.S. Bauer, H. Spitzer; Nucl. Instr. Meth. A 425, 57 (1999)

[2] C: Byloos (unpublished)

Effect of high helium concentrations on mechanical properties and microstructure of candidate structural materials of the ESS-target.

P.Jung, J.Chen, H.Klein, W.Schmitz,
Institute for Scattering Methods
J.Henry*, J.C. Brachet*, *CEA Saclay (F)

9Cr martensitic steels, homogeneously implantation with helium to 0.5 at% at 250°C and 550°C, were tensile tested at room temperature and at the implantation temperature. Implantation at 250°C caused complete embrittlement, while some ductility was retained at 550°C.

F&E-Nr: 23.80.5

Spallation of heavy nuclei by protons in the GeV energy range can be used for nuclear waste transmutation, breeding of fissile material, and for producing neutrons for research purposes. Advantages in the latter case are non-criticality of the neutron source and the possibility to impose a time structure on the source which can give orders of magnitude higher effective neutron fluxes. At present Europe is proceeding on two projects, ADS (accelerator driven system) for nuclear waste transformation, and ESS which is planned to replace the high flux research reactors, most of which soon will reach their end of life. In both projects the intended spallation targets are heavy liquid metals, eutectic Pb-Bi and Hg, respectively, which will be contained by steel structures. These structural materials, in particular the proton beam window and the entrance side of the liquid metal target container will experience, in addition to thermal and mechanical stresses, severe radiation damage by atomic displacements and production of large quantities of transmutation atoms from the intense fluxes of high energy protons and neutrons. Among these, helium is of particular concern as it has, next to hydrogen, the highest production rate (up to 1 at% per year), negligible solubility in solid metals, and unlike hydrogen, will be totally retained in the material. Effects of He on microstructure and mechanical properties of steels have been investigated in the fusion materials program, but accordingly mainly at higher temperatures (> 550°C) and at lower helium concentrations (<0.1 at%) than interesting for spallation sources.

Therefore in a co-operate program of FZJ and CEA, 100 μm thick specimens of two martensitic steels, 9Cr-1Mo (EM10) and 9Cr-1MoVNb (T91), which are candidate materials for ESS (European Spallation Source with Hg target), ADS (European Accelerator Driven System for transmutation of nuclear waste with PbBi target) and MEGAPIE (eutectic PbBi target for SINQ at PSI, CH), were homogeneously implanted with α particles to concentrations of 0.5 at% at the compact cyclotron of Forschungszentrum Jülich. Two implantation temperatures were selected, 250°C and 550 °C, corresponding to the maximum operating temperatures of ESS and ADS, respectively. Tensile testing of the specimens was performed both at room and implantation temperature. In the following only results for T91 are shown, which in essence are also representative for EM10. Fig.1 shows that implantation at 250 °C induced strong hardening and loss of ductility when tested at 250 °C, while no ductility was retained for testing at room temperature. Less severe hardening and embrittlement was observed after implantation at 550 °C and some plastic deformation occured before fracture.

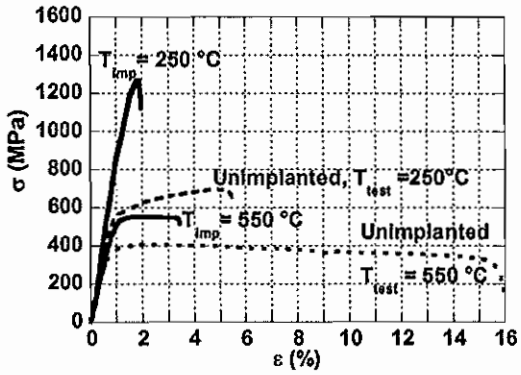

Figure 1. Stress-strain curves of T91 implanted to 0.5 at % He at 250°C and 550 °C. Tensile tests were performed at the

After tensile testing the fracture surfaces were characterised by scanning electron microscopy (Hitachi-F800 and JEOL 6004). Without implantation, fracture was fully ductile and transgranular while after implantation at 250 °C and testing at room temperature, specimens broke without any necking in predominantly intergranular fracture mode along prior austenitic grain boundaries (PAGs). Even some areas with cleavage-like features were found on the fracture surfaces. Tensile testing at 250 °C gave a more complex fracture mode. Fig 2a shows that necking had begun prior to rupture, in accordance with the tensile curve in Fig.1. Fracture occured partly along the necking line, which makes an angle of approximately 60 ° with the load axis. In this region of the fracture surface, the appearance is mixed: numerous intergranular facets are present, but some ductile features are also found (Fig.2c). This is not the case in that part of the specimen which broke perpendicular to the load axis. In this region, the fracture surface has a nearly fully intergranular

appearance (Fig.2b). After implantation at 550°C, some necking occured after both testing temperatures and less intergranular facets were seen than after implantation at 250 °C, in accordance with the tensile results.

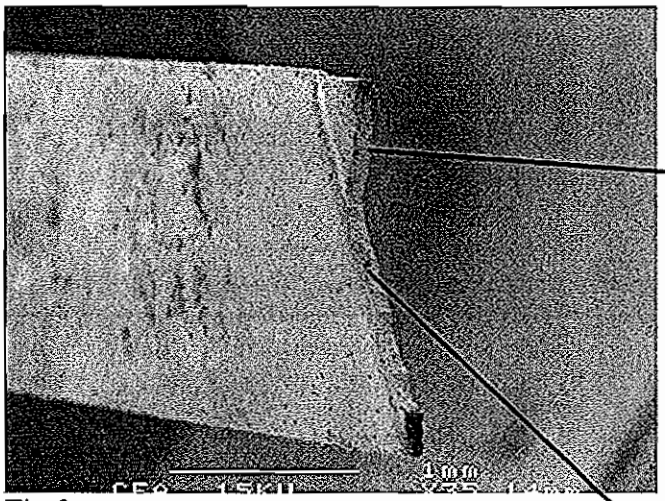

Fig. 2a.

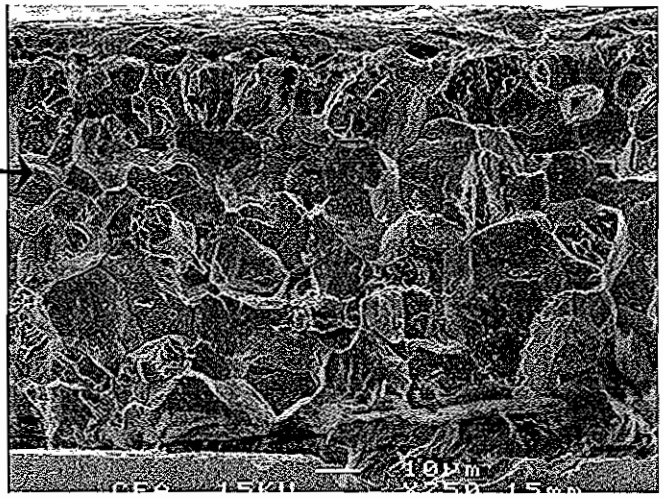

Fig. 2b.

Fig 2c.

Figure 2. T91 implanted to 0.5 at% He at 250°C and tested at 250 °C.
2a: general view of the broken specimen.
2b: fracture surface perpendicular to the the load axis.
2c: fracture surface perpendicular to the necking line.

After SEM analysis, 2 mm discs were punched from the gauge section of the tensile specimens and thin foils were prepared by jet electropolishing for microstructural examination by transmission electron microscopy (JEOL 2010 F, 200 kV and Philipps EM430, 300 kV). Again for a given implantation temperature, microstructures were very similar for both EM10 and T91. After implantation at 250 °C a large number density of small defect clusters but no bubbles were detected (Fig.3a). On the other hand, no point defect clusters but spherical as well as faceted bubbles were clearly observed in the specimens implanted at 550 °C which nucleated preferentially on dislocations inside the laths, sub-grains, laths, PAGs and on carbide-matrix interfaces

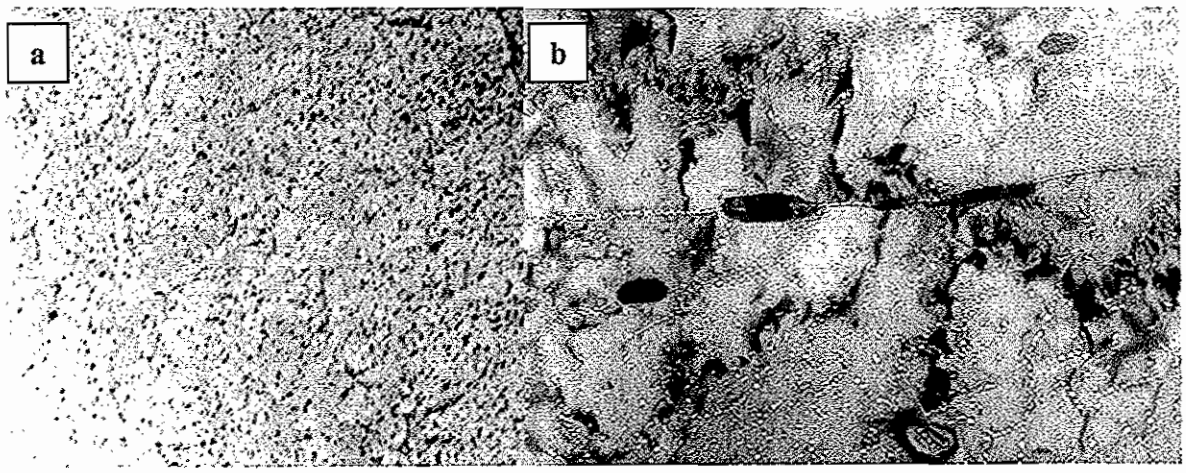

Figure 3. Bright field TEM micrograph of EM10 implanted to 0.5 at% He at 250 °C (a) and 550°C (b), respectively. At 250°C small defect clusters are observed (g=<110>, s>0), while at 55C°C He bubbles appear (under-focus imaging).

A discussion of the above tensile properties after implantation at 250 °C has to consider that a fully brittle intergranular fracture mode has never been reported for 9Cr martensitic steels before. The present He-implantations to 0.5 at% produce displacement damage of about 0.5 dpa. Neutron irradiation to this dose at similar temperatures in mixed-spectrum reactors which produces a few appm of He, yields much less hardening and embrittlement [1,2]. Indeed a calculation of hardening due to the defect clusters visible in Fig.3a gives good agreement with those results. Also He implantation both at lower temperatures [3] and at much higher rates [4] gave additional hardening only at higher concentrations. It may be speculated that under these conditions, He clusters are too small to significantly impede dislocation motion. Indeed Small-Angle-Neutron-Scattering (SANS) of the present specimens indicates the formation of small bubbles during implantation, with mean radii of less than 1 nm. Therefore it is proposed that not the displacement-induced black dot damage in Fig.3a, but a high density of small He bubbles is the main cause for the dramatic hardening and embrittlement following implantation at 250 °C, and that the brittle, intergranular fracture mode displayed by these specimens results from the combined effects of pronounced hardening of the grains and weakening of PAGs due to helium. Also the presence of a high carbide density on the PAG boundaries may promote crack nucleation and aid in the propagation of intergranular cracks.

A typical high-power spallation environment is characterised by a lower He creation rate and a higher damage rate than in the present imulation experiments. It is therefore expected that the helium distribution in the steels implanted at 250 °C is representative of spallation at lower temperature. Consequently, the severe embrittlement observed after implantation at 250 °C raises the question of the suitability of martensitic steels as structural materials for the ESS operation around 250 °C, while its use at the higher temperatures foreseen in ADS or MEGAPIE seems less problematic. In any case more data, both from simulation experiments (lower He concentrations, other temperatures and implantation rates, including TEM and SANS) and irradiations with a spallation spectrum, are obviously needed in order to obtain a more complete picture.

Part of this work was supported by the European Community under the SPIRE (Spallation and Irradiation Effects) project, Contract FIKW-CT-2000-00058.

[1] F. Abe, M. Narui and H. Kayano, Mater. Trans., JIM 34 (1993) 1053-1060
[2] K. Farrell, T.S. Byun, J. Nucl. Mater. 296 (2001) 129-138
[3] H. Ullmaier and E. Camus, J. Nucl. Mater. 251 (1997) 262-268
[4] J.D. Hunn, E.H. Lee, T.S. Byun and L.K. Mansur, J. Nucl. Mater. 282 (2000) 131-136

Publications in refereed journals

Brückel Th.; Hupfeld D.; Strempfer J.1; Caliebe W.; Mattenberger K.2; Stunault A.3; Bernhoeft N.4; McIntyre G. J.5
1APS at ANL, Argonne, USA
2ETH, Zürich, Switzerland
3ESRF, Grenoble, France
4CEA, Grenoble, France
5ILL, Grenoble, France
Antiferromagnetic order and phase transitions in GdS as studied with X-ray resonance-exchange scattering
Eur. Phys. J. B 19 (2001) 475 - 490
23.89.1

Brückel Th.; Strempfer J.1
1Northern Illinois University, DeKalb & ANL, Argonne, USA
Non-resonant Magnetic Diffraction at High X-ray Energies
Synchrotron Radiation News 14 (5) (2001) 16 - 20
23.89.1

Chen J.; Ullmaier H.; Floßdord T.; Kühnlein W.; Duwe R.; Carsughi F.1; Broome T.2
1University of Ancona, DIBIAGA, Italy
2Rutherford Appleton Laboratory, Chilton, UK
Mechanical properties of pure tantalum after 800 MeV proton irradiation
Journal of Nuclear Materials 298 (2001) 248 - 254
23.60.0

Dai Y.1; Jia X.1; Chen J.; Sommer W. F.2; Victoria M.3; Bauer G. S.1
1PSI, Spallation Neutron Source Division, Villigen, Switzerland
2Los Alamos National Laboratory, Neutron Science Center, USA
3Ecole Polytechnique Federal de Lausanne, Fusion Technology Materials, Switzerland
Microstructure of both as-irradiated and deformed 304L stainless steel irradiated with 800 MeV protons
Journal of Nuclear Materials 296 (2001) 174 - 182
23.60.0

Goerigk G.; Williamson D. L.1
1Colorado School of Mines, Dept. of Physics, Golden, USA
Comparative anomalous small-angle x-ray scattering study of hotwire and plasma grown amorphous silicon-germanium alloys
Journal of Applied Physics Volume 90, Number 11 (2001) 5808 - 5811
23.89.1

Goerigk G.; Williamson D. L.1
1Colorado School of Mines, Dept. of Physics, Golden, USA
Quantitative ASAXS of germanium inhomogeneities in amorphous silicon-germanium alloys
Journal of Non-Crystalline Solids 281 (2001) 181 - 188
23.89.1

Guilleaume B.1; Ballauff M.1; Goerigk G.; Wittemann M.2; Rehahn M.2
1Universität, Polymer-Institut, Karlsruhe
2TU, Institut für Makromolekulare Chemie, Darmstadt
Correlation of counterions with rodlike macroions as assessed by anomalous small-angle X-ray scattering
Colloid Polym Sci 279 (2001) 829 - 835
23.89.1

Haubold H.-G.; Vad Th.; Jungbluth H.; Hiller P.
Nano structure of NAFION: a SAXS study
Electrochimica Acta 46 (2001) 1559 - 1563
23.89.1

Ioffe A.; Mezei F.1,2
1HMI, Berlin
2Los Alamos National Laboratory, USA
4(-symmetry of the neutron wave function under space rotation
Physica B 297 (2001) 303 - 306
23.89.1

James M. R.1; Maloy S. A.1; Gac F. D.1; Sommer W. F.1; Chen J.; Ullmaier H.
1Los Alamos National Laboratory, USA
The mechanical properties of an Alloy 718 window after irradiation in a spallation environment
Journal of Nuclear Materials 296 (2001) 139 - 144
23.60.0

Jung P.; Liu C.; Chen J.
Retention of implanted hydrogen and helium in martensitic stainless steels and their effects on mechanical properties
Journal of Nuclear Materials 296 (2001) 165 - 173
23.60.0

Köbler U.; Fischer K.
The impact of fourth-order exchange interactions on the critical temperatures of EuxSr1-xS and EuxSr1-xTe
J. Phys.: Condens. Matter 13 (2001) 123 - 139
23.15.0

Köbler U.; Hoser A.1,2; Englich J.3; Snezhko A.3; Kawakami M.4; Beyss M.; Fischer K.
1HMI, Berlin
2RWTH, Institut für Kristallographie, Aachen
3Charles University, Faculty of Mathematics and Physics, Prag, Tschechische Republik
4University, Department of Physics, Kagoshima
On the Failure of the Bloch-Kubo-Dyson Spin Wave Theory
Journal of the Physical Society of Japan, Volume 70, Number 10 (2001) 3089 - 3097
23.15.0

Köbler U.; Hoser A.1; Kawakami M.2; Abens S.3
1RWTH, Institut für Kristallographie, Aachen
2Kagoshima University, Faculty of Science, Japan
3HMI, Berlin
Observation of a spin wave exponent of 5/2 in the uniaxial antiferromagnet MnF2
Physica B 307 (2001) 175 - 183
23.15.0

Köbler U.; Mueller R.; Brown P. J.1; Arons R. R.; Fischer K.
1ILL, Grenoble, France
Experimental identificaion of fourth-order exchange interactions in magnets with pure spin moments
J. Phys.: Condens. Matter 13 (2001) 6835 - 6852
23.15.0

Mezei F.1,2; Drabkin G.1,3; Ioffe A.
1HMI, Berlin
2Los Alamos National Laboratory, USA
3St. Petersburg Nuclear Physics Institute, Gatchina, Russia
Polarimetric neutron spin echo
Physica B 207 (2001) 9 - 13
23.89.1

Mueller R.
The Yb fiber laser for metastable 3He optical pumping at Jülich
Physica B 297 (2001) 277 - 281
23.89.1

Nerger S.; Kentzinger E.; Rücker U.; Voigt J.; Ott F.1; Seeck O. H.; Brückel Th.
1LLB (CEA/CNRS), Gif-sur-Yvette, France
Proximity effects in Fe1-xCox/Mn/Fe1-xCox trilayers
Physica B 297 (2001) 185 - 188
23.89.1

Nietubyc R.1; Sobczak E.1,2; Pelka J. B.1; Mackowski S.1; Janik E.1; Karczewski G.1; Goerigk G.
1Polish Academy of Sciences, Institute of Physics, Warsaw, Poland

2Polish Academy of Sciences, Center of Theoretical Physics, Warsaw, Poland
Anomalous small angle X-ray scattering study of CdTe quantum dots in ZnTe
Journal of Alloys and Compounds 328 (2001) 206 - 210
23.89.1

Pelka J. B.1; Paszkowics W.1; Dluzewski P.1; Dynowska E.1; Wawro A.1; Baczewski L. T.1; Koslowski M.1; Wisniewski A.1; Seeck O.; Messoloras S.2; Gamari-Seale H.3
1Polish Academy of Sciences, Warsaw, Poland
2NCSR Demokritos, Institute of Nuclear Technology, Attikis, Greece
3NCSR Demokritos, Institute of Materials Science, Attikis, Greece
Structural and magnetic study of Co/Gd multilayers deposited on Si and Si-N substrates
J. Phys. D: Appl. Phys. 34 (2001) A208 - A213
23.89.1

Pelka J. B.1; Paszkowicz W.1; Wawro A.1; Baczewski L. T.1; Seeck O.
1Polish Academy of Sciences, Warsaw, Poland
Structural study of Co/Gd multilayers by X-ray diffraction and GIXR
Journal of Alloys and Compounds 328 (2001) 253 - 258
23.89.1

Pinnow C. U.1; Bicker M.1; Geyer U.1; Schneider S.1; Goerigk G.
1Universität, I. Physikalisches Institut, Göttingen
Decomposition and nanocrystallization in reactively sputtered amorphous Ta-Si-N thin films
Journal of Applied Physics 90 (4) (2001) 1986 - 1991
23.89.1

Plakhty V. P.1; Maleyev S. V.1; Kulda J.2; Visser E. D.3,4,5; Wosnitza J.6; Moskvin E. V.1; Brückel Th.; Kremer R. K.7
1Petersburg Nuclear Physics Institute, Gatchina, Russia
2ILL, Grenoble, France
3University of Warwick, Dept. of Physics, Coventry, UK
4CLRC, ISIS Facility, RAL, Chilton, UK
5IRI, TU Delft, The Netherlands
6University, Physikalisches Institut, Karlsruhe
7MPI für Festkörperforschung, Stuttgart
Spin chirality and polarised neutron scattering
Physica B 297 (2001) 60 - 66
23.89.1

Plakhty V.1,2; Schweika W.; Brückel Th.; Kulda J.3; Gavrilov S. V.1; Regnault L.-P.4; Visser D.5
1Petersburg Nuclear Physics Institute, Russia
2FZJ, IFF-Streumethoden, Jülich
3ILL, Grenoble, France
4CEA, Grenoble, France
5CLRC, ISIS, Didcot, UK
Chiral criticality in helimagnet Ho studied by polarized neutron scattering
Physical Review B 64 100402(R) (2001) 100402-1 - 100402-4
23.89.1

Rücker U.; Bergs W.; Alefeld B.; Kentzinger E.; Brückel Th.
Polarization analysis for the 2D position-sensitive detector of the HADAS reflectometer in Jülich
Physica B 297 (2001) 140 - 142
23.89.1

Schweika W.; Böni P.1
1TUM, Garching
The instrument DNS: polarization analysis for diffuse neutron scattering
Physica B 297 (2001) 155 - 159
23.89.1

Schweika W.; Ice G. E.1; Robertson J. L.1; Sparks C J.1; Bai J.1
1Oak Ridge National Laboratory, USA
Diffuse Scattering of Cu3Au: Displacements and Fermi Surface Effects
Properties of Complex Inorganic Solids 2 (2000) 329 - 341
23.89.1

Shin K.1,2; Pu Y.2; Rafailovich M. H.2; Sokolov J.2; Seeck O.; Sinha S. K.3; Tolan M.4; Kolb R.5
1NIST, NCNR, Gaithersburg, USA
2SUNY, Stony Brook
3APS, ANL, USA
4University, Kiel
5Exxon Mobil
Correlated Surfaces of Free-Standing Polystyrene Thin Films
Macromolecules 34 (2001)5620 - 5626
23.89.1

Sobczak E.1; Nietubyc R.2; Pelka J. B.2; Mackowski S.2; Janik E.2; Karczewski G.2; Goerigk G.
1Institute of Physics and Center of Theoretical Physics PAS, Warsaw, Poland
2Institute of Physics PAS, Warsar, Poland
Anomalous Small Angle X-Ray Scattering Study of Self-Assembled Quantum Dots
Appl. Crystallogr. 18 (2001) 112 - 115
23.89.1

Syromyatnikov V. G.1; Toperverg B. P.1,2; Kentzinger E.2; Deriglazov V. V.1; Kampmann R.3; Pleshanov N. K.1; Pusenkov V. M.1; Schebetov A. F.1; Siebrecht R.4; Ul'yanov V. A.1
1Petersburg Nuclear Physics Institute, Gatchina, Russia
2FZJ, IFF, Jülich
3GKSS, Institut für Werkstofforschung, Geesthacht
4ILL, Grenoble, France
Off-specular polarized neutron scattering from periodic Co/Ti and aperiodic Fe/Al magnetic multilayers
Physica B 297 (2001) 175 - 179
23.89.1

Toperverg B.1,2; Nikonov O.3,4; Lauter-Pasyuk V.4,5; Lauter H. J.3
1Petersburg Nuclear Physics Institute, Gatchina, Russia
2FZJ, IFF, Jülich
3ILL, Grenoble, France
4Joint Institute for Nuclear Research, Dubna, Russia
5TUM, Garching
Towards 3D polarization analysis in neutron reflectometry
Physica B 297 (2001) 169 - 174
23.89.1

Toperverg B.1,2
1Petersburg Nuclear Physics Institute, Gatchina, Russia
2FZJ, IFF, Jülich
Specular reflection and off-specular scattering of polarized neutrons
Physica B 297 (2001) 160 - 168
23.89.1

Vasiliu-Doloc L.1; Osborn R.2; Rosenkranz S.2; Mesot J.2; Mitchell J. F.2; Sinha S. K.3; Seeck O.; Lynn J. W.4; Islam Z.1
1Northern Illinois University and APS/ANL, USA
2Materials Science Division, ANL, Argonne, USA
3APS/ANL, Argonne, USA
4NIST, USA
Neutron and x-ray evidence of charge melting in ferromagnetic layered colossal magnetoresistance manganites (invited)
Journal of Applied Physics 89, 11 (2001) 6840 - 6845
23.89.1

Vorobiev A.1; Gordeev G.1; Donner W.2; Dosch H.2; Nickel B.2,3; Toperverg B.1,4
1Petersburg Nuclear Physics Institute, Gatchina, Russia
2MPI für Metallforschung, Stuttgart
3ILL, Grenoble, France
4FZJ, IFF, Jülich
Reflectivity and off-specular neutron scattering from the free ferrofluid surface and silicon-ferrofluid interface

Physica B 297 (2001) 194 - 197
23.89.1

de Robillard Q.1; Guo X.1; Dingenouts N.1; Ballauff M.1; Goerigk G.
1University, Polymer-Institute, Karlsruhe
Application of Anomalous Small-Angle X-Ray Scattering to Spherical Polyelectrolyte Brushes
Macromol. Symp. 164 (2001) 81 - 90
23.89.1

Other publications

Brückel Th.
Elastic Scattering from Many-Body Systems
Schriften des Forschungszentrums Jülich: Materie und Material; Vol. 9 (2001) 3-1 - 3-28
23.89.1

Brückel Th.
Magnetism
Schriften des Forschungszentrums Jülich: Materie und Material; Vol. 9 (2001) 16-1 - 16-19
23.89.1

Conrad H.; Filges D.1; Hansen G.2; Neef R. D.1; Stelzer H.2; Tietze-Jaensch H.; Ullmaier H.
1FZJ, IKP, Jülich
2FZJ, ZAT, Jülich
Technische und methodische Entwicklungen am Target-Moderator-Reflektor-Komplex der ESS
Deutsche Neutronenstreutagung 2001, Schriften des Forschungszentrums Jülich, Reihe Materie und Material, Band 8 (2001) p. 83
23.89.1

Conrad H.; Ullmaier H.
Overview of the ESS Target and Moderator R&D
Proceedings of ICANS-XV, Tsukuba, Japan, 06. - 09.11.2000 (2001) 1137 - 1145
23.60.0

Conrad H.
German Neutron Users Meet in Jülich
Neutron News 12 (3) (2001), 4
23.89.1

Conrad H.
Neutron Sources
Schriften des Forschungszentrums Jülich: Materie und Material; Vol. 9 (2001) 1-1 - 1-15
23.89.1

Conrad H.
Status report on the Jülich ESS related activities
Proceedings of ICANS-XV, Tsukuba, Japan, 06. - 09.11.2000 (2001) 89 - 92
23.60.0

Goerigk G.; Williamson D. L.1
1Colorado School of Mines, Department of Physics, Golden, USA
Characterisation of Solar Cell Materials from Anomalous Small Angle X-Ray Scattering Studies
HASYLAB-Broschüre: Research at HASYLAB (2001) 18 - 20
23.89.1

Hupfeld D.; Brückel Th.; Schweika W.; Strempfer J.1; Mattenberger K.2; McIntyre G.3
1Northern Illinois University, de Kalb, USA
2ETH, Zürich, Switzerland
3ILL, Grenoble, France
Investigation of the magnetic properties of GdxEu1-xS with neutrons and x-rays
Deutsche Neutronenstreutagung 2001, Schriften des Forschungszentrums Jülich, Reihe Materie und Material, Band 8 (2001) p. 49
23.89.1

Ioffe A.; Conrad H.; Zeiske Th.; Mueller R.; Küssel E.; Massalovitch S.; Schlapp M.; Schmitz B.; Brückel Th.
Spektrometer SV30 für Polarisationsanalyse mit thermischen Neutronen am Forschungsreaktor FRJ-2
Deutsche Neutronenstreutagung 2001, Schriften des Forschungszentrums Jülich, Reihe Materie und Material, Band 8 (2001) p. 91
23.89.1

Kentzinger E.; Rücker U.; Toperverg B.; Brückel Th.
Reflectivity and off-specular scattering of neutrons from magnetic thin films
Deutsche Neutronenstreutagung 2001, Schriften des Forschungszentrums Jülich, Reihe Materie und Material, Band 8 (2001) p. 3
23.89.1

Köbler U.; Hoser A.1; Kawakami M.2
1RWTH, Institut für Kristallographie, Aachen
2Kagoshima University, Koorimoto, Japan
Beobachtung eines Bloch Exponent von 5/2 am Antiferromagneten MnF2 mit S=5/2 und axialer Austauschanisotropie
Deutsche Neutronenstreutagung 2001, Schriften des Forschungszentrums Jülich, Reihe Materie und Material, Band 8 (2001) p. 50
23.89.1

Lauter-Pasyuk V.1,2.3; Lauter H. J.3; Toperverg B.4,5; Nikonov O.3,2; Petrenko A.2; Schubert D.6; Petry W.1; Aksenov V.2
1TU, Physik Department, München
2Joint Institute for Nuclear Research, Dubna, Russia
3ILL, Grenoble, France
4PNPI, Gatchina, Russia
5FZJ, IFF, Jülich
6GKSS, Geesthacht
Off-specular neutron scattering studies of the interface and surface formation in self-assembled polymer multilayers
Proceedings of the ILL millennium symposium & european user meeting 06. - 07.04.2001 (2001) 84 - 85
23.89.1

Lauter-Pasyuk V.1,2; Lauter H. J.3; Toperverg B.4,5; Nikonov O.2,3; Kravtsov E.6; Ustinov V.6
1TUM, Physik Department, Garching
2Joint Institute for Nuclear Research, Dubna, Russia
3ILL, Grenoble, France
4PNPI, Gatchina, Russia
5FZJ, IFF, Jülich
6Institute of Metal Physics, Ekaterinburg, Russia
Magnetic domains in Fe/Cr multilayers
Deutsche Neutronenstreutagung 2001, Schriften des Forschungszentrums Jülich, Reihe Materie und Material, Band 8 (2001) p. 19
23.89.1

Lauter-Pasyuk V.1,2; Lauter H. J.3; Toperverg B.4,5; Nikonov O.2,3
1TUM, Physik Department, Garching
2Joint Institute for Nuclear Research, Dubna, Russia
3ILL, Grenoble, France
4PNPI, Gatchina, Russia
5FZJ, IFF, Jülich
Peculiar off-specular neutron scattering from islands on a lamellar film
Deutsche Neutronenstreutagung 2001, Schriften des Forschungszentrums Jülich, Reihe Materie und Material, Band 8 (2001) p. 159
23.89.1

Massalovitch S.; Ioffe A.; Küssel E.; Schlapp M.; Brückel Th.

Development of the large-area 2D neutron detector based on the imaging plate
Deutsche Neutronenstreutagung 2001, Schriften des Forschungszentrums Jülich, Reihe Materie und Material, Band 8 (2001) p. 102
23.89.1

Mueller R.; Brückel Th.; Horriar-Esser Ch.
Entwicklung einer Anlage zur Herstellung von kernspin-polarisiertem 3He am Forschungszentrum Jülich
Deutsche Neutronenstreutagung 2001, Schriften des Forschungszentrums Jülich, Reihe Materie und Material, Band 8 (2001) p. 105
23.89.1

Rücker U.; Alefeld B.; Bergs W.; Kentzinger E.; Heinen J.; Brückel Th.; Drochner M.1; Ackens A.1; Loevenich H.1; Reinhard P.1; Zwoll K.1
1FZJ, ZEL, Jülich
Das neue Neutronenreflektometer mit Polarisationsanalyse in Jülich
Deutsche Neutronenstreutagung 2001, Schriften des Forschungszentrums Jülich, Reihe Materie und Material, Band 8 (2001) p. 111
23.89.1

Rücker U.; Kentzinger E.; Toperverg B.; Brückel Th.; Ott F.1
1LLB, Gif sur Yvette, France
Spinaufgespaltene diffuse Streuung unter streifendem Einfall an polarisierenden Superspiegeln
Deutsche Neutronenstreutagung 2001, Schriften des Forschungszentrums Jülich, Reihe Materie und Material, Band 8 (2001) p. 60
23.89.1

Schlapp M.1,2, Kolb R.2; von Seggern H.2
1FZJ, IFF, Jülich
2TU, Fachbereich Materialwissenschaften, Darmstadt
Präparative Einflüsse auf die Empfindlichkeit des Speicherleuchtstoffs BaFBr:Eu2+ für Neutronen-Bildplatten
Deutsche Neutronenstreutagung 2001, Schriften des Forschungszentrums Jülich, Reihe Materie und Material, Band 8 (2001) p. 112
23.89.1

Schweika W.; Shramchenko N.1; Caudron R.1; Bellissent R.1
1LLB, Saclay, France
Phasonen in icosaedrischen AlPdMn Quasikristallen
Deutsche Neutronenstreutagung 2001, Schriften des Forschungszentrums Jülich, Reihe Materie und Material, Band 8 (2001) p. 183
23.89.1

Schweika W.
Polarization analysis
Schriften des Forschungszentrums Jülich: Materie und Material; Vol. 9 (2001) 4-1 - 4-23
23.89.1

Seeck O.; Mihaylova M.; Shin K.1
1SUNY, Department of Materials Science and Engineering, Stony Brook, USA
Investigation of Thin-Film Layer Systems with Synchrotron Radiation: Studies of Low-Contrast Polymer Interfaces
Research at HASYLAB (2001) 44 - 46
23.89.1

Seeck O.
Analytical Methods
Schriften des Forschungszentrums Jülich, Reihe Materie und Material; Band 7 (2001) B4.1 - B4.21
23.89.1

Seeck O.
Continuum description: Grazing Incidence Neutron Scattering
Schriften des Forschungszentrums Jülich: Materie und Material; Vol. 9 (2001) 6-1 - 6-18
23.89.1

Tietze-Jaensch H.; Conrad H.; Dietrich J.; Filges D.; Haft B.1; Hansen G.; Maier R.; Paul N.; Pohl C.; Prasuhn D.; Smirnov A.2; Stelzer K.; Ullmaier H.
1TU, ITP, Austria
2JINR, Dubna, Russia
JESSICA, the ESS-like target/reflector mock-up and cold moderator test facility
Proceedings of ICANS-XV, Tsukuba, Japan, 06. - 09.11.2000 (2001) 829 - 834
23.60.0

Toperverg B.1,2; Kentzinger E.1; Rücker U.1; Brückel Th.1
1FZJ, IFF, Jülich
2Petersburg Nuclear Physics Institute, Gatchina, Russia
Specular reflection and off-specular scattering of polarized neutrons from magnetic multilayers
Deutsche Neutronenstreutagung 2001, Schriften des Forschungszentrums Jülich, Reihe Materie und Material, Band 8 (2001) p. 70
23.89.1

Voigt J.; Schmidt W.; Ohl M.; Brückel Th.
Magnetische Ordnung in Erbium/Terbium-Schichtsystemen
Deutsche Neutronenstreutagung 2001, Schriften des Forschungszentrums Jülich, Reihe Materie und Material, Band 8 (2001) p. 71
23.89.1

Invited talks

Conrad H.; Byloos C.; Cates M.1; Riemer B.1; Hastings J.2; Spitzer H.3
1ORNL, Oak Ridge, USA
2BNL, Brookhaven, USA
3PSI, Villigen, Switzerland
Stress Wave Experiments with the ASTE Target
Seggau, Austria, 7th General ESS Meeting, 28.09.2001
23.60.0

Conrad H.
Materialprobleme in Targetkomponenten der ESS
Berlin, ESS-HGF-Projekt Meeting, 16.03.2001
23.60.0

Haubold H.-G.
In situ Small Angle X-Ray Scattering of Nafion and Pt Catalysts
Villigen, Switzerland, PSI-West, 16th PSI-Tagessymposium Elektrochemische Energiespeicherung, 23.10.2001
23.89.1

Hupfeld D.; Bos J.; Voigt J.; Seeck O.; Fischer K.; Brückel Th.
Resonante magnetische Röntgenstreuung an ferromagnetischem EuS
Hamburg, HASYLAB, Seminar, 15.11.2001
23.89.1

Hupfeld D.; Voigt J.; Brückel Th.
Investigation of element-specific magnetic correlations with synchrotron radiation
Berlin, 3rd Russian-German Workshop on Synchrotron Radiation Research, 18. - 20.11.2001
23.89.1

Hupfeld D.
High Energy X-Ray Scattering at μ-CAT
Chicago, USA, Workshop on High Energy X-Ray Scattering at the APS, 08.03.2001
23.89.1

Hupfeld D.
Untersuchung magnetischer Systeme mit resonanter Austauschstreuung
Kiel, Universität, Festkörperphysik Seminar, 15.02.2001

23.89.1

Ioffe A.
Simulations of the Neutron Speed Echo Spectrometer
Berlin, HMI, Workshop on VITESS 2 and other Packages for Simulations of Neutron Scattering, 25. - 27.06.2001
23.89.1

Jung P.
Irradiation effects and consequences on inservice properties under protron and neutron mixed spectrum: an overview
Paris, France, Journées d'Automne, 29. - 31.10.2001
23.60.0

Jung P.
Radiation Effects in Structural Materials of Spallation Sources
Brasimone, Italy, 2nd International Workshop on Materials for Hybrid Reactors and Related Technologies, 18. - 20.04.2001
23.60.0

Kentzinger E.; Rücker U.; Toperverg B.; Brückel Th.
Reflectivity and off-specular scattering of neutrons from magnetic thin films
Jülich, Deutsche Neutronenstreutagung 2001, 19. - 21.02.2001
23.89.1

Lucas G. E.; Odette G. R.; Sokolov M.; Spatig P.; Jung P.; Yamamoto T.
Current Status of Small Specimen Test Technology
Baden-Baden, 10th International Conference of Fusion Reactor Materials, 14. - 19.10.2001
23.60.0

Schweika W.
Temperature dependence of phason disorder in Al-Pd-Mn quasicrystals
Duisburg, Workshop on Dynamics in Quasicrystals, 04. - 07.12.2001
23.55.0

Seeck O.
Röntgenstreuexperimente an Flüssigkeitsfilmen in begrenzter Geometrie
Dortmund, Universität, Physikalisches Kolloquium, 03.07.2001
23.89.1

Seeck O.
Röntgenstreuexperimente an Flüssigkeitsfilmen in begrenzter Geometrie
Kiel, Universität, Kolloquium der Festkörperphysik + Materialwissenschaften, 22.11.2001
23.89.1

Toperverg B.
Grazing Incidence Scattering with Polarized Neutrons: A Tutorial
Argonne, USA, ANL-Seminar, 18.10.2001
23.89.1

Toperverg B.
Grazing Incidence Scattering with Polarized Neutrons: Examples and Applications
Argonne, USA, ANL-Seminar, 25.10.2001
23.89.1

Toperverg B.
Interphonon collisions
Grenoble, France, ILL, Lectures on lattice dynamics, 30.01. - 01.02.2001
23.89.1

Toperverg B.
Off-specular polarized neutron scattering from magnetic fluctuations in thin films and multilayers
München, ICNS-Konferenz, 09. - 13.09.2001
23.89.1

Toperverg B.
Phonon diffusion and localization
Grenoble, France, ILL, Lectures on lattice dynamics, 19. - 20.04.2001
23.89.1

Toperverg B.
Polarized Neutron Off-Specular Scattering from Magnetic Fluctuations in Films and Multilayers
Gaithersburg, USA, NIST-Seminar, 29.10.2001
23.89.1

Other talks

Brückel Th.
Hyperpolarisiertes 3He-Gas magnetisiert Neutronenstrahlen
Jülich, Workshop "Anwendung hyperpolarisierter Gase", 05.07.2001
23.89.1

Brückel Th.
Science at ILL - Plenary Discussion
Grenoble, France, ILL Millennium Symposium, 06. - 07.04.2001
23.89.1

Brückel Th.
Structural and Magnetic Characterization of Multilayers by Scattering Methods
Jülich, "Midterm Meeting Strategiefonds Magnetoelektronik", 22.11.2001
23.89.1

Chen J.; Carsughi F.1; Henry J.; Jung P.; Ullmaier H.
1University of Ancona, DIBIAGA, Italy
Summary of Radiation Damage Studies in ESS Target Structural Materials
Seggau, Austria, 7th General ESS Meeting, 27.- 29.09.2001
23.60.0

Chen J.; Ullmaier H.; Dai Y.1; Carsughi F.2; Maloy S. A.3; Sommer W.3; Broome T.4
1PSI, Spallation Neutron Source Division, Villigen, Switzerland
2University of Ancona, DIBIAGA, Italy
3Los Alamos National Laboratory, USA
4Rutherford Appleton Laboratory, Chilton, UK
Mechanical Properties of spent windows and target components from spallation sources
Brasimone, Italy, 2nd International Workshop on Materials for Hybrid Reactors and Related Technologies, 18. - 20.04.2001
23.60.0

Chen J.
Present and Future Work on Radiation Damage in ESS Target Structural Materials
Monschau, ESS-Tag, 10. - 11.05.2001
23.60.0

Conrad H.
Experimental results on intensities and life times of various target-moderator-reflector assemblies
Berlin, Moderator Concepts and Optimization for Spallation Neutron Sources, 13.03.2001
23.60.0

Conrad H.
Stress wave experiments with the ASTE mercury target
Oak Ridge, USA, 3rd International Workshop on Mercury Target Development, 19.11.2001
23.60.0

Goerigk G.
Materialforschung mit Synchrotronstrahlung am Beispiel der anomalen Röntgen-Kleinwinkelstreuung

Hamburg, Graduiertenkolleg des Fachbereichs Chemie der Universität, 19.12.2001
23.89.1

Ioffe A.; Vrana M.1
1CAS, Nuclear Physics Institute, Rez near Prague, Czech
A new neutron interferometry approach to the determination of the n-e interaction amplitude
Grenoble, France, ILL, PECNO Workshop, 01. - 04.03.2001
23.89.1

Ioffe A.
A new triple-axis spectrometer of polarized thermal neutrons at the FZ Jülich
Garching, Seminar, 19.01.2001
23.89.1

Ioffe A.
Monte Carlo simulations of Neutron Speed Echo Spectrometer
Didcot, UK, ENPI-Meeting, 27. - 30.06.2001
23.89.1

Jung P.; Liu C.
Desorption of Hydrogen from Pre-irradiated and Helium-Implanted Low Activation Martensitic Stainless Steels
Baden-Baden, 10th International Conference on Fusion Reactor Materials, 14. - 19.10.2001
23.60.0

Jung P.
Irradiation Effects on Hydrogen Diffusion and Permeation
Petten, The Netherlands, EU-EFDA 2000 Monitoring and 2001 Kick-off Meeting, 27. - 28.02.2001
23.60.0

Jung P.
Microstructure of C-containing materials, Be, W, SiC, and oxide ceramics with high helium concentrations
Garching, EU-EFDA Monitoring on Underlying Technology, 11. - 12.07.2001
23.60.0

Köbler U.
Experimentelle Fakten gegen die Gültigkeit der Bloch-Kubo-Dyson Spinwellentheorie
Karlsruhe, Universität, Seminar des Physikalischen Instituts, 14.05.2001
23.15.0

Köbler U.
The impact of fourth-order exchange interactions on spin dynamics, order parameters and critical magnetic behaviour
Prag, Tschechische Republik, Karls Universität, 07.05.2001
23.15.0

Lauter-Pasyuk V.1,2; Lauter H. J.3; Toperverg B.4,5; Nikonov O.2,3; Kravtsov E.6; Ustinov V.6
1TUM, Physik Department, Garching
2Joint Institute for Nuclear Research, Dubna, Russia
3ILL, Grenoble, France
4PNPI, Gatchina, Russia
5FZJ, IFF, Jülich
6Institute of Metal Physics, Ekaterinburg, Russia
Magnetic domains in Fe/Cr multilayers
Jülich, Deutsche Neutronenstreutagung 2001, 19. - 21.02.2001
23.89.1

Massalovitch S.
Neutron image plate detector
Mailand, Italy, TECHNI-Meeting, 03. - 04.05.2001
23.89.1

Rücker U.
Untersuchung lateral strukturierter magnetischer Vielfachschichten
Berlin, Hahn-Meitner-Institut, Workshop Magnetismus und Streumethoden, 22.06.2001
23.89.1

Schlapp M.
Development of neutron storage phosphors with low (-sensitivity
Mailand, Italy, TECHNI-Meeting, 03. - 04.05.2001
23.89.1

Seeck O.
Analysis by Diffraction and Fluorescence Methods
Jülich, 32. Ferienkurs des Instituts für Festkörperforschung, Neue Materialien für die Informationstechnik, 05. - 16.03.2001
23.89.1

Posters

Conrad H.; Filges D.1; Hansen G.2; Neef R. D.1; Stelzer H.2; Tietze-Jaensch H.; Ullmaier H.
1FZJ, IKP, Jülich
2FZJ, ZAT, Jülich
Technische und methodische Entwicklungen am Target-Moderator-Reflektor-Komplex der ESS
Jülich, Deutsche Neutronenstreutagung 2001, 19. - 21.02.2001
23.60.0

Doan T. D.1; Ott F.1; Menelle A.1; Rücker U.; Humbert P.2; Fermon C.2
1LLB, CEA/CNRS, Saclay, France
2SPEC, CEA Saclay, France
New evanescent wave surface diffractometer at the LLB
München, ICNS-Konferenz, 09. - 13.09.2001
23.89.1

Goerigk G.; Williamson D. L.1
1Colorado School of Mines, Dept. of Physics, Golden, USA
Quantitative ASAXS of Germanium Inhomogeneities in Amorphous Silicon-Germanium Alloys
Hamburg, HASYLAB User meeting, 26.01.2001
23.89.1

Hupfeld D.; Brückel Th.; Schweika W.; Strempfer J.1; Mattenberger K.2; McIntyre G.3
1Northern Illinois University, de Kalb, USA
2ETH, Zürich, Switzerland
3ILL, Grenoble, France
Investigation of the magnetic properties of GdxEu1-xS with neutrons and x-rays
Jülich, Deutsche Neutronenstreutagung 2001, 19. - 21.02.2001
23.89.1

Ioffe A.; Conrad H.; Zeiske Th.; Mueller R.; Küssel E.; Massalovitch S.; Schlapp M.; Schmitz B.; Brückel Th.
A New Thermal Neutron Spectrometer/Diffractometer for Polarization Analysis (SV30) at the research reactor FRJ-2
München, ICNS-Konferenz, 09. - 13.09.2001
23.89.1

Ioffe A.; Conrad H.; Zeiske Th.; Mueller R.; Küssel E.; Massalovitch S.; Schlapp M.; Schmitz B.; Brückel Th.
Spektrometer SV30 für Polarisationsanalyse mit thermischen Neutronen am Forschungsreaktor FRJ-2
Jülich, Deutsche Neutronenstreutagung 2001, 19. - 21.02.2001
23.89.1

Ioffe A.; Vrana M.1
1CAS, Nuclear Physics Institute, Rez near Prague, Czech
A new neutron interferometry approach to the determination of the neutron-electron interaction amplitude
München, ICNS-Konferenz, 09. - 13.09.2001
23.89.1

Köbler U.; Hoser A.1; Kawakami M.2
1RWTH, Institut für Kristallographie, Aachen
2Kagoshima University, Koorimoto, Japan
Beobachtung eines Bloch Exponent von 5/2 am Antiferromagneten MnF2 mit S=5/2 und axialer Austauschanisotropie
Jülich, Deutsche Neutronenstreutagung 2001, 19. - 21.02.2001
23.89.1

Köbler U.; Hoser A.1; Mueller R.; Fischer K.; Beyss M.
1HMI, Berlin
The impact of fourth-order exchange interactions on spin dynamics, order parameters and critical magnetic behaviour
München, ICNS-Konferenz, 09. - 13.09.2001
23.89.1

Lauter H. J.1; Lauter-Pasyuk V.2,3,1; Toperverg B.4,5; Nikonov O.1,3; Romashev L.6; Ustinov V.6; Kravtsov E.6; Vorobiev A.7; Major J.7
1ILL, Grenoble, France
2TU, Physik Department, München
3Joint Institute for Nuclear Research, Dubna, Russia
4PNPI, Gatchina, Russia
5FZJ, IFF, Jülich
6Institute of Metal Physics, Ekterinburg, Russia
7MPI Metallforschung, Stuttgart
Spin-resolved unpolarized neutron off-specular scattering for magnetic multilayers studies
München, ICNS-Konferenz, 09. - 13.09.2001
23.89.1

Lauter-Pasyuk V.1,2,3; Lauter H. J.3; Toperverg B.4,5; Nikonov O.3,2; Petrenko A.2; Schubert D.6; Schreiber J.7; Burcin M.7; Petry W.1; Aksenov V.2
1TUM, Physik Department, Garching
2Joint Institute for Nuclear Research, Dubna, Russia
3ILL, Grenoble, France
4PNPI, Gatchina, Russia
5FZJ, IFF, Jülich
6GKSS Forschungszentrum, Geesthacht
7Fraunhofer Institut für Zerstörungsfreie Prüfverfahren, Dresden
Interface and surface formation in self-assembled polymer multilayers by off-specular neutron scattering
München, ICNS-Konferenz, 09. - 13.09.2001
23.89.1

Lauter-Pasyuk V.1,2; Lauter H. J.3; Toperverg B.4,5; Nikonov O.2,3
1TUM, Physik Department, Garching
2Joint Institute for Nuclear Research, Dubna, Russia
3ILL, Grenoble, France
4PNPI, Gatchina, Russia
5FZJ, IFF, Jülich
Peculiar off-specular neutron scattering from islands on a lamellar film
Jülich, Deutsche Neutronenstreutagung 2001, 19. - 21.02.2001
23.89.1

Massalovitch S.; Ioffe A.; Küssel E.; Schlapp M.; Brückel Th.
Development of Image Plate Based Neutron Detector
Berlin, Hahn-Meitner-Institut, International Workshop on Position-Sensitive Neutron Detectors, 28. - 30.06.2001
23.89.1

Massalovitch S.; Ioffe A.; Küssel E.; Schlapp M.; Brückel Th.
Development of the large-area 2D neutron detector based on the imaging plate
Jülich, Deutsche Neutronenstreutagung 2001, 19. - 21.02.2001
23.89.1

Massalovitch S.; Ioffe A.; Küssel E.; Schlapp M.; von Seggern H.1; Brückel Th.
1Universität, Darmstadt
Development of neutron image plate for low flux measurements
München, ICNS-Konferenz, 09. - 13.09.2001
23.89.1

Mueller R.; Brückel Th., Horriar-Esser Ch.
Entwicklung einer Anlage zur Herstellung von kernspin-polarisiertem 3He am Forschungszentrum Jülich
Jülich, Deutsche Neutronenstreutagung 2001, 19. - 21.02.2001
23.89.1

Olligs D.; Bürgler D. E.; Wang Y.-G.; Kentzinger E.; Rücker U.; Schreiber R.; Brückel Th.; Grünberg P.
Unambiguous evidence for roughness-induced enhancement of Giant Magnetoresistance in epitaxial Fe/Cr/Fe (001) trilayers
Aachen, MML'01-Tagung, 25.06.2001
23.42.0

Rücker U.; Alefeld B.; Bergs W.; Kentzinger E.; Heinen J.; Brückel Th.; Drochner M.1; Ackens A.1; Loevenich H.1; Reinhard P.1; Zwoll K.1
1FZJ, ZEL, Jülich
Das neue Neutronenreflektometer mit Polarisationsanalyse in Jülich
Jülich, Deutsche Neutronenstreutagung 2001, 19. - 21.02.2001
23.89.1

Rücker U.; Alefeld B.; Bergs W.; Kentzinger E.; Heinen J.; Brückel Th.; Drochner M.1; Ackens A.1; Loevenich H.1; Reinhard P.1; Zwoll K.1
1FZJ, ZEL, Jülich
The new reflectometer with polarization analysis in Jülich
München, ICNS-Konferenz, 09. - 13.09.2001
23.89.1

Rücker U.; Grünberg P.; Demokritov S.1
1Universität, Kaiserslautern
Magnetic interlayer coupling across semiconducting EuS layers
Aachen, MML'01-Tagung, 25.06.2001
23.42.0

Rücker U.; Kentzinger E.; Toperverg B.; Brückel Th.; Ott F.1
1LLB, Gif sur Yvette, France
Spinaufgespaltene diffuse Streuung unter streifendem Einfall an polarisierenden Superspiegeln
Jülich, Deutsche Neutronenstreutagung 2001, 19. - 21.02.2001
23.89.1

Rücker U.; Kentzinger E.; Toperverg B.; Ott F.1; Brückel Th.
1LLB, Gif sur Yvette, France
Layer-by-layer magnetometry on polarizing supermirrors
München, ICNS-Konferenz, 09. - 13.09.2001
23.89.1

Rücker U.; Kentzinger E.
Characterization of thin layered structures for magnetoelectronic applications
Jülich, ESS-Begutachtung durch den Wissenschaftsrat, 10.12.2001
23.89.1

Schlapp M.1,2, Kolb R.2; von Seggern H.2
1FZJ, IFF, Jülich
2TU, Fachbereich Materialwissenschaften, Darmstadt
Präparative Einflüsse auf die Empfindlichkeit des Speicherleuchtstoffs BaFBr:Eu2+ für Neutronen-Bildplatten
Jülich, Deutsche Neutronenstreutagung 2001, 19. - 21.02.2001
23.89.1

Schlapp M.; von Seggern H.1; Massalovitch S.; Ioffe A.; Conrad H.; Brückel Th.

1Universität, Darmstadt
Materials for neutron image plates with low (sensitivity
München, ICNS-Konferenz, 09. - 13.09.2001
23.89.1

Schweika W.; Shramchenko N.1; Caudron R.1; Bellissent R.1; Widom M.2, Cousson A.1; Feuerbacher M.; Hennion B.1; Hupfeld D.; Mattauch S.3
Phason disorder in icosahedral AlPdMn quasicrystals
München, ICNS-Konferenz, 09. - 13.09.2001
23.89.1

Schweika W.; Shramchenko N.1; Caudron R.1; Bellissent R.1; Widom M.2
1LLB, Saclay, France
2Carnegie-Mellon University
Phason disorder in icosahedral AlPdMn quasicrystals
Jülich, Deutsche Neutronenstreutagung 2001, 19. - 21.02.2001
23.89.1

Schweika W.
Diffuse Neutron Scattering using time-of flight and polarization analysis
Jülich, ESS-Begutachtung durch den Wissenschaftsrat, 10.12.2001
23.89.1

Seeck O.; Kim H.1; Sinha S. K.1; Basu J. D.2; Kim H.3; Foster M. D.3
1APS/ANL, Argonne, USA
2University of Illinois, USA
3The University of Akron, USA
X-ray experiments on confined liquids
New London, USA, X-Ray Gordon Conference, 22. - 27.07.2001
23.89.1

Toperverg B.1,2; Kentzinger E.1; Rücker U.1; Brückel Th.1
1FZJ, IFF, Jülich
2Petersburg Nuclear Physics Institute, Gatchina, Russia
Specular reflection and off-specular scattering of polarized neutrons from magnetic multilayers
Jülich, Deutsche Neutronenstreutagung 2001, 19. - 21.02.2001
23.89.1

Voigt J.; Kentzinger E.; Rücker U.; Schweika W.; Brückel Th.; Schmidt W.; Ohl M.; Hupfeld D.
Proximity effects in Er/Tb superlattices: How Neutrons and X-Rays complement each other
München, ICNS-Konferenz, 09. - 13.09.2001
23.89.1

Voigt J.; Rücker U.; Kentzinger E.; Hupfeld D.; Brückel Th.
Proximity effects in Er/Tb superlattices
Aachen, MML'01-Tagung, 27.06.2001
23.89.1

Voigt J.; Schmidt W.; Ohl M.; Brückel Th.
Magnetische Ordnung in Erbium/Terbium-Schichtsystemen
Jülich, Deutsche Neutronenstreutagung 2001, 19. - 21.02.2001
23.89.1

Vorobiev A.1,2; Gordeev G.2; Major J.1; Toperverg B.2,3; Dosch H.1
1MPI für Metallforschung, Stuttgart
2PNPI, Gatchina, Russia
3FZJ, IFF, Jülich
The structure of ferrofluids in the vicinity of the interface with silicon
München, ICNS-Konferenz, 09. - 13.09.2001
23.89.1

Patents granted

Klatt K.H.; Wenzl H.; Chakraborty A.K.1; Rohde J.1; Konrad R.1
1GRS Köln
Katalysator zur Beseitigung von Wasserstoff aus einer Wasserstoff, Sauerstoff und Dampf enthaltenden Atmosphäre
CA: 2,046,820 (02.10.2001)
PT 1.1026
FE 23.42.0

Sonnenberg K.; Küssel E.; Bünger T.1; Flade T.1; Weinert B.1
1Fa. Freiberger
Verfahren und Vorrichtung zur Herstellung von Einkristallen sowie Kristallkeim
EP: 1038995 (08.08.2001) (BE,DE,FR,GB,IT,NL)
PT 1.1681
23.42.0

Wenzl H.; Oates W.
Verfahren zur aktiven Defektsteuerung bei der Züchtung von GaAs-Kristallen
EP: 0931184 (21.03.2001) (CH/LI,DE,FR,GB,IE)
PT 1.1405
23.42.0

Lecture courses

Brückel Th.
Elastic scattering from many-body systems
IFF, 5th Laboratory Course Neutron Scattering, 18.09.2001
23.89.1

Brückel Th.
Magnetism
IFF, 5th Laboratory Course Neutron Scattering, 21.09.2001
23.89.1

Conrad H.
Neutron Sources
IFF, 5th Laboratory Course Neutron Scattering, 18.09.2001
23.89.1

Schweika W.
Polarization analysis
IFF, 5th Laboratory Course Neutron Scattering, 19.09.2001
23.89.1

Seeck O.
Analysis by Diffraction and Fluorescence Methods
Jülich, 32. Ferienkurs des Instituts für Festkörperforschung, Neue Materialien für die Informationstechnik, 05. - 16.03.2001
23.89.1

Seeck O.
Continuum description: Grazing incidence neutron scattering
IFF, 5th Laboratory Course Neutron Scattering, 19.09.2001
23.89.1

Internal reports

Brückel Th.
Das Institut für Festkörperforschung
IFF, Informationsveranstaltung für den wissenschaftlichen Beirat, 26.04.2001
23.89.1

Brückel Th.
Elastic scattering from many-body systems
IFF, 5th Laboratory Course Neutron Scattering, 18.09.2001
23.89.1

Brückel Th.
Magnetism
IFF, 5th Laboratory Course Neutron Scattering, 21.09.2001

23.89.1

Conrad H.
JESSICA - die Jülicher 10 mW Spallation-Neutronenquelle
IFF, Informationsveranstaltung für den wissenschaftlichen Beirat, 26.04.2001
23.60.0

Conrad H.
Neutron Sources
IFF, 5th Laboratory Course Neutron Scattering, 18.09.2001
23.89.1

Ioffe A.
A New Thermal Neutron Spectrometer/Diffractometer for Polarization Analysis (SV30) at the Research Reactor FRJ-2
FZJ, DIDO operators meeting, 01. - 04.10.2001
23.89.1

Schweika W.
Polarization analysis
IFF, 5th Laboratory Course Neutron Scattering, 19.09.2001
23.89.1

Seeck O.
Continuum description: Grazing incidence neutron scattering
IFF, 5th Laboratory Course Neutron Scattering, 19.09.2001
23.89.1

Institute for Neutronscattering

General Overview

User program at the FRJ-2 reactor
From October 1st, 2001 the user operation at the FRJ-2 is funded by the *European Large Facility Access Program*, which supports the European use of the Jülich reactor in supporting foreign users to perform experiments at our facility. A first call for proposals was placed with a deadline of November 30, 2001 - 21 proposals for 180 days beamtime were received, which compares very favorable with the 45 days available within the program. An international review panel has been established and following the first reviewing process 89 days of beamtime were allocated to European users for the first four month of 2002.

In 2001 the FRJ-2 operation went smoothly delivering 129 days of beam time with good reliability. During that time altogether 149 experiments were performed, 64.43% with outside users. Figure 1 displays the origin of the different user groups, who partly came several times during 2001 to Jülich. Research groups from German and European universities took the majority of the beam time. In addition, we had users from industry and from national and international research centers.

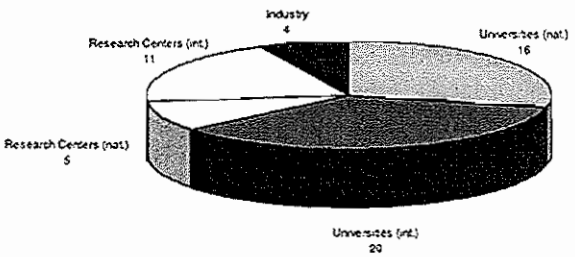

Figure 1: Origin of FRJ-2 users. Given is the number of different institutions, which have performed experiments in Jülich.

Figure 2 displays the distribution of internal and external experiments at a number of selected instruments. Most of the experiments were performed on the small angle scattering machines and the powder diffractometer SV7 operated by our institute and the University of Bonn respectively. Concerning inelastic scattering the most favored machine was the neutron spin echo spectrometer.

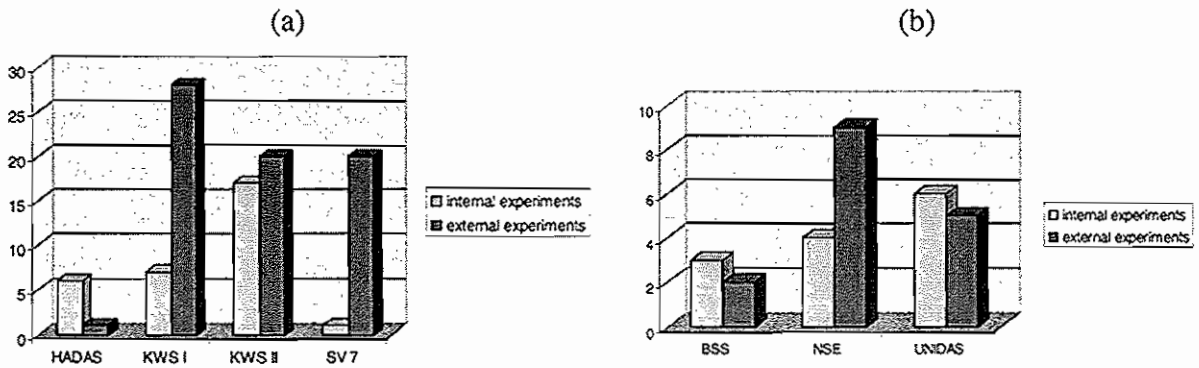

Figure 2: External and internal use of elastic (a) and inelastic instruments at the FRJ-2 by example. Given is the number of experiments.

In 2001 the 5th International Neutron Laboratory Course took place. This training course for students was supported by the European Neutron Round Table. Again the number of applicants (73) surpassed largely the available places. From the 40 accepted participants 14 came from outside Germany.

Neutron instrumentation (F&E-Nr. 23.89.1)
The development of neutron instrumentation and the construction of new neutron instruments is one of the focal points of the institute comprising activities in three areas.

- Preparation of instrumentation for 3rd generation neutron sources like the European Spallation Source (ESS).
- Construction of instrumentation for the FRM-2 reactor in Munich.
- Upgrading of existing instrumentation in Jülich.

The main endeavor in the field of spallation source instrumentation is the ongoing feasibility study (hardware) for a very high resolution neutron spin echo (NSE) spectrometer for the American spallation source (SNS) in Oak Ridge. The study is performed together with the HMI and should lead to the best of its class neutron spin echo instrument. Such an instrument will allow us to gain experience in the instrumentation of Megawatt spallation sources and at the same time will offer access to the use of SNS. The instrument was presented at the EFAC (Experimental Facilities Advisory Committee) in Oak Ridge and received very high marks. An increase of the time resolution to 1μs combined with a significant increase of the solid angle are the ambitious design goals. The feasibility study aims on the design of the magnetic fields using superconducting technology and the development of correction elements. For that purpose a test stand has been build facilitating very precise magnetic field measurements using NMR probes. Also computer simulations on the instrument performance are carried out.

Furthermore, a design study for a very high resolution backscattering instrument to be operated at the ESS was undertaken. The design goal is the combination of a large dynamic range, high resolution and significant intensity.

The work on the backscattering spectrometer for the FRM-2 in Munich proceeded according to plan. The main activities focused on the manufacturing of the analyzers and their mechanics. Furthermore, the design of the sample position and the concept of the spectrometer housing was finalized.

In Jülich, the upgrade of the small angle scattering machines was continued. In particular together with the ZEL a new two dimensional scintillation detector was developed allowing for an one order of magnitude higher counting rate. A number of sample environment devices like an elongational rheometer, a shear cell, a stretching machine for melts or rubbers and a cell for time resolved SANS studies of mineralization processes were constructed.

The focusing small angle scattering machine (KWS-3) was commissioned and inelastic fixed windows scans at the backscattering spectrometer as a new technique to monitor quasielastic scattering was developed.

Polymers, membranes and complex fluids (F&E-Nr. 23.30.0)
Most of the research in the institute concentrates on the study of soft condensed matter systems emphasizing polymers and complex fluids. Such research requires a close collaboration between synthetic chemists and physicists. In the institute this is realized by a synthetic laboratory which provides the samples for the physics research. Theoretical guidance is available through a close collaboration with the Institute Theory II of the IFF.

Polymer synthesis
Aside of standard preparations of homo- and blockcopolymers for particular physics problems, a number of items need to be emphasized:

- In the field of branched polymers, the synthesis of so called pom-pom polymers - these are star polymers which are joined by a cross bar was persued. The synthesis of a half-pom-pom – a A_5B_1-star - was achieved.
- Alkoxy-silanes as linking agents for branched polymers of the A_7B_1 or $A_{14}B_2$ type were explored. For an industrial collaboration with DSM nylons-6 star polymers were created.
- Polydienes and polyalkanes which are soluble in silicon oil were developed and likewise amphiphilic blockcopolymers with silicon oil soluble blocks were synthesized with the aim to boost silicon oil microemulsions.
- Polyalkane-PEO blockcopolymers as compatibilizers for nanocomposites with isotactic polypropylene were achieved.
- A number of triblockcopolymers for the study of interfaces in microphase separated diblockcopolymers as well as for the investigation of the reptation dynamics were created.
- Finally, the GPC triple detector for molecular weight analysis was tested and the limits of universal calibration using viscosity and light detection, were explored. In the molecular weight range from 1000g/mol to

500.000g/mol a molecular weight analysis on an absolute scale with a maximum error of 10% was found to be possible.

Polymer dynamics

We continued our studies on the dynamics of polymer chains covering all scales from the macroscopic motion to local dynamics including the motions of side groups.

- ***Large scale motion***

  One of this years highlights was the study of the single chain dynamic structure factor of polymer melts as a function of molecular weight. In a collaboration with Prof. T. McLeish from the University of Leeds these experiments facilitate a molecular identification of the often proposed tube length fluctuation process in the reptation model as the limiting mechanism to local reptation (see report A. Wischnewski). A study on the molecular weight dependence of the polymer melt viscosity to very high degrees of polymerization led to an observation of the viscosity cross over to so called pure reptation behavior ($\eta \sim M^{3.4} \rightarrow M^3$) for several polymers (PVCH, PI, PIB, PS).

- ***Intermediate scale dynamics***

  In the momentum transfer range Q below the first structure factor maximum the collective and self motion of polyisobutylene (PIB) melts were studied as a function of temperature. Unexpectedly and still not yet fully understood, we found that the relaxation of the short range order or the structural relaxation observed at the first structure factor maximum exhibits a stronger temperature dependence as the collective dynamics in the low Q regime – with decreasing temperature the short range order lives increasingly longer than the collective modes at low Q. The corresponding collective relaxation times observed with neutron spin echo agree quantitatively with the relaxation time of the shear stress. The self motion follows the temperature dependence of the collective modes (see report U. Buchenau).

  In the same spatial range but at picosecond time scales, the fast dynamics of polybutadiene (PB) was investigated. Comparing deuterated and protonated samples of the same scattering power, it was possible to show that the low Q inelastic scattering is purely coherent. The experiment demonstrated that this inelastic scattering is not due to large amplitude motion but rather due to a correlated small amplitude motion of many atoms. This finding supports strongly the concept of a strong coupling of the so called fast process to the longitudinal sound waves.

  Earlier studies of the fast process of glass forming materials in porous media have shown that the confinement reduces strongly the low frequency part of the Boson peak. At a first sight, this phenomenon appeared to be related to a cut off of long wave length sound waves due to the confining media. New studies using larger pore sizes displayed a similar effect invalidating the sound wave argument. The also observed slowing down and broadening of the α-relaxation could be explained by a model of an inhomogeneous distribution of relaxation times within the pores.

- ***Local dynamics***

  On polyisoprene melts, the methyl group dynamics was investigated using a combination of time of flight and backscattering experiments. The measurement validated a model of an Gaussian energy barrier distribution and led to a detailed determination of the corresponding parameters.

  In polymeric electrolytes (polypropyleneoxide/$LiClO_4$) measurements at the structure factor maximum displayed a slowing down and broadening of the structural relaxation depending on salt concentration. Studies of the self motion at small momentum transfers showed a temperature shift of the relaxational processes upon salt addition, while the characteristics of the entropy driven Rouse dynamics prevailed.

  Using dielectric techniques, the extend of the dipole fluctuations within the β-relaxation was studied in some detail. For PVAc the dipole fluctuation $\langle \delta\mu_\beta^2 \rangle$ of the β-relaxation was correlated with the mean squared displacement $\langle u^2 \rangle$ from backscattering experiments. A linear relation was found.

Cocrystallisation on polymeric and mineralisation on biomimetic templates

The study of cocrystallization processes of polymers, organic and nonorganic materials are a new field in our institute. Crystallization processes were studied first in connection with wax crystal modifiers for middle distillate fuels, where crystalline-amorphous diblockcopolymers were investigated. At present two lines are followed.

- ***Cocrystallization of paraffin with random crystalline-amorphous copolymers***

  The self assembly of PEB-n with $n = 7.5$ and 11 (n gives the number of ethyl side branches per 100 backbone carbons) copolymers in dilute decane solution and their effect on paraffin crystal formation ($C_{24}H_{50}$ and $C_{36}H_{74}$) were studied. Using contrast variation the structure of the polymers and the paraffin associates could be separately identified. At low temperature the two PEB-n copolymers by themselves selfassemble into needle shaped objects. For $n = 7.5$ and $n = 11$ the selfassembling process starts at different temperatures (60°C and 0°C respectively). The temperature of selfassembly strongly correlates with the wax crystal modification efficiency

of the polymeric additives. From the SANS data, we could conclude that the paraffin and the polymers cocrystallize into common two-dimensional structures (collaboration with Prof. R.K. Prud'homme, Univ. Princeton).

- *Mineralization in the presence of associating polymers and on biomimetic templates*
  Recently, it has been found, that double hydrophilic blockcopolymers which have an electrolytic and an neutral block, serve as efficient builders for Calcium binding and precipitation in $CaCO_3$ solutions. Despite of this extraordinary polymer effect, microscopic information on the conformation and the configuration of the polymer in the process is still not available. Using small angle neutron scattering (SANS) exploratory investigations of the nucleation and the growth processes as well as the final crystalline products were performed. First evidence for a nanometer internal structure of the minerals was found (collaboration with Prof. M. Antonietti, MPI Golm). As the second system, $CaCO_3$ mineralization on gold colloids (10nm size) which were covered with 4 dimethylaminopiridene was investigated (collaboration with Prof. W. Tremel, Univ. Mainz).

Branched polymers and rubbers

The study of the matrix deformation in filled elastomers was continued. An ideal cylindrical filler was prepared by microphase separation of a blockcopolymer and dispersed in homopolymer matrixes. Matching conditions were employed such, that only the matrix chains were visible. The SANS result indicate that rod like fillers do not lead to visible reinforcement effects of the polymer matrix reinforcement. Industrial silica filler were investigated by a combination of SAXS and SANS techniques, in order to observe the matrix deformation (SANS) and the deformation of the filler network (SAXS). The polymer chain deformation in the samples is an agreement with the hydrodynamic reinforcement effect, though, the dependence on the filler content is irregular (collaboration with Prof. E. Straube, Univ. Halle)

Real time SANS experiments combined with measurements of the dynamic moduli and the sol fraction allowed an identification of scission reactions during the cure of rubbers. It was found that due to the immobility and the recrosslinking of broken chains, random degradation processes do not effect the quality of the rubber.

Complex fluids

Complex fluids of three different types were investigated. Studies on the polymer efficiency boosting effect in microemulsions were continued on droplet phase systems. Bicontinuous polymeric microemulsions were characterized and star polymers/colloidal mixtures were investigated. Furthermore, dynamic experiments on microemulsions with three different morphologies were performed.

- **Droplet phase microemulsions containing amphiphilic diblockcopolymers**
  Droplet phase oil in water microemulsions consisting of water, decane and $C_{10}E_4$ surfactants containing amphiphilic diblockcopolymers of polyethylenepropylene-polyethyleneoxide PEP_5-PEO_y with the molecular weights (in 1000) $y = 15$ and 80 were investigated. The polymer concentration was chosen such that on the average one polymer was attached to one droplet. Systematic contrast variation experiments allowed the determination of the different partial structure functions. They could be described by a spherical core-shell-shell model. The core consists of oil, the first shell contains the surfactant, the next outer shell is a depletion zone, where the polymer is almost not present but beyond this shell the polymer is homogenously distributed. The observation of the depletion zone is in particularly clear for the larger chain system (collaboration with Prof. R. Strey, Univ. Köln).

- **Microemulsion dynamics**
  Extensive small angle scattering and neutron spin-echo experiments on a microemulsion system that exhibits boosting of its oil-in-water solubilization capability on the addition of polymeric cosurfactants have been performed. The dynamics in the bicontinuous phase and in the lamellar phase can be described consistently in the high wavevector regime by applying the model of free membrane patches of Zilman & Granek [PRL **77**, 4788 (1996)] if proper evaluation (partly) numerical is performed. The curvature elasticity κ extracted by this means from the dynamics is consistent with the expectations from other methods. The influence of the polymer cosurfactant on κ extracted from the dynamic scattering is only marginal. At larger length scales where the interference of membranes contributes to $S(Q)$ the dynamics exhibits deGennes narrowing. The investigations clearly showed the range of validity of the most recent theoretical concepts to describe the local and medium scale dynamics of these microemulsion phases and the conditions for and limits of their applicability.

- **Microemulsion phases in a three component polymer blend**
  Ternary polymer blends containing two partly incompatible homopolymers and the corresponding symmetric diblockcopolymer exhibit similar features as mixtures of amphiphilics with oil and water. The structure factor of a

ternary mixture of dPB/PS/dPB-PS polymers was investigated in the neighborhood of the Lifshitz line (LL). There, we observed a so called reentrance phase behavior with a two phase region limited by an upper and lower critical solution temperature T_u and T_l respectively. The temperature distance of the immiscibility $\Delta T = T_u - T_l$ decreased from 15K at a diblockcopolymer volume fraction $\varphi = 6.3\%$ to zero at the double critical point (DCP) at $\varphi \sim 7.05\%$. Approaching the DCP we observe an increase of the critical exponents to twice their values. If, however, the reduced temperature field $t_{ul} = |(T - T_u)(T_l - T)|/T^2$ instead of $t = |T - T_u|/T$ is used, the predicted Lifshitz critical exponents are evaluated. There is experimental evidence, that the observation of a reentrance phase behavior with a lower phase boundary is related to the formation of a droplet microemulsion phase which beyond the Lifshitz line becomes bicontinuous.

- **Star polymer/colloid mixtures**
  The influence of polymer branching on depletion forces was investigated by studying mixtures of hard sphere colloids and star branched polymers with increasing arm numbers $f = 2/32$ but constant $R_g \cong 50$nm. The position of the glass liquid demixing transition was found to be related to the amount of branching. Using SANS and SAXS partial structure factors in the star polymer colloid mixtures could be measured. The scattering data reflect the relative distance to the demixing transition (collaboration with Prof. P.N. Pusey, Univ. Edinburgh and Prof. H. Löwen, Univ. Düsseldorf).

Further research activities (F&E-Nr. 23.15.0)

Tunneling systems
The interpretation of rotational tunneling spectra, the phonon density of states and internal excitations on the basis of measured crystal structures and fundamental interactions - either transferable pair interaction potentials or united force fields - is successfully extended to the various isomers of xylene and the methyl halides.

Electron transfer between metal organic molecules containing methyl groups is related to the mechanism of hydrogen bond formation. The prominent example is trimethyl-aluminum. Studies have been extended to the respective gallium and indium alkyls.

Rotational tunneling as a probe of disorder is applied to a case - partially deuterated methane III - where the symmetry of the molecule is incompatible with the site symmetry. Large line broadenings allow an estimate of the distribution of barrier heights.

Biological macromolecules
The study on the interaction of DNA with its water hull was extended to a first example of a DNA-drug complex (planar aromatic complex). Experimental basis is the determination of the self correlation of hydrogen at the DNA on humidification with D_2O. Those spectra delver as typical information the ubiquitous onset of conformational fluctuations at around 200K for biomolecules and the characteristic sublinear relaxation. On this basis, no qualitative difference to pure DNA was observed. This absence of a difference speaks in favor of the intercalation of the drug between the bases - a position which hardly affects the conformational freedom.

Dieter Richter

Personnel 2001/2002 and areas of activity

Scientific Staff

Dr. J. Allgaier	Polymer synthesis, microemulsions	23.30.0
Prof. Dr. U. Buchenau	Dynamics of glassforming materials	23.30.0
Dr. H. Grimm	Molecular crystals, oriented macromolecules Instrument Responsible: Backscattering spectrometer BSS1	23.30.0
Dr. M. Monkenbusch	Dynamics of polymers and complex liquids, development of new spin echo techniques Instrument Responsible: Spinecho Spectrometer NSE	23.30.0
Dr. M. Prager	Rotational tunneling Instrument Responsible: Thermal time of flight spectrometer SV 29	23.15.0
Dr. W. Pyckhout-Hintzen	Polymer networks, branched polymers, rheology Instrument Responsible: Small angle neutron scattering KWS 1	23.30.0
Prof. Dr. D. Richter *Institute Director*	Structure and dynamics of polymers, glass transition, complex liquids ESS Science Director	23.30.0
Dr. D. Schwahn	Phase transitions in polymer systems, self assembly of crystalline copolymers, biomineralisation Instrument Responsible: Small angle neutron scattering KWS 1 and double crystal diffractometer DKD	23.30.0
Dr. L. Willner	Polymer synthesis, characterization kinetics of polymer micelles	23.30.0
Dr. habil. R. Zorn	Rubbery electrolytes, glass transition, dynamics in confinement, water dynamics in glasses	23.15.0

Technical Staff

U. Bünten	Technician at KWS 1 and NSE	23.89.1
Dr. W. Bünten	Development work on neutron spin echo spectrometer for SNS	23.89.1
Ms. M. Hintzen	Technician in the polymer characterization laboratory	23.30.0
Dipl.-Ing. M. Heiderich	Engineer responsible for the KWS 1 and DKD instruments	23.89.1
M. Jungen (until 31.08.01)	Technician at SV 29	23.89.1
Dipl.-Ing. T. Kozielewski	Engineer backscattering spectrometer FRM 2	23.89.1
Ms. U. Sausen-Malka	Electronic laboratory	23.89.1
J. Rademacher (until 31.07.01)	Technician at SV 29 and KWS 3	23.89.1
Dipl.-Ing. R. Schätzler	Head of technical service group	23.89.1
T. Starc	Technician at BSS 1 spectrometer	23.89.1
R. Stollenwerk	Technician at KWS 2, electronic data processing	23.89.1
Dipl.-Ing. G. Vehres	Electronics engineer, head of electronics laboratory Second Instrument Responsible: Thermal time of flight spectrometer SV 29	23.89.1
Ms. S. Oubenkhir	Secretary	

Scientists

Dr. L. Fetters (until 16.08.2001)	Self-assembly of crystalline: amorphous copolymers and rheological predictions of polymer systems.	23.30.0
Dr. H. Frielinghaus	Microemulsions Instrument Responsible: Small angle neutron scattering facility KWS 2	23.30.0
Dr. Ms. M. Heinrich	Polymer processing, influence of branched polymers	23.30.0
Dr. Ms. H. Hermes	Influence of solvent polymer interaction on the chain conformation of polyamide-6	23.30.0
Dr. S. Hoffmann	Dynamics of polymer blends	23.30.0

Dr. S. Kahle	Dielectric spectroscopy, relaxations in complex polymer systems, partially structure factor Second Instrument Responsible: Backscattering spectrometer BSS 1	23.30.0
Dr. G. Kali	Instrument Scientist at the IN 15 spectrometer at the ILL	23.89.1
Dr. O. Kirstein	Project scientist for backscattering instrument at FRM-II	23.89.1
Dr. M. Ohl (until 30.04.2001)	Second Instrument Responsible: D 23, IN 22 at the ILL	23.89.1
Dr. A. Radulescu	Aggregation behavior of copolymers and wax crystallization	23.30.0
Dr. W. Schmidt	Instrument Responsible: IN 12 at the ILL	23.89.1
Dr. J. Stellbrink	Star polymers, colloid mixtures and living polymerization	23.30.0
Dr. A. Wischnewski	Polymer dynamics, ESS Scientific Advisory Committee (SAC) Assistant	23.89.1

Thesis Students (University of Münster)

DI Ms. A. Blanchard	Relaxation mechanisms in entangled polymers by means of the small angle neutron scattering technique	23.30.0
Dipl.-Phys. A. Botti (until 30.05.01)	Microscopic deformation of filled networks	23.30.0
Dipl.-Phys. D. Byelov	Investigation of the role of polymers in microemulsions by small angle neutron scattering	23.30.0
M.Sc. H. Endo (until 31.03.01)	The role of amphiphilic polymers in the emulsification properties of microemulsions	23.30.0
Dipl.-Ing. H. Kaya (until 31.08.01)	Micellarisation of amphiphilic polymers	23.30.0
Dipl.-Chem. R. Lund	Exchange kinetics between polymer micelles	23.30.0
Dipl.-Ing. M. Ms. Mihailescu	Dynamic of microemulsions - influence of amphiphilic polymers	23.30.0
Dipl.-Phys. V. Pipich	Formation of structure in mixtures of two homopolymers and a diblockcopolymers	23.30.0
Dipl.-Phys. Ms M. Zamponi	Dynamics of entangled polymers	23.30.0

Guests

Dr. M. Abdel-Goad (El-Minia Univ. Egypt)	Investigation of the packing length concept by rheological methods of model polymers	23.30.0
Dr. Ms. A. Arbe (Univ. of San Sebastian, Spain)	Intermediate scale dynamics in polymer systems	23.30.0
Prof. Dr. J. Colmenero (Univ. of San Sebastian, Spain)	Partial structure factors in polymer melts	23.30.0
Prof. H. Yee-Madeira (Nat. Inst. of Polytechnique, New Mexico)	Phase separation in polymer blends	23.30.0
Dr. Y. Melnichenko (Oak Ridge Nat. Lab., USA)	Critical behavior in polymer blends	23.30.0
Dr. Ms. H. Montes (ESPCI Paris, France)	Concentration fluctuations and dynamics in diblock copolymers, neutron scattering approach	23.30.0
Prof. E. Straube (Univ. Halle)	The influence of topological constraints at the microscopic level in polymer networks and blends	23.30.0
Dr. G. Wignall (Oak Ridge Nat. Lab., USA)	Ordering behavior of triblockcopolymers and polymers in solution	23.30.0

Trainees

B. Pütz

M. Riemenschneider

T. Scymczyk

Molecular Observation of Contour Length Fluctuations Limiting Topological Confinement in Polymer Melts

A. Wischnewski, M. Monkenbusch, L. Willner, and D. Richter
Institut für Festkörperforschung,
Forschungszentrum Jülich, D-52425 Jülich, Germany

A.E. Likhtman and T.C.B. McLeish
IRC in Polymer Science and Technology, University of Leeds, Leeds LS2 9JT, United Kingdom

B. Farago
Institut Laue-Langevin, B.P. 156X, Avenue des Martyrs, F-38042 Grenoble Cedex 9, France
(Dated: December 10, 2001)

In order to study the mechanisms limiting the topological chain confinement in polymer melts, we have performed neutron spin echo investigations of the single chain dynamic structure factor from polyethylene melts over a large range of chain lengths. While at high molecular weight the reptation model is corroborated, a systematic loosening of the confinement with decreasing chain length is found. The dynamic structure factors are quantitatively described by the effect of contour length fluctuations on the confining tube establishing this mechanism on a molecular level in space and time.

F&E-Nr: 23.30.0

In the melt long chain polymers heavily interpenetrate each other and mutually restrict their motions in forming topological constraints. In his famous reptation model de Gennes described the effect of these entanglements by a tube (with diameter d) along the coarse grained chain profile localizing the chain and confining the chain motion [1, 2]. The dominating motional mechanisms in this model are (i) a curvilinear version of the Rouse motion at short times (also termed local reptation), (ii) and escape of the whole molecule from the tube at long times - the reptation process.

Exploiting the new capabilities of ultra high resolution neutron spin echo (NSE) spectroscopy the dynamic structure factor of polyethylene (PE) was explored deeply into the entangled regime. In this study the dynamic structure factor of the reptation model was corroborated, while all other competing models, which predict structure factors, performed far less well [3].

Thus, the assumption of tube confinement, enforcing one dimensional chain motion along the tube, is very effective in describing the chain dynamics for long chains. However, as it is known from broad cross-over phenomena like the molecular weight dependence of the melt viscosity, very important limiting mechanisms exist which effect the confinement and limit the reptation process [2]. These processes increase in importance as the chain length decreases. Theoretically, constraint release, where a constraining chain moves out of the way of a given chain, and tube contour length fluctuations removing the constraints from the ends have been identified as the most important of those processes but no direct microscopic observation exists. In this report we address the contour length fluctuation mechanism.

We present a systematic study of the single chain dynamic structure factor of polyethylene -melts with altogether 6 different molecular weights between 12.4 kg/mol $\leq M_w \leq$ 190 kg/mol. The experiments were performed at the IN15 spin echo spectrometer at Institute Laue Langevin in Grenoble covering a range of momentum transfers 0.03 $\text{Å}^{-1} \leq q \leq 0.115$ Å^{-1} at T = 509K. The wavelengths of the incoming neutrons were $\lambda = 8$ Å and 15 Å spanning a time range 0.3 ns $\leq$ t $\leq$ 170 ns. The experimental results were corrected for background and resolution. Fig.1 displays the obtained spectra for the highest and the lowest molecular weight.

The data were analysed both using the pure reptation model neglecting contour length fluctuations and by an alternative approach, where the contour length fluctuations are considered. The fits were performed fixing the elementary Rouse rate W taken from earlier measurements on PE at short-times [4] and varying the tube diameter d as the only parameter.

First the data were analysed in terms of the pure reptation model yielding a good fit of the data for the four higher M_w, while for the two lower M_w the fit is still acceptable. The constraint reduction is reflected in the pure reptation picture by an apparent tube diameter which increases with decreasing chain length. This is illustrated in Fig. 2.

In an alternative approach we took into account the contour length fluctuations. For times shorter than $\tau_R = N^2/(\pi^2 W)$ (N is the number of segments) the so called Rouse time which is the longest relaxation time of an unconfined chain, it was recently shown, that the effect of reptation on escaping from the tube is negligible in comparison to tube length fluctuations [5]. This time range corresponds to the times that are accessed in our experiment. For the shortest chain $M_w = 12.4$ kg/mol we have

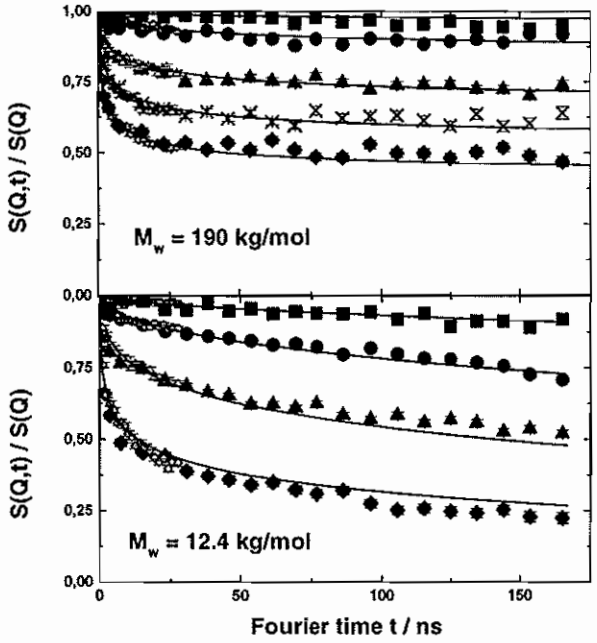

FIG. 1: Neutron spin echo spectra from polyethylene melts with $M_w = 190$ kg/mol and $M_w = 12.4$ kg/mol. The q-values correspond to: squares: q = 0.03 Å^{-1}; circles: q = 0.05 Å^{-1}; triangles: q = 0.077 Å^{-1}; crosses: q = 0.096 Å^{-1}; diamonds: q = 0.115 Å^{-1}. Lines: explanation see text.

$\tau_R = 186$ ns which is more or less the maximum time reached by NSE. In this regime the fraction of monomers released from the tube due to contour length fluctuations has a very simple form [5]:

$$\Psi(t) = \frac{1.5}{Z}\left(\frac{t}{\tau_e}\right)^{1/4} \qquad (1)$$

where $\tau_e = \tau_R/Z^2$ and Z is the number of entanglements per chain. Incorporating this in the calculation of the structure factor we come to the results displayed by the lines in Fig. 1. If we compare the experimental spectra with the model prediction, we generally find good agreement. The gradually increasing decay of S(q,t) with decreasing M_w is described very well both with respect to the magnitude of the effect as well as to the shape of S(q,t). We further note that in particular for smaller M_w the weighted error between fit and data is significantly smaller for this second approach.

The squares in Fig.2 show the resulting tube diameters. Aside from some small fluctuations they now stay constant, independent of M_w. At the highest molecular weight contour length fluctuations are insignificant and both lines of fitting yield the same d. At M_w = 36 kg/mol a slight difference appears which increases strongly with decreasing length. At $M_w = 12.4$ kg/mol the difference in the fitted tube diameters between both approaches rises to nearly 50 % emphasizing the strong effect of the contour length fluctuation in loosening the grip of the entanglements on a given chain.

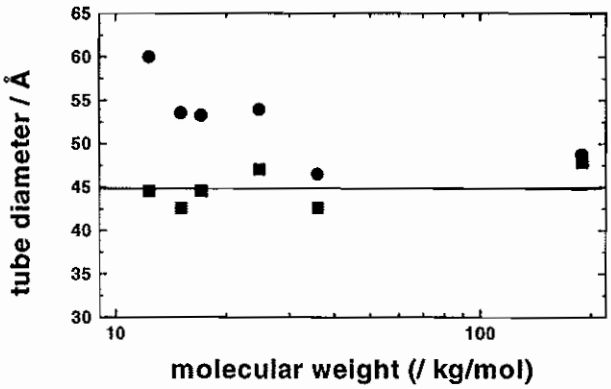

FIG. 2: Resulting tube diameters from the model fits with pure reptation (circles) and reptation and contour length fluctuations (squares) as a function of molecular weight. The line is a guide for the eye.

Thus, the comparison between the experimental chain length dependent dynamic structure factor and theoretical predictions clearly shows that in the time regime $t \leq \tau_R$ contour length fluctuations are the leading mechanism that limit the chain confinement inherent to the reptation picture. Without any further assumption or fitting parameter - the tube diameter d stays constant with M_w - it is possible to describe the full M_w dependence of S(q,t) in terms of local reptation and the contour length fluctuation mechanism.

In conclusion, our study of the chain length dependent dynamic structure factor in PE melts provides strong support to a theory of contour length fluctuations as the confinement limiting mechanism on a molecular scale.

[1] P.G. DeGennes, J. Physique **42**, 735 (1981)
[2] M. Doi and S.F. Edwards, The Theory of Polymer Dynamics, Oxford Science Publications, Clarendon Press, Oxford (1988) B. Ewen, Macromolecules **25**, 6156 (1992)
[3] P. Schleger, B. Farago, C. Lartigue, A. Kollmar, D. Richter, Phys. Rev. Lett. **81**, 124 (1998)
[4] D. Richter, B. Farago, R. Butera, L.J. Fetters, J.S. Huang and B. Ewen, Macromolecules **26**, 795 (1993)
[5] A.E. Likhtman, T.C.B. McLeish, Quantitative theory for linear rheology of linear polymer melts, to be published

Real Time SANS Study on Head Group Self-Assembly for Lithium Based Anionic Polymerisation

J. Stellbrink[1], J. Allgaier[1], L. Willner[1], T. Slawecki[2] and L. J. Fetters[3]

[1] *Institut für Neutronenstreuung*
[2] *NIST, Gaithersburg, MD 20899-8562, USA*
[3] *ExxonMobil, Annandale, NJ 08801 USA*

Small angle neutron scattering was used to *in situ* study the intermediate structures formed in the course of the polymerization of butadiene and isoprene in deuterated n-heptane. These *in situ* measurements showed that the start of the butadiene polymerization was accompanied by the presence of highly aggregated large-scale structures. The late stages of the isoprene polymerisation, on the other hand, can be well described by assuming a constant aggregation number f=4.

F&E-Nr: 23.30.0

Lithium based "living" anionic polymerisation [1] is an established method for preparing well-defined model polymers in laboratory as well as in industry. Nevertheless there exist still some unsolved questions concerning its detailed reaction mechanism: The "living" polymer chain R-$CH_2^-Li^+$ resembles surfactants in that way, that due to its zwitterionic head group it self-assembles if the polymerisation is performed in nonpolar solvents:

$$f\ \text{R-CH}_2^-\text{Li}^+ \quad (\text{R-CH}_2^-\text{Li}^+)_f \qquad (1)$$

In particular the detailed structure of these intermediate aggregates is still under discussion. The current textbook mechanism assumes a constant aggregation number f=4 for butadiene and isoprene. Recently we modelled the problem by investigating the aggregation behaviour of "living" polymer chains with different chain lengths by small angle neutron scattering (SANS) [2-4]. We found some evidence for i.) the existence of dense, large scale aggregates, R≈1000Å, which ii.) coexist with intermediate sized aggregates showing a concentration dependent aggregation number 4≤f≤12. Here we report real-time SANS studies perfomed directly on polymerizing solutions to investigate in more details the structure of the different species present during "living" anionic polymerisation [5].

Experimental: The SANS measurements were done on the NG-7 instrument at NIST, Gaithersburg(MD), USA. A detector setting of 12.75m with an offset of 25cm was used. The neutron wavelength of λ= 7Å was used with a spread $\Delta\lambda/\lambda$=15%. This in turn led to an experimental range of scattering vector $Q=4\pi \sin(\theta/2)\,\lambda^{-1}$ from 3×10^{-3} to 4×10^{-2} Å^{-1}, with θ the scattering angle. The SANS measurements were conducted at 22°C and 10°C to yield a convenient polymerization rate fitting to the temporal resolution of the SANS experiment. The polymerization solvent was deuterated n-heptane (Chemotrade, 99.2% d) while the initiator was sec-butyllithium, for details see[5].

Early reaction stages: Fig. 1 shows the raw intensity data (corrected only for empty cell scattering) for the butadiene system obtained in the very early stages of the polymerisation. In spite of the scatter at high Q the corresponding low Q data is seen to increase as Q is diminished. This is generic behavior for the presence of species with much larger length scales, R≈1000Å, than the tetramers predicted by the textbook mechanism. The enhanced forward scattering decreases with incrasing reaction time t, i.e. the large scale aggregates „melt". This corroborates our previous finding that aggregation number decreases with increasing chain length [4]. We note that neither the corresponding initiator nor the pure monomer solution show this type of scattering profile. For the isoprene system a similar behaviour is found, but the amount of forward scattering is not that large as for the butadiene system. This can be explained by the known much faster reaction rate of isoprene, which hinders us from covering the very early stages of the isoprene polymerisation even at 10°C.

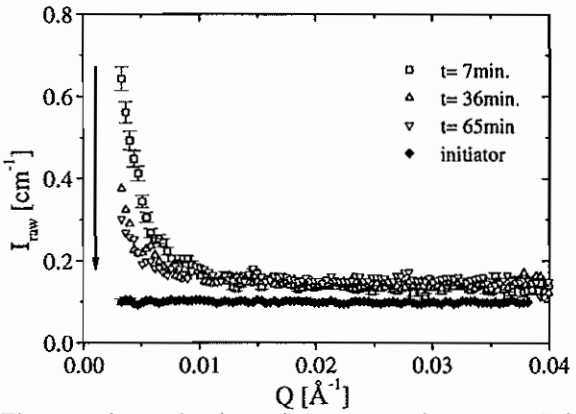

Figure 1: Scattering intensity vs. scattering vector Q for early stages of butadiene polymerisation at 22°C.

Late reaction stages: The polymerizing system can be considered to contain two types of monomers: i.) those incorporated into the growing polymer chains (passive) and ii.) those awaiting reaction (active). From mass conservation their volume fractions Φ_p and Φ_m are related by $\Phi_p(t)+\Phi_m(t)=\Phi_0$, with Φ_0 the given total monomer volume fraction. Therefore, the SANS scattering intensity as a function of reaction time t and scattering vector Q is given by:

$$I(Q,t)=\frac{\Phi_p(t)\left(1-\Phi_p(t)\right)}{\left[\dfrac{1}{f(t)V_w(t)P(Q,t)}+2A_2(t)\Phi_p(t)\right]}+\Phi_m V_m \qquad (2)$$

where P(Q,t) denotes the form factor of the polymer or the polymer aggregates, V_w the corresponding weight average

polymer volume per head group, A_2 the second virial coefficient, and V_m the monomer volume. In the first term, the scattering contribution of the growing polymer chains, we used a virial expansion for taking into account concentration effects in dilute polymer solution. In the second term, the scattering contribution of the monomers, we neglected the monomer form factor $P_m(Q)$, which equals 1 in the SANS Q-range under consideration.

If we transform to number density N_p, all time dependent

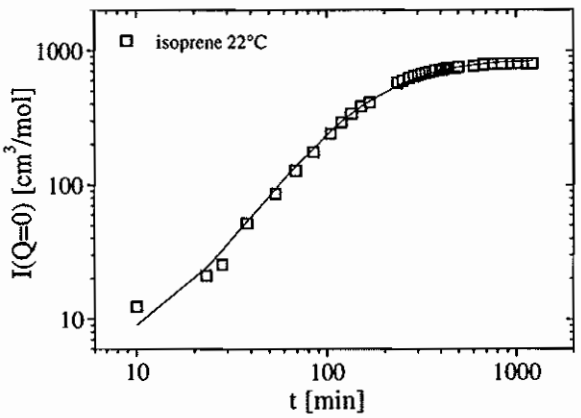

Figure 2: Forward scattering intensity as a function of reaction time for isoprene polymerisation at 22°C, solid line: fit to eq. 4, see text.

quantities in eq. (2) can be related to $N_p(t)$ if we i.) focus on the forward scattering I(Q=0, t), ii) assume a constant aggregation number f=4 as predicted by the current mechanism, iii) make use of the well known first order kinetics in monomer concentration:

$$N_p(t) = N_0\text{-}N_m(t) = N_0(1 - e^{-t/\tau_1}) \qquad (3)$$

and iv.) assume a M_w- and therefore also time-independent virial coeffcient A_2, which is justified by renormalisation group theory [6]:

$$I(Q=0) = \frac{N_p M_m}{\rho_p N_I \left(\frac{N_i N_p \rho_p}{f N_p M_m} + \frac{2 A_2 N_p M_m}{\rho_p N_I} \right)} + \frac{\left(\frac{c_0}{\rho_p} + \frac{N_p M_m}{\rho_p N_I} \right) M_m}{\rho_m} \qquad (4)$$

Here c_0 denotes the given total monomer concentration, M_m the monomer molecular weight, N_i the initiator concentration, and ρ_p, ρ_m the polymer and monomer density, respectively. Fig 2 shows a comparison between experimental data and fit according to eq. 4. We obtained the following results: τ_1=397±5min and A_2=(5.99±0.6)x10^{-4} cm^{3}mol/g^2. The virial coeffecient A_2 is within error bars the same as that for the corresponding terminated chain, $A_{2,term}$=(7.40±0.3)x10^{-4} cm^{3}mol/g^2 [7].

Finally, the complete Q-dependence can be described using the Benoit form factor [8], which links the radius of gyration R_g of star-like aggregates to the corresponding quantity of the building unit, i.e. in our case the growing polymer chain by $R_g = \sqrt{(3f-2)/f}\, R_{g,arm}$. The time dependence of R_g was modelled by a power law $R_g \sim M_w^{\nu}$, where prefactor and exponent are given by the terminated chain [7]. The result of the fit is shown in fig. 3. The agreement between calculation and experiment is striking: A complex data set of more than 4000 t- and Q-dependent points can be described by actually one single adjustable parameter, namely the characteristic time τ_1 of monomer consumption.

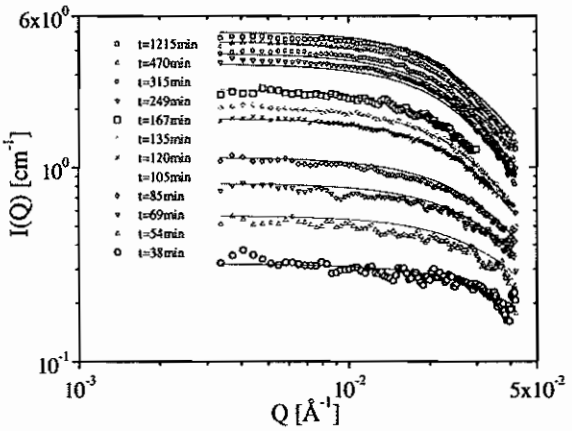

Figure 3: Scattering intensity vs. scattering vector Q as a function of reaction time for isoprene polymerisation.

Conclusions: SANS has been proven to be a powerfull tool for investigating reaction kinectics, which allows both, structure determination and evaluation of rate constants at the same time. The presented *insitu* SANS data on "living" anionic polymerisation show a large variety of intermediate aggregated species. In particular the large scale aggregates observed in the very early reaction stages, the post-initiation period, are somehow contradictory to current textbook mechanisms, and certainly need further investigation.

[1] M. Szwarc, M Van Beylen, *Ionic Polymerization and Living Polymers*, Chapman&Hall: N.Y./London (1993)

[2] L.J. Fetters, N. Balsara, J.S. Huang, H.S. Jeon, K. Almdal and M.Y. Lin, *Macromolecules*; **28**, 4996 (1995)

[3] J. Stellbrink, L. Willner, O. Jucknischke, D. Richter, P. Lindner, L.J. Fetters, J.S. Huang, *Macromolecules*; **31**, 4189 (1998)

[4] J. Stellbrink, L. Willner, D. Richter, P. Lindner, L.J. Fetters, J.S. Huang. *Macromolecules*, **32**,: 5321 (1999)

[5] J. Stellbrink, J. Allgaier, L. Willner, D. Richter, T. Slawecki, L.J. Fetters, submitted to *Polymer*

[6] H.G. Elias, *Makromoleküle*, Verl. Hüthig und Wepf, Heidelberg (1990)

[7] The final polymerisation product, the non-aggregated so called *terminated* chain, was analysed by an independent experiment with regard to M_w, R_g and A_2.

[8] H.J. Benoît, *Polym. Sci.*, *11*, 507 (1953)

A neutron scattering study on the structure and dynamics of oriented lamellar phase microemulsions

M.Mihailescu, M.Monkenbusch, J.Allgaier, H.Frielinghaus, D.Richter
Institute for Neutron Scattering

B.Jakobs, T.Sottmann
Institut für Physikalische Chemie, Universität zu Köln,
Luxemburger Str. 116, D-50939 Köln, Germany

Lamellar phases obtained by mixing water and oil with intervening surfactant monolayer interfaces (eventually containing low molecular weights amphiphilic block-copolymers) are studied. Structural and dynamical investigations of oriented lamellar phases at the length scale of the inter-membrane distance and beyond are performed using Small-Angle Neutrons Scattering (SANS) and Neutron Spin-Echo (NSE). The data analysis in terms of static and dynamic structure factors for a stack of elastic interfacial membranes yields information of the membrane curvature elasticity and membrane interactions in terms of membrane properties. The conditions of applicability of the available theoretical concepts to extract, e.g. the bending modulus from NSE data, are discussed.

F&E-Nr: 23.30.0

Long-range ordered lamellar phases consisting of an alternation of water and oil layers separated by surfactant monolayers are one of the various topologically distinct structures which can self-organize in a ternary aqueous-oil-surfactant system, see Fig.1. For very flexible membranes ($\kappa \simeq k_BT$), like those studied in this work, the large out-of-plane thermal fluctuations induce collisions between neighboring membranes. They give rise to a repulsive interaction which is caused by the reduction of entropy of the membrane fluctuations and is known under the name of Helfrich steric repulsion [1].

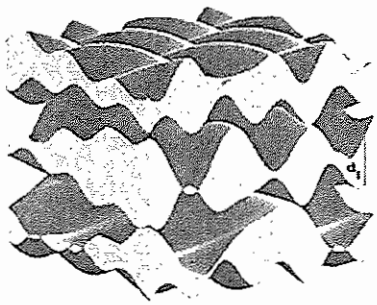

FIG. 1. Sketch of a lamellar phase with membrane fluctuations. The distance between two collisions relates to the lateral correlation length ξ.

It was shown [2,3], that anchoring amphiphilic block-copolymers (macromolecular surfactant analogs) on the interface has dramatic influences on the extension of the bicontinuous single-phase region in the phase diagram. Tethered polymers on surfactant layers modify the elastic moduli κ and $\overline{\kappa}$ [8,3]. The position and boundaries of a lamellar phase appearing in a basic surfactant system are also modified. Long polymers act on the phase diagram as to expand the random, bicontinuous phase domain, while suppressing the formation of the lamellar phase [2]. The polymers have profound effect on the correlation lengths of the structure and on the phase diagram. Upon addition of polymers, the appearance of lamellar islands, at higher dilution than normally expected for the pure $C_{10}E_4$ /water/decane system has been observed.

The lamellar phase is stabilized by the membrane-membrane interaction –expressed in terms of the layer compressibility modulus $\overline{B}$–, the bending energy contributions depend on $\kappa_c = \kappa/d_f$:

$$H = \frac{1}{2}\overline{B}(\frac{\partial u}{\partial z})^2 + \frac{1}{2}\kappa_c(\frac{\partial^2 u}{\partial x^2} + \frac{\partial^2 u}{\partial y^2})^2 \qquad (1)$$

Equipartition leads to the Fourier amplitudes of the membrane displacements U_k

$$\langle \mid U_k \mid^2 \rangle = \frac{k_BT}{\overline{B}k_z^2 + \kappa_c k_\perp^4} \qquad (2)$$

In general, we need to distinguish between the mode wave vector $\vec{k}$ and the momentum transfer $\vec{q}$ of the scattering experiment. In order to describe scattering intensities and NSE data around the $S(q)$ maxima, a theory of Caillé [4] (for NSE in a dynamical extension) may be used. It describes the off-peak intensity and the pseudo Bragg-peaks as power law divergencies. A consequence of the large fluctuation amplitudes is also that many modes with different $\vec{k}$ contribute to the observed dynamics at a given scattering wave vector $\vec{q}$. In the intermediate q-regime where the pseudo Bragg peaks occur the scattering behavior depends on both the membrane properties, κ, and the membrane interactions given in terms of the compressibility modulus of the stacks, $\overline{B}$.

In the regime of high-q ($qd_f \gg 1$), it may be assumed that the influence of the inter-membrane correlations on the dynamic structure factor are small, and the data can be described by the expression derived

by Zilman and Granek [9] that ignores $\overline{B}$ and assumes a system of decoupled membrane patches of size $\simeq \xi$. Interferences between adjacent membranes -due to the large fluctuation amplitudes- average to zero and motions probed there are no longer collective. In this asymptotic regime the relaxation mode of membrane fluctuation exhibits a simple dispersion of the relaxation rate [5,7,6]: $\omega(k) = k^3\kappa/[2(\eta_{\text{oil}} + \eta_{\text{water}})]$ since $\eta_{\text{oil, water}}$ are known this regime allows for the determination of single membrane properties -namely κ- by measurements of the relaxation dynamics. Neutron spin-echo spectroscopy covers the appropriate space and time regime. This membrane Zimm dynamics has already been studied in the bicontinuous phase of microemulsions of the same type by NSE and interpreted [10]. The orientation of the lamellar phase reduces the computational effort involved in the proper application of the Zilman Granek model compared to the bicontinuous version. However, the neglected membrane interactions are more important in the lamellar phase.

In a first data analysis in terms of stretched exponentials yielding Γ_q and β in the asymptotic regime ($q \gg q_{1f}$), i.e. $S(q,t)/S(q) = e^{-\Gamma_q{}^\beta}$ are compared with the predictions: $\Gamma_q \propto q^3$ and $\beta = 2/3$ of the single-membrane approach [9] (Figs.2,3).

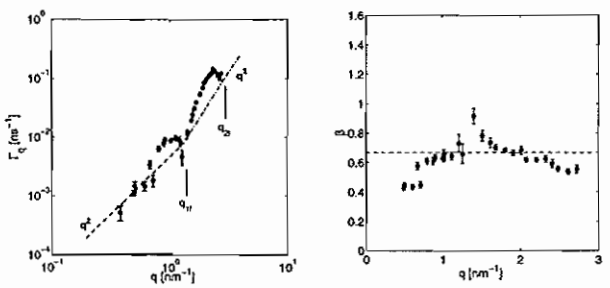

FIG. 2. Left: Relaxation rate $\Gamma_q(q)$ from the stretched exponential analysis based for the basic $C_{10}E_4$ system. Right: Corresponding $\beta(q)$ exponent.

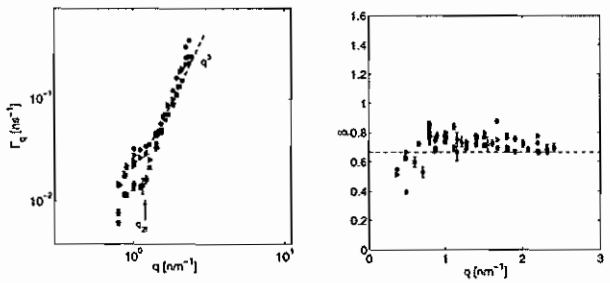

FIG. 3. Same type of data as shown in Fig. 2 but for polymer containing systems with larger d_f PEP_1-PEO_1 (circles), PEP_2-PEO_2 (triangles) and PEP_5-PEO_5 (*squares*).

Γ_q in Fig.2 shows clear evidence of deGennes narrowing at the pseudo Bragg peak positions and a $\propto q^2$ regime below the first peak, however, the expected asymptotic q^3 behavior is not reached. In contrast Fig. 3 displays a clear high-q behavior $\Gamma_q \propto q^3$ and the corresponding β values approach $\beta = 2/3$.

A complete analysis and the determination of the bending modulus κ, the full numerical procedure as described in Ref. [10] but without angular averaging was carried out, see Fig. 4.

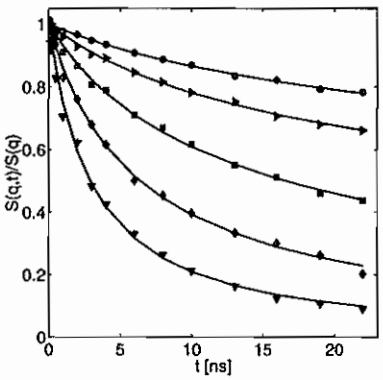

FIG. 4. NSE relaxation curves for oriented lamellar phase with PEP_5-PEO_5 corresponding, from top to bottom, to q=(0.5, 0.8, 1.0, 1.4, 1.8, 2.2) nm^{-1}. The solid lines are individual fits to the numerically integrated Zilman Granek model.

while at q in the peak region where the validity of the procedure is questionable fitted values of $\kappa(q < 2q_{1f}) \simeq 1k_BT$ are obtained, the extracted values of κ approach $2k_BT$ in the high-q limit. This somewhat large value for κ may indicate modified friction effects or higher order bending energy terms ? No clear dependence on polymer length beyond the 10% error bars was detected, however, a trend towards larger κ for the longest polymer is seen.

[1] W. Helfrich, Z. Naturforsch. bf 33a, 305 (1978)
[2] B. Jakobs et al., Langmuir **15**, 6707 (1999)
[3] H. Endo et al., J. Chem. Phys.**115**, 580 (2001)
[4] M. A. Caillé, C. R. Acad. Sci. Paris B **274**, 1733 (1972)
[5] S. Ramaswamy, J. Prost, W. Cai, T. C. Lubensky, Europhys. Lett, **23**, 271, (1993)
[6] T. Schilling, O. Theissen, and G. Gompper, Eur. Phys. J. E **4**, 103 (2001)
[7] R. Messager, P. Bassereau, G. Porte, J. Phys. (Paris) **51**, 1329 (1990)
[8] C. Hiergeist and R. Lipowsky , J. Phys. II France **6**, 1465 (1996)
[9] A.G. Zilman and R. Granek, Phys. Rev. Lett. **77**, 4788 (1996)
[10] M. Mihailescu et al., J. Chem. Phys. **115**, 9563 (2001)

Time evolution of strain relaxation in a model-branched H-polybutadiene

M. Heinrich, W. Pyckhout-Hintzen, D. Richter, E. Straube[1], T.C.B. McLeish[2], D.J. Read[3], A. Wiedenmann[4]
Institut für Neutronenstreuung
[1] *Martin-Luther-Universität Halle, Germany*
[2] *IRC in Polymer Science and Technology, Department of Physics, University of Leeds, U.K.*
[3] *Department of Applied Mathematics, University of Leeds, U.K.*
[4] *Hahn-Meitner-Institut, Berlin, Germany*

We present a study of the relaxation of strained H-shaped polymer melts by Small Angle Neutron Scattering. The structure functions corresponding to annealing times in the arm-relaxation range are interpreted in terms of a Random Phase Approximation theory. We show that the results obtained in non-linear deformation are in very good agreement with those obtained from the dynamical linear shear moduli.

F&E-Nr: 23.30.0

The relationship between the microscopic details of branched polymers dynamics on one hand and their enhanced ease of processing on the other hand compared to linear structures has been a challenge for decades in several disciplines of polymer research. Just shortly, new quantitative insights, especially in the linear response of simple architectures like linear chains and starlike structures, became available after an extensive theoretical modeling of stress relaxation concepts. The assignment of these processes, localised to specific time and length scales has led to the investigation of more complex hybrid architectures like H's which possess both linear and star dynamics features. An independent proof of this "molecular, rheological" pattern is ideally tackled by the technique of Small Angle Neutron Scattering (SANS), of which the scattering vector matches the length scales of interest.

In a former investigation of the short time relaxation dynamics, the feasability of the experimental decoupling of microscopic and macroscopic time scales by quenching the relaxation states was shown [1].The strongly non-linear experiments obtained in elongational flow failed to agree in quantitative way with the expected relaxation from small-amplitude linear shear data and sustained a slow-downed dynamics due to incipient crystallization under strain at low temperature. A follow-up with a non-crystallizable H-polymer, which was scaled to the first H in terms of its entanglement structure is presented here. The PB-polymer (40% vinyl structure) consists of a labeled bridge and unlabeled arms.

The stress relaxation which is a sensitive qualifier of the loss of topological contributions to the mechanical response provides the necessary microscopic features, detectable in a time-dependent small angle neutron scattering experiment. Fig. 1 and 2 show experimental dynamic shear moduli and estimated stress relaxation, reduced to $T_0 = 25°C$. The data points correspond to the states at which the SANS structure was investigated.

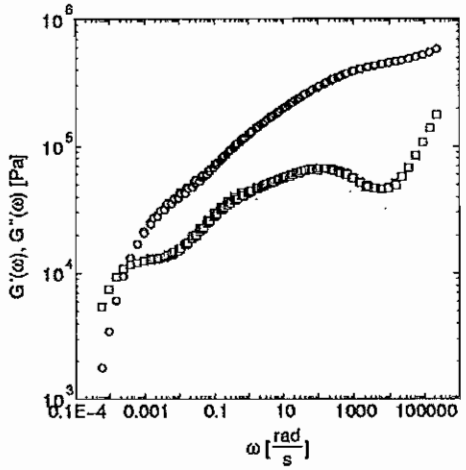

FIG. 1. Dynamic shear moduli G'(ω) (circles) and G"(ω) (squares) at $T_0 = 25°$.

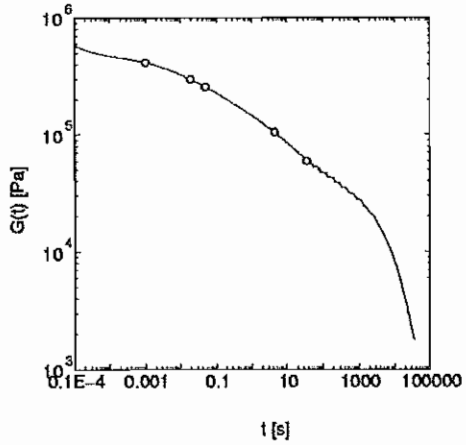

FIG. 2. Stress relaxation modulus G(t) at $T_0 = 25°$ (line) estimated from the measured dynamic moduli (Fig. 1). The points correspond to the states at which the SANS structure was investigated.

The Random Phase structure factor for the quenched system takes into account the presence of quenched and annealed variables. A rigorous treatment as well as a simplified treatment of interactions proved already to deliver comparable results [1].

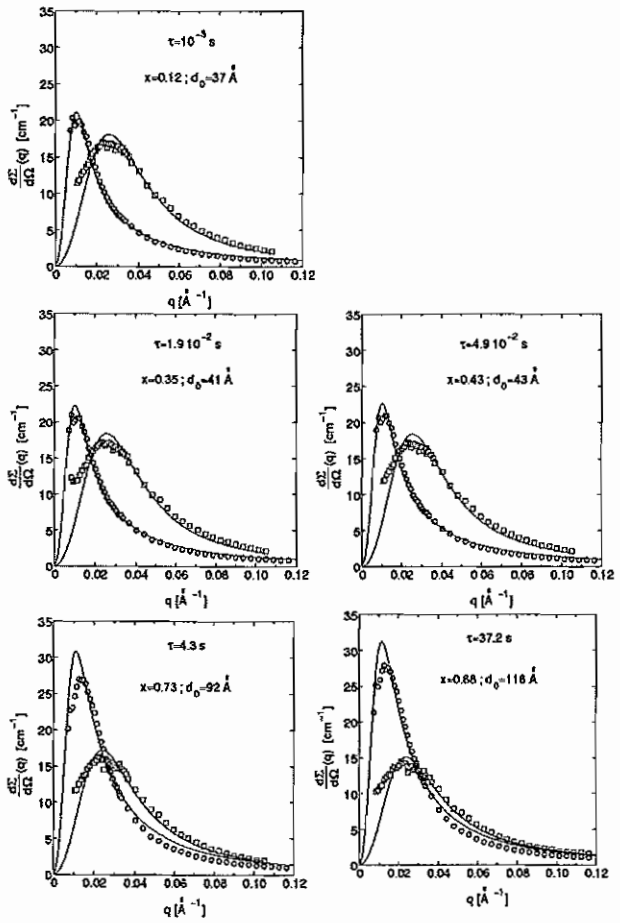

FIG. 3. Experimental structure functions along the axes parallel (circles) and perpendicular (squares) to the strain, measured after a strain of λ=2, after 10^{-3}, 1.9 10^{-2}, 4.9 10^{-2}, 4.3 and 37.2 s of annealing time at 25°. The lines represent the corresponding theoretical calculations.

The scattering data along both principal axes in Fig. 3 are presented in terms of the molecular rheology description [2]:

(1) The rapid end equilibration leads to an initial isotropization of arm segments of the order of the tube diameter. The arm is now consisting of isotropic segments and deformed segments with deformation λ.

(2) The typical non-linear retraction process, accompanied by contour length fluctuations is an entropic process and occurs to reach again the equilibrium tension in the arm. The strain depends on the Rouse time of the chain τ_R and the actual annealing time t as [3]:

$$\lambda(t) = 1 + (\alpha(G) - 1)exp(-t/\tau_R) \qquad (1)$$

where $\alpha(G)$ is the deformation tensor.

(3) The entropically unfavoured motion in direction of the branchpoint expresses itself in the increase of the diameter with relaxation. It reflects the loss of confinement by the dilution effect with isotropic chain ends. The diluted tube depends on the fraction x of relaxed segments.

(4) Branchpoint withdrawal and final reptation of a diluted bridge chain are not yet expected to appear.

The similarity of the predictions of linear shear and the fitted relaxation state of the arm as shown in Fig. 4 is striking.

It is encouraging to notice that typical non-linear phenomena can now be tackled from an input of linear data. This justifies the initial aim of constructing a rheological tool box for extensive non-linear predictive design.

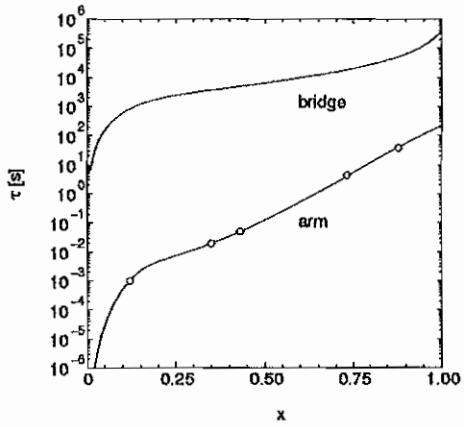

FIG. 4. Annealing times as a function of x, the fraction of relaxed segments in one arm. The lines represent predictions from linear shear and the points represent the results from SANS.

[1] M. Heinrich, W. Pyckhout-Hintzen, D. Richter, E. Straube, D.J. Read, T.C.B. McLeish, D.J. Groves, R.J. Blackwell, A.Wiedenmann, submitted to Macromolecules.

[2] T.C.B. McLeish, S.T. Milner, Adv.Polym.Sci. **143**, 195 (1999).

[3] M. Doi, S.F. Edwards, *The Theory of Polymer Dynamics* (Oxford Press, New York, 1986).

Unimer Exchange Kinetics of Block Copolymer Micelles

L. Willner, A. Poppe, J. Allgaier, M. Monkenbusch, D. Richter
Institute for Neutron Scattering

A time-resolved SANS technique was elaborated to study the unimer exchange kinetics in block copolymer micelles under equilibrium conditions exploiting the large difference in scattering length density between deuterated and protonated species. The technique was applied to the system PEP-PEO/DMF where in contrast to theoretical predictions the observed kinetics consists of two well separated processes. While the fast process can be associated with a single unimer exchange the second slow process could not yet be assigned to a microscopic picture.

F&E-Nr: 23.30.0

It is well known that block copolymers above a critical concentration self-assemble into micellar structures. According to the *Closed Association Concept* at equilibrium there is a dynamic exchange of block copolymers between solution and micelles. This equilibrium is characterized by a single equilibrium constant and a narrow micellar size distribution.

The equilibrium structures of block copolymer micelles have been extensively studied theoretically and experimentally using a large variety of different techniques, e.g. small angle neutron scattering, static light scattering, microscopy etc., while less attention has been payed to the kinetics of unimer exchange although interesting for both fundamental research and technical applications. Generally, the kinetic properties of a micellar equilibrium are difficult to access by experimental techniques. For block copolymer micelles fluorescence quenching [1,2] have been applied but this technique requires the preparation of block copolymers with bulky fluorescence labels preferably at the junction of the two blocks. This may influence the association behaviour of the underlying block copolymer/solvent system.

We have developed a time-resolved SANS method to study the exchange kinetics under equilibrium conditions [3]. The principles of the SANS-experiment are illustrated in FIG. 1. Two reservoirs consisting of deuterated (yellow) and protonated (blue) micelles are prepared in an isotopic solvent mixture whose scattering length density matches exactly the average scattering length density (green) of the two block copolymers. For the case that the block copolymers just carry different labels but are otherwise identical, scattering curves of the two reservoirs are equal. Since the square root of the scattered intensity $I(Q)^{1/2}$ is proportional to the difference in scattering length density between solvent and micelle, $\rho_{sol} - \rho_{mic}$, the excess concentration of a block copolymer species in a micelle can be determined. After mixing equal amounts of the two reservoirs the following time-dependence can be anticipated:
i) At $t = 0$ the contrast is maximal, the scattered intensity is identical with those of the two reservoirs since contrast and concentration do not change by mixing.
ii) As a function of t the intensity decreases because due to unimer exchange the contrast becomes smaller.
iii) At $t = \infty$ all micelles consist of a random mixture of h- and d-unimers, the contrast vanishes and scattering intensity is minimal.
Provided that the difference in $I(Q)$ at $t = 0$ and $t = \infty$ is sufficiently large and the residence time of a block copolymer in a micelle, which is determined by the expulsion rate, fits in the time-window of a typical SANS-measurement, time-resolved SANS is an ideal tool for a kinetic study.

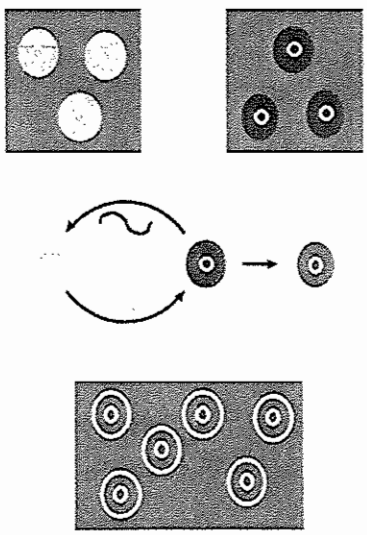

FIG. 1. Illustration of the SANS-experiment to determine the exchange kinetics of unimers in a micellar system.

This method was applied to study the exchange kinetics of micelles formed by the amphiphilic block copolymer poly(ethylene-alt-propylene) - polyethylene oxide (PEP-PEO) in water and in dimethylformamide (DMF) which are both selective solvents for PEO. In water we did not observe any decrease in intensity even not at high temperatures and long times. Apparently, the micelles are kinetically frozen due to the high interfacial tension between the strongly hydrophobic PEP and water ($\gamma \simeq 51\, Nm^{-1}$).

Despite of a strong reduction in the interfacial tension in DMF ($\gamma \simeq 3\,Nm^{-1}$) the unimer exchange is still to slow to be measured by the SANS method at room temperature. In order to accelerate the kinetics we have performed measurements at elevated temperatures. While at 65 °C the time dependence is still weak, the formation of mixed micelles is more pronounced at 70°C and is clearly visible at 80 °C. As an example the scattering curves at 70°C are shown as a function of time in FIG. 2.

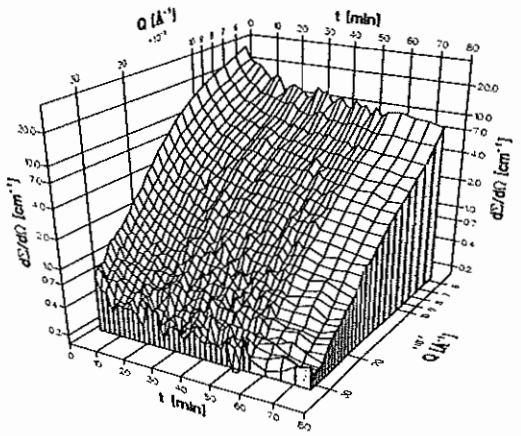

FIG. 2. Three dimensional plot of the scattering intensities as a function of scattering vector Q and time t of PEP-PEO micelles in DMF at $T = 70°C$.

For a quantitative evaluation the integral intensities were corrected by subtraction of the scattering of the sample at $t = \infty$ (Sample was prepared from a 50/50 blend of both polymers). The square root of this corrected intensity is then plotted versus time as shown for 80 °C in FIG. 3. Acceptable fits could only be obtained by a sum of two exponentials:

$$I(t) \sim a_1 exp\{-k_1 t\} + a_2 exp\{-k_2 t\} \qquad (1)$$

The fitted rate constants k_1 and k_2 differ by more than one order of magnitude, clearly indicating the existence of two well separated processes. The activation energies of the two processes were deduced from $\ln k$ *vs.* $1/T$ plots to be $29\,kJ/mol$ for the slow process and $12.2\,kJ/mol$ for the fast process. The existence of two processes stays in contradiction to theoretical conceivabilities. Halperin and Alexander [4] considered the association/dissociation of block copolymers to proceed solely via the insertion/expulsion of single unimers. For this process an expression for the activation energy was derived:

$$E_A = N_B^{2/3} \gamma l^2 \qquad (2)$$

where N_B denotes the degree of polymerization of the insoluble block and l the length of a repeat unit. With $l = 5.1$ Å and $N_{PEP} = 67$ an energy barrier of $7.5\,kJ/mol$ was calculated.

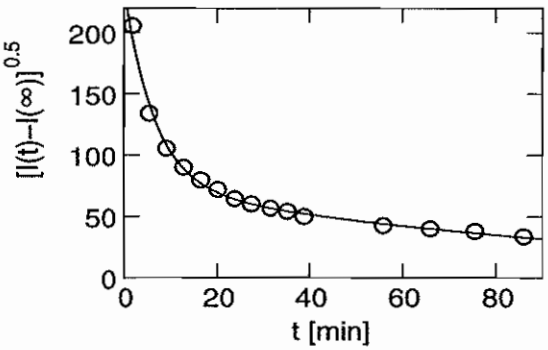

FIG. 3. Plot of the square root of the corrected integral intensity *vs.* time at 80°C. Solid line represents the fit with a sum of two exponentials

A comparison with the experimentally obtained energies implies that the fast process can be assigned to the single unimer exchange while the origin of the second slow process finds no basis in the scaling theory. A joint mechanism of unimer exchange and fusion and fission was considered in the scaling theory of Dormidontova [5]. However, since both mechanisms would exist in parallel, the corresponding rates would add and the signal decay would still be single exponential.

In order to explain the observed double exponential time decay we have considered an isotope effect for the interfacial tension. On the basis of eq.2 we have calculated a factor of 2.4 needed to account for the two rate constants. Such a large isotope effect would result in a more than a factor of 4 difference in the equilibrium aggregation of the two species which has not been observed by SANS. Moreover, due to umimer exchange a distribution of micelles with different interfacial tensions can be expected leading to a gradual rate change with changing composition which lead to a stretched exponential decay. Attempts to fit the data in such a way did not give satisfactory results.
Thus, the appearence of the second slow process has not yet been understood.

[1] K. Procházka K., B. Bednář, E. Mukhtar, P. Svoboda, J. Trněná, and M. Almgren, J. Phys. Chem. **95** 4563 (1991).
[2] Y. Wang, C. M. Kausch, M. Chun, R. P. Quirk, and W. L. Mattice, Macromolecules **28** 904 (1995).
[3] L. Willner, A. Poppe, J. Allgaier, M. Monkenbusch, and D. Richter, Europhys. Lett. **55** 667 (2001).
[4] A. Halperin, and S. Alexander, Macromolecules **22** 2403 (1989).
[5] E. E. Dormidontova, Macromolecules **32** 7630 (1999).

A step forward in understanding methane: rotational tunneling in phase III

M. Prager, W. Press[1], B. Asmussen[1], J. Combet[2]
Institute for Neutron Scattering
[1] *Institut für Experimentalphysik, Universität Kiel, D-24118 Kiel, FRG*
[2] *Institut Laue-Langevin, F-38042 Grenoble Cedex5, France*

Rotational tunneling of tetrahedral molecules is a sensitive probe of site symmetries and site multiplicities. However, the complexity of overlapping tunneling patterns can render a model free description of data impossible. Only on the basis of the recently determined low temperature crystal structure of phase III of methane the high resolution tunneling spectrum of 1.5% CH_4 in CD_4 could be quantitatively explained. The analysis is based on tunneling matrix elements and includes line positions and intensities. Barrier heights and disorder obtained with accuracies better than 0.1meV will allow to refine pair interaction potentials. Level specific spin conversion times show up in the intensities of tunneling transitions.

F&E-Nr: 23.15.0

Methane is the simplest organic molecule. It is of fundamental importance for any organic material to understand interactions between methane molecules. Like many supposedly simple molecular materials methane has a rich phase diagram with actually seven known phases. Fully solved crystal structures exist of the two cubic phases I and II only [1]. Phase I is a disordered plastic phase while in phase II 75% of the molecules become orientationally ordered. The structure of phase II was predicted on the basis of octupole-octupole interaction of methane tetrahedra [2] with the octupole moment calculated from pair interaction potentials [3]. Very recently phase III - known to exist since 1937 - could be solved using high resolution neutron powder diffractometry. In disagreement with predictions based on octupole-octupole interaction and a crystal field [4] it is not a subgroup of phase II but the cell is very slightly orthorhombic with all molecules ordered on two sublattices of m and 2 site symmetries, respectively, and equal occurrence probabilities [5]. Cuts through the unit cell at different heights are shown in Fig. 1.

Tunneling spectra were measured at the ILL, Grenoble, using the backscattering spectrometer IN10B with its variable temperature monochromators. A wide range of energy transfers $-7\mu eV \leq E \leq 180\mu eV$ at $\sim 1\mu eV$ energy resolution is obtained using the $KCl[200]$ and $NaCl[111]$ variable temperature monochromators. The lattice spacings of both monochromators allow only downscattering processes to be observed. The open symbols in fig. 2 show a composed spectrum representing 100h of counting time. The high energy resolution reveals many new details especially at low energy transfers. The signal to noise is limited by the low concentration of guest molecules, the high resolution and the large number of transitions. Long counting times lead to high background which amounts to about 30% of the most intense inelastic line. This constant background is subtracted.

The spectrum is further modified by inhomogeneous line broadening. Despite the concentration of guest molecules was limited to 1.5% disorder and the corresponding distribution of rotational barriers is still significant. Inhomogeneous line broadening is proportional to the energy transfer and thus reduces the quality of a spectrum especially at large energy transfers. In the present example we have $\Gamma(T) = \Gamma_{res}(1 + \frac{0.018}{\mu eV}\hbar\omega)$.

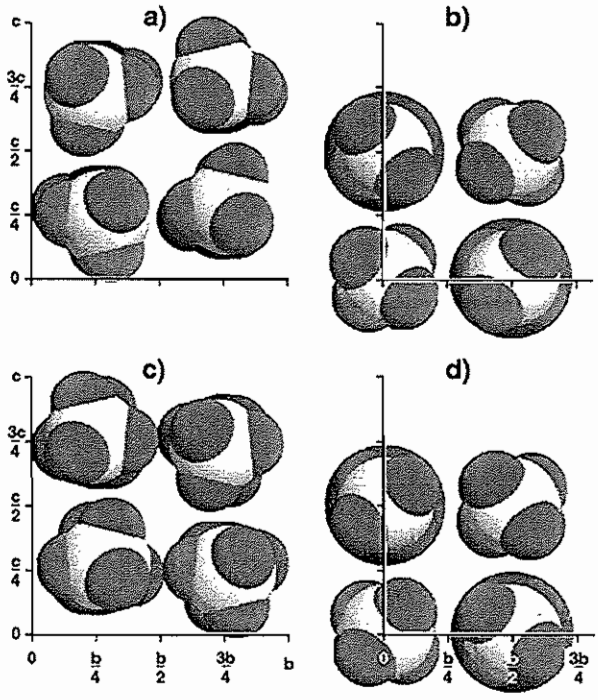

FIG. 1. Arrangement of the methane molecules in the b-c-plane of the *Cmca* space group of phase III. a) and c) show cuts through the planes $x = 0, \frac{1}{2}$ with m molecules, b) and d) represent planes $x = \frac{1}{4}, \frac{3}{4}$ with 2-site molecules. The underlying blue colour represents orientations in phase II.

Only the solution of the crystal structure of phase III [5] yielded a solid basis for a data analysis. The model

of single particle rotation offers the overlap matrix elements as the appropriate fit parameters [6]. In the general case the groundstate is a quintett (A, T_1, T_2, T_3, E) with nine allowed tunneling transitions. With increasing site symmetry T_i-levels become degenerate and the number of transitions is finally reduced to 2 for tetrahedral environment.

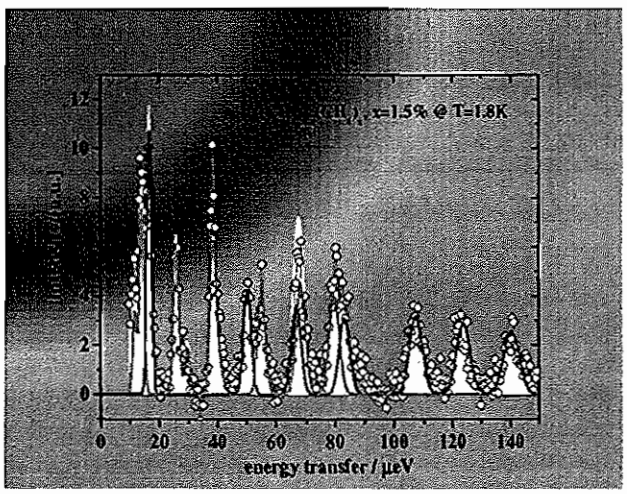

FIG. 2. Neutron spectrum of 1.5% CH_4 in CD_4. Energy resolution about $1\mu eV$. Sample temperature $T = 1.8K$. Experiment: open circles; red line: CH_4 on m-sites; blue line: CH_4 on 2-sites; yellow area: sum of both.

In the actual case we need the results for 2- and m-symmetries. Accordingly [6], the three equidistant lines of equal intensities at energy transfers $\geq 100\mu eV$ are identified as the $T_i \rightarrow A$ transitions of the site with 2-fold symmetry axis. This assignment and a small 180^o matrix element H determine all other transitions of this site. Final fit parameters are $h_1 = h_3 = -19.99\mu eV, h_2 = h_4 = -11.82\mu eV, H = 0.80\mu eV$ with levels $0(A^{(2)}), 107(T_1^{(2)}), 124(T_2^{(2)}), 140(T_3^{(2)}), 190(E^{(2)})\mu eV$.

The remaining inelastic intensity is explained by transitions of methane molecules at m-sites. Starting with attributing the unexplained inelastic intensity at the largest energy transfer to the $T_3 \rightarrow A$ transition a number of combinations of lines was explored. Final parameters are $h_1 = -2.09\mu eV, h_2 = -16.55\mu eV, h_3 = h_4 = -6.33\mu eV, H = 0.056\mu eV$ with levels $0(A^{(m)}), 39(T_1^{(m)}), 68(T_2^{(m)}), 79(T_3^{(m)}), 91(E^{(m)})\mu eV$.

Intensities are calculated for equal population of the tunnel sublevels. The good fit (yellow area of fig. 2) represents an independent support of the new crystal structure [5]. Based on the analogy to one-dimensional rotation barrier heights are derived from mean $E \rightarrow T$ transition energies via the Mathieu equation. The potential of molecules at 2-sites is ~16.6meV and significantly weaker than that of m-sites where it amounts to 21.5meV. This could be a residue of partial orientational disorder on this sublattice in phase II. Both potentials are stronger than any in phase II. The rotational potentials show a narrow distribution with a relative width below 1% ($\delta V = 0.12(0.13)meV$) due to chemical and excitational disorder.

The description with matrix elements is a first phenomenological step only. Next, the overlap matrix elements have to be related via the wave functions with the rotational potential $A(\omega_E)$, ω_E being the Eulerian angles. $A(\omega_E)$ must follow from the crystal structure and the intermolecular atom-atom potentials. Eventually, such refinement may lead to improved pair potential parameters beyond those of Bartell [3] which were successful for phases I and II.

A transition within the tunneling multiplet requires a nuclear spin flip. This prevents immediate equilibration with the phonon bath. Spin conversion times τ are of the order of days and usually different for different levels. This leads to differences in population. The fit shows a mismatch of intensity around 39 and $67\mu eV$ of m-site methane. The involved T_1 level converts faster, the T_2 level more slowly than the average.

After long stagnation the solution of the structure of phase III of CD_4 gives a new impact towards understanding dynamics and interactions of the simplest organic material.

[1] W. Press, J. Chem. Phys. **56**,2597(1972)
[2] H.M. James, T.A. Keenan, J. Chem. Phys. **31**,12(1959)
[3] L.S. Bartell, J. Chem. Phys. **32**,827(1960)
[4] K. Maki, Y. Kataoka, T. Yamamoto, J. Chem. Phys. **70**,655(1979)
[5] M. Neumann, W. Press, C. Noeldeke, B. Asmussen, M. Prager, R.M. Ibberson, to be published
[6] W. Press, *Single Particle Rotations in Molecular Crystals*, Springer Tracts in Modern Physics, Vol. 81, Springer, Berlin 1981

Stress Relaxation and Flow in a Polymer Melt

B. Farago[1], A. Arbe[2], J. Colmenero[2], D. Richter[3] and U. Buchenau[3]
[1] *Institut Laue-Langevin, BP 156 X, 38042 Grenoble Cedex 9, France*
[2] *Unidad de Fisica de Materiales (CSIC-UPV/EHU), Apartado 1072, 20080 San Sebastian, Spain*
[3] *Institut für Festkörperforschung, Forschungszentrum Jülich, Postfach 1913, 52425 Jülich, Germany*

Spin-echo measurements in deuterated polyisobutylene demonstrate unambiguously that the stress relaxation and the α relaxation of the flow process are two separate processes, with a slightly but clearly different temperature dependence. Obviously, the structural relaxation of the flow process sets in only *after* the stress has fully relaxed. Results in protonated polyisobutylene show that the proton diffusion shares the temperature dependence of the stress relaxation, so the diffusion distances required for the flow process get longer and longer with decreasing temperature.

F&E-Nr. 23.30.0

In viscoelastic fluids, one usually associates the flow process with the shear stress relaxation, identifying the relaxation time τ_α of the flow process with the shear stress relaxation time in terms of the Maxwell relation

$$\tau_\alpha = \frac{\eta}{G}, \tag{1}$$

where η is the viscosity and G is the infinite frequency shear modulus. This Maxwell idea is generally accepted, because it is obvious that the shear rigidity must disappear before the flow sets in. On the other hand, it is equally obvious that the disappearance of the shear rigidity is only the beginning of the flow process. The restructuring on the microscopic scale will also take time.

The present Letter evidences for the first time a measurable difference between the two time scales and their temperature dependence, using the neutron spin-echo technique. This method offers the unique possibility to measure both relaxation times in a single experimental setup. If one measures at the first sharp diffraction peak in $S(Q)$, one finds the structural relaxation time τ_α, with a temperature dependence which follows that of the viscosity. This was first shown for CKN, a mixed calcium-potassium nitrate [1], and later for several polymer glassformers [2–4] including polyisobutylene [4], a polymer with a glass temperature of 200 K. Since the first sharp diffraction peak mirrors the molecular packing, its lifetime is a direct measure of the structural relaxation time, providing a microscopic time scale for the viscosity.

In contrast, $S(Q)$ at small momentum transfer Q arises from the density fluctuation on a larger scale $1/Q$. In a viscoelastic fluid, it has three components: the Brillouin scattering from the high-frequency sound waves and two quasielastic components, one from the entropy fluctuations and another one from the stress relaxation [5]. The latter, sometimes denoted as Mountain scattering [6] allows to determine the structural relaxation time τ_s.

Here we present a new treatment of the scattering at small Q, based on the second moment sum rule [7]

$$\int_{-\infty}^{\infty} \omega^2 S(Q,\omega) d\omega = \frac{k_B T Q^2}{m}, \tag{2}$$

where m is the average atomic mass. In the absence of any damping of the sound waves, the Brillouin scattering [7]

$$S_{brill}(Q,\omega) = \frac{k_B T}{2m} \delta(\omega \pm v_l Q), \tag{3}$$

where v_l is the longitudinal sound velocity, *exhausts* the second moment sum rule. Consequently, any additional scattering at nonzero frequency, be it from the entropy fluctuations or from the Mountain scattering, must be connected with a weakening of the two Brillouin lines. More precisely, the visibility of the relaxational scattering is proportional to the square of the bilinear coupling between the corresponding relaxational mode and the Brillouin sound wave at the given Q. The bilinear coupling leads to a hybridization of the Brillouin sound wave and the relaxational mode. Thus the Brillouin scattering gets a bit weaker, and the relaxational mode becomes visible.

One can relate the strength of the relaxational scattering to the damping of the sound waves. A straightforward derivation [8] yields the low-Q scattering

$$S(Q,\omega) = \frac{k_B T \rho}{m} \frac{\chi_{11}''}{\omega}, \tag{4}$$

where χ_{11} is the inverse modulus $C_{11} = \rho v_l^2$ of the sound waves nd ρ is the density. This scattering has a quasielastic component reflecting the longitudinal stress relaxation time τ_s. In polyisobutylene, ultrasonic investigations [9] show that the longitudinal stress relaxation time equals the shear relaxation time within experimental error. Thus the spin-echo relaxation time determined at low Q should equal the shear stress relaxation time τ_s.

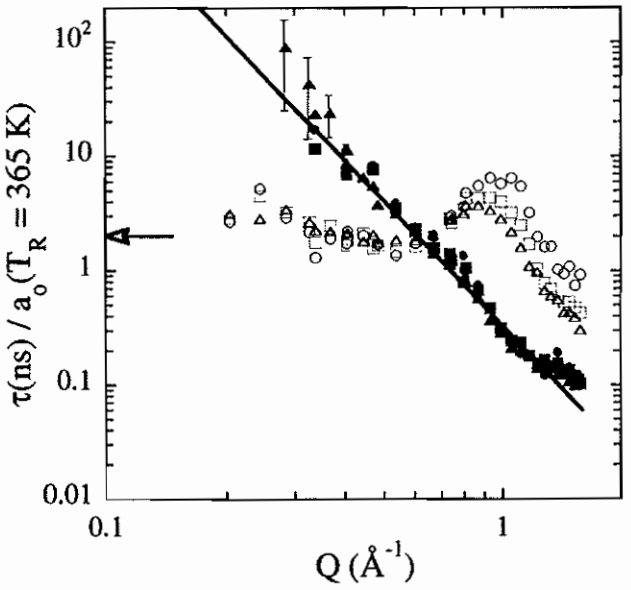

FIG. 1. Q-dependent relaxation times in polyisobutylene at 365 K. Full symbols: incoherent data from protonated sample; open symbols: coherent data from deuterated sample. Triangles are scaled from 390 K, circles from 335 K, both with an effective barrier height of 0.43 eV. The arrow corresponds to the hydrodynamic limit from the mechanical data, the line to $Q^{-3.6}$ (see text).

Fig. 1 shows the coherent spin-echo results at three different temperatures, plotted on a logarithmic scale against the momentum transfer Q. Also shown are data taken on protonated polyisobutylene, where the incoherent scattering from the proton dominates. At low Q, the incoherent relaxation time increases with $Q^{-2/0.55} = Q^{-3.6}$, as it should if the protons have a mean square displacement proportional to t^β with $\beta = 0.55$. This mean square displacement in turn is consistent with a Kohlrausch law with $\beta = 0.55$ in a scenario of homogeneous dynamics. The data at the three different temperatures 335, 365 and 390 K were scaled to 365 K, using an effective Arrhenius barrier of 0.43 eV, a procedure which works quite well for the incoherent relaxation times. It also seems to work quite well for the low-Q coherent relaxation times, but not for the data at the first sharp diffraction peak at 1 $\AA^{-1}$. There, the relaxation times are (i) larger than those at low Q (ii) change faster with temperature than those at low Q. In fact, their temperature dependence again follows closely that of the viscosity, while the temperature dependence at low Q is clearly slower.

We conclude that the shear relaxation time τ_s seen at low Q is not only shorter than the structural relaxation time τ_α seen at the first sharp diffraction peak, but that the ratio even increases with decreasing temperature. Further support for this conclusion comes from an interpolation of the longitudinal stress relaxation time in χ_{11} between an ultrasonic [9] and a Brillouin light scattering experiment [5] to the temperature 365 K, the arrow in Fig. 1, which agrees within experimental error with the low-Q coherent relaxation time reported here.

[1] F. Mezei, W. Knaak and B. Farago, Phys. Rev. Lett. **58**, 571 (1987); F. Mezei, W. Knaak and B. Farago, Phys. Scripta **19**, 363 (1987).

[2] D. Richter, B. Frick and B. Farago, Phys. Rev. Lett. **61**, 2465 (1988).

[3] R. Zorn, A. Arbe, J. Colmenero and D. Richter, unpublished.

[4] A. Arbe, J. Colmenero, B. Frick, M. Monkenbusch, and D. Richter, Macromolecules 31, 4926 (1998)

[5] G. D. Patterson, J. Polym. Sci., Polym. Phys. Ed. 15, 455 (1977)

[6] R. D. Mountain, Rev. Mod. Phys. **38**, 205 (1966)

[7] J.-P. Hansen and I. R. McDonald, in *Theory of simple liquids*, 2nd ed. (Academic Press, New York, 1986). Second moment sum rule: ch. 7.4, eq. (7.4.40), p. 220; Rayleigh-Brillouin scattering: ch. 8.5, p. 275 ff.

[8] B. Farago, A. Arbe, J. Colmenero, R. Faust, U. Buchenau and D. Richter, unpublished

[9] R. S. Marvin, R. Aldrich and H. S. Sack, J. Appl. Phys. 25, 1213 (1954)

Publications in refereed journals

Arbe A.1; Monkenbusch M.; Stellbrink J.; Richter D.; Farago B.2; Almdal K.3; Faust R.4
1Departamento de Fisica de Materiales, Universidad del Pais Vasco and Unidad de Fisica de Materiales (CSIC-UPV/EHU), San Sebastian, Spain
2Institut Laue Langevin, 156X, 38042 Grenoble, France
3The Danish Polymer Centre, Condensed Matter and Physics and Chemistry Department, Risø National Laboratory, Roskilde, Denmark
4Polymer Science Program, Dep. of Chemistry, University of Massachusetts-Lowell, Lowell, Massachusetts, USA
Origin of Internal Viscosity Effects in Flexible Polymers: A Comparative Neutron Spin-Echo and Light Scattering Study on Poly(dimethylsiloxane) and Polyisobutylene
Macromolecules 34, 1281-1290 (2001)
23.30.0

Buchenau U.
Dynamics of glasses
J. Phys.: Condens. Matter 13, 7827-7846 (2001)
23.15.0

Buchenau U.
Mechanical relaxation in glasses and the glass transition
Phys. Rev. B 63, 104203 (2001)
23.15.0

Carlsson P.1; Zorn R.; Andersson D.1; Farago B.2; Howells W.S.3; Börjesson L.1
1Department of Experimental and Applied Physics, Chalmers University of Technology, S-412 96 Göteborg, Sweden
2Institut Laue-Langevin, BP 156, F-38042 Grenoble Cedex, France
3Rutherford Appleton Laboratory, Chilton, Didcot OX11 0QX, United Kingdom
The segmental dynamics of a polymer electrolyte investigated by coherent quasi-elastic neutron scattering
J. Chem. Phys. 114, 9645-9656 (2001)
23.15.0

Caspary D.1; Eckold G.1; Güthoff F.1; Pyckhout-Hintzen W.
1Institut für Physiklaische Chemie und Sonderforschungsbereich 345, Univ. Göttingen, Tammanstr. 6, 37077 Göttingen
Kinetics of decomposition in ionic solids II: neutron scattering study of the system AgCl-NaCl"
J. Phys.: Condens. Matter 13, 11521-11530 (2001)
23.30.0

Dzubiella J.1; Jusufi A.1; Likos C.N.1; von Ferber C.1; Stellbrink J.; Allgaier J.; Richter D.; Schofield A.B.2; Poon W.C.K.2; Pusey P.N.2
1Institut für Theoretische Physik II, Heinrich-Heine-Universität Düsseldorf, Universitätsstraße 1, 40225 Düsseldorf
2Department of Physics and Astronomy, The University of Edinburgh, Mayfield Road, Edinburgh EH9 3JZ, UK
Phase Separation in Star Polymer-Colloid Mixtures
Phys. Rev. E64, 10401R (2001)
23.30.0

Edelmann K.1; Janich M.2; Hoinkis E.3; Pyckhout-Hintzen W.; Hoering S.1
1Fachbereich Chemie, Universität Halle
2Fachbereich Physik, Universität Halle
3Hahn Meitner Institut Berlin, Glienicker Str. 100, 14109 Berlin
The aggregation behaviour of poly(ethylene oxide)-poly(methyl methacrylate) diblock copolymers in organic solvents"
Macromol. Chem. Phys. 202, 1638-1644 (2001)
23.30.0

Endo H.; Mihailescu M.; Monkenbusch M.; Allgaier J.; Gompper G.; Richter D.; Jakobs B.1; Sottmann T.1; Strey R.1; Grillo I.2
1Institut für Physikalische Chemie, Universität Köln; Luxemburger Str. 116, 50939 Köln
2Institut Laue Langevin, 6, rue Jules Horowitz, BP 156, F-38042 Grenoble Cedex 9, France
Effect of amphiphilic block copolymers on the structure and phase behavior of oil-water-surfactant mixtures
J. Chem. Phys. 115, 580-600 (2001)
23.30.0

Erhardt R.1; Böker A.1; Zettl H.1; Kaya H.; Pyckhout-Hintzen W.; Krausch G.1,2; Abetz V.1; Müller A.1,2
1Fachbereich Chemie, Universität Bayreuth, 95440 Bayreuth
2Bayreuther Zentrum für Kolloide und Grenzflächen, 95440 Bayreuth
Janus Micelles
Macromolecules 34, 1069-1075 (2001)
23.30.0

Erhardt R.1; Böker A.1; Zettl H.1; Kaya H.; Pyckhout-Hintzen W.; Krausch G.1; Abetz V.1; Müller A.1
1Inst. für Makromolekulare Chemie, Universität Bayreuth, 95440 Bayreuth
Superstructures of janus micelles
Polymeric Materials: Science & Engineering 84 (2001)
23.30.0

Frielinghaus H.; Hermsdorf N.1; Sigel R.2; Almdal K.3; Mortensen K.3; Hamley I.W.4; Messé L.5; Corvazier L.5; Ryan A.J.5; van Dusschoten D.6; Wilhelm M.6; Floudas G.7; Fytas G.7
1Institut für Polymerforschung Dresden, 01069 Dresden
2MPI für Kolloid- und Grenzflächenforschung, 14424 Potsdam
3Risø National Laboratory, Danish Polymer Centre, DK-4000 Roskilde, Demark
4School of Chemistry, University of Leeds, Leeds LS2 9JT, UK
5Dept. of Chemistry, University of Sheffield, Sheffield S3 7HF, UK
6MPI for Polymer Research, 55021 Mainz
7Institute of Electronic Structure and Laser, GR-71110 Heraklion, Greece
Blends of AB/BC diblock copolymers with a large interaction parameter (
Macromolecules 34, 4907-4916 (2001)
23.30.0

Frielinghaus H.; Schwahn D.; Dudowicz J.1; Freed K.F.1; Foreman K.W.1
1The James Franck Institute and the Department of Chemistry, University of Chicago, Chicago, Illinois 60637, USA
Small-angle neutron scattering studies of polybutadiene/polystyrene blends as a function of pressure and microstructure: Comparison of experiment and theory
J. Chem. Phys. 114, 5016-5025 (2001)
23.30.0

Frielinghaus H.; Schwahn D.; Willner L.
Blends of polybutadiene with different vinyl contents and polystyrene studied with small-angle neutron scattering in varying temperature and pressure fields
Macromolecules 34, 1751-1763 (2001)
23.30.0

Gompper G.; Endo H.; Mihailescu M.; Allgaier J.; Monkenbusch M.; Richter D.; Jakobs B.1; Sottmann T.1; Strey R.1
1Institut für Physikalische Chemie, Universität Köln; Luxemburger Str. 116, 50939 Köln
Measuring bending rigidity and spatial renormalization in bicontinuous microemulsions
Europhys. Lett. 56, 683-689 (2001)
23.30.0

Gompper G.; Richter D.; Strey R.1
1Institut für Physikalische Chemie, Universität Köln, Luxemburger Str. 116, 50939 Köln
Amphiphilic block copolymers in oil-water-surfactant mixtures: Efficiency boosting, structure, phase behavior and mechanism
Journal of Physics: Condensed Matter 13, 9055-9074 (2001)

23.30.0

Graesseley W.W.1; Fetters L.J.
1Dept. of Chem. Engineering, Princeton University, Princeton, New Jersey 08544, USA
Thermoelasticity of Polymer Networks
Macromolecules 34, 7147-7151 (2001)
23.30.0

Götz H.1; Ewen B.1; Maschke U.2; Meier G.; Monkenbusch M.
1MPI für Polymerforschung, 55021 Mainz
2Laboratoire de Chimie Macromoléculaire, UPRESA CNRS No. 8009, Université des Science et Technologies de Lille, F-59655 Villeneuve d'Ascq Cedex, France
Neutron scattering investigations on the statics and dynamics of polydimethyl- and polyethylmethylsiloxane melts
Macromol. Chem. Phys. 202, 3334-3341 (2001)
23.30.0

Heinrich M.; Rawiso M.1; Zilliox J.G.1; Lesieur P.2; Simon J.P.3
1Institut Charles Sadron, CNRS-ULP, 6 rue Boussingault, 67083 Strasbourg Cedex, France
2Lab. pour l'Utilisation du Rayonnement Electromagnétique, Bât. 209 D, Centre Univ. Paris-Sud, 91405 Orsay Cedex, France
3Lab. de Thermodynamique et Physico-Chimie Métallurgiques, CNRS-INPG-UJF, BP 75, 38402 Saint Martin d'Hères Cedex, France
Small angle x-ray scattering from salt-free solutions of star-branched polyelectrolytes
Eur. Phys. J. E 4, 131-142 (2001)
23.30.0

Kemmerling G.1; Engels R.1; Bussmann N.1; Clemens U.1; Heiderich M.; Reinartz R.1; Rongen H.1; Schelten J.1; Schwahn D.; Zwoll K.1
1Zentrallabor für Elektronik, Forschungszentrum Jülich, 52425 Jülich
A new two-dimensional scintillation detector system for small angle neutron scattering experiments
Transactions on Nuclear Science 48, 1114 (2001)
23.89.1

Kirstein O.; Prager M.; Combet J.1; Johnson M.R.1
1Institut Laue Langevin, 6, BP 156, F-38042 Grenoble Cedex 9, France
Ammonia group rotation in . Zn(NH3)4J2
Molecular Physics Reports 31, 47-55 (2001)
23.15.0

Koizumi S.1; Monkenbusch M.; Richter D.; Schwahn D.; Annaka M.1
1Advanced Science Research Center, Japan Atomic Energy Research Institute, Tokai-mura, Ibaraki-ken 319-1195, Japan
Frozen Concentration Fluctuations of a Poly (N-isopropyl aclyamide) Gel Decomposed by Neutron Spin Echo
J Phys. Soc. Jpn. 70, Suppl. A p. 320. (2001)
23.30.0

Kramp S.1; Rotter M.2; Löwenhaupt M.3; Pyka N.M.4; Schmidt W.; van de Kamp R.5
1Institut Laue Langevin, BP 156 38042 Grenoble Cedex 9, France
2Institut für Experimentalphysik, Technische Universität Wien, Wiedner Hauptstraße 8-10, 1040 Wien, Austria
3Inst. für Angew. Physik u. Didaktik der Physik, TU Dresden, 01062 Dresden
4TU München, Zentrale Betriebseinheit FRM - II, 85747 Garching
5Hahn Meitner Institut, 14109 Berlin
Spin waves in the ferrimagnetic phase of NdCu2
J. Magn. Magn. Mat. 226-230, 470-472 (2001)
23.30.0

Matsuoka H.1; Yamamoto Y.1; Nakano M.1; Endo H.1; Yamaoka H.1; Zorn R.; Monkenbusch M.; Richter D.; Seto H.2; Kawabata Y.2; Nagao M.3
1Department of Polymer Chemistry, Kyoto University, Kyoto 606-8501, Japan
2FIAS, Hiroshima University, Higashi-Hiroshima, Hiroshima 739-8521, Japan
3Neutron Scattering Laboratory, Institute of Solid State Physics, The University of Tokyo, Tokai, Ibaraki 319-1106, Japan
Neutron Spin-Echo Study of the Dynamic Behavior of Amphiphilic Diblock Copolymer Micelles in Aqueous Solution
Langmuir 16, 9177-9185 (2000)
23.15.0

Maxelon M.1; Pundt A.1; Pyckhout-Hintzen W.; Barker J.2; Kirchheim R.1
1Institut für Materialphysik, Hospitalstraße 3-7, 37073 Göttingen
2NIST, Gaithersburg, Maryland 20899, USA
Interaction of hydrogen and deuterium with dislocations in palladium as observed by small angle neutron scattering
Acta Materialia 49, 2625-2634 (2001)
23.30.0

Maxelon M.1; Pundt A.1; Pyckhout-Hintzen W.; Kirchheim R.1
1Institut für Materialphysik, Hospitalstraße 3-7, 37073 Göttingen
Small angle neutron scattering of hydrogen segregation at dislocations on palladium
Scripta Materialia 44, 817-822 (2001)
23.30.0

Mihailescu M.; Monkenbusch M.; Endo H.; Allgaier J.; Gompper, G.; Stellbrink J.; Richter D.; Jakobs B.1; Sottmann T.1; Farago B.2
1Institut für Physikalische Chemie, Universität Köln, Luxemburger Str. 116, 50939 Köln
2Institut Laue Langevin, 6, rue Jules Horowitz, BP 156, F-38042 Grenoble Cedex 9, France
Dynamics of bicontinuous microemulsion phases with and without amphiphilic blockcopolymers
J. Chem. Phys. 115, 9563-9577 (2001)
23.30.0

Moreno A.J.1; Alegria A.1; Colmenero J.1; Prager M.; Grimm H.; Frick B.2
1Departamento de Fisica de Materiales y Centro Mixtor CSIC-UPV/EHU, Universidad del Pais Vasco (UPV/EHU), Apt. 1072, 20080 San Sebastian, Spain
2Institute Laue-Langevin, BP 156X, F-38042 Grenoble, France
Methyl group dynamics in glassy toluene: A neutron scattering study
J. Chem. Phys. 115, 8958-8966 (2001)
23.30.0

Perny S.; Allgaier J.; Cho D.1; Lee W.1; Chang T.1
1Dep. of Chemistry and Center for Integrated Molecular Systems, Pohang University of Science and Technology, Pohang, 790-784, China
Synthesis and structural analysis of an h-shaped polybutadiene
Macromolecules 34, 5408-5415 (2001)
23.30.0

Poon W.C.K.1; Egelhaaf S.U.1; Stellbrink J.; Allgaier J.; Schofield A.B.1; Pusey P.N.1
1Department of Physics and Astronomy, The University of Edinburgh, Mayfield Road, Edinburgh EH9 3JZ, UK
Beyond Simple Depletion: Phase Behaviour of Colloid-Star Polymer Mixtures
Phil. Trans. R. Soc. Lond. A, 359, 897-907 (2001)
23.30.0

Richter D.; Kahle S.; Monkenbusch M.; Willner L.; Arbe A.1; Colmenero J.1; Farago B.2

1Departamento de Fisica de Materiales, Universidad del Pais Vasco, San Sebastian, Spain
2Institut Laue-Langevin, BP 156, F-38042 Grenoble Cedex, France
Neutron scattering and the glass transition in polymers - present status and future opportunities
Contribution for the VI. Int. Workshop on Non-Crystalline Solids in Bilbao, Journal of Non-Crystalline Solids 287, 286-296 (2001)
23.30.0

Richter D.; Monkenbusch M.; Pyckhout-Hintzen W.; Arbe A.1; Colmenero J.1
1Departamento de Fisica de Materiales, Universidad del Pais Vasco, San Sebastian, Spain
Response to Comment on "From Rouse dynamics to local relaxation: A neutron spin echo on polyisobutylene melts"
J. Chem. Phys. 113, 11398-11399 (2000)
23.30.0

Rotter M.1; Löwenhaupt M.2; Kramp S.2,4; Reif T.; Pyka N.M.3; Schmidt W.; van de Kamp R.5
1Institut für Experimentalphysik, Technische Universität Wien, Wiedner Hauptstraße 8-10, 1040 Wien, Austria
2Institut für Angewandte Physik, Technische Universität Dresden, 01062 Dresden
3TU München, Zentrale Betriebseinheit FRM - II, 85747 Garching
4Institut Laue Langevin, BP 156 38042 Grenoble Cedex 9, France
5Hahn Meitner Institut, 14109 Berlin
Anisotropic magnetic exchange in orthorhombic RCu2 compounds (R = rare earth)
Eur. Phys. J. B 14, 29-42 (2000)

Schmidt W.; Ohl M.; Buchenau U.
Comment on: Experimental evidence for fast heterogeneous collective structural relaxation in a supercooled liquid near the glass transition
Phys. Rev. Lett. 85, 5669 (2000)
23.30.0

Schwahn D.; Frielinghaus H.; Mortensen K.1; Almdal K.1
1Risø National Laboratory, DK-4000 Roskilde, Demark
Abnormal pressure dependence of the phase boundaries in PEE-PDMS and PEP-PDMS binary homopolymer blends and diblock copolymers
Macromolecules 34, 1694-1706 (2001)
23.30.0

Smith G.D.1; Paul W.2; Monkenbusch M.; Richter D.
1Dep. of Mat. Science and Engineering, University of Utah, Salt Lake City, Utah 84112, USA
2Institut für Physik, Johannes-Gutenberg Universität, 55099 Mainz
On the non-Gaussianity of chain motion in unentangled polymer melts
J. Chem. Phys. 114, 4285-4288 (2001)
23.30.0

Tölle A.1; Zimmermann H.2; Fujara F.3; Petry W.4; Schmidt W.; Schober H.5; Wuttke J.4
1Fachbereich Physik, Universität Dortmund, 44221 Dortmund
2Max-Planck-Institut für medizinische Forschung, 69120 Heidelberg
3Institut für Festkörperphysik, Technische Universität Darmstadt, 64289 Darmstadt
4Physik-Department E13, Technische Universität München, 85747 Garching
5Institut Laue-Langevin, 38042 Grenoble, France
Vibrational states of glassy and crystalline orthoterphenyl
Eur. Phys. J. B 16, 73-80 (2000)
23.30.0

Westermann S.; Pyckhout-Hintzen W.; Richter D.; Straube E.1; Egelhaaf S.2; May R.2
1Martin-Luther-Universität Halle-Wittenberg, Fachbereich Physik, 06099 Halle
2Institut Laue Langevin, BP 156, F-38042 Grenoble Cedex 9, France
On The length scale dependence of microscopic strain by SANS
Macromolecules 34, 2186-2194 (2001)
23.30.0

Wignall G.D.1, Alamo R.G.2, Ritchon E.J.2; Mandelkern L.2; Schwahn D.
1Solid State Division, Oak Ridge National Laboratory, USA
2Chemical Engineering Department A&M University and Florida State University College of Engineering, Tallahasse, Florida, USA
SANS Studies of Liquid-Liquid Separation in Heterogeneous and Metallocene-Based Linear Low-Density Polyethylenes
Macromolecules 34, 8160 (2001)
23.30.0

Willner L.; Poppe A.; Allgaier J.; Monkenbusch M.; Richter D.
Time-resolved SANS for the determination of unimer exchange kinetics in block copolymer micelles
Europhys. Lett. 55, 667-673 (2001)
23.30.0

Other publications

Allenspach P.1; Andersen K.H.2; Colognesi D.2; Fak B.2; Kirstein O.; Zoppi M.3
1Laboratory for Neutron Scattering , ETHZ & PSI, CH-5232 Villigen PSI, Schweiz
2ISIS Department, Rutherford Appleton Laboratory, Chilton Didcot, Oxfordshire, OX11 0QX , UK
3Consiglio Nazionale delle Ricerche, Firenze, Italy
Indirect Geometry Spectrometer Performance of a Suite of Generic Instruments on ESS
ESS Instrumentation Group Reports, SAC Workshop, 03.-05.05.01, Ed.: F. Mezei and R. Eccleston, ESS 115-01-T, ISSN 1433-559X
23.89.1

Arbe A.1; Richter D.; Colmenero J.1,2; Monkenbusch M.; Farago B.3
1Dep. De Fisica de Materiales, Universidad del Pais Vasco and Unidad de Fisica de Materiales (CSIC-UPV/EHU), Apartado 1072, 20080 San Sebastian, Spain
2Donostia Internation Physics Center, Apartado 1072, 20080 San Sebastian, Spain
3Institut Laue Langevin, 156X, 38042 Grenoble Cedex, France
Single chain motions in flexible polymers by neutron spin echo
Conf. Proceed. ILL Millennium Symposium & European User Meeting, Grenoble/France, 06.-07.04.01, 69-70
23.30.0

Endo H.; Allgaier J.; Monkenbusch M.; Richter D.; Jakobs B.1; Sottmann T.1; Strey R.1
1Institut für Physikalische Chemie, Universität Köln; Luxemburger Str. 116, 50939 Köln
Polymeric efficiency boosters in microemulsions: A SANS investigation of the polymer's role
ILL Annual Report 2000, Scientific Highlights, 60-61 (2001)
23.30.0

Melnichenko Y.1; Wignall G.D.1; Schwahn D.
1Solid State Division, Oak Ridge National Laboratory, USA
Universal Behavior of Polymer Molecules in Blends, Solutions, and Supercritical Fluids
Polymeric Materials 85 (2001)
23.30.0

Richter D.
Neutronen für alle
Physikalische Blätter 57 (2001), Heft 9
23.30.0

Richter D.
Neutrons in Soft Condensed Matter
Conf. Proceed. ILL Millennium Symposium & European User Meeting, Grenoble/France, 06.-07.04.01, 38-44
23.30.0

Ronnow H.M.1; Regnault L.-P.1; Ulrich C.2; Keimer B.2; Ohl M.3; Bourges P.4
1CEA Grenoble, France
2MPI für Festkörperforschung, Stuttgart
3Institut Laue Langevin, 156X, 38042 Grenoble Cedex, France
4LLB Saclay, France
Incommensurate antiferromagnetic fluctuations in superconducitng Yba2Cu3O6.85
ILL Annual Report 2000, Scientific Highlights, 18-19 (2001)
23.89.1

Schreyer A.1; Wildes A.2; Schmidt W.2; Majkrzak C.F.3; Erwin R.W.3; Lee S.H.3; Hong M.4; Kwo R.4
1Ruhr-Universität Bochum and Institut Laue Langevin
2Institut Laue Langevin, 156X, 38042 Grenoble Cedex, France
3National Institute for Standards and Technology, Gaithersburg, USA
4Bell Laboratoires, Murray Hill
Spin excitations in a magnetic superlattice: the first inelastic neutron scattering measurements
ILL Annual Report 2000, Scientific Highlights, 26-27 (2001)
23.89.1

Schwahn D.; Willner L.
Phase Behavior of Binary Polybutadiene Copolymer Mixtures with different Vinyl Content as an Example of a Blend of Weak Interacting Polymers
Polymeric Materials 85 (2001)
23.30.0

Sokolov A.P.1; Kisliuk A.1; Grimm H.; Dianoux A.J.2
1University of Akron, USA
2Institut Laue Langevin, 156X, 38042 Grenoble Cedex, France
Slow relaxation process in DNS at different levels of hydration
ILL Annual Report 2000, Scientific Highlights, 56-57 (2001)
23.30.0

Invited Talks

Allgaier J.; Endo H.; Gompper G.; Mihailescu M.; Monkenbusch M.; Richter D.; Jakobs B.1; Sottmann T.1; Strey R.1
1Institut für Physikalische Chemie, Universität Köln; Luxemburger Str. 116, 50939 Köln
Amphiphilicity boosting in microemulsions: The effect of poly[ehyleneoxide-b-(ethylene-alt-propylene)] diblock copolymers
Int. Symp. on Ionic Polymerization, Heraklion, Greece, 22.-26.10.01
23.30.0

Allgaier J.; Endo H.; Richter D.; Sottmann T.1; Strey R.1;
1Institut für Physikalische Chemie, Universität Köln; Luxemburger Str. 116, 50939 Köln
Amphiphilic Block Copolymer as Efficiency Boosters for Surfactants
Wella AG, Darmstadt, 11.10.01
23.30.0

Allgaier J.
Amphiphile Blockcopolymere als Co-Emulgatoren in Wasser-Öl-Tensid Gemischen
Bayer AG, Landwirtschaftszentrum, Monheim, 01.06.01
23.30.0

Allgaier J.
From nonionic surfactants to their polymer analogues. Materials and micellar properties
University of Lever, Port Sunlight, UK, 11.07.01
23.30.0

Allgaier J.
Synthese, Neutronenkleinwinkelstreuung und Rheologie von verzweigten Modellpolymeren
Universität Bayreuth, 29.01.01
23.30.0

Buchenau U.; Wischnewski A.; Zorn R.; Hadjichristidis N.1
1Dep. of Chemistry, University of Athens, Industrial Chem. Lab. - Polymers, Panepistimiopolis - Zografou, Athens 15771, Greece
Relaxations in the glass phase of silica and PMMA
8th Int. Workshop on Disordered Systems, Andalo, Italy, 14.03.01
23.30.0

Buchenau U.
Dynamics of Glasses
Workshop on dynamics in Quasicrystals, Duisburg, 04.12.01
23.15.0

Buchenau U.
Mesoscale Dynamics in Glasses
Dynamical Properties of Solids XXVIII, Kerkrade, The Netherlands, 20.09.01
23.30.0

Buchenau U.
Relaxations in glasses and at the glass transition
4th Int. Discussion Meeting on Relaxations in Complex Systems, Crete, Greece, 21.06.01
23.15.0

Frielinghaus H.; Byelov D.; Endo H.; Allgaier J.; Stellbrink J.; Richter D.; Jakobs B.1; Sottmann T.1; Strey R.1
1Institut für Physikalische Chemie, Universität Köln, 50939 Köln
Polymer boosting effect in the Droplet Phase Studied by Small Angle Neutron Scattering
Jülich Soft Matter Days, Kerkrade, The Netherlands, 15.11.01
23.30.0

Hoffmann S.
Molecular Dynamics in Polymer Blends: First Steps towards an understanding of its heterogeneous behaviour
Institut Laue-Langevin, Grenoble, Frankreich, 13.03.01
23.30.0

Hoffmann S.
Molecular Dynamics in Polymer Mixtures: QENS and Dielectric Spectroscopy Study on the Origin of Dynamic Heterogeneity
4th Int. Discussion Meeting on the Relaxation in Complex Systems, Crete, Greece, 19.06.01
23.30.0

Kahle S.
Dynamic Neutron Scattering on Partially Deuterated Polybutadiene
4th Int. Discussion Meeting on Relaxations in Complex Systems, Crete, Greece, 20.06.01
23.30.0

Kirstein O.; Prager M.; Parker S.F.1; Johnson M.2
1ISIS Facility, Rutherford Appleton Lab., Chilton, Didcot, Oxon OX11 0QX, UK
2Institut Laue Langevin, F,38042 Grenoble Cedex 9, France
Lattice dynamics and methyl rotation of dimethylacetylene (DMA)
Int. Conf. on Neutron Scattering, TU München, 09.-13.09.01
23.15.0

Monkenbusch M.

High resolution neutron spin-echo spectroscopy - A tool for soft condensed matter research
Argonne National Lab., Chicago, USA, 14.06.01
23.30.0

Monkenbusch M.
Reptation dynamics observed by incoherent inelastic neutron scattering experiments
DYPROSO XXVIII, 16.-19.09.01, Kerkrade, The Netherlands
23.30.0

Prager M.; Schiebel P.1; Combet J.1
1Institut Laue Langevin, F-38042 Grenoble Cedex 9, France
Rotational tunnelling and disorder of 4-iodo-toluene
Conf. on Quantum Atomic and Molecular Tunnelling, Nottingham, UK, 05.09.01
23.15.0

Prager M.
Rotational tunnelling: from simple to complex systems
HMI Berlin, 18.06.01
23.15.0

Pyckhout-Hintzen W., Heinrich M.; Straube E.1; Richter D.; McLeish T.C.B.2
1Martin-Luther-Universität Halle-Wittenberg, Fachbereich Physik, 06099 Halle
2IRC in Polymer Science and Technology, University of Leeds, Leeds LS2 9JT, UK
A microscopic model for branched polymers in elongational flow by SANS
Seminar, MPI Golm, 23.10.01
23.30.0

Pyckhout-Hintzen W.; Westermann S.; Urban V.1; Richter D.; Straube E.2
1ESRF Grenoble, Frankreich
2Martin-Luther-Universität Halle-Wittenberg, Fachbereich Physik, 06099 Halle
The length scale dependence of microscopic strain in polymer networks by SANS
BPS Symposium, Universität Bayreuth, 16.-18.9.2001
23.30.0

Pyckhout-Hintzen W.
Fundamental polymer research and implications for industrial applications
El-Minia University, Egypt, 10.04.01
23.30.0

Richter D.; Monkenbusch M.; Willner L.; Wischnewski A.; Arbe A.1; Colmenero J.1
1Dep. de Fiscia de Materiales, Universidad del Pais Vasco, Facultad de Quimica, E-20080 San Sebastian, Spain
Experimental Aspects of Polymer Dynamics
Conf. on "Polymers in the Third Millennium", Univ. Montpellier, France, 02.-06.09.01
23.30.0

Richter D.
Neutronen und die Bewegung von Polymeren - Bernd Ewen und die Folgen
Festkolloquium, MPI für Polymerforschung, Mainz, 31.08.01
23.30.0

Richter D.
Neutrons in Soft Condensed Matter
ILL Millennium Symposium, Grenoble, France, 06.-07.04.01
23.30.0

Richter D.
Neutrons in Soft Condensed Matter
Kolloquium, Universität Bayreuth, 12.06.01
23.30.0

Richter D.
Soft Condensed Matter
OECD Workshop on Large Facilities for Studying the Structure and Dynamics of Matter, Kopenhagen, Sweden, 19.-21.09.01
23.30.0

Richter D.
The European Spallation Source Project
FZJ Kolloquium, FZ Jülich, 24.08.01
23.30.0

Richter D.
The European Spallation Source Project
Int. Conf. on Neutron Scattering, TU München, 09.-13.09.01
23.30.0

Richter D.
The European Spallation Source Project
Kolloquium, Universität Bochum, 19.11.01
23.30.0

Richter D.
The European Spallation Source Project
Kolloquium, Universität Darmstadt, 30.11.01
23.30.0

Richter D.
The European Spallation Source
Deutsche Neutronenstreutagung, FZ Jülich, 20.02.01
23.30.0

Richter D.
The Status of the European Spallation Source Project
Journée de la Diffusion Neutronique, Tregastel, France, 16.-17.05.01
23.30.0

Richter D.
The Status of the European Spallation Source Project
Russian Nat. Conf. on "The use of X-ray, Synchrotron, Neutron and Electron Scattering", Dubna, Russia, 25.05.01
23.30.0

Richter D.
Wax Crystal Modification by Random Copolymers of the PEB-n type
Seminar, University of Princeton, USA, 29.03.01
23.30.0

Schmidt W.1; Ohl M.1; Buchenau U.
1Institut Laue-Langevin, F-38042 Grenoble Cedex, France
Inelastic Neutron Scattering in Polybutadiene at Low Momentum Transfer
4th Int. Discussion Meeting on the Relaxation in Complex Systems, Crete, Greece, 17.-23.06.01
23.89.1

Stellbrink J.
Star polymer/colloid mixtures
University of Edinburgh, UK, 27.8.01
23.30.0

Willner L.
Unimer exchange kinetics in diblock copolymer micelles
DYPROSO XXVIII, 16.-19.09.01, Kerkrade, The Netherlands
23.30.0

Wischnewski A.; Richter D.; Monkenbusch M.; Willner L.; Farago B.1; Ehlers G.1; Schleger P.1
1Institut Laue-Langevin, F-38042 Grenoble Cedex, France
Kettendynamik in Polymerschmelzen: Grenzen des Reptationsmodells
Deutsche Neutronenstreutagung, FZ Jülich, 21.02.01
23.30.0

Wischnewski A.; Richter D.; Monkenbusch M.; Willner L.; Farago B.1; Ehlers G.1; Schleger P.1
1Institut Laue-Langevin, F-38042 Grenoble Cedex, France
Neutron spin echo spectroscopy on reptating polymers

4th Int. Discussion Meeting on Relaxations in Complex Systems, Crete, Greece, 18.06.01
23.30.0

Zorn R.; Hartmann L.1; Frick B.2; Richter D.; Kremer F.1
1Fakultät für Physik und Geowissenschaften, Universität Leipzig, Linnéstr. 5, 04103 Leipzig
2Institut Laue-Langevin, F-38042 Grenoble Cedex, France
Inelastic neutron scattering experiments on the dynamics of a glass forming material in mesoscopic confinements
DYPROSO XXVIII, Kerkrade, The Netherlands, 19.9.2001
23.15.0

Zorn R.; Hartmann L.1; Frick B.2; Richter D.; Kremer F.1
1Fakultät für Physik und Geowissenschaften, Universität Leipzig, Linnéstr. 5, 04103 Leipzig
2Institut Laue-Langevin, F-38042 Grenoble Cedex, France
Low frequency vibrations in a confined glassy system
4th Int. Discussion Meeting on Relaxations in Complex Systems, Crete, Greece, 21.06.01
23.15.0

Other talks

Kirstein O.; Kozielewski T.; Prager M.; Andersen K.H.1
1ISIS Facility, Rutherford Appleton Laboratory, Chilton, Didcot, Oxon, OX11 0QX, UK
A 0.9 micro eV backscattering spectrometer at the European Spallation Source (ESS)
7th General ESS Meeting, Seggau, Austria, 26.-29.09.01
23.89.1

Kirstein O.; Prager M.; Johnson M.R.1, Parker S.F.2
1Institut Laue Langevin, BP 156, F-38042 Grenoble Cedex 9, France
2ISIS Facility, Rutherford Appleton Laboratory, Chilton, Didcot, Oxon OX11, 0QX, UK
Lattice dynamics and methyl group rotation of 2-butyne
Int. Conf. on Neutron Scattering, TU München, 09.-13.09.01
23.15.0

Kirstein O.; Prager M.; Johnson M.R.1; Parker S.F.2
1Institut Laue Langevin, 6, rue Jules Horowitz, BP 156, F-38042 Grenoble Cedex 9, France
2ISIS Facility, Rutherford Appleton Laboratory, Chilton, Didcot, Oxon OX11, 0QX, UK
Lattice dynamics and methyl group rotation of dimethylacetylene
QAMTS 2001, Nottingham, UK, 05.-08.09.01
23.15.0

Monkenbusch M.; Mihailescu M.; Allgaier J.; Richter D.; Jakobs B.1; Sottmann T.1
1Institut für Physikalische Chemie, Universität zu Köln, Luxemburger Str. 116, 50939 Köln
Interface Dynamics in bicontinuous microemulsions investigated by neutron spin echo spectroscopy
75th ACS Conference "Colloids 2001", Pittsburgh, USA, 10.-13.06.01
23.30.0

Monkenbusch M.; Richter D.; Mezei F.1; Pappas C.1
1Hahn-Meitner-Institut, Glienicker Straße 100, 14109 Berlin
High resolution time-of-flight spin-echo spectrometer
EFAC Meeting, Oak Ridge, USA, 27.03.01
23.30.0

Monkenbusch M.
Neutron spin echo investigation of the membrane dynamics in bicontinuous microemulsions
Int. Conf. on Neutron Scattering, TU München, 09.-13.09.01
23.30.0

Pipich V.; Schwahn D.; Willner L.
Small angle neutron scattering in the vicinity of a double critical point in a ternary polymer blend
Physics of liquid matter: Modern problems, Kiev, Ukraine, 14.-19.09.01
23.30.0

Schwahn D.; Willner L.
Phase Behavior of Binary Polybutadiene Copolymer Mixtures as an Example of Weakly Interacting Polymers
Int. Conf. on Neutron Scattering, TU München, 09.-13.09.01
23.30.0

Schwahn D.; Willner L.
Phase Behavior of Binary Polybutadiene Copolymer Mixtures as an Example of
Weakly Interacting Polymers
Jülich Soft Matter Days, Kerkrade, The Netherlands, 14.11.01
23.30.0

Schwahn D.; Willner L.
Phase Behavior of weakly Interacting Binary Polybutadiene Copolymer Mixtures with different Vinyl Content
222nd ACS National Meeting, Chicago, USA, 27.08.01
23.30.0

Stellbrink J.
Partial Structure Factors in Star polymer/colloid mixtures
Int. Conf. on Neutron Scattering, TU München, 09.-13.09.01
23.30.0

Stellbrink J.
Partial Structure Factors in Star polymer/colloid mixtures
Jülich Soft Matter Days, Kerkrade, The Netherlands, 14.11.01
23.30.0

Willner L.; Poppe A.; Allgaier J.; Monkenbusch M.; Richter D.
Determination of the relaxation kinetics in a PEP-PEO/DMF micellar system by time-resolved SANS
ACS Conf., Colloids and Surface Science Symposium, Pittsburgh, USA, 10.-13.06.01
23.30.0

Wischnewski A.; Willner L.; Monkenbusch M.; Richter D.; Farago B.1; Ehlers G.1; Schleger P.1
1Institut Laue-Langevin, F-38042 Grenoble Cedex, France
Constraints of motion in polymer melts: coherent and incoherent scattering analyzed by neutron-spin-echo spectroscopy
Int. Conf. on Neutron Scattering, TU München, 09.-13.09.01
23.30.0

Posters

Allenspach P.1; Andersen K.2; Colognesi D.2; Fak B.2; Kirstein O.; Zoppi M.3
1Laboratory for Neutron Scattering , ETHZ & PSI, CH-5232 Villigen PSI, Schweiz
2ISIS Facility, Rutherford Appleton Laboratory, Chilton Didcot, Oxfordshire, OX11 0QX , UK
3Consiglio Nazionale delle Ricerche, Firenze, Italy
Indirect spectrometers at the European Spallation Source (ESS)
7th General ESS Meeting, Seggau, Austria, 26.-29.09.01
23.89.1

Botti A.; Pyckhout-Hintzen W.; Urban V.1; Richter D.; Straube E.1; Kohlbrecher J.3
1Institut Laue Langevin, F-38042 Grenoble Cedex 9, France
2Martin-Luther-Universität Halle-Wittenberg, Fachbereich Physik, 06099 Halle
3Abt. Spallationsquelle, Paul Scherrer Institut, 5232 Villigen PSI, Schweiz
Silica filled elastomers: polymer chain and filler characterization by a SANS-SAXS approach
Deutsche Neutronenstreutagung, FZ Jülich, 19.-21.02.01
23.30.0

Botti A.; Pyckhout-Hintzen W.; Urban V.1; Richter D.; Straube E.1; Kohlbrecher J.3
1Institut Laue Langevin, F-38042 Grenoble Cedex 9, France
2Martin-Luther-Universität Halle-Wittenberg, Fachbereich Physik, 06099 Halle
3Abt. Spallationsquelle, Paul Scherrer Institut, 5232 Villigen PSI, Schweiz
Silica filled elastomers: polymer chain and filler characterization by a SANS-SAXS approach
Int. Conf. on Neutron Scattering, TU München, 09.-13.09.01
23.30.0

Botti A.; Pyckhout-Hintzen W.; Urban V.1; Richter D.; Straube E.1
1Institut Laue Langevin, F-38042 Grenoble Cedex 9, France
2Martin-Luther-Universität Halle-Wittenberg, Fachbereich Physik, 06099 Halle
Composites reinforcement by rods: A SAS study
Int. Conf. on Neutron Scattering, TU München, 09.-13.09.01
23.30.0

Byelov D.; Frielinghaus H.; Endo H.; Allgaier J.; Richter D.
Polymer anti boosting. A small angle neutron scattering study of the bicontinuous microemulsion
Int. Summerschool "Fundamental Problems in Statistical Physics X", Odenthal-Altenberg, 25.08.01
23.30.0

Byelov D.; Frielinghaus H.; Endo H.; Allgaier J.; Richter D.
Polymer anti boosting. A small angle neutron scattering study of the bicontinuous microemulsion.
Jülich Soft Matter Days 2001, Kerkrade, The Netherlands, 15.11.01
23.30.0

Frielinghaus H.; Batsberg Pedersen W.1; Sommer Larsen P.1; Almdal K.1; Mortensen K.1
1Risø National Laboratory, Dep. of Solid State Physics, DK-4000 Roskilde; Denmark
Endeffekte in Polystyrol/Polyethylenoxid Copolymeren
Deutsche Neutronenstreutagung, FZ Jülich, 19.-21.02.01
23.30.0

Frielinghaus H.; Endo H.; Allgaier J.; Richter D.; Jakobs B.1; Sottmann T.1; Strey R.1
1Institut für Physikalische Chemie, Universität Köln, 50939 Köln
Polymer boosting effect in der Tröpfchenphase - eine Studie mit Neutronenkleinwinkelstreuung
Würzburger Tagung "Fortschritte für Wasch- und Reinigungsmittel", Würzburg, 02.04.01
23.30.0

Grimm H.
Relaxational dynamics in drug and humid DNA
Int. Conf. on Neutron Scattering, TU München, 09.-13.09.01
23.30.0

Grimm H.
Slow relaxation process in DNA at different levels of hydration
Deutsche Neutronenstreutagung, FZ Jülich, 19.-21.02.01
23.30.0

Heinrich M.; Pyckhout-Hintzen W.; Richter D.; Straube W.1; Wiedenmann A.2
1Martin-Luther-Universität Halle-Wittenberg, Fachbereich Physik, 06099 Halle
2Hahn Meitner Institut Berlin, Glienicker Str. 100, 14109 Berlin
Relaxation of entangled model H-shaped polymers: A SANS investigation
Int. Conf. on Neutron Scattering, TU München, 09.-13.09.01
23.30.0

Hoffmann S.; Richter D.; Arbe A.1; Colmenero J.1; Farago B.2
1Departamento de Física de Materiales, Universidad del País Vasco,Apt.1072, E-20080 San Sebastián, Spain
2Institut Laue Langevin, F-38042 Grenoble Cedex 9, France
Component Dynamics in Polymer Blends: A Combined QENS and Dielectric Spectroscopy Investigation
Int. Conf. on Neutron Scattering, TU München, 09.-13.09.01
23.30.0

Kahle S.; Willner L.; Monkenbusch M.; Richter D.; Arbe A.1; Colmenero J.1
1Dep. de Fiscia de Materiales, Universidad del Pais Vasco, Facultad de Quimica, E-20080 San Sebastian, Spain
Dynamic Neutron Scattering on Partially Deuterated Polybutadiene
ILL Millenium Symposium, Grenoble, France, 06.-08.04.01
23.30.0

Kahle S.; Willner L.; Monkenbusch M.; Richter D.; Arbe A.1; Colmenero J.1
1Dep. de Fiscia de Materiales, Universidad del Pais Vasco, Facultad de Quimica, E-20080 San Sebastian, Spain
Dynamic Neutron Scattering on Partially Deuterated Polybutadiene
Int. Conf. on Neutron Scattering, TU München, 09.-13.09.01
23.30.0

Kahle S.; Willner L.; Monkenbusch M.; Richter D.; Arbe A.1; Colmenero J.1
1Dep. de Fiscia de Materiales, Universidad del Pais Vasco, Facultad de Quimica, E-20080 San Sebastian, Spain
Dynamische Neutronenstreuung an partiell deuteriertem Polybutadien
Deutsche Neutronenstreutagung, FZ Jülich, 19.-21.02.01
23.30.0

Kirstein O.; Kozielewski T.; Prager M.; Andersen K.H.1
1ISIS Department, Rutherford Appleton Laboratory, Chilton, Didcot, Oxon, OX11 0QX, UK
A 0.9 micro eV backscattering spectrometer at the European Spallation Source (ESS)
7th General ESS Meeting, Seggau, Austria, 26.-29.09.01
23.89.1

Kirstein O.; Kozielewski T.; Prager M.; Richter D.
The high flux backscattering spectrometer (RSSM) for the FRM-II reactor in Munich
Int. Conf. on Neutron Scattering, TU München, 09.-13.09.01
23.89.1

Kirstein O.; Kozielewski T.; Prager M.
Conceptual analysis for a 1.4 micro eV backscattering spectrometer at the European Spallation Source (ESS)
Int. Conf. on Neutron Scattering, TU München, 09.-13.09.01
23.89.1

Kirstein O.; Prager M.; Parker S.F.1
1ISIS Facility, Rutherford Appleton Laboratory, Chilton, Didcot, Oxon OX11, 0QX, UK
Gitterdynamik und Methylgruppenrotation von Dimetyhlacetylen (DMA)
Deutsche Neutronenstreutagung, FZ Jülich, 19.-21.02.01
23.89.1

Kirstein O.; Prager M.
Methyl rotational excitations and lattice dynamics of o-, m-and p-xylene using transferable pair potentials
Int. Conf. on Neutron Scattering, TU München, 09.-13.09.01
23.15.0

Kirstein o.; Kozielewski T.; Prager M.; Richter D.
Das Rückstreuspektrometer (RSSM) hohen Flusses für den FRM-II Reaktor in München
Deutsche Neutronenstreutagung, FZ Jülich, 19.-21.02.01
23.89.1

Mihailescu M.; Monkenbusch M.; Endo H.; Allgaier J.; Richter D.; Jakobs B.1; Sottmann T.1; Farago B.2
1Institut für Physikalische Chemie, Universität zu Köln, 50939 Köln
2Institut Laue Langevin, F-38042 Grenoble Cedex 9, France

Dynamics of bicontinuous phase microemulsions with amphiphilic block-copolymer
Deutsche Neutronenstreutagung, FZ Jülich, 19.-21.02.01
23.30.0

Monkenbusch M.
Next generation NSE instruments - What are the challenges? - Where are the limits?
Deutsche Neutronenstreutagung, FZ Jülich, 19.-21.02.01
23.30.0

Neumann M.1; Press W.2; Nöldeke C.2; Asmussen B.2; Prager M.; Ibberson R.M.3
1MSI Europ. Headquarters 230/250, The Quorum Barnwell Road, Cambridge CB5 8RE, England
2Institut für Experimentelle und Angewandte Physik, Universität Kiel, Leibnitzstr. 19, 24098 Kiel
3ISIS Rutherford Appleton Laboratory, Chilton Didcot OX11 0QX, UK
The structure of the orientationally ordered phase III of solid methane
Int. Conf. on Neutron Scattering, TU München, 09.-13.09.01
23.15.0

Pipich V.; Schwahn D.; Willner L.
Complex phase behavior near the Lifshitz line in a ternary polymer blend
Int. Conf. on Neutron Scattering, TU München, 09.-13.09.01
23.30.0

Pipich V.; Schwahn D.; Willner L.
Formation of a microemulsion phase in a ternary polymer blend - a SANS study
Deutsche Neutronenstreutagung, FZ Jülich, 19.-21.02.01
23.30.0

Pipich V.; Schwahn D.; Willner L.
Influence of the reentrance criticality on isotropic Lifshitz critical behavior in a ternary polymer blend near the Lifshitz line
Jülich Soft Matter Days 2001, Kerkrade, NL, 13.-16.11.01
23.30.0

Prager M.; Press W.1; Asmussen B.1.; Combet J.2
1Institut für Experimentalphysik, Universität Kiel, Leibnitzstr. 19, 24098 Kiel
2Institut Laue-Langevin, F-38042 Grenoble Cedex 9, France
Phase III of ethane: basing rotational tunnelling on the crystal structure
Conf. on Quantum Atomic and Molecular Tunnelling 2001, Nottingham, UK, 07.09.01
23.15.0

Prager M.; Press W.1; Asmussen B.2; Combet J.2
1Institut für Experimentelle und Angewandte Physik, Universität Kiel, Leibnitzstr. 19, 24098 Kiel
2Institut Laue-Langevin, F-38042 Grenoble Cedex 9, France
Phase III of methane: crystal structure and rotational tunnelling
Int. Conf. on Neutron Scattering, TU München, 09.-13.09.01
23.15.0

Prager M.; Schiebel P.1; Grimm H.
1Inst. für Kristallographie, Universität Tübingen, 72070 Tübingen
Dipolar interaction in partially deuterated ammoniumhexachloroplatinate: rotational tunnelling spectroscopy
Int. Conf. on Neutron Scattering, TU München, 09.-13.09.01
23.15.0

Pyckhout-Hintzen W.
A microscopic model for branched polymers in elongational flow by SANS
GRC New Londen, NH, USA, 05.-12.08.01
23.30.0

Pyckhout-Hintzen W.
On the length scale dependence of microscopic strain
Deutsche Neutronenstreutagung, FZ Jülich, 19.-21.02.01
23.30.0

Pyckhout-Hintzen W.
On the length scale dependence of microscopic strain
Int. Conf. on Neutron Scattering, TU München, 09.-13.09.01
23.30.0

Pyckhout-Hintzen W.
Reinforcement of silica particles by SANS
GRC New Londen, NH, USA, 05.-12.08.01
23.30.0

Radulescu A.; Schwahn D.; Fetters L.J.; Richter D.
Crystallization of paraffin in decane in the presence of PEB-7 ethylene-butene random copolymers.
Int. Conf. on Neutron Scattering, TU München, 09.-13.09.01
23.30.0

Richter D.; Monkenbusch M.; Schwahn D.; Schweika W.
Scattering Experiments Relevant for Polymer Research at the Neutron Guide Laboratory of the Jülich Research Center
222nd ACS National Meeting Chicago, USA, 27.08.01
23.89.1

Schmidt W.1, Ohl M.1, Buchenau U., Koza M.1
1Institut Laue-Langevin, F-38042 Grenoble Cedex, France
Inelastic Neutron Scattering in Amorphous Systems at Low Momentum Transfer
Deutsche Neutronenstreutagung, FZ Jülich, 19.-21.02.01
23.89.1

Stellbrink J.; Allgaier J.; Monkenbusch M.; Richter D.
Self and Collective Dynamics of Ordered Star Polymer Solutions
DYPROSO XXVIII, Kerkrade, The Netherlands, 16.-19.09.01
23.30.0

Stellbrink J.; Allgaier J.; Monkenbusch M.; Richter D.
Self and Collective Dynamics of Ordered Star Polymer Solutions
Deutsche Neutronenstreutagung, FZ Jülich, 19.-21.02.01
23.30.0

Stellbrink J.; Allgaier J.; Monkenbusch M.; Richter D.
Self and Collective Dynamics of Ordered Star Polymer Solutions
Int. Conf. on Neutron Scattering, TU München, 09.-13.09.01
23.30.0

Stellbrink J.; Allgaier J.; Richter D.; Schofield A.B.1; Poon W.C.K.1; Pusey P.N.
1Department of Physics and Astronomy, The University of Edinburgh, Mayfield Road, Edinburgh EH9 3JZ, UK
Partial Structure Factors in Star polymer/colloid mixtures
Deutsche Neutronenstreutagung, FZ Jülich, 19.-21.02.01
23.30.0

Voigt J.; Schmidt W.1; Ohl M.1; Brückel T.
1Institut Laue-Langevin, F-38042 Grenoble Cedex, France
Magnetische Ordnung in Erbium/Terbium-Schichtsystemen
Deutsche Neutronenstreutagung, FZ Jülich, 19.-21.02.01
23.89.1

Willner L.
Bestimmung der Austauschkinetik von PEP-PEO Blockcopolymer-Mizellen mittels zeitaufgelöster NKWS
Deutsche Neutronenstreutagung, FZ Jülich, 19.-21.02.01
23.30.0

Zorn R.; Richter D.; Hartmann L.1; Kremer F.2; Frick B.1
1Institut Laue-Langevin, F-38042 Grenoble Cedex, France
2Fakultät für Physik und Geowissenschaften, Universität Leipzig, Linnéstr. 5, 04103 Leipzig
Inelastische Neutronenstreuungsexperimente zur Glasdynamik in eingeschränkter Geometrie

Deutsche Neutronenstreutagung, FZ Jülich, 20.02.01
23.15.0

Zorn R.; Richter D.; Hartmann L.1; Kremer F.2; Frick B.1
1Institut Laue-Langevin, F-38042 Grenoble Cedex, France
2Fakultät für Physik und Geowissenschaften, Universität Leipzig, Linnéstr. 5, 04103 Leipzig
Quasielastic neutron scattering experiments on the a relaxation in a confined glass-forming liquid
4th Int. Discussion Meeting on Relaxations in Complex Systems, Cheronissos, Greece, 21.06.01
23.15.0

Patents granted

Allgaier J.; Willner L., Richter D.
Synthese von lipophob-lipophilen polymeren Micellen
US: 6,284,847 (04.09.2001)
PT 1.1375
23.30.0

Lecture courses

Grimm H.
Crystal spectrometer: Triple-axis and backscattering spectrometer
WS 01/02, Laboratory Course Neutron Scattering, FZ Jülich, 18.-28.09.01
23.30.0

Monkenbusch M.
Neutron Spin-Echo Spectrometer (NSE)
WS 01/02, Laboratory Course Neutron Scattering, FZ Jülich, 18.-28.09.01
23.30.0

Monkenbusch M.
Polymer Dynamics
WS 01/02, Laboratory Course Neutron Scattering, FZ Jülich, 18.-28.09.01
23.30.0

Monkenbusch M.
Time-of-Flight Spectrometers
WS 01/02, Laboratory Course Neutron Scattering, FZ Jülich, 18.-28.09.01
23.30.0

Prager M.
Translation and Rotation
WS 01/02, Laboratory Course Neutron Scattering, FZ Jülich, 18.-28.09.01
23.15.0

Richter D.
Ferroelectricity
WS 00/01, IFF Ferienschule: Neue Materialien für die Informationstechnik, FZ Jülich, 05.-16.03.01
23.30.0

Richter D.
Properties of the neutron, elementary scattering processes
WS 01/02, Laboratory Course Neutron Scattering, FZ Jülich, 18.-28.09.01
23.30.0

Schmid D.1; Buchenau U.
1Univ. Düsseldorf, Inst. für Festkörperspektroskopie, Universitätsstraße 1 (Bereich 25), 40225 Düsseldorf
Experimentalphysik IV (Kern- und Elementarteilchenphysik)
Univ. Düsseldorf, SS 2001
23.15.0

Schwahn D.
Small-angle scattering and reflectometry
WS 01/02, Laboratory Course Neutron Scattering, FZ Jülich, 18.-28.09.2001
23.30.0

Schwahn D.
Soft Matter: Structure
WS 01/02, Laboratory Course Neutron Scattering, FZ Jülich, 18.-28.09.2001
23.30.0

Stellbrink J.
Reaktionskinetik
SS01, Universität Münster
23.30.0

Zorn R.
Correlation functions measured by scattering experiments
WS 01/02, Laboratory Course Neutron Scattering, FZ Jülich, 18.-28.09.2001
23.15.0

Zorn R.
Liquid Crystal Displays
WS00/01, IFF Ferienschule: Neue Materialien für die Informationstechnik, 05.-16.03.2001
23.15.0

Internal seminars

Monkenbusch M.; Richter D.; Wischnewski A.
Prototyp eines Neutronenspinecho-Spektrometers für Spallationsquellen
FZJ-HMI ESS HGF Projekt Meeting, FZ Jülich, 16.03.01
23.30.0

Monkenbusch M.; Wischnewski A.; Willner L.; Richter D.; Pyckhout-Hintzen W.; Farago B.1
1Institut Laue-Langevin, F-38042 Grenoble Cedex, France
Erste direkte Beobachtung des Übergangs von der Rouse- zur Reptationsdynamik in Polyethylen durch inkohärente Neutronenspinechospektroskopie
IFF Beirat, FZ Jülich, 26.04.01
23.30.0

Monkenbusch M.
Instrumentenwicklung für die ESS
ESS Tag, Monschau, 10.05.01
23.30.0

Institute of Electroceramic Materials

General Overview

Research Areas

The research areas of the institute comprise (1) technologies for the integration of electroceramic materials into microelectronics and nanoelectronics, (2) dielectric and ferroelectric properties of oxide ceramics, and (3) the defect structure in the vicinity of internal and external interfaces in oxides. These areas are complementary to the research areas of the Institute for Electronic Materials 2 (IWE 2) at the Aachen Technical University (RWTH). Project groups often comprise staff members and students from both institutes.

The 32nd IFF-Ferienschule which we organized in 2001 was entitled *Advanced Electronic Materials for the Information Technology*. This course turned out to be perfectly in time for preparation of the the new research programm *Information Technology and Nanoelectronics* in the frame-work of the HGF research area *Key Technologies*. One aspect of the new organization within the HGF will put more emphasis on the interdisciplinary of the research activities. In this respect, the course was strengthening the bridge between different institutes within the IFF and towards the ISG (Institut für Schichten und Grenzflächen).

Integration Technologies and Scaling Effects

The major project in the area of integration technologies and scaling effects is our HGF project *'Piccolo* – Scaling Effects in Integrated Electroceramic Materials' (2000 – 2003). This project is embedded in the former information technology program PGI (Physikalische Grundlagen der Informationstechnologie) of the Research Center Jülich. Beyond the Institut für Elektrokeramische Materialien (1), the (2) Institut für Mikrostrukturforschung IMF headed by K. Urban, (3) the Theorie III, headed by H. Müller-Krumbhaar, and (4) the Ion Technology (IT) group at the ISG headed by S. Mantl are involved. Several national and international universities and research centers participate in "Piccolo", too. The main focus of the proposal "Piccolo" is a fundamental as well as applied research on scaling effects of electroceramic materials. Today, typically polycrystalline films exhibit grain sizes much smaller than the feature sizes of the microelectronic devices. However, along with the sustaining trend towards further miniaturization, the decreasing feature sizes in microelectronic technology will approach the typical crystallite sizes of the perovskite-type oxide structures. Specific scaling effects are anticipated along this route, due to the long-range nature of the ferroelectric interaction of the oxides involved. The project aims at an (1) elucidation of the physical origin of these scaling effects, (2) an exploitation and extension of the limits to which the ferroelectric properties and high permittivities of the oxides involved can be used, and (3) the development of technological design rules for the integration of the perovskite-type oxides on a decreasing scale. The spectrum of designated results of the project comprises (semiquantitative) models for the superparaelectric limit of ferroelectric (FE) oxides, the dead layer at interfaces, the phase stability and segregation processes of perovskite films during annealing, the nucleation and growth of films by MOCVD, recipes for the deposition of single grain capacitors and ultrathin FE films as well as for reactive ion etching and a ferroelectric field-effect transistor (FE-FET) as a demonstrator. Scanning Probe Microscopy (SPM) techniques such as AFM and STM play an essential role in studying interrelationships on a microscopic base. Hence, the project "Piccolo" is an initiative to pursue research on the basic properties of electroceramic materials under scaling and on the relevance of these effects for the integration of perovskite-type oxides into microelectronics.

In cooperation with AIXTRON AG, our multiwafer MOCVD planetary reactor (MOCVD = Metal Organic Chemical Vapor Deposition) has been upgraded by the TriCent injector system which allows, in principle, the atomic layer-by-layer deposition of ultrathin films. This will be needed in the new Medea+ project which aims at the formation of alternative gate-oxide for future sub-100nm main-stream FETs and is useful as well for our FE-FET project.

As a supplement, we use high pressure oxygen sputtering for the deposition of ultrathin PZT film within the Piccolo project. For the patterning of the ceramic films and electrode / ceramic film stacks, the Reactive Ion Beam Etching (RIBE) technique is employed. In contrast to the situation in the standard Si and compound semiconductor technologies, dry etching processes of oxide ceramics have hardly been investigated yet and therefore represent a research area in which basic studies and industrially funded applied research can be linked in a beneficial manner. The integration processes are complemented by metallization methods based on electron beam and sputter techniques. Within this area, our studies aim at a better understanding of the processes and material parameters which govern the adhesion, the mechanical stress, the microstructure, and their effect on the dielectrical and ferroelectric properties.

Dielectric and ferroelectric properties

The second research area focuses on the *dielectric and ferroelectric properties* of oxide thin films and – for comparison - bulk ceramics, which are being investigated in Jülich as well as in Aachen. The material systems are based on compositions used for practical devices and model systems, e.g. $SrTiO_3$, $BaTiO_3$, $SrBi_2Ta_2O_9$, $Pb(Zr,Ti)O_3$. One of the research topics is the microscopic understanding of ferroelectric hysteresis including new approaches for the separation of *reversible* and *irreversible* contributions to polarisation based on the analysis of frequency-dependent small and large signals.

The polarisation studies are linked to the *aging* (imprint) phenomenon, i.e. the polarisation-dependent shift of the hysteresis curve with time and to the ferroelectric *fatigue* process, i. e. the reduction of the remanent polarisation by cycling. Both aging and fatigue processes play an important role in the operation of the novel non-volatile memories (Ferroelectric Random Access Memories, FeRAM). Impedance spectroscopy in the lower GHz regime is employed to determine the relaxation of the ferroelectric *domain wall* motion and to separate this contribution from the contribution of the crystal lattice. By varying the microstructure of the ceramics and by comparison between bulk ceramics and thin films, the model of Arlt will be extended with respect to the impact on 2D constraints imposed by mechanical stress due to the presence of substrates. The investigations of the ferroelectric properties are now additionally focussed on the scaling properties and nano-size effects. For *dielectric* ceramics, impedance spectroscopy is used to elucidate the interrelation of *extrinsic* losses and lattice defects. This activity includes the development and characterization of new microwave ceramics and is embedded into a cooperation with Norbert Klein's group at the ISG (Institut für Schichten und Grenzflächen) within the framework of a BMBF-Leitprojekt. In the case of ferroelectric materials, existing theories are further developed and extended towards a more quantitative description of the dielectric, piezoelectric, and elastic properties.

In addition, numerical *finite-element-methods* are used to describe the mutually coupled mechanical, thermal, and electrical properties of ceramic components such as multilayer capacitors and actuators.

Lattice disorder in the vicinity of internal interfaces

Our third research area comprises the *lattice disorder in the vicinity of internal interfaces* (grain boundaries) and external interfaces (surfaces and electrode interfaces) and their impact on electronic and ionic (oxygen ions and protons) charge transport. In the case of acceptor and donor doped titanate ceramics, the studies are focused on the formation of space charge depletion layers at grain boundaries as well as the related potential barriers and the transport of charge carriers along and across the grain boundary barrier. A hot-pressing technology has been developed to decorate the grain boundary area with additional dopants and to study the influence of these artifical grain boundary states. The coupling of the space-charge formation and the defect equilibria at the surface in the case of donor-doped titanates led us to a comprehensive explanation for long pending questions concerning the redox kinetics.

In some material systems, it is necessary to determine the equilibrium constants of the defect reactions and the diffusion constants of the system in order to create the basis for the research on interfaces. In this respect, the comparison of bulk ceramics and thin films of the same composition is of vital interest. In thin film systems, the significant influence of the electrode metals, the unexpectedly high stability under conditions of dc-voltage-induced resistance degradation, as well as the tolerance of the lattice concerning the incorporation of non-stoichiometries represent current research topics.

Rainer Waser

Institute of Electroceramic Materials

Head: Prof. Dr.-Ing. Rainer Waser
Secretary: Maria Garcia
Tel. +49(0)2461 61 5811; Fax: +49(0)2461 61 2550
e-mail: r.waser@fz-juelich.de/m.garcia@fz-juelich.de

Personnel 2001/2002 and their areas of activity

SCIENTISTS:

Dr. R. Dittmann	Pulsed laser deposition of dielectric and conducting oxide thin films and multilayers	23.42.0
Dr. P. Ehrhart	MOCVD methods for electroceramic thin films; X-ray diffraction and optical spectroscopy	23.42.0
Dr. R. Elsebrock	Processing of electroceramic bulk materials; microwave characterization; dielectric properties	23.42.0
Dr. S. Hoffmann-Eifert	High-permittivity electroceramic thin films: MOCVD, dielectric properties, charge transport, defect chemistry	23.42.0
Dr. S. Karthäuser	Self-assembly processes of oxidic and metallic nanostructures	23.42.0
Dr. H. Kohlstedt	Reactive ion beam etching of ceramic and metallic materials, magnetic and ferroelectric tunnel junctions	23.42.0
Dr. W. Krasser	Optical excitation-processes in electroceramic materials; light-annealing processes	23.42.0
Dr. P. Meuffels	Processing of electroceramic materials; studies of the defect chemistry	23.55.0
Dr. Ch. Pithan	Processing of hot pressed nanocrystalline and grain boundary decorated bulk electroceramics	23.55.0
Prof. T. Schober	High temperature proton conduction, thermogravimetry, impedance spectroscopy, transmission electron microscopy	23.55.0
Dr. H. Schroeder	Technology and properties of (metal) electrodes for electroceramic thin films; mechanical properties and electromigration in thin films and interconnects	23.42.0
Dr. K. Szot	Study of the surface layer of perovskite materials of ABO_3 structure	23.42.0
Prof. R. Waser	Electronic oxides and integration of electroceramic thin films	23.42.0

TECHNICAL ENGINEERS:

H. Bierfeld	Ceramic technology and sputtering techniques	23.55.0
DI J. Friedrich	Thermogravimetric analysis; Transmission electron microscopy	23.55.0
M. Gebauer	Metal organic chemical vapor deposition (MOCVD)of oxides; electrical measuring setups for atomic force microscopy (AFM)	23.42.0
M. Gerst	Measuring techniques; network administration	
DI H. Haselier	Metallization and thin film technology; clean-room technology	23.42.0
B. Hermanns	RIBE, sputtering of magnetic materials	23.42.0
DI H. John	Clean-room technology, microlithography and optical laboratory; LRP	23.42.0
DI C. Makovicka	Ceramic technology; powder processing	23.55.0

Ph.D. STUDENTS

O. Baldus (TH Aachen)	Laser annealing of CSD	23.42.0
F. Fitsilis (TH Aachen)	Thin film capacitors for future DRAM applications using the MOCVD technology	23.42.0
M. Fitsilis (Univ. of Thessaloniki)	Simulation and design concepts of ferroelectric field effect transistor circuits	23.42.0
R. Ganster (TH Aachen)	MOCVD growth of alkaline earth titanate-zirconate thin films; optimization of growth processes; layered structures; electrical characterization	23.42.0
A. Gerber (Uni Köln)	Epitaxial ferroelectric layers on silicon substrates and their use as field effect transistors	23.42.0
Ch. Ohly (TH Aachen)	Defect structures in doped titanate thin films: electrical and morphological properties	23.42.0
St. Regnery (TH Aachen)	MOCVD planetary reactor processes	23.42.0
S. Ritter (TH Aachen)	MOCVD growth of ultrathin ferroelectric films and electrical characterization	23.42.0
J. Rodriguez (Uni Köln)	Ferroelectric capacitors with oxide electrodes and tunneling	23.42.0
S. Schmitz, (TH Aachen)	Influence of the contact metal on the leakage current and dielectric permittivity of electroceramic thin film capacitors	23.42.0
St. Schneider (TH Aachen)	Reactive ion etching (RIE) and reactive ion beam etching (RIBE) of ceramic thin films	23.42.0
S. Stein (Uni Köln)	Spin injection devices	23.42.0

GRADUANTS:

C. Christidis (TH Aachen)	Leakage current investigations on $(Ba,Sr)TiO_3$ thin films in a multi-dimensional parameter space for their integration in the Gbit DRAM technology	23.42.0

GUEST SCIENTISTS:

Dr. N. Pertsev (A.F. Ioffe Institute St. Petersburg, Russia)	Theoretical calculations on the effects of strain and stress on the dielectric response of ferroelectric thin films grown on the sole substrates	23.42.0

POST-DOC:

Dr. D.J.D. Corcoran (Ireland)	Prototype mid-temperature SOFC assembly, performance analysis and testing, using thin-layer proton conducting oxide electrolytes. Investigation of thin layer deposition techniques.	23.55.0

The Network of Dislocations in the "Skin" Region of $SrTiO_3$ Crystals

K. Szot [(1)], W. Speier [(2)], R. Carius [(3)], U. Zastrow [(3)], R.Waser [(1)]

[1] *Institute of Electroceramic Materials,*

[2] *Institute of Chemistry and Dynamic of the Geosphere,*

[3] *Institute of Photovoltaics*

The defects in the perovskite materials of ABO_3-types show a tendency to accumulate in the form of linear or extended defects such as dislocation, shear planes and stacking faults. On the basis of SIMS measurements utilising tracer techniques and the observation of etch pits it is shown for model perovskite such as $SrTiO_3$ that the density of dislocations near the surface is of the order $10^9/cm^2$ and that these defects form an interconnected network. These defects provide easy diffusion paths which take the role of "short circuits".

F&E-Nr:23.42.0

In the surface region (the so-called "skin" region) of a ternary oxide with perovskite structure (ABO_3) solid state reactions take place at elevated temperatures as a result of the redistribution of AO complexes [1]. These solid state reactions lead to the formation of a chemically heterogeneous surface region with non-perovskite phases such as Ruddlesden–Popper and Magnéli type phases [2]. This is in contrast to the standard description based on point defect chemistry, which does not allow for the interaction between individual defects and the possibility of their accumulation [3]. New developments in defect chemistry account for this kind of restructuring phenomenon by including the possible existence of the new chemical phases on the surface. However these studies are still based on the assumption that the bulk of crystal is otherwise homogeneous in character and that the diffusion processes can be understood solely in terms of a random walk diffusion. This completely neglects the inherent structural inhomogeneity due to the existence of extended defects and their high density within the skin region. A prominent example of the special role of the dislocations in the ternary oxides is the recent discovery of super-plasticity in $SrTiO_3$ single crystals [4].

In our opinion, the segregation effects in the skin region of the perovskites are supported by fast diffusion along such extended defects. Already the use of simple chemical etching in order to mark the exits of dislocations on the surface in combination with analysis by AFM, allowed us to show for $SrTiO_3$ that a very large density of dislocations exists at the seemingly perfect surface of polished single crystals. In contrast to optical inspections with a light microscope (Fig. 1.) the AFM measurements have a very high resolution and allow the observation of etch pits in the early stages of chemical treatment. The measured density of dislocations (Fig. 2.) is close to the values found by Wang et al [5] in strontium titanate using the TEM technique ($10^9/cm^2$).

The dislocations provide the easy diffusion paths for oxygen, which becomes readily apparent from depth profile measurements by SIMS in conjunction with penetration experiments utilizing ^{18}O tracer.

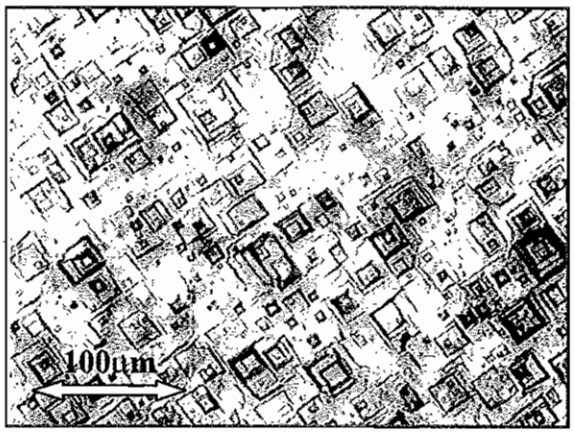

FIG. 1. Etch pits on the (100) $SrTiO_3$ (light microscope). The density of dislocation is of the order of magnitude $2*10^5/cm^2$

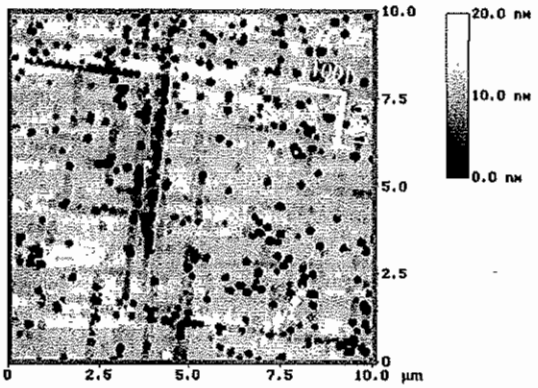

FIG. 2. AFM of etched (100) surface of strontium titanate with an estimated density of dislocations of $4*10^9/cm^2$

The depth concentration profile of the tracer obtained by SIMS follows closely the relation $\log (C_{18O}-C_N) \propto z^{6/5}$ (fig. 3a.) [6] corresponding to the so-called "B-regime" (after Harrison [7]) characteristic for the coexistence of statistical random walk diffusion (D_{latt}) and fast diffusion along preferential diffusion paths D_{disl} (Fig. 4.).

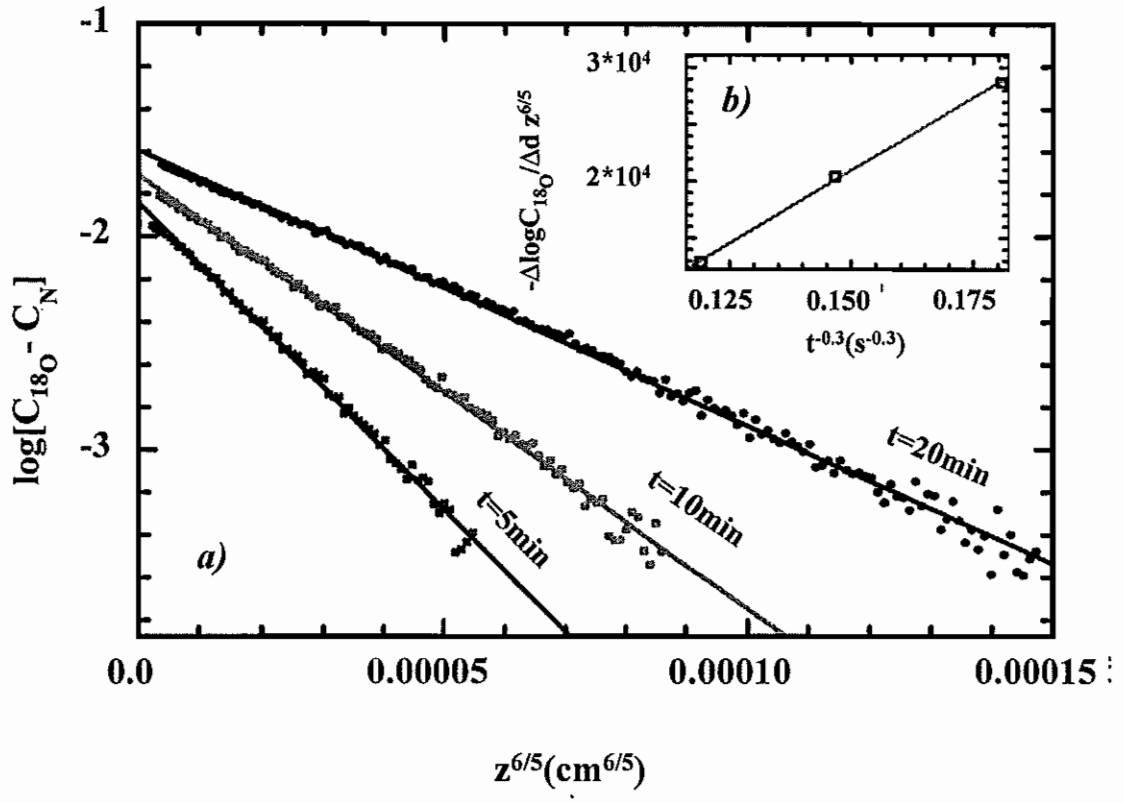

FIG. 3. The fraction of ^{18}O as detected by SIMS for reduced $SrTiO_3$ reoxidized in an ^{18}O-enriched atmosphere for different exposition times. The slope of the profiles as a function of penetration time (b) reveal diffusion along dislocation grouped in a network

Our experiments establish that the relation between the slope of $\delta \log C/\delta z^{6/5}$ as a function of penetration time($t^{-0.3}$) is linear (fig. 3b.) which provides a sensitive test for the fact that the diffusion proceeds along dislocations grouped in a network.

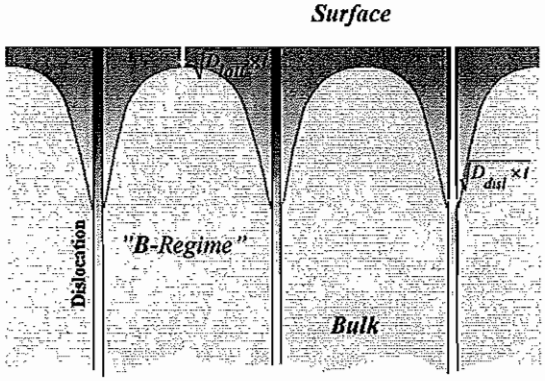

FIG. 4. Harison's "B" regime of diffusion along short-circuiting paths

The results presented for two model perovskites show that the extended defects play a very important role in the diffusion process and can "short-circuit" the lattice-random walk diffusion ($D_{disl} >> D_{latt}$). At low temperatures the network of extended defects may provide the only possible transport path for a material under mechanical, electrical, or chemical gradients. This concept, assuming preferential reduction of strontium titanate along extended defects, has been successfully applied for the first time to the analyses of the nature of the metal-insulator transition in reduced $SrTiO_{3-\delta}$ without at the same time violating the Mott criterion [8].

[1] K. Szot and W. Speier, Phys. Rev. B **60**, 5909 (1999)

[2] K. Szot, et al., Appl. Phys. A **64**, 55 (1997)

[3] F.A. Kröger and H.J. Vink , Solid State Physics,ed F. Seitz and D. Turnbull, Academic Press, New York, 1956, vol. 3

[4] P. Gumbsch, S. Taeri-Baghbadrani, D. Brunner, W.Sigle, and M.Rühle, Phys.Rev.Lett., **87**,085505 (2001)

[5] R. Wang, Y. Zhu, and S.M. Shapiro, Phys. Rev. Lett. **80** 2370 (1998)

[6] J. Philibert, *Atom movements - Diffusion and mass transport in solids,* Editions de physique, Les Ulis, France (1991

[7] L.G. Harrison, Trans. Faraday Soc. **57**, 1191(1961)

[8] K. Szot, W. Speier, R. Carius, U. Zastrow,and W. Bayer, Phys.Rev.Lett. (in press)

Structural and Ferroelectric Properties of Epitaxial $PbZr_{0.52}Ti_{0.48}O_3$ Thin Films Prepared on $SrRuO_3/SrTiO_3(100)$ Substrates

J. Rodríguez Contreras and H. Kohlstedt

Institute of Electroceramic Materials

We have prepared single crystalline epitaxial $PbZr_{0.52}Ti_{0.48}O_3$ (PZT) thin films on single crystalline epitaxial $SrRuO_3$ (SRO) thin films grown on $SrTiO_3$ (100) (STO) substrates. PZT and SRO thin films were grown using high-pressure on-axis sputtering. The film thickness ranged between 12 to 165 nm. Their excellent structural properties, surface smoothness and interface sharpness were demonstrated by X-Ray Diffraction measurements (XRD), High Resolution Transmission Electron Microscopy (HRTEM) and Atomic Force Microscopy (AFM). Rutherford Backscattering Spectrometry and Channeling measurements (RBS/C) were used to analyze stoichiometry and crystalline quality. Ferroelectric hysteresis loops were obtained for all films of a thickness down to 12 nm showing an increase in the coercive field E_c towards thinner film thickness. The decrease in the remanent polarization P_r, however, was found to depend on the patterning method. Furthermore tunnel junctions with a PZT barrier thickness of 3-6 nm have been prepared. Reproducible bi-stable I-V-curves and bias dependence of the conductance were obtained suggesting an influence of the ferroelectric properties of the barrier material on the tunnel current.

F&E-Nr: 23.42.0

The objective of this work is to investigate size effects in ferroelectrics such as PZT. Particularly interesting is the question of whether or not a switching in the polarization has an influence on the tunnel current in ultra thin ferroelectric films. The concept of a ferroelectric tunnel junction is described in [1].

To measure ferroelectric hysteresis loops Pt/PZT/SRO heterostructures with PZT thicknesses between 12 nm and 165 nm were patterned into capacitors with areas of 25 x 25 μm^2 to 200 x 200 μm^2 by conventional photolithography and lift-off or ion beam etching process. Ar-sputtered Pt was used as top electrode on PZT/SRO thin films, as SRO-top electrodes were found to increase the leakage current through PZT significantly. Ferroelectric hysteresis loops were obtained with the FE module of the aixACCT TF Analyzer 2000.

A more complex process was applied to pattern tunnel junctions [2,3]. In total, three photo mask steps allowed us to define tunnel junctions by conventional photolithography and ion beam etching. First Pt/PZT/SRO with a ferroelectric barrier thickness between 3 nm and 6 nm were Ar-etched to define the shape of the bottom electrode (Fig. 1a). Rectangular junctions with areas between 4 μm^2 and 200 μm^2 were then defined by using a second photo mask and ion milling, timed to end at the top surface of the bottom electrode (Fig. 1b). The surroundings of the mesas were isolated by 200 nm SiO_2. (Fig. 1c). After lift-off the third photo mask step defined the wiring layer, which served as an electrical contact to the top electrode of the tunnel junction (Fig. 1d). 100 x100 μm^2 crossovers without tunnel junctions served as test structures to measure the isolation resistance of the SiO_2 film. The resistance of these structures exceeded always 10 MΩ. Therefore, we neglected possible parallel current paths in the tunneling measurements through the isolating SiO_2 layer. In Fig. 1e, the top view of a tunnel junction including the current-voltage lead in a four-point arrangement is shown schematically. All I-V measurements were performed with a current source and a voltmeter. The bias-voltage dependence of the conductance was measured using a lock-in amplifier.

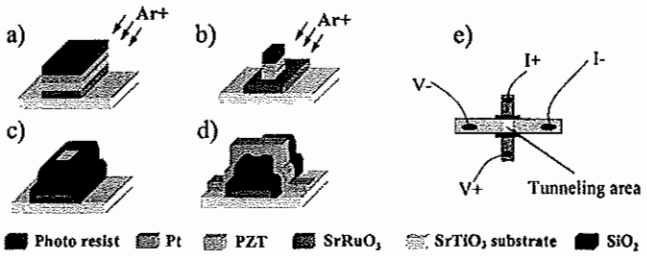

FIG. 1a-d Fabrication process of tunnel junctions in 4-point arrangement; FIG. 1e Top-view of a tunnel junction

X-ray diffraction indicates that both PZT and SRO layers are c-axis oriented and have an exact parallel orientation with the STO (100) substrate. The PZT films possess a small mosaicity (FWHM in $\omega \leq 0.05°$, FWHM in $\Phi < 1°$). For the SRO films these values are $\Delta\omega \leq 0.05°$ and $\Delta\Phi < 0.4°$. Atomic Force Microscopy reveals very smooth surfaces in the order of 2.8 Å, 6.4 Å and 8.9 Å (RMS roughness) for SRO, PZT and PZT/SRO films respectively. The stoichiometry has been verified by Rutherford Backscattering Spectrometry. As can be seen by channeling measurements the SRO buffer layer improves significantly the crystalline quality of the PZT film on top. This might be due to the smaller lattice mismatch of $SrRuO_3$ and $PbZr_{0.52}Ti_{0.48}O_3$. For example a 60 nm thick PZT film on STO shows a channeling yield (χ_{min}) of 16%, while the use of a SRO buffer layer improves this data to 8%. Note that

χ_{min} of the 90 nm thick SRO films is 1%. HRTEM shows very homogenous and atomically sharp interfaces without defects in 10 nm and 4 nm thick PZT films on SRO [4].

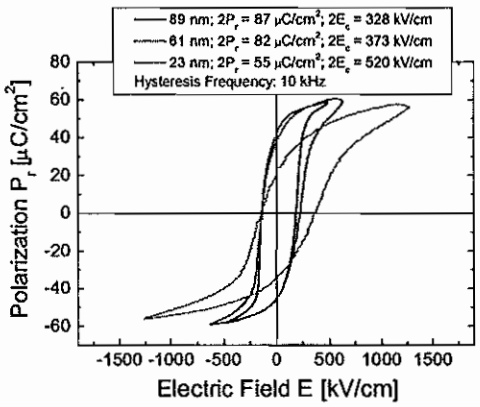

FIG. 2 Hysteresis loops of PZT thin film capacitors patterned by lift-off process

Well-saturated hysteresis loops with good square shapes were observed for all PZT capacitors with ferroelectric films thicker than 25 nm. Fig. 2 shows the P-E hysteresis loops for Pt/PZT/SRO capacitors with a PZT film thickness between 89 nm and 23 nm. With decreasing film thickness the rectangular form of the hysteresis curves is softened. Nevertheless, even 12 nm thick PZT films show clearly a ferroelectric hysteresis. The asymmetric electrodes used in Pt/PZT/SRO capacitors that result in different work functions at the interfaces between top electrode and PZT, and bottom electrode and PZT create an asymmetry of the hysteresis loops in PZT capacitors. Generally, the remanent polarization P_r decreases and the coercive field E_c increases for thinner films [5]. However, the ferroelectric properties are very sensitive to material quality and fabrication details. For example an increase of the remanent polarization from $2P_r = 64\ \mu C/cm^2$ to $2P_r = 105\ \mu C/cm^2$ for 23 nm thick PZT films has been obtained by substituting the initial used lift-off procedure by the ion beam etching procedure when patterning the capacitors. This higher P_r value is similar to the one obtained for 165 nm thick PZT films (Fig. 3).

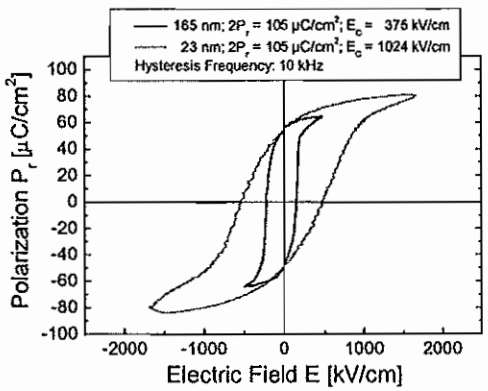

FIG. 3 Hysteresis loops of PZT thin film capacitors patterned by ion beam etching

Junctions with ultra thin PZT barriers (3-6 nm) have been fabricated. Fig. 4 shows a typical I-V-curve measured in a four-point arrangement to eliminate the lead resistance. One cycle, as indicated by the arrows, was measured in 15 minutes. Simultaneously the applied voltage dependence of the dynamic conductance was recorded with a lock-in amplifier (Fig. 4 inlet). The parabolic behavior of the dynamic conductance makes electron tunneling likely. Fitting the data to the Brinkman model at temperatures between 300 K and 4.2 K indicates additional current paths through the barrier. This non-tunneling current increases as the temperature is raised. A bi-stable and highly reproducible hysteresis in the I-V-curve is obtained. This effect can be caused by electromigration (creeping) [6], but also by a partial switching of the polarization in the ferroelectric barrier which may influence the tunneling current. Note that due to the increasing coercive field the applied electric field is probably not sufficient to polarize the whole ferro-electric film. The asymmetric shape of the I-V-curve and the bias voltage dependence of the dynamic conductance is due to the different work functions at the interfaces.

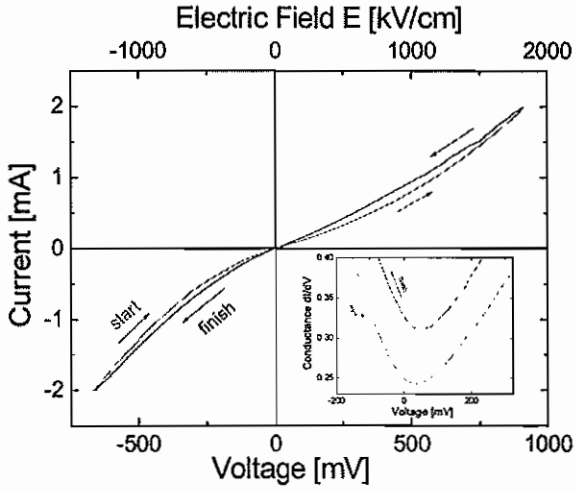

FIG. 4 IV-curve and dynamic conductance vs. bias V of a tunnel junction with an area of 16 μm^2 and a 5 nm thick PZT barrier at 300 K

In summary we have fabricated ferroelectric capacitors with a PZT film thickness in the range of 12 nm to 165 nm. Ferroelectric hysteresis loops have been obtained for these devices showing a decrease of the remanent polarization and an increase of the coercive field for thinner films. The decrease of the remanent polarization was found to depend on the crystalline quality and the fabrication process. Furthermore tunnel junctions with a barrier thickness of 3-6 nm have been prepared. A bi-stable and highly reproducible hysteresis in the I-V-curve and the bias dependence of the dynamic conductance has been measured. This behavior may be due to a partial switching of the polarization in the ferroelectric barrier.

[1] H. Kohlstedt, et al., Proceedings MRS Fall 2001
[2] J. Rodríguez Contreras, et al., Proceedings MRS Fall 2001
[3] Y. Lu, et al. Phys. Rev. B 54, 8357 (1996).
[4] C.L. Jia, et al., submittedt to Phys. Rev. Letters
[5] C. H. Lin, et al., J. Appl. Phys. 90, 1509 (2001).
[6] J. Z. Sun, et al., Phys. Rev. B 61, 11244 (2000).

Spin-injection Effects in Three Terminal Magnetic Tunnelling Junction Stacks

S. Stein and H. Kohlstedt

Institute of Electroceramic Materials

A magnetic tunnelling spin injection device (MAGTID) consisting of a stack of two ferromagnetic tunnelling junctions with access to the intermediate electrode has been developed. The layer structure is $Co/Al_2O_3/NiFe/Al_2O_3/Co$. The layers were deposited by dc-magnetron sputtering and the barriers were formed by ultraviolet-light assisted thermal oxidation. The performance of the upper and lower junctions within a stack were determined by current-voltage characteristics, the first derivatives (dV/dI vs. V) and the individual tunnelling magnetoresistances (TMR). A potential contact to an only 5.5 nm thick NiFe middle layer was successfully achieved. Using one junction in a stack as a spin injector and the second junction as a detector various magnetoresistance measurements were performed. The resistance of the detector junction was dependent on the magnetization of the common NiFe layer (parallel or antiparallel to the outer Co layers) and the injector current. The normalized TMR of the detector varied by up to 30%. This result will be discussed in the framework of non-equilibrium spin accumulation in the in the intermediate NiFe layer. For further improvement of the MAGTID we have studied $Ta/Ni_{79}Fe_{21}/Fe_{50}Mn_{50}/CoFe/Al_2O_3/CoFe/NiFe$ single barrier junctions using FeMn as an antiferromagnetic pinning layer. First results of these junctions will be presented.

F&E-Nr: 23.42.0

In the last years the field of magnetoelectronics evolved where not only the charge of electrons is used in electronic devices but also their spin information. Effects being used are the giant magnetoresistance and tunnelling magnetoresistance (TMR) of magnetic ultrathin film layer systems. Electronic applications have been proposed mainly in the area of non-volatile memories (magneto random access memory – MRAM) [1] and magnetic field sensors [2].

In this work we present a novel device which consists of two stacked magnetic tunnel junctions with an access to the intermediate electrode. This three terminal structure allows to determine the individual electrical properties of each junction. Moreover three terminal devices are an interesting approach to study spin-injection effects [3]. The schematic cross-section view is shown in Fig. (1).

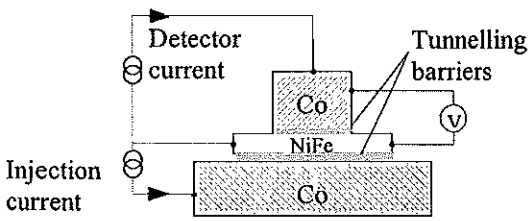

FIG. 1. Schematic view of the spin-injection measurement set-up.

Samples were fabricated with magnetron sputtering and structured with subsequent optical lithography and ion beam etching. For MAGTIDs the usual layer composition is Au(20nm)/ Co(15nm)/ Al_2O_3(1.3nm plus oxidation)/ NiFe(5.5...18.5nm)/ Al_2O_3(1.3nm plus oxidation)/ Co(15nm)/ Au(20nm). The multi layer was deposited on 2"-wafers in a multi-target sputtering system with a base pressure of 10^{-6} mbar. The metals were sputtered using a DC-magnetron source. For oxidation of the barriers first aluminium was deposited and then exposed for 1 hour to 10 mbar of O_2 and a UV-light source which enhances the thermal oxidation [4].

After deposition, the layer system was structured laterally in 5 lithography steps. The first three steps defined the three electrodes, the remaining two steps were used for deposition of SiO_2 insulation and wiring respectively. The areas fabricated in this way were $4x8\mu m^2$ for the upper junction and $8x20\mu m^2$ for the lower junction. It was possible to contact all three electrodes separately even with a common layer thickness as thin as 5.5 nm. The complete fabrication process is described in detail in ref. [5].

These junctions were subject of spin-injection experiments.

For improved TMR behaviour layer systems employing exchange biased electrodes with a single tunnelling barrier were also fabricated. The basic layer structure here was Substrate/
$Ta(5nm)/Ni_{81}Fe_{19}(3nm)/Cu(20nm)/NiFe(3nm)/Fe_{50}Mn_{50}(20$ nm)/$Co_{75}Fe_{25}(3nm)/Al_2O_3(1.6nm)/CoFe(3nm)/NiFe(20nm)/$ Au(20nm) (cf. [6]).The oxidation procedure was the same as mentioned above. The Ta and first NiFe layers were used as seed respectively texture layer for achieving the (111)-direction of the FeMn layer which is necessary for its antiferromagnetism. The magnetic tunnelling junction was deposited in no additional magnetic field. For aligning the antiferromagnetic FeMn samples were heated to 200°C – above the blocking temperature of FeMn – and then cooled down in a magnetic field of 130 Oe.

These single barrier tunnelling junctions were structured in three steps down to sizes of $1x5\mu m^2$.

I-V-characteristics and TMR measurements were performed in a four-point arrangement. For magnetic field dependence

an exterior coil could apply fields up to 0.6 T and a flow cryostat allowed measurements at temperatures from 4 to 300K.

Current-voltage characteristics of both lower and upper junctions in several MAGTIDs were measured. By calculating the first derivative of the I-V-curve parabolic behaviour characteristic of tunnelling junctions can be seen in Fig. (2, top left). Resistance-area products were in the range of 10 $k\Omega\mu m^2$ for both junctions. In a second experiment the magnetic field dependence of the resistance across each junction was measured as shown in Fig. (2, top right). For each junction the H-field was applied in a loop from negative values to positive and back again. Both junctions individually exhibited TMR like behaviour with values of about 3% at room temperature. Together with the tunnelling characteristic this is evidence enough that all electrodes were contacted properly.

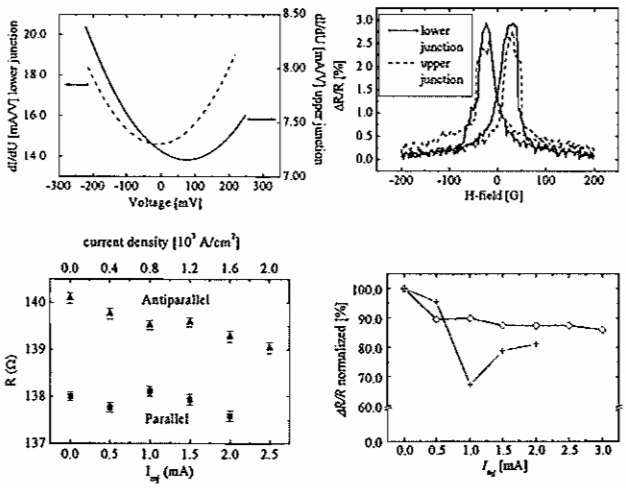

FIG. 2 Top left: G-V-curve of both junctions of a MAGTID sample. Top right: TMR curve of both junctions of MAGTID sample. Bottom left: Spin injection measurement, 5.5 nm common layer. Bottom right: TMR ratios for different common layer thickness d_{NiFe}, in dependence of the injected current. Values are normalized to $I_{inj} = 0$.

For the measurement of spin injection effects, the set-up as shown above (Fig. (1)) was used. The external magnetic field was chosen either to align all magnetic layers parallel or to align the common soft magnetic layer anti-parallel to the magnetization of both Co layers. In both cases the resistance across the upper junction was recorded in dependence of the spin-injector current (see Fig. (2, bottom left)). In Fig. (2, bottom right), there are plotted the ratios of the resistance in parallel to anti-parallel alignment (i.e. the TMR) for two different common layer thicknesses. With the 5.5nm sample there is an overall non-monotonous decrease of the normalized TMR by 30%, with the 18.5nm sample we find a decrease of around 12%.

If we take the current densities applied here into account (about 10^3 A/cm²) it seems unfeasible that we observed current induced switching effects like shown in [7].

Considering recent advances in spin valve transistors employing three-terminal ferromagnet/semiconductor devices [8,9] it might be noted that the fabrication process of the MAGTID can be used for these devices as well.

To increase the signal intensity of MAGTIDs single barrier MTJs for improved TMR performance were created. They were also characterized by their I-V-curves and TMR values. Fig. (3) shows the resistance change with a magnetic field sweep of one of these junctions. In this case oxidation of the barrier was done by exposure to 5 mbar of O_2 and UV-light for 1 hour. To align the antiferromagnet the junction was heated to 200°C for 10 minutes and cooled in a magnetic field of 130 G. The TMR value here reaches 48% at room temperature. Measurements at 4 K resulted in a TMR of 58%. It should be noted that the exchange bias based shift of the TMR curve is not optimised yet. This is a result of the rather low aligning field (130 Oe) during field-cooling.

Based on the performance of these MTJs we propose to fabricate further MAGTIDs employing as electrodes an exchange biased CoFe electrode, a NiFe common electrode and a third electrode simply consisting of CoFe. This system should show three different switching fields as well as much higher TMR values.

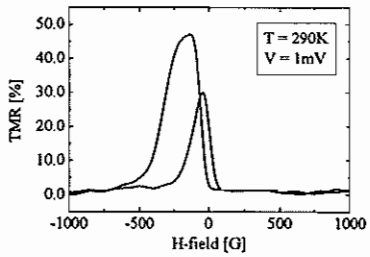

FIG. 3. TMR of a single barrier junction at room temperature.

REFERENCES

[1] S.S.P. Parkin et al., J. Appl. Phys. **85**, 5828 (1999).
[2] M. Tondra et al., J. Appl. Phys. **87**, 4679 (2000).
[3] M. Johnson, Phys. Rev. Lett. **70**, 2142 (1993); Science **260**, 320 (1993); J. Appl. Phys. **75**, 6714 (1994).
[4] P. Rottländer, H. Kohlstedt, P. Grünberg, and E. Girgis, J. Appl. Phys. **87**, 6067 (2000).
[5] S. Stein, R. Schmitz, and H. Kohlstedt, Solid state communications **117**, 599 (2001).
[6] X.F. Han et al., Appl. Phys. Lett., **77**, 283 (2000).
[7] J. Grollier et al., Appl. Phys. Lett. **78**, 3663 (2001).
[8] R. Vlutters et al., J. Appl. Phys. **89**, 7305 (2001).
[9] R. Jansen et al., J. Appl. Phys. **89**, 7431 (2001).

Crystallization and Thermal Stress in Laser-Treated Ceramic Thin Films

Oliver Baldus and Rainer Waser

Institute of Electroceramic Materials

The potential of perovskite type thin films for applications in electronic devices strongly relies on their compatibility to silicon substrates. Whereas the electrical properties of electroceramic films are investigated in detail, the deposition parameters (particularly the deposition temperature) still is above the critical value of 450°C in many cases. The subject of this work is to examine the possibility of laser sintering of thin ceramic films with nanosecond laser pulses to induce changes in their structural and electronic properties in the heated region only. A model for the crystallization process and the thermally induced stresses is presented.

F&E-Nr: 23.42.0

$(Ba_{1-x}Sr_x)TiO_3$ is one of the promising material systems for memory devices in microelectronics as well as for oxygen sensoring applications due to its exceptional electrical properties [1][2]. Thin films were prepared by a chemical solution deposition method from a stoichiometric $(Ba_{0.7}Sr_{0.3})Ti_1$ solution. The as-deposited coatings were pyrolized for ten minutes at 450°C on a hotplate. Usually a heat treatment of the amorphous as-deposited film is needed at high temperatures (> 600°C) for crystallization [3]. In this work, we report on the crystallization properties of ceramic thin films in which the substrate temperature is kept at room temperature [4]. Using UV-KrF-excimer laser pulses, sintering experiments result in x-ray crystalline and high-k thin films. Fig. 1a) shows the smooth film with sputtered top-electrode for electrical characterization. The film has been processed with 500 pulses of 100mJ/cm². A finite element model of the process has been developed. The model includes heat transfer, crystallization and thermal respectively phase transformation induced stress analysis. The temperature calculation of one 100mJ/cm² KrF-laser pulse shows the temperature during one heating cycle and the associated melting depth (Fig. 1b).

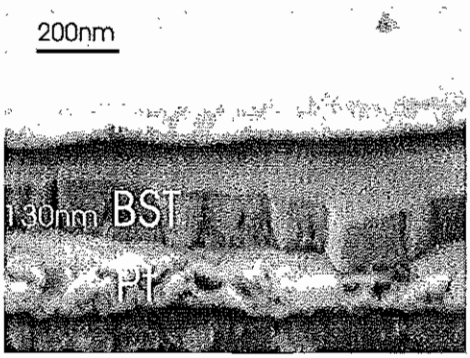

FIG. 1: a) SEM picture

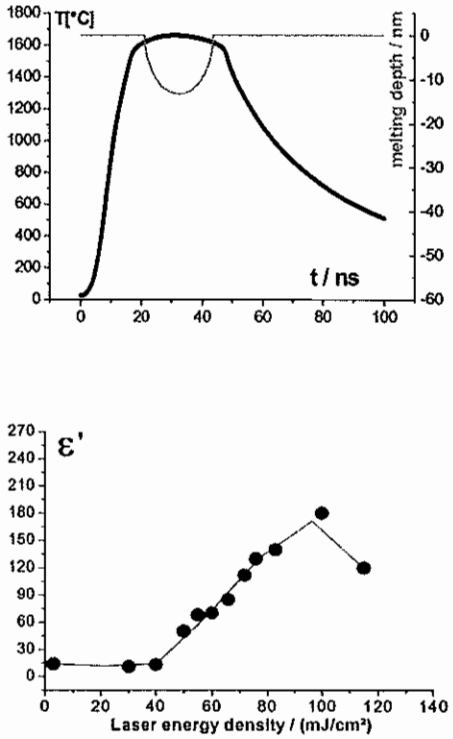

FIG. 1: b) calculated temperature c) measured permittivity of laser treated amorphous BST films.

The x-ray-pattern in Fig. 2 proves that the crystallization processes becomes more favourable with higher pulse energy density. By comparing the x-ray pattern and the corresponding electrical properties (fig. 1c) with the applied laser parameters a crystallization model has been developed based on the temperature calculation: The increasing temperature initiates the transformation from amorphous to a crystalline phase whereby the transformed phase X at time t is computed using the Johnson-Mehl-Avrami (JMA) kinetic equation in the modified version for non-isothermal temperature cycle (fig 4).

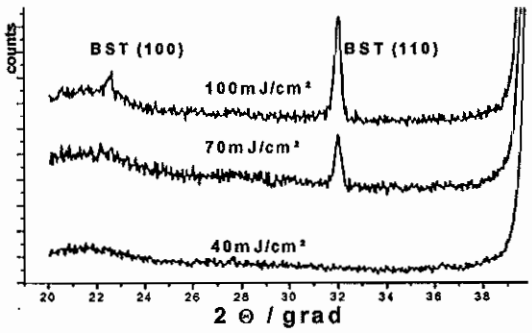

FIG. 2: XRD studies of laser treated BST thin films. With rising laser pulse energy density the Bragg reflexes become more intensive.

The laser crystallization is an incremental process whereby the desired fraction of crystallized phase has been attained by consecutive pulsed laser treatment. The stress distribution shows during the heating phase in the BST film exclusive compressive stress due to hindered thermal expansion (Fig. 4). After cooling down to total temperature homogenisation a tensile stress distribution remains due the material contraction after the amorphous to a crystalline phase transformation. This densification may lead to crack formation (Fig 3). The appropriate governing equations are as follows:
the heat equation:

$$\frac{\partial\ (\rho\ c_p T)}{\partial\ t} = \nabla\ (\ \lambda\ \nabla T\ ) + q_L$$

$$with: q_L = \frac{A \cdot I_L(r,t)}{\delta_{opt}} \cdot \exp\left(-\frac{z}{\delta_{opt}}\right) \quad (1)$$

$$X(t) = 1 - \exp\left[-(kt)^n\right] \quad (2)$$

$$with: k = \nu_o \cdot \exp\ (-E_a / RT)$$

the Johnson-Mehl-Avrami and the thermo-elastic stress/strain equations:

$$div\ \underline{\underline{\sigma}} = \frac{\partial\ \sigma_{ij}}{\partial\ x_j} = 0 \quad (3)$$

$$\sigma_{ij} = \frac{E}{1+\nu}\varepsilon_{ij} + \frac{E\ \nu}{(1+\nu)\ (1-2\nu)}\varepsilon_{kk}\delta_{ij}$$

$$-\frac{\alpha \cdot E \cdot \Delta T}{(1-2\nu)}\delta_{ij} - \frac{\alpha_c \cdot E \cdot X}{(1-2\nu)}\delta_{ij}$$

$$with: \varepsilon_{ij} = \frac{1}{2}\left(\frac{\partial u^i}{\partial x_j} + \frac{\partial u^j}{\partial x_i}\right)$$

The thermal expansion coefficient α_c in the above equation causes the experimentally observed contraction of the heated film depending on the crystallized part X. Probably because of this, the stepwise processing with the high power excimer laser leads to crack formation above a certain pulse number.

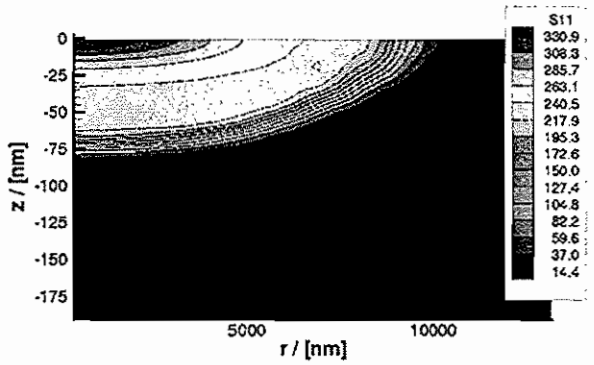

FIG.3: Residual radial stress component σ_{rr} / [N/nm^2] after temperature homogenization (parameters see Fig. 4).

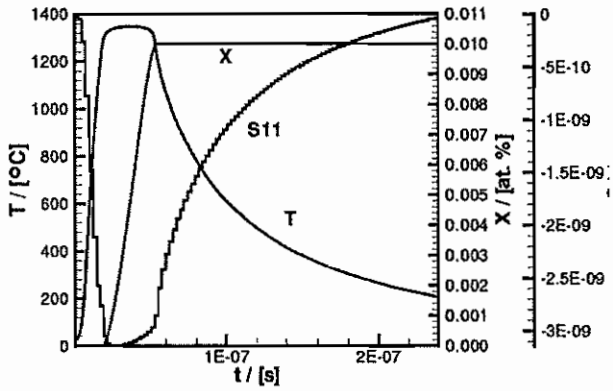

FIG.4: Temperature, crystalline phase and radial stress / [N/nm^2] at the center point (r=z=0) as a function of time, D=200nm, I=80mJ/cm, A=0.87, δ_{opt} =19nm

For the first time, BST thin films have been successful laser crystallized and electrically characterized. Describing the experimental results, a model is presented which contains the thermalization of optical energy, heating of a multilayer structure, crystallization, and stress development. The simulation results show that the crystallization has to be performed by application of consecutive laser pulses generating the desired fraction of crystallized phase. The temperature within the layers beneath the $(Ba,Sr)TiO_3$ film doesn't exceed the temperature limit of 450°C during laser treatment. With increasing fraction of crystallized phase the residual tensile stresses within the film increase.

1. Kotecki, D. et al., *IBM Journal of Research & Development*, 1999, **43**, 367-82.
2. York, R. A., Nagra, A. S., Speck, J. S., Auciello, O. H. & Streiffer, S. K., to be published in *Integr. Ferroelectrics*, (ISIF 2000).
3. U. Hasenkox, R. Waser, J. Sol-Gel Science a. Techn. **12** 67-79 1998
4. O. Baldus, R. Waser, Integrated Ferroelectrics 2000 **30** 129-138

Thin films of a High Temperature Proton Conductor Prepared by CSD Techniques

T. Schober[1] , T. Schneller[2], J. Friedrich[1], D. Corcoran[1]
[1]*Institute of Electroceramic Materials*
[2]*Institut Werkst. der Elektrotechnik II, RWTH Aachen*

Abstract – Thin films ($BaZr_{0.8}Y_{0.2}O_{(3-x)}$) were prepared by CSD techniques and were shown by impedance measurements to be high temperature proton conductors.

F&E-Nr: 23.55.0

Perovskite-type cerates and zirconates of the form ABO_3 (A=Ba, Sr; B=Ce, Zr) may dissolve significant amounts of water when doped with trivalent elements such as Y or Yb. Because the protons are mobile these systems become good proton conductors at elevated temperatures (1-9) (high temperature proton conductors, HTPCs).

For the preparation of the proton conducting Y-doped $BaZrO_3$ thin films a "hybrid type" CSD process has been developed. The 0.3 M precursor solution is chemically based on barium propionate ($Ba(OOCCH_2CH_3)_2$), zirconium tetrabutoxide, and yttrium acetate hydrate ($Y(OAc)_3 \cdot xH_2O$) which has been dehydrated by means of reaction with propionic acid anhydride. A mixture of propionic acid and n-butanol has been used as the solvent and the ($Zr(O^nBu)_4$ ^nBuOH) was chemically stabilized by addition of two moles of acetylacetone to avoid a premature hydrolysis and polycondensation reaction.

Prior to spin-coating, this solution was filtered with a 0.2µm PTFE filter. The solutions were spin-coated at 4000 rpm for 30s on platinized silicon substrates. After each coating process, the wet films were directly crystallized in a diffusion furnace at 900°C in O_2 atmosphere for 10 min. Thirteen coating cycles were carried out to reach a total thickness of approximately 500 nm. Finally top electrodes were deposited by sputtering Pt and patterning by lift off. The final sandwich was given an equilibrating anneal at 980 °C for 16 h.

The proton conducting properties were established by impedance spectroscopy using a Solatron 1260 analyzer. The first and second semicircle were investigated at the fixed temperature of 400 °C as a function of applied humidity (Fig. 1). The starting condition was always a carefully dried sample as obtained by annealing at 750 °C in dry 2%O_2 in Ar for several hours. A considerable decrease of the diameter of the first semicircle (bulk resistance) was obtained by humidifying the sample in moist 2%O_2 in Ar with $p_{H2O} \approx$ 23 mbar. This is already a firm evidence for proton conduction. Even more convincing is the response after exposure to moist Ar-4%H_2. It is seen that the first semicircle now has roughly a diameter of ~10% of the original (dry) value.

In a second experiment (Fig. 2) the temperature dependence of the totally dry conductivity and that after exposure to moist Ar-4%H_2 gas was determined. It is seen that the 'wet' conductivity is much larger than the 'dry' one. The slope of the 'wet' conductivity curve of 0.58 eV is very typical of proton conduction. Overall, the present evidence is a clear indication that the films are high temperature proton conductors.

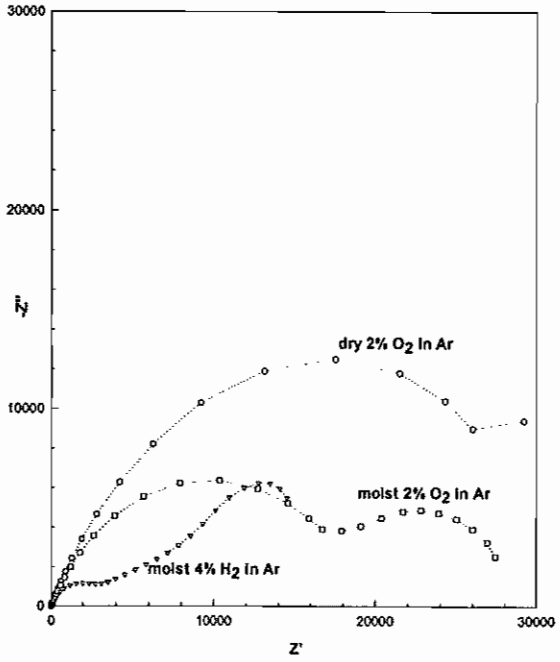

FIG.1 Impedance plots of a 0.5 µm thick $BaZr_{0.8}Y_{0.2}O_{(3-x)}$ thin film prepared by CSD techniques. The response to a hydrogen containing medium is clear evidence for proton conduction (see text).

The present thin films of $BaZr_{0.8}Y_{0.2}O_{(3-x)}$ may have the following applications:

- In the construction of a proton conducting high temperature fuel cell with a thin film electrolyte which would minimize the ohmic losses during operation.
- For sensors of hydrogen containing gaseous media. Such thin film sensors may be sensitive to water vapor and many organic vapors. Due to the low thickness of the film the response time would be ultra fast.
- In the construction of chemical reactors where protons are added or withdrawn from certain chemical compounds. A case in point is ammonia synthesis which has been shown to be possible with such proton conductors (10). Thin film technology could substantially lower the cost of such reactors.

- In the conditioning of gas streams, for instance Ar, where the addition of hydrogen may be desirable to lower the O_2 partial pressure.

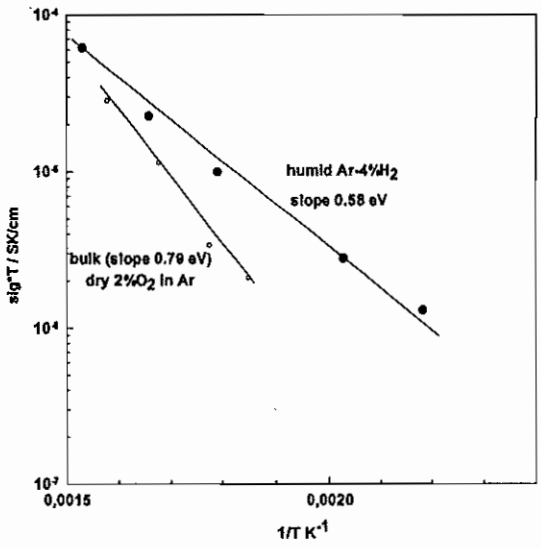

FIG. 2 Temperature dependence of conductivity in dry and humid state. Difference is due to proton conduction - for details see text.

References

1. T. Schober, Solid State Ionics, 144 (2001) 379-386
2. T. Schober, P. Meuffels, J. Am. Ceram. Soc. 84 (2001) 1996-2000
3. T. Schober, P. Meuffels, J. Vac. Sc. & Techn. A 19 (2001) 958-962
4. H. G. Bohn, T. Schober, J. Am. Ceram. Soc. 83 (2000) 768
5. T. Schober, H. G. Bohn, Solid State Ionics 127 (2000) 351
6. H.G. Bohn, T. Schober, T. Mono, W. Schilling, Solid State Ionics 117 (1999) 219
7. T. Schober, H. G. Bohn, T. Mono, W. Schilling, Solid State Ionics 118 (1999) 173
8. T. Schober, J. Friedrich, Solid State Ionics 125 (1999) 319
9. T. Schober, K. Szot, M. Barton, B. Kessler, U. Breuer, H.J. Penkalla, W. Speier, J. Solid State Chemistry 149 (2000) 262
10. G. Marnellos, M. Stoukides, Science 282 (1998) 98

Publications in refereed journals

Bachhofer H.; von Philipsborn H.; Hartner W.; Dehm C.; Jobst B.; Kiendl A.; Schroeder H.; Waser R.
Phase formation and crystal growth of Sr-Bi-Ta-O thin films grown by metalorganic chemical vapour deposition
J. Mat. Res. 16 (2001) 2966
23.42.0

Bartic A. T.1; Wouters D. J.1; Maes H.E.1; Rickes J.; Waser R.
1 imec, Leuven, Belgium
Preisach model for the simulation of ferroelectric capacitors
J. Appl. Phys. 89 (2001) 3420-3425
23.42.0

Bartic A.1; Rickes J.; Wouters D.1; Waser R.; Maes H.1
1 imec, Leuven, Belgium
Implementation of a Ferroelectric Capacitor Model using the Preisach Hysteresis Theory
Ferroelectrics 32 (2001) 295-302
23.42.0

Bolten D.1; Böttger U.1; Schneller T.1; Grossmann M.1; Lohse O.1; Waser R.
1 Institut für Werkstoffe der Elektrotechnik, RWTH Aachen
Irreversible Polarization in Donor Doped Pb(Zr, Ti)O3
Integrated Ferroelectrics 32 (2001) 93-99
23.42.0

Cassel D.; Pickartz G.; Siegel M.; Goldobin E.; Kohlstedt H.; Brinkman A.; Golubov A.A.; Kupriyanov M.Yu. ; Rogalla H.:
Influence of the transparency of tunnel barriers in Nb/Al2O3/Al/Al2O3/Nb junctions on transport properties
Physica C: Superconductivity 350 (2001) 276
23.42.0

Ehrhart P.; Fitsilis F.; Regnery S.; Jia C.; Waser R.; Schienle F.1; Schumacher M.1;
Dauelsberg M.1; Strzyzewski P.1; Jürgensen H.1
1 Aixtron AG, Aachen
Growth of (Ba,Sr)TiO3 thin films in a multi-wafer MOCVD reactor
in 'Ferroelectric thin Films IX '(P.C.McIntyre, S.R.Gilbert, Y.Miyasaka, R.W.Schwartz, D.Wouters eds,)
MRS Proc.Vol.655 (2001) p. CC9.4.1-CC9.4.6
23.42.0

Fitsilis F.; Regnery S.; Ehrhart P.; Waser R.; Schienle F.1; Schumacher M.1;
Dauelsberg M.1; Strzyzewski P.1; Jürgensen H.1
1 Aixtron AG, Aachen
BST thin films grown in a multi-wafer MOCVD reactor
J. Europ. Ceram. Soc. (2001) 1547-1551
23.42.0

Grossmann M.1; Lohse O.1; Bolten D.1; Böttger U.1; Waser R.; Tiedke S.2; Schmitz T.2; Kall U.2; Kastner M.; Schindler G.3; Hartner W.3
1 Institut für Werkstoffe der Elektrotechnik, RWTH Aachen
2 aixacct systems, Aachen
3 Infinion Technologies, München
Influence of the Measurement Parameters on the Reliability of Ferroelectric Thin Films
Integrated Ferroelectrics 32 (2001) 1-9
23.42.0

Haneder T.; Hönlein W.; Bachhofer H.; v. Philipsborn H.; Waser R.
Optimization of Pt/SBT/CeO2Si(100) Gate Stacks for Low Voltage Ferroelectric Field Effect Devices
Ferroelectrics 34 (2001) 47-54
23.42.0

Heinsohn J.-K.; Dittmann R.; Rodríguez Contreras J.; GoldobinE.; Klushin A.; Siegel M.; Hagedorn D.; Pöpel R.; Dolata R.; Buchholz F.; Niemeyer J.
Effect of the magnetic-field orientation on the modulation period of the critical current of ramp-type Josephson juction
J. Appl. Phys. 90 9 (2001) 4623-4631
23.42.0

Heinsohn J.-K.; Dittmann R.; Rodríguez Contreras J.; Scherbel J.; Klushin A.; Siegel M.; Jia C.; Golubov S.; Kupryanov M.
Current transport in ramp-type junctions with engineered interface
J. Appl. Phys. 89 7 (2001) 3852-3860
23.42.0

Hofer C.1; Weber U.1; Waser R.
1 Institut für Werkstoffe der Elektrotechnik, RWTH Aachen
Electrical characterization of grain boundary decorated SrTiO3 ceramics
J. Eur. Ceram. Soc. 1921 (2001) 1753-1757
23.42.0

Küppers H.1; Hoffmann M.1; Leuerer T.1; Schneller T.1; Böttger U.1; Waser R.; Mokwa W.1; Schnakenberg U.1
1 Institut für Werkstoffe der Elektrotechnik I+II, RWTH Aachen
Basic Investigations on a Piezoelectric Bending Actuator for Micro-Electro-Mechanical Applications
Ferroelectrics 35 (2001) 269-281
23.42.0

Küppers H.1; Leuerer T.1; Schnakenberg W.1; Mokwa W.1; Hoffmann M.1; Schneller T.1; Böttger U.1; Waser R.
1 Institut für Werkstoffe der Elektrotechnik I+II, RWTH Aachen
PZT thin films for piezoelectric micro-actuator applications
Transducers'01, Eurosensors XV, Springer-Verlag, Vol. 2,1018-1021
23.42.0

Lohse O.1; Grossmann M.1; Bolten D.1; Böttger U.1; Waser R.
1 Institut für Werkstoffe der Elektrotechnik, RWTH Aachen
Relaxation Mechanisms in Ferroelectric Thin Film Capacitors for FeRAM Application
Integrated Ferroelectrics 33 (2001) 39-48
23.42.0

Lohse O.1; Grossmann M.1; Bolten D.1; Böttger U.1; Waser R.
1 Institut für Werkstoffe der Elektrotechnik, RWTH Aachen
Transient Behavior of the Polarization in Ferroelectric Thin Film Capacitors
Mat. Res. Soc. Symp. Proc. 655 (2001) 761-769
23.42.0

Lohse O.1; Grossmann M.1; Böttger U.1; Bolten D.1; Waser R.
1 Institut für Werkstoffe der Elektrotechnik RWTH Aachen
Relaxation mechanism of Ferroelectric switching in Pb/Zr,Ti)O3 thin films
J. Appl. Phys. 89 (2001) 2332-2336
23.42.0

Ohly C.; Hoffmann S.; Szot K.; Waser R.
High temperature conductivity behavior of doped SrTiO3 thin films
Integrated Ferroelectrics 33 (2001) 363
23.42.0

Ohly C.; Hoffmann-Eifert S.; Szot K.; Waser R.
Electrical Conductivity and Segregation Effects of doped SrTiO3 Thin Films at High Temperatures,
J. Europ. Ceram. Soc. 21 (2001) 1673-1676
23.42.0

Partyka P.; Zhong Y.; Nordlund K.; Averback R. S. ; Robinson I. M.; Ehrhart P.:
Grazing incidence diffuse x-ray scattering investigation of the properties of irradiation-induced point defects in silicon
Phys.Rev. B64, 23, (2001) 235207-1 to 235207-8

23.42.0

Pertsev N.1 Koukhar V.1; Waser R.; Hoffmann S.
1 Ioffe Institute of Physics, St. Petersburg, Russia
Effects of Domain Formation on the Dielectric Properties of Ferroelectric Thin Films"
Ferroelectrics 32 (2001) 235-249
23.42.0

Petzelt J.; Ostapchuk T.; Gregora I.; Hoffmann S.; Lindner J.; Rafaja D.; Kamba S.; Pokorny J.; Bovtun V.; Porokhonsky V.; Savinov M.; Vanek P.; Rychetsky I.; Perina V.; Waser R.
Far Infrared and Raman Spectroscopy of Ferroelectric Soft Mode in SrTiO3 Thin Films and Ceramics
Ferroelectrics 32 (2001) 703
23.42.0

Petzelt J.; Ostapchuk T.; Gregora I.; Rychetsky I.; Hoffmann-Eifert S.; Pronin A. V.; Yuzyuk Y.; Gorshunov B. P.; Kamba S.; Bovtun V.; Pokorny J.; Savinov M.; Porokhonskyy V.; Rafaja D.; Vanek P.; Almeida A.; Chaves M. R.; Volkov A. A.; Dressel M.; Waser R.
Dielectric, infrared, and Raman response of undoped SrTiO3 ceramics: Evidence of polar grain boundaries
Phys. Rev. B 64 (2001) 184111/1
23.42.0

Prume K.1; Hoffmann S.; Waser R.:
1 Institut für Werkstoffe der Elektrotechnik, RWTH Aachen
Finite Element Simulations of Interdigital Electrode Structures on High Permittivity Thin Films
Integrated Ferrroelectrics 32 (2001) 63-72
23.42.0

Prume K.1; Hoffmann S.; Waser R.
1 Institut für Werkstoffe der Elektrotechnik, RWTH Aachen
Finite Element Simulations of Interdigital Electrode Stucture on High Permittivity Thin Films
Ferroelectrics 32 (2001) 755
23.42.0

Schneider St.
Etching Characteristic of Noble Metal Electrode Ferroelectric Thin Films IX
MRS Proceedings Volume 655, pp. CC2.5
23.42.0

Schober T.; Friedrich J.
The mixed perovskites BaCa(1+x)/3Nb(2-x)/3O3-x/2 (x=0...0.18): proton uptake
Solid State Ionics 136-137(2000) 161-165
23.42.0

Schober T.; Meuffels P.
Electrically operated hydrogen and oxygen vacuum leaks using ceramic high-temperature ionic conductors
J. Vac. Sc. Techn. A 19 (2001) 958-962
23.42.0

Schober T.; Meuffels P.
High-temperature proton conductors for the injection of hydrogen into a vacuum
J. Am. Ceram. Soc. 84 (2001) 1996-2001
23.42.0

Schober T.
High temperature proton conductors: hydrogen injection and pumping
Ionics 6 (2000)369
23.42.0

Schober T.
Solid state ionics applications in vacuum technology
Solid State Ionics 144 (201) 379-386
23.42.0

Schober T.
Tubular high-temperature proton conductors: transport numbers and hydrogen injection
Solid State Ionics 139 (2001) 95-104
23.42.0

Schober T.
Water vapor solubility and impedance of the high temperature proton conductor SrZr0.9Y0.1O2.95
Solid State Ionics 145 (2001)319-324
23.42.0

Sherman V.; Astafiev K.; Setter N.; Tagantsev A.; Vendik O.; Hoffmann-Eifert S.; Böttger U.; Waser R.
Digital Reflection-Type Phase Shifter Based on a Ferroelectric Planar Capacitor
IEEE Microwave and Wireless Components Letters 11, 10 (2001) 407-409
23.42.0

Stein S.; Schmitz R.; Kohlstedt H.
Magneto-tunneling injection device (MADTID)
Solid State Communications 117 (2001) 599 (2001)
23.42.0

Szot K.; Hoffmann S.; Speier W.; Breuer U.; Siegert M.; Waser R.
Segregation Phenomena in Thin Films of BaTiO3
Integrated Ferroelectrics 33 (2001) 303-310
23.42.0

Topolov V. Yu; Bolten D.1; Böttger U.1; Waser R.
1 Institut für Werkstoffe der Elektrotechnik, RWTH Aachen
Domain switching, rotation processes and dielectric response of polycrystalline Pb(ZrxTi1-x)O3 thin films
J. Phys. D: Appl. Phys. 34 (2001) 711-716
23.42.0

Weber U.1; Greuel G.; Böttger U.1; Weber S.1; Hennings D.2; Waser R.
1 Institut für Werkstoffe der Elektrotechnik, RWTH Aachen
2 Philips Forschungslabor, Aachen
Dielectric Properties of Ba(Zr.Ti)O3-based Ferroelectrics for Capacitor Applications
J. Am. Ceram. Soc. 84 (2001), 759-766
23.42.0

Wosik J.; Penkalla H.J.; Szot K.; Dubiel B.; Schubert F.; Czyrska-Filemonowicz A.
The Influence of Using Various Microscopic Techniques on the Quantification of g' Particles in Waspaloy alloy
Praktische Metallography 38 (2001) 1-15
23.42.0

Other publications

Ehrhart P.
Deposition Methods
32. IFF-Ferienkurs 2001 "Neue Materialien für die Informationstechnik
E23

Hoffmann M.1; Küppers H.1; Schneller T.1; Böttger U.1; Schnakenberg U.1; Mokwa W.1; Waser R.
1 Institut für Werkstoffe der Elektrotechnik I+II, RWTH Aachen
A new concept and first Development Results of a PZT Thin Film Actuator
ISAF Proc. 2001, Vol. I, 512-524
23.42.0

Hoffmann-Eifert S.
Dielectric and Optics
32. IFF-Ferienkurs 2001 "Neue Materialien für die Informationstechnik
23.42.0

Kohlstedt H.

Ferroelectric Field-Effect Transistors
32. IFF-Ferienkurs 2001 "Neue Materialien für die Informationstechnik
23.42.0

Schroeder H.
High-Permittivity Materials for DRAMs
32. IFF-Ferienkurs 2001 "Neue Materialien für die Informationstechnik
23.42.0

Waser R.
Molecular Electronics
32. IFF-Ferienkurs 2001 "Neue Materialien für die Informationstechnik
23.42.0

Wosik J.; Penkalla H.J.; Szot K.; Dubiel B.; Schubert F.; Czyrska-Filmemonowicz A.:
Quantitative Characterization of Wasopaloy Microstructure using various Microscopic Techniques
Proc. Europ. Metallographic Conf, EUROMET 2000, Saarbrücken, Germany, Special Edition of the Practical Metallography ed. by G. Petzow 32 (2001) 87-90
23.42.0

Invited Talks

Amano J.; Chi C.; Gilbert St.; Hunter St.; Lanham R.; Rickes J.; Ritchey D.; Aggarwal S.; Moise T.; Sakoda T.; Summerfelt S.
Embedded FeRAM for deep sub-micron SoC
1st Int. Meet. Ferroelectric Random Access Memories (FeRAM 2001), Gotemba, Japan, 19.11.-21.11.2001
23.42.0

Grossmann M.; Waser R.;. Lohse O.; Bolten D.; Böttger U.
Imprint in PZT thin films: A comparison of aging mechanisms in ferroelectric bulk material with ferroelectric thin films (O)
13th Int. Symp. Integrated Ferroelectrics, Colorado Springs, USA, 11.03.-14.03.01
23420

Hoffmann-Eifert S.; Schneller T.; Ehrhart P.; Waser R.
Advanced Chemical Deposition Techniques for Electroceramic Thin Films
Annual meeting of the Belgian ceramic Society, Limburgs Universitair Centrum, Diepenbeek, Belgium, 15.06.01
23420

Hoffmann-Eifert, S.
Ba1-xSrxTiO3 Dünnschichten: Abscheidung mittels CSD und MOCVD und Mikrostruktur-Eigenschaftsbeziehungen
Universität GHS Essen, 10.05.2001
23420

Kohlstedt H.
Hauptvortrag: Oxidische Dünnschichten
Etching of refractory metal electrodes and complex oxides
DPG-Tagung 2001, Hamburg, 26.-30.03.01
23420

Kohlstedt H.
Magnetische Tunnelkontake mit FeMn als Anti-ferromagnet und CoFe als Elektroden
Universität Kassel, 11.07.01
23420

Kohlstedt H.
Nicht-flüchtige Informationsspeicherung: eine neue Generation von Bauelementen für das 21. Jahrhundert
Universität Tübingen, 07.11.01
23.42.0

Kohlstedt H.
Structural and ferroelectric properties of BaTiO3/SrRuO3 and PbZr0.52Ti0.48O3/SrRuO3 thin films on SrTiO3 substrates
University of Liege, Belgium, 25.10.01
23.42.0

Meyer R.; Waser R.
RESTRUCTURING the SURFACE REGION of DONOR DOPED SrTiO3 SINGLE CRYSTALS UNDER OXIDIZING CONDITIONS
112th Annual Meeting of American Ceramic Society, Indianapolis, 22.04.-25.04.01
23420

Rickes J.; Summerfelt S.R.; Lanham R.H.; Waser R.
Circuit design issues affecting present and future deep sub-micron ferroelectric random-access memories
13th Int. Symp. Integrated Ferroelectrics, Colorado Springs, USA, 11.03.-14.03.01
23420

Schneider St.
Patterning of BST thin films by reactive ion etching
Workshop on "Patterning of Thin Oxide Films", Bratislava, Slovak Republic, 21.-22.06.01
23420

Schneider St.
Platinum high temperature etching characteristics
EMC, Notre Dame, Indicana, USA, 25.-29.06.01
23420

Schneider St.
Quadrupole mass spectroscopy studies of high temperature platinum etch processes
American Vacuum Society, San Francisco, USA, 29.10.-02.11.01
23.42.0

Szot K.
Segregation in Perowskite
Schlesische Universität Katowice, Polen, 05.04.01

Waser R.; Meyer R.; Szot K.
Defektchemie in der Nähe von Grenzflächen dotierter Perowskite
Bunsenkolloquium "100. Geburtstag von Carl Wagner", RWTH Aachen, 09.11.01
23.42.0

Waser R.
Advanced chemical deposition techniques - from research to production
13th Int. Symp. Integrated Ferroelectrics, Colorado Springs, USA, 11.03.-14.03.01
E2 Waser R.
Nano-sized single grains and continuous films of ferroelectric oxides - chemical synthesis and scanning probe analysis
2001 Swiss Workshop on Materials with Novel Electronic Properties, Les Diablerets, Switzerland, 02.10.-04.10.2001
23420

Waser R.
Am Vorabend der nächsten Evolutionsstufe?
FZJ-Kolloquium
09.02.2001
23420

Waser R.
Chemical Synthesis and swtiching properties of ferroelectric thin films
IBM, Rüschlikon, Zürich, Switzerland
05.01.2001
23420

Waser R.
FeRAM - eine Alternative zu herkömmlichen Speichermedien ?

Technical Universität Dresden
09.01.01
23420

Waser R.
Ferroelektrische Oxide in der Mikro- und Nanoelektronik - Chancen und Perspektiven
Physikalisches Kolloquium, RWTH Aachen
22.01.01
23420

Waser R.
Neue oxidische Materialien in der Informationstechnik: Forschung für die Praxis
Gesprächskreis Management und Informatik, Gesellschaft für Informatik - Bonn, FZJ, 09.05.2001
23420

Waser R.
On robots and cats: the next evolution step
Advanced Materials, EPFL-ETHZ-UCSB-WIS, Cret-Bérard (Puidoux), Schweiz,
09.09.-13.09.2001
23420

Waser R.
Technology and design challenges of the next FeRAM generation
1st Int. Meet. Ferroelectric Random Access Memories (FeRAM 2001), Gotemba, Japan, 19.11.-21.11.2001
23.42.0

Other talks

Bachhofer H.; Reisinger H.; Steinlesberger G.; Nagel N.; Cerva H.; von Philipsborn H.; Schroeder H.; Waser R.
Interfacial layers and their effect on leakage current in MOCVD-deposited SBT thin films
13th Int. Symp. Integrated Ferroelectrics, Colorado Springs, USA, 11.03.-14.03.01
23.42.0

Böttger U.; Hoffmann-Eifert S.
Dielelectric high frequency characteristics of (Ba,Sr)TiO3 thin films on silicon for microwave device applications
13th Int. Symp. Integrated Ferroelectrics, Colorado Springs, USA, 11.03.-14.03.01
23.42.0

Böttger U.; Lohse O.; Grossmann M.; Waser R.
Inherent contributions to the frequency dependence of the coercive voltage of ferroelectric thin films
MRS 2001, Boston, USA, 25.11.-29.11.01
23.42.0

Fitsilis F.; Regnery S.; Waser R.; Ehrhart P.
Structure property relations of BST thin films
13th Int. Symp. Integrated Ferroelectrics, Colorado Springs, USA, 11.03.-14.03.01
23.42.0

Hoffmann M.; Böttger U.; Waser R.
PZT and PMN-PT thin films cantilevers: Comparison between monomorph and bimorph structures
MRS 2001, Boston, USA, 25.11.-29.11.01
23.42.0

Hoffmann-Eifert S.; Ohly C.; Waser R.
Influence of morphology on the high-temperature conduction behavior of SrTiO3 and BaTiO3 thin films
MRS Fall meeting 2001, Boston, USA, 25.11.-29.11.01
23.42.0

Hoffmann-Eifert S.; Ohly Ch.; Szot K.; Waser R.
High temperature conduction behavior and segregation phenomena in SrTiO3 and BaTiO3 thin films:
MRS 2001, Boston, USA, 25.11.-29.11.01
23.42.0

Hoffmann-Eifert S.; Ritter S.; Waser R.
Growth of lead barium titanate thin films by MOCVD: structural and electrical characterization
MRS 2001, Boston , USA, 25.11.-29.11.01
23.42.0

Kohlstedt H.; Pertsev N.A.; Waser R.
Size Effects on polarization in epitaxial ferroelectric thin films
MRS 2001, Boston, USA, 25.11.-29.11.01
23.42.0

Kohlstedt H.; Pertsev N.A.; Waser R.
Size effects on polarization in epitaxial ferroelectric thin films
MRS 2001, Boston, USA, 25.11.-29.11.01
23.42.0

Lohse O.; Böttger U. Grossmann M.; Bolten D.; Waser R.
Polarization switching behavior of Nb doped PZT thin films
13th Int. Symp. Integrated Ferroelectrics, Colorado Springs, USA, 11.03.-14.03.01
23.42.0

Ohly Ch.; Hoffmann-Eifert S.; Szot K.; Waser R.
Alkaline earth titanate thin films - the conduction behavior of doped BST
13th Int. Symp. Integrated Ferroelectrics, Colorado Springs, USA, 11.03.-14.03.01
23.42.0

Pithan Ch.
Synthese von nano-BatiO3 Pulvern über Mikroemulsionen
NANOMAT-Workshop "Trend", Reinstorf, Lüneburger Heide, 21.-23.10.2001
23.42.0

Rodriguez Contreras J.R.; Poppe U.; Szot K.; Jia C.L.; Kohlstedt R.; Waser R.
Structural and ferroelectric properties of PbZr0.52Ti0.48O3/SrRuO3 thin films on SrTiO3 substrates
MRS 2001, Boston, USA, 25.11.-29.11.01
23.42.0

Rodriguez-Contreras J.
Experimental Approach to Investigate the Influence of Ferroelectricity on a Tunnel Current
MRS 2001, boston, USA, 25.11.-29.11.01
E223.42.002

Rodriguez-Contreras J.
Sputtered PbZr0.52Ti0.48O3/SrRuO3 films on SrTiO3-substrates
DPG Tagung, Hamburg, 26.-30.03.01
23.42.0

Roelofs A.; Pertsev N.A.; Waser R.
Depolarizing-field-induced 180o switching of a-domains in polydomain epitaxial PZT thin films by AFM
MRS 2001, Boston USA, 25.11.-29.11.01
23.42.0

Schmitz S.; Schroeder H.
Electrical characterization of SrTiO3 thin films
13th Int. Symp. Integrated Ferroelectrics, Colorado Springs, USA, 11.03.-14.03.01
23.42.0

Schneider St.; Kohlstedt H.; Waser R.
The role of carbonylchemistry to pattern platinum electrodes
MRS 2001, Boston, USA, 25.11.-29.11.01
23.42.0

Schneider St.
Anisotropic plasma etching of BST thin films for Gigabit-DRAM integration and what to learn for MOCVD reactor cleaning

Aixtron AG, Aachen, 20.09.01
23.42.0

Schneider St.
High temperature platinum etch processes
Texas Instruments, Dallas, USA 05.11.01
23.42.0

Schneider St.
SiO2 etch with the ICP sources of OPT's Ionfab300+:
Reliability and contamination issues
Characterizing the wafer clamping and heat conduction efficiency in OPT's Ionfab300+ with a SensArray wafertemperature probe
Characterizing of OPT's Ionfab300 + Ionsource by energy dispersive quadrupole mass spectrometry using Hiden's EPQ
Seminar at Oxford Plasmatechnology, Yatton, Great Britain, 07.-08.08.01
23.42.0

Shur V.; Nikolaeva E.; Shishkin E.; Baturin I.; Lohse O.; IBolten D.; Waser R.
Fatigue and rejunenation phenomena in PZT thin films
13th Int. Symp. Integrated Ferroelectrics, Colorado Springs, USA, 11.03.-14.03.01
23.42.0

Stein S.; Kohlstedt H.
Influence of spin-polarized injection currents on magnetic tunnelling junctions (O)
JEMS, Grenoble, 28.08.-01.09.01
23.42.0

Stein S.; Kohlstedt H.
Magneto tunneling injection device
DPG-Tagung, Hamburg, 26.-30.03.01
23.42.0

Stein S.; Kohlstedt H.
Spin-injection effects in three terminal magnetic tunnelling junctions
MRS 2001, Boston, USA, 25.-30.11.01
23.42.0

Steinlesberger G.; Reisinger H.; Bachhofer H.; Schroeder H.; Werner W.
Dielectric relaxation and charge carrier transport mechanisms in (Ba,Sr)TiO3 thin films
13th Int. Symp. Integrated Ferroelectrics, Colorado Springs, USA, 11.03.-14.03.01
23.42.0

Waser R.
Oxidkeramische Materialien in der Mikroelektronik und Nanotechnologie
NANOMAT-Meeting 2. Szene, Karlsruhe, 05.04.01
E234

Wosik J.; Penkalla H.J.; Szot K.; Dubiel B.; Buffat P.A.; Czyrska-Filemonowicz A.
Combination of various microscopical methods for quantitative microstructure analysis of Waspaloy
Conf. on Modern Microscopical Methods, Innsbruck, Austria, 09.-14.09.01
23.42.0

Posters

Ganpule C.; Stanishevsky A.; Hill B.K.; Nagarajan V:; Alpay S.P.; Melngailis J.; Williams E.D.; Ramesh R.; Roelofs R.; Waser R.; Tiedke S.; De. Wolf P.; Joshi V.; Paz de Araujo,C.
Scaling of ferroelectric properties in thin films (P)
13th Int. Symp. Integrated Ferroelectrics, Colorado Springs, USA, 11.03.-14.03.01
23.42.0

Hofer C.; Hoffmann-Eifert S.; Waser R.
Dielectric and Raman spectroscopy of SrTiO3 ceramics compared with single crystals
Advanced Electroceramics: Grain Boundary Engineering Kick-off Workshop, Madrid, 24.-28.03.01
23.42.0

Ohly C.; Hoffmann-Eifert S.; Waser R.
The electrical conductivity of SrTiO3 thin films under changing oxygen ambients
CECAM/PSIK Workshop on Oxide-Metal Interfaces: Theoretical Progress and Challenges, Lyon, 4.10.-6.10.01
23.42.0

Ohly Ch.; Hoffmann-Eifert S.; Szot K.; Waser R.
Defects in alkaline earth titanate thin films - structural and morphological aspects
13th Int. Symp. Integrated Ferroelectrics, Colorado Springs, USA, 11.03.-14.03.01
23.42.0

Regnery S.; Fitsilis F.; Ehrhart P.; Waser R.; Schienle F.; Schumacher M.; Jürgensen H.
Nucleation and growth of ultra thin (Ba,Sr)TiO3 films in a MOCVD reactor
MRS 2001, Boston, USA, 25.11.-29.11.01
23.42.0

Ritter S.; Hoffmann-Eifert S.; Bolten D.; Waser R.
(Pb1xxBax)TiO3 thin films prepared by liquid delivery MOCVD: Influence of the process parameters on film formation and electrical propertie
Int. Meeting on Ferroelectricity, Madrid, 03.-07.09.01
23.42.0

Ritter S.; Schäfer P.; Hoffmann-Eifert S.; Waser R.
(Pb1-xBax)TiO3 thin films prepared by liquid delivery MOCVD: Influence of process parameters on film formation and electrical properties
13th Int. Symp. Integrated Ferroelectrics, Colorado Springs, USA, 11.03.-14.03.01
23.42.0

Rodriguez-Contreras J.;
High-pressure sputtering of PbZr0.52Ti0.48O3/SrRuO3 thin films on SrTiO3 substrates
Int. Meeting on Ferroelectricty, Madrid, 03.-07.09.01
23.42.0

Rodriguez-Contreras J.
Characterization of ferroelectric thin films prepared by High-Pressure Oxygen Sputtering and PLD
MRS 2001, Boston, USA, 25.11.-29.11.01
23.42.0

Schneider S.; Kohlstedt H.; Waser R.
High temperature etching characteristics of noble metal electrode
13th Int. Symp. Integrated Ferroelectrics, Colorado Springs, USA, 11.03.-14.03.01
23.42.0

Schneller T.; Waser R.
Chemical origin of different electrical and morphological qualities in CSD derived PZT thin films
13th Int. Symp. Integrated Ferroelectrics, Colorado Springs, USA, 11.03.-14.03.01
23.42.0

Shur W.; Blankov E.; NEgashev S.; Borisova E.; Barannikov A.; Schneller T.; Gerhardt R.; Waser R.
In situ study of crystallization kinetics during rapid thermal annealing of sol-gel PZT and PLZT films
13th Int. Symp. Integrated Ferroelectrics, Colorado Springs, USA, 11.03.-14.03.01
23.42.0

Patents granted

Kohlstedt H.; Stein S.
Dreitorbauelement, insbesondere Spininjektionstransistor
DE: 100 31 401 (22.11.2001)
PT 1.1810
23.42.0

Patents applied for

Kohlstedt H.; Rodriguez Contrearas J.
Verfahren zur Erzeugung eines Tunnelkontaktes sowie Vorrichtung umfassend Mittel zur Erzeugung eines Tunnelkontaktes
PCT: PCT/DE01/04447 (23.11.2001) (EP,US,JP,KR)
PT 1.1859
23.42.0

Kohlstedt H.; Stein S.
Dreitorbauelement, insbesondere Spininjektionstransistor
PCT: PCT/EP01/07143 (23.06.2001) (EP;US,JP;KR)
PT 1.1810
23.42.0

Kohlstedt H.
Anordnung zum Messen eines Magnetfeldes und Verfahren zum Herstellen einer Anordnung zum Messen eines Magnetfeldes
PCT: PCT/EP01/01305 (07.02.2001) (EP,US,JP,KR)
PT 1.1782
23.42.0

Kohlstedt H.
Matrix für einen Magneto-Random-Access Memory (MRAM)
DE: 298 24 631.7 (2001)
PT 1.1583
23.42.0

Lecture courses

Ehrhart P.
Deposition methods
32. IFF-Ferienkurs, Jülich, 05.03.2001
23.42.0

Hoffmann-Eifert S.
Dielectrics and Optics
32. IFF-Ferienkurs, Jülich, 05.03.2001
23.42.0

Kohlstedt H.
Ferroelectric field-effect transistors
32. IFF-Ferienkurs, Jülich, 05.03.2001
23.42.0

Kohlstedt H.
Grundlagen und Anwendungen supraleitender Bauelemente (WS 00/01)
Universität zu Köln
23.42.0

Kohlstedt H.
Halbleiterphysik (SS 01)
Universität zu Köln
23.42.0

Schroeder H.
Ausgewählte Kapitel der Metallphysik
Vertiefungsfach II: Metallphysik
Fakultät für Bergbau, Hüttenwesen und Geowissenschaften der RWTH Aachen, WS 00/01 und WS 01/02
23.42.0

Schroeder H.
High-permittivity materials for DRAMs
32. IFF-Ferienkurs, Jülich, 05.03.2001.
23.42.0

Waser R.; Ehrhart P. Hoffmann S.; Kohlstedt H.; Schroeder H.
Neue Materialien und Bauelemente für die Informationstechnik I (WS 01/02)
Vertiefungsfach II
Fakultät für Elektrotechnik der RWTH Aachen
23.42.0

Waser R.
Molecular electronics
32. IFF-Ferienkurs, Jülich, 05.03.2001.
23.42.0

Waser R.
Vorlesung Werkstoffe der Elektrotechnik
Sensoren und Sensormeßtechnik I+II
RWTH Aachen
23.42.0

Internal seminars

Ehrhart P.
Metal Organic Chemical Vapor Deposition
Klausurtagung des Instituts Elektrokeramische Materialien
Hirschegg, 27.08.01-30.08.01
23.42.0

Elsebrock R.
Mikrowellen-Keramiken
Klausurtagung des Instituts Elektrokeramische Materialien
Hirschegg, 27.08.01-30.08.01
23.42.0

Hoffmann-Eifert S.
Defektchemie dünner Schichten
Klausurtagung des Instituts Elektrokeramische Materialien
Hirschegg, 27.08.01-30.08.01
23.42.0

Kohlstedt H.
TMR&MRAM, Ultradünne FE-Schichten
Klausurtagung des Instituts Elektrokeramische Materialien
Hirschegg, 27.08.01-30.08.01
23.42.0

Pithan C.
Pulver- und Keramiksynthese
Klausurtagung des Instituts Elektrokeramische Materialien
Hirschegg, 27.08.01-30.08.01
23.42.0

Schroeder H.
Ladungstransport durch dünne Schichten
Klausurtagung des Instituts Elektrokeramische Materialien
Hirschegg, 27.08.01-30.08.01
23.42.0

Waser R.
Integration elektrokeramischer Materialien
Klausurtagung des Instituts Elektrokeramische Materialien
Hirschegg, 27.08.01-30.08.01
23.42.0

Waser R.
Überblick und Ausblick Forschungsarbeiten des Instituts
Klausurtagung des Instituts Elektrokeramische Materialien
Hirschegg, 27.08.01-30.08.01
23.42.0

Institute for Soft Condensed Matter Physics

General Overview

The Institute "Weiche Materie" was founded in jan. 2000. The main focus of the Institute is to understand macroscopic properties and microstructural order of colloidal systems, under equilibrium- and non-equilibrium conditions, on a microscopic level. To make progress in this area it is necessary to be able to synthesize model colloidal systems, where monodispersity of the desirable interaction potential is one of the main goals.. The properties of these model systems should be tuned in such a way that it exhibits the phenomena that one wishes to study.

The research in the Institute is done within "projects", which will be described below.

At this moment the further development of the Institute is severely hindered by lack of laboratory facilities. Most of the planned laboratories are not yet ready for use, for reasons that go beyond the jurisdiction of the FZJ. Some of the planned research can not be started, while other research themes can only be performed in part in improvised laboratories.

The following projects have been defined within the Institute Weiche Materie,

Non-equilibrium Phenomena

Project leader :	**Prof. J.K.G. Dhont**
Personnel :	D. Triefenbach (Technical Engineer)
	Dr. S. Rathgeber (Habilitand)
	Dr. P. Lettinga (Post Doc)
	Dr. T. Lenstra (Post Doc)
	Dr. Z. Dogic (Humboldt Fellow, started march 2001)
	Dr. P. Carletto (EU Post Doc, started june 2001)
	Dr. R. Tuinier (started october 2001)

The subjects under investigation in this project are :

Shear-banding and Rheology of "hairy Colloids" and Suspensions of rod-like Particles (S. Rathgeber, P. Carletto, P. Lettinga, Z. Dogic)

Shear-banding is a hydrodynamic instability in systems under flow that occurs whenever the stress decreases with increasing shear-rate, or the stress is a multivalued function of the shear-rate. The stationary state is now a state where regions of different microstructure and sometimes different shear-rates "coexist". The kinetics of the shear-banding instability and the possible stationary states that can occur are studied for two kinds of systems : "hairy colloids" (colloidal spheres coated with long polymer chains) and rigid rod-like particles. A system of hairy colloids where shear-banding has been observed will be investigated in cooperation with Dr. J. Vermant (University of Leuven). Another, well-defined hairy colloid has been developed in the Institut for Neutron Scattering (see the next theme). So far, our investigations are focused on the shear-induced polymer brush defoprmation at lower concentrations. Simulations on hairy colloids in shear flow will be performed in the Insitute Theory II. We recently observed a very clear shear-banding transition in suspensions of fd-virus (a semi-flexible colloid). By adding free polymer, the rate of the transition can be tuned, so that kinetic studies will be feasible in these systems. At this moment we are determining, by rheology and light scattering, the full non-equilibirum phase diagram of these kind of systems (where the shear-rate is on of the control variables). The shear-banding transition lines will be located as well. There is an ongoing collaboration with prof. W. Briels (University of Twente) on the theory of the shear-banding transition in systems of rigid rods.

Shear induced Polymer Brush Deformation (S. Rathgeber, P. Carletto)

As was mentioned above, colloidal particles with a small core in comparison to the length of the polymers that are attached to their surface have been developed in the Institute for Neutron Scattering by Dr J. Allgaier and Dr. L. Willner. These systems will be used to study the polymer brush deformation under shear flow by means of birefringence measurements and small angle neutron scattering on very dilute samples, in cooperation with Dr. L. Willner and Dr. W Pyckhout (Institute for Neutron Scattering) and Dr. P. Lindner (ILL, Grenoble). For this purpose we developed a quartz shear cell in cooperation with Dr. W. Pyckhout and Dr. P. Lindner. In a later stage we will also perform rheology experiments and scattering experiments at larger concentrations, in order to probe the effect of the brush deformation on the microstructure. It has been found that appreciable brush deformation in water occurs only at very high shear-rates, where the onset of a Taylor instability occurs. We therefore investigate at the moment the possibility to use more viscous solvents. These investigations are part of a European project (HUSC, Hard to Ultra Soft Colloids).

Critical Phenomena under Shear Flow (P. Lettinga, H. Wang)

In mixtures of stearyl silica spheres and small PDMS polymers (Poly Di Methyl Siloxane) in cyclohexane, depletion attractions can give rise to gas-liquid phase separation. Non-linear microstructural response to stationary and oscillatory shear flow near the gas-liquid critical point in these systems is studied by means of time resolved small angle light scattering. The results of the static experiments are being analysed at the moment, also by Dr. H. Wang. The analysis of the time dependent response is currently in progress.

Dynamics and Structure of "Polymer-colloids" (S. Rathgeber)

Suspensions of polymeric particles of a colloidal size are studied by means of small angle neutron scattering and neutron spin echo experiments. This concerns the shape, internal structur and dynamics of the colloidal particles. The systems that are studied are two different kinds of dendrimers, cellulose derivatives and bottlebrush macomolecules, in cooperation with T. Pakula (Max Planck Institute for Polymer Research in Mainz). Scattering experiments and rheology measurements at higher concentration are planned.

Nucleation and Crystal Growth under Shear Flow Conditions (R. Tuinier)

Small angle, time resolved static light scattering will be used to examine nucleation and crystal growth under the influence of shear flow. The shear induced shift of the liquid-solid binodal will be a point of interest also. Since the crystals will probably be anisometric, scattering experiments are planned where the incident light beam is either directed along the gradient direction or the vorticity direction. High angular resolution is achieved with a 2D CCD camera , with the photosensitive chip placed directly at the position of Bragg scattering angles.

Negative Thixotropy of Polymer Solutions (J. Buitenhuis)

This project has been started at the Technical University Berlin and was continued at the FZ-Jülich. Negative thixotropy is the phenomenon of a time-of-flow dependent shear thickening, which is not well understood. A new explanation is proposed and compared to experimental results.

Structure and Dynamics of Colloids at Interfaces

Project leader : **Dr. P. Lang**
Personnel : M. Hoelzle (Technician, started june 2000)

The subjects under investigation in this project are :

Structure and Dynamics of Interfaces between Coexisting Phases

The colloidal systems that will be investigated are rigid rods, like silica coated boehmite rods and semi-flexible fd-virus (in isotropic-nematic coexistence), soft systems like internally crosslinked cylindrical micelles (in isotropic-columnar coexistence), and spheres (in gas-liquid or liquid-crystal coexistence).

Structure and Dynamics close to a Wall

Like in the previous theme, rods and spheres will be investigated. We also plan to investigate depletion forces near a wall in mixtures of long polymers and small colloidal spheres. This will be done in cooperation with Dr. E. Eisenriegler (Institute Theory II).

To study the above mentioned phenomena, it is necessary to apply surface and interface sensitive measuring techniques. At this moment, Dr. P. Lang is constructing two instruments with options for static and dynamic light scattering of evanescent waves (EWLS), total internal reflection microscopy (TIRM), capillary wave spectroscopy (CWS), ellipsometry and Brewster angle microscopy (BAM). The TIRM option is being built in cooperation with Dr. C. Bechinger (University of Konstanz).

In addition, P. Lang is working on the synthesis of "soft colloidal rods" (see the project "Synthesis").

Within the entire project "Structure and Dynamics of Colloids at Interfaces", the yet non-existing laboratories are essential for it's further development.

Dynamics in Equilibrium Systems

Project leader :	**Dr. G. Meier**
Personnel :	M. Hoelzle (Technician, started june 2000)

The subjects under investigation in this project are :

Dynamics of Polymer Mixtures and Colloids under high Pressure

Pressure is an external variable that can be used to continuously vary the compatibility of polymers. The polymers can either be free polymers or polymers bound to the surface of colloidal particles. Besides by pressure, monomer-monomer pair-interaction potentials can also be changed systematically by changing the H/D composition of the polymers. This offers the possibility to gain insight in the microscopic origin of the rich phase behaviour and dynamics of these systems. The phase behaviour and (critical) dynamics of polymer mixtures and mixtures of polymers and polymer-coated colloidal particles will be the topic of this project.

Phonon Dispersion in heterogeneous Systems

Colloidal systems represent heterogeneous systems, in which the dynamics of acoustic modes will be studied. There will almost certainly be a dependence of the properties of acoustic exitations on the structural properties of the colloidal suspensions. The degree of heterogeneity can be changed continously by changing the size and/or concentration of the colloidal particles.

Rotational Diffusion of Rods near Phasetransition Lines

Rotational diffusion of rod like colloids and polymers in the neighbourhood of a gas-liquid and isotropic-nematic phase boundary will be studied. Near a gas-liquid phase transition line, the attractive interactions between the rods will probably lead to a severe change of the rotational diffusion coefficient, since attractions favor parallel alignment of neigbouring rods over perpendicular alignment. On approach of the isotropic-nematic spinodals, the rotational diffusion coefficient tends to zero in a way that is not known, that is, the critical exponent for the rotational diffusion coefficient is as yet unknown.

Rotational Diffusion away from Phasetransition Lines (P. Lettinga)

Rotational diffusion coefficients of colloidal spheres and rods in bulk solution and within porous media are investigated by means of Time resolved Phosphorescence Anisotropy (TPA) and Recovery After Photobleaching (FRAP). These experiments are performed at the University of Utrecht in collaboration G. Koenderink and prof. A.P. Philipse. Also of

interest is rotational diffusion of rigid rods under stationary shear flow, where FRAP and heterodyne dynamic light scattering experiments are planned.

We plan to built a combination of set ups which allows one to investigate dynamics in the time range 10^{-13}-10^{2} s. Dynamic light scattering covers a dynamic range of 10^{-7}-10^{2} s. A Sandercock tandem interferometer will be used to cover the time range 10^{-9}-10^{-11}s. The gap between these time ranges can be covered employing a confocal interferometer. The very fast dynamics will be studied by means of Raman scattering.

The project "Dynamics in Equilibrium Systems" can not start yet due lack of laboratory facilities.

Correlation between Interactions and ordered Structures

Project leader : **Dr. J. Hauck**

Dr. J. Hauck has been at the IFF for a longer time. His work in the Institute Weiche Materie is a continuation of part of the work that has been done by J. Hauck during the past, applied to ordered structures in various colloidal systems.

Synthesis

Project leaders :	**Dr. J. Buitenhuis (started in march 2001)**
	Dr. W. Sager (started in april 2001)
Personnel	K. Sellinghoff
	D. Triefenbach (Technical Engineer)

The aim of this project is the development of new colloidal systems, the investigation of synthesis mechanisms and the synthesis of (known) colloidal systems for cooperation projects.

Synthesis of known Colloidal Model Systems for Cooperation Projects

The first aim will be to build up additional know how concerning the synthesis of known colloidal model systems (like coated silica spheres, latex spheres, coated boehmite rods and gibbsite platelets, fd-virus and DNA fragments). D. Jablonski and D. Triefenbach have already synthesized silica-coated boehmite rods under the guidance of J. van Wijnhoven (Colloid Synthesis Facility in Utrecht, the facility was closed down recently). J. Buitenhuis synthesized aluminium chloro hydrate coated boehmite rods.

Synthesis of Soft Colloidal Rods (P. Lang, L. Willner)

The aim is to develop a model system for soft colloidal rods. These rods are synthesized by radically crosslinking of cylindrical micelles, which consist of amphiphilic blockcopolymers.. This will lead to flexible colloidal rods, of which the length is about 200 nm and the aspect ratio about 20. The main problem will be to fractionate the system in order to reduce the polydispersity in length.

Synthesis of Silica Coated fd-virusses (J. Buitenhuis)

The fd-virus is a slightly flexible rod of about 800 nm length and 6 nm width. The aim is to coat the virus by a silica layer to obtain rigid rods of variable diameter, which after using a variety of standard coatings of the silica, can be dispersed in apolar solvent to obtain cylinders with a variety of well defined interactions. This subject is just starting.

Optimization and Mechanism of the Synthesis of Colloidal Boehmite Rods (J. Buitenhuis)

Colloidal boehmite rods can be synthesized with an average length ranging from 70 to 500 nm. Although several studies on dispersions of these rods were successful, the system still contains a small degree of aggregates or is to polydisperse

for certain other studies. To improve the quality of the rods is the aim of this project. To do so it will be important to obtain some knowledge about the mechanism of the particles formation. This subject is just starting.

In addition, J. Buitenhuis has been working on the "Negative thixotropy of polymer solutions" (see the project "Non-equilibrium Phenomena").

The polymer synthesis know how that is available in the Institute for Neutron Scattering (Dr. L. Willner and Dr. J. Allgaier) will be of great advantage in developing certain classes of new colloidal systems.

Preparation of Nanostructured Materials in Self-organising Systems (W. Sager)

This project is concerned with the characterisation of microemulsions as precipitation media for inorganic materials with at least one dimension in the nanometer range and the development of synthesis routes for nanostructured inorganic/organic composites employing the different structures encountered in microemulsion systems as templates. It is part of the PhD-project of Aurelie Autin and is performed together with Prof. R. Nolte at the University of Nijmegen.
Though microemulsions have increasingly been utilised over the last 2 decades, and in some cases even established themselves as precipitation medium for the preparation of small uniform inorganic particles of mostly spherical geometry, little systematic work has been performed on what actually controls the size, shape, crystallinity and stability of the particles formed. Until now there is no global picture at hand describing nucleation and growth processes for the different microemulsion morphologies investigated and a generally valid theory is still out of reach.

In this project we want to perform a systematic study on precipitation in well defined and characterised microemulsions with different morphology ranging from droplet-type microemulsions to cylindrical aggregate structures and bicontinuous microemulsions. The latter consist of an interwoven network of water and oil channels stabilised by the interfacial surfactant film. To establish a direct relation between microemulsion structure and particle morphology, the microemulsions and the precipitated inorganic materials will be characterised by phase diagram and conductivity studies, electron and atomic force microscopy, X-ray diffraction and scattering techniques. Underlying nucleation and growth processes will be studied with respect to microemulsion morphology, specific inorganic nuclei/surfactant interactions and properties of the interfacial surfactant film. Emphasis will be laid on solidifying bicontinuous structures which is of special interest for inorganic/organic nanocomposites. Employing microemulsions systems as templates for nanostructured composite materials has the advantage of offering the possibility of both simultaneous and consecutive formation of the organic and the inorganic solid phase by bringing in one precursor with the water and the other with the oil phase or the interfacial surfactant layer.

The project "Synthesis" can not be realized yet, due to the lack of laboratory facilities.

Theory

Project leader :	**Dr. G. Naegele (started jan. 2001)**
Personnel :	Dr. M. Kollmann (started in april 2001)
	Dr. H. Wang (started in march 2001)

The aim of this project is two-fold : (i) developing theory on subjects that are, or may become, of experimental interest to the Institute, and (ii) to assist experimentalists with devising new experiments and with data interpretation.

Currently, the following subjects are being investigated :

Electrokinetic Effects in Colloids

In particular, electrolyte friction is studied on the basis of mode coupling theory for a binary system : the large colloidal particles and the counter ions. A remarkable result is that hydrodynamic interactions play an essential role. A treatment of non-linear electrolyte friction response is within the validity of the present approach.

Diffusion in Two-dimensional Space

Inspired by experiments that are performed by Dr. K. Zahn and Prof. G. Maret (University of Konstanz), diffusion coefficients have been calculated in case of a spatial dimension equal to 2. The surprising divergence of the ensemble averaged hydrodynamic interaction function (commonly denoted as H(q)) is confirmed by theory. In addition, unexpected scaling behaviour has been predicted theoretically.

Linear Viscoelastic Behaviour of spherical Colloids

A Green-Kubo formula for the linear shear viscosity of colloids, where hydrodynamic interactions are important, has been derived and evaluated numerically on the basis of a mode coupling approach.

Jan Dhont

Personnel 2000/2001 and areas of activity

Scientific Staff

Prof. Dr. J.K.G. Dhont	Non-equilibrium structure and dynamics	23.15.0
Dr. J. Hauck	Structures and Interactions of Colloids, Polymers, Lipids and Bacteriae	23.15.0
Dr. G. Meier	Dynamics of mixtures, critical scattering, high pressure techniques	23.15.0
Prof. G. Nägele	Theory and Simulation	23.15.0

Technical Staff

Ms. K. Sellinghoff	Technician	23.15.0
Dipl.-Ing. D. Triefenbach	Chemical Engineer	23.15.0
Ms M.-L. Schüsseler	Secretary	

Scientists

Dr. J. Buitenhuis (ab 01.03.01)	Synthesis	23.15.0
Dr. P. Carletto (ab 01.06.01)	Shear-banding of very soft colloids	23.15.0
Dr. Z. Dogic	Synthesis and phase behaviour of di-block colloids	23.15.0
Dr. M. Kollmann (ab 01.05.01)	Electrokinetic effects in colloidal systems	23.15.0
Dr. P. Lang (ab 01.10.00)	Structure and dynamics of interfaces in colloidal systems	23.30.0
Dr. T. Lenstra (ab 01.03.01)	Inhomogeneous flow of colloids	23.15.0
Dr. P. Lèttinga (ab 01.07.00)	Study of the non-linear and linear viscoelastic, response of colloidal dispersions	23.15.0
Dr. S. Rathgeber	Structure and dynamics of polymer – colloids, polymer & colloid mixtures and biological colloids	23.15.0
Dr. W. Sager (ab 01.04.01)	Synthesis	23.15.0
Dr. R. Tuinier (ab 01.11.01)	Phase behaviour, phase separation kinetics	23.15.0
Dr. H. Wang (ab 01.04.01)	Structure under shear flow	23.15.0

Trainees

M. Hölzle	Technician	23.15.0

Microstructural Response of a near-Critical Colloidal Dispersion to Oscillatory Shear Flow

M. P. Lettinga and J. K. G. Dhont
Institut für Festkörperforschung
Teilinstitut Weiche Materie
(Dated: December 20, 2001)

The viscoelastic response to a strong externally imposed shear flow is generally non-linear. This behaviour is the result of shear induced microstructural distortion. Such non-linear microstructural response is particularly pronounced close to a gas-liquid critical point, since there the dynamics is very slow and microstructural order extends over large distances. In order to investigate the frequency dependence of the microstructural response, we perform time resolved small angle light scattering experiments on a polymer-colloid mixture under oscillatory shear flow. The slow dynamics near the gas-liquid critical point allows to perform experiments at frequencies that are much larger then inverse microstructural relaxation times, but still small enough to avoid surface loading effects.

The objective of this study is to gain insight in the (non-linear) response of the microstructure to an externally imposed, oscillatory shear flow of a near-critical colloidal fluid. The control variables of interest here are : the amplitude of the applied shear field, its frequency, and the distance of the colloidal sample to the critical point as measured by the correlation length ξ in the absence of shear flow. We are thus interested in "the Ornstein-Zernike structure factor under oscillatory shear flow conditions". Time resolved measurements of the critical, small scattering angle behaviour of the structure factor have been performed. A small angle light scattering (SALS) set up with an optical shear cell is used, where the wavevector dependence of the structure factor in the flow-vorticity plane is probed. The inner cylinder oscillates with angular amplitudes between $A = 10$and 130^o and frequencies between $0.025$and$0.1Hz$. Sequences of images are taken with a CCD camera, which is triggered by a function generator. Experimental results are compared with a solution of the Smoluchowski equation for the small wavevector behaviour of the structure factor.[1] The system used in this study consists of silica spheres

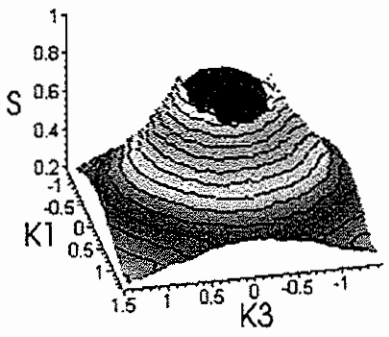

FIG. 1: The Ornstein-Zernike structure factor in the absence of shear flow, corresponding to a correlation length of $\xi = 650nm$.K1 and K3 are the dimensionless wave vector components in the flow and velocity direction, respectively.

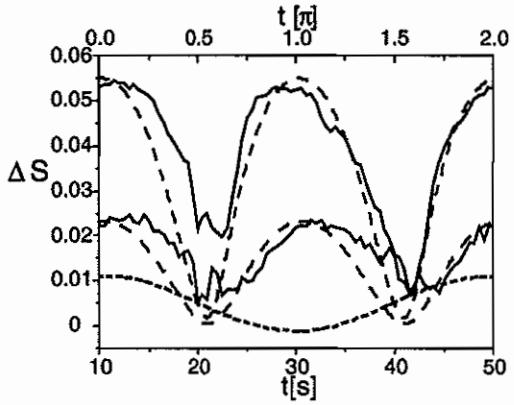

FIG. 2: Effect of the shear rate on the response of a near-critical colloidal dispersion, for $\Omega = 0.9, \omega = 2\pi 0.025 s^{-1}$, measured at $K1 = 1.4$ and $K3 = 0$. The experimental curves are given by the solid lines: $\dot{\gamma} = 0.72 s^{-1}$ (red) and $\dot{\gamma} = 3.26 s^{-1}$ (blue). The theoretical lines are given by the solid lines: $\lambda = 2.0$ (red) and $\lambda = 4.5$ (blue).

(102 nm diameter) grafted with stearyl alcohol, dissolved in cyclohexane. Polydimethylsiloxane (radius of gyration = 23 nm) is added to the solution to induce depletion attractions. Due to these attractive forces between the colloidal spheres, this system undergoes a gas-liquid phase transition. The distance to the critical point can be tuned by gently evaporating or adding solvent [2]. As a typical example, we shall describe some of the data that we obtained for a system with a correlation length of $\xi = 650nm$. The correlation length is obtained from the Ornstein-Zernike structure factor in the absence of shear flow (see Fig. 1). The two relevant parameters describing the response of the colloidal dispersion are the dressed Péclet number,

$$\lambda = \frac{\gamma \dot{\xi}^4}{2 D_0 \beta \Sigma},$$

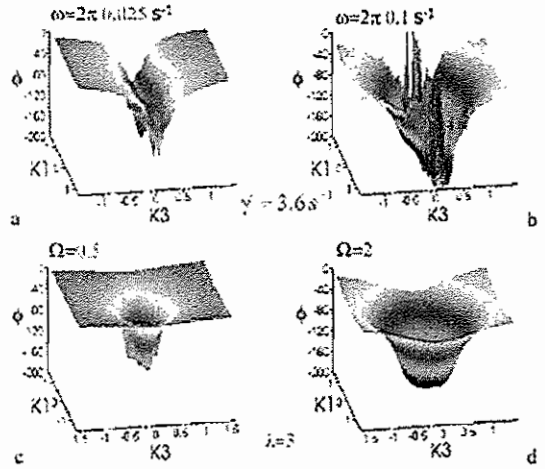

FIG. 3: Frequency and wavevector dependence of the phase shift. (a and b), experiment. (c and d), theory.

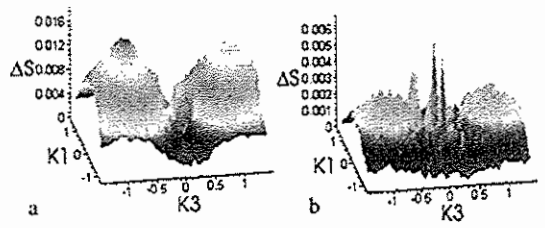

FIG. 4: The amplitude of the second (a) and fourth (b) harmonic Fourier amplitudes for $\dot{\gamma} = 3.92s^{-1}$ and an angular amplitude of 65^o

and the dressed Deborah number,

$$\Omega = \frac{\omega \xi^4}{2 D_0 \beta \Sigma},$$

where $\dot{\gamma}$ is the shear rate, D_0 is the single particle diffusion coefficient, $\beta = 1/k_B T$, and Σ is the Cahn-Hilliard square gradient coefficient. The dimensionless numbers λ and Ω characterize the long-wavelength shear induced distortion and the phase shift of the structure factor response, respectively. For $\lambda > 1$, the structure will be significantly affected by the shear flow. For $\Omega > 1$, the response of microstructure will not be in-phase with the externally applied shear field. In Fig. 2, time traces at a fixed frequency and for a fixed wavevector vector are plotted (the wavevector is always expressed in dimensionless units : $K = k\xi$, with k the physical wavevector) . It is evident that shear flow indeed affects the microstructure. Note that the response is non-linear : in fact, it can be shown from the above mentioned theory, that in the flow-vorticity plane the response of the structure factor to shear flow is always non-linear, even for very small values of λ. The degree of non-linearity as well as the phase shift of the microstructural response with respect to the applied field can be quantified by Fourier analysis of time traces like those plotted in Fig. 2.

In Fig. 3 the phase shift is calculated for each wavevector at two different frequencies. The expected increase in the phase shift on increasing the frequency is observed. Furthermore, the phase shift increases dramatically when $K = 0$ is approached. This is the result of small diffusion relaxation times at small wavevectors (which scale like $\sim K^2$). We also note that the degree of non-linearity seems to diminish with increasing frequency at fixed shear rate (data are not shown). As mentioned above, the response in the flow-vorticity plane is always non-linear, so that the first harmonic (the Fourier mode with the same frequency as the externally applied field) is always zero. The contribution to the response with a frequency equal to twice of that of the external field, the amplitude of the second harmonic, and the amplitude of the fourth harmonic are plotted in Fig. 4 as functions of the wavevector. Here we find a maximum at a specific wavevector for both the second- and fourth harmonic Fourier amplitudes. This wavevector is oriented parallel to the shear flow, due to the fact that structures perpendicular to the shear flow are not distorted (e.g. where $K1 = 0$).

To summarize, we have characterized the response of a near-critical colloidal dispersion to an oscillatory shear flow by small angle, time resolved, static light scattering. All features seen experimentally are, at least qualitatively, in accordance with theory. A more quantitative comparison will be made in the near future. Furthermore, the microstructural response seen in our experiments is the microscopic origin for the rheological behaviour of these near-critical colloidal suspensions. One could therefore measure the (linear and non-linear) viscoelastic response of near critical colloidal systems and compare with theory, once the connection between microstructural response and viscoelastic response has been made[3].

[1] J. K. G. Dhont and G. Nagele, Phys. Rev. E **58**, 7710 (1998).
[2] T. A. J. Lenstra and J. K. G. Dhont, Phys. Rev. E. **63**, 61401 (2000).
[3] I. Bodnár and J. K. G. Dhont, Phys. Rev. Lett. **77**, 5304 (1996).

Properties of Two- and Three-dimensional Colloidal Suspensions: Scaling and related Freezing Criteria

Gerhard Nägele and Markus Kollmann
Institut für Festkörperforschung
Teilinstitut Weiche Materie

We explore static and dynamic properties of two- and three-dimensional systems of strongly interacting colloidal spheres. Quasi-two-dimensional (Q2D) dispersions of particles interacting by long-range electrostatic and dipolar magnetic forces are investigated using Brownian Dynamics computer simulations. The dynamics of three-dimensional suspensions of charge-stabilized and neutral colloidal spheres is determined from a self-consistent mode coupling scheme. Particular focus is given to the implication of scaling and hydrodynamic interactions on the relation between static and dynamic freezing criteria. New freezing criteria are provided in terms of collective diffusion coefficients.

Typical examples of Q2D systems studied in this work are monolayers of charged colloidal spheres between two glass plates interacting by long-range screened electrostatic interactions, and super-paramagnetic colloidal spheres located at a liquid-air interface and interacting by repulsive dipolar magnetic forces induced by a perpendicularly applied external magnetic field. We have employed a Brownian Dynamics (BD) simulation method with the dominant far-field part of the hydrodynamic interactions (HI) included, to study the statics and dynamics of these Q2D systems with its implications on related static and dynamic freezing criteria [1,2]. For this purpose, various measurable quantities are calculated like the radial distribution function $g(r)$, the static structure factor $S(q)$, the mean squared displacement $W(t)$, the dynamic structure factor $S(q,t)$, and the distinct and self van Hove space-time correlation functions $G_d(r,t)$ and $G_s(r,t)$, respectively. An analogous study for three-dimensional dispersions of neutral and of charge-stabilized particles was performed using a fully self-consistent mode-coupling scheme [3,8].

The radial distribution functions, $g(r) = G_d(r, t = 0)/n$, of systems with long-range particle repulsions reveal a pronounced principal peak located at a distance, r_m, nearly equal to the geometric mean particle distance, $r_0 = n^{-1/d}$. Here, n is the particle number density, and d is the dimension. Since r_m is the only physically relevant static length scale, different systems sharing the same peak height $g(r_m)$ have radial distribution functions which superimpose nearly perfectly as functions of reduced distance r/r_0 (cf. Fig. 1). The static scaling of the $g(r)$'s implies that the corresponding static structure factors nearly coincide when plotted versus the reduced wave number q/q_0 with $q_0 = 2\pi/r_0$. Without HI, there is a single characteristic time scale $\tau_0 = r_0^2/D_0$ associated with r_0. This implies dynamic scaling, i.e. systems with strong and long-range particle repulsion and identical peak heights $g(r_m)$ (likewise, identical $S(q_m)$) show nearly identical dynamical properties, e.g., nearly identical $G_d(r,t)/n$, , $W(t)/r_0^2$ and $S(q,t)$ as functions of reduced time $\tau = t/\tau_0$, distance $x = r/r_0$ and wave number $y = q/q_0$ (cf. Fig. 1 displaying $G_d(r,t)/n$ at time $t/\tau_0 = 0.035$).

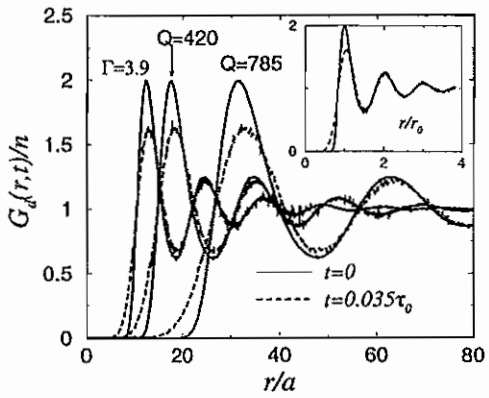

FIG. 1: BD results for the distinct van Hove function $G_d(r,t)/n$ versus r/a of a magnetic dispersion with coupling parameter $\Gamma = 3.9$ and of two charge-stabilized Q2D systems of particle charge numbers $Q = 420$ and $Q = 785$, respectively. Note that $G_d(r, t = 0)/n = g(r)$ at $t = 0$. The inset exemplifies the static and dynamic scaling (from [1,2]).

Hydrodynamic interactions introduce the particle radius a as another relevant length scale since particles are in contact with the solvent. With HI, a more restricted form of dynamic scaling holds where, e.g., the master curves for $G_d(x,\tau)/n$ and $D(\tau)$, defined by $D(\tau) = W(t)/(D_0 t)$, depend on the characteristic length ratio a/r_0. Furthermore, HI cause a modest enhancement of self-diffusion which becomes stronger with increasing a/r_0. The enhancement of self-diffusion is indicative of systems with prevailing influence of the far-field part of HI (cf. Fig. 2 showing $D(\tau)$).

The dynamic scaling behavior of systems with strong and long-range repulsion implies in particular a one-to-one correspondence between $S(q_m)$ and the non-dimensionalized long-time self-diffusion coefficient $D_S^L/D_0 = D(t \to \infty)$. Fig. 3a includes the master curve for D_S^L/D_0 vs. $S(q_m)$ as obtained for deionized three-dimensional dispersions of charge-stabilized parti-

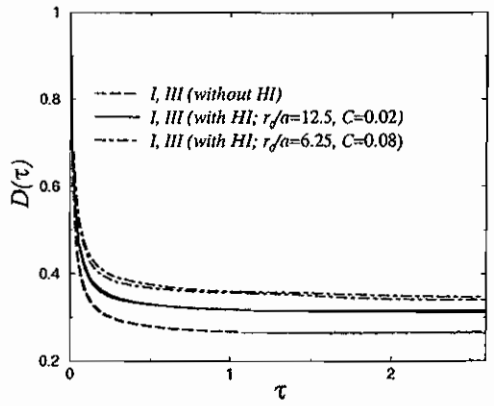

FIG. 2: BD results with/without HI for the normalized self-diffusion coefficient $D(t) = W(t)/(D_0 t)$ of a magnetic systems, labeled by I, and a charged Q2D system, labeled by III, versus reduced time τ. Here, $C = \pi n a^2$ is the area fraction, and $S(q_m) = 2.2$ is constant for all systems considered in this figure (from [1,2]).

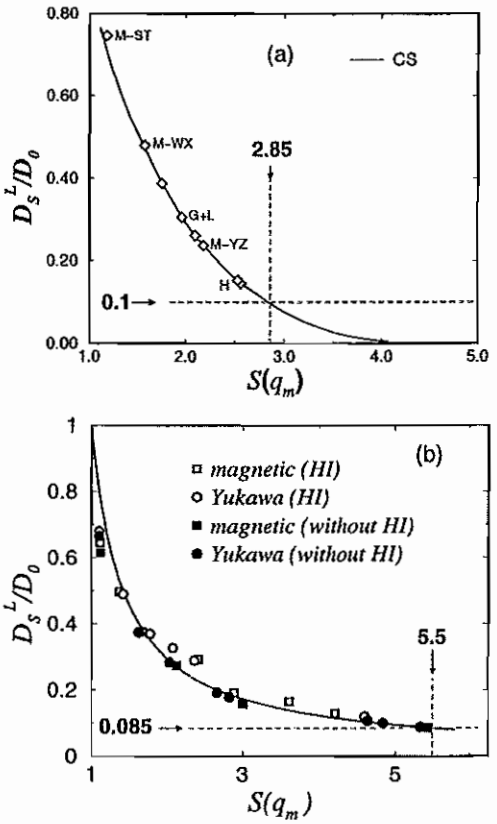

FIG. 3: Reduced long-time self-diffusion coefficient D_S^L/D_0 vs. liquid static structure factor peak height $S(q_m)$. Mode-coupling theory results without HI (from [3]) for deionized three-dimensional bulk dispersions of charge-stabilized particles are included in (a). The particle interactions in (a) are described by a Yukawa-like screened Coulomb potential of DLVO type. BD results with/without HI for magnetic and charge-stabilized Q2D systems are shown in (b) (from [2,3]).

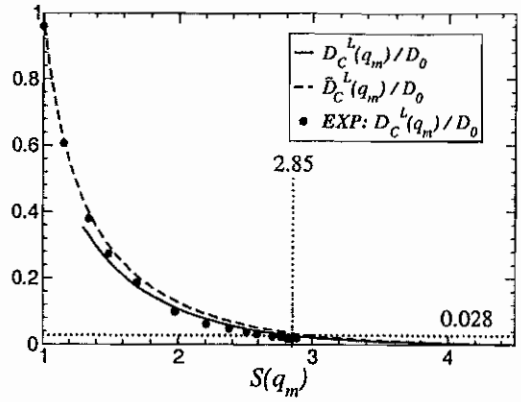

FIG. 4: HI-rescaled mode coupling theory results for the hard-sphere long-time and mean collective diffusion coefficients $D_C^L(q_m)/D_0$ and $\tilde{D}_C^L(q_m)/D_0$ vs $S(q_m)$. The dotted lines indicate the freezing values. Further included are the experimental data for $D_C^L(q_m)/D_0$ (from [8]).

cles using a fully self-consistent mode-coupling scheme without HI. Note that a peak height of $S(q_m) = 2.85$ corresponds to $D_S^L/D_0 = 0.1$. This result is in accord with an empirical static freezing criterion of Hansen and Verlet [4], which states that the onset of freezing in three-dimensional systems should occur when $S(q_m) \approx 2.85$, and with a dynamic criterion of Löwen, Palberg and Simon [5], which localizes the freezing line of three-dimensional Brownian systems at $D_S^L/D_0 \approx 0.1$.

Our BD results of D_S^L/D_0 vs. $S(q_m)$ for magnetic and charged Q2D dispersions with and without HI are displayed in Fig. 3b. Without HI, there is for Q2D systems again a single master curve, but now with $D_S^L/D_0 \approx 0.085$ and $S(q_m) \approx 5.5$ at freezing. This finding is in excellent accord with an empirically found dynamic criterion for two-dimensional freezing of Löwen [6] stating that $D_S^L/D_0 \approx 0.085$ at the freezing line independent of the pair potential and the nature of the freezing process. Moreover, a value of $S(q_m) \approx 5.5$ at freezing was indeed found from computer simulations of Broughton et al. [7]

For three-dimensional and Q2D dispersions with strong and long-range particle repulsion we have thus shown that dynamic scaling is at the origin of the equivalence of related static and dynamic freezing criteria. According to Fig. 3b, the value of D_S^L/D_0 close to freezing is only modestly enlarged by HI, indicating that the dynamic freezing rule of Löwen et al. applies also when far-field HI are considered.

For systems with strong near-field HI and lubrication forces acting between the particles like dispersions of colloidal hard spheres, $D_S^S < D_0$, where D_S^S is the short-time self-diffusion coefficient. We have shown that the dynamic freezing criterion can then be reestablished in terms of D_S^L/D_S^S rather than D_S^L/D_0. [8]

In [8], we propose and explore novel dynamic freezing criteria in terms of long-time and mean collective diffu-

sion coefficients, $D_C^L(q_m)$ and $\tilde{D}_C^L(q_m)/D_0$, respectively. In Fig. 4, we compare HI-rescaled mode coupling theory results (cf. [8]) for the reduced hard-sphere collective diffusion coefficients $D_C^L(q_m)/D_0$ and $\tilde{D}_C^L(q_m)/D_0$ vs $S(q_m)$ with experimental data for $D_C^L(q_m)/D_0$ by Segrè and coworkers [9]. There is good agreement between theory and experiment for volume fractions Φ, and peak heights $S(q_m)$ (i.e. $\Phi \geq 0.22$ and $S(q_m) \geq 1.27$) where, according to mode coupling theory, $D_C^L(q_m)$ exists. For the freezing value $S(q_m) = 2.85$, the hard-sphere long-time coefficient $D_C^L(q_m)$ is reduced to $D_C^L(q_m) \approx 0.028 D_0$.

Finally, we point out that any of the proposed freezing criteria may be used, depending on what is most convenient from the experimental point of view.

---

[1] R. Pesché, M. Kollmann and G. Nägele, Phys. Rev. E **64**, 052401 (2001)

[2] R. Pesché, M. Kollmann and G. Nägele, J. Chem. Phys. **114**, 8701 (2001)

[3] A.J. Banchio, G. Nägele and J. Bergenholtz, J. Chem. Phys. **113**, 3381 (2000)

[4] J.-P. Hansen and L. Verlet, Phys. Rev. **184**, 151 (1969)

[5] H. Löwen, T. Palberg and R. G. Simon, Phys. Rev. Lett. **70**, 1557 (1993)

[6] H. Löwen, Phys. Rev. E **53**, R29 (1996)

[7] J.Q. Broughton, G. H. Gilmer and Y. D. Weeks, Phys. Rev. B **25**, 4651 (1982)

[8] G. Nägele, M. Kollmann, R. Pesché and A.J. Banchio, Mol. Phys., in press (2002)

[9] P.N. Segrè, S.P. Meeker, P.N. Pusey and W.C.K. Poon, Phys. Rev. Lett. **75**, 958 (1995)

Properties of Two- and Three-dimensional Colloidal Suspensions: Scaling and related Freezing Criteria

Gerhard Nägele and Markus Kollmann
Institut für Festkörperforschung
Teilinstitut Weiche Materie

We explore static and dynamic properties of two- and three-dimensional systems of strongly interacting colloidal spheres. Quasi-two-dimensional (Q2D) dispersions of particles interacting by long-range electrostatic and dipolar magnetic forces are investigated using Brownian Dynamics computer simulations. The dynamics of three-dimensional suspensions of charge-stabilized and neutral colloidal spheres is determined from a self-consistent mode coupling scheme. Particular focus is given to the implication of scaling and hydrodynamic interactions on the relation between static and dynamic freezing criteria. New freezing criteria are provided in terms of collective diffusion coefficients.

Typical examples of Q2D systems studied in this work are monolayers of charged colloidal spheres between two glass plates interacting by long-range screened electrostatic interactions, and super-paramagnetic colloidal spheres located at a liquid-air interface and interacting by repulsive dipolar magnetic forces induced by a perpendicularly applied external magnetic field. We have employed a Brownian Dynamics (BD) simulation method with the dominant far-field part of the hydrodynamic interactions (HI) included, to study the statics and dynamics of these Q2D systems with its implications on related static and dynamic freezing criteria [1,2]. For this purpose, various measurable quantities are calculated like the radial distribution function $g(r)$, the static structure factor $S(q)$, the mean squared displacement $W(t)$, the dynamic structure factor $S(q,t)$, and the distinct and self van Hove space-time correlation functions $G_d(r,t)$ and $G_s(r,t)$, respectively. An analogous study for three-dimensional dispersions of neutral and of charge-stabilized particles was performed using a fully self-consistent mode-coupling scheme [3,8].

The radial distribution functions, $g(r) = G_d(r, t = 0)/n$, of systems with long-range particle repulsions reveal a pronounced principal peak located at a distance, r_m, nearly equal to the geometric mean particle distance, $r_0 = n^{-1/d}$. Here, n is the particle number density, and d is the dimension. Since r_m is the only physically relevant static length scale, different systems sharing the same peak height $g(r_m)$ have radial distribution functions which superimpose nearly perfectly as functions of reduced distance r/r_0 (cf. Fig. 1). The static scaling of the $g(r)$'s implies that the corresponding static structure factors nearly coincide when plotted versus the reduced wave number q/q_0 with $q_0 = 2\pi/r_0$. Without HI, there is a single characteristic time scale $\tau_0 = r_0^2/D_0$ associated with r_0. This implies dynamic scaling, i.e. systems with strong and long-range particle repulsion and identical peak heights $g(r_m)$ (likewise, identical $S(q_m)$) show nearly identical dynamical properties, e.g., nearly identical $G_d(r,t)/n$, , $W(t)/r_0^2$ and $S(q,t)$ as functions of reduced time $\tau = t/\tau_0$, distance $x = r/r_0$ and wave number $y = q/q_0$ (cf. Fig. 1 displaying $G_d(r,t)/n$ at time $t/\tau_0 = 0.035$).

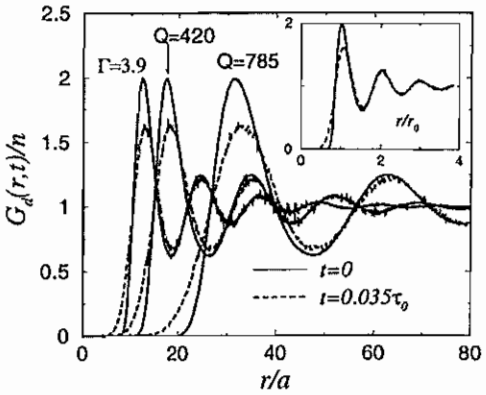

FIG. 1: BD results for the distinct van Hove function $G_d(r,t)/n$ versus r/a of a magnetic dispersion with coupling parameter $\Gamma = 3.9$ and of two charge-stabilized Q2D systems of particle charge numbers $Q = 420$ and $Q = 785$, respectively. Note that $G_d(r, t = 0)/n = g(r)$ at $t = 0$. The inset exemplifies the static and dynamic scaling (from [1,2]).

Hydrodynamic interactions introduce the particle radius a as another relevant length scale since particles are in contact with the solvent. With HI, a more restricted form of dynamic scaling holds where, e.g., the master curves for $G_d(x,\tau)/n$ and $D(\tau)$, defined by $D(\tau) = W(t)/(D_0 t)$, depend on the characteristic length ratio a/r_0. Furthermore, HI cause a modest enhancement of self-diffusion which becomes stronger with increasing a/r_0. The enhancement of self-diffusion is indicative of systems with prevailing influence of the far-field part of HI (cf. Fig. 2 showing $D(\tau)$).

The dynamic scaling behavior of systems with strong and long-range repulsion implies in particular a one-to-one correspondence between $S(q_m)$ and the non-dimensionalized long-time self-diffusion coefficient $D_S^L/D_0 = D(t \to \infty)$. Fig. 3a includes the master curve for D_S^L/D_0 vs. $S(q_m)$ as obtained for deionized three-dimensional dispersions of charge-stabilized parti-

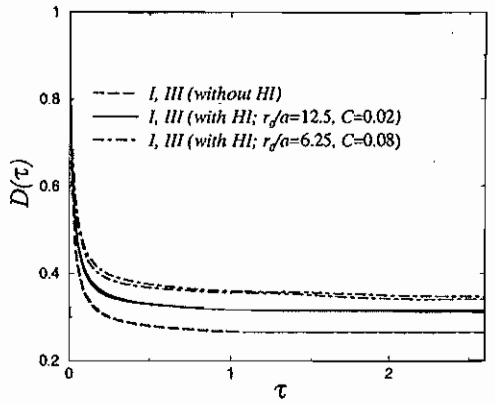

FIG. 2: BD results with/without HI for the normalized self-diffusion coefficient $D(t) = W(t)/(D_0 t)$ of a magnetic systems, labeled by I, and a charged Q2D system, labeled by III, versus reduced time τ. Here, $C = \pi n a^2$ is the area fraction, and $S(q_m) = 2.2$ is constant for all systems considered in this figure (from [1,2]).

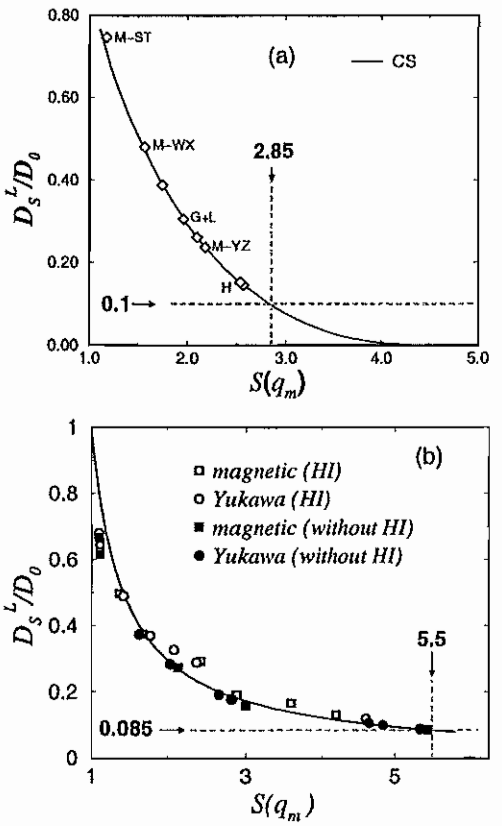

FIG. 3: Reduced long-time self-diffusion coefficient D_S^L/D_0 vs. liquid static structure factor peak height $S(q_m)$. Mode-coupling theory results without HI (from [3]) for deionized three-dimensional bulk dispersions of charge-stabilized particles are included in (a). The particle interactions in (a) are described by a Yukawa-like screened Coulomb potential of DLVO type. BD results with/without HI for magnetic and charge-stabilized Q2D systems are shown in (b) (from [2,3]).

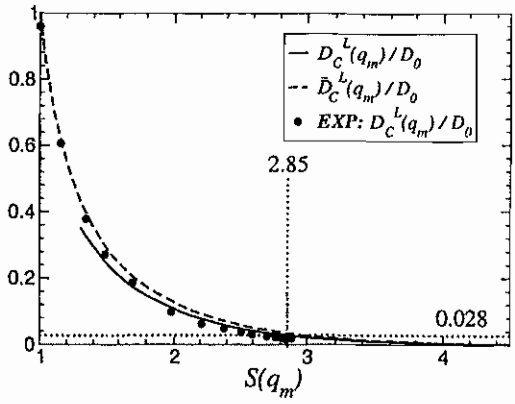

FIG. 4: HI-rescaled mode coupling theory results for the hard-sphere long-time and mean collective diffusion coefficients $D_C^L(q_m)/D_0$ and $\tilde{D}_C^L(q_m)/D_0$ vs $S(q_m)$. The dotted lines indicate the freezing values. Further included are the experimental data for $D_C^L(q_m)/D_0$ (from [8]).

cles using a fully self-consistent mode-coupling scheme without HI. Note that a peak height of $S(q_m) = 2.85$ corresponds to $D_S^L/D_0 = 0.1$. This result is in accord with an empirical static freezing criterion of Hansen and Verlet [4], which states that the onset of freezing in three-dimensional systems should occur when $S(q_m) \approx 2.85$, and with a dynamic criterion of Löwen, Palberg and Simon [5], which localizes the freezing line of three-dimensional Brownian systems at $D_S^L/D_0 \approx 0.1$.

Our BD results of D_S^L/D_0 vs. $S(q_m)$ for magnetic and charged Q2D dispersions with and without HI are displayed in Fig. 3b. Without HI, there is for Q2D systems again a single master curve, but now with $D_S^L/D_0 \approx 0.085$ and $S(q_m) \approx 5.5$ at freezing. This finding is in excellent accord with an empirically found dynamic criterion for two-dimensional freezing of Löwen [6] stating that $D_S^L/D_0 \approx 0.085$ at the freezing line independent of the pair potential and the nature of the freezing process. Moreover, a value of $S(q_m) \approx 5.5$ at freezing was indeed found from computer simulations of Broughton et al. [7]

For three-dimensional and Q2D dispersions with strong and long-range particle repulsion we have thus shown that dynamic scaling is at the origin of the equivalence of related static and dynamic freezing criteria. According to Fig. 3b, the value of D_S^L/D_0 close to freezing is only modestly enlarged by HI, indicating that the dynamic freezing rule of Löwen et al. applies also when far-field HI are considered.

For systems with strong near-field HI and lubrication forces acting between the particles like dispersions of colloidal hard spheres, $D_S^S < D_0$, where D_S^S is the short-time self-diffusion coefficient. We have shown that the dynamic freezing criterion can then be reestablished in terms of D_S^L/D_S^S rather than D_S^L/D_0. [8]

In [8], we propose and explore novel dynamic freezing criteria in terms of long-time and mean collective diffu-

sion coefficients, $D_C^L(q_m)$ and $\tilde{D}_C^L(q_m)/D_0$, respectively. In Fig. 4, we compare HI-rescaled mode coupling theory results (cf. [8]) for the reduced hard-sphere collective diffusion coefficients $D_C^L(q_m)/D_0$ and $\tilde{D}_C^L(q_m)/D_0$ vs $S(q_m)$ with experimental data for $D_C^L(q_m)/D_0$ by Segrè and coworkers [9]. There is good agreement between theory and experiment for volume fractions Φ, and peak heights $S(q_m)$ (i.e. $\Phi \gtrsim 0.22$ and $S(q_m) \geq 1.27$) where, according to mode coupling theory, $D_C^L(q_m)$ exists. For the freezing value $S(q_m) = 2.85$, the hard-sphere long-time coefficient $D_C^L(q_m)$ is reduced to $D_C^L(q_m) \approx 0.028 D_0$.

Finally, we point out that any of the proposed freezing criteria may be used, depending on what is most convenient from the experimental point of view.

---

[1] R. Pesché, M. Kollmann and G. Nägele, Phys. Rev. E **64**, 052401 (2001)

[2] R. Pesché, M. Kollmann and G. Nägele, J. Chem. Phys. **114**, 8701 (2001)

[3] A.J. Banchio, G. Nägele and J. Bergenholtz, J. Chem. Phys. **113**, 3381 (2000)

[4] J.-P. Hansen and L. Verlet, Phys. Rev. **184**, 151 (1969)

[5] H. Löwen, T. Palberg and R. G. Simon, Phys. Rev. Lett. **70**, 1557 (1993)

[6] H. Löwen, Phys. Rev. E **53**, R29 (1996)

[7] J.Q. Broughton, G. H. Gilmer and Y. D. Weeks, Phys. Rev. B **25**, 4651 (1982)

[8] G. Nägele, M. Kollmann, R. Pesché and A.J. Banchio, Mol. Phys., in press (2002)

[9] P.N. Segrè, S.P. Meeker, P.N. Pusey and W.C.K. Poon, Phys. Rev. Lett. **75**, 958 (1995)

Micellar properties of Polybutadiene-b-poly(ethyleneoxide) blockcopolymers

Peter Lang and Lutz Willner
Institut für Festkörperforschung
Teilinstitut Weiche Materie

Amphiphilc polybutadiene-b-poly(ethyleneoxide) (PBPEO) blockcopolymers with two different ratios of blocklengths were synthezised by anionic polymerisation. The properties of the PBPEO micelles in aqueous solution were investigated by static light scattering and small-angle neutron scattering. Surprisingly the micellar shape of PBPEO aggregates differs grossly from that of the corresponding poly(ethylene-propylene)-b-poly(etyleneoxide) PEPPEO micelles.

The properties of blockcopolymer aggragtes in solutions have been studied in great detail during the last decade [1]. However, except from the work on polyelectrolyte systems, the vast majority of the contributions was dedicated either to non-equilibrium systems or to the structure determination of spherical micelles. Actually the first reports on cylindrical non-polyelectrolyte aggregates are not older than two years [2, 3]. There the authors showed for a series of PBPEO samples that the micellar shape may be tuned by the volume ratio of the hydrophobic and the hydrophilic block respectively. This feature, which is well known from low molar mass amphiphiles implies that blockcopolymers with a short hydrophobic chain and a large hydrophilic moiety form spherical micelles in aqueous solutions, while cylindrical aggregates are expected to form, if the hydrophobic chain is much longer than the water soluble part.

We have synthesized PB(I)PEO(J) blockcopolymers by anionic polymerization. The numbers I an J denote the molar mass of the respective block expressed in kg/mol. Static light scattering experiments on aqueous solutions of various concentration c_m were conducted using a commercial setup by ALV. For all polymer mass concentrations the inverse of the scattered intensity $I(Q)$ was depending strictly linearly on the scattering vector squared, Q^2. Consequently, the quantity $M_{app}(c_m) = M_w S(Q=0)$ could be reliably determined by linear extrapolation of $I(Q)$ to $Q = 0$. Here M_w is the mass average molar mass of the scattering particles and $S(Q=0)$ is the structure factor at zero scattering vector. Further, for low concentrations $M_{app}(c_m)$ depends linearly on the concentration, such that M_w can be determined by linear extrapolation of M_{app} to infinite dilution. As a result one obtains the concentration dependence of $S(Q=0)$, which is a characteristic feature, depending on the shape and the interaction potential of the scattering entities.

In Fig. 1 we have plotted $S(Q=0)^{-1}$ versus the reduced concentration $X \propto A_2 M_w c_m$, where A_2 is the second osmotic virial coefficient, and the proportionality constant depends on the theoretical model applied. The graph displays experimental data for PB5-PEO15 together with theoretical predictions for solutions of hard spheres [4], semi-flexible polymers [5] and rigid rods [6]. For comparison we have also plotted the data from

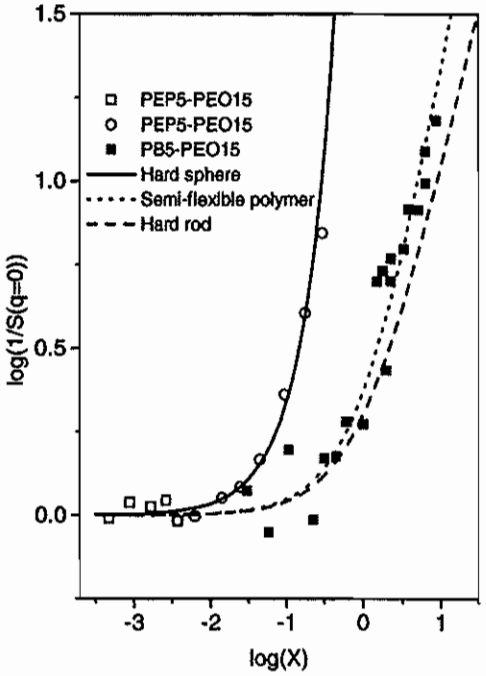

FIG. 1: Structure factor at zero scattering vector as a function of reduced concentration from aqueous blockcopolymer solutions as determined by static light scattering. The symbols are experimental data, while the lines represent theoretical prediction for the models indicated in the legend

PEP5–PEO15, which is known to form spherical micelles in aqueous soluion [7].While the experimental data of the latter system follow perfectly the theoretical prediction for a solution of hard spheres, the PBPEO aggregates obviously are elongated objects, i. e. cylindrical micelles.

To confirm these finding we performed small-angle neutron scattering (SANS) experiments on PBPEO polymers in D_2O solution. The radially averaged, background and solvent corrected scatttering curves are displayed in Figs, 2 and 3. As to be seen from Fig, 2 where the scattering curves from two solutions of PB5–PEO15 with polymer weight fractions of $w_p = 0.01$ and 0.1 respectively are plotted, the scattered intensity is proportional to the solute content over the entire range of scattering vectors probed. In the Q-range $Q \leq 6 \cdot 10^{-3}$ Å^{-1} the scattering curves decay as $I(Q) \propto Q^{-1}$, which is typi-

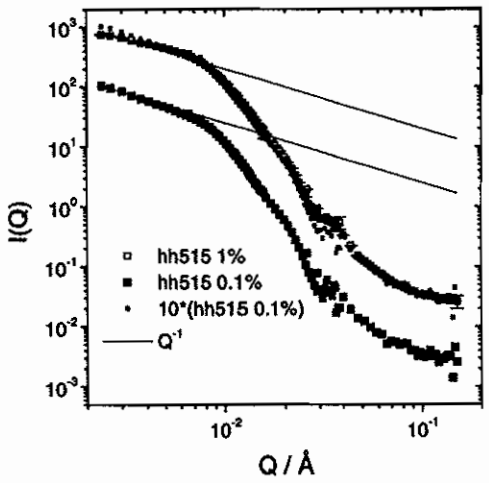

FIG. 2: SANS curves from two solutions of PB5–PEO15 in D_2O at different weight fractions of the polymer as indicated by the legend. The scattered intensity is proportional to the polymer content in the entire Q–range.

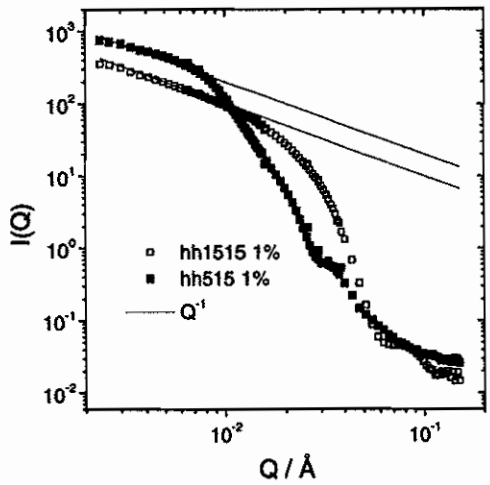

FIG. 3: SANS curves from solutions of PB5–PEO15 and PB1.5–PEO1.5 in D_2O with a polymer mass fraction of ten percent. Both curves show the typical Q^{-1} dependence of cylindrical micelles.

cal for locally cylindrical structures. For PB1.5–PEO1.5 solutions we find the same behavior. However in this case the deviation of the scattering curve from the Q^{-1}–behavior occurs at higher values of the scattering vector. This indicates that the cross sectional dimensions of the PB1.5–PEO1.5 micelles are smaller than those of the PB5–PEO15 aggregates.

This estimate may be quantified by a cross sectional Guinier–extrapolation. In the appropriate Q–range the scattered intensity from a locally cylindrical particle may be approximated as

$$I(c_m, Q) \propto \frac{1}{Q} \exp\left(-R_{g,cs}^2 Q^2/2.\right) \qquad (1)$$

where $R_{g,cs}$is the cross sectional radius of gyration. From the linear extrapolation of $\ln(I(Q) \cdot Q)$ versus Q^2 we determined the cross sectional radii to be $R_{g,cs} = 61$ Å for the PB1.5–1.5PEO micelles, while that of the PB5–PEO15 micelles was found to be$R_{g,cs} = 99$ Å.

We therefore conclude that PB–PEO form cylindrical micelles in aqueous solution, the cross sectional diameter of which can be tuned by the overall length of the polymeric unimers. It is however, striking that PB5–PEO15 blockcopolymers form cylindrical micelles, while PEP5–PEO15 polymers definitely form spherical aggregates. This would imply that very minor differences in the chemical structure of the polimeric unimers can have a drastic influence on their aggregation behavior.

[1] For an overview see: Förster, S.; Zisenis, M.; Wenz, E.; Antonietti, A. *J. Chem. Phys.* **104**, 9959 (1996). Zhang, L.; Shen, H.; Eisenberg, A. *Macromolecules* **30**, 1001 (1997). Desbaumes, L.; Eisenberg, A. *Langmuir* **15**, 36 (1999). and references therein.
[2] Hentze, H. P.; Krämer, E.; Berton, B.; Förster, S.; Antonietti, M.; Dreja, M. *Macromolecules* **32**, 5803 (1999).
[3] Egger, H.; Nordskog, A.; Lang, P.; Brandt, A. *Macromol. Symp.* **162**, 291 (2000).
[4] Carnahan, N. F.; Starling, K. E. *J. Chem. Phys.* **51**, 635 (1969).
[5] Otha, T.; Oono, Y. *Phys. Lett.* **89A**, 460 (1982).
[6] Onsager, L. *Ann. N. Y. Acad. Sci.* **51**, 627 (1949).
[7] Willner, L.; Poppe, A.; Allgaier, J.; Monkenbusch, M.; Lindner, P.; Richter, D. *Europhys. Lett.* **51**, 628 (2000).

Publications in refereed journals

Blokhuis E.M.1; Sager W.
1University of Leiden, Niederlande
Sphere to cylinder transition in a single phase microemulsion system: A theoretical investigation
Journal of Chemical Physics, 115, 1073-1085, 2001
23.30.0

Dhont J.; Wagner N.J.1
1University of Delaware, USA
Superposition rheology
Phys.Rev.E.; 63, 021406, 2001
23.30.0

Figolio A.1; Sager W.; Mulder M.1
1University of Twente, Niederlande
Facilitated oxygen transport in liquid membranes: review and new concepts
Journal of Membrane Science, 181, 97-110, 2001
23.30.0

Götz H.1; Ewen B.1; Maschke U.2; Meier G.; Monkenbusch M.
1MPI in Mainz
2Université de Lille, France
Neutron Scattering Investigations on the Statics and Dynamics of Polydimethyl- and Polyethylmethylsiloxane Melts
Macromol.Chem.Phys. 202, 3334-3341 (2001
23.30.0

Hauck J.; Mika K.
Ordering and interactions
Phys.Low-Dim. Struct., 7/8, 41-54, 2001
23.30.0

Hauck J; Henkel D; Mika K.
The evolution processes of DNA sequences, languages and carols
Elsevier, Physica A, 293, 540-548, 2001
23.30.0

Hauck J; Mika K.
Ground-State Structures of Polymers
Journal of Computational Chem.; 22, 1944-1955, 2001
23.30.0

Hauck J; Mika K.
Interactions in Sphere Packings
Zeitschrift f. Physikalische Chemie, 215, 5, 637-652, 2001
23.30.0

Hauck J; Mika K.
Ordering and interactions
Colloids and Surfaces A: Physicochem. and Eng. Aspects, 190, 99-109, 2001
23.30.0

Koenderink G.H.1; Zhang H.2; Lettinga P.; Nägele G.; Philipse A.P.1
1University of Utrecht
2University of Shanghai
Rotational tracer diffusion in binary colloidal sphere mixtures
Physical Rev.E., 64, 22401, 2001

Lenstra T.; Dhont J.
Flow dichroism in critical colloidal fluids
Physical Rev. E., 63, 61401-12, 2001
23.30.0

Lenstra T.; Dogic Z.; Dhont J.
Shear-induced displacement of isotropic-nematic spinodals
Journal of Chem. Phys., 114, 10151, 2001
23.30.0

Patkowski A.1,2; Fischer E.W.1; Steffen W.1; Gläser H.1; Baumann M.1; Ruths T.1; Meier G.
1MPI in Mainz
2University of Poznan, Poland
Unusual features of long-range density fluctuations in glass-forming organic liquids: A Rayleigh and Rayleigh-Brillouin light scattering study
Physical Rev.E., 63, 061503, 2001
23.30.0

Pesché R.1; Kollmann M.; Nägele G.
1University of Delaware, Newark, USA
Brownian dynamics study of dynamic scaling and related freezing criteria in quasi-two-dimensional dispersions
Journal of Chemical Physics, 114, 8701-8707, 2001
23.30.0

Pesché R.1; Kollmann M.; Nägele G.
1University of Delaware, Newark, USA
Dynamic scaling and freezing criteria in quasi-two-dimensional dispersions
Phys.Rev.E., 64, 2001
23.30.0

Woudenberg F.1; Sager W.; Sibelt N.1; Verweij H.1
1University of Twente, Niederlande
Dense nanostructured t-ZrO2 coatings at low temperatures via modified emulsion precipitation
Advanced Materials, 13, 514, 2001
23.30.0

Other publications

Figoli A.1; Wessling M.1; Sager W.
1Universität Twente
Synthesis of nanostructured mixed matrix membranes for facilitated gas separation
23.30.0

Hauck J; Mika K.
Aperiodische Kreispackungen
9. Jahrestagung der Deutschen Gesellschaft für Kristallographie (DGK) im März 2001
Zeitschrift Krist. Suppl.; 17, 72, 2001
23.30.0

Hauck J; Mika K.
Correlation between Interactions and ordered structures
20th European Crystallographie Meeting
Krakow, 25.08.-31.08.01
Zeitschrift Krist. Suppl.; 18, 95, 2001
23.30.0

Kollmann M.
Dynamics and Microstructure of Interacting Brownian Systems: Electreokinetic Effects,
Quasi-two-dimensional Systems and Sphere Caging
Universität Konstanz, 03.08.01
23.30.0

Woundenberg F.C.M.1; Verweij H.1; Sager W.
1Universität Twente
Nanostructured oxide coatings via emulsion precipitation
23.15.0

Invited talks

Dhont J.
Dynamics of Colloids
Winterschool "Physical Chemistry"
Han sur Lesse; Belgien; 05.-09.02.01
23.30.0

Dhont J.
Flow Instability in Complex Fluids
General Physics Colloquium
Univ. Groningen; The Netherlands, 05.04.01
23.30.0

Dhont J.
Spinodal Decomposition of Colloids
Winterschool "Sensing and Manipulating in the Nanoworld"
Mauterndorf; Austria, 18.-23.02.01
23.30.0

Dhont J.
The Shear-banding Transition in Colloids
4th International Discussion, Meeting on Relaxations in Complex Systems
Heraklion, Greece, 17.06.-24.06.01
23.30.0

Dhont J.
The Shear-banding Transition in Complex Fluids
Complex Materials in External Fields
Manchester, UK, 29.08.-31.08.01
23.30.0

Lang P.
Grenzflächeninduzierte Ordnungsphänomene von fluiden Phasen: Untersuchungen mittels Streumethoden
TU-Clausthal-Zellerfeld, 10. Juli 2001
23.30.0

Meier G.
Photon Correlation Spectroscopy with visible light: Concepts, experimental methods and scientific applications
Lecture at Research Courses on New X-Ray Sciences
Desy, Hasylab, Hamburg, 15.10.-17.10.01
23.30.0

Nägele G.; Pesché R.1
1Universität Konstanz (???)
Dynamic Scaling and Freezing Criteria of Quasi-two-dimensional and three-dimensional Colloidal Dispersions
IUAP 21st International Conference on Statistical Physics
Cancum, Mexiko, 15.07.-20.07.01
23.30.0

Nägele G.
Dynamic Properties, Scaling and Related Freezing Criteria of Quasi-two-dimensional and Three-dimensional Colloidal Dispersions
Applied Statistical Physics Molecular Engineering Conference
Cancum, Mexiko, 23.07.-27.07.01
23.30.0

Nägele G.
Dynamische Eigenschaften ladungsstabilisierter Kolloide
MPI in Mainz, 12.02.01
23.30.0

Sager W.
Phase behaviour and structural evolution in surfactant self assemblies and their employment in the preparation of (inorganic) nanoparticles and nanoporous/nanostructured (composite) materials
1st Meeting of Young Academic Chemists in the Netherlands
Nijmwegen, 27.09.-28.09.2001
23.30.0

Other talks

Hauck J., Mika K.
Self-Assembly of homogeneous systems
Steinfurter-Keramik-Seminar v. 28.11.-01.12.01
23.30.0

Hauck J.
Self-Assembly of Homogeneous Systems
XV Conference of the European Colloid and Interface Society
Coimbra, Portugal; 16.09.-21.09.2001
23.30.0

Sager W., Woudenberg F.C.M.1, Sibelt N.G.M.1, Verweij H.1
1Universität Twente
Characterisation of nanosized oxide particles and ceramic nanocomposite coatings prepared via modified emulsion precipitation
Steinfurter-Keramik-Seminar v. 28.11.-01.12.01
23.30.0

Posters

Eckert S.1; Hoffmann S.; Meier G.; Alig I.1
1DKI Darmstadt
Critical fluctuations in non-critical and critical mixtures of polyethylene glycol and propylene glycol studied by ultrasonic and light scattering experiments
4th IDMRCS, Crete, Greece; 18.06.-26.06.01
23.30.0

Hauck J.; Mika K.
Ground State Structures of Polymers
Europhysics Conference on Computational Physics
Aachen, 05.09.-08.09.2001
23.30.0

Kollmann M.; Näglele G.
Electrokinetic Effects in Charged Colloids: the Role of Hydrodynamic Interactions
Jülich Soft Matter Days 2001 in Kerkrade; 13.11.-16.11.01
23.30.0

Näglele G.; Kollmann M.; Pesché R.1; Banchio A.J.2
1University of Delaware, Newark; USA
2CALTECH Institute in Pasadena, USA
Dynamic properties, scaling and related freezing criteria of 2D and 3D dispersions
Jülich Soft Matter Days 2001 in Kerkrade; 13.11.-16.11.01
23.30.0

Näglele G.
Electrokinetic Effects in Charged Colloids: the Role of Hydrodynamic Interactions
IUAP 21st International Conference on Statistical Physics
Cancum, Mexico; 15.07.-20.07.01
23.30.0

Sager W.; Blokhuis E.1; Smeets J.1; Svergun D.I.2,3; Koch M.2; Konarev P.2,3; Volkov V.3
1University of Leiden, The Netherlands
2DESY in Hamburg
3Institute of Crystallography, Moscow
Aggregation and shape transformations in w/o AOT microemulsions
Conference on Assembly and Self Assembly at the Interface of Biology, Chemistry and Physics
Il Ciocco, Italy, 20.08.-25.08.01
23.30.0

Sager W.; Blokhuis E.1; Smeets J.1; Svergun D.I.2,3; Koch M.2; Konarev P.2,3; Volkov V.3
1University of Leiden, The Netherlands
2DESY in Hamburg
3Institute of Crystallography, Moscow
Aggregation and shape transformations in w/o AOT microemulsions
Jülich Soft Matter Days in Kerkrade v. 13.11.-16.11.01
23.30.0

Sager W.; Woudenberg F.1; Urban J.2; Weiss K.2; Verweij H.1
1University of Twente; The Netherlands
2MPI in Berlin
Characterisation of nanosized oxide particles and nanocomposite coatings prepared via modified emulsion precipitation
Il Ciocco, Italy, 20.08.-25.08.01

23.30.0

Sager W.; Woudenberg F.1; Urban J.2; Weiss K.2; Verweij H.1
1University of Twente; The Netherlands
2MPI in Berlin
Characterisation of nanosized oxide particles and nanocomposite coatings prepared via modified emulsion precipitation
Jülich Soft Matter Days in Kerkrade v. 13.11.-16.11.01
23.30.0

Vass S.1; Haimer K.2; Meier G.; Grimm H.; Klapper M.2; Borberly S.1
1KFKI, Budapest
2MPI, Mainz
Sequence-dependent hydration properties of ionic ABA and BAB triblock copolymer micelles for SANS
Deutsche Neutronenstreutagung in Jülich vom 19.02.-21.02.2001
23.30.0

Lecture courses

Lang P.
Streuung an fluiden Grenzflächen und biologischen Modellsystemen
TU Berlin, Sommersemester 2001
23.30.0

Nägele G.
Kolloide als Modellsysteme weicher Materie: strukturelle und dynamische Eigenschaften
Universität Konstanz, Wintersemester Okt./Nov. 2001
23.30.0

Sager W.
Kolloide und Grenzschichten
Universität in Twente, Wintersemester 2000/2001
23.30.0

Internal seminars

Dhont J.
The Smoluchowski Equation and Spinodal Decomposition
Soft Matter Seminar - Jülich
Heimbach, 18.01.01
23.30.0

Lettinga P.
Microscopic Origin of the non-linear viscoelastic response of colloidal dispersions
IFF, Informationsveranstaltung für den wiss. Beirat, 26.04.01
23.30.0

Institute for Microstructure Research

General Overview

The Institut für Mikrostrukturforschung (Institute for Microstructure Research) is working in a number of fields selected with an emphasis on the atomistic and microstructural understanding of materials properties and the possibility to contribute to the development of technology. In some of these fields the competence spans the whole range from materials preparation via basic research to technical devices. In others access to interesting materials and problems is provided by qualified collaborations. Besides this general-physics and technology part of the institute there is a second part of special competence. This is structure research by means of modern transmission electron microscopy and scanning tunnelling microscopy. This work is carried out within the Jülich Centre for High-Resolution Electron Microscopy operated by the institute.

Research Fields

(1) *Ceramic Superconductors*: Thin-film and heterostructure production, Josephson effects, and their application in magnetometer systems and spectroscopic techniques.

(2) *Semiconductors*: Structural investigations, mainly by transmission electron microscopy, of thin films and heterostructures. In collaboration with various research groups we are studying growth-related problems, like the relaxation mechanisms in SiGe films or the influence of doping on the microstructure in as-grown and annealed low-temperature grown GaAs films. Another topic is the study of electronic states in compound semiconductors by scanning tunnelling microscopy employing a technique developed in our group. It permits, via the detection of the far-reaching Debye screening cloud at the surface, an investigation of charged doping or impurity atoms in the bulk.

(3) *Metallic Alloys*: This concerns two major fields, quasicrystalline alloys and structurally complex alloy phases (SCAP). We are growing large single quasicrystals and SCAP crystals for our own research but also for users world-wide. Our own work on quasicrystals and SCAP concentrates on phase-diagrams, plasticity and surface physics.

(4) *Electroceramics*: In the field of electroceramic materials we take advantage of our long-standing experience with respect to perovskitic materials both in preparation and in transmission electron microscopy. In collaboration with the Institut für Elektrokeramische Materialien (Prof. Waser) we dedicate a large research capacity to the investigation of the structural aspects of the production and properties of electroceramic thin films.

(5) *High-Resolution Electron Microscopy*: The theoretical and technical aspects of atomic-resolution transmission electron microscopy are one of the central fields of interest of our group. Computer program packages for the exit wave-function reconstruction developed in the institute are in use world-wide. The institute co-developed and houses the world's first aberration-corrected transmission electron microscope with a record resolution of 1.3 Å at 200 kV.

Equipment

The institute has at its disposal sputtering deposition machines, some of them with three-target facilities, which were developed and built in the institute for the high-quality deposition of ceramic superconductor thin films and heterostructures. For device production local clean room, structuring and packaging facilities are available. The institute operates the Jülich Centre for High-Resolution Electron Microscopy with two 400 kV JEOL machines of the type 4000 EX/FX, a JEOL 2000 EX, a PHILIPS CM20 FEG, the spherical-aberration corrected PHILIPS CM200 FEG and a JEOL 840A scanning microscope. The priority in scanning tunnelling microscopy is on high-temperature investigations. Our instruments: Two microscopes with *in-situ* cleaving facilities and *ex-situ* heating up to 750 °C. An *in-situ* heating STM (Omicron) was installed in 2000. For the work on alloy plasticity a Zwick mechanical testing system is available. The institute operates together with the Institut für Streumethoden (Prof. Brückel) the IFF laboratory for crystal growth.

Special results and developments in 2001

Our *dc*-SQUIDs on the basis of ramp-type and bicrystal junction geometry continue their success with world record in sensitivity. As a supplier of TRISTAN (USA, formerly Conductus) our devices are used commercially. The market demands represent challenges to science and technology, and our work in this field will be continued as long as we can derive good science from it. We have a unique position with respect to the development of Hilbert-transform spectroscopy on the basis of the *ac*-Josephson effect. This technique provides an excellent tool for spectroscopy in the frequency range of 10^{10} to 10^{13} Hertz. It is broad band and orders of magnitude faster than Fourier spectroscopy. Here we have an excellent collaboration with the Institute for Radioelectronics (IRE) in Moscow with which we operate a joint superconductivity group. After our successful demonstration of the applicability of Hilbert spectroscopy for the determination of the shape of electron bunches in the TESLA test facility in Hamburg the joint project with DESY was brought to an end. Experiments will be resumed as soon as the TESLA facility has reached a stable beam situation. The BMBF project of a fast gas spectrometer was finished successfully. Current developments are focussing on two aspects. (1) Still the relatively high noise level of HTc devices represents a principle obstacle for application. Our studies have shown that fabrication conditions of Josephson junctions can be still substantially improved with corresponding gains in performance. (2) The lack of high-intensity broad-band radiation sources in the

far infrared is one of the major obstacles on the way to a wider application of Hilbert spectroscopy (e.g. using the rotation bands of molecules). We are currently testing ultra-short pulse lasers as novel far-infrared sources.

Our project of a SQUID microscope is continuing. There is extraordinary strong interest in such instruments in semiconductor industry. The first prototypic parts have been built and tested successfully. We expect, after delays due to loss in personnel and difficulties with suppliers, that a prototype microscope can start operation during 2002.

The successful project of the spherical-aberration corrected transmission electron microscope in which Jülich was a partner has triggered new activities in electron optics world wide. In Germany this concerns the SATEM (our institute) and the SESAM (MPI Stuttgart) projects in collaboration with ZEISS-LEO, Oberkochen, and CEOS, Heidelberg. SATEM will be the world's first Subangström-Instrument. The delivery had to be postponed by LEO by 1 year to summer 2003. SATEM will maintain the institute's position as a pioneer in advanced instrumentation. However, this success has to been seen in connexion with the problem that the abundant technical problems with these prototypes require an extraordinary commitment in personnel and the need to accept excessive down times. On the other hand, the institute's basic microscope equipment is after 15 years of service definitely out of date. The result is a rather problematic situation, in particular with respect to modern materials applications. This is at the origin of plans to apply for financial support for the replacement of the JEOL 2000EX TEM and the 860A SEM.

Another field in which our institute is respected as an international leader is exit wave-function reconstruction for atomic resolution imaging in transmission electron microscopy. End of 2001 FEI has purchased our complete software package for implementation in the Tecnai series of advanced transmission electron microscopes.

The alloy physics group has successfully started an extended research program in a new field which we termed structurally complex alloy phases (SCAP). This concerns intermetallics with giant unit cells containing hundreds to thousands of atoms on which essentially nothing is known with respect to physical properties. A special Symposium is organized by us at the DPG Frühjahrstagung 2002 in Regensburg. This field will also play a role in a Chinese-German research program on Modern Metallic Materials Design organized on behalf of the DFG and the NSFC by Profs. Herlach, Köln, and Urban, Jülich, whose kick-off meeting was held at Beijing in November 2001. We are, together with Prof. Dubois, Nancy, in the process of organizing an EU network on this subject.

In recent years great efforts went into joint doctor student programs with foreign universities. Formal contracts were signed with the Russian Academy of Sciences, the University of Kiev, the Tsinghua University and the Institute of Physics, Beijing, the Dalian University and Wuhan University, China. In the framework of this special program the doctor students are working up to three years in Jülich on a grant supervised by the Jülich Doktorandenausschuß, but they will pass their examina in their home university.

Outstanding results of the year 2001:

- The principal possibility to measure broadband spectra in the sub-teraherz range by Hilbert spectroscopy has been successfully demonstrated. The transmission spectra of CO-gas and mesh filters could be measured by Hilbert spectroscopy using a Hg-lamp as a broadband source of radiation.
- The interface structure, epitaxial strain and interfacial defect formation in the STO/SRO/LAO and BTO/MgO film systems could be elucidated by means of high-resolution TEM.
- By means of quantitative contrast analysis of electron micrographs the interdiffusion coefficient in AlSb/GaSb heterostructures could be measured for the first time. Under Sb rich conditions interdiffusion is significantly faster than under Ga rich conditions. This can be explained by different diffusion mechanisms.
- By He implantation followed by subsequent temperature treatment it was possible to produce nearly entirely stress-free $Si_{0.7}Ge_{0.3}$ layers on Si (100). This technologically relevant result can be explained on the basis of our TEM analyses which demonstrate that He bubbles are acting as sources for dislocations involved in stress relaxation.
- By extension of the exit wave-function reconstruction technique a method was developed by which all relevant optical parameters of atomically resolving TEM images can be determined directly in the area in which the structure is studied. These parameters are required as input in quantum-mechanical calculations of the images or the wave function.
- By cross sectional STM the roughness of the *electronic interfaces* of *p-n* GaAs multilayers was investigated. The high roughness level can be explained by dopant atom clustering induced by many-body interactions. This effect is limiting the precision of the spatial and energetic positioning of the Fermi energy in nanoscale semiconductor structures. Thus dopant atom clustering may induce an ultimate limit to miniaturization in semiconductor devices.

Prof. Dr. Knut Urban

Institute for Microstructure Research

Personnel 2000/2001 and areas of activity

Scientific Staff	Field of Activity	No.
Dr. Y. Divin	Hilbert-spectroscopy	(23.42.0)
Dr. Ph. Ebert	Scanning tunneling microscopy of semiconductors and quasicrystals	(23.55.0, 23.42.0)
Dr. M. Faley	High-T_c-Superconductor SQUIDs, Multilayer structures, SQUID-Microscopy	(23.42.0)
Dr. M. Feuerbacher	Plasticity of quasicrystals	(23.55.0)
Dr. B. Grushko	Crystal growth, phase diagrams of alloys	(23.55.0)
Dr. C.L. Jia	Characterization of superconductors, diamond and electroceramic films by high-resolution electron microsopy	(23.42.0)
Dr. M. Lentzen	Reconstruction techniques in high-resolution electron microscopy, Cs-corrected transmission electron microscopy for imaging of interfaces in semiconductors and of superconducting materials	(23.42.0, 23.55.0)
Dr. M. Luysberg	Transmission electron microscopy of semiconductor heterostructures, low-temperature GaAs and microcrystalline silicon	(23.42.0)
Dr. U. Poppe	Superconductivity, tunneling spectroscopy, High-T_c superconductor thin films and multilayers, SQUID-Microscopy	(23.42.0)
Dr. A. Thust	Reconstruction techniques in high-resolution electron microscopy, Cs-corrected transmission electron microscopy for imaging of interfaces in semiconductors, electron microscopy of superconducting materials	(23.42.0, 23.55.0)
Prof. Dr. K. Urban	Head of Institute	(23.42.0, 23.55.0)
Technical Staff		
M. Beyss	Crystal growth, Materials preparation and characterization	(23.55.0)
DI W. Evers	Physical experimental technique, low temperature technique, thin film production	(23.55.0, 23.42.0)
A. Fattah	Crystal growth, Materials preparation and characterization	(23.55.0)
K. Fischer	Crystal growth, Materials preparation and characterization	(23.55.0)
R. Fischer	Metallography, Materials preparation and characterization	(23.55.0)
DI K.-H. Graf	Electronics, Electronic data processing, scanning tunneling microscopy	(23.55.0, 23.42.0)
D. Meertens	Metallography, semiconductor preparation, scanning- and transmission electron microscopy	(23.55.0, 23.42.0)
W. Pieper	Technical supervisor, Centre for High Resolution Electron Microscopy	(23.55.0, 32.42.0)
I. Rische-Radloff	Secretary	
K. Schwill	Trainee	
R. Speen	SQUID-Microscopy, Sputtering systems	
C. Thomas	Crystal growth, Materials preparation and characterization	(23.55.0)
G. Waßenhoven	Photolaboratory, photography technique	(23.55.0, 23.42.0)
E. Würtz	Metallography, semiconductor preparation, scanning and transmission electron microscopy	(23.55.0, 23.42.0)

Junior scientists		
Dr. Y. Qin	Cs-corrected transmission electron microscopy of electroceramic thin films	(23.42.0)
Dr. L. Houben	Structure characterization of microcrystalline silicon thin films and solar cells. Investigation of potential distributions at grain boundaries in semiconductors and semiconductor devices by holographic imaging.	(23.42.0)
Dr. K. Tillmann	Quantitative analysis of semiconductor heterostructures by high-resolution transmission electron microscopy and finite element simulations	(23.42.0)
Doctor students		
V. Chirotov	Broadband Hilbert-Transform Spectroscopy with high-T_c Josephson junctions	(23.42.0)
M. Heggen	Plasticity of quasicrystals and complex intermetallic phases	(23.55.0)
B. Jahnen	Interdiffusion in antimonide-based heterostructures	(23.42.0)
H.Z. Jin	Investigation of electroceramic thin films by high resolution electron microscopy	(23.42.0)
P. Schall	Plasticity of quasicrystals and related intermetallic phases	(23.55.0)
F. Kluge	Scanning tunneling microscopy of quasicrystals	(23.55.0)
S. Mi	Formation of intermetallic and quasicrystalline phases in ternary alloys of aluminium with transition metals	(23.55.0)
U. Semmler	Diffusion and dynamic effects on compound semiconductor surfaces	(23.42.0)
J. Wang	The nature of plasticity in quasicrystalline alloys and related approximants	(23.42.0)
M. Winter	Microwave frequency standards	(23.42.0)
M. Yurechko	Formation of intermetallic phases in ternary alloys of aluminium with transition metals	(23.55.0)
M.Liatti	Signal/noise optimisation in heterostructures	(23.55.0)
He	Investigation of electroceramic thin films by high resolution electron microscopy	(23.42.0)
S. Balanetsky	Formation of intermetallic phases in ternary alloys of aluminium with palladium and a second transition metal	(23.55.0)
Diploma students		
D. Kirch	He-Implantation into SiGe/Si Heterostructures	(23.42.0)
Th. Lange	Microstructural investigations of icosahedral Zn-Mg-RE quasicrystals	(23.42.0)
C. Scholten	Influence of the microstructure of microcrystalline silicon solar cells on their optoelectronic properties	(23.42.0)
Guests		
P. Shadrin	AFM and LSM of high T_c Josephson junctions	(23.55.0)
Dr. J. Wu	Electronmicroscopy and production of oxide films	(23.42.0)
Prof. Ohnuki	Irradiated metallic heterostructures	(23.55.0)
Prof. F. Spaepen	Plasiticity of bulk metallic glosses	
Dr. Chr. Kisielowski	Cs-corrected transmission electron microscopy of semiconductors	(23.55.0)

Prof. T. Velikanova	Formation of intermetallic phases in ternary alloys of aluminium with transition metals	(23.55.0)

Investigation of the Al-Pd-Co alloy system

B. Grushko, M. Yurechko and S. Mi
Institut für Mikrostrukturforschung

The Al-Pd-Co alloy system was studied in the range of 50 to 100 at.% Al. Isothermal sections at 1050, 1000, 940 and 790°C were determined. Six stable ternary compounds designated W, Y_2, U, V, F and C_2 were revealed and characterized.

F&E-Nr: 23550

A search for new quasicrystalline and related phases leads us to the replacement of Ni by Pd (element from the same column of the periodic table) in Al-Ni-Co, the extensively studied alloy system exhibiting formation of decagonal quasicrystals. Only a few works have been dedicated till now to the Al-Pd-Co alloy system [1]. The total of 90 ternary alloys of this system was studied in the range of 50 to 100 at.% Al using SEM, TEM, XRD and DTA. Isothermal sections at 1050, 1000, 940 and 790°C were determined. Six stable ternary compounds designated W, Y_2, U, V, F and C_2 were revealed and characterized. The results of this work are reported in [2-5] and in related contribution [6] where the Al-Pd binary alloy system was updated.

The crystallographic data of the ternary phases are compiled in Table 1. For example, the results concerning one of the phases (the U-phase) are presented here in more details, for others only briefly.

The monoclinic U-phase was found in an elongated compositional range between about $Al_{69.1}Pd_{18.5}Co_{12.4}$ and $Al_{70.2}Pd_{11.4}Co_{18.4}$. It melts between 1000 and 1050°C. TEM examinations of the U-phase revealed pronounced sixfold diffraction patterns (Fig.1c) whose dense nets of reflections are typical of a principal zone axis.

However, neither hexagonal nor cubic lattice could be proved for the U-phase, rotation experiments confirmed a monoclinic unit cell. The diffraction patterns in Fig.1 are associated with the principal zone axis of a *C*-centered monoclinic structure and the following reflection conditions: *hk0*: $h+k=2n$; *h00*, *00l*: $h=2n$ and *0k0*: $k=2n$. The lattice parameters determined from the electron diffractograms were refined from the powder XRD data (see Table 1). The [001] diffraction pattern of the U-phase is surprisingly sixfold. Indeed the interplanar spacings of (020) and (110) are 1.4500 nm and 1.4609 nm respectively and the angle between them is 59.75° as obtained by calculation from the refined lattice parameters.

The W-phase is closely related to the decagonal quasicrystals [7]. It solidifies from the liquid above 1050°C and decomposes between 1050 and 1000°C. A similar structure was observed in Al-Ni-Co alloys where under different conditions a stable decagonal phase can be formed.

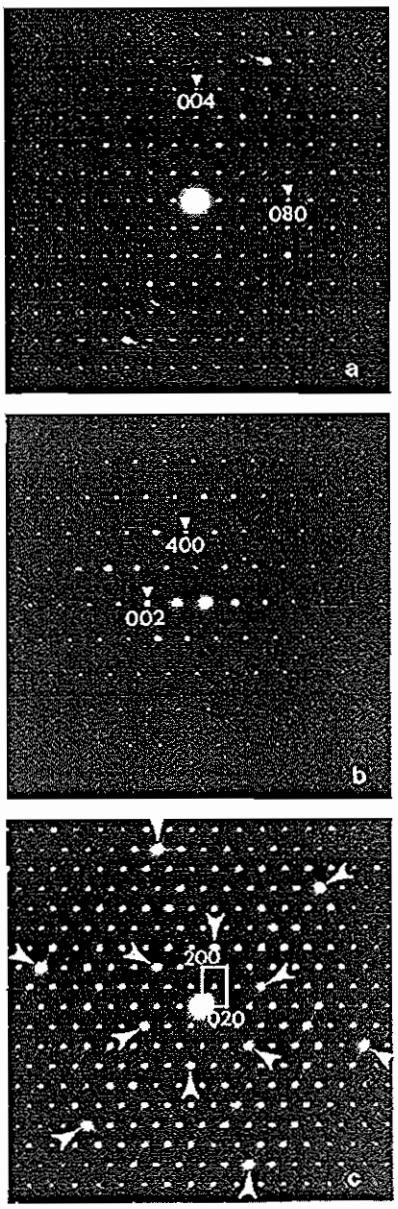

Fig. 1. Electron diffraction patterns of the U-phase: (a) [100], (b) [0-10] and (c) [001] zone axis. In (c) the strong spots displaying a slightly distorted hexagon are marked by arrows.

The V-phase has a monoclinic structure. It solidifies from the liquid above 1050°C and decomposes between 1000 and 940°C. The cubic F-phase was found in a compositional range between about $Al_{71.3}Pd_{12.2}Co_{16.5}$ and $Al_{72.5}Pd_{8.0}Co_{19.5}$. The formation temperature of the F-phase was determined between 1000 and 1050 °C, the phase was observed down to the lowest temperature of the investigation (790°C). The Y_2-phase was observed below 1000°C. This orthorhombic phase is isostructural to that in Al-Ni-Co and is formed at similar compositions. The C_2-phase was observed in a small compositional range around $Al_{63.0}Pd_{26.5}Co_{10.5}$ at 790°C.

Both Al-Pd ε_6 and ε_{28} [6] dissolve Co but their separation in ternary compositions was not clearly observed by metallography. Therefore, in the ternary diagram they are shown as one phase designated ε. The Co solubility limit of ε_6 is quite low and not yet specified. The ε_{28}-phase extends probably up to 16.1 at.% determined by EDX, it was observed by electron diffraction in a number of samples belonging to the ε range, the highest-Co sample contained 15.6 at.% Co. In this range two other structures designated ε_{22} and ε_{34} were also observed. Their lattice parameters are included in Table 1.

The partial isothermal section of Al-Pd-Co at 1050°C is presented in Fig.2. The ternary phases W, F and V were observed in equilibrium with the liquid which occupies a significant part of the diagram. M, Z and Al_5Co_2 dissolves several at.% Pd. At 790°C (Fig.3) the extended ε range can be seen. The Al_9Co_2 dissolves up to 2.6 at.% Pd. The range of the Y_2-phase extends from 2.7 to 5.2 at.% Pd. The U and F phases are also observed at this temperature.

References

[1] B. Grushko and M. Yurechko, IFF report 1999.
[2] M. Yurechko and B. Grushko, Mater. Sci. Eng. A294-296 (2000) 139.
[3] S. Mi, M. Yurechko, J.S. Wu and B. Grushko, J. Alloys Comp. 329 (2001) L1.
[4] M. Yurechko, T. Velikanova and B. Grushko, Dopovidi NAN Ukrainy, (in Russian) accepted.
[5] M. Yurechko, B. Grushko, T. Velikanova, and K. Urban, J. Alloys Comp. in press.
[6] M. Yurechko, A. Fattah, T. Velikanova and B. Grushko J. Alloys Comp. 329 (2001) 173.
[7] K. Yubuta, W. Sun, K. Hiraga Phil. Mag. A75 (1997) 273.

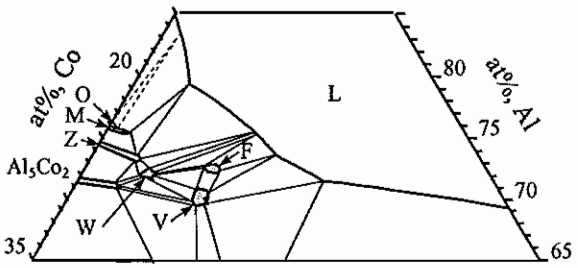

Fig.2 Partial isothermal section of Al-Pd-Co at 1050°C. The provisional tie-lines are shown by broken lines. The liquid is designated L.

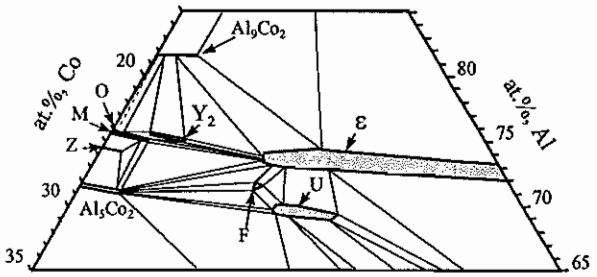

Fig.3 Partial isothermal section of Al-Pd-Co at 790°C.

Table 1. Crystallographic data of the ternary Al-Pd-Co phases. The lattice parameters are given for the mentioned compositions.

Phase	Space group or crystal symmetry	Lattice parameters				at composition, at.%		
		a, nm	*b*, nm	*c*, nm	β, °	Al	Pd	Co
W [a]	$Pmn2_1$	2.36	0.82	2.07	-	72.0	4.8	23.2
V	*P*121, *P*1*m*1 or *P*12/*m*1	1.0068	0.3755	0.6512	102.38	70.0	10.0	20.0
U	*C*121, *C*1*m*1 or *C*12/*m*1	1.9024	2.9000	1.3140	117.26	69.1	16.5	14.4
F	$P2_1/a\bar{3}$	2.4397	-	-	-	72.8	9.0	18.2
C_2	$Fm\bar{3}$	1.5507	-	-	-	63.0	26.5	10.5
Y_2	*Immm*	1.5451	1.2105	0.7590	-	75.5	3.8	20.7
ε_{22} [a]	orthorh.	2.35	1.68	5.70	-	72.0	20.0	8.0
ε_{34} [a]	orthorh.	2.35	1.68	7.01	-	70.0	15.0	15.0

Effect of Helium Ion Implantation and Annealing on the Relaxation Behaviour of Pseudomorphic $Si_{1-x}Ge_x$ Buffer Layers

D.Kirch, M. Luysberg

Institut für Mikrostrukturforschung

The influence of He implantation and annealing on the relaxation of $Si_{0.72}Ge_{0.28}$ layers on Si substrates is investigated. Proper choice of the implantation energy results in a narrow defect band underneath the substrate/epilayer interface. During annealing at 700°C to 1000°C, He-filled bubbles are created, which act as dislocation sources for misfit dislocation generation. Complete annihilation of the threading dislocations is theoretically predicted, if a certain bubble density with respect to the buffer layer thickness is maintained. The variation of the implantation dose and the annealing conditions changes the density and size of He bubbles resulting in characteristic differences of the dislocation structure. A strain relaxation of 70% of $Si_{1-x}Ge_x$ layers with Ge fractions up to 30 at.% is obtained at temperatures as low as 850°C. Simultaneously low threading dislocation densities of 10^7 cm^{-2} are achieved.

F&E-Nr: 2342 8000

"Virtual" substrates of strain relaxed $Si_{1-x}Ge_x$ layers are the key to control the strain and therefore the bandgap and bandoffset of Si layers grown onto such substrates within heterostructure devices, like e.g. heterobipolar transistors. The promising application in high speed electronic devices based on Si technology has triggered many efforts to tackle the basic problem: Initially, $Si_{1-x}Ge_x$ layers deposited onto Si (100) substrates below the critical thickness are metastable, dislocation free and tetragonally distorted according to the lattice mismatch. These $Si_{1-x}Ge_x$ layers have to be transformed into the relaxed state without introducing threading dislocations into the films. Many approaches have been developed to overcome this problem: by growth of several µm thick compositionally graded layers, by use of Ge implantation into thin Si layers, by growing thick $Si_{1-x}Ge_x$ layers silicon-on-insulator wafers, or by depositing SiGe buffer layers onto a low-temperature grown Si or SiGe buffer layer (see references in [1]). None of these approaches gives satisfactory results with respect to high degree of relaxation, low threading dislocation densities, or implementation of the method into Si device processing.

In our work we investigate the relaxation behaviour of MBE grown $Si_{1-x}Ge_x$ layers on Si (100) substrates in dependence on He implantation and annealing conditions [1]. Transmission electron microscopy is applied for structural characterization

The effect of different He implantation doses and annealing temperatures on the microstructure of a $Si_{0.72}Ge_{0.28}$/Si(100) heterostructure is shown in the cross-sectional electron micrographs (Fig. 1). In all cases, a He bubble layer can be clearly seen to be separated by about 80 nm from the interface. For the implantation dose of $2.0x10^{16}$ cm^{-2} and annealing at 850°C no bubbles are located within the interface (Fig. 1a). This is in contrast to the higher implantation dose and/or higher annealing temperature

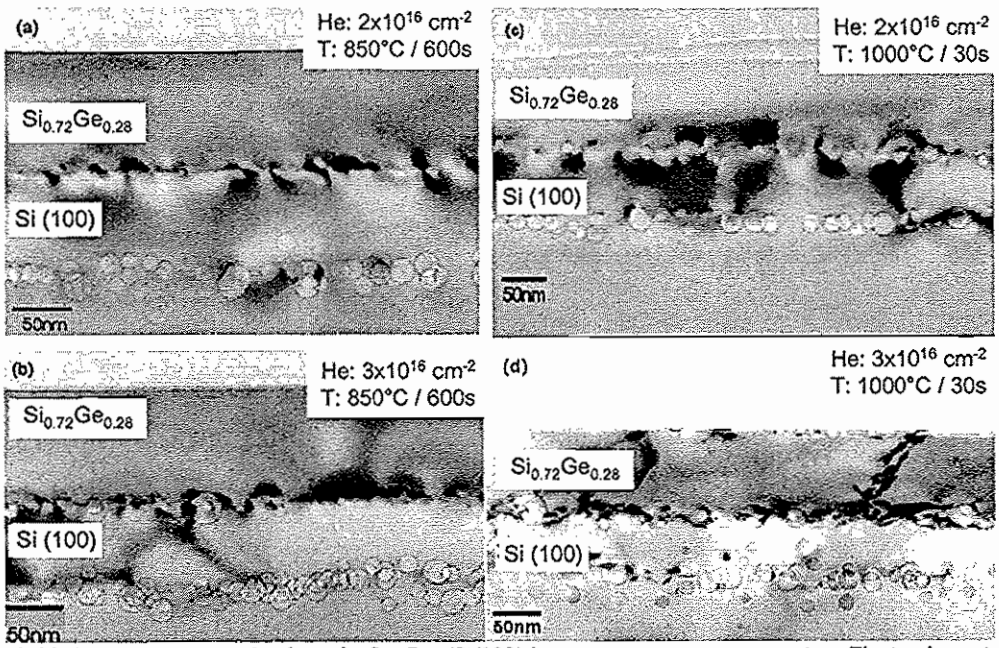

Fig. 1: The bright field electron micrographs show the $Si_{72}Ge_{28}$/Si(100) heterostructure in cross section. The implantation dose and annealing conditions are indicated. Note the cavity layer about 80 nm below the interface. The strain fields of the misfit dislocation network make the interface clearly distinguishable.

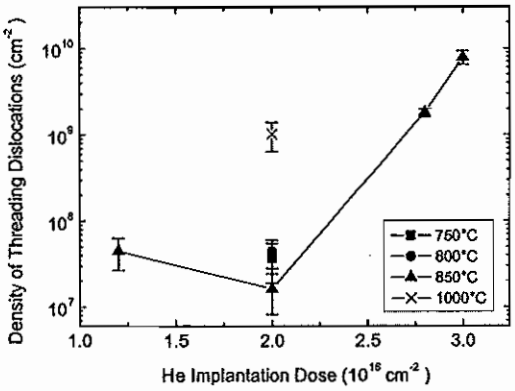

Fig. 2: Threading dislocation density plotted versus the He implantation dose for the different annealing temperatures indicated.

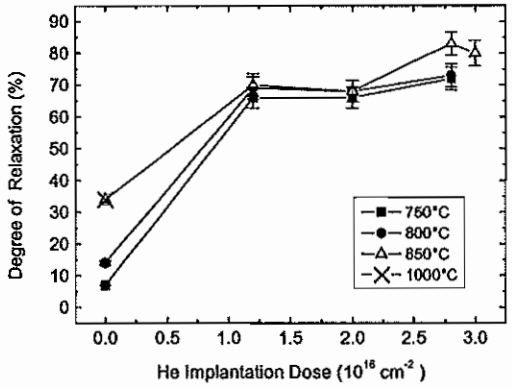

Fig. 3: Degree of relaxation versus the impla-tation dose for different annealing tempera-tures. Samples at 0 cm^{-2} were annealed only.

(Figs. 1b-d), where considerable densities of He bubbles are found within the interface. Furthermore, the bubble layer is much broader in the case of the highest dose and temperature (Fig. 1d), where also a high density of threading dislocations is present within the $Si_{72}Ge_{28}$ layer. In all cases the $Si_{72}Ge_{28}$/Si(100) interface is marked by strain contrast associated with the misfit dislocation network. Nearly all of the misfit dislocations are of 60° type, which was determined from contrast analyses using weak beam dark field images of plan-view samples.

The threading dislocation density shown in Figure 2 was determined from plan view samples by counting the number of dislocations within a defined area. The threading dislocation density obtained after annealing at 1000°C or at high implantation doses is always larger than 10^9 cm^{-2}, which is unacceptably high for any device applications. A minimum threading dislocation density of about 10^7 cm^{-2} is observed for a He implantation dose of $2.0x10^{16}$ cm^{-2} and an annealing temperature of 850°C.

The degree of relaxation (Fig. 3) was measured by use of ion channeling angular yield scans A high degree of relaxation of up to 85% is obtained if high He implantation doses and an annealing at 850°C are applied. Considerably lower values of only 35% are achieved if the samples are annealed only. Since the lowest threading dislocation density was observed for an He implantation dose of $2.0x10^{16}$ cm^{-2} and annealing at 850°C, this condition seems to be the most favourable so far with respect to a high degree of relaxation connected with a low threading dislocation density.

The He bubbles formed after implantation and subsequent annealing promote the formation of misfit dislocations. This can be concluded from the fact that the degree of relaxation is considerably lower in unimplanted and only annealed samples as in those containing He bubbles. Recently, a theoretical model was proposed attributing the strain relaxation to the He filled cavities acting as efficient nucleation sources for dislocations [2]. Dislocation loops punched out by the He filled overpressurized cavities glide to the interface. When a loop comes into contact with the SiGe layer it experiences an asymmetric force. As a consequence one side of the loop is pinned at the interface where it forms a strain relieving misfit segment. The other side is driven by the mismatch stress to the surface where an atomic step is generated. The accompanied threading dislocations annihilate efficiently by a combined climb-glide mechanism. Obviously the density of dislocation sources, i.e. He bubbles, has to be sufficiently high to allow the generation of a large number of misfit dislocations to relax the SiGe layer. In addition, the distance between threading dislocations has to be smaller than the annihilation radius of two dislocations with opposite Burgers vectors. For all of our samples the density of He bubbles fulfils the requirements of the model. So, even samples with high He implantation doses and/or high annealing temperatures agree with the model, where high threading dislocation densities are observed. This may indicate that in these cases the conventional relaxation mechanism still operates, introducing threading dislocations, which cannot effectively annihilate. In addition, these samples contain a considerable density of bubbles within the interface. These react with the dislocations, and therefore impede motion of the threading dislocations necessary for annihilation. On the other hand, the initial overpressure within the bubbles is not known to date, which hinders quantitative evaluation of their strength as dislocation source. Qualitatively, our experimental observations of the bubble structure and types of dislocation agree with the model.

Acknowledgements

The fruitful cooperation with B. Holländer, St. Lenk, S. Mantl (ISG, Forschungszentrum Jülich), H. Trinkaus (IFF), Th. Hackbarth, H.-J. Herzog (DaimlerChrysler AG Ulm) and P.F.P. Fihtner (University of Porto Allegre, Brazil) is greatfully acknowedged.

References

[1] M Luysberg, D Kirch, H Trinkaus, B Holländer, St Lenk, S Mantl, H-J Herzog, T Hackbarth, and P F P Fichtner 2001, Inst. Phys. Conf. Ser., will appear

[2] Trinkaus H, Holländer B, Rongen St, Mantl S, Herzog H-J, Kuchenbecker J and Hackbarth T 2000 Appl. Phys. Lett. **76**, 3552

Interdiffusion of GaSb/$Al_xGa_{1-x}Sb$ Heterostructures

B. Jahnen, M. Luysberg

Institut für Mikrostrukturforschung

Interdiffusion of heterostructures based on the GaSb/AlSb material system is investigated by means of bright-field transmission electron microscopy (TEM). Samples grown by metal organic molecular beam epitaxy (MOMBE) are subjected to annealing experiments under both Sb-rich and Ga-rich conditions. Changes of concentration profiles of the group-III elements are determined by evaluating thickness fringes of cleaved 90° wedge specimens on a nanometer scale. Interdiffusion is found to be significantly slower under Ga-rich conditions than under Sb-rich conditions and can be described numerically by an interdiffusion coefficient with non-linear concentration dependency. The experimental results are interpreted in terms of a diffusion mechanism by group-III vacancies. F&E-Nr: 2342 8000

Current research activities in the field of optoelectronic devices for the infrared range are focused on semiconductor heterostructures based on group-III antimonides, a low-eV material system [1]. The low-misfit GaSb/AlSb system is of particular interest because of its potential use as quantum wells and walls in the active region of emitters for optical data transmission. In the last years, this has led to an increased interest in the investigation of diffusion phenomena in antimonides and primarily in the nature of interdiffusion in the GaSb/AlSb system. Recently, self-diffusion experiments in GaSb were carried out that suggest a good agreement between the mechanisms of self-diffusion in GaSb and GaAs on an atomic scale and emphasise the importance of Ga vacancies for diffusion [2].

For the systematic investigation of post-growth interdiffusion of GaSb/$Al_xGa_{1-x}Sb$ heterostructures reported on here, well-defined Sb-rich and Ga-rich annealing conditions were established that lead to different equilibrium point defect concentrations in the samples during the annealing experiments. To this end, quartz ampoules were fabricated in which the samples were subjected to thermal treatment under a residual pressure of less than 5×10^{-6} Torr. The samples consist of a seven-fold 120 nm GaSb/ 8 nm AlSb superlattice and a 500 nm GaSb cap layer grown by MOMBE onto a (001)-oriented, nominally undoped GaSb substrate. The individual layers of the superlattice serve to reveal changes of the local annealing conditions as a function of distance from the sample surface. The experiments cover a temperature range of 600 °C to 700 °C and annealing times from 10 minutes to 360 minutes. For TEM characterisation, the samples were cleaved along {110} planes to obtain wedge specimens with a fixed 90° thickness gradient. Concentration profiles were acquired by use of the bright-field imaging technique [3], resulting in thickness fringes with chemical contrast due to the dynamical interaction of the chemically sensitive {200}-beams with the direct beam (fig. 1). At a field of view of 150 nm, lateral resolution of 1.8 nm is achieved. The uncertainty of measurement is 4.5 at-% to 11 at-% aluminium.

Fig. 2 shows a typical set of aluminium concentration profiles of several layers after annealing under Sb-rich conditions at 620 °C for 60 minutes, 90 minutes and 120 minutes, respectively. There are no significant differences between the individual layers of the superlattice after a given annealing time, indicating homogeneous annealing conditions and thus a homogeneous depth distribution of the point defect that mediates interdiffusion. The long tails

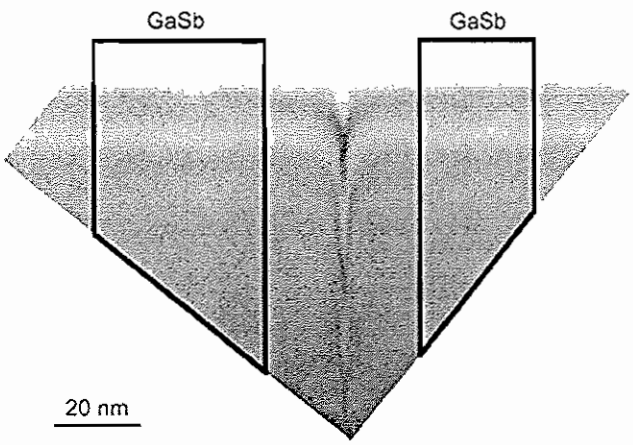

Fig. 1: Bright-field electron micrograph of a sample after annealing, <100> zone axis orientation. Part of the superlattice with a layer of high aluminium concentration is visible in the central part of the image due to changes of the thickness fringes. Annealing conditions:620 °C, 90 minutes, Sb-rich conditions.

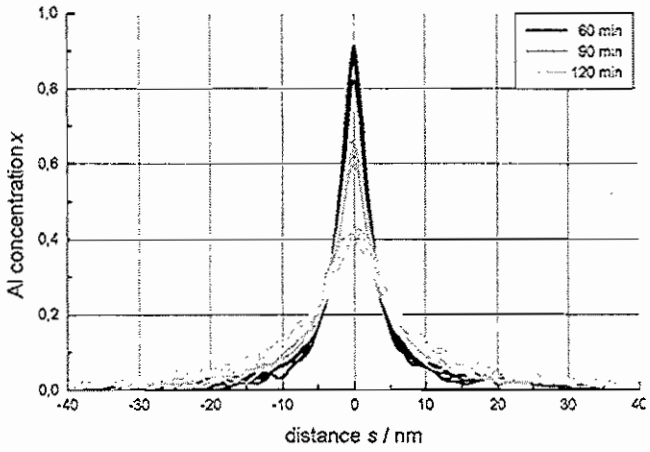

Fig. 2: Experimentally obtained aluminium concentration profiles across layers of high aluminium concentration. Each curve corresponds to one layer. Annealing conditions: 620 °C, 60 minutes, 90 minutes and 120 minutes, respectively, Sb-rich conditions.

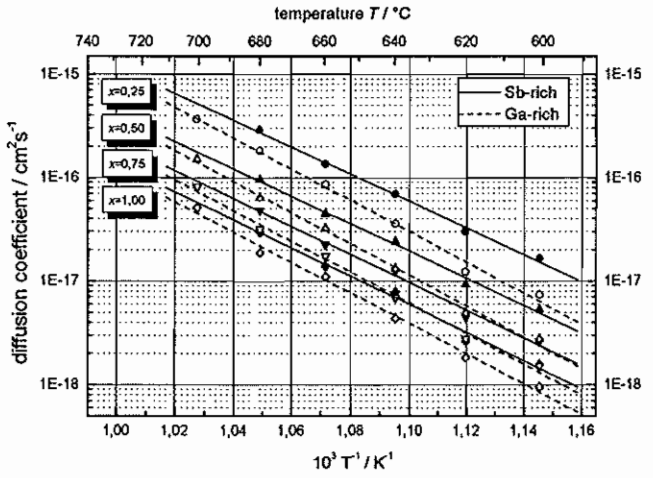

Fig. 3: Diffusion coefficient versus reciprocal annealing temperature for four selected aluminium concentrations and both Sb-rich and Ga-rich annealing conditions.

of the profiles indicate a comparably fast diffusion of aluminium into GaSb, whereas the steep peaks show a slower diffusion of gallium into regions of high aluminium concentration. These findings can be accounted for quantitatively by a concentration dependent interdiffusion coefficient D, with D decreasing for increasing aluminium concentration x of the $GaSb/Al_xGa_{1-x}Sb$ solid solution. By solving Fick's second law of diffusion numerically, we find that the experimentally obtained concentration profiles are best reproduced with a non-linear concentration dependency of D with x:

$$D(x) = \frac{D_{Al}}{(D_{Al}/D_{Ga} - 1)x^{\gamma} + 1} \quad (1)$$

In this equation, D_{Al} and D_{Ga} represent the diffusion coefficients of aluminium in GaSb and gallium in AlSb, respectively. γ is an additional fit parameter with values of 1.5 to 1.9. At a given concentration x, $D(x)$ varies by about one order of magnitude within the range of temperatures. In this range also, the diffusion coefficient D_{Al} of aluminium in GaSb is larger than the diffusion coefficient D_{Ga} of gallium in AlSb by more than one order of magnitude at a given temperature. Fig. 3 shows that our results of $D(x)$ closely follow an Arrhenius behaviour when plotted versus the reciprocal annealing temperature. Under Sb-rich conditions, an activation enthalpy of about 2.6 eV is obtained.

Under Ga-rich conditions, the shapes of the concentration profiles closely resemble the one shown in fig. 2 for the Sb-rich conditions. Thus, similar results are found for the concentration dependency of $D(x)$. However, interdiffusion is significantly slower under Ga-rich conditions than under Sb-rich conditions (dashed lines in fig. 3), with the differences decreasing for increasing annealing temperature, and an activation enthalpy of about 3.0 eV. In addition, under Ga-rich conditions, a deviation from uniformity of the concentration profiles is observed for intermediate annealing temperatures and times that is not found under Sb-rich conditions: in these cases, broadening of the profiles is systematically less pronounced for layers further away from the sample surface. Thus, for these experimental conditions, a temporal change in the local concentration of the point defect that mediates interdiffusion is observed.

For a model of the mechanisms of interdiffusion on an atomic scale, we interpret our experimental results in terms of vacancies on the group-III sublattice. This is in accordance with previous analyses of diffusion in nominally undoped III-V semiconductor materials. For the arsenides, this model has been confirmed both by self-diffusion and interdiffusion experiments [4]. For pure GaSb, similar conclusions have been drawn from self-diffusion experiments [2]. We therefore attribute the differences in interdiffusion caused by the ambient conditions to different concentrations of vacancies on the group-III sublattice, i.e. Ga vacancies (V_{Ga}) and Al vacancies (V_{Al}). Sb-rich conditions should favour these point defects [5]. Thus, under Sb-rich conditions, a large concentration of group-III vacancies is rapidly supplied from the sample surface. Equilibrium with the ambience is reached quickly, leading to fast interdiffusion and to no apparent inhomogeneity of the diffusion conditions within the sample. In contrast, the comparably slow interdiffusion under Ga-rich conditions can be attributed to a small concentration of group-III vacancies. In fact, with group-III vacancies being the defects that mediate interdiffusion, a strong decrease of interdiffusion could be expected, since Ga-rich conditions should favour Sb vacancies (V_{Sb}) and Ga interstitials (Ga_i). However, we find significantly but moderately reduced values of $D(x)$ and enhanced interdiffusion of the layers closest to the sample surface. These findings are in good agreement with calculations [5] and indirect measurements [6] of point defect concentrations in antimonides that suggest that even under Ga-rich conditions, group-III vacancies are created by way of a reaction which transforms Ga atoms (Ga_{Ga}) to Ga antisites (Ga_{Sb}) and simultaneously creates Ga vacancies (V_{Ga}):

$$Ga_{Ga} + V_{Sb} \Leftrightarrow V_{Ga} + Ga_{Sb} \quad (2)$$

Accordingly, the group-III vacancy concentration is increased indirectly by a growing supply of Sb vacancies from the sample surface. Thus, interdiffusion of the group-III elements can take place via vacancies on their own sublattice, even under Ga-rich conditions. These conclusions are supported by annealing experiments that show that Sb self-diffusion in GaSb is strongly suppressed under Ga-rich conditions due to a lack of Sb vacancies [2].

Acknowledgements

The work presented here was done in co-operation with A. Fattah (Institut für Streumethoden) and H. Bracht (University of Münster). The authors would like to thank R. Schmidt (ISG) and T. Bleuel (University of Würzburg) for providing the samples.

References

[1] P.S. Dutta, H.L. Bhat, J. Appl. Phys. **81**, 5821 (1997)

[2] H. Bracht, S.P. Nicols, E.E. Haller, J.P. Silveira, F. Briones, Nature **408**, 69 (2000)

[3] H. Kakibayashi, F. Nagata, Jpn. J. Appl. Phys. **24**, L905 (1985)
[4] D. Deppe, N. Holonyak, J. Appl. Phys. **64**, R93 (1988)
[5] M. Ichimura, K. Higuchi, Y. Hattori, T. Wada, N. Kitamura, J. Appl. Phys. **68** (12), 6153 (1990)
[6] G. Edelin, D. Mathiot, Phil. Mag. B **42**, 95 (1980)

Dopant atom clustering and charge screening induced roughness of electronic interfaces in GaAs *p-n* multilayers

N. D. Jäger [1], K. Urban [1], E. R. Weber [2], and Ph. Ebert [1]
[1] *Institut für Festkörperforschung, Forschungszentrum Jülich, 52425 Jülich, Germany*
[2] *University of California and Lawrence Berkeley Laboratory, Berkeley, CA 94720, U.S.A.*

The roughness of the *electronic* interfaces of *p-n* GaAs multilayers has been investigated by cross-sectional scanning tunneling microscopy. Two physically different contributions to the roughness were found, both much larger than the underlying atomically sharp 'metallurgical' interface. The roughness arises from the individual electrostatic screening fields around each dopant atom near the interface and from a clustering of dopant atoms. The latter leads to charge carrier depleted zones extending locally through the entire nominally homogeneously doped layer for layer thicknesses close to the cluster dimension, hence limiting the precision of the spatial and energetic positioning of the Fermi energy in nanoscale semiconductor structures.

Currently the dimensions of integrated semiconductor devices on microships in industrial production are characterized by a transistor gate length of about 70 nm and the research is focusing on a further reduction to 20-30 nm [1]. An endless downsizing is, however, limited by physical constraints, such as the loss of the desired band structure in atomic-scale dimensions, i.e., structures with dimensions of 1 to 2 nm. The functionality of all semiconductor devices is, however, not only depending on the band structure alone. It is critically depending on the ability to dope the semiconductor materials with foreign atoms (dopant atoms). The dopant atoms govern the position of the Fermi energy with respect to the band edges. The precise spatial and energetic positioning of the Fermi energy in nanoscale semiconductor structures is the key to the realization of devices. The smaller the devices get, the sharper the changes between differently doped sections or layers in the device structure need to be.

We investigated the physics governing the properties of interfaces between differently doped layers by analyzing GaAs *p-n* multilayers by cross-sectional scanning tunneling microscopy. We demonstrate that the *electronic p-n* interface exhibits a much larger roughness than the underlying essentially perfect 'metallurgical' interface, due to long range electrostatic screening effects of individual dopant atoms near the interfaces and due to a clustering of dopant atoms. The clustering and the inherently connected local lack of dopant atoms give rise to charge carrier depletion zones extending locally through entire nominally homogeneously doped layers once their thickness is close to the cluster dimensions.

Figure 1a shows a large scale cross-sectional scanning tunneling microscopy (STM) overview of several 30 nm wide *p*- and *n*-doped GaAs layers cleaved along a (110) plane (C and Si dopant atom concentrations of $(5\pm1)\times10^{18}$ and $(4\pm1)\times10^{18}$ cm^{-3}, respectively). An atomically resolved image is shown in Fig. 1b. The *p*- and *n*-doped layers are separated by lines with a darker contrast, whereas the doped layers themselves appear both bright. We identified the *n*- and *p*-doped layers on basis of the growth sequence, secondary ion mass spectra, and tunneling spectra.

The dark lines between the *p*- and *n*-doped layers were found to be the image of the depletion zones localized at *p-n* interfaces, where the Fermi-energy is close to midgap [2]. Thus the dark lines mark the *electronic* interface between the *n*-doped and the *p*-doped layers. It is important to note that this interface is *not* the atomically sharp metallurgical or chemical interface (marked by dashes), where the doping changes from C_{As} to Si_{Ga} or vice versa. Fig. 1 shows that the electronic interface (dark lines) exhibits a roughness much larger than one atomic layer. The white arrows in Fig. 1a point out examples of a local electronically very narrow and wide *p*-type 'layer'. Note that the individual bright hillocks with about 3 to 5 nm diameter, visible in the *p*- as well as *n*-doped layers, are the signatures of negatively charged C_{As} and positively charged Si_{Ga} dopant atoms, respectively [3]. Their contrast is essentially given by the image of the screened Coulomb potential [3], which arises from the screening of the dopant charge by free charge carriers [4]. Figure 1b shows that the depletion zone imaged as dark line circumvents each individual dopant atom. Undoubtedly each dopant atom near the metallurgical interface causes a short range

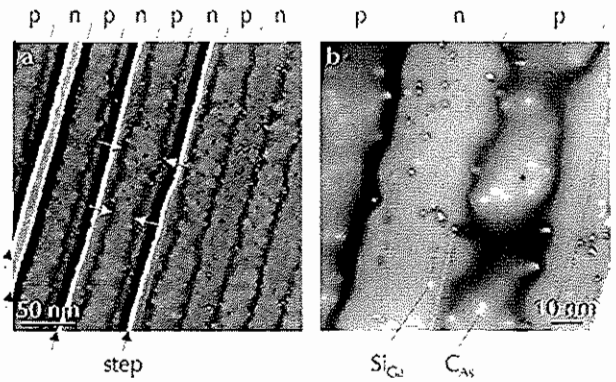

Fig. 1 Large scale (a) and atomically resolved (b) cross-sectional scanning tunneling microscopy images of multiple *p*- and *n*-doped GaAs layers. The bright hillocks marked by Si_{Ga} and C_{As} arise from individual dopant atoms. The dark lines between the *p*- and *n*-type layers are the signatures of the depletion zone at each *p-n* interface and show the position of the electronic interface. Note its pronounced roughness and its correlation with the dopant atoms.

meandering of the electronic interface on the scale of 2-5 nm. Careful inspection of large scale STM images reveals a further contribution to the interface roughness on a longer length scale, leading to the electronically wide and narrow layers (see examples marked by white arrows in Fig. 1).

In order to quantify the amplitude and correlation length of the two different roughness contributions, we computed the power spectral density, $\tilde{G}(k) = \left|\tilde{A}(k)\right|^2$, on basis of the deviation from mean of the interface lines $A(x)$ visible in the STM images, with $\tilde{A}(k)$ being the discrete Fourier transform of $A(x)$ [5]. Figure 2 shows the results for the *p-n* and *n-p* interfaces. Two separate frequency ranges are visible, one at small k values with a large slope and another one at large k values with a smaller slope. We first concentrate one the latter one, which exhibits a clear exponential decay characteristic for all our interfaces. The exponential decay, $\tilde{G}(k) = \pi a b^{-1} \cdot e^{-b \cdot k}$, corresponds to a Lorenzian functional dependence of the *real space* autocorrelation function, $G(x) = a/(x^2 + b^2)$. $(a/b^2)^{0.5}$ and b are the amplitude (equivalent to the root mean square roughness) and the correlation length of the interface roughness, respectively.

The entire data sets in Fig. 2 can be well described by *two* exponential decays and we extracted the corresponding values for the amplitudes and the correlation lengths from the fits (lines in Fig. 2). For large k values the amplitudes are (1.5±0.3) and (1.2±0.2) nm and the correlation lengths are (2.9±0.5) and (2.9±0.5) nm for the *p-n* and *n-p* interfaces, respectively. For small k values we obtained (2.2±0.5) and (2.7±0.4) nm as amplitudes and (26±8) and (23±5) nm as correlation lengths, respectively. No difference between *p-n* and *n-p* interfaces can be observed within the error margin. The quantitative analysis in Fig. 2 confirms our above observation of two different contributions to the roughness. Note, the roughness amplitudes and correlation lengths are about one order of magnitude larger than those found for heterojunction interfaces between different compounds [6], because the latter probe primarily the metallurgical interface.

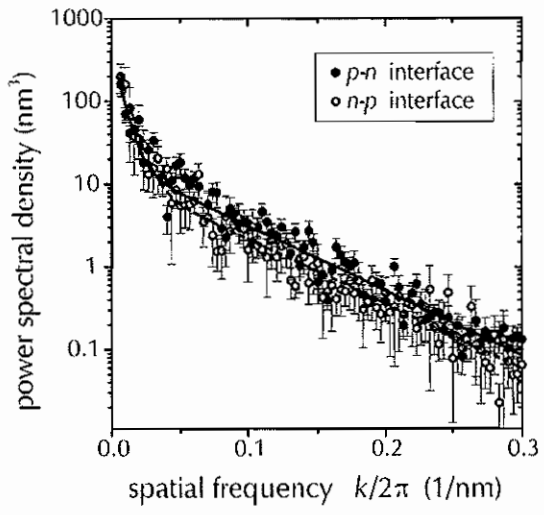

Fig. 2 Power spectral density of the electronic *p-n* (●) and *n-p* (○) GaAs interfaces obtained from STM images as seen in Fig. 1. Each data set is fitted to a sum of two exponentials representing two scales of roughness found in each interface type. The solid (dashed) line is a fit to the data of the *p-n* (*n-p*) interface.

At this stage we discuss the origin of the two contributions to the roughness of the electronic interface. First, the roughness with correlation lengths of about 3 nm and amplitudes of about 1.5 nm can be correlated to the meandering of the electronic interface around the *individual* dopant atoms. The meandering is on the same scale as the spatial extension of the charge screening clouds around individual dopants (bright area of each dopant atom). Thus the screening length of the screened Coulomb potential around the individual charged dopants governs the roughness.

Second, the physical origin of the long range contribution to the roughness can be perhaps best discussed using Fig. 1b, which shows that dopant atoms within nominally homogeneously doped layers exhibit large variations in the local concentration leading to a cluster of dopant atoms. Above and below are areas locally free of dopant atoms. This clustering induces the long range roughness of the electronic interfaces with correlation lengths of about 25 nm and amplitudes of approximately 2.5 nm.

Finally, the presence of the dopant cluster locally enlarges the electronic *p*-type layer, whereas the lack of dopant atoms nearby leads to a completely depleted zone extending locally through the entire *p*-type layer (Fig. 1b). Thus the Fermi energy is near mid gap and not near the valence-band maximum as intended. These results show that local variations in the dopant atom distribution lead in nanoscale semiconductor structures to uncontrolled Fermi-energy positions in space and energy, effectively limiting the miniaturization of semiconductor devices.

1. Intel Corporation, http://www.intel.com/research/silicon/micron.htm and references therein.
2. R. M. Feenstra *et al.*, in: *Semiconductor Interfaces at the Sub-Nanometer Scale*, Eds. H. W. M. Salemink and M. D. Pashley (Kluwer Academic, Dordrecht, 1993), p. 127; R. M. Feenstra *et al.*, Appl. Phys. Lett. **61**, 795 (1992).
3. Ph. Ebert, Surf. Sci. Rep. **33**, 121 (1999) and references therein.
4. R. B. Dingle, Phil. Mag. **46**, 831 (1955).
5. J. M. Bennett and L. Mattsson, *Introduction to surface roughness and scattering* (Optical Society of America, Washington D.C., 1989).
6. R. M. Feenstra et al., Phys. Rev. Lett. **72**, 2749 (1994); J. Harper et al., Appl. Phys. Lett. **73**, 2805 (1998); W. Barvosa-Carter et al., *Phys. Rev. B* **63**, 245311 (2001).

Publications in refereed journals

Divin Y.; Volkov O.Y.1; Pavlovskii V.V.1; Poppe U.; Urban K.
1 Institute of Radioengineering & Electronics of RAS, Moscow 103907, Russian FederationTerahertz Spectral Analysis by ac Josephson Effect in High-Tc Bicrystal Junctions
IEEE Transactions on Appl. Supercond., Vol. 11, No. 1, 582-585 (2001)
23.42.0

Divin Y.Y.; Poppe U.; Jia C.L.; Shadrin P.; Urban K.
Structural and electrical properties of YBa2Cu3O7 [100]-tilt grain boundary Josephson junctions with high IcRn-products on SrTiO3 bicrystals
Physica C, 2002 (accepted for publications)
23.42.0

Divin Y.Y.; Volkov O.Y.1; Laytti M.; Shirotov V.; Pavlovskii V.V.1; Poppe U.; Shadrin P.; Urban K.
1 Institute of Radioengineering & Electronics of RAS, Moscow 103907, Russian Federation
Hilbert spectroscopy from microwave to terahertz frequencies by high-Tc Josephson junctions
Physica C, 2002 (accepted for publications)
23.42.0

Dolinsek J.1; Klanjsek M.1; Apih T.1; Gavilano J.L.2; Giannò K.2; Ott H.R.2; Dubois J.M.3; Urban K.
1 J. Stefan Institute, University of Ljubljana, Jamova 39, SI-1000 Ljubljana, Slovenia
2 Laboratorium für Festkörperphysik, ETH Hönggerberg, CH-8093 Zürich / Schweiz
3 Ecole des Mines de Nancy, LSG2M, Nancy / F
Mn magnetism in icosahedral quasicrystalline Al72.4Pd20.5Mn7.1
Phys. Rev. B, Vol. 64, 024203-1 - 024203-7 (2001)
23.42.0

Döblinger M.1; Wittmann R.1; Gerthsen D.1; Grushko B.
1 Lab. Elektronenmikroskopie, Univ. Karlsruhe, 76128 Karlsruhe
A Transition State between Quasicrystal and Approximant in the System Al-Ni-Co
Ferroelectrics, Vol. 250, 241-244 (2001)
23.55.0

Döblinger M.1; Wittmann R.1; Grushko B.
1 Lab. Elektronenmikroskopie, Univ. Karlsruhe, 76128 Karlsruhe
Metastable transformation states of decagonal Al-Co-Ni due to inhibited decomposition
Phys. Rev. B, Vol. 64, 134208-1-134208-9 (2001)
23.55.0

Ebert Ph.; Domke C.; Urban K.
Direct observation of electrical charges at dislocations in GaAs by cross-sectional scanning tunneling microscopy
Appl. Phys. Lett. 78, No. 4, 480-482 (2001)
23.55.0

Ebert Ph.; Domke C.; Urban K.
Direct observation of electrical charges at dislocations in GaAs by cross-sectional scanning tunneling microscopy
Appl. Phys. Lett., Vol. 78, 480-482 (2001).
23.42.0

Ebert Ph.; Quadbeck P.; Urban K.; Henninger B.1; Horn K.1; Schwarz G.1; Neugebauer J.1; Scheffler M.1
Identification of surface anion antisite defects in (110) surfaces of III-V semiconductors
Appl. Phys. Lett., Vol. 79, 2877-2879 (2001).
23.42.0

Ebert Ph.
Atomic structure of Point Defects in Compound Semiconductor Surfaces.
Current Opinion in Solid State and Materials Science 5, 211-250 (2001)
23.55.0

Ebert Ph.
Defects in III-V semiconductor surfaces
Appl. Phys. A, in press (2001).
23.42.0

Estermann M.A.1; Lemster K.1; Steurer W.1; Grushko B.; Döblinger M.2
1 Laboratory of Crystallography Swiss Federal Institute of Technology, CH-8092 Zürich
2 Lab. Elektronenmikroskopie, Univ. Karlsruhe, 76128 Karlsruhe
Structure Solution of a High-Order Decagonal Approximant Al71Co14.5Ni14.5 by Maximum Entropy Patterson Deconvolution
Ferroelectrics, Vol. 250, 245-248 (2001)
23.55.0

Faley M.I.; Poppe U.; Urban K.; Paulson D.N.1; Starr T.N.1; Fagaly R.L.1
1 Tristan Technologies Inc., CA 92121, USA
Low noise HTS dc-SQUID flip-chip magnetometers and gradiometers
IEEE Transactions on Appl. Supercond., Vol. 11, No. 1, 1383-1386 (2001)
23.42.0

Faley M.I.; Poppe U.; Urban K.; Paulson D.N.1; Starr T.N.1; Fagaly R.L.1
1 Tristan Technologies Inc., CA 92121, USA
Sensitive HTS gradiometers for magnetic evaluation applications accepted for publication in
Physica C (2002)
23.42.0

Feuerbacher M.; Klein H.1; Urban K.
1 ESRF, Pluo E, B.P. 220, 38043 Grenoble Cedex, France
Plastic deformation properties of the orthorhombic ('-(Al-Pd-Mn) quasicrystal approximant
Phil. Mag. Lett., Vol. 81, No. 9, 639-647 (2001)
23.55.0

Feuerbacher M.; Schall P.; Estrin Y.1; Bréchet Y.2
1 Institut für Werkstoffkunde und Werkstofftechnik, Technische Universität Clausthal, Agricolastrasse 6, D-38678 Clausthal-Zellerfeld, Germany
2 Laboratoire de Thermodynamique et Physicochimie Metallurgiques, Institut National Polytechnique de Grenoble, F-38402 Saint Martin d'Heres Cedex, France
A constitutive model for quasicrystal plasticity
Phil. Mag. Lett. Vol. 81, No. 7, 473-482 (2001)
23.55.0

Gebauer J.1; Krause-Rehberg R.2; Domke C.; Ebert Ph.; Urban K.; Staab T.E.M.3
1 ISG, FZ Jülich
2 FB Physik, Universität Halle
3 Lab. of Physics, Helsinki University of Technology
Direct identification of As vacancies in GaAs using positron annihilation calibrated by scanning tunneling microscopy
Phys. Rev. B, Vol. 63, 045203 (2001)
23.55.0

Heggen M.; Feuerbacher M.; Schall P.; Urban K.; Wang R.1
1 Department of Physics, Wuhan University, 430072 Wuhan, People's Republic of China
Antiphase domains in plastically deformed Zn-Mg-Dy single quasicrystals
Phys. Rev. B, Vol. 64, 014202-1-014202-6 (2001)
23.55.0

Highfield J.G.1; Oguro K.1; Grushko B.
1 Osaka National Research Institute, Midorigaoka 1-8-31, Ikeda-shi, Osaka 563, Japan

Raney multi-metallic electrodes from regular crystalline and quasi-crystalline precursors: I. Cu-stabilized Ni/Mo cathodes for hydrogen evolution in acid
Electrochimica Acta 47, 465-481 (2001)
23.55.0

Holländer B.1; Lenk St.1; Mantl S.1; Trinkaus H.; Kirch D.; Luysberg M.; Hackbarth T.1; Herzog H.-J.2; Fichtner P.F.P.3
1 ISG, FZ Jülich
2 Daimler Crysler AG, Research and Technology, 89081 Ulm
3 Dept. de Metallurgia, Univ. Fed Do Rio Grande do Sul, 91501-970 Porto
Strain relaxation of pseudomorphic Si1-xGex/Si(100) heterostructures after hydrogen or helium ion implantation for virtual substrate fabrication
Nuclear Instruments and Methods in Physics Research B 175-177, 357-367 (2001)
23.42.0

Houben L.; Luysberg M.; Carius R.1
1 IPV, FZ Jülich
Microtwinning in microcrystalline silicon and ist effect on grain-size measurements
Phys. Rev. B
submitted 09.05.2001
23.42.0

Houben L.; Scholten C.; Luysberg M.; Vetterl O.1; Finger F.1; Carius R.1
1 IPV, FZ Jülich
Growth of microcrystalline nip solar cells: Role of local epitaxy
Journal of Non-Crystalline Solids
accepted
23.42.0

Jia C.L.; Siegert M.1; Urban K.
1 ISI, FZ Jülich
The Structure of the interface between BaTiO3 thin films and MgO substrates
Acta mater. 49, 2783-2789 (2001)
23.42.0

Jia C.L.; Zeng X.H.1; Xi X.X.1; Urban K.
1 Dept. of Physics, The Pennsylvania State University, University Park, PN 16802, USA
Microstructure and residual strain in La2CuO4 thin films on LaSrAlO4-buffered SrTiO3 substrates
Phys. Rev. B, Vol. 64, 075416-1-075416-6 (2001)

Jiang C. S.1; Yu H.1; Wang X. D.1; Shih C. K.1; Ebert Ph.
Scanning tunneling spectroscopy of quantum well and surface states of thin Ag films grown on GaAs (110)
Phys. Rev. B, Vol. 64, 235410, 1-5 (2001).
23.42.0

Jiang X.1; Jia C.L.; Szameitat M.1; Rickers C.1
1 Fraunhofer-Institut für Schicht und Oberflächentechnik, Bienroder Weg 54E, D-38108 Braunschweig
Epitaxy of diamond on Si(100) and surface-roughening-induced crystal misorientation
Phys. Rev. B, Vol. 64, 245413-1 - 245413- 5 (2001)
23.42.0

Jin H.Z.1; Zhu J.1; Ehrhart P.; Fitsilis F.; Jia C.L.; Regnery S.; Urban K.; Waser R.
1 Department of Materials Science and Engineering, Tsinghua University, Beijing 100084 China
A Study of (Ba,Sr)TiO3 thin films on Pt-electrodes by transmission electron microscopy
Appl. Phys. Lett., submitted
23.42.0

Khoukaz C.1; Galler R.1; Feuerbacher M.; Mehrer H.1
1 Institut für Metallforschung, Universität Münster, 48149 Münster
Self-Diffusion of Ni and Co in decagonal Al-Ni-Co quasicrystals.
Defect and Diffusion Forum 194-199 (2001) in press
23.55.0

Kisielowski C.1; Hetherington C.J.D.1,2; Wang Y.C.1,3; Kilaas R.1; O'Keefe M.A.1; Thust A.
1 Department of Materials Science, University of California, Berkeley, CA 94720, USA
2 Department of Materials, University of Oxford, Oxford / UK
3 FEI Company, Hilsboro OR 97124, USA
Imaging columns of the light elements carbon, nitrogen and oxygen with sub Angstrom resolution
Ultramicroscopy 89, 243-263 (2001)
23.42.0

Klein H.1; Feuerbacher M.; Urban K.
1 ESRF, Pluo E, B.P. 220, 38043 Grenoble Cedex, France
Structure of Dislocations and Stacking Faults in a Large-Unit-Cell Intermetallic Compound.
Phys. Rev. B, submitted
23.55.0

Krause H.-J.1; Wolf W.1; Glaas W.1; Zimmermann E.1; Faley M.I.; Sawade G.2; Mattheus R.2; Neudert G.3; Gampe U.3; Krieger J.4
1 ISG, FZ Jülich
2 Forschungs- und Materialprüfungsanstalt Baden-Württemberg, 70569 Stuttgart
3 Siempelkamp, Prüf- und Gutachtergesellschaft mbH, 01099 Dresden
4 Bundesanstalt für Straßenwesen, 51427 Bergisch-Gladbach
SQUID Array for Magnetic Inspection of Prestressed Concrete Bridges accepted for publication in
Physica C (2002)
23.42.0

Lentzen M.; Jahnen B.; Jia C.L.; Thust A.; Tillmann K.; Urban K.
High-resolution imaging with an aberration-corrected transmission electron microscope
Ultramicrocopy 2001 (eingereicht)
23.42.0

Mi S.; Yurechko M.; Wu J.; Grushko B.
Ternary Al-Pd-Co monoclinic phases
Journal of Alloys and Compounds 329, L1-L4 (2001)
23.55.0

O'Keefe M.A.1; Hetherington C.J.D.1,2; Wang Y.C.1,3; Nelson E.C.1; Turner J.H.1; Kisielowski C.1; Malm J.-O.4; Müller R.3; Ringnalda J.3; Pan M.5; Thust A.
1 Department of Materials Science, University of California, Berkeley, CA 94720, USA
2 Department of Materials, University of Oxford, Oxford / UK
3 FEI Company, Hilsboro OR 97124, USA
4 Materials Chemistry 2, Lund University, SE-22100 Lund / Schweden
5 Gatan, Inc. Pleasanton, CA 94588, USA
Sub-Angstrom high-resolution transmission electron microscopy at 300 keV
Ultramicroscopy 89, 215-241 (2001)
23.42.0

O'Keefe M.A.1; Nelson E.C.1; Wang Y.C.1; Thust A.
1 Department of Materials Science, University of California, Berkeley, CA 94720, USA
Sub-Angström resolution of atomistic structures below 0.8 A
Phil. Mag. B, Vol. 81, No. 11, 1861-1878 (2001)
23.42.0

Poppe U.; Divin Y.Y.; Faley M.I.; Wu J.S.; Jia C.L.; Shadrin P.; Urban K.
Properties of YBa2Cu3O7 Thin Films Deposited on Substrates and Bicrystals with Vicinal Offcut and Realization of High IcRn Junctions
IEEE Transactions on Appl. Supercond., Vol. 11, No. 1, 3768-3771 (2001)
23.42.0

Schall P.; Feuerbacher M.; Urban K.
Plastic deformation behaviour of decagonal Al70Ni15Co15 single quasicrystals
Phil. Mag. Lett. Vol. 81, No. 5, 339-349 (2001)
23.55.0

Schall P.; Feuerbacher M.; Urban K.
Plastic deformation of decagonal Al-Ni-Co single quasicrystals
Mat. Sci. Eng. A309-310, 548-551 (2001)
23.55.0

Semmler U.; Simon M.; Ebert Ph.; Urban K.
Stoichiometry changes by selective vacancy formation on (110) surfaces of III-V semiconductors: Influence of electronic effects
J. Chem. Phys. 114, No. 1, 445-451 (2001)
23.55.0

Shadrin P.; Divin Y.
Spread of critical currents in thin-film YBa2Cu3O7-x bicrystal junctions
IEEE Transactions on Appl. Supercond., Vol. 11, No. 1, 414-417 (2001)
23.42.0

Shadrin P.; Jia C.L.; Divin Y.Y.
Spread of critical currents in thin-film YBa2Cu3O7-x bicrystal junctions and faceting of grain boundary
Physica C, 2002 (accepted for publications)
23.42.0

Shirotov V.; Divin Y.; Urban K.
Dynamic Range of Frequency-Selective Response of High-Tc Josephson Detector to Millimeter-Wave Radiation
IEEE Transactions on Appl. Supercond., Vol. 11, No. 1, 955-957 (2001)
23.42.0

Shirotov V.; Divin Y.Y.; Urban K.
Far-infrared broadband measurements with Hilbert-transform spectroscopy
Physica C, 2002 (accepted for publications)
23.42.0

Staab T.E.M.1; Nieminen R.M.1; Gebauer J.2; Krause-Rehberg R.2; Luysberg M.; Haugk M.3; Frauenheim Th.3
1 Lab. of Physics, Helsinki University of Technology
2 FB Physik, Universität Halle3 Dept. of Physic, University GH Paderborn, 33098 Paderborn
Do Arsenic Interstitials Really Exist in As-Rich GaAs?
Phys. Rev. Lett., Vol. 87, No. 4, 045504-1 - 045504-4 (2001)
23.42.0

Tillmann K.; Luysberg M.; Specht P.1; Weber E.R.1
1 Department of Materials Science, University of California, Berkeley, CA 94720, USA
Direct determination of local layer compositions by the reciprocal space segmentation of high-resolution micrographs
Ultramicroscopy
submitted October 2001
23.42.0

Wu J.S., Jia C.L., Urban K., Hao J.H.1 Xi X.X.1
1 Dept. of Physics, The Pennsylvania State University, University Park, PN 16802, USA
Conservative antiphase boundary in SrTiO3 films on LaAlO3 substrates with SrRuO3 buffer layers
Journal of Applied Physics, Vol. 89, No. 10, 5653-5656 (2001)
23.42.0

Wu J.S.; Jia C.L.; Urban K.; Hao J.H.1; Xi X.X.1
1 Dept. of Physics, The Pennsylvania State University, University Park, PN 16802, USA
A new mechanism for misfit dislocation generation: superdislocations associated with Ruddlesden-Popper planar defects
Journal of Crystal Growth 234, 603-609 (2001)
23.42.0

Wu J.S.; Jia C.L.; Urban K.; Hao J.H.1; Xi X.X.1
1 Dept. of Physics, The Pennsylvania State University, University Park, PN 16802, USA
Microstructure and misfit relaxation in SrTiO3 /SrRuO3 bilayer films on LaAlO3 (100) substrates
J. Mat. Res. 16, 3443-3450 (2001)

Wu J.S.; Jia C.L.; Urban K.; Hao J.H.1; Xi X.X.1
1 Dept. of Physics, The Pennsylvania State University, University Park, PN 16802, USA
Stair-rod dislocations in perovskite films on LaAlO3 substrates
Phil. Mag. Lett. Vol. 81, No. 6, 375-383 (2001)
23.42.0

Yu H.1; Jiang C. S.1; Ebert Ph; Wang X. D.1; White J. M.1; Niu Q.1; Zhang Z.1; Shih C. K.1
1 University of Texas, Austin
2 Oak Ridge National Laboratory
Quantitative Determination of the Metastability of Flat Ag Overlayers on GaAs(110)
Phys. Rev. Lett., Vol. 88, 016102, 1-4 (2002).
23.42.0

Yurechko M.; Fattah A.; Velikanova T.1; Grushko B.
1 Ukrainian Academy of Sciences, Kiev
A contribution to the Al-Pd phase diagram
Journal of Alloys and Compounds 329, 173-181 (2001)
23.55.0

Yurechko M.; Grushko B.; Urban K.; Velikanova T.1
1 Ukrainian Academy of Sciences, Kiev
The Al-Rh phase diagram
Poroshkovaia Metallurgia 7-8, 75-80 (2001)
23.55.0

Yurechko M.; Grushko B.; Velikanova T.1; Urban K.
1 Ukrainian Academy of Sciences, Kiev
Isothermal sections of the Al-Pd-Co alloy system for 50-100 at.% Al
Journal of Alloys and Compounds 1 (2001)
23.55.0

Other publications

Baier F.1; Müller M.A.1; Sprengel W.1; Grushko B.; Sterzel R.2; Assmus W.2; Schäfer H.E.1
1 ITAP, Universität Stuttgart, 70550 Stuttgart
2 Johann Wolfgang Goethe-Universität, 60325 Frankfurt/Main
Atomic defects in Al-Pd-Mn: a study by means of positron annihilation spectroscopy.
Int. Conf. Positron Annihilation ICPA-13, München.
Materials Science Forum 363-365, 179-181 (2001)
23.55.0

Divin Y.; Volkov O.1; Pavlovskii V.1; Shirotov V.; Shadrin P.; Poppe U.; Urban K.
1 Institute of Radioengineering & Electronics of RAS, Moscow 103907, Russian Federation
Terahertz Hilbert spectroscopy by high-Tc Josephson junctions
In: Advances in Solid State Physics, 41, ed. B. Kramer (Springer, Berlin, 2001), 301-313 (2001)
23.42.0

Duckham A.1; Shechtman D.2; Grushko B.
1 National Institute of Standards and Technology, MSEL, Gaitherburg, MD 20899 USA
2 Department of Materials Engineering, Technion Haifa 32000, Israel

Influence of Grain Orientation on Friction and Wear Behavior in Quasicrystalline Alloys
Mat. Res. Soc. Symp. Proc., Vol. 643, K8.1.1-6 (2001)
23.55.0

Ebert Ph.; Szot K.
Scanning Probe Microscopy
in: Neue Materialien für die Informationstechnik, Forschungszentrum Jülich, 2001, B5.1-B5.40.
23.42.0

Ebert Ph.
Point Defects in Compound Semiconductor Surfaces
Berichte des Forschungszentrums Jülich, Nr. 3850, 235 p., Forschungszentrum Jülich, 2001.
23.42.0

Faley M.I.; Poppe U.; Urban K.; Paulson D.N.1; Starr T.1; Fagaly R.L.1
1 Tristan Technologies Inc., CA 92121, USA
HTS dc-SQUID flip-chip magnetometers and gradiometers
Biomag2000, Proc. 12th Int. Conf. on Biomagnetism, J. Nenonen, R.J. Ilmoniemi, and T. Katila, eds. (Helsinki Univ. of Technology, Espoo, Finland, 2001), pp.931-934.
23.42.0

Feuerbacher M.; Schall P.; Estrin Y.1; Bréchet Y.2; Urban K.
1 Institut für Werkstoffkunde und Werkstofftechnik, Technische Universität Clausthal, Agricolastrasse 6, D-38678 Clausthal-Zellerfeld, Germany
2 Laboratoire de Thermodynamique et Physicochimie Metallurgiques, Institut National Polytechnique de Grenoble, F-38402 Saint Martin d'Heres Cedex, France
Modelling Quasicrystal Plastic Deformation By Means of Constituive Equations
Mat. Res. Soc. Symp. Proc., Vol. 643, K.7.2.1-6 (2001)
23.55.0

Jahnen B.; Luysberg M.; Urban K.; Bracht H.1; Schmidt R.2; Ungermanns C.2; Bleuel T.3
1 Institut für Materialphysik, Universität Münster
2 ISG, FZ Jülich
3 Fachbereich Physik, Universität Würzburg
Interdiffusion in GaSb/AlxGa1-xSb heterostructures
Proceedings of the XIIth Conference on Microscopy of Semiconducting Materials, 22-25 March 2001, Oxford, Microscopy of Seminconducting Materials 2001, Inst. Phys. Conf. Ser., in press.
23.42.0

Luysberg M.; Kirch D.; Trinkaus H.; Holländer B.1; Lenk St.1; Mantl S.1; Herzog H.-J.2; Hackbarth T.2; Fichtner P.F.P.3
1 ISG, FZ Jülich
2 Daimler Crysler AG, Research and Technology, 89081 Ulm
3 Dept. de Metallurgia, Univ. Fed Do Rio Grande do Sul, 91501-970 Porto
Relaxation of Si1-xGex Buffer Layers on Si(100) through Helium Ion Implantation
Proceedings of the XIIth Conference on Microscopy of Semiconducting Materials, 22-25 March 2001, Oxford, Microscopy of Seminconducting Materials 2001, Inst. Phys. Conf. Ser., in press.
23.42.0

Luysberg M.; Meertens D.; Herfort J.1; Ulrici W.1; Moreno M.1; Ploog K.H.1
1 Paul Drude Institut, Hausvogteiplatz 5-7, 10117 Berlin
Structural properties of Carbon doped LT-GaAs
Proc. of the 3rd Symposium on non-stoichiometric III-V compounds, Erlangen (2001) in:
Physik mikrostrukturierter Halbleiter, Vol. 23 ed.: S. Malzer, T. Marek and P. Kiesel, Verlag: Lehrstuhl für Mikrocharakterisierung, Universität Erlangen, P. 91
23.42.0

Luysberg M.; Scholten C.; Houben L.; Carius R.1; Finger F.1; Vetterl O.1
1 IPV, FZ Jülich
Structural Properties of microcrystalline Si solar cells
Proceedings of the MRS Spring Meeting, San Francisco, in press (2001)
23.42.0

Messerschmidt U.1; Bartsch M.1; Geyer B.1; Ledig L.; Feuerbacher M.; Wollgarten M; Urban K.
1 MPI für Mikrostrukturphysik, Halle
Dislocation Dynamics in Icosahedral Al-Pd-Mn Single Quasicrystal
Mat. Res. Soc. Symp. Proc., Vol. 643, K.6.5.1-6 (2001)
23.55.0

Tillmann K.; Förster A.1; Houben L.
1 ISG, FZ Jülich
Critical dimensions for the formation of misfit dislocations in In0.6Ga0.4As island on GaAs(001)
Proceedings of the XIIth Conference on Microscopy of Semiconducting Materials, 22-25 March 2001, Oxford, Microscopy of Seminconducting Materials 2001, Inst. Phys. Conf. Ser., in press.
23.42.0

Tillmann K.; Luysberg M.; Fattah A.; Specht P.1; Weber E.R.1
1 Department of Materials Science, University of California, Berkeley, CA 94720, USA
Mechanism of interdiffusion and thermal stability upon annealing of AlAs/GaAs: Be quantum wells grown under low temperature conditions
Proceedings of the XIIth Conference on Microscopy of Semiconducting Materials, 22-25 March 2001, Oxford, Microscopy of Seminconducting Materials 2001, Inst. Phys. Conf. Ser., in press.

Tillmann K.; Luysberg M.; Specht P.1; Cich M.J.1; Weber E.R.1
1 Department of Materials Science, University of California, Berkeley, CA 94720, USA
Beryllium dopant induced stabilization against in-termixing and precipitation upon annealing of LT-AlAs/GaAs:Be Multiple quantum wells
Proc. of the 3rd Symposium on non-stoichiometric III-V compounds, Erlangen (2001) in:
Physik mikrostrukturierter Halbleiter, Vol. 23 ed.: S. Malzer, T. Marek and P. Kiesel, Verlag: Lehrstuhl für Mikrocharakterisierung, Universität Erlangen, p. 79
23.42.0

Yang W.; Feuerbacher M.; Urban K.
Cluster structure and low-energy planes in icosahedral Al-Pd-Mn quasicrystals
Conference Quasicrystals 2001, Sendai/Japan, 24.-28. September (2001)
23.55.0

Invited Talks

Divin Y.Y.; Volkov O.Y.1; Pavlovskii V.V.1; Shirotov V.; Shadrin P.; Poppe U.; Urban K.
1 Institute of Radioengineering & Electronics of RAS, Moscow 103907, Russian FederationTerahertz Hilbert spectroscopy by high-Tc Josephson junctions
Hauptvortrag, DPG Frühjahrstagung, Hamburg 26.-30. März (2001)
23.42.0

Ebert Ph.
Defects in III-V semiconductor surfaces
Université de Fribourg, Switzerland, May 15, 2001.
23.42.0

Ebert Ph.
Defekte auf III-V-Halbleiteroberflächen
Hauptvortrag, 65. Physikertagung der Deutschen Physikalischen Gesellschaft, Symposium Rekonstruktion und

Wachstum von III-V-Halbleiteroberflächen der Fachverbände Halbleiter- und Oberflächenphysik, Hamburg, Germany, 26.-30.3.2001.

Ebert Ph.
Festkörperforschung auf atomarer Skala mittels Rastertunnelmikroskopie
Kolloquium in Physik, Mathematisch-Naturwissenschaftliche Fakultät, Université de Fribourg, Switzerland, 7. Dezember 2001.
23.42.0

Ebert Ph.
Leuchtendes Silizium
RWTH Aachen, Germany, February 14, 2001.
23.42.0

Ebert Ph.
Scanning Tunneling Microscopy in Materials Physics
Institute of Physics, Chinese Academy of Sciences, The International Center of Quantum Structures, Peking, China, October 12, 2001.
23.42.0

Ebert Ph.
Scanning Tunneling Microscopy in Materials Physics
Nanoscale Physics and Device Laboratory, Chinese Academy of Sciences, Peking, China, October 29, 2001.
23.42.0

Feuerbacher M.
Mechanical properties of quasicrystals
Quasicrystals 2001, Sendai, Japan, September 2001.
23.55.0

Luysberg M.
Microcrystalline silicon for electronic devices
Dreiländertagung über Elektronenmikroskopie, Innsbruck, September 2001
23.42.0

Luysberg M.
Mikrokristallines Silizium: Ein Material für elektronische Bauelemente
Uni Göttingen, Dezember 2001
23.42.0

Luysberg M.
Relaxation von SiGe-Schichten durch He Implantation
Uni Kiel, November 2001
23.42.0

Luysberg M.
Structural properties of Be doped LT-GaAs
HUT, Helsinki, Februar 2001
23.42.0

Luysberg M.
Strukturelle Eigenschaften von mikrokristallinem Silizium
HMI Berlin, Januar 2001
23.42.0

Urban K.
Application of spherical-aberration corrected transmission electron microscopy in materials science
Dreiländertagung für Elektronenmikroskopie, Innsbruck/A, 9. - 14.09.2001
23.42.0

Urban K.
Application of spherical-aberration corrected transmission electron microscopy in materials science
Dreiländertagung für Elektronenmikroskopie, Innsbruck/A, 9. - 14.09.2001
MRS Spring Meeting, San Francisco / USA, April 2001
23.42.0

Urban K.
Das neue Paradigma der Elektronenmikroskopie - Aberrationskorrektur und Austrittswellenfunktionsrekonstruktion
Kolloquiumsvortrag am IFW Dresden, Dresden
23.42.0

Urban K.
Das neue Paradigma der Elektronenmikroskopie - Aberrationskorrektur und Austrittswellenfunktionsrekonstruktion
Kolloquiumsvortrag an der Universität Münster, Münster
23.42.0

Urban K.
Plasticity of Quasicrystals and related intermetallics
AMT Conference, Gdansk / Polen, September 2001
23.42.0

Urban K.
Structurally complex alloy phases
Chinese - German Workshop on "Modern Metallic Materials Design"
Beijing, 5 - 8 November 2001
23.42.0

Urban K.
The new paradigm of transmission electron microscopy
Institute of Physics, Chinese Academy of Science, Beijing, 13 July 2001
23.42.0

Urban K.
Wellen - Basis der Materie und der Kommunikation
Schulvorträge im "Jahr der Lebenswissenschaften", Berlin, Juni 2001
23.42.0

Other talks

Divin Y.Y.; Poppe U.; Jia C.L.; Shadrin P.M.; Urban K.
Structural and electrical properties of YBa2Cu3O7 [100]-tilt grain boundary Josephson junctions with high IcRn-products on SrTiO3 bicrystals
5th European Conf. Appl. Supercond., Copenhagen/Dänemark, 26.-30. August (2001)
23.42.0

Divin Y.Y.; Volkov O. Y.1; Laytti M.; Shirotov V. V.; Pavlovskii V.V.1; Poppe U.; Shadrin P.M.; Urban K.
1 Institute of Radioengineering & Electronics of RAS, Moscow 103907, Russian Federation
Hilbert spectroscopy from gigahertz to terahertz frequencies by high-Tc Josephson junctions
26th Int. Conf. Infrared and Millimeter Waves, September 10-14, 2001, Toulouse, France
23.42.0

Divin Y.Y.; Volkov O.Y.1; Laytti M.; Shirotov V.V.; Pavlovskii V.V.1; Poppe U.; Shadrin P.M.; Urban K.
1 Institute of Radioengineering & Electronics of RAS, Moscow 103907, Russian Federation
Hilbert spectroscopy from microwave to terahertz frequencies by high-Tc Josephson junctions
5th European Conf. Appl. Supercond., Copenhagen/Dänemark, 26.-30. August (2001)
23.42.0

Ebert Ph.; Kluge F.; Cai T.1; Grushko B.; Thiel P.A.1; Urban K.
1 Ames Laboratory, Ames, Iowa
Surface structure of Al-Pd-Mn quasicrystals: effect of bulk vacancies.
Quasicrystals 2001, Sendai, Japan, September 24-28, 2001
23.55.0

Ebert Ph.; Semmler U.; Simon M.; Urban K.

Stoichiometry changes by selective vacancy formation on (110) surfaces of III-V semiconductors: Influence of electronic effects.
Materials Research Society Fall Meeting, Boston, Massachusetts, November 26-30, 2001.
23.42.0

Faley M.I.; Poppe U.; Urban K.; Paulson D.N.1; Starr T.N.1; Fagaly R.L.1
1 Tristan Technologies Inc., CA 92121, USA
Low noise HTS dc-SQUID flip-chip magnetometers and gradiometers
DPG Frühjahrstagung, Hamburg 26.-30. März (2001)
23.42.0

Houben L.
Growth of microcrystalline nip solar cells: role of local epitaxy
ICAMS 19, Nizza, August 2001
23.42.0

Jahnen B.; Luysberg M.; Urban K.; Bracht H.1; Schmidt R.2; Ungermanns C.2; Bleuel T.3
1 Institut für Materialphysik, Universität Münster
2 ISG, FZ Jülich
3 Fachbereich Physik, Universität Würzburg
Interdiffusion in GaSb/AlxGa1-xSb heterostructures
XIIth Conference on Microscopy of Semiconducting Materials, 22-25 March 2001, Oxford, Microscopy of Seminconducting Materials 2001.
23.42.0

Jahnen B.
Interdiffusion in GaSb/AlxGa1-xSb heterostructures
XIIth Conference on Microscopy of Semiconducting Materials, 22-25 March 2001, Oxford
23.42.0

Kirch D.
Relaxationsmechanismen in He-implantierten SiGe Pufferschichten
DPG Frühjahrstagung Hamburg, März 2001
23.42.0

Luysberg M.; Kirch D.; Trinkaus H.; Holländer B.1; Lenk St.1; Mantl S.1; Herzog H.-J.2; Hackbarth T.2; Fichtner P.F.P.3
1 ISG, FZ Jülich
2 Daimler Crysler AG, Research and Technology, 89081 Ulm
3 Dept. de Metallurgia, Univ. Fed Do Rio Grande do Sul, 91501-970 Porto
Relaxation of Si1-xGex Buffer Layers on Si(100) through Helium Ion Implantation
MRS Spring Meeting, San Francisco, April 2001
23.42.0

Luysberg M.; Kirch D.; Trinkaus H.; Holländer B.1; Lenk St.1; Mantl S.1; Herzog H.-J.2; Hackbarth T.2; Fichtner P.F.P.3
1 ISG, FZ Jülich
2 Daimler Crysler AG, Research and Technology, 89081 Ulm
3 Dept. de Metallurgia, Univ. Fed Do Rio Grande do Sul, 91501-970 Porto
Relaxation of Si1-xGex Buffer Layers on Si(100) through Helium Ion Implantation
Proceedings of the XIIth Conference on Microscopy of Semiconducting Materials, 22-25 March 2001, Oxford/UK
23.42.0

Luysberg M.; Meertens D.; Herfort J.1; Ulrici W.1; Moreno M.1; Ploog K.H.1
1 Paul Drude Institut, Hausvogteiplatz 5-7, 10117 Berlin
Structural Properties of Carbon doped LT-GaAs
3rd Symposium on non-stoichiometric III-V compounds, Erlangen, Oktober 2001
23.42.0

Luysberg M.; Scholten C.; Houben L.; Carius R.1; Finger F.1; Vetterl O.1
1 IPV, FZ Jülich
Structural Properties of microcrystalline Si solar cells
MRS Spring Meeting, San Francisco, April 2001
23.42.0

Semmler U.; Simon M.; Ebert Ph.; Urban K.
Stöchiometrieänderungen durch selektive Leerstellenbildung auf (110)-Oberflächen von III-V-Halbleitern: Einfluß elektronischer Effekte
Frühjahrtagung der Deutschen Physikalischen Gesellschaft, Hamburg, Germany, 26.-30.3.2001.
23.42.0

Tillmann K.
Beryllium dopant induced stabilization against intermixing and precipitation upon annealing of LT-GaAs/GaAs:Be multiple quantum wells
3rd Symposium on non-stoichiometric III-V Compounds, Erlangen, Oktober 2001
23.42.0

Tillmann K.
Mechanisms of interdiffusion and thermal stability during annealing of AlAs/GaAs:Be quantum wells grown under low temperature conditions
XIIth Conference on Microscopy of Semiconducting Materials, 22-25 March 2001, Oxford
23.42.0

Posters

Faley M.I.; Poppe U.; Urban K.; Paulson D. N.1, Starr T. N.1, Fagaly R. L.1
1 Tristan Technologies Inc., CA 92121, USA
Sensitive HTS sensors for magnetic evaluation applications
Tagung Kryoelektronische Bauelemente 2001, 30. Sept. - 2. Okt. 2001, Congrescentrum Rolduc, Kerkrade, Niederlande.
23.42.0

Faley M.I.; Poppe U.; Urban K.; Paulson D.N.1; Starr T.N.1; Fagaly R.L1.
1 Tristan Technologies Inc., CA 92121, USA
Sensitive HTS gradiometers for magnetic evaluation applications
5th European Conference on Applied Superconductivity, Kopenhagen, Dänemark, 26.-30. August (2001)
23.42.0

Jahnen B.; Luysberg M.; Urban K.; Bracht H.1; Schmidt R.2; Ungermanns C.2; Bleuel T.3
1 Institut für Materialphysik, Universität Münster
2 ISG, FZ Jülich
3 Fachbereich Physik, Universität Würzburg
Interdiffusion in GaSb/AlxGa1-xSb heterostructures
XIIth Conference on Microscopy of Semiconducting Materials, 22-25 March 2001, Oxford, Microscopy of Seminconducting Materials 2001.
23.42.0

Krause H.-J.1; Wolf W.1; Glaas W.1; Zimmermann E.1; Faley M.I.; Sawade G.2; Mattheus R.2; Neudert G.3; Gampe U.3; Krieger J.4
1 ISG, FZ Jülich
2 Forschungs- und Materialprüfungsanstalt Baden-Württemberg, 70569 Stuttgart
3 Siempelkamp, Prüf- und Gutachtergesellschaft mbH, 01099 Dresden
4 Bundesanstalt für Straßenwesen, 51427 Bergisch-Gladbach
SQUID Array for Magnetic Inspection of Prestressed Concrete Bridges
Conference SQUID2001, Gothenburg, Schweden, 31.08.-03.09. (2001)
23.42.0

Shadrin P. M.; Jia C.L.; Divin Y.Y.
Spread of critical currents in thin-film YBa2Cu3O7-x bicrystal junctions and faceting of grain boundary

5th European Conf. Appl. Supercond.,
Copenhagen/Dänemark, 26.-30. August (2001)
23.42.0

Shirotov V. V.; Divin Y.Y.; Urban K.
Far-infrared broadband measurements with Hilbert-transform spectroscopy
5th European Conf. Appl. Supercond.,
Copenhagen/Dänemark, 26.-30. August (2001)
23.42.0

Patents granted

Divin Y.Y.; Seo J.W.; Poppe U.
Schichtfolge mit wenigstens einem epitaktischen, nahezu a-Achsen orientierten HTSL-Dünnfilm oder mit einer Schicht aus einem mit HTSL kristallographisch vergleichbarer Struktur, sowie Verfahren zu ihrer Herstellung
US: 6,156,706 (05.12.2000)
PT 1.1333
23.42.0

Hojczyk R.; Poppe U.; Jia C.L.
Schichtenfolge sowie ein diese enthaltendes Bauelement
US: 6,191,073 (20.02.2001)
PT 1.1385
34.42.0

Zhang Y.; Zander W.; Banzet M.; Schubert J.1; Soltner H.
1ISG
Anordnung zur Ankopplung eines rf-SQUID-Magnetometers an einen supraleitenden Tankschwingkreis auf einem Substrat
US: 6,225,800 (01.05.2001)
PT 1.1356
29.85.0

Patents applied for

Zimmermann E.; Glaas W.; Halling H.1; Faley M.; Soltner H.2
1ZEL
2ESS
SQUID-Mikroskop
EP: 01.125102.2 (23.10.2001)
(AT,BE,CH/Li,CY,DE,DK,ES,FI,FR,GB,GR;IE,IT,LU,MC,NL,PT,SE,TR)
US: (2001)
PT 1.1838
23.42.0

Lecture courses

Urban K.; Ebert Ph.
Neue Materialien: Von der Präparation zur Anwendung
Seminar an der RWTH Aachen, SS 2001.

Institute for Electronic Properties

General Overview

In any condensed matter system, electrons are the "glue" that hold the atoms together. Therefore the electronic structure constitutes a microscopic base for all material properties. The electronic interactions determine whether a solid is metallic, insulating or semiconducting, whether it is transparent or exhibits a distinctive color, whether it is a magnet or a superconductor.

The research program of the Institute for Electronic Properties is devoted towards the investigation of the electronic structure of atoms, clusters, nonostructures, and solids. The ultimate goal is the development of an understanding and thus a base for the control of the properties of new materials. The research efforts of the institute are concentrated in the areas: **Magnetism of thin films and nanostructures, clusters as new materials,** and **methods and instrumentation.**

The major event in the year 2001 was the departure of Prof. Wolfgang Eberhardt from his position as an institute director. He left to take up a position as a scientific director of BESSY in conjunction with a professorship at the TU Berlin. Dr. H. Dürr followed him to BESSY in the late summer. Since Dr. C. Carbone and Dr. S. Blügel had left the institute already in the year 2000 to take up positions as professors in Trieste and Osnabrück, respectively, many of the group leaders have left the institute. Several of the PhD students have followed or are following Prof. Eberhardt to BESSY. Major equipment, which has been bought by the BESSY GmbH, will be transferred to Berlin.

The investigation of the electronic properties is fundamental for any condensed matter research. Therefore, at the Forschungszentrum, it has been decided to keep an Institute for Electronic Properties within the condensed matter department IFF. As a consequence of the successful HGF magneto-electronic project within the research center, the research on magnetic nanostructures will be strengthened in the future.

Despite the fact that the institute is in a transition period, a lot of research activities were going on in 2001, leading to many exciting results. Some examples are given below and others in the attached detailed reports.

In the group **magneto-electronics**, the research efforts have concentrated on Fe/Al/Fe trilayers (see attached report), Fe/AlO/Fe TMR (tunnel magneto resistance) devices, and Fe/Si/Fe trilayers. The latter system, where a semiconductor is sandwiched between two metallic layers, shows a surprisingly high interlayer coupling of up to 8 mJ/m^2, which cannot be understood within the conventional models. Nanocontacts in Fe/Cr/Fe trilayers structures have been prepared with electron beam lithography to study a new effect, which can be described as the reverse of the GMR effect: the current-induced magnetic coupling. A switching between ferromagnetic and antiferromagnetic coupling can be achieved just by reversing the electron current. Finally, in the small theory group working in very close contact with the experimental magneto-electronic group, a novel ab-initio Green function formulation of the transfer matrix has been developed and applied to complex band-structures.

Within the **cluster group**, a new magnetron sputter source for the deposition of clusters has been constructed (see attached report). This continuous source is superior to pulsed cluster sources due to the more stable operation conditions and higher cluster intensities. The research efforts in the cluster group were concentrated on scanning tunneling spectroscopy of endohedral fullerenes and femtosecond time resolved studies. Small endohedral fullerenes $Ce@C_n$ (n = 36,44,50,60) have been produced in a laser vaporization cluster source, mass selected and non-destructively deposited on a highly oriented pyrolytic graphite substrate. The density of states has been determined by scanning tunneling spectroscopy. A semiconductor-like density of states at the Fermi level is observed with energy gaps between 0.55 and 1.1 eV. Metal-adsorbate-clusters have been studied using femtosecond time resolved photoelectron spectroscopy. Information concerning the dissociation dynamics of these systems could be deduced. The photodisscociation process of $Pt_2N_2^-$ occurs on a time scale of 100(25) ps and involves different reaction pathways. Another example of the ongoing research involves the relaxation dynamics of opticly excited electrons in free Ni_3^- cluster. By means of femtosecond two-color pump-probe photoelectron spectroscopy, the electronic relaxation of excited electrons via inelastic electron-electron-scattering could be observed in real-time. The inelastic electron-electron relaxation time was determined to be 190 fs.

One highlight in the development of **methods and instrumentation** was the successful commissioning of the spin-polarized photoelectron emission microscope (PEEM) with the application to magnetic nanostructures. Combining a femtosecond pump-probe laser with a photoelectron emission microscope, the spin dynamics in nanostructures can be studied on a femtosecond time scale. Magnetic sensitivity is obtained by analyzing the spin-polarization of the emitted photoelectrons. The technique has been successfully applied to Co/Pt nanoscale magnetic dots. The institute also operates two synchrotron beamlines. The beamline for soft x-rays at BESSY II has been commissioned. Within the entire energy range the experimental resolution exceeded the design-resolution of $E/\Delta E = 10.000$. With the linear or circular polarized radiation available, the electronic properties of novel materials are now being examined. The systems include nanotubes, magnetic multilayers or organic semiconductors. The VUV-beamline at the DELTA storage ring in Dortmund suffered in the past due to storage ring problems. Many of these problems, such as beam position fluctuations and beam losses, have now been solved and thus in 2001 a first stable operation of the beamline became possible. As a consequence, a first scientific result has been obtained: the electronic structure of Co-quantum-wires has been determined.

The successful scientific work of the institute is documented by the following personal awards and achievements:
Dr. S. Blügel has received an offer for a C4 professorship at the University of Kaiserslautern in the field of Theoretical Solid State Physics. Dr. D.E. Bürgler has received an offer for a C4 professorship at the Martin-Luther-University, Halle/Saale, in the field of Experimental Physics. Prof. Dr. W. Eberhardt and Dr. J. Morenzin have been awarded the first prize of the "Mitteldeutscher Rundfunk", MDR, for the invention of counterfeit-prove magnetic stripes. The following students have been awarded their diploma or PhD degrees in 2001:

Diploma:

Ariane Blanchard	Production and electronic properties of endohedrally doped fullerenes
Jan Sievers	Ultrafast electron dynamics of image potential states on Ni surfaces
Florian Kronast	Spinaufgelöste Photoelektronen-Emissions-Mikroskopie an magnetischen Nanostrukturen

Doctorate:

Sven Link	Femtosecond electron dynamics of image-potential states on the transition-metal surfaces of Pt and Ni
Ricardo Scherer	Soft X-ray emission and resonant inelastic scattering study of polycyclic hydrocarbons
Rainer Klingeler	Erzeugung und elektronische Struktur von endohedral dotierten Fullerenen
Ingo Wirth	Untersuchung des Einflusses unterschiedlicher Dotierungen auf die elektronische Struktur von deponierten Einzelfullerenen mittels Rastertunnelspektroskopie
Gunnar Lüttgens	Photoelektronenspektroskopie an reagierten Metallclustern – Dynamik der Ligandendesorption, elektronische Struktur und Geometrie
Niko Pontius	Ultraschnelle Relaxation optisch angeregter Elektronen in kleinen Übergangsmetallclustern
Cristina Malagoli	Magnetic and electronic properties of local-moment systems: Rare earth metals and oxides

I would like to close this report by thanking all members of the institute for their dedicated work during the past year.

Thomas Brückel

Personnel 2001/2002 and areas of activity

Director: Prof. Dr. W. Eberhardt *until30.04.01*
Tel.: 4428
Prof. Dr. Th. Brückel (interims director)
Tel. 4699

Secretary: J. Gollnick
Tel.: 5814, Fax: 2620

Groups	Research Areas
M. Malagoli (PhD-student) *until31.08.01*	Thin film magnetism Spin-polarized photoemission and CMXD with synchrotron radiation
Dr. L. Baumgarten Dr. H. Dürr *until 30.09.01* C. Zilkens (PhD-student) F. Kronast (PhD-student) *until 30.04.01* S. Link (PhD-student) *until 30.06.01* H. Rhie (PhD-student) *until 31.07.01* J. Sievers (Diploma-student) B. Heitkamp (Diploma-student)	F-sec laser photoemission and high resolution photoemission from solids Photoelectron microscopy
Dr. S. Cramm M. Freiwald (PhD-student) D. Schondelmaier (PhD-student) *until 31.08.01*	Beamlines at DELTA and BESSY II Characterization of functionalized surfaces
Dr. S. Eisebitt *until 31.12.01* R. Scherer (PhD-student) *until 30.04.01* I. Wirth (PhD-student) M. Lörgen (PhD-student) *until 30.09.01* A. Zimina (PhD-student) *until 31.12.01*	Soft x-ray emission spectroscopy STM microscopy and spectroscopy
Dr. S. Blügel *until 31.03.01* Dr. G. Bihlmayer D. Wortmann (PhD-student) M. Heide (PhD-student)	Electronic structure theory of solids and multilayers STM-theory
Dr. P.S. Bechthold Dr. M. Neeb R. Klingeler (PhD-student) *until 31.10.01* G. Lüttgens (PhD-student) N. Pontius (PhD-student) *until 30.09.01* A. Blanchard (Diploma-student) *until 03.08.01* Ch. Breuer (Diploma-student)	Electronic structure, geometry and materials properties of clusters F-sec dynamics of clusters
Dr. J. Morenzin	Development of a magnetic security system
J. Lauer H. Pfeifer	Electronic-Laboratory
K. Bickmann B. Küpper	Vacuum-Laboratory

Research Group "Magnetic Multilayers"

Prof. Dr. P. Grünberg
Dr. D. Bürgler
Dr. R. Gareev
Prof. B. Kuanr *until 30.06.01*
Dr. A. Paul
J. Wingbermühle (PhD-student)
M. Buchmeier (PhD-student)
M. Breidbach (PhD-student)
F.-J. Köhne
R. Schreiber
T. Damm (PhD-student)
H. Dassow (Diploma-student)
L. Pohlmann (Diploma-student)

Magnetic multilayers for sensors and memory applications

Studies of strongly coupled epitaxial Fe(001)/Al/Fe trilayers by Brillouin Light Scattering

M. Buchmeier, B. K. Kuanr, R. Schreiber, D. E. Bürgler and P. Grünberg
Institute "Electronic Properties"

We report experiments on the interlayer exchange coupling in epitaxial Fe/Al/Fe structures. The total coupling is as high as 3 mJ/m^2 and leads to the formation of a partial domain wall in the ferromagnetic films parallel to the interfaces due to the competition between the torques excerted by the interlayer coupling and the external field. Using micromagnetic calculations to simulate magnetizations loops and Brillouin light scattering spectra we show that the twisted state results in higher saturation fields than expected for coupled uniform films. Hence, for strongly coupled systems the twisted state must be taken into account to reliably determine interlayer coupling constants.

F&E-Nr.: 23.42.0

Magnetic interlayer exchange coupling was discovered in 1986 by Grünberg *et al.* [1]. Meanwhile, its origin is well understood, although there is still quite some discrepancy between the theoretically predicted and experimentally measured coupling strengths [2]. On the other hand there is an increasing interest in interlayer coupling, in particular in systems showing strong coupling, due to applications as artificial antiferromagnets or antiferrimagnets in magnetic sensors [3] or more recently in antiferromagnetically coupled (AFC) storage media for harddisk drives [4]. Here, we report on strong coupling in Fe/Al/Fe structures and on general consequences of strong coupling on the magnetization state of magnetic multilayers.

Epitaxial Fe(50Å)/Al(wedge)/Fe(70Å) trilayers are prepared by molecular beam epitaxy (MBE) on top of a GaAs(001)/Fe(10Å)/Ag(1500Å) buffer system [5] at background pressures of about 10^{-10} mbar. Deposition rates of 0.1 Å/s are controlled by a quartz crystal monitor, and the layers are characterized by AES, LEED, and RHEED. The best growth temperatures in order to obtain strong coupling were found to be 300 °C for the first Fe layer and 80 °C for the Al layer. The magnetic properties are measured by Brillouin light scattering (BLS) using a Sandercock-type interferometer and the longitudinal magneto-optic Kerr effect (MOKE).

In a BLS experiment the frequency of spin-waves (or magnons) ν_m is measured via inelastic scattering of monochromatic light. The frequency of the photons can be shifted either down or up by ν_m corresponding to the creation (Stokes condition) or annihilation (Anti-Stokes condition) of a magnon, respectively. As the in-plane momentum is conserved, the in-plane wavevector of the probed magnons q is well defined by the scattering geometry. In analogy to coupled harmonic oscillators (i.e. phonons), the magnon modes in magnetic doublelayers can be classified into optic (O) and acoustic (A) depending on whether their frequency depends on the interlayer coupling strength or not. With increasing antiferromagnetic (AFM) coupling strength the optic mode frequency shifts up for antiparallel (AP) alignment and down for parallel (P) alignment of the magnetizations. In contrast the acoustic mode frequency only depends indirectly on the coupling via the direction of magnetizations.

The spin-wave frequencies observed by BLS were modeled using a thin-film approximation following Ref. [6], which underestimates the optic mode frequency with increasing coupling strength. The comparison with the full

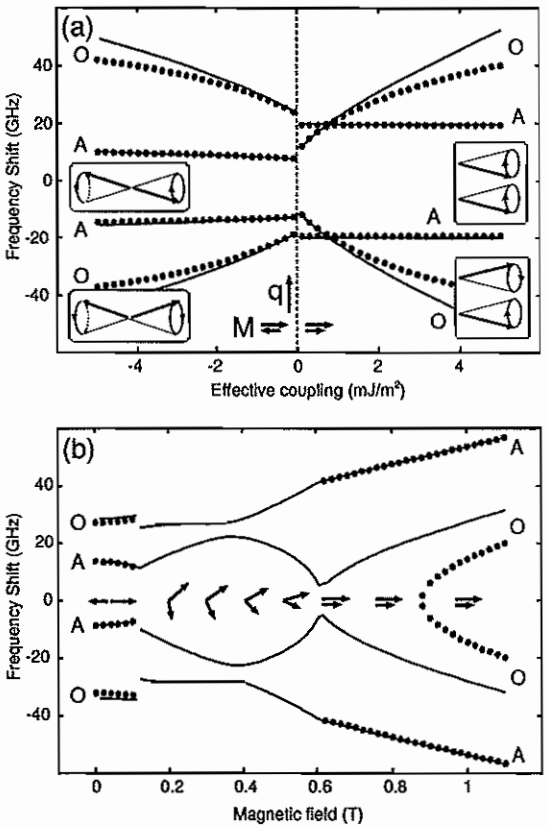

FIG. 1. Calculated acoustic (A) and optic (O) spin-wave frequencies of a Fe(001)(50Å)/spacer/Fe(70Å) system. Solid lines: thin film approximation [6], dotted lines: full calculation [7]. The parameters are: $M_s = 1.65 \times 10^6$ A/m, $K_1 = 45000$ J/m^3, $\gamma = 28$ GHz/T, $A = 2 \times 10^{11}$ J/m, $q = 1.67 \times 10^7$ m^{-1}. (a): BLS frequencies in zero field as a function of effective coupling which is defined as $J_1 - 2J_2$ for AP and $J_1 + 2J_2$ for P alignment. Insets show the precession directions of the magnetizations, bold arrows are in the plane. (b): BLS frequencies as a function of field applied along the easy axis. Coupling constants are $J_1 = -2.4$ mJ/m^2, $J_2 = -0.4$ mJ/m^2 corresponding to Fig. 2. The softening of the optic mode in the full calculation at about 0.9 T results in a dynamic instability giving rise to non-uniform magnetization in the magnetic films.

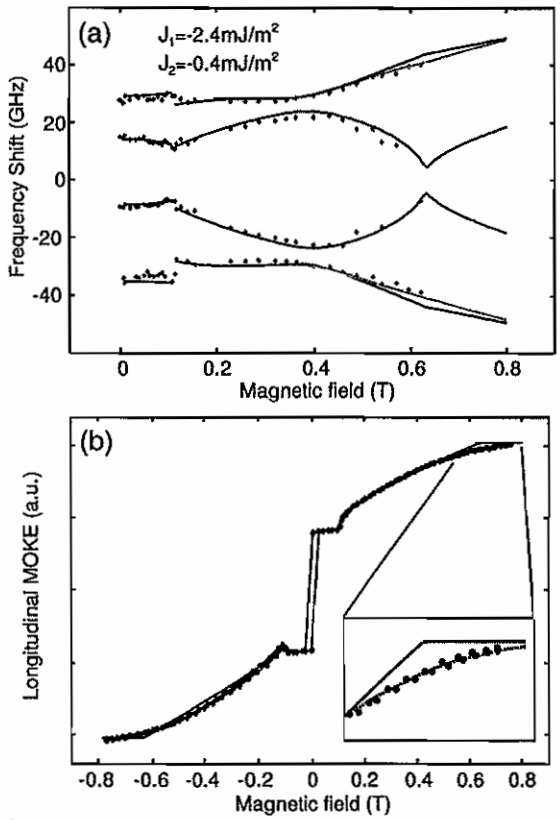

FIG. 2. Easy axis field variation curves of a sample with constant Al thickness (6 Å). Dots: experimental data, solid lines: fit assuming uniform magnetization. (a) BLS fitting J_1 and J_2. (b) MOKE loop obtained using J_1 and J_2 from (a) and fitting phenomenological MOKE constants including quadratic effects [9]. Dashed lines in the high field part of (a) and in the inset of (b) are the results of a micromagnetic calculation allowing a nonuniform magnetization.

calculation using the formalism of Ref. [7] (only possible in P or AP alignment) is shown in Fig. 1 and reveals that the approximation is good in the range between -2 mJ/m^2 and 1 mJ/m^2 effective coupling strength for our samples. We obtain the bilinear (J_1) and biquadratic (J_2) contribution to the coupling defined by $E_c = -J_i \cos^i(\Delta\theta)$ [2] by fitting the dependence of the BLS frequency on the magnetic field. Comparing the J_1 and J_2 values derived from BLS with those from MOKE loops shows excellent agreement (Fig. 2). However, while both the full and approximated approach assume a single domain configuration with uniform magnetization, this is not strictly the case for strongly coupled samples. As a result of the competitive torques exerted by the interlayer coupling at the interface and by the external field in the bulk, a partial domain wall parallel to the interface forms, if coupling and external field are strong enough compared to the magnetic intralayer exchange stiffness A [8]. As can be seen in Fig. 1(b) the optic mode frequency in the full calculation approaches zero at a field of about 0.9 T indicating a destabilization of the uniform P state of the magnetizations. This happens at a field significantly higher than the saturation field of about 0.6 T obtained by assuming uniform magnetizations (solid line). Micromagnetic calculations reveal that

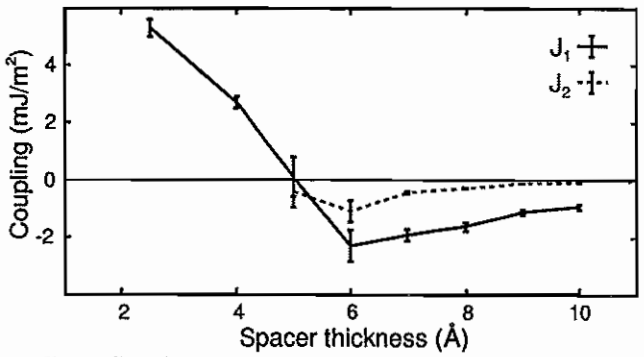

FIG. 3. Coupling versus spacer thickness of a wedge-type Fe/Al/Fe sample.

the configuration is indeed twisted. Below saturation the magnetizations turn about 10° more out of the field direction at the interface than at the outer boundaries. Therefore, the observed saturation field corresponds to the softening of the optic mode. This nonuniform behavior is also in agreement with the experimental curves (Fig. 2). While the deviations from the uniform model are not so pronounced in this case, they must be taken into account when dealing with thicker magnetic layers or stronger coupling.

We find a non-oscillatory behavior of the coupling versus spacer thickness (Fig. 3). The AFM coupling decays slowly with increasing spacer thickness and is present for Al thicknesses of at least 20 Å. The maximum total coupling strength ($J_1 + J_2$) at an interlayer thickness of 6 Å is about -3 mJ/m^2 which is among the largest values observed so far. With increasing interlayer thickness the biquadratic coupling contribution J_2 decreases more quickly than the bilinear part J_1. However, for spacer thicknesses below $\approx$ 5 Å J_2 dominates but is overcome by pinhole-induced ferromagnetic coupling below 4 Å. This suggests that the biquadratic coupling arises from the competition between pinholes and the intrinsic bilinear AFM coupling.

In conclusion, we observe strong interlayer coupling across Al spacers which is about one order of magnitude larger than previously reported (e.g. [5]). The strong coupling leads to a twisted magnetization state which shows up in BLS and MOKE measurements. We expect much stronger effects in systems with even higher coupling, e.g. Fe/Si/Fe [10].

[1] P. Grünberg *et al.*, Phys. Rev. Lett. **57**, 2442 (1986).
[2] D. E. Bürgler *et al.*, Handbook of Magnetic Materials, Vol. 13, p. 14, edited by K. H. J. Buschow, Elsevier Science B. V. (2001).
[3] van den Berg *et al.*, IEEE Trans. Mag. **32**, 4624 (1996).
[4] E. E. Fullerton *et al.*, Appl. Rev. Lett. **77**, 3806 (2000).
[5] A. Fuß *et al.*, J. Magn. Magn. Mater. **103**, L221 (1992).
[6] S. M. Rezende *et al.*, J. Appl. Phys. **84**, 958 (1998).
[7] J. Barnas and P. Grünberg, J. Magn. Magn. Mater. **82**, 186 (1989).
[8] J. F. Cochran, J. Magn. Magn. Mater. **147**, 101 (1995).
[9] K. Postava *et al.*, J. Appl. Phys., to be published (2002).
[10] R. R. Gareev *et al.*, J. Magn. Magn. Mater. to be published (2002).

A Green-function formulation of the transfer matrix for electronic structure calculations: First application to complex bandstructures

D. Wortmann,[1] G. Bihlmayer,[1] H. Ishida,[2] and S. Blügel[3]

[1]*Institute "Electronic Properties"*
[2]*College for Humanities and Sciences, Nihon University, Sakura-josui, Tokyo 156, Japan*
[3]*Fachbereich Physik, Universiät Osnabrück, 49069 Osnabrück, Germany*

A new method for the first-principles calculation of the transfer matrix is presented. The method is based on a Green-function formulation and allows to relate the wavefunctions and their derivatives on boundaries at opposite sides of a film or junction of finite thickness. Both the underlying theory and an actual implementation in the full-potential linearized augmented planewave (FLAPW) method are described. Applications of the transfer-matrix method include the calculations of the complex bandstructure and the calculation of ballistic electron transport relevant in realistic magnetic multilayers and magnetic tunneljunctions used in spin- and magnetoelectronics.

An electron propagating through a crystal towards an interface can either reflect or transmit. This rather simple statement is at the heart of fields such as nanoelectronics, magnetoelectronics, spin-electronics, or molecular-electronics – areas of great importance for future technology. Understanding the transport properties on the basis of the underlying electronic structure is a key issue. On the other hand, over the past decades, the core of methods developed to perform *ab initio* electronic structure calculations based on density functional theory focussed on finding eigenstates for electrons in increasingly more complex material systems. These eigenstates are usually calculated within some slab or supercell geometry with periodic boundary conditions, and are used to calculate the total energy of the system or forces exerted on the atoms. In the field of transport, however, in particular ballistic transport, one has to consider a scattering problem. In the asymptotic region, i.e. in the interior of the electrodes on both sides of the interface, transmitted and reflected electron waves are expressed as the superposition of generalized Bloch states. The generalized Bloch states include the propagating Bloch waves as well as evanescent states that decay exponentially. The amplitudes of these waves are determined such that the total wavefunction connects smoothly to the solutions of the Schrödinger equation in the interface region.

In the past a number of methods have been developed which address the problem of calculating the transmission of ballistic electrons through interfaces. We present [1] a new general method which can be applied to a wide variety of problems. For example it can be used to calculate the complex bandstructure of bulk crystals, ballistic transport properties of interfaces, and the electronic structure of semi-infinite surfaces. It is based on a transfer matrix for one-electron wavefunctions which is calculated using a Green function in the LAPW basis. The method should therefore inherit from the FLAPW method the generality in the choice of systems and the accuracy in the description of the underlying electronic structure which was often missing in previous approaches. In our method we consider a region of space,

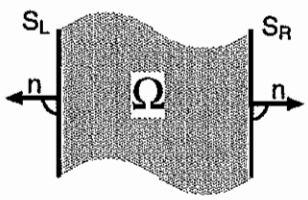

FIG. 1: Setup used to calculate the transfer matrix. The region of interest is a slab Ω between the two boundaries S_L and S_R. Ω is infinite in two dimensions and of finite size normal to the boundaries. The surface normals indicated by arrows are assumed to point outwards.

Ω, which has the shape of a slab (see Fig. 1), i.e. we assume that Ω is infinite in two dimensions and of finite size in the third dimension. To get an idea of what we have in mind, the slab could consist of a single layer of atoms of bulk material with two-dimensional translation symmetry, a monolayer, or of a few monolayers, forming a heterostructure or describing an interface between two semi-infinite crystals. The boundary surface of the slab volume Ω is divided into two parts: the left boundary, S_L, and the right one, S_R. Given a local and spin independent potential energy defined in Ω and on S, $V(\vec{r})$, we consider solutions of the Schrödinger equation corresponding to this potential. Since the Schrödinger equation is a second order differential equation, its solution $\psi(\vec{r})$ in Ω with complex energy $Z \equiv \epsilon + i\delta$ is completely determined by specifying the value $\psi(\vec{r}_{L/R})$ and its local normal derivative, $\partial_n \psi_{L/R} = \partial_n \psi(\vec{r}_{L/R}) = \frac{\partial}{\partial n}\psi(\vec{r}_{L/R})$, on one of the boundary surfaces, $S_{L/R}$. The key quantity of the method presented in this paper is the transfer matrix T. It maps the left boundary values of a solution of the Schrödinger equation onto the right ones:

$$\begin{pmatrix} \psi(\vec{r}_R) \\ \partial_n \psi(\vec{r}_R) \end{pmatrix} = T \begin{pmatrix} \psi(\vec{r}_L) \\ \partial_n \psi(\vec{r}_L) \end{pmatrix}. \qquad (1)$$

The transfer matrix can be expressed in terms of the Green function $(\hat{H} - Z)\, G(\vec{r}, \vec{r}\,'; Z) = -\delta(\vec{r} - \vec{r}\,')$, where

$\hat{H}$ is the usual Hamiltonian consisting of the potential and kinetic energy terms. A particularly simple form is obtained by choosing a Green function which satisfies the von Neumann boundary condition of vanishing normal derivative on the boundary surface: $\frac{\partial}{\partial n} G(\vec{r}, \vec{r}_{L/R}; Z) = 0$ In this case one can derive a simple matrix expression for the transfer matrix in terms of surface Green-functions,

$$T = \begin{pmatrix} G_{RR} G_{LR}^{-1} & -\frac{1}{2} G_{RL} + \frac{1}{2} G_{RR} G_{LR}^{-1} G_{LL} \\ -2 G_{LR}^{-1} & -G_{LR}^{-1} G_{LL} \end{pmatrix}, \quad (2)$$

where the surface Green-functions G_{LL}, G_{LR}, G_{RL}, and G_{RR} are defined by placing $\vec{r}$ and $\vec{r}'$ onto the boundary surfaces. For example $G_{LR}(Z) = G(\vec{r}_L, \vec{r}_R; Z)$, with the first argument of the Green function placed on S_L and the second on S_R.

With the transfer matrix we can calculate various quantities of which we will present the complex bandstructure and the calculation of transport properties.

Most fundamental is the calculation of the complex bandstructure as it is the basis of further applications of the theory. Generally, the term complex bandstructure [2] refers to the so called "real bands" consisting of the solutions $\epsilon(\vec{k})$ with real energy ϵ and in general complex Bloch vectors $\vec{k} = \vec{q} + i\vec{\kappa}$. In the bulk of a crystal, the translation symmetry requires that the Bloch vectors are purely real. But near a crystal surface or interface the wavefunctions of complex $\vec{k}$ vectors can match with wavefunctions in the crystal, and thus are describing evanescent surface, interface, or metal induced gap states.

To calculate these generalized Bloch states with complex $\vec{k}$ one assumes that the region Ω is a principle layer of a bulk crystal with three-dimensional translation symmetry. Thus, there exists a translation vector $\vec{d}$ between S_L and S_R, which is a lattice vector and one can exploit this translation symmetry by the generalized Bloch theorem. This leads to the following eigenvalue equation for the transfer matrix which defines the complex $\vec{k}$-vectors:

$$T \begin{pmatrix} \psi(\vec{r}_R) \\ \partial_n \psi(\vec{r}_R) \end{pmatrix} = \exp(i\vec{k}\vec{d}) \begin{pmatrix} \psi(\vec{r}_R) \\ -\partial_n \psi(\vec{r}_R) \end{pmatrix}. \quad (3)$$

In Fig. 2 we present the complex bandstructure of Cu with $\vec{k}_\parallel$ corresponding to the $\overline{\text{M}}$-point of the two-dimensional Brillouin zone and the k_z along the [100]-direction. The (propagating) Bloch states, i.e. real bands with $\kappa_z = 0$, are plotted as black dots in the center panel of the figure. The complex bandstructure includes all propagating Bloch states $(\vec{k}_\parallel, q_z)$ along the line in a first bulk Brillouin zone connecting the high-symmetry points X ($q_z = 0$) and W ($q_z \neq 0$). The imaginary part κ_z of the wave vectors of the complex bands are plotted in the right- and left-hand panels of the figures in units of $a.u.^{-1}$. Red and green dots denote states corresponding to a wave vector q_z at the left (X) and right (W) high-symmetry point, respectively. Complex bands with general k_z-values are indicated in the figures by two yellow dots corresponding to a projection of k_z onto the real and the imaginary plane. The real component q_z is plotted in the center panel together with the Bloch states with $\kappa_z = 0$ and the imaginary component κ_z is shown in the left-hand panel together with the evanescent states with $q_z = 0$.

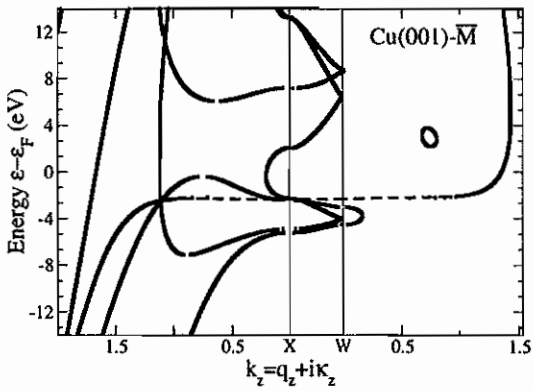

FIG. 2: Complex bandstructure of Cu. The black lines show the propagating Bloch states, colored dots denote evanescent states. κ_z is given in absolute units of $a.u.^{-1} = 1.89$ Å^{-1}.

After having obtained the complex bandstructure we can use our transfer matrix to evaluate the transmission coefficients $t_{nn'}$ for each incoming Bloch wave. To define the problem, we will consider a ballistic electron approaching the left boundary surface from the left and being reflected in Ω or being transmitted into a lead to the right. The total setup now consists of three regions, the left and right leads, and the region Ω. We assume that the scattering potential is confined within Ω, i.e. the potential in the leads is assumed to be the bulk crystal potential. Within the the formulation of Landauer and Büttiker [3] for ballistic transport the ballistic conductance of the system is obtained as

$$G = \frac{e^2}{h} \sum_n \sum_{n'} |t_{nn'}|^2. \quad (4)$$

By expanding the reflected and transmitted waves in the leads in terms of the eigenstates Ψ_{Left} and Ψ_{Right} determined from Eq. (3) for these regions one can easily determine the transmission ($t_{nn'}$) and reflection (r_{nm}) coefficients by applying the transfer matrix for the interface region Ω:

$$\sum_{n'} t_{nn'} \Psi^{n'}_{\text{Right}} = T \Psi^{n}_{\text{incomming}} + \sum_m r_{nm} T \Psi^{m}_{\text{Left}}. \quad (5)$$

This method enables us to calculate the ballistic transport through realistic tunneljunctions and magnetic multilayers.

References

1. D. Wortmann, H. Ishida, and S. Blügel, accepted by Phys. Rev. B
2. V. Heine, Surf. Sci. **2**, 1 (1964)
3. M. Büttiker, Phys. Rev. Lett. **57**, 1761 (1986)

Spin-Polarized Photoelectron Emission Microscopy of Magnetic Nanostructures

F. Kronast, B. Heitkamp, H.A. Dürr, and W. Eberhardt
Institute "Electronic Properties"

The development of high performance magnetic data storage devices requires the further miniaturization of bit sizes and the shortening of read/write cycles. For these future generations of magnetic data storage devices a fundamental understanding of the magnetization dynamics in nanostructures is indispensable. We realized a novel experimental setup which allows us to study the fundamental limits in magnetization dynamics on nm length scales. We operate a photoemission electron microscope (PEEM) with a fs-laser light source. The fs temporal resolution is achieved by laser based pump-probe techniques and the magnetic sensitivity is obtained by analyzing the spin of the emitted photoelectrons. We will present an application of the technique to CoPt nanoscale magnetic dots [6].

The development of pump-probe techniques using ultrashort laser pulses has recently led to a tremendous advance in the investigation of time dependent magnetic phenomena [1, 2, 4]. This method utilizes two subsequent laser pulses with a variable time delay focussed on the same spot on the sample. The pump laser pulse is used to induce a local demagnetization of the sample via electronic excitations. The delayed probe laser pulse creates a photoelectron yield that carries information about changes in the sample magnetization. Qualitatively these processes can be described by the energy transfer between different quasiparticle reservoirs such as electrons, spins and phonons. The absorption of the pump pulse leads to a non-equilibrium electron distribution which thermalizes within several 100 fs. Although still controversial in its magnitude it is obvious that during this time spin-flip transitions can occur that reduce the sample magnetization to a certain degree. On a longer (ps) time scale energy is transferred to the lattice providing an additional path for demagnetization. Not much is known about the lateral extent of the demagnetized sample area since all techniques have averaged over the pump and probe laser spots. However, the determination of lateral energy transport mechanisms leading to a reduction of the sample magnetization contributes significantly to the interpretation of previous experiments [1, 2, 4]. Here we describe a first attempt to determine the possibility of a 'non-local' reduction of the magnetization.

The experimental setup is shown schematically in Fig. 1. We use a commercial PEEM (Omicron/Focus IS-PEEM) where the magnification is achieved by three sets of electrostatic lenses. The heart of the PEEM is the objective lens whose aberrations determine the limit of the achievable lateral resolution. The sample is an integral part of this lens. Between the sample surface and the so-called extractor an electrical voltage typically of 15kV is applied. This results in a very efficient extraction of low-energy photoelectrons emitted from the sample surface. For threshold photoemission the chromatic aberration is reduced due to the small energy spread of photoelectrons. Astigmatism can be corrected by a stigmator/deflector unit (not shown in Fig. 1). A contrast aperture (not shown) in the backfocal plane of the objective lens determines the size of spherical aberration. This contrast aperture can also be used to separate photoelectrons emitted from the surface at different emission angles. An adjustable iris aperture is mounted in the first image plane of the PEEM. This allows us to select the width of the transmitted photoelectron beam, i.e. only photoelectrons emitted from a certain sample area are transmitted. This is instrumental for achieving lateral magnetic resolution. In this case the photoelectron beam is electrostatically deflected into a spin detector (Omicron/Focus SPLEED). Here the spin dependent scattering of low-energy electrons from a W(100) single crystal surface is used. The asymmetry, $A = (N_+ - N_-)/(N_+ + N_-)$, of the count rates, N_{+-}, for two symmetrically positioned electron detectors is proportional to the photoelectron spin polarization [6].

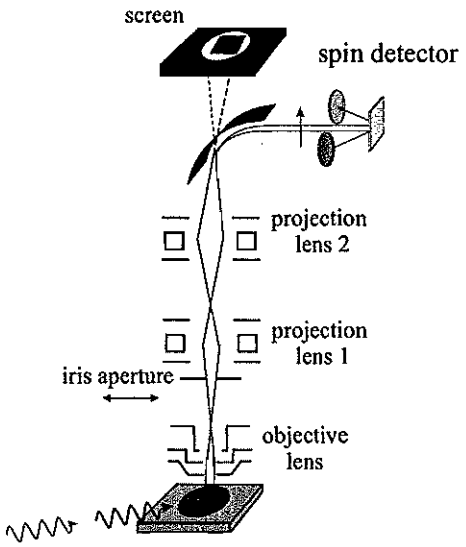

FIG. 1: Schematic diagram of the spin-polarized photoemission electron microscope

Photoelectrons were excited using a Ti:sapphire laser

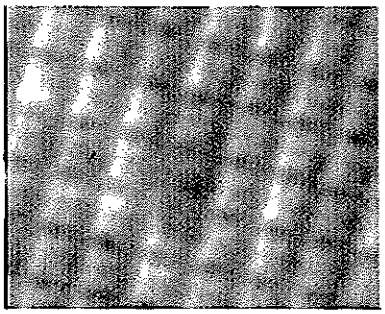

FIG. 2: Typical PEEM image of the sample taken with 3eV s-polarized light. The 200nm x 200nm nanodots are clearly resolved.

system operating with a repetition rate of 76 MHz (Coherent Mira pumped by a Coherent Innova 400 Ar-ion laser). Mode locking results in 150 fs long laser pulses of 1.5eV photon energy and a pulse energy of up to 20nJ. The pulses were frequency doubled using β-BBO crystals. The fundamental and second harmonics (3eV) were separated by dichroic mirrors.

Our sample consisted of 200nm x 200nm wide magnetic structures separated from each other by 100nm wide and 200nm deep troughs [5]. A Pt(1.8nm)[Co(0.5nm)Pt(1.8nm)]$_4$ multilayer was sputter deposited on top of a patterned Si substrate. The CoPt multilayer structure induced a spin alignment along the surface normal due to a large perpendicular magnetic anisotropy at the CoPt interfaces [5]. PEEM images of the nanodot arrays with 3eV photons show photoemission mainly from the fringes. This can be explained by a Mie plasmon enhancement of the laser field inside the nanodots. This process enhances the photoemission yield by a factor of 240 as was determined by comparing with an unstructured area of the sample.

For a non-local pump probe experiment we generated a spatially strongly varying laser intensity profile across the illuminated sample spot by interference patterns. They were generated by splitting each 3eV laser pulse in two and subsequently focusing them on the same sample spot. By varying the optical delay between the two pulses interference patterns could be varied as shown in Fig. 3. The two PEEM images show the illuminated area on the CoPt sample. The top image shows the interference pattern for an optical delay of half a wavelength, i.e. 205nm. In the bottom image the two laser pulses arrive at the sample without an optical delay. We set the iris aperture to the positions indicated in the images and detected only photoelectrons emitted from these sample areas. The measured spin asymmetry is plotted in Fig. 3 as a function of the laser pulse energy. With increasing laser intensity the spin polarization in the center of the brightly illuminated laser spot is reduced (solid symbols) indicating an increasing demagnetization of the CoPt sample. It is interesting to note that this decrease sets in at fluences that are about a factor of 1000 lower than those reported for a $CoPt_3$ sample [3]. We consider this a clear indication that for our multilayered sample the electric field becomes strongly enhanced through the dielectric response of the Pt layers. This leads to effectively similar laser intensities as those reported by Beaurepaire et al. [3], causing a similar sample demagnetization. Interestingly we also find a reduction of the sample magnetization in the areas where the laser intensity is reduced by interference effects (open symbols). This demonstrates that heat transport away from the high intensity regions sets in. We note that it should also be possible to determine the time constants for this process from time-resolved pump-probe experiments which are presently underway.

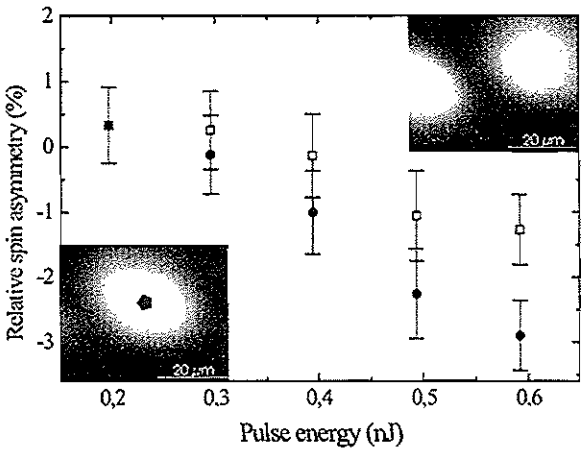

FIG. 3: Laser induced demagnetization: Two 3eV laser pulses interfere with each other and produce footprints on the sample as shown by the PEEM images in the insets for different optical delays. The spin asymmetry measured for the indicated regions is shown as a function of the laser pulse energy (open and solid symbols correspond to the aperture positions as indicated in the top and bottom inserts, respectively).

[1] A. Scholl L. Baumgarten, R. Jacquemin, W. Eberhardt, Phys. Rev. Lett. **79**, 5146 (1997)

[2] B. Koopmans, M. van Kampen, J. T. Kohlhepp, W. J. M. de Jonge, Phys. Rev. Lett. **85**, 844 (2000)

[3] E. Beaurepaire, J.-C. Merle, V. Halt, A. Daunois, J.-Y Bigot, Phys. Rev. B **58**, 12134 (1998)

[4] G.P. Zhang, W. Hübner, Phys. Rev. Lett. **85**, 3025 (2000)

[5] S. Landis, B. Rodmacq, B. Dieny, B. Dal'Zatto, S. Tedesco, M. Heitzmann, Appl. Phys. Lett. **75**, 2473 (1999)

[6] H.A. Dürr, F. Kronast, W. Eberhardt, Advances in Solid State Physics, **41**, Springer-Verlag (2001)

Magnetron Cluster Sputter Source at the IEE

C. Breuer*, N. Pontius†, I. Wirth‡, P.S. Bechthold, M. Neeb§, and W. Eberhardt¶
Institute "Electronic Properties"
(Dated: December 20, 2001)

A magnetron cluster aggregation source has been constructed and successfully implemented into the existing cluster deposition apparatus at the IEE. The cluster source can be used to produce clusters of almost any conducting and semiconducting material. The reliability, stability and first mass spectra are exemplarily demonstrated for copper clusters.

PACS numbers: F&E-Nr: 23200

A magnetron cluster sputter source [1] has been constructed and built at the IEE during the last year. The cluster source combines a magnetron gas discharge with the cluster aggregation technique. The plasma source is driven by a dc-power supply and can be used to produce a continuous beam of clusters from all conducting and semiconducting solid materials. The new cluster source has been implemented into the existing cluster deposition machine. The whole cluster beam apparatus can be used for controlled deposition of mass-selected clusters up to 10000 amu, i.e. Fe_{180}, Cu_{140}, C_{800}, Pt_{50}. Mass selection prior to soft-landing is provided by a magnetic sector field. Depending on the slit width a maximum ion transmission of 50 % and a mass resolution ($m/\Delta m$) of 300 has been demonstrated recently for doped fullerene clusters [2,3]. Because the magnetron source runs in a continuous mode it is ideally suited to be used with the magnetic cluster ion selector.

A picture of the magnetron cluster source is shown in Fig. 1. Under working conditions (Ar-pressure: 1-10 Torr, He-pressure: ~100 Torr, ~250 V, 200 W) a stationary plasma is formed between the target cathode and anode. Electrons are guided in the vicinity of the target surface by a magnetic field. This enhances the rare gas cation yield which sputters the target (diameter 2").

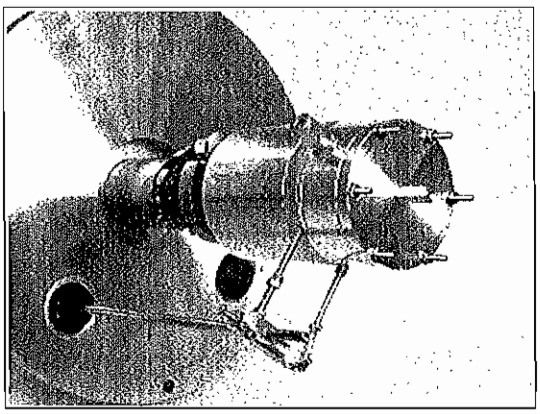

FIG. 1: Magnetron cluster source

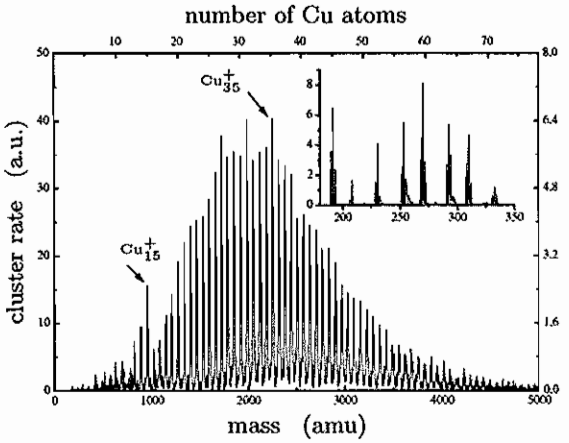

FIG. 2:Cu^+ mass spectrum as produced by the magnetron cluster source. The inset shows the isotopic distribution of smaller clusters.

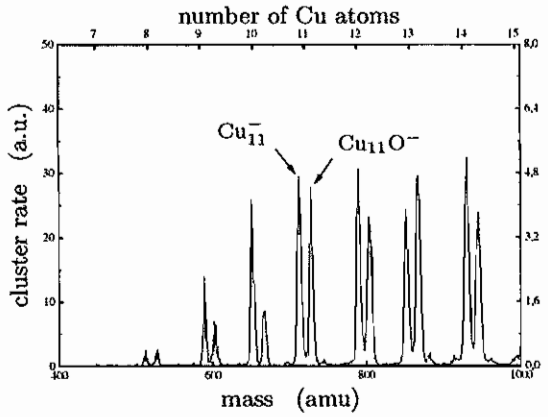

FIG. 3:Cu^- mass spectrum.

A condensation cell has been adapted immediately behind the cathode for cluster aggregation. The particle flow entering the condensation cell can externally be controlled by a adjustable iris aperture. An important

*till 2002-01-07
†till 2001-10-01
‡till 2001-12-31
§till 2002-01-01
¶till 2001-05-01

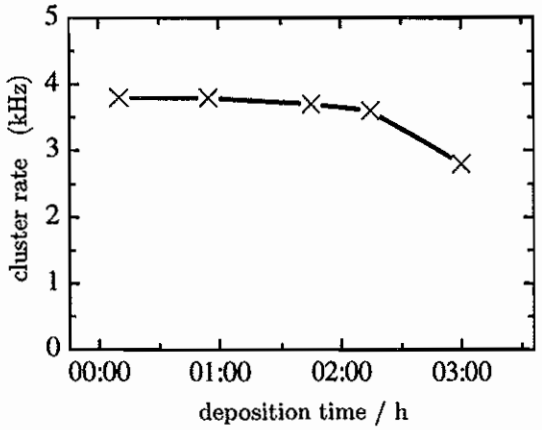

FIG. 4: Cluster intensity as a function of deposition time.

parameter to control the cluster size distribution is the length of the condensation tube which, so far, cannot be adjusted in situ but only after opening the chamber.

A typical mass spectrum of Cu clusters is shown in Fig. 2. Cluster sizes between 10 and 70 atoms are seen. The homogenous size distribution and intensity pattern is typical for clusters produced in a aggregation source. The sharp peaks demonstrate the well defined thermal energy distribution of the supersonic cluster beam. Note the natural isotopic intensity pattern which is resolved for very small Cu clusters (see inset). From this a mass resolution of ca. 200 is deduced. Also, no contamination with oxygen is observed in Fig. 3. This is different for negatively charged Cu clusters which seem to be more reactive than the cations since each Cu_n^- peak is accompanied by an adjacent $Cu_nO_m^-$ peak.

The source runs stable over a couple of hours as is demonstrated in Fig. 4 where the cluster intensity of Cu_{15}^+ is shown as a function of the deposition time. The intensity has been measured behind the exit slit of the magnetic cluster selector using a channeltron detector.

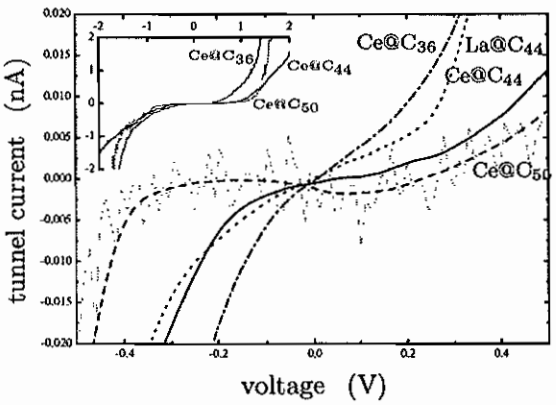

FIG. 5: $I(V)$-curves of deposited small endohedral fullerenes on graphite. The lines represent smoothed experimental data.

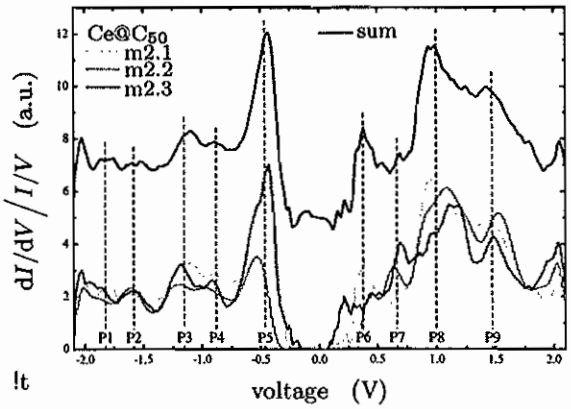

FIG. 6: Scanning tunneling spectroscopy on $Ce@C_{50}$/HOPG at 27 K. The total result (bold line) is the sum of single spectra (m2.1, m2.2, m2.3) taken on three different clusters. The total sum is shifted vertically. Zero refers to the Fermi level; peaks at negative voltages correspond to occupied electronic levels while positive voltages are due to empty orbitals.

From the scientific point of view, doped endohedral metallofullerenes have been deposited on HOPG and investigated by STM/STS. The metallofullerenes were produced in a laser evaporation cluster source using Ce-doped carbon targets. $I(V)$-curves of the deposited endohedral metallofullerenes are shown in Fig 5 which have been taken with a chemically etched tungsten tip on top of individual clusters. The $I(V)$-curves show the different metallic behaviour of the deposited metallofullerenes. While $Ce@C_{36}$/HOPG shows the most metallic character $Ce@C_{50}$ is definitely semiconducting, showing a gap of ~0.8 eV. The gap is clearly obvious by the normalized differential conductivity, the so called scanning tunneling spectrum, which is shown in Fig. 6. The STS-spectrum shows the local density of states immediately below and above the Fermi level.

Supposing a charge transfer of 3 electrons from the lanthanoide to the carbon cage the gap can be explained by a metal-to-insulator transition. Supposing a Mott-Hubbard model the gap of 0.8 eV is equal to the Coulomb interaction between the electrons in the highest occupied orbital. Due to the small dispersion of the molecular-like orbitals the Coulomb energy should be much larger than the bandwidth causing the semiconducting character of the open shell cluster $Ce@C_{50}$.

[1] H. Haberland, M. Karrais, M. Mall, Z. Phys. D 20, 413 (1991).

[2] Klingeler, R., Bechthold, P.S., Neeb, M., Eberhardt, W., J. Chem. Phys. 113, 1420 (2000).

[3] Klingeler, R., Kann, G., Wirth, I., Eisebitt, S, Bechthold, P.S., Neeb, M., Eberhardt, W., J.Chem.Phys. 115, 7215 (2001)

Monitoring ultrafast relaxation dynamics of optically excited electrons in Ni_3^- using two-color pump-probe photoelectron spectroscopy

N. Pontius, G. Lüttgens, P.S. Bechthold, M. Neeb, and W. Eberhardt
Institute "Electronic Properties"

The relaxation dynamics of optically excited electrons in free Ni_3^- has been investigated. By means of femtosecond two-color pump-probe photoelectron spectroscopy the relaxation of excited electrons via inelastic electron-electron-scattering could be observed in real-time. The unexpected short electron-electron-scattering time of 190 fs is caused by the relatively large density of states in the vicinity of the highest occupied cluster orbital. This large density of states is results from the narrow bandwidth of the partially filled d-levels in the transition metal clusters. Other aspects for the enhancement of inelastic electron-electron scattering are the spread of the electronic levels by vibrational broadening and the spill-out of the s/p-electron wave functions intensifying the Coulomb-interaction between the electrons.

Electron scattering processes play a key role within many phenomena in solid state physics. If an electron in a bulk metal is excited about 1 eV or more above the Fermi level the predominant relaxation process is inelastic electron-electron scattering as bulk metals generally exhibit a continuous DOS. The mean scattering time τ_{e-e} of inelastically scattered electrons usually amounts to few tens of femtoseconds [1]. τ_{e-e} considerably depends on the density of states (DOS) around the Fermi level.

If the size of a metallic system is reduced to the sub nanometer scale, the DOS is substantially affected by quantum confinement leading to a rather discrete electronic structures. Consequently inelastic electron-electron scattering should be less probable in small metal clusters. This is in particular evident from experiments on small noble and simple metal clusters (e.g. Ag, Na) where inelastic scattering of electrons has not yet been observed. In time resolved photoemission studies on small Pd- and Pt-clusters, however, we could demonstrate for the first time that inelastic electron-electron-scattering takes place on a femtosecond time scale [2–4]. In these transition metal clusters the ultrafast relaxations are enabled by the large DOS around the HOMO (highest occupied molecular orbital) which is caused by the partially filled d-levels. This creates a rather dense electronic level structure in the upper valence region. During the last year we additionally succeeded in observing ultrafast electron relaxations in Ni_3^- in a two-color pump-probe experimental setup.

Fig.1 shows photoelectron spectra of Ni_3^- taken with fs-laser pulses of 80 fs width. The uppermost spectrum was recorded with single fs-pulses of 3 eV photon energy and reveals mainly direct photoemission. Hence in first-order approximation the spectrum reflects the DOS of the occupied orbitals in the electronic ground state configuration of Ni_3^-. Below the HOMO (dotted line at 1.3 eV) the electron intensity drops to zero as here the electronic levels are not occupied.

Fig. 1b) shows a photoelectron spectrum of Ni_3^- but this time being optically excited 130 fs before photoemission by a 1.5 eV photon. A significant change in the binding energy region above the HOMO can be observed. Upon absorption of a pump photon unoccupied orbitals are populated by electrons from occupied levels. The photoelectrons between 0 and 1.3 eV originate form these excited electrons. Increasing the delay between pump and probe up to 600 fs (fig. 1c) the electron intensity distribution above the HOMO changes distinctly. This indicates a fast relaxation of the excited electrons by inelastic electron-electron-scattering as it is well known from similar experiments on metal surfaces [5].

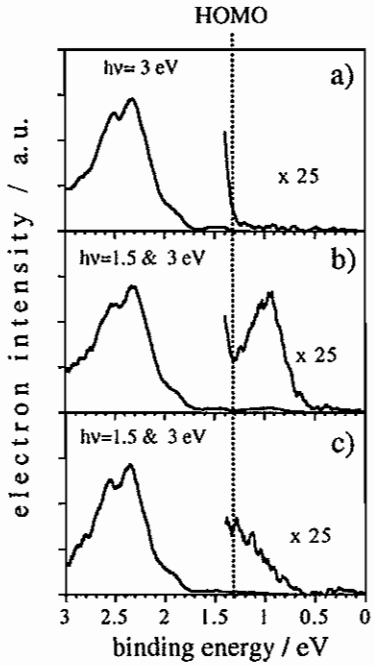

FIG. 1: Femtosecond photoelectron spectra of Ni_3^- taken with fs-pulses. a) shows single-photon photoemission from the Ni_3^- ground state with 3 eV photon energy. b) and c) represent photoemission spectra after optical excitation with a 1.5 eV photon either 130 fs (b) or 600 fs (c) before the probe pulse detaches an electron from the excited cluster.

To study this relaxation process in detail a complete series of pump-probe photoelectron spectra is shown in

fig. 2. Here the electron intensity distribution is plotted in a contour graph as a function of the delay $\Delta\tau$ between pump and probe pulse in the binding energy range above the HOMO (plotted in red in fig. 1). At strong negative delays hardly any intensity can be observed above HOMO (see fig 1a). With increasing delay a broad peak arround 0.9 eV grows into a maximum at about 140 fs (see fig. 1b). Subsequently the electron intensity begins to diminish and to shift towards higher binding energies. After 2 ps, the intensity distribution remains almost constant slightly dropping at decreasing binding energy.

The optically excited electrons scatter with electrons below the HOMO with it transferring a fraction of their excitation energy to their scattered counterpart. After the scattering process both electrons reside above the HOMO at larger binding energies with respect to the binding energy of the initially excited electron. This induces the observed intensity shift. Later on, the relaxation proceeds in a cascade of many further scattering events.

After sufficient scattering processes the electron system attains more or less thermal equilibrium involving a thermal electron intensity distribution ($\Delta\tau \gtrsim$1ps). The decrease of the *total* intensity is caused by the drain of excitation energy from the electronic into the vibrational system via internal conversion.

To quantify a mean scattering time τ_{e-e} of the excited electrons the evolution of the partial electron intensity in the binding energy range between 0 eV to 0.8 eV was

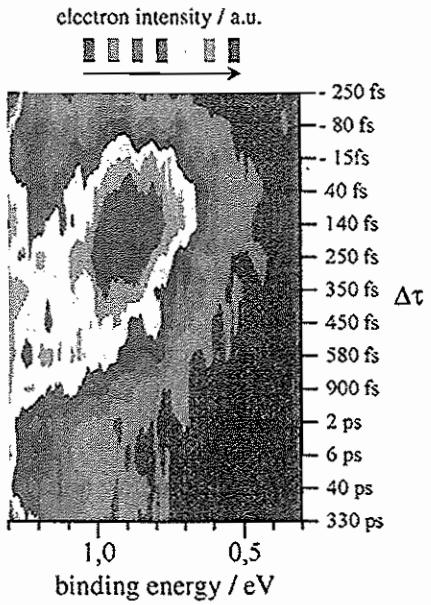

FIG. 2: Evolution of the electron intensity distribution in the energy range above the HOMO of Ni_3^- observed by pump probe photoelectron spectroscopy in real time. The change of the distribution clearly indicates the ultrafast relaxation of the optically excited electrons towards the HOMO by inelastic electron-electron-scattering.

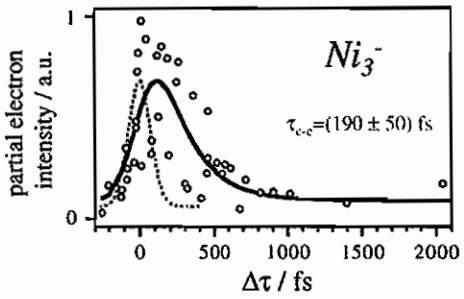

FIG. 3: Population dynamics of the highest excited electrons in the binding energy interval 0 - 0.8 eV. Assuming a first order exponential decay of the initially excited electrons the scattering time τ_{e-e} for inelastic electron-electron-scattering could be deduced. The dotted line shows the calculated cross correlation curve.

analyzed in detail (see fig. 3). The intensity in this energy range represents the electron population which is initially created by the pump pulse. Afterwards it undergoes a simple exponential decay with the time constant τ_{e-e}. This assumption is justified by the fact that electrons usually release half their excitation energy in a single scattering event leading to the removal of the electron from that energy range. Moreover secondary electrons are not expected in that area. Fitting this model to the data in fig. 3 leads to a mean scattering time of τ_{e-e}=(190 ± 50) fs.

The absorbed energy keeps localized in the small cluster (in contrast to similar experiments on bulk metal surfaces). Therefore all electronic states of the cluster have to be energetically degenerate during the dissipation process (within the exciting laser pulse bandwidth and the Heisenberg uncertainty). Thus it is plausible that the more electronic states are located in the immediate vicinity of the excitation energy the faster the relaxation can proceed. From this consideration the above mentioned different relaxation behavior of small noble and transition metal clusters gets clear as the mean number of excited states per energy in transition metal clusters is estimated to be two orders of magnitude larger as in noble metal clusters.

We thank A. Bringer, Forschungszentrum Jülich GmbH (IFF), for stimulating and valuable discussions.

[1] H. Petek, S. Ogawa, Prog. Surf. Sci. **56**, 239 (1997)
[2] N. Pontius, P.S. Bechthold, M. Neeb, W. Eberhardt, Phys. Rev. Lett. **84**, 1132 (2000)
[3] N. Pontius, P. S. Bechthold, M. Neeb, W. Eberhardt, Appl. Phys. **B 71**, 351 (2000)
[4] N. Pontius, G. Lüttgens, P. S. Bechthold, M. Neeb, W. Eberhardt, J. Chem. Phys. **115**, 10479 (2001)
[5] E. Knoesel, A. Hotzel, T. Hertel, M. Wolf, G. Ertl, Surf. Sci **368**, 76 (1996)

Depth Resolved Soft X-ray Emission Spectroscopy of Si-based Materials

A. Zimina, S.Eisebitt, W.Eberhardt
Institute of ''Solid State Research Electronic Properties''

Abstract. We discuss a soft X-ray emission (SXE) valence band (VB) spectroscopy method for the study of the electronic structure and chemical phase composition of solids in a near-surface region with depth resolution. The depth information is obtained by variation of the energy of the incident electron beam used to excite the SXE spectra. As the information depth can be varied from about 1 nm to 1 μm in silicon, this method is suitable for the investigation of materials of modern micro- and nano-electronics. VB → core level (Si 2p or Al 2p) transitions in Si- based materials are used to demonstrate the technique. It was found that the contribution of the signal from the near-surface region (<1.5 nm) can be substantial (up to 50%) when the primary electron energy does not exceed the Si $L_{2,3}$ threshold by more than 150 eV. The technique is applied to Al impurities in a Si matrix, produced by ion implantation. The electronic structure at the Al sites and the depth distribution of the Al impurity change markedly after post implantation annealing. The observed electronic structure after annealing is in agreement with electronic structure calculations for substitutional Al impurities in a crystalline Si lattice.

Characteristic soft X-ray emission (SXE) valence band (VB) spectroscopy is a well-known method of investigation of the electronic structure of solids. In the initial state a vacancy on the core level of the element under investigation is created by photons or electrons. Then the core holes decay by transition of electrons from the VB and the intensity of photon emission is monitored. The shape of a SXE spectrum thus reflects the VB local and partial density of occupied electronic states (LPDOS), i.e. the DOS can be determined with atom and angular momentum selectivity due to the certain dipole selection rules.

Variation of the primary electron beam energy (E_0) allows for the non-destructive depth-resolved study of the electronic structure, atomic concentration and chemical phase composition in the surface region of solids by means of the SXE [1]. The main goals of the work presented here are:

(i) to estimate the contribution of the top surface atomic layers to the total SXE signal (surface sensitivity) and its dependence on the primary electron energy and angle of incidence;

(ii) to apply this SXE technique to the investigation of materials with depth distributed parameters even without sharp interfaces.

The SXE spectra were recorded with the Rowland spectrometer at the IFF [2]. Electron excitation of SXE was performed by commercial electron guns. Synchrotron radiation from the storage ring DORIS at HASYLAB (Hamburg, Germany) from the beamline BW3 was used for the photon excitation of SXE.

Si-based materials were used as model systems due to their technological importance. For the study of surface sensitivity we used Si(100) wafers covered with SiO_2 films of two different thicknesses. For one sample (sample 1) the thickness was known from ellipsometry (1,5±0,2 nm). The surface of the other sample was etched in HF acid before its introduction into the vacuum chamber of the spectrometer (sample 2). The thickness of the oxide layer on the surface of this sample was unknown. The angle between the electron beam and the surface of the sample 1 was 22°±5° while the SXE measurements on sample 2 were carried out under normal incidence. The SXE $L_{2,3}$ emission bands of silicon were measured. As the LPDOS of crystalline Si and SiO_2 differ markedly, the contributions of the oxide layer to the total intensity can be determined from the observed spectral shape.

For electron excited SXE a probing depth is determined by the penetration properties of the incident electrons and it depends on details of the electron scattering processes in solids and the core shells ionization cross section of electrons with certain energy. As a result, the SXE spectra represent a superposition of photons emitted from different depths of the sample. For the theoretical description of electron impact excitation of SXE we used a phenomenological model of Borovsky-Rydnik [3] based on experimentally obtained parameters of electron scattering in isotropic solids. This model was modified to describe the case of non-isotropic solids.

To estimate the contribution of SXE from top-surface atomic layers to the total SXE intensity one has to be able to distinguish between near-surface and bulk emission. We used the model system SiO_2-Si for this task because (a) the parameters used for the theoretical description of the processes in Si and SiO_2 are close to each other, (b) the relative fluorescence yield of the Si $L_{2,3}$ emission band for Si and SiO_2 is known [4] and (c) the Si $L_{2,3}$ emission bands in Si and SiO_2 can be distinguished due to their different spectral shape. This allows both to simplify the theoretical calculation and to break down the experimental spectra into Si ("bulk") and SiO_2 ("surface") contributions with a large accuracy for each E_0 into following way: 'surface phase'= $I(SiO_2)$ / $I(Si+SiO_2)$.

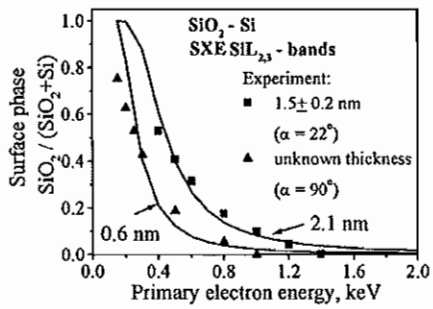

FIG.1. *Si $L_{2,3}$ SXE "surface phase" contribution: comparison of experimentally obtained values with the model calculation. Squares: sample 1, triangles: sample 2. α is the incidence angle of the electron beam.*

The theoretical curve describes the experimental results for the sample 1 well if we assume that the plume generated by the primary electron beam in SiO_2 layer is 2.1 nm long instead of the expected geometrical path length of 4.0 nm (1.5 nm / sin (22°)). It is possible to explain this at first sight surprising effect by the approximately isotropic character of scattering of low energy electron beams (< 2.5 keV) even in the thin near-surface region of the solid [5].
The thickness of the oxide from experimental data for the sample 2 via calculation was determined to be 0.6 nm by using a standard fit procedure. This value seems reasonable for the sample treatment procedure used.
The experiment proves that the contribution of the characteristic Si $L_{2,3}$ emission from a near-surface region less than 1 nm thick can easily exceed 50% of the total signal if $E_{Si2p}<E_0<250$ eV, i.e. in the energy range of about 150 eV in excess of the Si 2p ionization threshold.
Moreover, it was established that due to the approximately isotropic character of the low energy electron scattering in the surface region a grazing incidence of the primary electrons does not increase the surface sensitivity significantly.

Al implanted into Si(100) was investigated as a system with depth dependent parameters such as the Al concentration and local bonding configuration, as reflected in the LPDOS.
Al was implanted into a Si (100) n-doped wafer at room temperature with 30 keV energy and a dose of $5\cdot10^{16}$ cm^{-2}. The depth distribution of Al atoms inside the wafer in the as-implanted state was calculated to have a maximum at 50 nm depth with a FWHM of 48 nm using a standard TRIM program. A part of the samples were investigated in the as-implanted state while the other samples were annealed at 1000°C for 100s in N_2 atmosphere. This sample part was subsequently etched in HF solution in order to remove the silicon oxide formed during annealing at the wafer surface.
The analysis of the band shape clearly demonstrates than even a short heat treatment initiates a fast redistribution of the Al atoms.

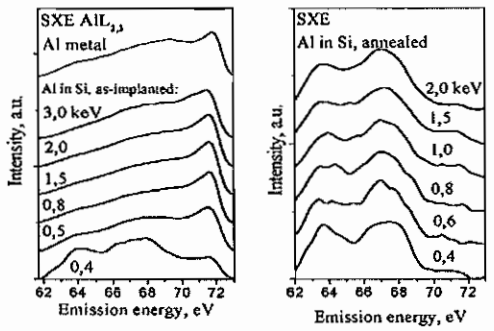

a b

FIG.2. *Electron excited Al $L_{2,3}$ SXE VB spectra from the as-implanted sample (a) and from the annealed sample (b) for different excitation energies. The SXE of a pure Al crystal metal is shown for comparison as well.*

The metallic-like SXE shape in the as-implanted sample suggests that Al atoms form metallic conglomerates or clusters dominated by Al – Al chemical bonds in a highly damaged Si matrix. After annealing, the Al – Si chemical bonds become dominant and the Al atoms are dispersed in the crystal as electronically decoupled impurities. The similar shape of SXE spectra for different E_0 indicates the uniform chemical state of Al atoms at different depths of samples. Spectra obtained with photon excitation have the shape similar to the electron excited SXE spectra. Comparison of the theoretical calculation [6] with the experimental results confirms that the most of Al atoms in the annealed sample are in the substitutional position in Si lattice.
Analysis of the dependence of the Al $L_{2,3}$ SXE intensity on E_0 ($I_{Al}(E_0)$) allows resolving the Al impurity depth profiles before and after annealing. As we restricted our study to maximum electron energy of 2 keV and certain incident geometry, we were not able to investigate the entire implantation profile till 50nm but we were able to see finer details on the low-depth side of the profile.

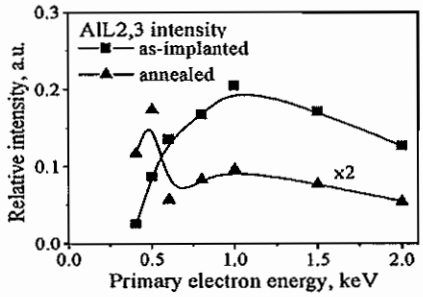

FIG.3. *Intensity of Al $L_{2,3}$ emission band normalized to the intensity of Si $L_{2,3}$ emission as a function of the primary electron energy for the as-implanted and annealed samples.*

To interpret the $I_{Al}(E_0)$ dependencies in more detail depth profiles were simulated by means of the modified Borovsky-Rydnik model, assuming particular Al concentration profiles near surface in addition to the TRIM profile. The coincident between calculated and experimental results gives the assumption of a relatively narrow Al concentration peak in the as-implanted sample situated at a depth of approximately 15 nm and additional concentration max at the surface in the annealed sample.

In summary, this work demonstrates that the electron exited SXE can be an useful method for the investigation of surfaces, films and materials with depth distributed parameters.

1. A. S. Shulakov, Crist. Res. Technol., 23, 6, 835 (1988).
2. J. E. Rubensson, *Electronic structure determined by soft X-ray emission spectroscopy* in 23.IFF Ferienkurs, Forschungszentrum Juelich (1992)
3. I. V. Borovsky, V. I. Rydnik, Izvestiya Akademii Nauk SSSR, seriya fizicheskaya, 31, 6, 1009 (1967) (in Russian)
4. A.S.Shulakov, A.P.Brajko, Phys.Solid State **39**, 11, 1880 (1997).
5. I.M.Bronshtejn, B.S.Frajman, "Secondary Electron Emission", "Nauka" publ., Moskow (1969) (in Russian)
6. A. Settels, *Electronische Structure und Hyperfeineigenschaften von Stoerstellen in Halbleitern*, Diplomarbeit in Physik, Rheinische-Westfaelischen Technischen Hochschule Aachen, IFF Forschungszentrum Juelich(1996)

Publications in refereed journals

Clarke S.; Bihlmayer G.; Blügel S.
Chemical effects in rare gas adsorption: FLAPW calculations for Ag(001)c(2x2)-Xe
Phys. Rev. B 63, 085416-1 (2001)
23.20.0

Dallmeyer A.; Maiti K.; Rader O.1; Pasquali L.2; Carbone C.; Eberhardt W.
1Bessy, Berlin
2INFM and Dipartimento di Fisica, Universita di Modena e Reggio Emilia, Modena
Magnetism and interlayer coupling in fcc Fe/Co films
Phys. Rev. B 63, 104413 (2001)
23.20.0

Gareev R.R.; Bürgler D.E.; Buchmeier M.; Olligs D.; Schreiber R.; Grünberg P.
Metallic-type oscillatory interlayer exchange coupling across an epitaxial FeSi spacer
Phys. Rev. Lett. 87, 157202 (2001)
23.42.0

Grünberg P.
Exchange anisotropy, interlayer exchange coupling and GMR in research and application
Sensors and Actuators A 91, 153-160 (2001)
23.42.0

Grünberg P.
Layered magnetic structures: History, highlights, applications
Physics Today, S. 31-37, (2001)
23.42.0

Grünberg P.
Layered magnetic structures: history, facts and figures
J. of Magnetism and Magnetic Materials 226, 1688 (2001)
23.42.0

Heinze S.; Blügel S.
Magnetische Ordnung wird sichtbar
Physik in unserer Zeit, 32, Juli (2001)
23.20.0

Kim H.-J.1; Vescovo E.1; Heinze S.; Blügel S.
1Brookhaven National Laboratory, Upton, N.Y.
Surface electronic structure of Fe(110): the importance of surface resonances
Surf. Sci. 478, 193 (2001)
23.20.0

Klingeler R.; Kann G.; Wirth I.; Eisebitt S.; Bechthold P.S.; Neeb M.; Eberhardt W.
La@C60: A metallic endohedral fullerene
J. of Chemical Physics 115, 7215 (2001)
23.20.0

Kurz P.; Bihlmayer G.; Blügel S.; Hirai K.1; Asada T.2
1Department of Physics, Nara Mecial University, Kashihara, Nara, Japan
2Faculty of Engineering, Shizuoka University, Hamamatsu, Japan
Comment on "Ultrathin Mn films on Cu(111) substrates: Frustrated antiferromagnetic order"
Phys. Rev. B 63, 096401 (2001)
23.20.0

Kurz P.; Bihlmayer G.; Hirai K.1; Blügel S.
1Department of Physics, Nara Mecial University, Kashihara, Nara, Japan
Three-dimensional spin structure on a two-dimensional lattice: Mn/Cu(111)
Phys. Rev. Lett. 86, 1106 (2001)
23.20.0

Link S.; Dürr H.A.; Bihlmayer G.; Blügel S.; Eberhardt W.; Chulkov E.V.1; Silkin V.M.1; Echenique P.M.1
1Donostia International Physics Center, San Sebastian, Spain
Femtosecond electron dynamics of image-potential states on clean and oxygen-covered Pt(111)
Phys. Rev. B 63, 115420 (2001)
23.20.0

Link S.; Dürr H.A.; Bihlmayer G.; Blügel S.; Eberhardt W.; Chulkov E.V.1
1Donostia International Physics Center (DIPC), San Sebastian, Spain
Electron dynamics of image potential states on the clean and oxygen covered Pt(111) surface
Pys. Rev. B 63, 115420 (2001)
23.20.0

Link S.; Dürr H.A.; Eberhardt W.
Femtosecond spectroscopy
Journal of Physics: Condensed Matter 13, 7873 (2001)
23.20.0

Lüttgens G.; Pontius N.; Friedrich C.; Klingeler R.; Bechthold P.S.; Neeb M.; Eberhardt W.
Chemisorption of benzene on metal dimer anions: A study by photoelectron detachment spectroscopy
J. Chem. Phys. 114, 8414 (2001)
23.20.0

Maiti K.; Dallmeyer A.; Malagoli M.; Carbone C.; Eberhardt W.; Rader O.1; Pasquali L.2; Banerjee, A.3; Turchini S.4; Zennaro S.4; Zema N.4
1BESSY Berlin
2INFM and Dipartimento di Fisica, Universita di Modena e Reggio Emilia, Italy
3Inter University Consortium for DAE Facilities, Indore, India
4Consiglio Nazionale delle Recerche, Roma, Italy
Oscillary interlayer coupling mediated by fcc-Fe/Co(100) films
Appl Surf. Science 182, 302 (2001)
23.20.0

Maiti K.; Malagoli M.C.; Magnano E.; Dallmeyer A.; Carbone C
Electronic band structure of Gd: A consistent description
Phys. Rev. Lett 86, 2846 (2001)
23.20.0

Morenzin J.; Kietzmann H.; Bechthold P.S.; Ganteför G.; Eberhardt W.
Localization and bandwidth of the 3d-orbitals in magnetic Ni and Co clusters
Pure Appl. Chem. 72, 2149 (2000) (erschienen 2001)
23.20.0

Neeb M.; Klingeler R.; Bechthold P.S.; Kann G.; Wirth I.; Eisebitt S.; Eberhardt W.
Deposition of endohedral fullerenes from a laser evaporation cluster source
Appl. Phys. A 72 , 289 (2001)
23.20.0

Panaccione G.1; van der Laan G.1; Dürr H.A.; Vogel J.1
1Department of Physics, University of Durham, UK
Magnetic circular dichroism in Co 2p photoemission of Co/Cu (1 1 13): Separation of the fundamental spectra
Eur. Phys. J. B 19, 281 (2001)
23.20.0

Schmidt C.M.1; Bürgler D.E.; Schaller D.M.1; Meisinger F.1; Güntherodt H.-J.1; Temst K.1
1Universität Basel
Interface morphology of a Cr(001)/Fe(001) superlattice determined by scanning tunneling microscopy and X-ray diffraction: A comparison
J. Appl. Phys. 89, 181 (2001)
23.42.0

Wortmann D.; Heinze S.; Kurz Ph.; Bihlmayer G.; Blügel S.

Resolving complex atomic-scale spin structures by spin polarized scanning tunneling microscopy
Phys. Rev. Lett 86, 4132 (2001)
23.20.0

Other publications

Bürgler D.E.; Grünberg P.; Demokritov S.O.1; Johnson M.T.2
1Universität Kaiserslautern
2Philips Research, Eindhoven, NL
Interlayer exchange coupling in layered magnetic structures
In: Handbook of Magnetic Materials, Vol. 13, Ed. K.H.J. Buschow, Elsevier (2001)
23.42.0

Bürgler D.E.; Grünberg P.
Magnetoelectronics: Exchange anisotropy, interlayer exchange coupling, GMR, TMR, and current-induced magnetic switching
In: 32. Ferienkurs des IFF: "Neue Materialien für die Informationstechnik" (2001)
23.42.0

Dürr H.A.; Kronast F.; Eberhardt W.
Spin-polarized photoelectron emission microscopy of magnetic nanostructures
Advances in Solid State Physics, Vol. 41, ed. B. Kramer, Springer Verlag (2001)
23.20.0

Dürr H.A.
Anisotropic magnetic ground-state moments probed by soft x-ray spectroscopy
In: Bandferromagnetism: Ground-state and Finite-temperature Phenomena, ed. K. Baberschke, M. Donath, W. Nolting, Springer Verlag Berlin, Heidelberg, New York, Barcelona, Hong Kong, London, Milan, Paris, Singapore, Tokyo (2001), p. 46-59
23.20.0

Dürr H.A.
Magnetic random access memory devices
In: 32. Ferienkurs des Instituts für Festkörperforschung "Neue Materialien für die Informationstechnik"
23.20.0

Eberhardt W.; Klingeler R.; Kann G.; Wirth I.; Bürgler D.E.; Bechthold P.S.; Neeb M.
Metal doped fullerenes: Mircoscopy and spectroscopy
XVth International Winterschool on Electronic Properties of Novel Materials (IWEPNM)
Kirchberg, Tirol (2001)
23.20.0

Grünberg P.; Bürgler D.E.
Vom Kompass zum Datenspeicher: Magnetoelektronik
In: ....und Er würfelt doch!, Ed. H. Müller-Krumbhaar, H.-F. Wagner,
Wiley-VCH, Weinheim (2001)
23.42.0

Link S.; Dürr H.A.; Eberhardt W.
Lifetimes of image potential states on Pt(111) probed by time-resolved two-photon photoemission spectroscopy
Appl. Phys. A 71, 524 (2001)
23.20.0

Link S.; Sievers J.; Dürr H.A.; Eberhardt W.
Lifetimes of image-potential states on the clean and hydrogen-covered Ni(111) surface
J. of Electron Spectroscopy and Related Phenomena 114-116, 349 (2001)
23.20.0

Pontius N.; Bechthold P.S.; Neeb M.; Eberhardt W.
Time-resolved photoelectron spectra of optically excited states in Pd3-
J. of Electron Spectroscopy and Related Phenomena 114, 163 (2001)
23.20.0

Invited talks

Blügel S.
Novel surface nanoprobes - scanning probe microscopies
IUVSTA 15th International Vacuum Congress, AVS 48th International Symposium, 11th International Congress on Solid Surfaces, San Francisco, CA
29.10.01 - 02.11.01
23.20.0

Bürgler D.E.
Ag(001) Pufferschichten auf GaAs: Präparation und Verwendung als Substrate für magnetische Schichtstrukturen
Seminar Universität Mainz
20.06.2001
23.42.0

Bürgler D.E.
Coupling across silicon and iron-silicide spacers
Argonne National Laboratory, Chicago (USA)
20.11.2001
23.42.0

Bürgler D.E.
The role of the spacer layer for magnetic interlayer exchange coupling and for giant magnetoresistance (GMR)
Michigan State University, East Lansing (USA)
19.11.2001
23.42.0

Dürr H.A.
Fsec electron and spin relaxation at surfaces
Van der Waals-Zeeman Kolloquium, Universität Amsterdam
22.05.2001
23.20.0

Dürr H.A.
Fsec spin dynamics in CoPt nanostructures
Seminar Experimentelle Physik, Universität Würzburg
06.06.2001
23.20.0

Dürr H.A.
Magnetic ordering phenomena in nanostructured materials
Sonderkolloquium Physikalisches Institut, TU Berlin
08.05.2001
23.20.0

Dürr H.A.
Magnetic quantumphenomena in nanostructures
Sonderkolloquium, Institut für Angewandte Physik, Universität Düsseldorf
23.02.2001
23.20.0

Dürr H.A.
Magnetism in nanostructures
Greifswalder Physikalisches Kolloquium, Ernst-Moriz-Arndt-Universität Greifswald
01.02.2001
23.20.0

Dürr H.A.
Spin-polarized photoelectron emission microscopy with femtosecond temporal resolution
Symposium on Dynamics of Magnetic Switching, DPG March Meeting, Hamburg
29.03.2001
23.20.0

Grünberg P.; Buchmeier M.; Bürgler D.E.; Gareev R.; Kuanr B.
Zwischenschichtkopplung: Grundlagen, aktuelle Forschung, Anwendungen
Symposium über "Magnetoresistive Sensoren", Wetzlar
13.03.2001
23.42.0

Grünberg P.
Interlayer exchange coupling across metallic and semiconducting interlayers
Institute for Electrical Engineering, Slovak Ac. Of Science, Bratislava, Slowakei
04.10.2001
23.42.0

Grünberg P.
Interlayer exchange coupling in Fe/FeSi/Fe and Fe/AlSi/Fe layered structures
1st Seeheim Conference on Magnetism, Seeheim, Germany
10.09.2001
23.42.0

Grünberg P.
Interlayer exchange couöling across metals, semimetals and semiconductors: Experiments
The European Graduate School on Condensed Matter (EGSCM Prague '01), Prag
10.06.2001
23.42.0

Grünberg P.
Layered magnetic structures in research and application
International Workshop on Physics of Magnetoresistance Effects, Peking
28.08.2001
23.42.0

Grünberg P.
Magnetische Multilagen: Austauschkopplungder ferromagnetischen Schichten über metallische und halbleitende Zwischenschichten
Seminar, TU Hannover, Institut für Mikrosystemtechnik
02.11.2001
23.42.0

Grünberg P.
Magnetische Multilagen: Austauschkopplungder ferromagnetischen Schichten über metallische und halbleitende Zwischenschichten
Seminar, TU Wien, Center for Computational Material Science
05.10.2001
23.42.0

Grünberg P.
Magnetoelektronik in Forschung und Anwendung
Graduiertenkolleg "Materialien und Komponenten der Mikrosystemtechnik" der Gesamthochschule Kassel
12.07.2001
23.42.0

Grünberg P.
Magnetoelektronik: Vom Kompass zum Datenspeicher
Kolloquium Universität-Gesamthochschule Siegen
26.04.2001
23.42.0

Grünberg P.
Zwischenschicht-Austauschkopplung und GMR-Effekt
WE Heraeus Ferienkurs: "Komplexe magnetische Phänomene in Festkörpern", Dresden
05.09.01
23.42.0

Other talks

Bürgler D.E.
Interlayer exchange coupling across conducting and non-conducting iron-silicide spacers with varying Si content
46th Annual Conference on Magnetism & Magnetic Materials
Seattle, Washington
14.11.2001
23.42.0

Bürgler D.E.
Magnetic interlayer exchange coupling in Fe/Si/Fe systems
CNRS Strasbourg, Frankreich
02.07.2001
23.42.0

Bürgler D.E.
Magnetische Zwischenschichtkopplung in Fe/FeSi/Fe Systemen
IFF-Beiratssitzung
26.04.2001
23.42.0

Dürr H.A.
Magnetic ordering phenomena probed by soft x-ray spectroscopy
Plenary Talk, 4th International Conference on Inelastic X-ray Scattering, Haikko, Finland
22.08.2001
23.20.0

Gareev R.R.
Very strong interlayer exchange coupling in Fe/Fe1-xSix/Fe (x=0.4-1.0) epitaxial trilayers
4th International Symposium on Metallic Multilayers, Aachen, Deutschland
27.06.2001
23.42.0

Grünberg P.; Bürgler D.E.; Gareev R.; Kuanr B.
Magnetoelektronik: Vom Kompass zum Datenspeicher
Plenarvortrag auf der 65. Physikertagung Hamburg 2001
30.03.2001
23.42.0

Klingeler R.
A metallic endohedral fullerene: La@C60
7th European Conference on Atomic and Molecular Physics (ECAMP) und DPG-Frühjahrstagung
2. - 6. April 2001, Berlin
23.20.0

Lüttgens G.; Pontius N.; Bechthold P.S.; Neeb M.; Eberhardt W.
Femtosecond-time-resolved fragmentation of metal-carbonylclusters
The 7th European Conference on Atomic and Molecular Physics (ECAMP) und
DPG-Frühjahrstagung Berlin,
03.04.01
23.20.0

Neeb M.
Pump-probe Elektronenspektroskopie an Metall und Metall-Carbonylclustern
268. WE-Heraeus Seminar, Cluster 2001, Herzogenhorn
07.10. - 12.10.2001
23.20.0

Wirth I.
Scanning tunneling spectroscopy of endohedrally doped fullerenes
The 7th European Conference on Atomic and Molecular Physics (ECAMP) und
DPG-Frühjahrstagung Berlin
03.04.01
23.20.0

Wortmann D.; Bihlmayer G.; Blügel S.; Ishida H.1

1College of Humanities and Science, Nihon University, Sakura-josui, Tokyo, Japan
A transfer matrix method for ballistic transport: MgO(Fe(001)
1st Annual Meeting of the Research Training Network "Computational Magnetoelectronics", Budapest, Hungary
27. - 30.09.2001
23.20.0

Posters

Bürgler D.E.; Gareev R.R.; Buchmeier M.; Olligs D.; Schreiber R.; Grünberg P.
Oscillatory interlayer exchange coupling across epitaxial FeSi spacer layers
Edgar-Lüscher-Seminar, Serneus, Schweiz
06.02.2001-08-06
23.42.0

Eberhardt W.
Breuer C.; Blanchard A.; Klingeler R.; Wirth I.; Bürgler D.E.; Bechthold P.S.; Neeb M.;
Eberhardt W.
Production and scanning tunneling investigations of deposited endohedrally-doped fullerenes Ce@50, Ce@C44 and Ce@C36
Cluster 2001, 268. WE-Heraeus-Seminar, Herzogenhorn
07. - 12.10.2001
23.20.0

Gareev R.R.; Buchmeier M.; Breidbach M.; Schreiber R.; Bürgler D.E.; Grünberg P.
Antiferromagnetic exchange coupling in excess of 8 mJ/m2 in Fe/Si/Fe expitaxial trilayers with thin boundary layers
46th Annual Conference on Magnetism & Magnetic Materials
Seattle, Washington
12. - 16.11.2001
23.42.0

Klingeler R.
La@C60, a metallic endohedral fullerene
15th International Winterschool on Electronic Properties of Novel Materials
3. - 10. März 2001, Kirchberg, Tirol
23.20.0

Kronast F.; Dürr H.A.; Eberhardt W.; Bihlmayer G.; Blügel S.; Liebsch A.
Femtosecond spin dynamics of magnetic nanodots
XIII International Conference on Vacuum Ultraviolet Radiation Physics, Trieste, Italy
23. - 27. Juli 2001
23.20.0

Kronast F.; Dürr H.A.; Eberhardt W.; Landis S.
Non-local pump-probe spectromicroscopy of layered magnetic structures
International Workshop on Ultrafast Surface Dynamics, San Sebastian, Spain
09. - 11. Juli 2001
23.20.0

Kronast F.; Dürr H.A.; Eberhardt W.
Spin-polarized two-photon photoemission microscopy of magnetic nanostructures
DPG-Frühjahrstagung, Hamburg
März.2001
23.20.0

Kuanr B.K.; Buchmeier M.; Bürgler D.E.; Grünberg P.
Broadening of the frequency linewidth in exchange-biased or exchange-coupled systems observed by FMR and BLS
4th International Symposium on Metallic Multilayers, Aachen, Deutschland
27.06.2001
23.42.0

Kuanr B.K.; Buchmeier M.; Bürgler D.E.; Grünberg P.
Exchange coupling of MBE grown Fe/Al/Fe by dynamic techniques
MMM'01, Seattle, USA
16.11.2001
23.42.0

Malagoli M.
Lifetime effects on Gd valence band structure
XIII International Conference on Vacuum Ultraviolet Radiation Physics, Trieste, Italy
23. - 27. Juli 2001
23.20.0

Olligs D.; Bürgler D.E.; Wang Y.G.; Kentzinger E.; Rücker U.; Schreiber R.; Brückel Th.; Grünberg P.
Unambiguous evidence for roughness-induced enhancement of giant magnetoresistance in epitaxial Fe/Cr/Fe(001) trilayers
4th International Symposium on Metallic Multilayers , Aachen, Deutschland
25.06.2001
23.42.0

Pontius N.; Lüttgens G.; Bechthold P.S.; Neeb M., Eberhardt W.
Hot-electron dynamics in mass-selected transition metal clusters probed by femtosecond pump-probe photoelectron spectroscopy
Cluster 2001, 268. WE-Heraeus-Seminar, Herzogenhorn
07. - 12.10.2001
23.20.0

Rhie H.-S.; Link S.; Sievers J.; Dürr H.A.; Eberhardt W.; Smith N.V.1
1NSLS Berkeley, USA
Femtosecond electron dynamics of image potential states on Ni surface
XIII International Conference on Vacuum Ultraviolet Radiation Physics, Trieste, Italy
23. - 27. Juli 2001
23.20.0

Sievers J.; Rhie H.-S.; Link S.; Dürr H.A.; Eberhardt W.
Ultrafast electron dynamics of image potential states on Ni surfaces
DPG-Frühjahrstagung, Hamburg
März 2001
23.20.0

Patents applied for

Morenzin J.; Eberhardt W.; Schondelmeier D.
Markierungseinrichtung sowie Verfahren zum Auslesen einer solchen Markierungseinrichtung
a) PCT: PCT/EP01/00246 (10.01.2001) (alle Länder)
b) PCT: PCT/EP01/00247 (10.01.2001) (alle Länder)
AR: P0101 00762 (21.02.2001)
CL: 403-01 (21.02.2001)
c) PCT: PCT/EP01/00244 (10.01.2001 (alle Länder)
AR: P0101 00763 (21.02.2001)
CL: 404-01 (21.02.2001)
PT 1.1777
23.55.0

Morenzin J.; Schondelmeier D.
Markierungseinrichtung sowie Verfahren zum Auslesen der Markierungseinrichtung
DE: 101 30 553.2 (25.06.2001)
PT 1.1922
23.42.0

Nie X.
Magnetisches Schichtsystem sowie ein solches Schichtsystem aufweisendes Bauelement
PCT: PCT/DE01/03631 (19.09.2001) (EP,US,CA,JP)

PT 1.1832
23.42.0

Schondelmeier D.; Eberhardt W.
Verfahren zur Behandlung von Oberflächen sowie mit diesen Verfahren hergestellte Gegenstände und Verwendung von Verbindungen als photochemisch spaltbare Reagenzien
PCT: PCT/DE01/02315 (21.06.2001) (EP,US,JP)
PT 1.1798
23.42.0

Lecture courses

Bechthold P.S.
Experimentalphysik für Studierende der Medizin und der Wirtschafts- und Sozialwissenschaften
Vorlesung WS 2001
Universität zu Köln
23.20.0

Bechthold P.S.
Symmetrie und Spektroskopie
Vorlesung SS 2001
Universität zu Köln
23.20.0

Bürgler D.E.; Grünberg P.
Magnetoelectronic: Exchange anisotropy, interlayer exchange coupling, GMR, TMR and current induced magnetic switching
Vorlesung während des 32. IFF Ferienkurs 2001 "Neue Materialien für die Informationstechnik"
23.42.0

Bürgler D.E.
Magnetoelektronik (Teil 2)
IFF-Ferienschule 2001 "Neue Materialien für die Informationstechnik"
05. - 16. March 2001, FZJ
23.42.0

Dürr H.A.
Magnetic random access memory devices
IFF-Ferienschule 2001 "Neue Materialien für die Informationstechnik"
05. - 16. March 2001, FZJ
23.20.0

Grünberg P.; Bürgler D.E.
Magnetoelektronik in Forschung und Anwendung
Universität zu Köln, SS 2001
23.42.0

Internal seminars

Bürgler D.E.
Magnetische Zwischenschichtkopplung in Fe/FeSi/Fe Systemen
IFF-Beiratssitzung
26.04.2001
23.42.0

The number at the end of each contribution characterize the associated R&D program:

23.06.0	Special and guest program in solid state research
23.15.0	Cooperative phenomena in condensed matter
23.20.0	Electronic structure of solids, surfaces and layered systems
23.30.0	Polymer, membranes and complex fluids
23.42.0	Solid State Research for information technology
23.55.0	Research on novel and advanced materials
23.60.0	Material problems in target components
23.80.5	Materials under high doses of radiation
23.89.1	Applications of synchrotron and neutron radiation

Publications in refereed journals

IFF-01-11-001
Akola J.; M. Manninen1
1 Dept. of Physics, University of Jyväskylä, Finland
Heating of Al13 and Al14 clusters
Phys. Rev. B 63, 193410 (2001)
23.20.0

IFF-01-11-002
Akola J.; Rytkönen K.1; Manninen M.1
1 Dept. of Physics, University of Jyväskylä, Finland
Metallic evolution of small magnesium clusters
Eur. Phys. J. D 16, 21 (2001)
23.20.0

IFF-01-11-003
Arbe A.1; Monkenbusch M.; Stellbrink J.; Richter D.; Farago B.2; Almdal K.3; Faust R.4
1Departamento de Fisica de Materiales, Universidad del Pais Vasco and Unidad de Fisica de Materiales (CSIC-UPV/EHU), San Sebastian, Spain
2Institut Laue Langevin, 156X, 38042 Grenoble, France
3The Danish Polymer Centre, Condensed Matter and Physics and Chemistry Department, Risø National Laboratory, Roskilde, Denmark
4Polymer Science Program, Dep. of Chemistry, University of Massachusetts-Lowell, Lowell, Massachusetts, USA
Origin of Internal Viscosity Effects in Flexible Polymers: A Comparative Neutron Spin-Echo and Light Scattering Study on Poly(dimethylsiloxane) and Polyisobutylene
Macromolecules 34, 1281-1290 (2001)
23.30.0

IFF-01-11-004
Bachhofer H.; von Philipsborn H.; Hartner W.; Dehm C.; Jobst B.; Kiendl A.; Schroeder H.; Waser R.
Phase formation and crystal growth of Sr-Bi-Ta-O thin films grown by metalorganic chemical vapour deposition
J. Mat. Res. 16 (2001) 2966
23.42.0

IFF-01-11-005
Ballone P.1; Jones R.O.
1 University of Messina, Italy
Equilibrium polymerization of cyclic carbonate oligomers
J. Chem. Phys. 115, 3895-3905 (2001)
23.20.0

IFF-01-11-006
Barashev A.V. 1; Golubov S.I. 2; Trinkaus H.
1 Materials Science and Engineering, University of Liverpool, UK
2 Scientific Center of Russian Federation, Obninsk, Russian Federation
Reaction kinetics of glissile interstitial clusters in a crystal containing voids and dislocations
Phil. Mag. A 81, 2515-2532 (2001)
23.15.0

IFF-01-11-007
Barman S.R.1; Häberle P.2; Horn K.3; Maytorena J.; Liebsch A.
1 Inter University Consortium, Indore, India
2 Universidad Técnica, Valparaíso, Chile
3 Fritz Haber Institut Berlin
Quantum well behavior without confining barrier observed via dynamically screened photon field
Phys. Rev. Lett. 86, 5108 (2001)
23.20.0

IFF-01-11-008
Bartic A. T.1; Wouters D. J.1; Maes H.E.1; Rickes J.; Waser R.
1 imec, Leuven, Belgium
Preisach model for the simulation of ferroelectric capacitors
J. Appl. Phys. 89 (2001) 3420-3425
23.42.0

IFF-01-11-009
Bartic A.1; Rickes J.; Wouters D.1; Waser R.; Maes H.1
1 imec, Leuven, Belgium
Implementation of a Ferroelectric Capacitor Model using the Preisach Hysteresis Theory
Ferroelectrics 32 (2001) 295-302
23.42.0

IFF-01-11-010
Belitsky V.1; Krug J.2; Jordao Neves I.1; Schütz G.M.
1 Univ. Sao Paolo, Brazil
2 Univ. Essen, Germany
A Cellular Automaton for Two-Lane Traffic
J. Stat. Phys. 103, 945-971 (2001)
23.15.0

IFF-01-11-011
Bellini V.; Papanikolaou N.; Zeller R; Dederichs P.H.
Magnetic 4d monoatomic rows on Ag vicinal surfaces
Phys. Rev. B 64, 094403 (2001)
23.20.0

IFF-01-11-012
Bellini V.; Zeller R.; Dederichs P.H.
Cd hyperfine fields at the bcc Fe/Co interface
Phys. Rev. B 64, 144427 (2001)
23.20.0

IFF-01-11-013
Blokhuis E.M.1; Sager W.
1University of Leiden, Niederlande
Sphere to cylinder transition in a single phase microemulsion system: A theoretical investigation
Journal of Chemical Physics, 115, 1073-1085, 2001
23.30.0

IFF-01-11-014
Bolten D.1; Böttger U.1; Schneller T.1; Grossmann M.1; Lohse O.1; Waser R.
1 Institut für Werkstoffe der Elektrotechnik, RWTH Aachen
Irreversible Polarization in Donor Doped Pb(Zr, Ti)O3
Integrated Ferroelectrics 32 (2001) 93-99
23.42.0

IFF-01-11-015
Brener E. A.; Müller-Krumbhaar H.; Spatschek R.
Coarsening of cracks in a uniaxially strained solid
Phys. Rev. Lett. 86, 1291 (2001)
23.15.0

IFF-01-11-016
Brückel Th.; Hupfeld D.; Strempfer J.1; Caliebe W.; Mattenberger K.2; Stunault A.3; Bernhoeft N.4; McIntyre G. J.5
1APS at ANL, Argonne, USA
2ETH, Zürich, Switzerland
3ESRF, Grenoble, France
4CEA, Grenoble, France
5ILL, Grenoble, France
Antiferromagnetic order and phase transitions in GdS as studied with X-ray resonance-exchange scattering
Eur. Phys. J. B 19 (2001) 475 - 490
23.89.1

IFF-01-11-017
Brückel Th.; Strempfer J.1
1Northern Illinois University, DeKalb & ANL, Argonne, USA
Non-resonant Magnetic Diffraction at High X-ray Energies
Synchrotron Radiation News 14 (5) (2001) 16 - 20
23.89.1

IFF-01-11-018
Buchenau U.
Dynamics of glasses
J. Phys.: Condens. Matter 13, 7827-7846 (2001)
23.15.0

IFF-01-11-019
Buchenau U.
Mechanical relaxation in glasses and the glass transition
Phys. Rev. B 63, 104203 (2001)
23.15.0

IFF-01-11-020
Caprion D.; Schober H. R.
Is diffusion in selenium heterogeneous or homogeneous?
Defect and Diffusion Forum 194-199, 841-848 (2001)
23.30.0

IFF-01-11-021
Caprion D.; Schober H. R.
Vibrational density of states of selenium through the glass transition
J. Chem. Phys. 114, 3236 (2001)
23.30.0

IFF-01-11-022
Carlsson P.1; Zorn R.; Andersson D.1; Farago B.2; Howells W.S.3; Börjesson L.1
1Department of Experimental and Applied Physics, Chalmers University of Technology, S-412 96 Göteborg, Sweden
2Institut Laue-Langevin, BP 156, F-38042 Grenoble Cedex, France
3Rutherford Appleton Laboratory, Chilton, Didcot OX11 0QX, United Kingdom
The segmental dynamics of a polymer electrolyte investigated by coherent quasi-elastic neutron scattering
J. Chem. Phys. 114, 9645-9656 (2001)
23.15.0

IFF-01-11-023
Caspary D.1; Eckold G.1; Güthoff F.1; Pyckhout-Hintzen W.
1Institut für Physiklaische Chemie und Sonderforschungsbereich 345, Univ. Göttingen, Tammanstr. 6, 37077 Göttingen
Kinetics of decomposition in ionic solids II: neutron scattering study of the system AgCl-NaCl"
J. Phys.: Condens. Matter 13, 11521-11530 (2001)
23.30.0

IFF-01-11-024
Cassel D.; Pickartz G.; Siegel M.; Goldobin E.; Kohlstedt H.; Brinkman A.; Golubov A.A.; Kupriyanov M.Yu. ; Rogalla H.:
Influence of the transparency of tunnel barriers in Nb/Al2O3/Al/Al2O3/Nb junctions on transport properties
Physica C: Superconductivity 350 (2001) 276
23.42.0

IFF-01-11-025
Chen J.; Ullmaier H.; Floßdord T.; Kühnlein W.; Duwe R.; Carsughi F.1; Broome T.2
1University of Ancona, DIBIAGA, Italy
2Rutherford Appleton Laboratory, Chilton, UK
Mechanical properties of pure tantalum after 800 MeV proton irradiation
Journal of Nuclear Materials 298 (2001) 248 - 254
23.60.0

IFF-01-11-026
Clarke S.; Bihlmayer G.; Blügel S.
Chemical effects in rare gas adsorption: FLAPW calculations for Ag(001)c(2x2)-Xe
Phys. Rev. B 63, 085416-1 (2001)
23.20.0

IFF-01-11-027
Dai Y.1; Jia X.1; Chen J.; Sommer W. F.2; Victoria M.3; Bauer G. S.1
1PSI, Spallation Neutron Source Division, Villigen, Switzerland
2Los Alamos National Laboratory, Neutron Science Center, USA
3Ecole Polytechnique Federal de Lausanne, Fusion Technology Materials, Switzerland
Microstructure of both as-irradiated and deformed 304L stainless steel irradiated with 800 MeV protons
Journal of Nuclear Materials 296 (2001) 174 - 182
23.60.0

IFF-01-11-028
Dallmeyer A.; Maiti K.; Rader O.1; Pasquali L.2; Carbone C.; Eberhardt W.
1Bessy, Berlin
2INFM and Dipartimento di Fisica, Universita di Modena e Reggio Emilia, Modena
Magnetism and interlayer coupling in fcc Fe/Co films
Phys. Rev. B 63, 104413 (2001)
23.20.0

IFF-01-11-029
Dhont J.; Wagner N.J.1
1University of Delaware, USA
Superposition rheology
Phys.Rev.E.; 63, 021406, 2001
23.30.0

IFF-01-11-030
Divin Y.Y.; Volkov O.Y.1; Pavlovskii V.V.1; Poppe U.; Urban K.
1 Institute of Radioengineering & Electronics of RAS, Moscow 103907, Russian FederationTerahertz Spectral Analysis by ac Josephson Effect in High-Tc Bicrystal Junctions
IEEE Transactions on Appl. Supercond., Vol. 11, No. 1, 582-585 (2001)
23.42.0

IFF-01-11-031
Divin Y.Y.; Poppe U.; Jia C.L.; Shadrin P.; Urban K.
Structural and electrical properties of YBa2Cu3O7 [100]-tilt grain boundary Josephson junctions with high IcRn-products on SrTiO3 bicrystals
Physica C, 2002 (accepted for publications)
23.42.0

IFF-01-11-032
Divin Y.Y.; Volkov O.Y.1; Laytti M.; Shirotov V.; Pavlovskii V.V.1; Poppe U.; Shadrin P.; Urban K.
1 Institute of Radioengineering & Electronics of RAS, Moscow 103907, Russian Federation
Hilbert spectroscopy from microwave to terahertz frequencies by high-Tc Josephson junctions
Physica C, 2002 (accepted for publications)
23.42.0

IFF-01-11-033
Dolinsek J.1; Klanjsek M.1; Apih T.1; Gavilano J.L.2; Giannò K.2; Ott H.R.2; Dubois J.M.3; Urban K.
1 J. Stefan Institute, University of Ljubljana, Jamova 39, SI-1000 Ljubljana, Slovenia
2 Laboratorium für Festkörperphysik, ETH Hönggerberg, CH-8093 Zürich / Schweiz
3 Ecole des Mines de Nancy, LSG2M, Nancy / F
Mn magnetism in icosahedral quasicrystalline Al72.4Pd20.5Mn7.1
Phys. Rev. B, Vol. 64, 024203-1 - 024203-7 (2001)
23.42.0

IFF-01-11-034
Dzubiella J.1; Jusufi A.1; Likos C.N.1; von Ferber C.1; Stellbrink J.; Allgaier J.; Richter D.; Schofield A.B.2; Poon W.C.K.2; Pusey P.N.2
1Institut für Theoretische Physik II, Heinrich-Heine-Universität Düsseldorf, Universitätsstraße 1, 40225 Düsseldorf
2Department of Physics and Astronomy, The University of Edinburgh, Mayfield Road, Edinburgh EH9 3JZ, UK
Phase Separation in Star Polymer-Colloid Mixtures
Phys. Rev. E64, 10401R (2001)
23.30.0

IFF-01-11-035
Döblinger M.1; Wittmann R.1; Gerthsen D.1; Grushko B.

1 Lab. Elektronenmikroskopie, Univ. Karlsruhe, 76128 Karlsruhe
A Transition State between Quasicrystal and Approximant in the System Al-Ni-Co
Ferroelectrics, Vol. 250, 241-244 (2001)
23.55.0

IFF-01-11-036
Döblinger M.1; Wittmann R.1; Grushko B.
1 Lab. Elektronenmikroskopie, Univ. Karlsruhe, 76128 Karlsruhe
Metastable transformation states of decagonal Al-Co-Ni due to inhibited decomposition
Phys. Rev. B, Vol. 64, 134208-1-134208-9 (2001)
23.55.0

IFF-01-11-037
Ebert Ph.; Domke C.; Urban K.
Direct observation of electrical charges at dislocations in GaAs by cross-sectional scanning tunneling microscopy
Appl. Phys. Lett. 78, No. 4, 480-482 (2001)
23.55.0

IFF-01-11-038
Ebert Ph.; Domke C.; Urban K.
Direct observation of electrical charges at dislocations in GaAs by cross-sectional scanning tunneling microscopy
Appl. Phys. Lett., Vol. 78, 480-482 (2001).
23.42.0

IFF-01-11-039
Ebert Ph.; Quadbeck P.; Urban K.; Henninger B.1; Horn K.1; Schwarz G.1; Neugebauer J.1; Scheffler M.1
Identification of surface anion antisite defects in (110) surfaces of III-V semiconductors
Appl. Phys. Lett., Vol. 79, 2877-2879 (2001).
23.42.0

IFF-01-11-040
Ebert Ph.
Atomic structure of Point Defects in Compound Semiconductor Surfaces.
Current Opinion in Solid State and Materials Science 5, 211-250 (2001)
23.55.0

IFF-01-11-041
Ebert Ph.
Defects in III-V semiconductor surfaces
Appl. Phys. A, in press (2001).
23.42.0

IFF-01-11-042
Edelmann K.1; Janich M.2; Hoinkis E.3; Pyckhout-Hintzen W.; Hoering S.1
1Fachbereich Chemie, Universität Halle
2Fachbereich Physik, Universität Halle
3Hahn Meitner Institut Berlin, Glienicker Str. 100, 14109 Berlin
The aggregation behaviour of poly(ethylene oxide)-poly(methyl methacrylate) diblock copolymers in organic solvents"
Macromol. Chem. Phys. 202, 1638-1644 (2001)
23.30.0

IFF-01-11-043
Ehrhart P.; Fitsilis F.; Regnery S.; Jia C.; Waser R.; Schienle F.1; Schumacher M.1;
Dauelsberg M.1; Strzyzewski P.1; Jürgensen H.1
1 Aixtron AG, Aachen
Growth of (Ba,Sr)TiO3 thin films in a multi-wafer MOCVD reactor
in 'Ferroelectric thin Films IX '(P.C.McIntyre, S.R.Gilbert, Y.Miyasaka, R.W.Schwartz, D.Wouters eds,)
MRS Proc.Vol.655 (2001) p. CC9.4.1-CC9.4.6
23.42.0

IFF-01-11-044
Endo H.; Mihailescu M.; Monkenbusch M.; Allgaier J.; Gompper G.; Richter D.; Jakobs B.1; Sottmann T.1; Strey R.1; Grillo I.1
1 Univ. Köln, Germany
Effect of amphiphilic block copolymers on the structure and phase behavior of oil-water-surfactant mixtures
J. Chem. Phys. 115, 580-600 (2001)
23.30.0

IFF-01-11-045
Endo H.; Mihailescu M.; Monkenbusch M.; Allgaier J.; Gompper G.; Richter D.; Jakobs B.1; Sottmann T.1; Strey R.1; Grillo I.2
1Institut für Physikalische Chemie, Universität Köln; Luxemburger Str. 116, 50939 Köln
2Institut Laue Langevin, 6, rue Jules Horowitz, BP 156, F-38042 Grenoble Cedex 9, France
Effect of amphiphilic block copolymers on the structure and phase behavior of oil-water-surfactant mixtures
J. Chem. Phys. 115, 580-600 (2001)
23.30.0

IFF-01-11-046
Erhardt R.1; Böker A.1; Zettl H.1; Kaya H.; Pyckhout-Hintzen W.; Krausch G.1,2; Abetz V.1; Müller A.1,2
1Fachbereich Chemie, Universität Bayreuth, 95440 Bayreuth
2Bayreuther Zentrum für Kolloide und Grenzflächen, 95440 Bayreuth
Janus Micelles
Macromolecules 34, 1069-1075 (2001)
23.30.0

IFF-01-11-047
Erhardt R.1; Böker A.1; Zettl H.1; Kaya H.; Pyckhout-Hintzen W.; Krausch G.1; Abetz V.1; Müller A.1
1Inst. für Makromolekulare Chemie, Universität Bayreuth, 95440 Bayreuth
Superstructures of janus micelles
Polymeric Materials: Science & Engineering 84 (2001)
23.30.0

IFF-01-11-048
Estermann M.A.1; Lemster K.1; Steurer W.1; Grushko B.; Döblinger M.2
1 Laboratory of Crystallography Swiss Federal Institute of Technology, CH-8092 Zürich
2 Lab. Elektronenmikroskopie, Univ. Karlsruhe, 76128 Karlsruhe
Structure Solution of a High-Order Decagonal Approximant Al71Co14.5Ni14.5 by Maximum Entropy Patterson Deconvolution
Ferroelectrics, Vol. 250, 245-248 (2001)
23.55.0

IFF-01-11-049
Faley M.I.; Poppe U.; Urban K.; Paulson D.N.1; Starr T.N.1; Fagaly R.L.1
1 Tristan Technologies Inc., CA 92121, USA
Low noise HTS dc-SQUID flip-chip magnetometers and gradiometers
IEEE Transactions on Appl. Supercond., Vol. 11, No. 1, 1383-1386 (2001)
23.42.0

IFF-01-11-050
Faley M.I.; Poppe U.; Urban K.; Paulson D.N.1; Starr T.N.1; Fagaly R.L.1
1 Tristan Technologies Inc., CA 92121, USA
Sensitive HTS gradiometers for magnetic evaluation applications accepted for publication in
Physica C (2002)
23.42.0

IFF-01-11-051
Feuerbacher M.; Klein H.1; Urban K.
1 ESRF, Pluo E, B.P. 220, 38043 Grenoble Cedex, France

Plastic deformation properties of the orthorhombic ('-(Al-Pd-Mn) quasicrystal approximant
Phil. Mag. Lett., Vol. 81, No. 9, 639-647 (2001)
23.55.0

IFF-01-11-052
Feuerbacher M.; Schall P.; Estrin Y.1; Bréchet Y.2
1 Institut für Werkstoffkunde und Werkstofftechnik, Technische Universität Clausthal, Agricolastrasse 6, D-38678 Clausthal-Zellerfeld, Germany
2 Laboratoire de Thermodynamique et Physicochimie Metallurgiques, Institut National Polytechnique de Grenoble, F-38402 Saint Martin d'Heres Cedex, France
A constitutive model for quasicrystal plasticity
Phil. Mag. Lett. Vol. 81, No. 7, 473-482 (2001)
23.55.0

IFF-01-11-053
Figolio A.1; Sager W.; Mulder M.1
1University of Twente, Niederlande
Facilitated oxygen transport in liquid membranes: review and new concepts
Journal of Membrane Science, 181, 97-110, 2001
23.30.0

IFF-01-11-054
Fitsilis F.; Regnery S.; Ehrhart P.; Waser R.; Schienle F.1; Schumacher M.1;
Dauelsberg M.1; Strzyzewski P.1; Jürgensen H.1
1 Aixtron AG, Aachen
BST thin films grown in a multi-wafer MOCVD reactor
J. Europ. Ceram. Soc. (2001) 1547-1551
23.42.0

IFF-01-11-055
Frielinghaus H.; Hermsdorf N.1; Sigel R.2; Almdal K.3; Mortensen K.3; Hamley I.W.4; Messé L.5; Corvazier L.5; Ryan A.J.5; van Dusschoten D.6; Wilhelm M.6; Floudas G.7; Fytas G.7
1Institut für Polymerforschung Dresden, 01069 Dresden
2MPI für Kolloid- und Grenzflächenforschung, 14424 Potsdam
3Risø National Laboratory, Danish Polymer Centre, DK-4000 Roskilde, Demark
4School of Chemistry, University of Leeds, Leeds LS2 9JT, UK
5Dept. of Chemistry, University of Sheffield, Sheffield S3 7HF, UK
6MPI for Polymer Research, 55021 Mainz
7Institute of Electronic Structure and Laser, GR-71110 Heraklion, Greece
Blends of AB/BC diblock copolymers with a large interaction parameter (
Macromolecules 34, 4907-4916 (2001)
23.30.0

IFF-01-11-056
Frielinghaus H.; Schwahn D.; Dudowicz J.1; Freed K.F.1; Foreman K.W.1
1The James Franck Institute and the Department of Chemistry, University of Chicago, Chicago, Illinois 60637, USA
Small-angle neutron scattering studies of polybutadiene/polystyrene blends as a function of pressure and microstructure: Comparison of experiment and theory
J. Chem. Phys. 114, 5016-5025 (2001)
23.30.0

IFF-01-11-057
Frielinghaus H.; Schwahn D.; Willner L.
Blends of polybutadiene with different vinyl contents and polystyrene studied with small-angle neutron scattering in varying temperature and pressure fields
Macromolecules 34, 1751-1763 (2001)
23.30.0

IFF-01-11-058
Galanakis I.; Alouani M.1; Oppeneer P.M.2; Dreysse H.1; Eriksson O.3
1 Institut de Physique et Chimie des Materiaux de Strasbourg, Strasbourg, France
2 Institute of Solid State and Materials Research, Dresden
3 Department of Physics, Uppsala University, Uppsala, Sweden
Tuning the orbital moment in transition metal compounds using ligand states
J. Phys.: Condens. Matter 13, 4553-4566 (2001)
23.20.0

IFF-01-11-059
Gallos L.K.1; Argyrakis P.1; Kehr K.W.
1 Univ. Thessaloniki
Trapping and survival probability in two dimensions
Phys. Rev. E63, 021104 (2001)
23.15.0

IFF-01-11-060
Gareev R.R.; Bürgler D.E.; Buchmeier M.; Olligs D.; Schreiber R.; Grünberg P.
Metallic-type oscillatory interlayer exchange coupling across an epitaxial FeSi spacer
Phys. Rev. Lett. 87, 157202 (2001)
23.42.0

IFF-01-11-061
Gebauer J.1; Krause-Rehberg R.2; Domke C.; Ebert Ph.; Urban K.; Staab T.E.M.3
1 ISG, FZ Jülich
2 FB Physik, Universität Halle
3 Lab. of Physics, Helsinki University of Technology
Direct identification of As vacancies in GaAs using positron annihilation calibrated by scanning tunneling microscopy
Phys. Rev. B, Vol. 63, 045203 (2001)
23.55.0

IFF-01-11-062
Goerigk G.; Williamson D. L.1
1Colorado School of Mines, Dept. of Physics, Golden, USA
Comparative anomalous small-angle x-ray scattering study of hotwire and plasma grown amorphous silicon-germanium alloys
Journal of Applied Physics Volume 90, Number 11 (2001) 5808 - 5811
23.89.1

IFF-01-11-063
Goerigk G.; Williamson D. L.1
1Colorado School of Mines, Dept. of Physics, Golden, USA
Quantitative ASAXS of germanium inhomogeneities in amorphous silicon-germanium alloys
Journal of Non-Crystalline Solids 281 (2001) 181 - 188
23.89.1

IFF-01-11-064
Golubov S.I. 1; Singh B.N. 1; Trinkaus H.
1 Department of Materials Research, Riso National Laboratory, Roskilde, Denmark
Defect accumulation in fcc and bcc metals and alloys under cascade damage conditions - Towards a generalisation of the production bias model
J. Nucl. Mat. 276, 78-89 (2000)
23.15.0

IFF-01-11-065
Gompper G.; Endo H.; Mihailescu M.; Allgaier J.; Monkenbusch M.; Richter D.; Jakobs B.1; Sottmann T.1; Strey R.1
1 Univ. Köln, Germany
Measuring Bending Rigidity and Spatial Renormalization in Bicontinuous Microemulsions
Europhys. Lett. 56, 683-689 (2001)
23.30.0

IFF-01-11-066

Gompper G.; Endo H.; Mihailescu M.; Allgaier J.; Monkenbusch M.; Richter D.; Jakobs B.1; Sottmann T.1; Strey R.1
1Institut für Physikalische Chemie, Universität Köln; Luxemburger Str. 116, 50939 Köln
Measuring bending rigidity and spatial renormalization in bicontinuous microemulsions
Europhys. Lett. 56, 683-689 (2001)
23.30.0

IFF-01-11-067
Gompper G.; Richter D.; Strey R.1
1 Univ. Köln, Germany
Amphiphilic block copolymers in oil-water-surfactant mixtures: efficiency boosting, structure, phase behaviour and mechanism
J. Phys.: Condens. Matter 13, 9055-9074 (2001)
23.30.0

IFF-01-11-068
Gompper G.; Richter D.; Strey R.1
1Institut für Physikalische Chemie, Universität Köln, Luxemburger Str. 116, 50939 Köln
Amphiphilic block copolymers in oil-water-surfactant mixtures: Efficiency boosting, structure, phase behavior and mechanism
Journal of Physics: Condensed Matter 13, 9055-9074 (2001)
23.30.0

IFF-01-11-069
Gozdz W.1,3; Gompper G.
1 Academy of Sciences, Warsaw, Poland
3 MPI Golm
Shape Transformations of Two-Component Membranes under Weak Tension
Europhys. Lett. 55, 587-593 (2001)
23.30.0

IFF-01-11-070
Graesseley W.W.1; Fetters L.J.
1Dept. of Chem. Engineering, Princeton University, Princeton, New Jersey 08544, USA
Thermoelasticity of Polymer Networks
Macromolecules 34, 7147-7151 (2001)
23.30.0

IFF-01-11-071
Grossmann M.1; Lohse O.1; Bolten D.1; Böttger U.1; Waser R.; Tiedke S.2; Schmitz T.2; Kall U.2; Kastner M.; Schindler G.3; Hartner W.3
1 Institut für Werkstoffe der Elektrotechnik, RWTH Aachen
2 aixacct systems, Aachen
3 Infinion Technologies, München
Influence of the Measurement Parameters on the Reliability of Ferroelectric Thin Films
Integrated Ferroelectrics 32 (2001) 1-9
23.42.0

IFF-01-11-072
Grünberg P.
Exchange anisotropy, interlayer exchange coupling and GMR in research and application
Sensors and Actuators A 91, 153-160 (2001)
23.42.0

IFF-01-11-073
Grünberg P.
Layered magnetic structures: History, highlights, applications
Physics Today, S. 31-37, (2001)
23.42.0

IFF-01-11-074
Grünberg P.
Layered magnetic structures: history, facts and figures
J. of Magnetism and Magnetic Materials 226, 1688 (2001)
23.42.0

IFF-01-11-075
Guilleaume B.1; Ballauff M.1; Goerigk G.; Wittemann M.2; Rehahn M.2
1Universität, Polymer-Institut, Karlsruhe
2TU, Institut für Makromolekulare Chemie, Darmstadt
Correlation of counterions with rodlike macroions as assessed by anomalous small-angle X-ray scattering
Colloid Polym Sci 279 (2001) 829 - 835
23.89.1

IFF-01-11-076
Gutheim F.; Müller-Krumbhaar H.; Brener E. A.
Epitaxial growth with elastic interaction: Submonolayer island formation
Phys. Rev. E 63, 041603 (2001)
23.15.0

IFF-01-11-077
Götz H.1; Ewen B.1; Maschke U.2; Meier G.; Monkenbusch M.
1MPI für Polymerforschung, 55021 Mainz
2Laboratoire de Chimie Macromoléculaire, UPRESA CNRS No. 8009, Université des Science et Technologies de Lille, F-59655 Villeneuve d'Ascq Cedex, France
Neutron scattering investigations on the statics and dynamics of polydimethyl- and polyethylmethylsiloxane melts
Macromol. Chem. Phys. 202, 3334-3341 (2001)
23.30.0

IFF-01-11-078
Götz H.1; Ewen B.1; Maschke U.2; Meier G.; Monkenbusch M.
1MPI in Mainz
2Université de Lille, France
Neutron Scattering Investigations on the Statics and Dynamics of Polydimethyl- and Polyethylmethylsiloxane Melts
Macromol.Chem.Phys. 202, 3334-3341 (2001
23.30.0

IFF-01-11-079
Haneder T.; Hönlein W.; Bachhofer H.; v. Philipsborn H.; Waser R.
Optimization of Pt/SBT/CeO2SI(100) Gate Stacks for Low Voltage Ferroelectric Field Effect Devices
Ferroelectrics 34 (2001) 47-54
23.42.0

IFF-01-11-080
Haubold H.-G.; Vad Th.; Jungbluth H.; Hiller P.
Nano structure of NAFION: a SAXS study
Electrochimica Acta 46 (2001) 1559 - 1563
23.89.1

IFF-01-11-081
Hauck J.; Henkel D.; Mika K.
The evolution processes of DNA sequences, languages and carols
Elsevier, Physica A, 293, 540-548, 2001
23.30.0

IFF-01-11-082
Hauck J.; Mika K.
Ground-State Structures of Polymers
Journal of Computational Chem.; 22, 1944-1955, 2001
23.30.0

IFF-01-11-083
Hauck J.; Mika K.
Interactions in Sphere Packings
Zeitschrift f. Physikalische Chemie, 215, 5, 637-652, 2001
23.30.0

IFF-01-11-084
Hauck J.; Mika K.
Ordering and interactions
Colloids and Surfaces A: Physicochem. and Eng. Aspects, 190, 99-109, 2001
23.30.0

IFF-01-11-085

Hauck J.; Mika K.
Ordering and interactions
Phys.Low-Dim. Struct., 7/8, 41-54, 2001
23.30.0

IFF-01-11-086
Heggen M.; Feuerbacher M.; Schall P.; Urban K.; Wang R.1
1 Department of Physics, Wuhan University, 430072 Wuhan, People's Republic of China
Antiphase domains in plastically deformed Zn-Mg-Dy single quasicrystals
Phys. Rev. B, Vol. 64, 014202-1-014202-6 (2001)
23.55.0

IFF-01-11-087
Heinrich M.; Rawiso M.1; Zilliox J.G.1; Lesieur P.2; Simon J.P.3
1Institut Charles Sadron, CNRS-ULP, 6 rue Boussingault, 67083 Strasbourg Cedex, France
2Lab. pour l'Utilisation du Rayonnement Electromagnétique, Bât. 209 D, Centre Univ. Paris-Sud, 91405 Orsay Cedex, France
3Lab. de Thermodynamique et Physico-Chimie Métallurgiques, CNRS-INPG-UJF, BP 75, 38402 Saint Martin d'Hères Cedex, France
Small angle x-ray scattering from salt-free solutions of star-branched polyelectrolytes
Eur. Phys. J. E 4, 131-142 (2001)
23.30.0

IFF-01-11-088
Heinsohn J.-K.; Dittmann R.; Rodríguez Contreras J.; GoldobinE.; Klushin A.; Siegel M.; Hagedorn D.; Pöpel R.; Dolata R.; Buchholz F.; Niemeyer J.
Effect of the magnetic-field orientation on the modulation period of the critical current of ramp-type Josephson juction
J. Appl. Phys. 90 9 (2001) 4623-4631
23.42.0

IFF-01-11-089
Heinsohn J.-K.; Dittmann R.; Rodríguez Contreras J.; Scherbel J.; Klushin A.; Siegel M.; Jia C.; Golubov S.; Kupryanov M.
Current transport in ramp-type junctions with engineered interface
J. Appl. Phys. 89 7 (2001) 3852-3860
23.42.0

IFF-01-11-090
Heinze S.; Blügel S.
Magnetische Ordnung wird sichtbar
Physik in unserer Zeit, 32, Juli (2001)
23.20.0

IFF-01-11-091
Highfield J.G.1; Oguro K.1; Grushko B.
1 Osaka National Research Institute, Midorigaoka 1-8-31, Ikeda-shi, Osaka 563, Japan
Raney multi-metallic electrodes from regular crystalline and quasi-crystalline precursors: I. Cu-stabilized Ni/Mo cathodes for hydrogen evolution in acid
Electrochimica Acta 47, 465-481 (2001)
23.55.0

IFF-01-11-092
Hofer C.1; Weber U.1; Waser R.
1 Institut für Werkstoffe der Elektrotechnik, RWTH Aachen
Electrical characterization of grain boundary decorated SrTiO3 ceramics
J. Eur. Ceram. Soc. 1921 (2001) 1753-1757
23.42.0

IFF-01-11-093
Hofmann T.1; Winkler R.G.; Reineker P.1
1 Univ. Ulm, Germany
Integral equation theory approach to rodlike polyelectrolytes: Counterion condensation
J. Chem. Phys., 114, 10181 (2001)
23.30.0

IFF-01-11-094
Holländer B.1; Lenk St.1; Mantl S.1; Trinkaus H.; Kirch D.; Luysberg M.; Hackbarth T.1; Herzog H.-J.2; Fichtner P.F.P.3
1 ISG, FZ Jülich
2 Daimler Crysler AG, Research and Technology, 89081 Ulm
3 Dept. de Metallurgia, Univ. Fed Do Rio Grande do Sul, 91501-970 Porto
Strain relaxation of pseudomorphic Si1-xGex/Si(100) heterostructures after hydrogen or helium ion implantation for virtual substrate fabrication
Nuclear Instruments and Methods in Physics Research B 175-177, 357-367 (2001)
23.42.0

IFF-01-11-095
Houben L.; Luysberg M.; Carius R.1
1 IPV, FZ Jülich
Microtwinning in microcrystalline silicon and ist effect on grain-size measurements
Phys. Rev. B
submitted 09.05.2001
23.42.0

IFF-01-11-096
Houben L.; Scholten C.; Luysberg M.; Vetterl O.1; Finger F.1; Carius R.1
1 IPV, FZ Jülich
Growth of microcrystalline nip solar cells: Role of local epitaxy
Journal of Non-Crystalline Solids
accepted
23.42.0

IFF-01-11-097
Ioffe A.; Mezei F.1,2
1HMI, Berlin
2Los Alamos National Laboratory, USA
4(-symmetry of the neutron wave function under space rotation
Physica B 297 (2001) 303 - 306
23.89.1

IFF-01-11-098
James M. R.1; Maloy S. A.1; Gac F. D.1; Sommer W. F.1; Chen J.; Ullmaier H.
1Los Alamos National Laboratory, USA
The mechanical properties of an Alloy 718 window after irradiation in a spallation environment
Journal of Nuclear Materials 296 (2001) 139 - 144
23.60.0

IFF-01-11-099
Jia C.L.; Siegert M.1; Urban K.
1 ISI, FZ Jülich
The Structure of the interface between BaTiO3 thin films and MgO substrates
Acta mater. 49, 2783-2789 (2001)
23.42.0

IFF-01-11-100
Jia C.L.; Zeng X.H.1; Xi X.X.1; Urban K.
1 Dept. of Physics, The Pennsylvania State University, University Park, PN 16802, USA
Microstructure and residual strain in La2CuO4 thin films on LaSrAlO4-buffered SrTiO3 substrates
Phys. Rev. B, Vol. 64, 075416-1-075416-6 (2001)

IFF-01-11-101
Jiang C. S.1; Yu H.1; Wang X. D.1; Shih C. K.1; Ebert Ph.
Scanning tunneling spectroscopy of quantum well and surface states of thin Ag films grown on GaAs (110)
Phys. Rev. B, Vol. 64, 235410, 1-5 (2001).
23.42.0

IFF-01-11-102

Jiang X.1; Jia C.L.; Szameitat M.1; Rickers C.1
1 Fraunhofer-Institut für Schicht und Oberflächentechnik, Bienroder Weg 54E, D-38108 Braunschweig
Epitaxy of diamond on Si(100) and surface-roughening-induced crystal misorientation
Phys. Rev. B, Vol. 64, 245413-1 - 245413- 5 (2001)
23.42.0

IFF-01-11-103
Jin H.Z.1; Zhu J.1; Ehrhart P.; Fitsilis F.; Jia C.L.; Regnery S.; Urban K.; Waser R.
1 Department of Materials Science and Engineering, Tsinghua University, Beijing 100084 China
A Study of (Ba,Sr)TiO3 thin films on Pt-electrodes by transmission electron microscopy
Appl. Phys. Lett., submitted
23.42.0

IFF-01-11-104
Jones R.O.; Ballone P.1
1 University of Messina, Italy
A combined density functional and Monte Carlo study of polycarbonate
Mat. Res. Soc. Symp. 677, AA3.1.1-12 (2001)
23.20.0

IFF-01-11-105
Jones R.O.; Ballone P.1
1 University of Messina, Italy
Density functional calculations for polymers and clusters - progress and limitations
Comput. Materials Science 22, 1-6 (2001)
23.20.0

IFF-01-11-106
Jones R.O.; Clare B.W.1; Jennings P.J.1
1 Murdoch University, Perth, Australia
Si-H clusters, defects, and hydrogenated silicon
Phys. Rev. B 64, 125203-1-9 (2001)
23.20.0

IFF-01-11-107
Jung P.; Liu C.; Chen J.
Retention of implanted hydrogen and helium in martensitic stainless steels and their effects on mechanical properties
Journal of Nuclear Materials 296 (2001) 165 - 173
23.60.0

IFF-01-11-108
Kaufmann Z.1; Lustfeld H.
1 Dept. of Physics of Complex Systems, Eötvös University, Budapest
Comparison of averages of flows and maps
Phys. Rev. E RC. 64, 1 (2001)
23.20.0

IFF-01-11-109
Kemmerling G.1; Engels R.1; Bussmann N.1; Clemens U.1; Heiderich M.; Reinartz R.1; Rongen H.1; Schelten J.1; Schwahn D.; Zwoll K.1
1Zentrallabor für Elektronik, Forschungszentrum Jülich, 52425 Jülich
A new two-dimensional scintillation detector system for small angle neutron scattering experiments
Transactions on Nuclear Science 48, 1114 (2001)
23.89.1

IFF-01-11-110
Khoukaz C.1; Galler R.1; Feuerbacher M.; Mehrer H.1
1 Institut für Metallforschung, Universität Münster, 48149 Münster
Self-Diffusion of Ni and Co in decagonal Al-Ni-Co quasicrystals.
Defect and Diffusion Forum 194-199 (2001) in press
23.55.0

IFF-01-11-111
Kim H.-J.1; Vescovo E.1; Heinze S.; Blügel S.
1Brookhaven National Laboratory, Upton, N.Y.
Surface electronic structure of Fe(110): the importance of surface resonances
Surf. Sci. 478, 193 (2001)
23.20.0

IFF-01-11-112
Kirstein O.; Prager M.; Combet J.1; Johnson M.R.1
1Institut Laue Langevin, 6, BP 156, F-38042 Grenoble Cedex 9, France
Ammonia group rotation in . Zn(NH3)4J2
Molecular Physics Reports 31, 47-55 (2001)
23.15.0

IFF-01-11-113
Kisielowski C.1; Hetherington C.J.D.1,2; Wang Y.C.1,3; Kilaas R.1; O'Keefe M.A.1; Thust A.
1 Department of Materials Science, University of California, Berkeley, CA 94720, USA
2 Department of Materials, University of Oxford, Oxford / UK
3 FEI Company, Hilsboro OR 97124, USA
Imaging columns of the light elements carbon, nitrogen and oxygen with sub Angstrom resolution
Ultramicroscopy 89, 243-263 (2001)
23.42.0

IFF-01-11-114
Klein H.1; Feuerbacher M.; Urban K.
1 ESRF, Pluo E, B.P. 220, 38043 Grenoble Cedex, France
Structure of Dislocations and Stacking Faults in a Large-Unit-Cell Intermetallic Compound.
Phys. Rev. B, submitted
23.55.0

IFF-01-11-115
Klingeler R.; Kann G.; Wirth I.; Eisebitt S.; Bechthold P.S.; Neeb M.; Eberhardt W.
La@C60: A metallic endohedral fullerene
J. of Chemical Physics 115, 7215 (2001)
23.20.0

IFF-01-11-116
Kluge M.; Schober H. R.
Simulation of diffusion in amorphous solids and liquids
Defect and Diffusion Forum 194-199, 849-854 (2001)
23.30.0

IFF-01-11-117
Koenderink G.H.1; Zhang H.2; Lettinga P.; Nägele G.; Philipse A.P.1
1University of Utrecht
2University of Shanghai
Rotational tracer diffusion in binary colloidal sphere mixtures
Physical Rev.E., 64, 22401, 2001

IFF-01-11-118
Koizumi S.1; Monkenbusch M.; Richter D.; Schwahn D.; Annaka M.1
1Advanced Science Research Center, Japan Atomic Energy Research Institute, Tokai-mura, Ibaraki-ken 319-1195, Japan
Frozen Concentration Fluctuations of a Poly (N-isopropyl aclyamide) Gel Decomposed by Neutron Spin Echo
J Phys. Soc. Jpn. 70, Suppl. A p. 320. (2001)
23.30.0

IFF-01-11-119
Korhonen T.1; Settels A.; Papanikolaou N.; Zeller R.; Dederichs P.H.
1 Lab. of Physics, Helsinki University of Technology, Finland
Effect of lattice relaxations on the hyperfine fields of heavy impurities in Fe
J. Mag. Mag. Mat. 226-230, 1024-1026 (2001)
23.20.0

IFF-01-11-120

Kramp S.1; Rotter M.2; Löwenhaupt M.3; Pyka N.M.4; Schmidt W.; van de Kamp R.5
1Institut Laue Langevin, BP 156 38042 Grenoble Cedex 9, France
2Institut für Experimentalphysik, Technische Universität Wien, Wiedner Hauptstraße 8-10, 1040 Wien, Austria
3Inst. für Angew. Physik u. Didaktik der Physik, TU Dresden, 01062 Dresden
4TU München, Zentrale Betriebseinheit FRM - II, 85747 Garching
5Hahn Meitner Institut, 14109 Berlin
Spin waves in the ferrimagnetic phase of NdCu2
J. Magn. Magn. Mat. 226-230, 470-472 (2001)
23.30.0

IFF-01-11-121
Krause H.-J.1; Wolf W.1; Glaas W.1; Zimmermann E.1; Faley M.I.; Sawade G.2; Mattheus R.2; Neudert G.3; Gampe U.3; Krieger J.4
1 ISG, FZ Jülich
2 Forschungs- und Materialprüfungsanstalt Baden-Württemberg, 70569 Stuttgart
3 Siempelkamp, Prüf- und Gutachtergesellschaft mbH, 01099 Dresden
4 Bundesanstalt für Straßenwesen, 51427 Bergisch-Gladbach
SQUID Array for Magnetic Inspection of Prestressed Concrete Bridges accepted for publication in
Physica C (2002)
23.42.0

IFF-01-11-122
Kurz P.; Bihlmayer G.; Blügel S.; Hirai K.1; Asada T.2
1Department of Physics, Nara Mecial University, Kashihara, Nara, Japan
2Faculty of Engineering, Shizuoka University, Hamamatsu, Japan
Comment on "Ultrathin Mn films on Cu(111) substrates: Frustrated antiferromagnetic order"
Phys. Rev. B 63, 096401 (2001)
23.20.0

IFF-01-11-123
Kurz P.; Bihlmayer G.; Hirai K.1; Blügel S.
1Department of Physics, Nara Mecial University, Kashihara, Nara, Japan
Three-dimensional spin structure on a two-dimensional lattice: Mn/Cu(111)
Phys. Rev. Lett. 86, 1106 (2001)
23.20.0

IFF-01-11-124
Köbler U.; Fischer K.
The impact of fourth-order exchange interactions on the critical temperatures of EuxSr1-xS and EuxSr1-xTe
J. Phys.: Condens. Matter 13 (2001) 123 - 139
23.15.0

IFF-01-11-125
Köbler U.; Hoser A.1,2; Englich J.3; Snezhko A.3; Kawakami M.4; Beyss M.; Fischer K.
1HMI, Berlin
2RWTH, Institut für Kristallographie, Aachen
3Charles University, Faculty of Mathematics and Physics, Prag, Tschechische Republik
4University, Department of Physics, Kagoshima
On the Failure of the Bloch-Kubo-Dyson Spin Wave Theory
Journal of the Physical Society of Japan, Volume 70, Number 10 (2001) 3089 - 3097
23.15.0

IFF-01-11-126
Köbler U.; Hoser A.1; Kawakami M.2; Abens S.3
1RWTH, Institut für Kristallographie, Aachen
2Kagoshima University, Faculty of Science, Japan
3HMI, Berlin
Observation of a spin wave exponent of 5/2 in the uniaxial antiferromagnet MnF2
Physica B 307 (2001) 175 - 183
23.15.0

IFF-01-11-127
Köbler U.; Mueller R.; Brown P. J.1; Arons R. R.; Fischer K.
1ILL, Grenoble, France
Experimental identificaion of fourth-order exchange interactions in magnets with pure spin moments
J. Phys.: Condens. Matter 13 (2001) 6835 - 6852
23.15.0

IFF-01-11-128
Küppers H.1; Hoffmann M.1; Leuerer T.1; Schneller T.1; Böttger U.1; Waser R.; Mokwa W.1; Schnakenberg U.1
1 Institut für Werkstoffe der Elektrotechnik I+II, RWTH Aachen
Basic Investigations on a Piezoelectric Bending Actuator for Micro-Electro-Mechanical Applications
Ferroelectrics 35 (2001) 269-281
23.42.0

IFF-01-11-129
Küppers H.1; Leuerer T.1; Schnakenberg W.1; Mokwa W.1; Hoffmann M.1; Schneller T.1; Böttger U.1; Waser R.
1 Institut für Werkstoffe der Elektrotechnik I+II, RWTH Aachen
PZT thin films for piezoelectric micro-actuator applications
Transducers'01, Eurosensors XV, Springer-Verlag, Vol. 2,1018-1021
23.42.0

IFF-01-11-130
Lamura A.; Burkhardt T.W.1; Gompper G.
1 Univ. Philadelphia, USA
Semi-Flexible Polymer in a Uniform Force Field in Two Dimensions
Phys. Rev. E 64, 061801 [1-8] (2001)
23.30.0

IFF-01-11-131
Lamura A.; Gompper G.; Ihle T.1; Kroll D.M.1
1 Univ. Minnesota, USA
Multi-particle-collision dynamics: Flow around a circular and a square cylinder
Europhys. Lett. 56, 319-325 (2001)
23.30.0

IFF-01-11-132
Lamura A.; Gonnella G.1
1 Univ. Bari, Italy
Lattice Boltzmann simulations of segregating binary fluid mixtures in shear flow
Physica A, 294, 295 (2001)
23.30.0

IFF-01-11-133
Lenstra T.; Dhont J.
Flow dichroism in critical colloidal fluids
Physical Rev. E., 63, 61401-12, 2001
23.30.0

IFF-01-11-134
Lenstra T.; Dogic Z.; Dhont J.
Shear-induced displacement of isotropic-nematic spinodals
Journal of Chem. Phys., 114, 10151, 2001
23.30.0

IFF-01-11-135
Lentzen M.; Jahnen B.; Jia C.L.; Thust A.; Tillmann K.; Urban K.
High-resolution imaging with an aberration-corrected transmission electron microscope
Ultramicrocopy 2001 (eingereicht)
23.42.0

IFF-01-11-136
Liebsch A.; Kim B.-O.1; Plummer E.W.1
1 Depart. of Physics, University of Tennessee, Knoxville, Tennessee, USA

Collective excitations in adsorbed alkali-metal films: Critical analysis of photoyield and electron-energy-loss spectra for K on Al(111)
Phys. Rev. B 63, 125416-1-10 (2001)
23.20.0

IFF-01-11-137
Liebsch A.
Comment on: ``Fermi Surface, Surface States and Surface Reconstruction in Sr2RuO4"
Phys. Rev. Lett. 87, 239701 (2001)
23.20.0

IFF-01-11-138
Link S.; Dürr H.A.; Bihlmayer G.; Blügel S.; Eberhardt W.; Chulkov E.V.1; Silkin V.M.1; Echenique P.M.1
1Donostia International Physics Center, San Sebastian, Spain
Femtosecond electron dynamics of image-potential states on clean and oxygen-covered Pt(111)
Phys. Rev. B 63, 115420 (2001)
23.20.0

IFF-01-11-139
Link S.; Dürr H.A.; Bihlmayer G.; Blügel S.; Eberhardt W.; Chulkov E.V.1
1Donostia International Physics Center (DIPC), San Sebastian, Spain
Electron dynamics of image potential states on the clean and oxygen covered Pt(111) surface
Pys. Rev. B 63, 115420 (2001)
23.20.0

IFF-01-11-140
Link S.; Dürr H.A.; Eberhardt W.
Femtosecond spectroscopy
Journal of Physics: Condensed Matter 13, 7873 (2001)
23.20.0

IFF-01-11-141
Lohse O.1; Grossmann M.1; Bolten D.1; Böttger U.1; Waser R.
1 Institut für Werkstoffe der Elektrotechnik, RWTH Aachen
Relaxation Mechanisms in Ferroelectric Thin Film Capacitors for FeRAM Application
Integrated Ferroelectrics 33 (2001) 39-48
23.42.0

IFF-01-11-142
Lohse O.1; Grossmann M.1; Bolten D.1; Böttger U.1; Waser R.
1 Institut für Werkstoffe der Elektrotechnik, RWTH Aachen
Transient Behavior of the Polarization in Ferroelectric Thin Film Capacitors
Mat. Res. Soc. Symp. Proc. 655 (2001) 761-769
23.42.0

IFF-01-11-143
Lohse O.1; Grossmann M.1; Böttger U.1; Bolten D.1; Waser R.
1 Institut für Werkstoffe der Elektrotechnik RWTH Aachen
Relaxation mechanism of Ferroelectric switching in Pb/Zr,Ti)O3 thin films
J. Appl. Phys. 89 (2001) 2332-2336
23.42.0

IFF-01-11-144
Lustfeld H.; Pohlmeier A.1
1 FZ-ICG IV
Electric potential and reaction rates at charged surfaces in asymmetric electrolytes - an analytic approach
J. Colloid Interface Science 181, 45 (2001)
23.20.0

IFF-01-11-145
López Bastidas C.; Liebsch A.; Mochán W.L.1
1 Centro de Ciencias Fisicas, UNAM, Cuernavaca, Mexico
Influence of d electrons on the dispersion relation of Ag surface plasmons for different single-crystal faces
Phys. Rev. B 63, 165407-1-12 (2001)
23.20.0

IFF-01-11-146
Lüttgens G.; Pontius N.; Friedrich C.; Klingeler R.; Bechthold P.S.; Neeb M.; Eberhardt W.
Chemisorption of benzene on metal dimer anions: A study by photoelectron detachment spectroscopy
J. Chem. Phys. 114, 8414 (2001)
23.20.0

IFF-01-11-147
Maassen R.1; Eisenriegler E.1; Bringer A.
1 Theory II, IFF
Density depletion profile and solvation free energy of a colloidal particle in a polymer solution
J. Chem. Phys. 115, 5292 (2001)
23.20.0

IFF-01-11-148
Maassen R.; Eisenriegler E.; Bringer A.
Density depletion profile and solvation free energy of a colloidal particle in a polymer solution
Journal of Chem. Phys. 115, 5292-5309 (2001)
23.30.0

IFF-01-11-149
Maiti K.; Dallmeyer A.; Malagoli M.; Carbone C.; Eberhardt W.; Rader O.1; Pasquali L.2; Banerjee, A.3; Turchini S.4; Zennaro S.4; Zema N.4
1BESSY Berlin
2INFM and Dipartimento di Fisica, Universita di Modena e Reggio Emilia, Italy
3Inter University Consortium for DAE Facilities, Indore, India
4Consiglio Nazionale delle Recerche, Roma, Italy
Oscillary interlayer coupling mediated by fcc-Fe/Co(100) films
Appl Surf. Science 182, 302 (2001)
23.20.0

IFF-01-11-150
Maiti K.; Malagoli M.; Magnano E.; Dallmeyer A.; Carbone C.
Electronic band structure of Gd: A consistent description
Phys. Rev. Lett 86, 2846 (2001)
23.20.0

IFF-01-11-151
Matsuoka H.1; Yamamoto Y.1; Nakano M.1; Endo H.1; Yamaoka H.1; Zorn R.; Monkenbusch M.; Richter D.; Seto H.2; Kawabata Y.2; Nagao M.3
1Department of Polymer Chemistry, Kyoto University, Kyoto 606-8501, Japan
2FIAS, Hiroshima University, Higashi-Hiroshima, Hiroshima 739-8521, Japan
3Neutron Scattering Laboratory, Institute of Solid State Physics, The University of Tokyo, Tokai, Ibaraki 319-1106, Japan
Neutron Spin-Echo Study of the Dynamic Behavior of Amphiphilic Diblock Copolymer Micelles in Aqueous Solution
Langmuir 16, 9177-9185 (2000)
23.15.0

IFF-01-11-152
Maxelon M.1; Pundt A.1; Pyckhout-Hintzen W.; Barker J.2; Kirchheim R.1
1Institut für Materialphysik, Hospitalstraße 3-7, 37073 Göttingen
2NIST, Gaithersburg, Maryland 20899, USA
Interaction of hydrogen and deuterium with dislocations in palladium as observed by small angle neutron scattering
Acta Materialia 49, 2625-2634 (2001)
23.30.0

IFF-01-11-153
Maxelon M.1; Pundt A.1; Pyckhout-Hintzen W.; Kirchheim R.1

1Institut für Materialphysik, Hospitalstraße 3-7, 37073 Göttingen
Small angle neutron scattering of hydrogen segregation at dislocations on palladium
Scripta Materialia 44, 817-822 (2001)
23.30.0

IFF-01-11-154
Mezei F.1,2; Drabkin G.1,3; Ioffe A.
1HMI, Berlin
2Los Alamos National Laboratory, USA
3St. Petersburg Nuclear Physics Institute, Gatchina, Russia
Polarimetric neutron spin echo
Physica B 207 (2001) 9 - 13
23.89.1

IFF-01-11-155
Mi S.; Yurechko M.; Wu J.; Grushko B.
Ternary Al-Pd-Co monoclinic phases
Journal of Alloys and Compounds 329, L1-L4 (2001)
23.55.0

IFF-01-11-156
Mihailescu M.; Monkenbusch M.; Endo H.; Allgaier J.; Gompper G.; Stellbrink J.; Richter D.; Jakobs B.1; Sottmann T.1; Farago B.1
1 Univ. Köln, Germany
Dynamics of bicontinuous microemulsion phases with and without amphiphilic block-copolymers
J. Chem. Phys. 115, 9563-9577 (2001)
23.30.0

IFF-01-11-157
Mihailescu M.; Monkenbusch M.; Endo H.; Allgaier J.; Gompper G.; Stellbrink J.; Richter D.; Jakobs B.1; Sottmann T.1; Farago B.2
1Institut für Physikalische Chemie, Universität Köln, Luxemburger Str. 116, 50939 Köln
2Institut Laue Langevin, 6, rue Jules Horowitz, BP 156, F-38042 Grenoble Cedex 9, France
Dynamics of bicontinuous microemulsion phases with and without amphiphilic blockcopolymers
J. Chem. Phys. 115, 9563-9577 (2001)
23.30.0

IFF-01-11-158
Moreno A.J.1; Alegria A.1; Colmenero J.1; Prager M.; Grimm H.; Frick B.2
1Departamento de Fisica de Materiales y Centro Mixtor CSIC-UPV/EHU, Universidad del Pais Vasco (UPV/EHU), Apt. 1072, 20080 San Sebastian, Spain
2Institute Laue-Langevin, BP 156X, F-38042 Grenoble, France
Methyl group dynamics in glassy toluene: A neutron scattering study
J. Chem. Phys. 115, 8958-8966 (2001)
23.30.0

IFF-01-11-159
Morenzin J.; Kietzmann H.; Bechthold P.S.; Ganteför G.; Eberhardt W.
Localization and bandwidth of the 3d-orbitals in magnetic Ni and Co clusters
Pure Appl. Chem. 72, 2149 (2000) (erschienen 2001)
23.20.0

IFF-01-11-160
Mueller R.
The Yb fiber laser for metastable 3He optical pumping at Jülich
Physica B 297 (2001) 277 - 281
23.89.1

IFF-01-11-161
Müller-Krumbhaar H.; Gutheim F.; Spatschek R.; Brener E. A.
Elastic effect on growth processes
Appl. Surface Science 182, 265 (2001)
23.15.0

IFF-01-11-162
Neeb M.; Klingeler R.; Bechthold P.S.; Kann G.; Wirth I.; Eisebitt S.; Eberhardt W.
Deposition of endohedral fullerenes from a laser evaporation cluster source
Appl. Phys. A 72 , 289 (2001)
23.20.0

IFF-01-11-163
Nerger S.; Kentzinger E.; Rücker U.; Voigt J.; Ott F.1; Seeck O.; Brückel Th.
1LLB (CEA/CNRS), Gif-sur-Yvette, France
Proximity effects in Fe1-xCox/Mn/Fe1-xCox trilayers
Physica B 297 (2001) 185 - 188
23.89.1

IFF-01-11-164
Nietubyc R.1; Sobczak E.1,2; Pelka J. B.1; Mackowski S.1; Janik E.1; Karczewski G.1; Goerigk G.
1Polish Academy of Sciences, Institute of Physics, Warsaw, Poland
2Polish Academy of Sciences, Center of Theoretical Physics, Warsaw, Poland
Anomalous small angle X-ray scattering study of CdTe quantum dots in ZnTe
Journal of Alloys and Compounds 328 (2001) 206 - 210
23.89.1

IFF-01-11-165
Nonas B.; Cabria I.; Zeller R.; Dederichs P.H.; Huhne T.1; Ebert H.1
1 Institut für Phys. Chemie, Universität München
Strongly enhanced orbital moments and anisotropies of adatoms on the Ag(001) surface
Phys. Rev. Lett. 86, 2146 (2001)
23.20.0

IFF-01-11-166
O'Keefe M.A.1; Hetherington C.J.D.1,2; Wang Y.C.1,3; Nelson E.C.1; Turner J.H.1; Kisielowski C.1; Malm J.-O.4; Müller R.3; Ringnalda J.3; Pan M.5; Thust A.
1 Department of Materials Science, University of California, Berkeley, CA 94720, USA
2 Department of Materials, University of Oxford, Oxford / UK
3 FEI Company, Hilsboro OR 97124, USA
4 Materials Chemistry 2, Lund University, SE-22100 Lund / Schweden
5 Gatan, Inc. Pleasanton, CA 94588, USA
Sub-Angstrom high-resolution transmission electron microscopy at 300 keV
Ultramicroscopy 89, 215-241 (2001)
23.42.0

IFF-01-11-167
O'Keefe M.A.1; Nelson E.C.1; Wang Y.C.1; Thust A.
1 Department of Materials Science, University of California, Berkeley, CA 94720, USA
Sub-Angström resolution of atomistic structures below 0.8 A
Phil. Mag. B, Vol. 81, No. 11, 1861-1878 (2001)
23.42.0

IFF-01-11-168
Ohly C.; Hoffmann S.; Szot K.; Waser R.
High temperature conductivity behavior of doped SrTiO3 thin films
Integrated Ferroelectrics 33 (2001) 363
23.42.0

IFF-01-11-169
Ohly C.; Hoffmann-Eifert S.; Szot K.; Waser R.
Electrical Conductivity and Segregation Effects of doped SrTiO3 Thin Films at High Temperatures,
J. Europ. Ceram. Soc. 21 (2001) 1673-1676
23.42.0

IFF-01-11-170
Panaccione G.1; van der Laan G.1; Dürr H.A.; Vogel J.1
1Department of Physics, University of Durham, UK
Magnetic circular dichroism in Co 2p photoemission of Co/Cu (1 1 13): Separation of the fundamental spectra
Eur. Phys. J. B 19, 281 (2001)
23.20.0

IFF-01-11-171
Partyka P.; Zhong Y.; Nordlund K.; Averback R. S. ; Robinson I. M.; Ehrhart P.:
Grazing incidence diffuse x-ray scattering investigation of the properties of irradiation-induced point defects in silicon
Phys.Rev. B64, 23, (2001) 235207-1 to 235207-8
23.42.0

IFF-01-11-172
Patkowski A.1,2; Fischer E.W.1; Steffen W.1; Gläser H.1; Baumann M.1; Ruths T.1; Meier G.
1MPI in Mainz
2University of Poznan, Poland
Unusual features of long-range density fluctuations in glass-forming organic liquids: A Rayleigh and Rayleigh-Brillouin light scattering study
Physical Rev.E., 63, 061503, 2001
23.30.0

IFF-01-11-173
Pelka J. B.1; Paszkowics W.1; Dluzewski P.1; Dynowska E.1; Wawro A.1; Baczewski L. T.1; Kosiowski M.1; Wisniewski A.1; Seeck O.; Messoloras S.2; Gamari-Seale H.3
1Polish Academy of Sciences, Warsaw, Poland
2NCSR Demokritos, Institute of Nuclear Technology, Attikis, Greece
3NCSR Demokritos, Institute of Materials Science, Attikis, Greece
Structural and magnetic study of Co/Gd multilayers deposited on Si and Si-N substrates
J. Phys. D: Appl. Phys. 34 (2001) A208 - A213
23.89.1

IFF-01-11-174
Pelka J. B.1; Paszkowicz W.1; Wawro A.1; Baczewski L. T.1; Seeck O.
1Polish Academy of Sciences, Warsaw, Poland
Structural study of Co/Gd multilayers by X-ray diffraction and GIXR
Journal of Alloys and Compounds 328 (2001) 253 - 258
23.89.1

IFF-01-11-175
Perny S.; Allgaier J.; Cho D.1; Lee W.1; Chang T.1
1Dep. of Chemistry and Center for Integrated Molecular Systems, Pohang University of Science and Technology, Pohang, 790-784, China
Synthesis and structural analysis of an h-shaped polybutadiene
Macromolecules 34, 5408-5415 (2001)
23.30.0

IFF-01-11-176
Persson B.N.J.; Tosatti E.1
1 ICTP Trieste, Italy
The effect of surface roughness on the adhesion of elastic solids
J. Chem. Phys. 115, 5597 (2001)
23.20.0

IFF-01-11-177
Persson B.N.J.
Elastic instabilities at a sliding interface
Phys. Rev. B 63, 104101 (2001)
23.20.0

IFF-01-11-178
Persson B.N.J.
Elastoplastic contact between randomly rough surfaces
Phys. Rev. Lett. 87, 116101 (2001)
23.20.0

IFF-01-11-179
Persson B.N.J.
Theory of Rubber Friction and Contact Mechanics
J. Chem. Phys. 115, 3840 (2001)
23.20.0

IFF-01-11-180
Pertsev N.1 Koukhar V.1; Waser R.; Hoffmann S.
1 Ioffe Institute of Physics, St. Petersburg, Russia
Effects of Domain Formation on the Dielectric Properties of Ferroelectric Thin Films"
Ferroelectrics 32 (2001) 235-249
23.42.0

IFF-01-11-181
Pesché R.1; Kollmann M.; Nägele G.
1University of Delaware, Newark, USA
Brownian dynamics study of dynamic scaling and related freezing criteria in quasi-two-dimensional dispersions
Journal of Chemical Physics, 114, 8701-8707, 2001
23.30.0

IFF-01-11-182
Pesché R.1; Kollmann M.; Nägele G.
1University of Delaware, Newark, USA
Dynamic scaling and freezing criteria in quasi-two-dimensional dispersions
Phys.Rev.E., 64, 2001
23.30.0

IFF-01-11-183
Petzelt J.; Ostapchuk T.; Gregora I.; Hoffmann S.; Lindner J.; Rafaja D.; Kamba S.; Pokorny J.; Bovtun V.; Porokhonsky V.; Savinov M.; Vanek P.; Rychetsky I.; Perina V.; Waser R.
Far Infrared and Raman Spectroscopy of Ferroelectric Soft Mode in SrTiO3 Thin Films and Ceramics
Ferroelectrics 32 (2001) 703
23.42.0

IFF-01-11-184
Petzelt J.; Ostapchuk T.; Gregora I.; Rychetsky I.; Hoffmann-Eifert S.; Pronin A. V.; Yuzyuk Y.; Gorshunov B. P.; Kamba S.; Bovtun V.; Pokorny J.; Savinov M.; Porokhonskyy V.; Rafaja D.; Vanek P.; Almeida A.; Chaves M. R.; Volkov A. A.; Dressel M.; Waser R.
Dielectric, infrared, and Raman response of undoped SrTiO3 ceramics: Evidence of polar grain boundaries
Phys. Rev. B 64 (2001) 184111/1
23.42.0

IFF-01-11-185
Pinnow C. U.1; Bicker M.1; Geyer U.1; Schneider S.1; Goerigk G.
1Universität, I. Physikalisches Institut, Göttingen
Decomposition and nanocrystallization in reactively sputtered amorphous Ta-Si-N thin films
Journal of Applied Physics 90 (4) (2001) 1986 - 1991
23.89.1

IFF-01-11-186
Plakhty V. P.1; Maleyev S. V.1; Kulda J.2; Visser E. D.3,4,5; Wosnitza J.6; Moskvin E. V.1; Brückel Th.; Kremer R. K.7
1Petersburg Nuclear Physics Institute, Gatchina, Russia
2ILL, Grenoble, France
3University of Warwick, Dept. of Physics, Coventry, UK
4CLRC, ISIS Facility, RAL, Chilton, UK
5IRI, TU Delft, The Netherlands
6University, Physikalisches Institut, Karlsruhe
7MPI für Festkörperforschung, Stuttgart
Spin chirality and polarised neutron scattering
Physica B 297 (2001) 60 - 66
23.89.1

IFF-01-11-187

Plakhty V.1,2; Schweika W.; Brückel Th.; Kulda J.3; Gavrilov S. V.1; Regnault L.-P.4; Visser D.5
1Petersburg Nuclear Physics Institute, Russia
2FZJ, IFF-Streumethoden, Jülich
3ILL, Grenoble, France
4CEA, Grenoble, France
5CLRC, ISIS, Didcot, UK
Chiral criticality in helimagnet Ho studied by polarized neutron scattering
Physical Review B 64 100402(R) (2001) 100402-1 - 100402-4
23.89.1

IFF-01-11-188
Poon W.C.K.1; Egelhaaf S.U.1; Stellbrink J.; Allgaier J.; Schofield A.B.1; Pusey P.N.1
1Department of Physics and Astronomy, The University of Edinburgh, Mayfield Road, Edinburgh EH9 3JZ, UK
Beyond Simple Depletion: Phase Behaviour of Colloid-Star Polymer Mixtures
Phil. Trans. R. Soc. Lond. A, 359, 897-907 (2001)
23.30.0

IFF-01-11-189
Popkov V.; Hager J.1; Krug J.2; Schütz G.M.
1 RWTH Aachen, Germany
2 Univ. Essen, Germany
Minimal current phase and boundary layers in driven diffusive systems
Phys. Rev. E 63 (2001), 056110
23.15.0

IFF-01-11-190
Popkov V.; Peschel I.1
1 FU Berlin, Germany
Symmetry breaking and phase coexistence in a driven diffusive two-channel system
Phys. Rev. E, 64 (2001)026126
23.15.0

IFF-01-11-191
Popkov V.; Santen L.1; Schadschneider A.2; Schütz G.M.
1 Univ. Nancy, France
2 Univ. Köln, Germany
Boundary-induced phase transition in traffic flow
J. Phys. A 34,L1 - L8 (2001)
23.15.0

IFF-01-11-192
Poppe U.; Divin Y.Y.; Faley M.I.; Wu J.S.; Jia C.L.; Shadrin P.; Urban K.
Properties of YBa2Cu3O7 Thin Films Deposited on Substrates and Bicrystals with Vicinal Offcut and Realization of High IcRn Junctions
IEEE Transactions on Appl. Supercond., Vol. 11, No. 1, 3768-3771 (2001)
23.42.0

IFF-01-11-193
Prume K.1; Hoffmann S.; Waser R.:
1 Institut für Werkstoffe der Elektrotechnik, RWTH Aachen
Finite Element Simulations of Interdigital Electrode Structures on High Permittivity Thin Films
Integrated Ferrroelectrics 32 (2001) 63-72
23.42.0

IFF-01-11-194
Prume K.1; Hoffmann S.; Waser R.
1 Institut für Werkstoffe der Elektrotechnik, RWTH Aachen
Finite Element Simulations of Interdigital Electrode Stucture on High Permittivity Thin Films
Ferroelectrics 32 (2001) 755
23.42.0

IFF-01-11-195
Richter D.; Kahle S.; Monkenbusch M.; Willner L.; Arbe A.1; Colmenero J.1; Farago B.2
1Departamento de Fisica de Materiales, Universidad del Pais Vasco, San Sebastian, Spain
2Institut Laue-Langevin, BP 156, F-38042 Grenoble Cedex, France
Neutron scattering and the glass transition in polymers - present status and future opportunities
Contribution for the VI. Int. Workshop on Non-Crystalline Solids in Bilbao, Journal of Non-Crystalline Solids 287, 286-296 (2001)
23.30.0

IFF-01-11-196
Richter D.; Monkenbusch M.; Pyckhout-Hintzen W.; Arbe A.1; Colmenero J.1
1Departamento de Fisica de Materiales, Universidad del Pais Vasco, San Sebastian, Spain
Response to Comment on "From Rouse dynamics to local relaxation: A neutron spin echo on polyisobutylene melts" J. Chem. Phys. 113, 11398-11399 (2000)
23.30.0

IFF-01-11-197
Rotter M.1; Löwenhaupt M.2; Kramp S.2,4; Reif T.; Pyka N.M.3; Schmidt W.; van de Kamp R.5
1Institut für Experimentalphysik, Technische Universität Wien, Wiedner Hauptstraße 8-10, 1040 Wien, Austria
2Institut für Angewandte Physik, Technische Universität Dresden, 01062 Dresden
3TU München, Zentrale Betriebseinheit FRM - II, 85747 Garching
4Institut Laue Langevin, BP 156 38042 Grenoble Cedex 9, France
5Hahn Meitner Institut, 14109 Berlin
Anisotropic magnetic exchange in orthorhombic RCu2 compounds (R = rare earth)
Eur. Phys. J. B 14, 29-42 (2000)

IFF-01-11-198
Rücker U.; Bergs W.; Alefeld B.; Kentzinger E.; Brückel Th.
Polarization analysis for the 2D position-sensitive detector of the HADAS reflectometer in Jülich
Physica B 297 (2001) 140 - 142
23.89.1

IFF-01-11-199
Sambeth R.; Baumgaertner A.
Autocatalytic Polymerization Generates Persistent Random Walk of Crawling Cells
Phys. Rev. Lett. 86,(2001)
23.30.0

IFF-01-11-200
Sambeth R.; Baumgaertner A.
Locomotion of a two dimensional keratocyte model
J. Biol. Systems 9, 201-219 (2001)
23.30.0

IFF-01-11-201
Santos J.E.1; Schütz G.M.
1 TU München, Germany
Exact time-dependent correlation functions for the symmetric exclusion process with open boundary
Phys. Rev. E. 64, 036107 (2001)
23.15.0

IFF-01-11-202
Schall P.; Feuerbacher M.; Urban K.
Plastic deformation behaviour of decagonal Al70Ni15Co15 single quasicrystals
Phil. Mag. Lett. Vol. 81, No. 5, 339-349 (2001)
23.55.0

IFF-01-11-203
Schall P.; Feuerbacher M.; Urban K.
Plastic deformation of decagonal Al-Ni-Co single quasicrystals
Mat. Sci. Eng. A309-310, 548-551 (2001)
23.55.0

IFF-01-11-204
Scharte M.1; Porath R.1; Ohms T.1; Aeschlimann M.1; Krenn J.R.2; Ditlbacher H.2; Aussenegg F.R.2; Liebsch A.
1 Dept. of Physics, University of Kaiserslautern
2 Inst. for Experimental Physics, University of Graz, Austria
Do Mie Plasmons have a longer lifetime on resonance than off-resonance?
Appl. Phys. Lett. B73, 305-310 (2001)
23.20.0

IFF-01-11-205
Schilling T.; Theissen O.; Gompper G.
Dynamics of the swollen lamellar phase
Eur. Phys. J E4, 103-114 (2001)
23.30.0

IFF-01-11-206
Schmidt C.M.1; Bürgler D.E.; Schaller D.M.1; Meisinger F.1; Güntherodt H.-J.1; Temst K.1
1Universität Basel
Interface morphology of a Cr(001)/Fe(001) superlattice determined by scanning tunneling microscopy and X-ray diffraction: A comparison
J. Appl. Phys. 89, 181 (2001)
23.42.0

IFF-01-11-207
Schmidt W.; Ohl M.; Buchenau U.
Comment on: Experimental evidence for fast heterogeneous collective structural relaxation in a supercooled liquid near the glass transition
Phys. Rev. Lett. 85, 5669 (2000)
23.30.0

IFF-01-11-208
Schneider St.
Etching Characteristic of Noble Metal Electrode Ferroelectric Thin Films IX
MRS Proceedings Volume 655, pp. CC2.5
23.42.0

IFF-01-11-209
Schober H. R.
Isotope effect in the diffusion of binary liquids
Solid State Commun. 119, 73-77 (2001)
23.30.0

IFF-01-11-210
Schober T.; Friedrich J.
The mixed perovskites BaCa(1+x)/3Nb(2-x)/3O3-x/2 (x=0...0.18): proton uptake
Solid State Ionics 136-137(2000) 161-165
23.42.0

IFF-01-11-211
Schober T.; Meuffels P.
Electrically operated hydrogen and oxygen vacuum leaks using ceramic high-temperature ionic conductors
J. Vac. Sc. Techn. A 19 (2001) 958-962
23.42.0

IFF-01-11-212
Schober T.; Meuffels P.
High-temperature proton conductors for the injection of hydrogen into a vacuum
J. Am. Ceram. Soc. 84 (2001) 1996-2001
23.42.0

IFF-01-11-213
Schober T.
High temperature proton conductors: hydrogen injection and pumping
Ionics 6 (2000)369
23.42.0

IFF-01-11-214
Schober T.
Solid state ionics applications in vacuum technology
Solid State Ionics 144 (201) 379-386
23.42.0

IFF-01-11-215
Schober T.
Tubular high-temperature proton conductors: transport numbers and hydrogen injection
Solid State Ionics 139 (2001) 95-104
23.42.0

IFF-01-11-216
Schober T.
Water vapor solubility and impedance of the high temperature proton conductor SrZr0.9Y0.1O2.95
Solid State Ionics 145 (2001)319-324
23.42.0

IFF-01-11-217
Schwahn D.; Frielinghaus H.; Mortensen K.1; Almdal K.1
1Risø National Laboratory, DK-4000 Roskilde, Demark
Abnormal pressure dependence of the phase boundaries in PEE-PDMS and PEP-PDMS binary homopolymer blends and diblock copolymers
Macromolecules 34, 1694-1706 (2001)
23.30.0

IFF-01-11-218
Schwarz U.S.1; Gompper G.
1 Weizmann Inst.,Rehovot, Israel
Bending Frustration of Lipid-Water Mesophases Based on Cubic Minimal Surfaces
Langmuir 17, 2084-2096 (2001)
23.30.0

IFF-01-11-219
Schweika W.; Böni P.1
1TUM, Garching
The instrument DNS: polarization analysis for diffuse neutron scattering
Physica B 297 (2001) 155 - 159
23.89.1

IFF-01-11-220
Schweika W.; Ice G. E.1; Robertson J. L.1; Sparks C J.1; Bai J.1
1Oak Ridge National Laboratory, USA
Diffuse Scattering of Cu3Au: Displacements and Fermi Surface Effects
Properties of Complex Inorganic Solids 2 (2000) 329 - 341
23.89.1

IFF-01-11-221
Schütz G.M.; Ispolatov I.1; Barkema G.2; Widom B.1
1 Cornell Univ. USA
2 Univ. Utrecht, Netherlands
Symmetries and Equivalences in a lattice model for hydrophobic
interaction.
Physica A 291, 24 - 38 (2001)
23.30.0

IFF-01-11-222
Schütz G.M.; Santos J.1
1 TU München, Germany
Nonequilibrium tube-length fluctuations of entangled polymers
J. Chem. Phys. (Comm.) 114, 8733- 8736 (2001)
23.30.0

IFF-01-11-223
Semmler U.; Simon M.; Ebert Ph.; Urban K.
Stoichiometry changes by selective vacancy formation on (110) surfaces of III-V semiconductors: Influence of electronic effects
J. Chem. Phys. 114, No. 1, 445-451 (2001)
23.55.0

IFF-01-11-224
Shadrin P.; Divin Y.Y.
Spread of critical currents in thin-film YBa2Cu3O7-x bicrystal junctions
IEEE Transactions on Appl. Supercond., Vol. 11, No. 1, 414-417 (2001)
23.42.0

IFF-01-11-225
Shadrin P.; Jia C.L.; Divin Y.Y.
Spread of critical currents in thin-film YBa2Cu3O7-x bicrystal junctions and faceting of grain boundary
Physica C, 2002 (accepted for publications)
23.42.0

IFF-01-11-226
Sherman V.; Astafiev K.; Setter N.; Tagantsev A.; Vendik O.; Hoffmann-Eifert S.; Böttger U.; Waser R.
Digital Reflection-Type Phase Shifter Based on a Ferroelectric Planar Capacitor
IEEE Microwave and Wireless Components Letters 11, 10 (2001) 407-409
23.42.0

IFF-01-11-227
Shin K.1,2; Pu Y.2; Rafailovich M. H.2; Sokolov J.2; Seeck O.; Sinha S. K.3; Tolan M.4; Kolb R.5
1NIST, NCNR, Gaithersburg, USA
2SUNY, Stony Brook
3APS, ANL, USA
4University, Kiel
5Exxon Mobil
Correlated Surfaces of Free-Standing Polystyrene Thin Films
Macromolecules 34 (2001)5620 - 5626
23.89.1

IFF-01-11-228
Shirotov V.; Divin Y.Y.; Urban K.
Dynamic Range of Frequency-Selective Response of High-Tc Josephson Detector to Millimeter-Wave Radiation
IEEE Transactions on Appl. Supercond., Vol. 11, No. 1, 955-957 (2001)
23.42.0

IFF-01-11-229
Shirotov V.; Divin Y.Y.; Urban K.
Far-infrared broadband measurements with Hilbert-transform spectroscopy
Physica C, 2002 (accepted for publications)
23.42.0

IFF-01-11-230
Smith G.D.1; Paul W.2; Monkenbusch M.; Richter D.
1Dep. of Mat. Science and Engineering, University of Utah, Salt Lake City, Utah 84112, USA
2Institut für Physik, Johannes-Gutenberg Universität, 55099 Mainz
On the non-Gaussianity of chain motion in unentangled polymer melts
J. Chem. Phys. 114, 4285-4288 (2001)
23.30.0

IFF-01-11-231
Sobczak E.1; Nietubyc R.2; Pelka J. B.2; Mackowski S.2; Janik E.2; Karczewski G.2; Goerigk G.
1Institute of Physics and Center of Theoretical Physics PAS, Warsaw, Poland
2Institute of Physics PAS, Warsar, Poland
Anomalous Small Angle X-Ray Scattering Study of Self-Assembled Quantum Dots
Appl. Crystallogr. 18 (2001) 112 - 115
23.89.1

IFF-01-11-232
Spatschek R.; Brener E. A.
Grinfeld instability on crack surfaces
Phys. Rev. E 64, 046120 (2001)
23.15.0

IFF-01-11-233
Staab T.E.M.1; Nieminen R.M.1; Gebauer J.2; Krause-Rehberg R.2; Luysberg M.; Haugk M.3; Frauenheim Th.3
1 Lab. of Physics, Helsinki University of Technology
2 FB Physik, Universität Halle3 Dept. of Physic, University GH Paderborn, 33098 Paderborn
Do Arsenic Interstitials Really Exist in As-Rich GaAs?
Phys. Rev. Lett., Vol. 87, No. 4, 045504-1 - 045504-4 (2001)
23.42.0

IFF-01-11-234
Stein S.; Schmitz R.; Kohlstedt H.
Magneto-tunneling injection device (MADTID)
Solid State Communications 117 (2001) 599 (2001)
23.42.0

IFF-01-11-235
Sunil Kumar P.B.1; Gompper G.; Lipowsky R.2
1 IIT, Chennai, India
2 MPI Potsdam, Germany
Budding dynamics of multicomponent membranes
Phys. Rev. Lett. 86, 3911 (2001)
23.30.0

IFF-01-11-236
Syromyatnikov V. G.1; Toperverg B. P.1,2; Kentzinger E.2; Deriglazov V. V.1; Kampmann R.3; Pleshanov N. K.1; Pusenkov V. M.1; Schebetov A. F.1; Siebrecht R.4; Ul'yanov V. A.1
1Petersburg Nuclear Physics Institute, Gatchina, Russia
2FZJ, IFF, Jülich
3GKSS, Institut für Werkstofforschung, Geesthacht
4ILL, Grenoble, France
Off-specular polarized neutron scattering from periodic Co/Ti and aperiodic Fe/Al magnetic multilayers
Physica B 297 (2001) 175 - 179
23.89.1

IFF-01-11-237
Szot K.; Hoffmann S.; Speier W.; Breuer U.; Siegert M.; Waser R.
Segregation Phenomena in Thin Films of BaTiO3
Integrated Ferroelectrics 33 (2001) 303-310
23.42.0

IFF-01-11-238
Tillmann K.; Luysberg M.; Specht P.1; Weber E.R.1
1 Department of Materials Science, University of California, Berkeley, CA 94720, USA
Direct determination of local layer compositions by the reciprocal space segmentation of high-resolution micrographs
Ultramicroscopy
submitted October 2001
23.42.0

IFF-01-11-239
Toperverg B.1,2; Nikonov O.3,4; Lauter-Pasyuk V.4,5; Lauter H. J.3
1Petersburg Nuclear Physics Institute, Gatchina, Russia
2FZJ, IFF, Jülich
3ILL, Grenoble, France
4Joint Institute for Nuclear Research, Dubna, Russia
5TUM, Garching
Towards 3D polarization analysis in neutron reflectometry
Physica B 297 (2001) 169 - 174
23.89.1

IFF-01-11-240
Toperverg B.1,2
1Petersburg Nuclear Physics Institute, Gatchina, Russia
2FZJ, IFF, Jülich
Specular reflection and off-specular scattering of polarized neutrons

Physica B 297 (2001) 160 - 168
23.89.1

IFF-01-11-241
Topolov V. Yu; Bolten D.1; Böttger U.1; Waser R.
1 Institut für Werkstoffe der Elektrotechnik, RWTH Aachen
Domain switching, rotation processes and dielectric response of polycrystalline Pb(ZrxTi1-x)O3 thin films
J. Phys. D: Appl. Phys. 34 (2001) 711-716
23.42.0

IFF-01-11-242
Trinkaus H.; Singh B.N. 1; Golubov S.I. 2
1 Department of Materials Research, Riso National Laboratory, Roskilde, Denmark
2 Scientific Center of Russian Federation, Obninsk, Russian Federation
Progress in modelling the microstructural evolution in metals under cascade damage conditions
J. Nucl. Mat. 283-287, 89-98 (2000)
23.15.0

IFF-01-11-243
Trinkaus H.; Ullmaier H.
Does pulsing in spallation neutron sources affect radiation damage?
J. Nucl. Mat. 296, 101-111 (2001)
23.15.0

IFF-01-11-244
Tölle A.1; Zimmermann H.2; Fujara F.3; Petry W.4; Schmidt W.; Schober H.5; Wuttke J.4
1Fachbereich Physik, Universität Dortmund, 44221 Dortmund
2Max-Planck-Institut für medizinische Forschung, 69120 Heidelberg
3Institut für Festkörperphysik, Technische Universität Darmstadt, 64289 Darmstadt
4Physik-Department E13, Technische Universität München, 85747 Garching
5Institut Laue-Langevin, 38042 Grenoble, France
Vibrational states of glassy and crystalline orthoterphenyl
Eur. Phys. J. B 16, 73-80 (2000)
23.30.0

IFF-01-11-245
Valadares A.A.1; Alvarez F.1; Liu Z.2; Sticht J.3; Harris J.
1 Instituto de Investigaciones en Materiales, UNAM, Mexico
2 Molecular Simulations Inc., San Diego, USA
3 Materials Design Inc., Oceanside, USA
Ab-initio studies of the atomic and electronic structure of pure and hydrogonated -Silicon
Eur. Phys. J. B 22, 443 (2001)
23.20.0

IFF-01-11-246
Vasiliu-Doloc L.1; Osborn R.2; Rosenkranz S.2; Mesot J.2; Mitchell J. F.2; Sinha S. K.3; Seeck O.; Lynn J. W.4; Islam Z.1
1Northern Illinois University and APS/ANL, USA
2Materials Science Division, ANL, Argonne, USA
3APS/ANL, Argonne, USA
4NIST, USA
Neutron and x-ray evidence of charge melting in ferromagnetic layered colossal magnetoresistance manganites (invited)
Journal of Applied Physics 89, 11 (2001) 6840 - 6845
23.89.1

IFF-01-11-247
Volokitin A.I.1; Persson B.N.J.
1 Samara University, Russia
Frictional drag between quantum wells mediated by fluctuating electromagnetic field
J. Phys. C 13, 859 (2001)
23.20.0

IFF-01-11-248
Volokitin A.I.1; Persson B.N.J.
1 Samara University, Russia
Radiative heat transfer between nanostructures
Phys. Rev. B63, 205404 (2001)
23.20.0

IFF-01-11-249
Vorobiev A.1; Gordeev G.1; Donner W.2; Dosch H.2; Nickel B.2,3; Toperverg B.1,4
1Petersburg Nuclear Physics Institute, Gatchina, Russia
2MPI für Metallforschung, Stuttgart
3ILL, Grenoble, France
4FZJ, IFF, Jülich
Reflectivity and off-specular neutron scattering from the free ferrofluid surface and silicon-ferrofluid interface
Physica B 297 (2001) 194 - 197
23.89.1

IFF-01-11-250
Weber U.1; Greuel G.; Böttger U.1; Weber S.1; Hennings D.2; Waser R.
1 Institut für Werkstoffe der Elektrotechnik, RWTH Aachen
2 Philips Forschungslabor, Aachen
Dielectric Properties of Ba(Zr.Ti)O3-based Ferroelectrics for Capacitor Applications
J. Am. Ceram. Soc. 84 (2001), 759-766
23.42.0

IFF-01-11-251
Westermann S.; Pyckhout-Hintzen W.; Richter D.; Straube E.1; Egelhaaf S.2; May R.2
1Martin-Luther-Universität Halle-Wittenberg, Fachbereich Physik, 06099 Halle
2Institut Laue Langevin, BP 156, F-38042 Grenoble Cedex 9, France
On The length scale dependence of microscopic strain by SANS
Macromolecules 34, 2186-2194 (2001)
23.30.0

IFF-01-11-252
Wignall G.D.1, Alamo R.G.2, Ritchon E.J.2; Mandelkern L.2; Schwahn D.
1Solid State Division, Oak Ridge National Laboratory, USA
2Chemical Engineering Department A&M University and Florida State University College of Engineering, Tallahasse, Florida, USA
SANS Studies of Liquid-Liquid Separation in Heterogeneous and Metallocene-Based Linear Low-Density Polyethylenes
Macromolecules 34, 8160 (2001)
23.30.0

IFF-01-11-253
Willner L.; Poppe A.; Allgaier J.; Monkenbusch M.; Richter D.
Time-resolved SANS for the determination of unimer exchange kinetics in block copolymer micelles
Europhys. Lett. 55, 667-673 (2001)
23.30.0

IFF-01-11-254
Wortmann D.; Heinze S.; Kurz P.; Bihlmayer G.; Blügel S.
Resolving complex atomic-scale spin structures by spin polarized scanning tunneling microscopy
Phys. Rev. Lett 86, 4132 (2001)
23.20.0

IFF-01-11-255
Wosik J.; Penkalla H.J.; Szot K.; Dubiel B.; Schubert F.; Czyrska-Filemonowicz A.
The Influence of Using Various Microscopic Techniques on the Quantification of g' Particles in Waspaloy alloy
Praktische Metallography 38 (2001) 1-15
23.42.0

IFF-01-11-256
Woudenberg F.1; Sager W.; Sibelt N.1; Verweij H.1
1University of Twente, Niederlande
Dense nanostructured t-ZrO2 coatings at low temperatures via modified emulsion precipitation

Advanced Materials, 13, 514, 2001
23.30.0

IFF-01-11-257
Wu J.S., Jia C.L.; Urban K., Hao J.H.1 Xi X.X.1
1 Dept. of Physics, The Pennsylvania State University, University Park, PN 16802, USA
Conservative antiphase boundary in SrTiO3 films on LaAlO3 substrates with SrRuO3 buffer layers
Journal of Applied Physics, Vol. 89, No. 10, 5653-5656 (2001)
23.42.0

IFF-01-11-258
Wu J.S.; Jia C.L.; Urban K.; Hao J.H.1; Xi X.X.1
1 Dept. of Physics, The Pennsylvania State University, University Park, PN 16802, USA
A new mechanism for misfit dislocation generation: superdislocations associated with Ruddlesden-Popper planar defects
Journal of Crystal Growth 234, 603-609 (2001)
23.42.0

IFF-01-11-259
Wu J.S.; Jia C.L.; Urban K.; Hao J.H.1; Xi X.X.1
1 Dept. of Physics, The Pennsylvania State University, University Park, PN 16802, USA
Microstructure and misfit relaxation in SrTiO3 /SrRuO3 bilayer films on LaAlO3 (100) substrates
J. Mat. Res. 16, 3443-3450 (2001)

IFF-01-11-260
Wu J.S.; Jia C.L.; Urban K.; Hao J.H.1; Xi X.X.1
1 Dept. of Physics, The Pennsylvania State University, University Park, PN 16802, USA
Stair-rod dislocations in perovskite films on LaAlO3 substrates
Phil. Mag. Lett. Vol. 81, No. 6, 375-383 (2001)
23.42.0

IFF-01-11-261
Yu H.1; Jiang C. S.1; Ebert Ph; Wang X. D.1; White J. M.1; Niu Q.1; Zhang Z.1; Shih C. K.1
1 University of Texas, Austin
2 Oak Ridge National Laboratory
Quantitative Determination of the Metastability of Flat Ag Overlayers on GaAs(110)
Phys. Rev. Lett., Vol. 88, 016102, 1-4 (2002).
23.42.0

IFF-01-11-262
Yurechko M.; Fattah A.; Velikanova T.1; Grushko B.
1 Ukrainian Academy of Sciences, Kiev
A contribution to the Al-Pd phase diagram
Journal of Alloys and Compounds 329, 173-181 (2001)
23.55.0

IFF-01-11-263
Yurechko M.; Grushko B.; Urban K.; Velikanova T.1
1 Ukrainian Academy of Sciences, Kiev
The Al-Rh phase diagram
Poroshkovaia Metallurgia 7-8, 75-80 (2001)
23.55.0

IFF-01-11-264
Yurechko M.; Grushko B.; Velikanova T.1; Urban K.
1 Ukrainian Academy of Sciences, Kiev
Isothermal sections of the Al-Pd-Co alloy system for 50-100 at.% Al
Journal of Alloys and Compounds 1 (2001)
23.55.0

IFF-01-11-265
Zilberman S.1; Persson B.N.J.; Nitzan A.1, Mugele F.2; Salmeron M.2
1 School of Chemistry, Tel Aviv University, Israel
2 Materials Science Division, University of California, Berkeley, USA
Boundary lubrication: dynamics of squeeze-out
Phys. Rev. B 63, 55103-1 (2001)
23.20.0

IFF-01-11-266
Zilberman S.1; Persson B.N.J.; Nitzan A.1
1 School of Chemistry, Tel Aviv University, Israel
Theory and simulations of squeeze-out dynamics in boundry lubrication
J. Chem. Phys. 115, 11268 (2001)
23.20.0

IFF-01-11-267
de Robillard Q.1; Guo X.1; Dingenouts N.1; Ballauff M.1; Goerigk G.
1University, Polymer-Institute, Karlsruhe
Application of Anomalous Small-Angle X-Ray Scattering to Spherical Polyelectrolyte Brushes
Macromol. Symp. 164 (2001) 81 - 90
23.89.1

List of references

Akola J.	IFF-01-11-001	IFF-01-11-002	
Alefeld B.	IFF-01-11-198		
Allgaier J.	IFF-01-11-034	IFF-01-11-044	IFF-01-11-045
	IFF-01-11-065	IFF-01-11-066	IFF-01-11-156
	IFF-01-11-157	IFF-01-11-175	IFF-01-11-188
	IFF-01-11-253		
Arons R. R.	IFF-01-11-127		
Baumgaertner A.	IFF-01-11-199	IFF-01-11-200	
Bechthold P.S.	IFF-01-11-115	IFF-01-11-146	IFF-01-11-159
	IFF-01-11-162		
Bellini V.	IFF-01-11-011	IFF-01-11-012	
Bergs W.	IFF-01-11-198		
Beyss M.	IFF-01-11-125		
Bihlmayer G.	IFF-01-11-026	IFF-01-11-122	IFF-01-11-123
	IFF-01-11-138	IFF-01-11-139	IFF-01-11-254
Blügel S.	IFF-01-11-026	IFF-01-11-090	IFF-01-11-111
	IFF-01-11-122	IFF-01-11-123	IFF-01-11-138
	IFF-01-11-139	IFF-01-11-254	
Brener E. A.	IFF-01-11-015	IFF-01-11-076	IFF-01-11-161
	IFF-01-11-232		
Bringer A.	IFF-01-11-147	IFF-01-11-148	
Brückel Th.	IFF-01-11-016	IFF-01-11-017	IFF-01-11-163
	IFF-01-11-186	IFF-01-11-187	IFF-01-11-198
Buchenau U.	IFF-01-11-018	IFF-01-11-019	IFF-01-11-207
Buchmeier M.	IFF-01-11-060		
Bürgler D.E.	IFF-01-11-060	IFF-01-11-206	
Cabria I.	IFF-01-11-165		
Caliebe W.	IFF-01-11-016		
Caprion D.	IFF-01-11-020	IFF-01-11-021	
Carbone C.	IFF-01-11-028	IFF-01-11-149	IFF-01-11-150
Chen J.	IFF-01-11-025	IFF-01-11-027	IFF-01-11-098
	IFF-01-11-107		
Clarke S.	IFF-01-11-026		
Dallmeyer A.	IFF-01-11-028	IFF-01-11-149	IFF-01-11-150
Dederichs P.H.	IFF-01-11-011	IFF-01-11-012	IFF-01-11-119
	IFF-01-11-165		
Dhont J.	IFF-01-11-029	IFF-01-11-133	IFF-01-11-134
Divin Y.Y.	IFF-01-11-030	IFF-01-11-031	IFF-01-11-032
	IFF-01-11-192	IFF-01-11-224	IFF-01-11-225
	IFF-01-11-228	IFF-01-11-229	
Dogic Z.	IFF-01-11-134		
Domke C.	IFF-01-11-037	IFF-01-11-038	IFF-01-11-061
Duwe R.	IFF-01-11-025		
Dürr H.A.	IFF-01-11-138	IFF-01-11-139	IFF-01-11-140
	IFF-01-11-170		

Heggen M.	IFF-01-11-086		
Heiderich M.	IFF-01-11-109		
Heinrich M.	IFF-01-11-087		
Heinze S.	IFF-01-11-090	IFF-01-11-111	IFF-01-11-254
Henkel D.	IFF-01-11-081		
Hiller P.	IFF-01-11-080		
Hoffmann S.	IFF-01-11-168 IFF-01-11-194	IFF-01-11-180 IFF-01-11-237	IFF-01-11-193
Hoffmann-Eifert S.	IFF-01-11-169	IFF-01-11-184	IFF-01-11-226
Hoser A.	IFF-01-11-125		
Houben L.	IFF-01-11-095	IFF-01-11-096	
Hupfeld D.	IFF-01-11-016		
Ioffe A.	IFF-01-11-097	IFF-01-11-154	
Jahnen B.	IFF-01-11-135		
Jia C.L.	IFF-01-11-031 IFF-01-11-102 IFF-01-11-192 IFF-01-11-258	IFF-01-11-099 IFF-01-11-103 IFF-01-11-225 IFF-01-11-259	IFF-01-11-100 IFF-01-11-135 IFF-01-11-257 IFF-01-11-260
Jones R.O.	IFF-01-11-005 IFF-01-11-106	IFF-01-11-104	IFF-01-11-105
Jung P.	IFF-01-11-107		
Jungbluth H.	IFF-01-11-080		
Kahle S.	IFF-01-11-195		
Kann G.	IFF-01-11-115	IFF-01-11-162	
Kaya H.	IFF-01-11-046	IFF-01-11-047	
Kehr K.W.	IFF-01-11-059		
Kentzinger E.	IFF-01-11-163	IFF-01-11-198	IFF-01-11-236
Kietzmann H.	IFF-01-11-159		
Kirch D.	IFF-01-11-094		
Kirstein O.	IFF-01-11-112		
Klingeler R.	IFF-01-11-115	IFF-01-11-146	IFF-01-11-162
Kluge M.	IFF-01-11-116		
Kohlstedt H.	IFF-01-11-024	IFF-01-11-234	
Kollmann M.	IFF-01-11-181	IFF-01-11-182	
Kurz P.	IFF-01-11-122	IFF-01-11-123	IFF-01-11-254
Köbler U.	IFF-01-11-124 IFF-01-11-127	IFF-01-11-125	IFF-01-11-126
Kühnlein W.	IFF-01-11-025		
Lamura A.	IFF-01-11-130	IFF-01-11-131	IFF-01-11-132
Laytti M.	IFF-01-11-032		
Lenstra T.	IFF-01-11-133	IFF-01-11-134	
Lentzen M.	IFF-01-11-135		

Poppe A.	IFF-01-11-253		
Poppe U.	IFF-01-11-030	IFF-01-11-031	IFF-01-11-032
	IFF-01-11-049	IFF-01-11-050	IFF-01-11-192
Prager M.	IFF-01-11-112	IFF-01-11-158	
Pyckhout-Hintzen W.	IFF-01-11-023	IFF-01-11-042	IFF-01-11-046
	IFF-01-11-047	IFF-01-11-152	IFF-01-11-153
	IFF-01-11-196	IFF-01-11-251	
Quadbeck P.	IFF-01-11-039		
Regnery S.	IFF-01-11-043	IFF-01-11-054	IFF-01-11-103
Richter D.	IFF-01-11-003	IFF-01-11-034	IFF-01-11-044
	IFF-01-11-045	IFF-01-11-065	IFF-01-11-066
	IFF-01-11-067	IFF-01-11-068	IFF-01-11-118
	IFF-01-11-151	IFF-01-11-156	IFF-01-11-157
	IFF-01-11-195	IFF-01-11-196	IFF-01-11-230
	IFF-01-11-251	IFF-01-11-253	
Rickes J.	IFF-01-11-008	IFF-01-11-009	
Rodriguez Contreras	IFF-01-11-088	IFF-01-11-089	
Rücker U.	IFF-01-11-163	IFF-01-11-198	
Sager W.	IFF-01-11-013	IFF-01-11-053	IFF-01-11-256
Sambeth R.	IFF-01-11-199	IFF-01-11-200	
Schall P.	IFF-01-11-052	IFF-01-11-086	IFF-01-11-202
	IFF-01-11-203		
Schilling T.	IFF-01-11-205		
Schmidt W.	IFF-01-11-120	IFF-01-11-197	IFF-01-11-207
	IFF-01-11-244		
Schmitz R.	IFF-01-11-234		
Schneider St.	IFF-01-11-208		
Schober H. R.	IFF-01-11-020	IFF-01-11-021	IFF-01-11-116
	IFF-01-11-209		
Schober T.	IFF-01-11-210	IFF-01-11-211	IFF-01-11-212
	IFF-01-11-213	IFF-01-11-214	IFF-01-11-215
	IFF-01-11-216		
Scholten C.	IFF-01-11-096		
Schreiber R.	IFF-01-11-060		
Schroeder H.	IFF-01-11-004		
Schwahn D.	IFF-01-11-056	IFF-01-11-057	IFF-01-11-109
	IFF-01-11-118	IFF-01-11-217	IFF-01-11-252
Schweika W.	IFF-01-11-187	IFF-01-11-219	IFF-01-11-220
Schütz G.M.	IFF-01-11-010	IFF-01-11-189	IFF-01-11-191
	IFF-01-11-201	IFF-01-11-221	IFF-01-11-222
Seeck O.	IFF-01-11-163	IFF-01-11-173	IFF-01-11-174
	IFF-01-11-227	IFF-01-11-246	
Semmler U.	IFF-01-11-223		
Settels A.	IFF-01-11-119		
Shadrin P.	IFF-01-11-031	IFF-01-11-032	IFF-01-11-192
	IFF-01-11-224	IFF-01-11-225	
Shirotov V.	IFF-01-11-032	IFF-01-11-228	IFF-01-11-229

Simon M.	IFF-01-11-223		
Spatschek R.	IFF-01-11-015	IFF-01-11-161	IFF-01-11-232
Stein S.	IFF-01-11-234		
Stellbrink J.	IFF-01-11-003	IFF-01-11-034	IFF-01-11-156
	IFF-01-11-157	IFF-01-11-188	
Szot K.	IFF-01-11-168	IFF-01-11-169	IFF-01-11-237
	IFF-01-11-255		
Theissen O.	IFF-01-11-205		
Thust A.	IFF-01-11-113	IFF-01-11-135	IFF-01-11-166
	IFF-01-11-167		
Tillmann K.	IFF-01-11-135	IFF-01-11-238	
Toperverg B.	IFF-01-11-236	IFF-01-11-239	IFF-01-11-240
	IFF-01-11-249		
Trinkaus H.	IFF-01-11-006	IFF-01-11-064	IFF-01-11-094
	IFF-01-11-242	IFF-01-11-243	
Ullmaier H.	IFF-01-11-025	IFF-01-11-098	IFF-01-11-243
Urban K.	IFF-01-11-030	IFF-01-11-031	IFF-01-11-032
	IFF-01-11-033	IFF-01-11-037	IFF-01-11-038
	IFF-01-11-039	IFF-01-11-049	IFF-01-11-050
	IFF-01-11-051	IFF-01-11-061	IFF-01-11-086
	IFF-01-11-099	IFF-01-11-100	IFF-01-11-103
	IFF-01-11-114	IFF-01-11-135	IFF-01-11-192
	IFF-01-11-202	IFF-01-11-203	IFF-01-11-223
	IFF-01-11-228	IFF-01-11-229	IFF-01-11-257
	IFF-01-11-258	IFF-01-11-259	IFF-01-11-260
	IFF-01-11-263	IFF-01-11-264	
Vad Th.	IFF-01-11-080		
Voigt J.	IFF-01-11-163		
Waser R.	IFF-01-11-004	IFF-01-11-008	IFF-01-11-009
	IFF-01-11-014	IFF-01-11-054	IFF-01-11-071
	IFF-01-11-079	IFF-01-11-092	IFF-01-11-103
	IFF-01-11-128	IFF-01-11-129	IFF-01-11-141
	IFF-01-11-142	IFF-01-11-143	IFF-01-11-168
	IFF-01-11-169	IFF-01-11-180	IFF-01-11-183
	IFF-01-11-184	IFF-01-11-193	IFF-01-11-194
	IFF-01-11-226	IFF-01-11-237	IFF-01-11-241
	IFF-01-11-250		
Westermann S.	IFF-01-11-251		
Willner L.	IFF-01-11-057	IFF-01-11-195	IFF-01-11-253
Winkler R.G.	IFF-01-11-093		
Wirth I.	IFF-01-11-115	IFF-01-11-162	
Wortmann D.	IFF-01-11-254		
Wu J.	IFF-01-11-155		
Wu J.S.	IFF-01-11-192	IFF-01-11-257	IFF-01-11-258
	IFF-01-11-259	IFF-01-11-260	
Yurechko M.	IFF-01-11-155	IFF-01-11-262	IFF-01-11-263
	IFF-01-11-264		
Zeller R.	IFF-01-11-011	IFF-01-11-012	IFF-01-11-119
	IFF-01-11-165		
Zorn R.	IFF-01-11-022	IFF-01-11-151	

Other publications

IFF-01-12-001
Allenspach P.1; Andersen K.H.2; Colognesi D.2; Fak B.2; Kirstein O.; Zoppi M.3
1Laboratory for Neutron Scattering , ETHZ & PSI, CH-5232 Villigen PSI, Schweiz
2ISIS Department, Rutherford Appleton Laboratory, Chilton Didcot, Oxfordshire, OX11 0QX , UK
3Consiglio Nazionale delle Ricerche, Firenze, Italy
Indirect Geometry Spectrometer Performance of a Suite of Generic Instruments on ESS
ESS Instrumentation Group Reports, SAC Workshop, 03.-05.05.01, Ed.: F. Mezei and R. Eccleston, ESS 115-01-T, ISSN 1433-559X
23.89.1

IFF-01-12-002
Antons A.
First-principles investigation of initial stages of surfactant Me diated growth on the Si(111) substrate
Dissertation, RWTH Aachen, Juli 2001
23.42.0

IFF-01-12-003
Arbe A.1; Richter D.; Colmenero J.1,2; Monkenbusch M.; Farago B.3
1Dep. De Fisica de Materiales, Universidad del Pais Vasco and Unidad de Fisica de Materiales (CSIC-UPV/EHU), Apartado 1072, 20080 San Sebastian, Spain
2Donostia Internation Physics Center, Apartado 1072, 20080 San Sebastian, Spain
3Institut Laue Langevin, 156X, 38042 Grenoble Cedex, France
Single chain motions in flexible polymers by neutron spin echo
Conf. Proceed. ILL Millennium Symposium & European User Meeting, Grenoble/France, 06.-07.04.01, 69-70
23.30.0

IFF-01-12-004
Baier F.1; Müller M.A.1; Sprengel W.1; Grushko B.; Sterzel R.2; Assmus W.2; Schäfer H.E.1
1 ITAP, Universität Stuttgart, 70550 Stuttgart
2 Johann Wolfgang Goethe-Universität, 60325 Frankfurt/Main
Atomic defects in Al-Pd-Mn: a study by means of positron annihilation spectroscopy.
Int. Conf. Positron Annihilation ICPA-13, München.
Materials Science Forum 363-365, 179-181 (2001)
23.55.0

IFF-01-12-005
Bellini V.
Electronic structure of low-dimensional magnetic systems
Berichte des Forschungszentrums Jülich, Jül-3856 (2001)
23.20.0

IFF-01-12-006
Brückel Th.
Elastic Scattering from Many-Body Systems
Schriften des Forschungszentrums Jülich: Materie und Material; Vol. 9 (2001) 3-1 - 3-28
23.89.1

IFF-01-12-007
Brückel Th.
Magnetism
Schriften des Forschungszentrums Jülich: Materie und Material; Vol. 9 (2001) 16-1 - 16-19
23.89.1

IFF-01-12-008
Bürgler D.E.; Grünberg P.; Demokritov S.O.1; Johnson M.T.2
1Universität Kaiserslautern
2Philips Research, Eindhoven, NL
Interlayer exchange coupling in layered magnetic structures
In: Handbook of Magnetic Materials, Vol. 13, Ed. K.H.J. Buschow, Elsevier (2001)
23.42.0

IFF-01-12-009
Bürgler D.E.; Grünberg P.
Magnetoelectronics: Exchange anisotropy, interlayer exchange coupling, GMR, TMR, and current-induced magnetic switching
In: 32. Ferienkurs des IFF: "Neue Materialien für die Informationstechnik" (2001)
23.42.0

IFF-01-12-010
Conrad H.; Filges D.1; Hansen G.2; Neef R. D.1; Stelzer H.2; Tietze-Jaensch H.; Ullmaier H.
1FZJ, IKP, Jülich
2FZJ, ZAT, Jülich
Technische und methodische Entwicklungen am Target-Moderator-Reflektor-Komplex der ESS
Deutsche Neutronenstreutagung 2001, Schriften des Forschungszentrums Jülich, Reihe Materie und Material, Band 8 (2001) p. 83
23.89.1

IFF-01-12-011
Conrad H.; Ullmaier H.
Overview of the ESS Target and Moderator R&D
Proceedings of ICANS-XV, Tsukuba, Japan, 06. - 09.11.2000 (2001) 1137 - 1145
23.60.0

IFF-01-12-012
Conrad H.
German Neutron Users Meet in Jülich
Neutron News 12 (3) (2001), 4
23.89.1

IFF-01-12-013
Conrad H.
Neutron Sources
Schriften des Forschungszentrums Jülich: Materie und Material; Vol. 9 (2001) 1-1 - 1-15
23.89.1

IFF-01-12-014
Conrad H.
Status report on the Jülich ESS related activities
Proceedings of ICANS-XV, Tsukuba, Japan, 06. - 09.11.2000 (2001) 89 - 92
23.60.0

IFF-01-12-015
Divin Y.; Volkov O.1; Pavlovskii V.1; Shirotov V.; Shadrin P.; Poppe U.; Urban K.
1 Institute of Radioengineering & Electronics of RAS, Moscow 103907, Russian Federation
Terahertz Hilbert spectroscopy by high-Tc Josephson junctions
In: Advances in Solid State Physics, 41, ed. B. Kramer (Springer, Berlin, 2001), 301-313 (2001)
23.42.0

IFF-01-12-016
Duckham A.1; Shechtman D.2; Grushko B.
1 National Institute of Standards and Technology, MSEL, Gaitherburg, MD 20899 USA
2 Department of Materials Engineering, Technion Haifa 32000, Israel
Influence of Grain Orientation on Friction and Wear Behavior in Quasicrystalline Alloys
Mat. Res. Soc. Symp. Proc., Vol. 643, K8.1.1-6 (2001)
23.55.0

IFF-01-12-017
Dürr H.A.; Kronast F.; Eberhardt W.
Spin-polarized photoelectron emission microscopy of magnetic nanostructures

Advances in Solid State Physics, Vol. 41, ed. B. Kramer, Springer Verlag (2001)
23.20.0

IFF-01-12-018
Dürr H.A.
Anisotropic magnetic ground-state moments probed by soft x-ray spectroscopy
In: Bandferromagnetism: Ground-state and Finite-temperature Phenomena, ed. K. Baberschke, M. Donath, W. Nolting, Springer Verlag Berlin, Heidelberg, New York, Barcelona, Hong Kong, London, Milan, Paris, Singapore, Tokyo (2001), p. 46-59
23.20.0

IFF-01-12-019
Dürr H.A.
Magnetic random access memory devices
In: 32. Ferienkurs des Instituts für Festkörperforschung "Neue Materialien für die Informationstechnik"
23.20.0

IFF-01-12-020
Eberhardt W.; Klingeler R.; Kann G.; Wirth I.; Bürgler D.E.; Bechthold P.S.; Neeb M.
Metal doped fullerenes: Mircoscopy and spectroscopy
XVth International Winterschool on Electronic Properties of Novel Materials (IWEPNM)
Kirchberg, Tirol (2001)
23.20.0

IFF-01-12-021
Ebert Ph.; Szot K.
Scanning Probe Microscopy
In: Neue Materialien für die Informationstechnik, Forschungszentrum Jülich, 2001, B5.1-B5.40.
23.42.0

IFF-01-12-022
Ebert Ph.
Point Defects in Compound Semiconductor Surfaces
Berichte des Forschungszentrums Jülich, Nr. 3850, 235 p., Forschungszentrum Jülich, 2001.
23.42.0

IFF-01-12-023
Ehrhart P.
Deposition Methods
32. IFF-Ferienkurs 2001 "Neue Materialien für die Informationstechnik
E23

IFF-01-12-024
Endo H.; Allgaier J.; Monkenbusch M.; Richter D.; Jakobs B.1; Sottmann T.1; Strey R.1
1Institut für Physikalische Chemie, Universität Köln; Luxemburger Str. 116, 50939 Köln
Polymeric efficiency boosters in microemulsions: A SANS investigation of the polymer's role
ILL Annual Report 2000, Scientific Highlights, 60-61 (2001)
23.30.0

IFF-01-12-025
Faley M.I.; Poppe U.; Urban K.; Paulson D.N.1; Starr T.1; Fagaly R.L.1
1 Tristan Technologies Inc., CA 92121, USA
HTS dc-SQUID flip-chip magnetometers and gradiometers
Biomag2000, Proc. 12th Int. Conf. on Biomagnetism, J. Nenonen, R.J. Ilmoniemi, and T. Katila, eds. (Helsinki Univ. of Technology, Espoo, Finland, 2001), pp.931-934.
23.42.0

IFF-01-12-026
Feuerbacher M.; Schall P.; Estrin Y.1; Bréchet Y.2; Urban K.
1 Institut für Werkstoffkunde und Werkstofftechnik, Technische Universität Clausthal, Agricolastrasse 6, D-38678 Clausthal-Zellerfeld, Germany
2 Laboratoire de Thermodynamique et Physicochimie Metallurgiques, Institut National Polytechnique de Grenoble, F-38402 Saint Martin d'Heres Cedex, France
Modelling Quasicrystal Plastic Deformation By Means of Constituive Equations
Mat. Res. Soc. Symp. Proc., Vol. 643, K.7.2.1-6 (2001)
23.55.0

IFF-01-12-027
Figoli A.1; Wessling M.1; Sager W.
1Universität Twente
Synthesis of nanostructured mixed matrix membranes for facilitated gas separation
23.30.0

IFF-01-12-028
Goerigk G.; Williamson D. L.1
1Colorado School of Mines, Department of Physics, Golden, USA
Characterisation of Solar Cell Materials from Anomalous Small Angle X-Ray Scattering Studies
HASYLAB-Broschüre: Research at HASYLAB (2001) 18 - 20
23.89.1

IFF-01-12-029
Grünberg P.; Bürgler D.E.
Vom Kompass zum Datenspeicher: Magnetoelektronik
In: ....und Er würfelt doch!, Ed. H. Müller-Krumbhaar, H.-F. Wagner,
Wiley-VCH, Weinheim (2001)
23.42.0

IFF-01-12-030
Hauck J.; Mika K.
Aperiodische Kreispackungen
9. Jahrestagung der Deutschen Gesellschaft für Kristallographie (DGK) im März 2001
Zeitschrift Krist. Suppl.; 17, 72, 2001
23.30.0

IFF-01-12-031
Hauck J.; Mika K.
Correlation between Interactions and ordered structures
20th European Crystallographie Meeting
Krakow, 25.08.-31.08.01
Zeitschrift Krist. Suppl.; 18, 95, 2001
23.30.0

IFF-01-12-032
Hoffmann M.1; Küppers H.1; Schneller T.1; Böttger U.1; Schnakenberg U.1; Mokwa W.1; Waser R.
1 Institut für Werkstoffe der Elektrotechnik I+II, RWTH Aachen
A new concept and first Development Results of a PZT Thin Film Actuator
ISAF Proc. 2001, Vol. I, 512-524
23.42.0

IFF-01-12-033
Hoffmann-Eifert S.
Dielectric and Optics
32. IFF-Ferienkurs 2001 "Neue Materialien für die Informationstechnik
23.42.0

IFF-01-12-034
Hupfeld D.; Brückel Th.; Schweika W.; Strempfer J.1; Mattenberger K.2; McIntyre G.3
1Northern Illinois University, de Kalb, USA
2ETH, Zürich, Switzerland
3ILL, Grenoble, France
Investigation of the magnetic properties of GdxEu1-xS with neutrons and x-rays
Deutsche Neutronenstreutagung 2001, Schriften des Forschungszentrums Jülich, Reihe Materie und Material, Band 8 (2001) p. 49
23.89.1

IFF-01-12-035
Ioffe A.; Conrad H.; Zeiske Th.; Mueller R.; Küssel E.; Massalovitch S.; Schlapp M.; Schmitz B.; Brückel Th.
Spektrometer SV30 für Polarisationsanalyse mit thermischen Neutronen am Forschungsreaktor FRJ-2
Deutsche Neutronenstreutagung 2001, Schriften des Forschungszentrums Jülich, Reihe Materie und Material, Band 8 (2001) p. 91
23.89.1

IFF-01-12-036
Jahnen B.; Luysberg M.; Urban K.; Bracht H.1; Schmidt R.2; Ungermanns C.2; Bleuel T.3
1 Institut für Materialphysik, Universität Münster
2 ISG, FZ Jülich
3 Fachbereich Physik, Universität Würzburg
Interdiffusion in GaSb/AlxGa1-xSb heterostructures
Proceedings of the XIIth Conference on Microscopy of Semiconducting Materials, 22-25 March 2001, Oxford, Microscopy of Seminconducting Materials 2001, Inst. Phys. Conf. Ser., in press.
23.42.0

IFF-01-12-037
Kentzinger E.; Rücker U.; Toperverg B.; Brückel Th.
Reflectivity and off-specular scattering of neutrons from magnetic thin films
Deutsche Neutronenstreutagung 2001, Schriften des Forschungszentrums Jülich, Reihe Materie und Material, Band 8 (2001) p. 3
23.89.1

IFF-01-12-038
Kienle D.
Forschungszentrum Jülich: "Fließt wie geschmiert" - Computersimulationen helfen Verhalten einzelner Polymermoleküle zu verstehen
IHK Aachen, Wirtschaftliche Nachrichten WN 4/2001
23.30.0

IFF-01-12-039
Kienle D.
Verankerte Polymere in einfache Strömungen
Dissertation, Universität des Saarlandes, Saarbrücken (2001)
23.30.0

IFF-01-12-040
Kluge M.
Molekulardynamik-Simulation der Diffusion in binären unterkühlten metallischen Schmelzen und Gläsern aus Cu33Zr67
Jül-Bericht 3913, Forschungszentrum Jülich (2001)
23.30.0

IFF-01-12-041
Kohlstedt H.
Ferroelectric Field-Effect Transistors
32. IFF-Ferienkurs 2001 "Neue Materialien für die Informationstechnik
23.42.0

IFF-01-12-042
Kollmann M.
Dynamics and Microstructure of Interacting Brownian Systems: Electreokinetic Effects,
Quasi-two-dimensional Systems and Sphere Caging
Universität Konstanz, 03.08.01
23.30.0

IFF-01-12-043
Kromen Wi.
Die Projector Augmented Wave-Methode: Ein schnelles Allelektronenverfahren für die ab-initio-Molekulardynamik
Jül-Bericht 3887, Forschungszentrum Jülich (2001)
23.42.0

IFF-01-12-044
Köbler U.; Hoser A.1; Kawakami M.2
1RWTH, Institut für Kristallographie, Aachen
2Kagoshima University, Koorimoto, Japan
Beobachtung eines Bloch Exponent von 5/2 am Antiferromagneten MnF2 mit S=5/2 und axialer Austauschanisotropie
Deutsche Neutronenstreutagung 2001, Schriften des Forschungszentrums Jülich, Reihe Materie und Material, Band 8 (2001) p. 50
23.89.1

IFF-01-12-045
Lauter-Pasyuk V.1,2.3; Lauter H. J.3; Toperverg B.4,5; Nikonov O.3,2; Petrenko A.2; Schubert D.6; Petry W.1; Aksenov V.2
1TU, Physik Department, München
2Joint Institute for Nuclear Research, Dubna, Russia
3ILL, Grenoble, France
4PNPI, Gatchina, Russia
5FZJ, IFF, Jülich
6GKSS, Geesthacht
Off-specular neutron scattering studies of the interface and surface formation in self-assembled polymer multilayers
Proceedings of the ILL millennium symposium & european user meeting 06. - 07.04.2001 (2001) 84 - 85
23.89.1

IFF-01-12-046
Lauter-Pasyuk V.1,2; Lauter H. J.3; Toperverg B.4,5; Nikonov O.2,3; Kravtsov E.6; Ustinov V.6
1TUM, Physik Department, Garching
2Joint Institute for Nuclear Research, Dubna, Russia
3ILL, Grenoble, France
4PNPI, Gatchina, Russia
5FZJ, IFF, Jülich
6Institute of Metal Physics, Ekaterinburg, Russia
Magnetic domains in Fe/Cr multilayers
Deutsche Neutronenstreutagung 2001, Schriften des Forschungszentrums Jülich, Reihe Materie und Material, Band 8 (2001) p. 19
23.89.1

IFF-01-12-047
Lauter-Pasyuk V.1,2; Lauter H. J.3; Toperverg B.4,5; Nikonov O.2,3
1TUM, Physik Department, Garching
2Joint Institute for Nuclear Research, Dubna, Russia
3ILL, Grenoble, France
4PNPI, Gatchina, Russia
5FZJ, IFF, Jülich
Peculiar off-specular neutron scattering from islands on a lamellar film
Deutsche Neutronenstreutagung 2001, Schriften des Forschungszentrums Jülich, Reihe Materie und Material, Band 8 (2001) p. 159
23.89.1

IFF-01-12-048
Link S.; Dürr H.A.; Eberhardt W.
Lifetimes of image potential states on Pt(111) probed by time-resolved two-photon photoemission spectroscopy
Appl. Phys. A 71, 524 (2001)
23.20.0

IFF-01-12-049
Link S.; Sievers J.; Dürr H.A.; Eberhardt W.
Lifetimes of image-potential states on the clean and hydrogen-covered Ni(111) surface
J. of Electron Spectroscopy and Related Phenomena 114-116, 349 (2001)
23.20.0

IFF-01-12-050
Luysberg M.; Kirch D.; Trinkaus H.; Holländer B.1; Lenk St.1; Mantl S.1; Herzog H.-J.2; Hackbarth T.2; Fichtner P.F.P.3
1 ISG, FZ Jülich
2 Daimler Crysler AG, Research and Technology, 89081 Ulm

3 Dept. de Metallurgia, Univ. Fed Do Rio Grande do Sul, 91501-970 Porto
Relaxation of Si1-xGex Buffer Layers on Si(100) through Helium Ion Implantation
Proceedings of the XIIth Conference on Microscopy of Semiconducting Materials, 22-25 March 2001, Oxford, Microscopy of Seminconducting Materials 2001, Inst. Phys. Conf. Ser., in press.
23.42.0

IFF-01-12-051
Luysberg M.; Meertens D.; Herfort J.1; Ulrici W.1; Moreno M.1; Ploog K.H.1
1 Paul Drude Institut, Hausvogteiplatz 5-7, 10117 Berlin
Structural properties of Carbon doped LT-GaAs
Proc. of the 3rd Symposium on non-stoichiometric III-V compounds, Erlangen (2001) in:
Physik mikrostrukturierter Halbleiter, Vol. 23 ed.: S. Malzer, T. Marek and P. Kiesel, Verlag: Lehrstuhl für Mikrocharakterisierung, Universität Erlangen, P. 91
23.42.0

IFF-01-12-052
Luysberg M.; Scholten C.; Houben L.; Carius R.1; Finger F.1; Vetterl O.1
1 IPV, FZ Jülich
Structural Properties of microcrystalline Si solar cells
Proceedings of the MRS Spring Meeting, San Francisco, in press (2001)
23.42.0

IFF-01-12-053
Massalovitch S.; Ioffe A.; Küssel E.; Schlapp M.; Brückel Th.
Development of the large-area 2D neutron detector based on the imaging plate
Deutsche Neutronenstreutagung 2001, Schriften des Forschungszentrums Jülich, Reihe Materie und Material, Band 8 (2001) p. 102
23.89.1

IFF-01-12-054
Melnichenko Y.1; Wignall G.D.1; Schwahn D.
1Solid State Division, Oak Ridge National Laboratory, USA
Universal Behavior of Polymer Molecules in Blends, Solutions, and Supercritical Fluids
Polymeric Materials 85 (2001)
23.30.0

IFF-01-12-055
Messerschmidt U.1; Bartsch M.1; Geyer B.1; Ledig L.; Feuerbacher M.; Wollgarten M; Urban K.
1 MPI für Mikrostrukturphysik, Halle
Dislocation Dynamics in Icosahedral Al-Pd-Mn Single Quasicrystal
Mat. Res. Soc. Symp. Proc., Vol. 643, K.6.5.1-6 (2001)
23.55.0

IFF-01-12-056
Mueller R.; Brückel Th.; Horriar-Esser Ch.
Entwicklung einer Anlage zur Herstellung von kernspin-polarisiertem 3He am Forschungszentrum Jülich
Deutsche Neutronenstreutagung 2001, Schriften des Forschungszentrums Jülich, Reihe Materie und Material, Band 8 (2001) p. 105
23.89.1

IFF-01-12-057
Pontius N.; Bechthold P.S.; Neeb M.; Eberhardt W.
Time-resolved photoelectron spectra of optically excited states in Pd3-
J. of Electron Spectroscopy and Related Phenomena 114, 163 (2001)
23.20.0

IFF-01-12-058
Richter D.
Neutronen für alle
Physikalische Blätter 57 (2001), Heft 9
23.30.0

IFF-01-12-059
Richter D.
Neutrons in Soft Condensed Matter
Conf. Proceed. ILL Millennium Symposium & European User Meeting, Grenoble/France, 06.-07.04.01, 38-44
23.30.0

IFF-01-12-060
Ronnow H.M.1; Regnault L.-P.1; Ulrich C.2; Keimer B.2; Ohl M.3; Bourges P.4
1CEA Grenoble, France
2MPI für Festkörperforschung, Stuttgart
3Institut Laue Langevin, 156X, 38042 Grenoble Cedex, France
4LLB Saclay, France
Incommensurate antiferromagnetic fluctuations in superconducitng Yba2Cu3O6.85
ILL Annual Report 2000, Scientific Highlights, 18-19 (2001)
23.89.1

IFF-01-12-061
Rücker U.; Alefeld B.; Bergs W.; Kentzinger E.; Heinen J.; Brückel Th.; Drochner M.1; Ackens A.1; Loevenich H.1; Reinhard P.1; Zwoll K.1
1FZJ, ZEL, Jülich
Das neue Neutronenreflektometer mit Polarisationsanalyse in Jülich
Deutsche Neutronenstreutagung 2001, Schriften des Forschungszentrums Jülich, Reihe Materie und Material, Band 8 (2001) p. 111
23.89.1

IFF-01-12-062
Rücker U.; Kentzinger E.; Toperverg B.; Brückel Th.; Ott F.1
1LLB, Gif sur Yvette, France
Spinaufgespaltene diffuse Streuung unter streifendem Einfall an polarisierenden Superspiegeln
Deutsche Neutronenstreutagung 2001, Schriften des Forschungszentrums Jülich, Reihe Materie und Material, Band 8 (2001) p. 60
23.89.1

IFF-01-12-063
Schlapp M.1,2; Kolb R.2; von Seggern H.2
1FZJ, IFF, Jülich
2TU, Fachbereich Materialwissenschaften, Darmstadt
Präparative Einflüsse auf die Empfindlichkeit des Speicherleuchtstoffs BaFBr:Eu2+ für Neutronen-Bildplatten
Deutsche Neutronenstreutagung 2001, Schriften des Forschungszentrums Jülich, Reihe Materie und Material, Band 8 (2001) p. 112
23.89.1

IFF-01-12-064
Schreyer A.1; Wildes A.2; Schmidt W.2; Majkrzak C.F.3; Erwin R.W.3; Lee S.H.3; Hong M.4; Kwo R.4
1Ruhr-Universität Bochum and Institut Laue Langevin
2Institut Laue Langevin, 156X, 38042 Grenoble Cedex, France
3National Institute for Standards and Technology, Gaithersburg, USA
4Bell Laboratoires, Murray Hill
Spin excitations in a magnetic superlattice: the first inelastic neutron scattering measurements
ILL Annual Report 2000, Scientific Highlights, 26-27 (2001)
23.89.1

IFF-01-12-065
Schroeder H.
High-Permittivity Materials for DRAMs
32. IFF-Ferienkurs 2001 "Neue Materialien für die Informationstechnik
23.42.0

IFF-01-12-066
Schwahn D.; Willner L.
Phase Behavior of Binary Polybutadiene Copolymer Mixtures with different Vinyl Content as an Example of a Blend of Weak Interacting Polymers
Polymeric Materials 85 (2001)
23.30.0

IFF-01-12-067
Schweika W.; Shramchenko N.1; Caudron R.1; Bellissent R.1
1LLB, Saclay, France
Phasonen in icosaedrischen AlPdMn Quasikristallen
Deutsche Neutronenstreutagung 2001, Schriften des Forschungszentrums Jülich, Reihe Materie und Material, Band 8 (2001) p. 183
23.89.1

IFF-01-12-068
Schweika W.
Polarization analysis
Schriften des Forschungszentrums Jülich: Materie und Material; Vol. 9 (2001) 4-1 - 4-23
23.89.1

IFF-01-12-069
Seeck O.; Mihaylova M.; Shin K.1
1SUNY, Department of Materials Science and Engineering, Stony Brook, USA
Investigation of Thin-Film Layer Systems with Synchrotron Radiation: Studies of Low-Contrast Polymer Interfaces
Research at HASYLAB (2001) 44 - 46
23.89.1

IFF-01-12-070
Seeck O.
Analytical Methods
Schriften des Forschungszentrums Jülich, Reihe Materie und Material; Band 7 (2001) B4.1 - B4.21
23.89.1

IFF-01-12-071
Seeck O.
Continuum description: Grazing Incidence Neutron Scattering
Schriften des Forschungszentrums Jülich: Materie und Material; Vol. 9 (2001) 6-1 - 6-18
23.89.1

IFF-01-12-072
Sokolov A.P.1; Kisliuk A.1; Grimm H.; Dianoux A.J.2
1University of Akron, USA
2Institut Laue Langevin, 156X, 38042 Grenoble Cedex, France
Slow relaxation process in DNS at different levels of hydration
ILL Annual Report 2000, Scientific Highlights, 56-57 (2001)
23.30.0

IFF-01-12-073
Tietze-Jaensch H.; Conrad H.; Dietrich J.; Filges D.; Haft B.1; Hansen G.; Maier R.; Paul N.; Pohl C.; Prasuhn D.; Smirnov A.2; Stelzer K.; Ullmaier H.
1TU, ITP, Austria
2JINR, Dubna, Russia
JESSICA, the ESS-like target/reflector mock-up and cold moderator test facility
Proceedings of ICANS-XV, Tsukuba, Japan, 06. - 09.11.2000 (2001) 829 - 834
23.60.0

IFF-01-12-074
Tillmann K.; Förster A.1; Houben L.
1 ISG, FZ Jülich
Critical dimensions for the formation of misfit dislocations in In0.6Ga0.4As island on GaAs(001)
Proceedings of the XIIth Conference on Microscopy of Semiconducting Materials, 22-25 March 2001, Oxford, Microscopy of Seminconducting Materials 2001, Inst. Phys. Conf. Ser., in press.
23.42.0

IFF-01-12-075
Tillmann K.; Luysberg M.; Fattah A.; Specht P.1; Weber E.R.1
1 Department of Materials Science, University of California, Berkeley, CA 94720, USA
Mechanism of interdiffusion and thermal stability upon annealing of AlAs/GaAs: Be quantum wells grown under low temperature conditions
Proceedings of the XIIth Conference on Microscopy of Semiconducting Materials, 22-25 March 2001, Oxford, Microscopy of Seminconducting Materials 2001, Inst. Phys. Conf. Ser., in press.

IFF-01-12-076
Tillmann K.; Luysberg M.; Specht P.1; Cich M.J.1; Weber E.R.1
1 Department of Materials Science, University of California, Berkeley, CA 94720, USA
Beryllium dopant induced stabilization against in-termixing and precipitation upon annealing of LT-AlAs/GaAs:Be Multiple quantum wells
Proc. of the 3rd Symposium on non-stoichiometric III-V compounds, Erlangen (2001) in:
Physik mikrostrukturierter Halbleiter, Vol. 23 ed.: S. Malzer, T. Marek and P. Kiesel, Verlag: Lehrstuhl für Mikrocharakterisierung, Universität Erlangen, p. 79
23.42.0

IFF-01-12-077
Toperverg B.1,2; Kentzinger E.1; Rücker U.1; Brückel Th.1
1FZJ, IFF, Jülich
2Petersburg Nuclear Physics Institute, Gatchina, Russia
Specular reflection and off-specular scattering of polarized neutrons from magnetic multilayers
Deutsche Neutronenstreutagung 2001, Schriften des Forschungszentrums Jülich, Reihe Materie und Material, Band 8 (2001) p. 70
23.89.1

IFF-01-12-078
Voigt J.; Schmidt W.; Ohl M.; Brückel Th.
Magnetische Ordnung in Erbium/Terbium-Schichtsystemen
Deutsche Neutronenstreutagung 2001, Schriften des Forschungszentrums Jülich, Reihe Materie und Material, Band 8 (2001) p. 71
23.89.1

IFF-01-12-079
Waser R.
Molecular Electronics
32. IFF-Ferienkurs 2001 "Neue Materialien für die Informationstechnik
23.42.0

IFF-01-12-080
Wosik J.; Penkalla H.J.; Szot K.; Dubiel B.; Schubert F.; Czyrska-Filmemonowicz A.:
Quantitative Characterization of Wasopaloy Microstructure using various Microscopic Techniques
Proc. Europ. Metallographic Conf, EUROMET 2000, Saarbrücken, Germany, Special Edition of the Practical Metallography ed. by G. Petzow 32 (2001) 87-90
23.42.0

IFF-01-12-081
Woundenberg F.C.M.1; Verweij H.1; Sager W.
1Universität Twente
Nanostructured oxide coatings via emulsion precipitation
23.15.0

IFF-01-12-082
Yang W.; Feuerbacher M.; Urban K.
Cluster structure and low-energy planes in icosahedral Al-Pd-Mn quasicrystals
Conference Quasicrystals 2001, Sendai/Japan, 24.-28. September (2001) 23.55.0

List of references

Alefeld B.	IFF-01-12-061		
Allgaier J.	IFF-01-12-024		
Antons A.	IFF-01-12-002		
Bechthold P.S.	IFF-01-12-020	IFF-01-12-057	
Bellini V.	IFF-01-12-005		
Bergs W.	IFF-01-12-061		
Brückel Th.	IFF-01-12-006	IFF-01-12-007	IFF-01-12-034
	IFF-01-12-035	IFF-01-12-037	IFF-01-12-053
	IFF-01-12-056	IFF-01-12-061	IFF-01-12-062
	IFF-01-12-077	IFF-01-12-078	
Bürgler D.E.	IFF-01-12-008	IFF-01-12-009	IFF-01-12-020
	IFF-01-12-029		
Conrad H.	IFF-01-12-010	IFF-01-12-011	IFF-01-12-012
	IFF-01-12-013	IFF-01-12-014	IFF-01-12-035
	IFF-01-12-073		
Dietrich J.	IFF-01-12-073		
Divin Y.	IFF-01-12-015		
Dürr H.A.	IFF-01-12-017	IFF-01-12-018	IFF-01-12-019
	IFF-01-12-048	IFF-01-12-049	
Eberhardt W.	IFF-01-12-017	IFF-01-12-020	IFF-01-12-048
	IFF-01-12-049	IFF-01-12-057	
Ebert Ph.	IFF-01-12-021	IFF-01-12-022	
Ehrhart P.	IFF-01-12-023		
Endo H.	IFF-01-12-024		
Faley M.I.	IFF-01-12-025		
Fattah A.	IFF-01-12-075		
Feuerbacher M.	IFF-01-12-026	IFF-01-12-055	IFF-01-12-082
Filges D.	IFF-01-12-073		
Goerigk G.	IFF-01-12-028		
Grimm H.	IFF-01-12-072		
Grushko B.	IFF-01-12-004	IFF-01-12-016	
Grünberg P.	IFF-01-12-008	IFF-01-12-009	IFF-01-12-029
Hansen G.	IFF-01-12-073		
Hauck J.	IFF-01-12-030	IFF-01-12-031	
Heinen J.	IFF-01-12-061		
Hoffmann-Eifert S.	IFF-01-12-033		
Horriar-Esser Ch.	IFF-01-12-056		
Houben L.	IFF-01-12-052	IFF-01-12-074	
Hupfeld D.	IFF-01-12-034		
Ioffe A.	IFF-01-12-035	IFF-01-12-053	
Jahnen B.	IFF-01-12-036		
Kann G.	IFF-01-12-020		

Kentzinger E.	IFF-01-12-037 IFF-01-12-077	IFF-01-12-061	IFF-01-12-062
Kienle D.	IFF-01-12-038	IFF-01-12-039	
Kirch D.	IFF-01-12-050		
Kirstein O.	IFF-01-12-001		
Klingeler R.	IFF-01-12-020		
Kluge M.	IFF-01-12-040		
Kohlstedt H.	IFF-01-12-041		
Kollmann M.	IFF-01-12-042		
Kromen Wi.	IFF-01-12-043		
Kronast F.	IFF-01-12-017		
Köbler U.	IFF-01-12-044		
Küssel E.	IFF-01-12-035	IFF-01-12-053	
Ledig L.	IFF-01-12-055		
Link S.	IFF-01-12-048	IFF-01-12-049	
Luysberg M.	IFF-01-12-036 IFF-01-12-052	IFF-01-12-050 IFF-01-12-075	IFF-01-12-051 IFF-01-12-076
Maier R.	IFF-01-12-073		
Massalovitch S.	IFF-01-12-035	IFF-01-12-053	
Meertens D.	IFF-01-12-051		
Mihaylova M.	IFF-01-12-069		
Mika K.	IFF-01-12-030	IFF-01-12-031	
Monkenbusch M.	IFF-01-12-003	IFF-01-12-024	
Mueller R.	IFF-01-12-035	IFF-01-12-056	
Neeb M.	IFF-01-12-020	IFF-01-12-057	
Ohl M.	IFF-01-12-060	IFF-01-12-078	
Paul N.	IFF-01-12-073		
Pohl C.	IFF-01-12-073		
Pontius N.	IFF-01-12-057		
Poppe U.	IFF-01-12-015	IFF-01-12-025	
Prasuhn D.	IFF-01-12-073		
Richter D.	IFF-01-12-003 IFF-01-12-059	IFF-01-12-024	IFF-01-12-058
Rücker U.	IFF-01-12-037 IFF-01-12-077	IFF-01-12-061	IFF-01-12-062
Sager W.	IFF-01-12-027	IFF-01-12-081	
Schall P.	IFF-01-12-026		
Schlapp M.	IFF-01-12-035	IFF-01-12-053	IFF-01-12-063
Schmidt W.	IFF-01-12-064	IFF-01-12-078	
Schmitz B.	IFF-01-12-035		

Scholten C.	IFF-01-12-052		
Schroeder H.	IFF-01-12-065		
Schwahn D.	IFF-01-12-054	IFF-01-12-066	
Schweika W.	IFF-01-12-034	IFF-01-12-067	IFF-01-12-068
Seeck O.	IFF-01-12-069	IFF-01-12-070	IFF-01-12-071
Shadrin P.	IFF-01-12-015		
Shirotov V.	IFF-01-12-015		
Sievers J.	IFF-01-12-049		
Stelzer K.	IFF-01-12-073		
Szot K.	IFF-01-12-021	IFF-01-12-080	
Tietze-Jaensch H.	IFF-01-12-073		
Tillmann K.	IFF-01-12-074	IFF-01-12-075	IFF-01-12-076
Toperverg B.	IFF-01-12-037 IFF-01-12-047	IFF-01-12-045 IFF-01-12-062	IFF-01-12-046 IFF-01-12-077
Trinkaus H.	IFF-01-12-050		
Ullmaier H.	IFF-01-12-011	IFF-01-12-073	
Urban K.	IFF-01-12-015 IFF-01-12-036	IFF-01-12-025 IFF-01-12-055	IFF-01-12-026 IFF-01-12-082
Voigt J.	IFF-01-12-078		
Waser R.	IFF-01-12-032	IFF-01-12-079	
Willner L.	IFF-01-12-066		
Wirth I.	IFF-01-12-020		
Wollgarten M.	IFF-01-12-055		
Yang W.	IFF-01-12-082		
Zeiske Th.	IFF-01-12-035		

Invited Talks

IFF-01-21-001
Akola J.; Ballone P.1; Jones R.O.
1 University of Messina, Italy
Improved Classical Force Fields for Hydrogen Bonds
Leverkusen (Bayer): BMBF project meeting
3.5.2001
23.20.0

IFF-01-21-002
Akola J.; Ballone P.1; Jones R.O.
1 University of Messina, Italy
Polymer Modelling based on Density Functional Calculations
SISSA, Trieste
21.9.2001
23.20.0

IFF-01-21-003
Allgaier J.; Endo H.; Gompper G.; Mihailescu M.; Monkenbusch M.; Richter D.; Jakobs B.1; Sottmann T.1; Strey R.1
1Institut für Physikalische Chemie, Universität Köln; Luxemburger Str. 116, 50939 Köln
Amphiphilicity boosting in microemulsions: The effect of poly[ehyleneoxide-b-(ethylene-alt-propylene)] diblock copolymers
Int. Symp. on Ionic Polymerization, Heraklion, Greece, 22.-26.10.01
23.30.0

IFF-01-21-004
Allgaier J.; Endo H.; Richter D.; Sottmann T.1; Strey R.1;
1Institut für Physikalische Chemie, Universität Köln; Luxemburger Str. 116, 50939 Köln
Amphiphilic Block Copolymer as Efficiency Boosters for Surfactants
Wella AG, Darmstadt, 11.10.01
23.30.0

IFF-01-21-005
Allgaier J.
Amphiphile Blockcopolymere als Co-Emulgatoren in Wasser-Öl-Tensid Gemischen
Bayer AG, Landwirtschaftszentrum, Monheim, 01.06.01
23.30.0

IFF-01-21-006
Allgaier J.
From nonionic surfactants to their polymer analogues. Materials and micellar properties
University of Lever, Port Sunlight, UK, 11.07.01
23.30.0

IFF-01-21-007
Allgaier J.
Synthese, Neutronenkleinwinkelstreuung und Rheologie von verzweigten Modellpolymeren
Universität Bayreuth, 29.01.01
23.30.0

IFF-01-21-008
Amano J.; Chi C.; Gilbert St.; Hunter St.; Lanham R.; Rickes J.; Ritchey D.; Aggarwal S.; Moise T.; Sakoda T.; Summerfelt S.
Embedded FeRAM for deep sub-micron SoC
1st Int. Meet. Ferroelectric Random Access Memories (FeRAM 2001), Gotemba, Japan, 19.11.-21.11.2001
23.42.0

IFF-01-21-009
Baumgaertner A.
Advancements in Molecular Dynamics Simulations
Meeting of EC network "Protein-Lipid Interactions"
Bruessel, Belgien
1.6.2001
23.30.0

IFF-01-21-010
Baumgaertner A.
Molecular dynamics simulations of membrane proteins
Biophysics School on Lipid-Protein Interactions and the Organization of Membranes.
Szeged, Ungarn
29.6.2001
23.30.0

IFF-01-21-011
Baumgaertner A.
Molekulardynamik eines Ionenkanals
Universitaet Duisburg
22.5.2001
23.30.0

IFF-01-21-012
Baumgaertner A.
Simulations of gating properties of the KcsA ion channel
University of Ljubljana, Slowenien
2.11.2001
23.30.0

IFF-01-21-013
Baumgaertner A.
The protein-lipid interface
Conference on "Protein-Lipid Interaction".
Zagreb, Croatia
31.8.2001
23.30.0

IFF-01-21-014
Baumgaertner A.
Why cells are persistent
Int.Center of Theoret.Phys., Trieste
20.9.2001
23.30.0

IFF-01-21-015
Bene J.1; Lustfeld H.
1 Institute for Theoretical Physics, Eötvös University, Budapest
Simulating viscuous 2D Flows using wavelet dynamics
General Assembly der European Geophysical Society, Nizza
26.3.2001
23.20.0

IFF-01-21-016
Blügel S.
Novel surface nanoprobes - scanning probe microscopies
IUVSTA 15th International Vacuum Congress, AVS 48th International Symposium, 11th International Congress on Solid Surfaces, San Francisco, CA
29.10.01 - 02.11.01
23.20.0

IFF-01-21-017
Buchenau U.; Wischnewski A.; Zorn R.; Hadjichristidis N.1
1Dep. of Chemistry, University of Athens, Industrial Chem. Lab. - Polymers, Panepistimiopolis - Zografou, Athens 15771, Greece
Relaxations in the glass phase of silica and PMMA
8th Int. Workshop on Disordered Systems, Andalo, Italy, 14.03.01
23.30.0

IFF-01-21-018
Buchenau U.
Dynamics of Glasses
Workshop on dynamics in Quasicrystals, Duisburg, 04.12.01
23.15.0

IFF-01-21-019
Buchenau U.
Mesoscale Dynamics in Glasses

Dynamical Properties of Solids XXVIII, Kerkrade, The Netherlands, 20.09.01
23.30.0

IFF-01-21-020
Buchenau U.
Relaxations in glasses and at the glass transition
4th Int. Discussion Meeting on Relaxations in Complex Systems, Crete, Greece, 21.06.01
23.15.0

IFF-01-21-021
Bürgler D.E.
Ag(001) Pufferschichten auf GaAs: Präparation und Verwendung als Substrate für magnetische Schichtstrukturen
Seminar Universität Mainz
20.06.2001
23.42.0

IFF-01-21-022
Bürgler D.E.
Coupling across silicon and iron-silicide spacers
Argonne National Laboratory, Chicago (USA)
20.11.2001
23.42.0

IFF-01-21-023
Bürgler D.E.
The role of the spacer layer for magnetic interlayer exchange coupling and for giant magnetoresistance (GMR)
Michigan State University, East Lansing (USA)
19.11.2001
23.42.0

IFF-01-21-024
Conrad H.; Byloos C.; Cates M.1; Riemer B.1; Hastings J.2; Spitzer H.3
1ORNL, Oak Ridge, USA
2BNL, Brookhaven, USA
3PSI, Villigen, Switzerland
Stress Wave Experiments with the ASTE Target
Seggau, Austria, 7th General ESS Meeting, 28.09.2001
23.60.0

IFF-01-21-025
Conrad H.
Materialprobleme in Targetkomponenten der ESS
Berlin, ESS-HGF-Projekt Meeting, 16.03.2001
23.60.0

IFF-01-21-026
Dederichs P.H.
Ballistic spininjection
Seminar Universität Kyoto, 12.12.2001
23.20.0

IFF-01-21-027
Dederichs P.H.
Ballistic spininjection from Fe into ZnSe and GaAs
Center of Excellence Symposium, Osaka, Japan, 13.12.2001
23.20.0

IFF-01-21-028
Dederichs P.H.
Ballistic spininjection from Fe into ZnSe and GaAs
Symposium "Selforganizing Nanostructures and Magnetic Heterostructures", Universität Duisburg, 29.11.2001
23.20.0

IFF-01-21-029
Dederichs P.H.
Ballistic spininjection from Fe into ZnSe and GaAs
Symposium on Magnetoelectronics, Regensburg, 25.07.2001
23.20.0

IFF-01-21-030
Dederichs P.H.
Complex band structure and resonant states in the barrier problem
APS March Meeting, Seattle, USA, 15.03.2001
23.20.0

IFF-01-21-031
Dederichs P.H.
Importance of complex band structure and resonant states for tunneling
Symposium on Metallic Multilayers, Aachen, 26.06.2001
23.20.0

IFF-01-21-032
Dederichs P.H.
Surface magnetism
The European Graduate School on Condensed Matter: Physics of Magnetic Multilayers, Prag, 09.06.2001
23.20.0

IFF-01-21-033
Dhont J.
Dynamics of Colloids
Winterschool "Physical Chemistry"
Han sur Lesse; Belgien; 05.-09.02.01
23.30.0

IFF-01-21-034
Dhont J.
Flow Instability in Complex Fluids
General Physics Colloquium
Univ. Groningen; The Netherlands, 05.04.01
23.30.0

IFF-01-21-035
Dhont J.
Spinodal Decomposition of Colloids
Winterschool "Sensing and Manipulating in the Nanoworld"
Mauterndorf; Austria, 18.-23.02.01
23.30.0

IFF-01-21-036
Dhont J.
The Shear-banding Transition in Colloids
4th International Discussion, Meeting on Relaxations in Complex Systems
Heraklion, Greece, 17.06.-24.06.01
23.30.0

IFF-01-21-037
Dhont J.
The Shear-banding Transition in Complex Fluids
Complex Materials in External Fields
Manchester, UK, 29.08.-31.08.01
23.30.0

IFF-01-21-038
Divin Y.Y.; Volkov O.Y.1; Pavlovskii V.V.1; Shirotov V.; Shadrin P.; Poppe U.; Urban K.
1 Institute of Radioengineering & Electronics of RAS, Moscow 103907, Russian FederationTerahertz Hilbert spectroscopy by high-Tc Josephson junctions
Hauptvortrag, DPG Frühjahrstagung, Hamburg 26.-30. März (2001)
23.42.0

IFF-01-21-039
Dürr H.A.
Fsec electron and spin relaxation at surfaces
Van der Waals-Zeeman Kolloquium, Universität Amsterdam
22.05.2001
23.20.0

IFF-01-21-040
Dürr H.A.
Fsec spin dynamics in CoPt nanostructures
Seminar Experimentelle Physik, Universität Würzburg
06.06.2001

23.20.0

IFF-01-21-041
Dürr H.A.
Magnetic ordering phenomena in nanostructured materials
Sonderkolloquium Physikalisches Institut, TU Berlin
08.05.2001
23.20.0

IFF-01-21-042
Dürr H.A.
Magnetic quantumphenomena in nanostructures
Sonderkolloquium, Institut für Angewandte Physik, Universität Düsseldorf
23.02.2001
23.20.0

IFF-01-21-043
Dürr H.A.
Magnetism in nanostructures
Greifswalder Physikalisches Kolloquium, Ernst-Moriz-Arndt-Universität Greifswald
01.02.2001
23.20.0

IFF-01-21-044
Dürr H.A.
Spin-polarized photoelectron emission microscopy with femtosecond temporal resolution
Symposium on Dynamics of Magnetic Switching, DPG March Meeting, Hamburg
29.03.2001
23.20.0

IFF-01-21-045
Ebert Ph.
Defects in III-V semiconductor surfaces
Université de Fribourg, Switzerland, May 15, 2001.
23.42.0

IFF-01-21-046
Ebert Ph.
Defekte auf III-V-Halbleiteroberflächen
Hauptvortrag, 65. Physikertagung der Deutschen Physikalischen Gesellschaft, Symposium Rekonstruktion und Wachstum von III-V-Halbleiteroberflächen der Fachverbände Halbleiter- und Oberflächenphysik, Hamburg, Germany, 26.-30.3.2001.

IFF-01-21-047
Ebert Ph.
Festkörperforschung auf atomarer Skala mittels Rastertunnelmikroskopie
Kolloquium in Physik, Mathematisch-Naturwissenschaftliche Fakultät, Université de Fribourg, Switzerland, 7. Dezember 2001.
23.42.0

IFF-01-21-048
Ebert Ph.
Leuchtendes Silizium
RWTH Aachen, Germany, February 14, 2001.
23.42.0

IFF-01-21-049
Ebert Ph.
Scanning Tunneling Microscopy in Materials Physics
Institute of Physics, Chinese Academy of Sciences, The International Center of Quantum Structures, Peking, China, October 12, 2001.
23.42.0

IFF-01-21-050
Ebert Ph.
Scanning Tunneling Microscopy in Materials Physics
Nanoscale Physics and Device Laboratory, Chinese Academy of Sciences, Peking, China, October 29, 2001.

23.42.0

IFF-01-21-051
Eisenriegler E.
Polymer depletion potentials: Center of mass distribution of a polymer
Chain near a repulsive wall
Jülich Soft Matter Days, Rolduc, Kerkrade, Niederlande
14. 11. 2001
23.30.0

IFF-01-21-052
Feuerbacher M.
Mechanical properties of quasicrystals
Quasicrystals 2001, Sendai, Japan, September 2001.
23.55.0

IFF-01-21-053
Frielinghaus H.; Byelov D.; Endo H.; Allgaier J.; Stellbrink J.; Richter D.; Jakobs B.1; Sottmann T.1; Strey R.1
1Institut für Physikalische Chemie, Universität Köln, 50939 Köln
Polymer boosting effect in the Droplet Phase Studied by Small Angle Neutron Scattering
Jülich Soft Matter Days, Kerkrade, The Netherlands, 15.11.01
23.30.0

IFF-01-21-054
Gompper G.; Theissen O.
Lattice-Boltzmann Study of Spontaneous Emulsification
Dynamic Days 2001, Dresden
05.-08. Juni 2001
23.30.0

IFF-01-21-055
Gompper G.
Dynamics of the Swollen Lamellar Phase in Ternary Amphiphilic
Systems
4th International Discussion Meeting on Relaxation in Complex Systems, Kreta, Greece
17.-23. Juni 2001
23.30.0

IFF-01-21-056
Gompper G.
Effect of amphiphilic block copolymers on membrane elasticity and
phase behavior
Adriatico Research Conference on "Interaction and Assembly of Biomolecules", International Center for Theoretical Physics, Trieste
27.-31. August 2001
23.30.0

IFF-01-21-057
Gompper G.
Lebendige Membranen
Antrittsvorlesung, Mathematisch-Naturwissenschaftliche Fakultät,
Universität zu Köln
29.05.2001
23.30.0

IFF-01-21-058
Gompper G.
Struktur und Phasenverhalten von Mikroemulsionen und Schwammphasen
Seminarvortrag, Physikalische Chemie, Universität zu Köln
20.04.2001
23.30.0

IFF-01-21-059
Grossmann M.; Waser R.;. Lohse O.; Bolten D.; Böttger U.
Imprint in PZT thin films: A comparison of aging mechanisms in ferroelectric bulk material with ferroelectric thin films (O)

13th Int. Symp. Integrated Ferroelectrics, Colorado Springs, USA, 11.03.-14.03.01
23420

IFF-01-21-060
Grünberg P.; Buchmeier M.; Bürgler D.E.; Gareev R.; Kuanr B.
Zwischenschichtkopplung: Grundlagen, aktuelle Forschung, Anwendungen
Symposium über "Magnetoresistive Sensoren", Wetzlar
13.03.2001
23.42.0

IFF-01-21-061
Grünberg P.
Interlayer exchange coupling across metallic and semiconducting interlayers
Institute for Electrical Engineering, Slovak Ac. Of Science, Bratislava, Slowakei
04.10.2001
23.42.0

IFF-01-21-062
Grünberg P.
Interlayer exchange coupling in Fe/FeSi/Fe and Fe/AlSi/Fe layered structures
1st Seeheim Conference on Magnetism, Seeheim, Germany
10.09.2001
23.42.0

IFF-01-21-063
Grünberg P.
Interlayer exchange couöling across metals, semimetals and semiconductors: Experiments
The European Graduate School on Condensed Matter (EGSCM Prague '01), Prag
10.06.2001
23.42.0

IFF-01-21-064
Grünberg P.
Layered magnetic structures in research and application
International Workshop on Physics of Magnetoresistance Effects, Peking
28.08.2001
23.42.0

IFF-01-21-065
Grünberg P.
Magnetische Multilagen: Austauschkopplungder ferromagnetischen Schichten über metallische und halbleitende Zwischenschichten
Seminar, TU Hannover, Institut für Mikrosystemtechnik
02.11.2001
23.42.0

IFF-01-21-066
Grünberg P.
Magnetische Multilagen: Austauschkopplungder ferromagnetischen Schichten über metallische und halbleitende Zwischenschichten
Seminar, TU Wien, Center for Computational Material Science
05.10.2001
23.42.0

IFF-01-21-067
Grünberg P.
Magnetoelektronik in Forschung und Anwendung
Graduiertenkolleg "Materialien und Komponenten der Mikrosystemtechnik" der Gesamthochschule Kassel
12.07.2001
23.42.0

IFF-01-21-068
Grünberg P.
Magnetoelektronik: Vom Kompass zum Datenspeicher
Kolloquium Universität-Gesamthochschule Siegen
26.04.2001
23.42.0

IFF-01-21-069
Grünberg P.
Zwischenschicht-Austauschkopplung und GMR-Effekt
WE Heraeus Ferienkurs: "Komplexe magnetische Phänomene in Festkörpern", Dresden
05.09.01
23.42.0

IFF-01-21-070
Gutheim F.; Müller-Krumbhaar H.
Epitaktisches Wachstum unter elastischer Wechselwirkung: Inselbildung im Submonolagenbereich
DGKK, Arbeitskreis Kinetik, 22.02.2001, Erlangen
23.15.0

IFF-01-21-071
Harris J.
Calculation of Elastic Constants of Materials using Density Functional Theory
University of Dortmund: Gemeinsames Kolloquim Physik/Chemie
17.7.2001
23.20.0

IFF-01-21-072
Harris J.
Computation and Information in Materials Science
University of Kyoto, Japan
24.10.2001
23.20.0

IFF-01-21-073
Harris J.
Computational Methods in Materials Science
Ecole Polytechnique de Montreal, Canada
6.6.2001
23.20.0

IFF-01-21-074
Harris J.
Computational Methods in Materials Science
General Motors Research Center, Warren, Michigan
21.2.2001
23.20.0

IFF-01-21-075
Hartmann M.
Strukturbildung an fest-flüssig Phasengrenzen unter hydrodynamischer Wechselwirkung
Universität Magdeburg, 15.01.2001
23.15.0

IFF-01-21-076
Haubold H.-G.
In situ Small Angle X-Ray Scattering of Nafion and Pt Catalysts
Villigen, Switzerland, PSI-West, 16th PSI-Tagessymposium Elektrochemische Energiespeicherung, 23.10.2001
23.89.1

IFF-01-21-077
Hoffmann S.
Molecular Dynamics in Polymer Blends: First Steps towards an understanding of its heterogeneous behaviour
Institut Laue-Langevin, Grenoble, Frankreich, 13.03.01
23.30.0

IFF-01-21-078
Hoffmann S.
Molecular Dynamics in Polymer Mixtures: QENS and Dielectric Spectroscopy Study on the Origin of Dynamic Heterogeneity
4th Int. Discussion Meeting on the Relaxation in Complex Systems, Crete, Greece, 19.06.01
23.30.0

IFF-01-21-079
Hoffmann-Eifert S.; Schneller T.; Ehrhart P.; Waser R.
Advanced Chemical Deposition Techniques for Electroceramic Thin Films
Annual meeting of the Belgian ceramic Society, Limburgs Universitair Centrum, Diepenbeek, Belgium, 15.06.01
23420

IFF-01-21-080
Hoffmann-Eifert S.
Ba1-xSrxTiO3 Dünnschichten: Abscheidung mittels CSD und MOCVD und Mikrostruktur-Eigenschaftsbeziehungen
Universität GHS Essen, 10.05.2001
23420

IFF-01-21-081
Hupfeld D.; Bos J.; Voigt J.; Seeck O.; Fischer K.; Brückel Th.
Resonante magnetische Röntgenstreuung an ferromagnetischem EuS
Hamburg, HASYLAB, Seminar, 15.11.2001
23.89.1

IFF-01-21-082
Hupfeld D.; Voigt J.; Brückel Th.
Investigation of element-specific magnetic correlations with synchrotron radiation
Berlin, 3rd Russian-German Workshop on Synchrotron Radiation Research, 18. - 20.11.2001
23.89.1

IFF-01-21-083
Hupfeld D.
High Energy X-Ray Scattering at μ-CAT
Chicago, USA, Workshop on High Energy X-Ray Scattering at the APS, 08.03.2001
23.89.1

IFF-01-21-084
Hupfeld D.
Untersuchung magnetischer Systeme mit resonanter Austauschstreuung
Kiel, Universität, Festkörperphysik Seminar, 15.02.2001
23.89.1

IFF-01-21-085
Ioffe A.
Simulations of the Neutron Speed Echo Spectrometer
Berlin, HMI, Workshop on VITESS 2 and other Packages for Simulations of Neutron Scattering, 25. - 27.06.2001
23.89.1

IFF-01-21-086
Jones R.O.
A combined density functional and Monte Carlo study of polycarbonate
Spring Meeting, Materials Research Society, San Francisco, USA
19.4.2001
23.20.0

IFF-01-21-087
Jones R.O.
Density functional calculations for some real materials - thermal expansion in glass ceramics, and reactions in polycarbonate (the stuff of CD's)
Department of Physics, University of California, Berkeley, USA
16.4.2001
23.20.0

IFF-01-21-088
Jones R.O.
Density functional calculations on supercomputers
Supercomputing Global Workshop (Denver, Jülich)
15.11.2001
23.20.0

IFF-01-21-089
Jones R.O.
Density functional/Monte Carlo study of ring-opening polymerization
Conference on Computational Physics, Aachen
6.9.2001
23.20.0

IFF-01-21-090
Jones R.O.
Ring-opening polymerization and ``living polymers'' - density functional calculations and beyond
NIC-Symposium 2001, Jülich
6.12.2001
23.20.0

IFF-01-21-091
Jung P.
Irradiation effects and consequences on inservice properties under protron and neutron mixed spectrum: an overview
Paris, France, Journées d'Automne, 29. - 31.10.2001
23.60.0

IFF-01-21-092
Jung P.
Radiation Effects in Structural Materials of Spallation Sources
Brasimone, Italy, 2nd International Workshop on Materials for Hybrid Reactors and Related Technologies, 18. - 20.04.2001
23.60.0

IFF-01-21-093
Kahle S.
Dynamic Neutron Scattering on Partially Deuterated Polybutadiene
4th Int. Discussion Meeting on Relaxations in Complex Systems, Crete, Greece, 20.06.01
23.30.0

IFF-01-21-094
Kentzinger E.; Rücker U.; Toperverg B.; Brückel Th.
Reflectivity and off-specular scattering of neutrons from magnetic thin films
Jülich, Deutsche Neutronenstreutagung 2001, 19. - 21.02.2001
23.89.1

IFF-01-21-095
Kirstein O.; Prager M.; Parker S.F.1; Johnson M.2
1ISIS Facility, Rutherford Appleton Lab., Chilton, Didcot, Oxon OX11 0QX, UK
2Institut Laue Langevin, F,38042 Grenoble Cedex 9, France
Lattice dynamics and methyl rotation of dimethylacetylene (DMA)
Int. Conf. on Neutron Scattering, TU München, 09.-13.09.01
23.15.0

IFF-01-21-096
Kohlstedt H.
Hauptvortrag: Oxidische Dünnschichten
Etching of refractory metal electrodes and complex oxides
DPG-Tagung 2001, Hamburg, 26.-30.03.01
23420

IFF-01-21-097
Kohlstedt H.
Magnetische Tunnelkontake mit FeMn als Anti-ferromagnet und CoFe als Elektroden
Universität Kassel, 11.07.01
23420

IFF-01-21-098
Kohlstedt H.
Nicht-flüchtige Informationsspeicherung: eine neue Generation von Bauelementen für das 21. Jahrhundert
Universität Tübingen, 07.11.01
23.42.0

IFF-01-21-099

Kohlstedt H.
Structural and ferroelectric properties of BaTiO3/SrRuO3 and PbZr0.52Ti0.48O3/SrRuO3 thin films on SrTiO3 substrates
University of Liege, Belgium, 25.10.01
23.42.0

IFF-01-21-100
Lang P.
Grenzflächeninduzierte Ordnungsphänomene von fluiden Phasen: Untersuchungen mittels Streumethoden
TU-Clausthal-Zellerfeld, 10. Juli 2001
23.30.0

IFF-01-21-101
Liebsch A.
Do Mie Plasmons have a longer lifetime on resonance than off-resonance?
San Sebastian, Spanien
12.7.2001
23.20.0

IFF-01-21-102
Liebsch A.
Dynamischer Response an Metalloberflächen
Universität Konstanz
11.5.2001
23.20.0

IFF-01-21-103
Liebsch A.
Hot electron lifetimes at noble metal surfaces
Fritz Haber Institut Berlin
28.5.2001
23.20.0

IFF-01-21-104
Liebsch A.
Hot electron lifetimes at noble metal surfaces
LEPES-CNRS, Grenoble, France
23.3.2001
23.20.0

IFF-01-21-105
Liebsch A.
Hot electron lifetimes at noble metal surfaces
San Sebastian, Spanien
5.7.2001
23.20.0

IFF-01-21-106
Liebsch A.
Modern Materials Research in Jülich
DAAD Promotion Tour; Delhi, Pune, Chennai, Colcatta, India
29.10.-9.11.2001
23.20.0

IFF-01-21-107
Lucas G. E.; Odette G. R.; Sokolov M.; Spatig P.; Jung P.; Yamamoto T.
Current Status of Small Specimen Test Technology
Baden-Baden, 10th International Conference of Fusion Reactor Materials, 14. - 19.10.2001
23.60.0

IFF-01-21-108
Lustfeld H.; D. Poppe1
1 FZ-ICG II
Fast/slow behavior in realistic pollutant reaction equations of the troposphere
Hamburg, Frühjahrstagung der Arbeitsgemeinschaft Exterrestrische Forschung der DPG
22.3.2001
23.20.0

IFF-01-21-109
Lustfeld H.
Relevanter Informationsverlust bei Poincaré Abbildungen?
Universität Duisburg
10.7.2001
23.20.0

IFF-01-21-110
Lustfeld H.
Ursache und Beschreibung kleinskaliger Konzentrationsschwankungen von Spurengasen in der Atmosphaere
Universität Duisburg
3.7.2001
23.20.0

IFF-01-21-111
Luysberg M.
Microcrystalline silicon for electronic devices
Dreiländertagung über Elektronenmikroskopie, Innsbruck, September 2001
23.42.0

IFF-01-21-112
Luysberg M.
Mikrokristallines Silizium: Ein Material für elektronische Bauelemente
Uni Göttingen, Dezember 2001
23.42.0

IFF-01-21-113
Luysberg M.
Relaxation von SiGe-Schichten durch He Implantation
Uni Kiel, November 2001
23.42.0

IFF-01-21-114
Luysberg M.
Structural properties of Be doped LT-GaAs
HUT, Helsinki, Februar 2001
23.42.0

IFF-01-21-115
Luysberg M.
Strukturelle Eigenschaften von mikrokristallinem Silizium
HMI Berlin, Januar 2001
23.42.0

IFF-01-21-116
Meier G.
Photon Correlation Spectroscopy with visible light: Concepts, experimental methods and scientific applications
Lecture at Research Courses on New X-Ray Sciences
Desy, Hasylab, Hamburg, 15.10.-17.10.01
23.30.0

IFF-01-21-117
Meyer R.; Waser R.
RESTRUCTURING the SURFACE REGION of DONOR DOPED SrTiO3 SINGLE CRYSTALS UNDER OXIDIZING CONDITIONS
112th Annual Meeting of American Ceramic Society, Indianapolis, 22.04.-26.04.01
23420

IFF-01-21-118
Monkenbusch M.
High resolution neutron spin-echo spectroscopy - A tool for soft condensed matter research
Argonne National Lab., Chicago, USA, 14.06.01
23.30.0

IFF-01-21-119
Monkenbusch M.
Reptation dynamics observed by incoherent inelastic neutron scattering experiments
DYPROSO XXVIII, 16.-19.09.01, Kerkrade, The Netherlands
23.30.0

IFF-01-21-120

Müller-Krumbhaar H.
Elastic effects on pattern formation
Calcutta, Indien, 07.03.2001
23.15.0

IFF-01-21-121
Müller-Krumbhaar H.
Elastische Effekte beim Cluster-Wachstum
Erlangen, 22.02.2001
23.15.0

IFF-01-21-122
Müller-Krumbhaar H.
Growth-morphologies in solidification and hydrodynamics
AFI-Conference, Sendai, Japan, 05.10.2001
23.15.0

IFF-01-21-123
Müller-Krumbhaar H.
Phase-field models for crystal growth
ICCG-13, Kyoto, Japan, 31.07.2001
23.15.0

IFF-01-21-124
Müller-Krumbhaar H.
Physik, das ungeliebte Schulfach
Institut für Lehrerbildung, Soest, 04.05.2001
23.15.0

IFF-01-21-125
Müller-Krumbhaar H.
Propagation fraktaler Fronten
Heraeus-Seminar, Bad Honnef, 23.03.2001
23.15.0

IFF-01-21-126
Müller-Krumbhaar H.
Propagation fraktaler Fronten
Universität Leipzig, 09.10.2001
23.15.0

IFF-01-21-127
Müller-Krumbhaar H.
Schulphysik - Kooperation zwischen Schule und Universität
GDNÄ-Tagung Schulphysik, Frankfurt, 05.11.2001
23.15.0

IFF-01-21-128
Nägele G.; Pesché R.1
1Universität Konstanz (???)
Dynamic Scaling and Freezing Criteria of Quasi-two-dimensional and three-dimensional Colloidal Dispersions
IUAP 21st International Conference on Statistical Physics
Cancum, Mexiko, 15.07.-20.07.01
23.30.0

IFF-01-21-129
Nägele G.
Dynamic Properties, Scaling and Related Freezing Criteria of Quasi-two-dimensional and Three-dimensional Colloidal Dispersions
Applied Statistical Physics Molecular Engineering Conference
Cancum, Mexiko, 23.07.-27.07.01
23.30.0

IFF-01-21-130
Nägele G.
Dynamische Eigenschaften ladungsstabilisierter Kolloide
MPI in Mainz, 12.02.01
23.30.0

IFF-01-21-131
Persson B.N.J.
Rubber Friction
ACS Rubber Division meeting on Rubber Friction, Ohio, USA
October 16-19, 2001
23.20.0

IFF-01-21-132
Persson B.N.J.
Rubber Friction
Colmar-Berg, Luxembourg
05.12.2001
23.20.0

IFF-01-21-133
Persson B.N.J.
Rubber Friction
Deutsches Institut für Kautschuktechnologie e.V., Hannover, Germany
09.10.2001
23.20.0

IFF-01-21-134
Persson B.N.J.
Rubber Friction
Pirelli Reifenwerke, Höchts/Odenwald
11.01.2001
23.20.0

IFF-01-21-135
Persson B.N.J.
Rubber Friction
Pirelli, Milano, Italy
12.10.2001
23.20.0

IFF-01-21-136
Persson B.N.J.
Sliding Friction
ACS Symposium on MOLECULAR TRIBOLOGY, San Diego, USA
1.4.2001
23.20.0

IFF-01-21-137
Persson B.N.J.
Sliding Friction
CECAM-SIMU Workshop on ``Simulation and theory of solid friction", Lyon, France
August 27-30, 2001
23.20.0

IFF-01-21-138
Persson B.N.J.
Sliding Friction
DIP meeting, Mainz
4.5.2001
23.20.0

IFF-01-21-139
Persson B.N.J.
Sliding Friction
Nonlinear Phenomena in Materials Science, Dresden, Germany
September 10-15, 2001
23.20.0

IFF-01-21-140
Persson B.N.J.
Sliding Friction
Ohio State University, Columbus, OH, USA
15.10.2001
23.20.0

IFF-01-21-141
Persson B.N.J.
Sliding Friction
SISSA, Trieste, Italy
26.01.2001
23.20.0

IFF-01-21-142
Persson B.N.J.

Sliding Friction
Sensing and Manipulating in the Nanoworld, Mauterndorf, Austria
18.2.2001
23.20.0

IFF-01-21-143
Persson B.N.J.
Sliding Friction
The second Stig Lundqvist research conference on Advancing Frontiers in Condensed Matter Physics: ``Non-Conventional Systems and New Directions", Trieste, Italy
July,2-6, 2001
23.20.0

IFF-01-21-144
Persson B.N.J.
Sliding Friction
University of Delf, The Netherlands
24.01.2001
23.20.0

IFF-01-21-145
Persson B.N.J.
Sliding Friction
University of Düsseldorf, Germany
20.12.2001
23.20.0

IFF-01-21-146
Persson B.N.J.
Sliding Friction
University of Erlangen, Germany
18.01.2001
23.20.0

IFF-01-21-147
Persson B.N.J.
Sliding Friction
University of Essen, Germany
07.06.2001
23.20.0

IFF-01-21-148
Persson B.N.J.
Sliding Friction
University of Illmenau, Germany
12.12.2001
23.20.0

IFF-01-21-149
Persson B.N.J.
Sliding Friction
University of Ulm, Germany
23.01.2001
23.20.0

IFF-01-21-150
Persson B.N.J.
Sliding Friction
Workshop on ``Computational Materials Science", Sardinia, Italy
September 17-23, 2001
23.20.0

IFF-01-21-151
Persson B.N.J.
Surface Vibrations
Vibrations at Surfaces 10, Saint Malo, France
17.6.2001
23.20.0

IFF-01-21-152
Persson B.N.J.
Vibrational Dynamics at Surfaces
University of Heidelberg, Germany
28.11.2001
23.20.0

IFF-01-21-153
Popkov V.
A sufficient criterion of integrability for nonequilibrium statistical models
International Conference "Theory of Functions and Mathematical Physics", Kharkov, Ukraine
10.-17. August, 2001
23.15.0

IFF-01-21-154
Prager M.; Schiebel P.1; Combet J.1
1Institut Laue Langevin, F-38042 Grenoble Cedex 9, France
Rotational tunnelling and disorder of 4-iodo-toluene
Conf. on Quantum Atomic and Molecular Tunnelling, Nottingham, UK, 05.09.01
23.15.0

IFF-01-21-155
Prager M.
Rotational tunnelling: from simple to complex systems
HMI Berlin, 18.06.01
23.15.0

IFF-01-21-156
Pyckhout-Hintzen W.; Heinrich M.; Straube E.1; Richter D.; McLeish T.C.B.2
1Martin-Luther-Universität Halle-Wittenberg, Fachbereich Physik, 06099 Halle
2IRC in Polymer Science and Technology, University of Leeds, Leeds LS2 9JT, UK
A microscopic model for branched polymers in elongational flow by SANS
Seminar, MPI Golm, 23.10.01
23.30.0

IFF-01-21-157
Pyckhout-Hintzen W.; Westermann S.; Urban V.1; Richter D.; Straube E.2
1ESRF Grenoble, Frankreich
2Martin-Luther-Universität Halle-Wittenberg, Fachbereich Physik, 06099 Halle
The length scale dependence of microscopic strain in polymer networks by SANS
BPS Symposium, Universität Bayreuth, 16.-18.9.2001
23.30.0

IFF-01-21-158
Pyckhout-Hintzen W.
Fundamental polymer research and implications for industrial applications
El-Minia University, Egypt, 10.04.01
23.30.0

IFF-01-21-159
Richter D.; Monkenbusch M.; Willner L.; Wischnewski A.; Arbe A.1; Colmenero J.1
1Dep. de Fiscia de Materiales, Universidad del Pais Vasco, Facultad de Quimica, E-20080 San Sebastian, Spain
Experimental Aspects of Polymer Dynamics
Conf. on "Polymers in the Third Millennium", Univ. Montpellier, France, 02.-06.09.01
23.30.0

IFF-01-21-160
Richter D.
Neutronen und die Bewegung von Polymeren - Bernd Ewen und die Folgen
Festkolloquium, MPI für Polymerforschung, Mainz, 31.08.01
23.30.0

IFF-01-21-161
Richter D.
Neutrons in Soft Condensed Matter
ILL Millennium Symposium, Grenoble, France, 06.-07.04.01
23.30.0

IFF-01-21-162
Richter D.
Neutrons in Soft Condensed Matter
Kolloquium, Universität Bayreuth, 12.06.01
23.30.0

IFF-01-21-163
Richter D.
Soft Condensed Matter
OECD Workshop on Large Facilities for Studying the Structure and Dynamics of Matter, Kopenhagen, Sweden, 19.-21.09.01
23.30.0

IFF-01-21-164
Richter D.
The European Spallation Source Project
FZJ Kolloquium, FZ Jülich, 24.08.01
23.30.0

IFF-01-21-165
Richter D.
The European Spallation Source Project
Int. Conf. on Neutron Scattering, TU München, 09.-13.09.01
23.30.0

IFF-01-21-166
Richter D.
The European Spallation Source Project
Kolloquium, Universität Bochum, 19.11.01
23.30.0

IFF-01-21-167
Richter D.
The European Spallation Source Project
Kolloquium, Universität Darmstadt, 30.11.01
23.30.0

IFF-01-21-168
Richter D.
The European Spallation Source
Deutsche Neutronenstreutagung, FZ Jülich, 20.02.01
23.30.0

IFF-01-21-169
Richter D.
The Status of the European Spallation Source Project
Journée de la Diffusion Neutronique, Tregastel, France, 16.-17.05.01
23.30.0

IFF-01-21-170
Richter D.
The Status of the European Spallation Source Project
Russian Nat. Conf. on "The use of X-ray, Synchrotron, Neutron and Electron Scattering", Dubna, Russia, 25.05.01
23.30.0

IFF-01-21-171
Richter D.
Wax Crystal Modification by Random Copolymers of the PEB-n type
Seminar, University of Princeton, USA, 29.03.01
23.30.0

IFF-01-21-172
Rickes J.; Summerfelt S.R.; Lanham R.H.; Waser R.
Circuit design issues affecting present and future deep sub-micron ferroelectric random-access memories
13th Int. Symp. Integrated Ferroelectrics, Colorado Springs, USA, 11.03.-14.03.01
23420

IFF-01-21-173
Sager W.
Phase behaviour and structural evolution in surfactant self assemblies and their employment in the preparation of (inorganic) nanoparticles and nanoporous/nanostructured (composite) materials
1st Meeting of Young Academic Chemists in the Netherlands Nijmwegen, 27.09.-28.09.2001
23.30.0

IFF-01-21-174
Schmidt W.1; Ohl M.1; Buchenau U.
1Institut Laue-Langevin, F-38042 Grenoble Cedex, France
Inelastic Neutron Scattering in Polybutadiene at Low Momentum Transfer
4th Int. Discussion Meeting on the Relaxation in Complex Systems, Crete, Greece, 17.-23.06.01
23.89.1

IFF-01-21-175
Schneider St.
Patterning of BST thin films by reactive ion etching
Workshop on "Patterning of Thin Oxide Films", Bratislava, Slovak Republic, 21.-22.06.01
23420

IFF-01-21-176
Schneider St.
Platinum high temperature etching characteristics
EMC, Notre Dame, Indicana, USA, 25.-29.06.01
23420

IFF-01-21-177
Schneider St.
Quadrupole mass spectroscopy studies of high temperature platinum etch processes
American Vacuum Society, San Francisco, USA, 29.10.-02.11.01
23.42.0

IFF-01-21-178
Schober H. R.; Caprion D.; Kluge M.
Collectivity of motion in undercooled liquids and amorphous solids
4th International Discussion Meeting on Relaxations in Complex Systems, Heraklion, Kreta, Griechenland, 21.06.2001
23.30.0

IFF-01-21-179
Schober H. R.; Caprion D.; Kluge M.
Collectivity of motion in undercooled liquids and amorphous solids
8th International workshop on disordered solids, Andalo, Trento, Italien, 12.03.2001
23.30.0

IFF-01-21-180
Schober H. R.
Atomic motion in amorphous solids
ISS PMS '2001, Jasowiec, Polen 28.-29.09.2001
23.30.0

IFF-01-21-181
Schober H. R.
Dynamik in Gläsern
Universität Heidelberg, 05.11.2001
23.30.0

IFF-01-21-182
Schober H. R.
Niederenergetische Anregungen in Gläsern
Universität Freiburg, 16.05.2001
23.30.0

IFF-01-21-183
Schweika W.
Temperature dependence of phason disorder in Al-Pd-Mn quasicrystals
Duisburg, Workshop on Dynamics in Quasicrystals, 04. - 07.12.2001

23.55.0

IFF-01-21-184
Schütz G.
Aging in quantum spin chains
Universität Nancy
25.5.2001
23.15.0

IFF-01-21-185
Schütz G.
Boundary-induced phase transitions in driven diffusive systems
Max-Planck-Institut für Kolloid- und Grenzflächenforschung, Golm
19.2.2001
23.15.0

IFF-01-21-186
Schütz G.
Diffusion and interaction of shocks in exactly solvable many-body systems
Summer School on Fundamental Problems in Statistical Mechanics, Altenberg
30.8.2001
23.15.0

IFF-01-21-187
Schütz G.
Diffusion und Wechselwirkung von Schocks in exakt lösbaren Vielteilchensystemen
Hauptvortrag der DPG-Tagung, Bonn
26.3.2001
23.15.0

IFF-01-21-188
Schütz G.
From Many Interacting Particles to Collective Few-Body Modes: Motion of Shocks in Driven Diffusive Systems
Universität Utrecht
28.3.2001
23.15.0

IFF-01-21-189
Schütz G.
From many individual particles to single collective modes: Diffusion and
interaction of shocks in nonequilibrium systems
German-American Frontiers of Science Symposium, Bad Homburg
9.6.2001
23.15.0

IFF-01-21-190
Schütz G.
Getriebene diffusive Systeme fern vom Gleichgewicht
Physikalisches Kolloquium, Universität Leipzig
15.5.2001
23.15.0

IFF-01-21-191
Schütz G.
Getriebene diffusive Systeme fern vom Gleichgewicht,
Physikalisches Kolloquium, Universitaet Ulm
22.1.2001
23.15.0

IFF-01-21-192
Schütz G.
Nonequilibrium relaxation law for entangled polymers
Dynamics Days, Dresden
5.6.2001
23.30.0

IFF-01-21-193
Schütz G.
Nonequilibrium relaxation law for entangled polymers
University of Leeds
5.10.2001
23.30.0

IFF-01-21-194
Schütz G.
Von diffundierenden Teilchen zu nichtlinearen Wellen: Phasendiagramm von
Vielteilchensystemen fern vom Gleichgewicht
Universität GH Wuppertal
29.5.2001
23.15.0

IFF-01-21-195
Schütz G.
q-deformed symmetries and multiple shocks in the asymmetric simple
exclusion process
Nankai Symposium, Tianjin
9.10.2001
23.15.0

IFF-01-21-196
Seeck O.
Röntgenstreuexperimente an Flüssigkeitsfilmen in begrenzter Geometrie
Dortmund, Universität, Physikalisches Kolloquium, 03.07.2001
23.89.1

IFF-01-21-197
Seeck O.
Röntgenstreuexperimente an Flüssigkeitsfilmen in begrenzter Geometrie
Kiel, Universität, Kolloquium der Festkörperphysik + Materialwissenschaften, 22.11.2001
23.89.1

IFF-01-21-198
Stellbrink J.
Star polymer/colloid mixtures
University of Edinburgh, UK, 27.8.01
23.30.0

IFF-01-21-199
Szot K.
Segregation in Perowskite
Schlesische Universität Katowice, Polen, 05.04.01

IFF-01-21-200
Toperverg B.
Grazing Incidence Scattering with Polarized Neutrons: A Tutorial
Argonne, USA, ANL-Seminar, 18.10.2001
23.89.1

IFF-01-21-201
Toperverg B.
Grazing Incidence Scattering with Polarized Neutrons: Examples and Applications
Argonne, USA, ANL-Seminar, 25.10.2001
23.89.1

IFF-01-21-202
Toperverg B.
Interphonon collisions
Grenoble, France, ILL, Lectures on lattice dynamics, 30.01. - 01.02.2001
23.89.1

IFF-01-21-203
Toperverg B.
Off-specular polarized neutron scattering from magnetic fluctuations in thin films and multilayers
München, ICNS-Konferenz, 09. - 13.09.2001
23.89.1

IFF-01-21-204

Toperverg B.
Phonon diffusion and localization
Grenoble, France, ILL, Lectures on lattice dynamics, 19. - 20.04.2001
23.89.1

IFF-01-21-205
Toperverg B.
Polarized Neutron Off-Specular Scattering from Magnetic Fluctuations in Films and Multilayers
Gaithersburg, USA, NIST-Seminar, 29.10.2001
23.89.1

IFF-01-21-206
Urban K.
Application of spherical-aberration corrected transmission electron microscopy in materials science
Dreiländertagung für Elektronenmikroskopie, Innsbruck/A, 9. - 14.09.2001
23.42.0

IFF-01-21-207
Urban K.
Application of spherical-aberration corrected transmission electron microscopy in materials science
Dreiländertagung für Elektronenmikroskopie, Innsbruck/A, 9. - 14.09.2001
MRS Spring Meeting, San Francisco / USA, April 2001
23.42.0

IFF-01-21-208
Urban K.
Das neue Paradigma der Elektronenmikroskopie - Aberrationskorrektur und Austrittswellenfunktionsrekonstruktion
Kolloquiumsvortrag am IFW Dresden, Dresden
23.42.0

IFF-01-21-209
Urban K.
Das neue Paradigma der Elektronenmikroskopie - Aberrationskorrektur und Austrittswellenfunktionsrekonstruktion
Kolloquiumsvortrag an der Universität Münster, Münster
23.42.0

IFF-01-21-210
Urban K.
Plasticity of Quasicrystals and related intermetallics
AMT Conference, Gdansk / Polen, September 2001
23.42.0

IFF-01-21-211
Urban K.
Structurally complex alloy phases
Chinese - German Workshop on "Modern Metallic Materials Design"
Beijing, 5 - 8 November 2001
23.42.0

IFF-01-21-212
Urban K.
The new paradigm of transmission electron microscopy
Institute of Physics, Chinese Academy of Science, Beijing, 13 July 2001
23.42.0

IFF-01-21-213
Urban K.
Wellen - Basis der Materie und der Kommunikation
Schulvorträge im "Jahr der Lebenswissenschaften", Berlin, Juni 2001
23.42.0

IFF-01-21-214
Waser R.; Meyer R.; Szot K.
Defektchemie in der Nähe von Grenzflächen dotierter Perowskite
Bunsenkolloquium "100. Geburtstag von Carl Wagner", RWTH Aachen, 09.11.01
23.42.0

IFF-01-21-215
Waser R.
Advanced chemical deposition techniques - from research to production
13th Int. Symp. Integrated Ferroelectrics, Colorado Springs, USA, 11.03.-14.03.01
E2 Waser R.
Nano-sized single grains and continuous films of ferroelectric oxides - chemical synthesis and scanning probe analysis
2001 Swiss Workshop on Materials with Novel Electronic Properties, Les Diablerets, Switzerland, 02.10.-04.10.2001
23420

IFF-01-21-216
Waser R.
Am Vorabend der nächsten Evolutionsstufe?
FZJ-Kolloquium
09.02.2001
23420

IFF-01-21-217
Waser R.
Chemical Synthesis and swtiching properties of ferroelectric thin films
IBM, Rüschlikon, Zürich, Switzerland
05.01.2001
23420

IFF-01-21-218
Waser R.
FeRAM - eine Alternative zu herkömmlichen Speichermedien ?
Technical Universität Dresden
09.01.01
23420

IFF-01-21-219
Waser R.
Ferroelektrische Oxide in der Mikro- und Nanoelektronik - Chancen und Perspektiven
Physikalisches Kolloquium, RWTH Aachen
22.01.01
23420

IFF-01-21-220
Waser R.
Neue oxidische Materialien in der Informationstechnik: Forschung für die Praxis
Gesprächskreis Management und Informatik, Gesellschaft für Informatik - Bonn, FZJ, 09.05.2001
23420

IFF-01-21-221
Waser R.
On robots and cats: the next evolution step
Advanced Materials, EPFL-ETHZ-UCSB-WIS, Cret-Bérard (Puidoux), Schweiz,
09.09.-13.09.2001
23420

IFF-01-21-222
Waser R.
Technology and design challenges of the next FeRAM generation
1st Int. Meet. Ferroelectric Random Access Memories (FeRAM 2001), Gotemba, Japan, 19.11.-21.11.2001
23.42.0

IFF-01-21-223
Willner L.
Unimer exchange kinetics in diblock copolymer micelles

DYPROSO XXVIII, 16.-19.09.01, Kerkrade, The Netherlands
23.30.0

IFF-01-21-224
Winkler R.G.; Hofmann T.1; Reineker P.1
1 Univ. Ulm, Germany
Influence of Counterions and Salt on the Structure of Polyelectrolyte Solutions
Schwerpunkt "Polyelektrolyte", Berlin
13.09.01 – 14.09.01
23.30.0

IFF-01-21-225
Winkler R.G.
Structure of Polyelectrolyte Solutions
Fachbereich Physik
Bergische Universität Wuppertal
10.12.01
23.30.0

IFF-01-21-226
Wischnewski A.; Richter D.; Monkenbusch M.; Willner L.; Farago B.1; Ehlers G.1; Schleger P.1
1Institut Laue-Langevin, F-38042 Grenoble Cedex, France
Kettendynamik in Polymerschmelzen: Grenzen des Reptationsmodells
Deutsche Neutronenstreutagung, FZ Jülich, 21.02.01
23.30.0

IFF-01-21-227
Wischnewski A.; Richter D.; Monkenbusch M.; Willner L.; Farago B.1; Ehlers G.1; Schleger P.1
1Institut Laue-Langevin, F-38042 Grenoble Cedex, France
Neutron spin echo spectroscopy on reptating polymers
4th Int. Discussion Meeting on Relaxations in Complex Systems, Crete, Greece, 18.06.01
23.30.0

IFF-01-21-228
Zeller R.
Recent developments in the full-potential KKR-method
International Conference on Applied Density Functional Theory, 14.-17.01.2001, Wien, Österreich
23.20.0

IFF-01-21-229
Zorn R.; Hartmann L.1; Frick B.2; Richter D.; Kremer F.1
1Fakultät für Physik und Geowissenschaften, Universität Leipzig, Linnéstr. 5, 04103 Leipzig
2Institut Laue-Langevin, F-38042 Grenoble Cedex, France
Inelastic neutron scattering experiments on the dynamics of a glass forming material in mesoscopic confinements
DYPROSO XXVIII, Kerkrade, The Netherlands, 19.9.2001
23.15.0

IFF-01-21-230
Zorn R.; Hartmann L.1; Frick B.2; Richter D.; Kremer F.1
1Fakultät für Physik und Geowissenschaften, Universität Leipzig, Linnéstr. 5, 04103 Leipzig
2Institut Laue-Langevin, F-38042 Grenoble Cedex, France
Low frequency vibrations in a confined glassy system
4th Int. Discussion Meeting on Relaxations in Complex Systems, Crete, Greece, 21.06.01
23.15.0

List of references

Akola J.	IFF-01-21-001	IFF-01-21-002	
Allgaier J.	IFF-01-21-003	IFF-01-21-004	IFF-01-21-005
	IFF-01-21-006	IFF-01-21-007	IFF-01-21-053
Baumgaertner A.	IFF-01-21-009	IFF-01-21-010	IFF-01-21-011
	IFF-01-21-012	IFF-01-21-013	IFF-01-21-014
Blügel S.	IFF-01-21-016		
Bos J.	IFF-01-21-081		
Brückel Th.	IFF-01-21-081	IFF-01-21-082	IFF-01-21-094
Buchenau U.	IFF-01-21-017	IFF-01-21-018	IFF-01-21-019
	IFF-01-21-020	IFF-01-21-174	
Buchmeier M.	IFF-01-21-060		
Byelov D.	IFF-01-21-053		
Byloos C.	IFF-01-21-024		
Bürgler D.E.	IFF-01-21-021	IFF-01-21-022	IFF-01-21-023
	IFF-01-21-060		
Caprion D.	IFF-01-21-178	IFF-01-21-179	
Conrad H.	IFF-01-21-024	IFF-01-21-025	
Dederichs P.H.	IFF-01-21-026	IFF-01-21-027	IFF-01-21-028
	IFF-01-21-029	IFF-01-21-030	IFF-01-21-031
	IFF-01-21-032		
Dhont J.	IFF-01-21-033	IFF-01-21-034	IFF-01-21-035
	IFF-01-21-036	IFF-01-21-037	
Divin Y.Y.	IFF-01-21-038		
Dürr H.A.	IFF-01-21-039	IFF-01-21-040	IFF-01-21-041
	IFF-01-21-042	IFF-01-21-043	IFF-01-21-044
Ebert Ph.	IFF-01-21-045	IFF-01-21-046	IFF-01-21-047
	IFF-01-21-048	IFF-01-21-049	IFF-01-21-050
Eisenriegler E.	IFF-01-21-051		
Endo H.	IFF-01-21-003	IFF-01-21-004	IFF-01-21-053
Feuerbacher M.	IFF-01-21-052		
Fischer K.	IFF-01-21-081		
Frielinghaus H.	IFF-01-21-053		
Gareev R.	IFF-01-21-060		
Gompper G.	IFF-01-21-003	IFF-01-21-054	IFF-01-21-055
	IFF-01-21-056	IFF-01-21-057	IFF-01-21-058
Grünberg P.	IFF-01-21-060	IFF-01-21-061	IFF-01-21-062
	IFF-01-21-063	IFF-01-21-064	IFF-01-21-065
	IFF-01-21-066	IFF-01-21-067	IFF-01-21-068
	IFF-01-21-069		
Gutheim F.	IFF-01-21-070		
Harris J.	IFF-01-21-071	IFF-01-21-072	IFF-01-21-073
	IFF-01-21-074		
Hartmann M.	IFF-01-21-075		
Haubold H.-G.	IFF-01-21-076		
Heinrich M.	IFF-01-21-156		

Hoffmann S.	IFF-01-21-077	IFF-01-21-078	
Hoffmann-Eifert S.	IFF-01-21-079	IFF-01-21-080	
Hupfeld D.	IFF-01-21-081	IFF-01-21-082	IFF-01-21-083
	IFF-01-21-084		
Ioffe A.	IFF-01-21-085		
Jones R.O.	IFF-01-21-086	IFF-01-21-087	IFF-01-21-088
	IFF-01-21-089	IFF-01-21-090	
Jung P.	IFF-01-21-091	IFF-01-21-092	IFF-01-21-107
Kahle S.	IFF-01-21-093		
Kentzinger E.	IFF-01-21-094		
Kirstein O.	IFF-01-21-095		
Kluge M.	IFF-01-21-178	IFF-01-21-179	
Kohlstedt H.	IFF-01-21-096	IFF-01-21-097	IFF-01-21-098
	IFF-01-21-099		
Kuanr B.	IFF-01-21-060		
Lang P.	IFF-01-21-100		
Liebsch A.	IFF-01-21-101	IFF-01-21-102	IFF-01-21-103
	IFF-01-21-104	IFF-01-21-105	IFF-01-21-106
Lustfeld H.	IFF-01-21-015	IFF-01-21-108	IFF-01-21-109
	IFF-01-21-110		
Luysberg M.	IFF-01-21-111	IFF-01-21-112	IFF-01-21-113
	IFF-01-21-114	IFF-01-21-115	
Meier G.	IFF-01-21-116		
Mihailescu M.	IFF-01-21-003		
Monkenbusch M.	IFF-01-21-003	IFF-01-21-118	IFF-01-21-119
	IFF-01-21-159	IFF-01-21-226	IFF-01-21-227
Müller-Krumbhaar H.	IFF-01-21-070	IFF-01-21-120	IFF-01-21-121
	IFF-01-21-122	IFF-01-21-123	IFF-01-21-124
	IFF-01-21-125	IFF-01-21-126	IFF-01-21-127
Nägele G.	IFF-01-21-128	IFF-01-21-129	IFF-01-21-130
Persson B.N.J.	IFF-01-21-131	IFF-01-21-132	IFF-01-21-133
	IFF-01-21-134	IFF-01-21-135	IFF-01-21-136
	IFF-01-21-137	IFF-01-21-138	IFF-01-21-139
	IFF-01-21-140	IFF-01-21-141	IFF-01-21-142
	IFF-01-21-143	IFF-01-21-144	IFF-01-21-145
	IFF-01-21-146	IFF-01-21-147	IFF-01-21-148
	IFF-01-21-149	IFF-01-21-150	IFF-01-21-151
	IFF-01-21-152		
Popkov V.	IFF-01-21-153		
Poppe U.	IFF-01-21-038		
Prager M.	IFF-01-21-095	IFF-01-21-154	IFF-01-21-155
Pyckhout-Hintzen W.	IFF-01-21-156	IFF-01-21-157	IFF-01-21-158
Richter D.	IFF-01-21-003	IFF-01-21-004	IFF-01-21-053
	IFF-01-21-157	IFF-01-21-159	IFF-01-21-160
	IFF-01-21-161	IFF-01-21-162	IFF-01-21-163
	IFF-01-21-164	IFF-01-21-165	IFF-01-21-166
	IFF-01-21-167	IFF-01-21-168	IFF-01-21-169
	IFF-01-21-170	IFF-01-21-171	IFF-01-21-226
	IFF-01-21-227	IFF-01-21-229	IFF-01-21-230

Rickes J.	IFF-01-21-008	IFF-01-21-172	
Rücker U.	IFF-01-21-094		
Sager W.	IFF-01-21-173		
Schneider St.	IFF-01-21-175	IFF-01-21-176	IFF-01-21-177
Schober H. R.	IFF-01-21-178	IFF-01-21-179	IFF-01-21-180
	IFF-01-21-181	IFF-01-21-182	
Schweika W.	IFF-01-21-183		
Schütz G.	IFF-01-21-184	IFF-01-21-185	IFF-01-21-186
	IFF-01-21-187	IFF-01-21-188	IFF-01-21-189
	IFF-01-21-190	IFF-01-21-191	IFF-01-21-192
	IFF-01-21-193	IFF-01-21-194	IFF-01-21-195
Seeck O.	IFF-01-21-081	IFF-01-21-196	IFF-01-21-197
Shadrin P.	IFF-01-21-038		
Shirotov V.	IFF-01-21-038		
Stellbrink J.	IFF-01-21-053	IFF-01-21-198	
Szot K.	IFF-01-21-199	IFF-01-21-214	
Toperverg B.	IFF-01-21-094	IFF-01-21-200	IFF-01-21-201
	IFF-01-21-202	IFF-01-21-203	IFF-01-21-204
	IFF-01-21-205		
Urban K.	IFF-01-21-038	IFF-01-21-206	IFF-01-21-207
	IFF-01-21-208	IFF-01-21-209	IFF-01-21-210
	IFF-01-21-211	IFF-01-21-212	IFF-01-21-213
Voigt J.	IFF-01-21-081	IFF-01-21-082	
Waser R.	IFF-01-21-059	IFF-01-21-079	IFF-01-21-117
	IFF-01-21-172	IFF-01-21-214	IFF-01-21-215
	IFF-01-21-216	IFF-01-21-217	IFF-01-21-218
	IFF-01-21-219	IFF-01-21-220	IFF-01-21-221
	IFF-01-21-222		
Willner L.	IFF-01-21-159	IFF-01-21-223	IFF-01-21-226
	IFF-01-21-227		
Winkler R.G.	IFF-01-21-224	IFF-01-21-225	
Wischnewski A.	IFF-01-21-017	IFF-01-21-159	IFF-01-21-226
	IFF-01-21-227		
Zeller R.	IFF-01-21-228		
Zorn R.	IFF-01-21-017	IFF-01-21-229	IFF-01-21-230

Other talks

IFF-01-22-001
Antons A.; Berger R.; Blügel S.; Schroeder K.
Ab-initio Untersuchung des Wachstums kleiner Si Cluster auf As und Sb bedecktem Si(111)
DPG-Frühjahrstagung, Hamburg, 29.03.2001
23.42.0

IFF-01-22-002
Bachhofer H.; Reisinger H.; Steinlesberger G.; Nagel N.; Cerva H.; von Philipsborn H.; Schroeder H.; Waser R.
Interfacial layers and their effect on leakage current in MOCVD-deposited SBT thin films
13th Int. Symp. Integrated Ferroelectrics, Colorado Springs, USA, 11.03.-14.03.01
23.42.0

IFF-01-22-003
Blügel S.; Kromen Wi.; Schroeder K.
Implementierung und Anwendung einer Projektor-Augmentierten Wellen (PAW) Methode für die ab-initio Molekulardynamik
DPG-Frühjahrstagung, Hamburg, 29.03.2001
23.42.0

IFF-01-22-004
Brückel Th.
Hyperpolarisiertes 3He-Gas magnetisiert Neutronenstrahlen
Jülich, Workshop "Anwendung hyperpolarisierter Gase", 05.07.2001
23.89.1

IFF-01-22-005
Brückel Th.
Science at ILL - Plenary Discussion
Grenoble, France, ILL Millennium Symposium, 06. - 07.04.2001
23.89.1

IFF-01-22-006
Brückel Th.
Structural and Magnetic Characterization of Multilayers by Scattering Methods
Jülich, "Midterm Meeting Strategiefonds Magnetoelektronik", 22.11.2001
23.89.1

IFF-01-22-007
Böttger U.; Hoffmann-Eifert S.
Dielelectric high frequency characteristics of (Ba,Sr)TiO3 thin films on silicon for microwave device applications
13th Int. Symp. Integrated Ferroelectrics, Colorado Springs, USA, 11.03.-14.03.01
23.42.0

IFF-01-22-008
Böttger U.; Lohse O.; Grossmann M.; Waser R.
Inherent contributions to the frequency dependence of the coercive voltage of ferroelectric thin films
MRS 2001, Boston, USA, 25.11.-29.11.01
23.42.0

IFF-01-22-009
Bürgler D.E.
Interlayer exchange coupling across conducting and non-conducting iron-silicide spacers with varying Si content
46th Annual Conference on Magnetism & Magnetic Materials
Seattle, Washington
14.11.2001
23.42.0

IFF-01-22-010
Bürgler D.E.
Magnetic interlayer exchange coupling in Fe/Si/Fe systems
CNRS Strasbourg, Frankreich
02.07.2001
23.42.0

IFF-01-22-011
Bürgler D.E.
Magnetische Zwischenschichtkopplung in Fe/FeSi/Fe Systemen
IFF-Beiratssitzung
26.04.2001
23.42.0

IFF-01-22-012
Cao Y.; Antons A.; Berger R.; Kromen Wi.; Schroeder K.; Blügel S.
Stability and adatom dynamics on surfactant covered growing Ge(111) films
DPG-Frühjahrstagung, Hamburg, 29.03.2001
23.42.0

IFF-01-22-013
Chen J.; Carsughi F.1; Henry J.; Jung P.; Ullmaier H.
1University of Ancona, DIBIAGA, Italy
Summary of Radiation Damage Studies in ESS Target Structural Materials
Seggau, Austria, 7th General ESS Meeting, 27.- 29.09.2001
23.60.0

IFF-01-22-014
Chen J.; Ullmaier H.; Dai Y.1; Carsughi F.2; Maloy S. A.3; Sommer W.3; Broome T.4
1PSI, Spallation Neutron Source Division, Villigen, Switzerland
2University of Ancona, DIBIAGA, Italy
3Los Alamos National Laboratory, USA
4Rutherford Appleton Laboratory, Chilton, UK
Mechanical Properties of spent windows and target components from spallation sources
Brasimone, Italy, 2nd International Workshop on Materials for Hybrid Reactors and Related Technologies, 18. - 20.04.2001
23.60.0

IFF-01-22-015
Chen J.
Present and Future Work on Radiation Damage in ESS Target Structural Materials
Monschau, ESS-Tag, 10. - 11.05.2001
23.60.0

IFF-01-22-016
Conrad H.
Experimental results on intensities and life times of various target-moderator-reflector assemblies
Berlin, Moderator Concepts and Optimization for Spallation Neutron Sources, 13.03.2001
23.60.0

IFF-01-22-017
Conrad H.
Stress wave experiments with the ASTE mercury target
Oak Ridge, USA, 3rd International Workshop on Mercury Target Development, 19.11.2001
23.60.0

IFF-01-22-018
Dederichs P.H.; Cabria I.; Nonas B.; Zeller R.
Spin- und Bahnmagnetismus von Übergangsmetall-Adatomen und -Clustern auf Ag und Au-Oberflächen
DPG-Frühjahrstagung, Hamburg, 28.03.2001
23.20.0

IFF-01-22-019
Dederichs P.H.; Cabria I.; Nonas B.; Zeller R.
Strongly enhanced orbital moments and anisotropies of single adatoms and small clusters on Ag(001) and Pt(111)
APS March Meeting, Seattle, USA, 12.03.2001
23.20.0

IFF-01-22-020
Dederichs P.H.

Ballistic spininjection from Fe into ZnSe and GaAs
Midterm-Meeting-Strategiefonds Magnetoelektronik,
22.11.2001, Jülich
23.20.0

IFF-01-22-021
Divin Y.Y.; Poppe U.; Jia C.L.; Shadrin P.M.; Urban K.
Structural and electrical properties of YBa2Cu3O7 [100]-tilt grain boundary Josephson junctions with high IcRn-products on SrTiO3 bicrystals
5th European Conf. Appl. Supercond.,
Copenhagen/Dänemark, 26.-30. August (2001)
23.42.0

IFF-01-22-022
Divin Y.Y.; Volkov O. Y.1; Laytti M.; Shirotov V.V.; Pavlovskii V.V.1; Poppe U.; Shadrin P.M.; Urban K.
1 Institute of Radioengineering & Electronics of RAS, Moscow 103907, Russian Federation
Hilbert spectroscopy from gigahertz to terahertz frequencies by high-Tc Josephson junctions
26th Int. Conf. Infrared and Millimeter Waves, September 10-14, 2001, Toulouse, France
23.42.0

IFF-01-22-023
Divin Y.Y.; Volkov O.Y.1; Laytti M.; Shirotov V.V.; Pavlovskii V.V.1; Poppe U.; Shadrin P.M.; Urban K.
1 Institute of Radioengineering & Electronics of RAS, Moscow 103907, Russian Federation
Hilbert spectroscopy from microwave to terahertz frequencies by high-Tc Josephson junctions
5th European Conf. Appl. Supercond.,
Copenhagen/Dänemark, 26.-30. August (2001)
23.42.0

IFF-01-22-024
Dürr H.A.
Magnetic ordering phenomena probed by soft x-ray spectroscopy
Plenary Talk, 4th International Conference on Inelastic X-ray Scattering, Haikko, Finland
22.08.2001
23.20.0

IFF-01-22-025
Ebert Ph.; Kluge F.; Cai T.1; Grushko B.; Thiel P.A.1; Urban K.
1 Ames Laboratory, Ames, Iowa
Surface structure of Al-Pd-Mn quasicrystals: effect of bulk vacancies.
Quasicrystals 2001, Sendai, Japan, September 24-28, 2001
23.55.0

IFF-01-22-026
Ebert Ph.; Semmler U.; Simon M.; Urban K.
Stoichiometry changes by selective vacancy formation on (110) surfaces of III-V semiconductors: Influence of electronic effects.
Materials Research Society Fall Meeting, Boston, Massachusetts, November 26-30, 2001.
23.42.0

IFF-01-22-027
Faley M.I.; Poppe U.; Urban K.; Paulson D.N.1; Starr T.N.1; Fagaly R.L.1
1 Tristan Technologies Inc., CA 92121, USA
Low noise HTS dc-SQUID flip-chip magnetometers and gradiometers
DPG Frühjahrstagung, Hamburg 26.-30. März (2001)
23.42.0

IFF-01-22-028
Fitsilis F.; Regnery S.; Waser R.; Ehrhart P.
Structure property relations of BST thin films
13th Int. Symp. Integrated Ferroelectrics, Colorado Springs, USA, 11.03.-14.03.01
23.42.0

IFF-01-22-029
Galanakis I.; Papanikolaou N.*; Dederichs P.H.
*Martin-Luther-Universität Halle-Wittenberg, FB Physik, Halle
Half-metallic Heusler alloys: bulk and surface properties
1st Annual Meeting of the Research Training Network "Computational Magnetoelectronics", 27.-30.09.2001, Budapest, Ungarn
23.20.0

IFF-01-22-030
Gareev R.
Very strong interlayer exchange coupling in Fe/Fe1-xSix/Fe (x=0.4-1.0) epitaxial trilayers
4th International Symposium on Metallic Multilayers, Aachen, Deutschland
27.06.2001
23.42.0

IFF-01-22-031
Goerigk G.
Materialforschung mit Synchrotronstrahlung am Beispiel der anomalen Röntgen-Kleinwinkelstreuung
Hamburg, Graduiertenkolleg des Fachbereichs Chemie der Universität, 19.12.2001
23.89.1

IFF-01-22-032
Gompper G.
Structure and Phase Behavior of Membrane Ensembles
Vortrag auf der "2nd Conference on Spatial Statistics and Statistical Physics", Wuppertal
05.-09. März 2001
23.30.0

IFF-01-22-033
Grünberg P.; Bürgler D.E.; Gareev R.; Kuanr B.
Magnetoelektronik: Vom Kompass zum Datenspeicher
Plenarvortrag auf der 65. Physikertagung Hamburg 2001
30.03.2001
23.42.0

IFF-01-22-034
Gutheim F.; Brener E. A.; Müller-Krumbhaar H.
Epitaktisches Wachstum unter elastischer Wechselwirkung: Lagen und Cluster-Wachstum
DPG-Frühjahrstagung, Hamburg, 26.-30.03.01
23.15.0

IFF-01-22-035
Hauck J., Mika K.
Self-Assembly of homogeneous systems
Steinfurter-Keramik-Seminar v. 28.11.-01.12.01
23.30.0

IFF-01-22-036
Hauck J.
Self-Assembly of Homogeneous Systems
XV Conference of the European Colloid and Interface Society
Coimbra, Portugal; 16.09.-21.09.2001
23.30.0

IFF-01-22-037
Hoffmann M.; Böttger U.; Waser R.
PZT and PMN-PT thin films cantilevers: Comparison between monomorph and bimorph structures
MRS 2001, Boston, USA, 25.11.-29.11.01
23.42.0

IFF-01-22-038
Hoffmann-Eifert S.; Ohly Ch.; Szot K.; Waser R.
High temperature conduction behavior and segregation phenomena in SrTiO3 and BaTiO3 thin films:
MRS 2001, Boston, USA, 25.11.-29.11.01
23.42.0

IFF-01-22-039

Hoffmann-Eifert S.; Ohly Ch.; Waser R.
Influence of morphology on the high-temperature conduction behavior of SrTiO3 and BaTiO3 thin films
MRS Fall meeting 2001, Boston, USA, 25.11.-29.11.01
23.42.0

IFF-01-22-040
Hoffmann-Eifert S.; Ritter S.; Waser R.
Growth of lead barium titanate thin films by MOCVD: structural and electrical characterization
MRS 2001, Boston , USA, 25.11.-29.11.01
23.42.0

IFF-01-22-041
Houben L.
Growth of microcrystalline nip solar cells: role of local epitaxy
ICAMS 19, Nizza, August 2001
23.42.0

IFF-01-22-042
Ioffe A.; Vrana M.1
1CAS, Nuclear Physics Institute, Rez near Prague, Czech
A new neutron interferometry approach to the determination of the n-e interaction amplitude
Grenoble, France, ILL, PECNO Workshop, 01. - 04.03.2001
23.89.1

IFF-01-22-043
Ioffe A.
A new triple-axis spectrometer of polarized thermal neutrons at the FZ Jülich
Garching, Seminar, 19.01.2001
23.89.1

IFF-01-22-044
Ioffe A.
Monte Carlo simulations of Neutron Speed Echo Spectrometer
Didcot, UK, ENPI-Meeting, 27. - 30.06.2001
23.89.1

IFF-01-22-045
Jahnen B.; Luysberg M.; Urban K.; Bracht H.1; Schmidt R.2; Ungermanns C.2; Bleuel T.3
1 Institut für Materialphysik, Universität Münster
2 ISG, FZ Jülich
3 Fachbereich Physik, Universität Würzburg
Interdiffusion in GaSb/AlxGa1-xSb heterostructures
XIIth Conference on Microscopy of Semiconducting Materials, 22-25 March 2001, Oxford, Microscopy of Seminconducting Materials 2001.
23.42.0

IFF-01-22-046
Jahnen B.
Interdiffusion in GaSb/AlxGa1-xSb heterostructures
XIIth Conference on Microscopy of Semiconducting Materials, 22-25 March 2001, Oxford
23.42.0

IFF-01-22-047
Jung P.; Liu C.
Desorption of Hydrogen from Pre-irradiated and Helium-implanted Low Activation Martensitic Stainless Steels
Baden-Baden, 10th International Conference on Fusion Reactor Materials, 14. - 19.10.2001
23.60.0

IFF-01-22-048
Jung P.
Irradiation Effects on Hydrogen Diffusion and Permeation
Petten, The Netherlands, EU-EFDA 2000 Monitoring and 2001 Kick-off Meeting, 27. - 28.02.2001
23.60.0

IFF-01-22-049
Jung P.
Microstructure of C-containing materials, Be, W, SiC, and oxide ceramics with high helium concentrations
Garching, EU-EFDA Monitoring on Underlying Technology, 11. - 12.07.2001
23.60.0

IFF-01-22-050
Kirch D.
Relaxationsmechanismen in He-implantierten SiGe Pufferschichten
DPG Frühjahrstagung Hamburg, März 2001
23.42.0

IFF-01-22-051
Kirstein O.; Kozielewski T.; Prager M.; Andersen K.H.1
1ISIS Facility, Rutherford Appleton Laboratory, Chilton, Didcot, Oxon, OX11 0QX, UK
A 0.9 micro eV backscattering spectrometer at the European Spallation Source (ESS)
7th General ESS Meeting, Seggau, Austria, 26.-29.09.01
23.89.1

IFF-01-22-052
Kirstein O.; Prager M.; Johnson M.R.1, Parker S.F.2
1Institut Laue Langevin, BP 156, F-38042 Grenoble Cedex 9, France
2ISIS Facility, Rutherford Appleton Laboratory, Chilton, Didcot, Oxon OX11, 0QX, UK
Lattice dynamics and methyl group rotation of 2-butyne
Int. Conf. on Neutron Scattering, TU München, 09.-13.09.01
23.15.0

IFF-01-22-053
Kirstein O.; Prager M.; Johnson M.R.1; Parker S.F.2
1Institut Laue Langevin, 6, rue Jules Horowitz, BP 156, F-38042 Grenoble Cedex 9, France
2ISIS Facility, Rutherford Appleton Laboratory, Chilton, Didcot, Oxon OX11, 0QX, UK
Lattice dynamics and methyl group rotation of dimethylacetylene
QAMTS 2001, Nottingham, UK, 05.-08.09.01
23.15.0

IFF-01-22-054
Klingeler R.
A metallic endohedral fullerene: La@C60
7th European Conference on Atomic and Molecular Physics (ECAMP) und DPG-Frühjahrstagung
2. - 6. April 2001, Berlin
23.20.0

IFF-01-22-055
Kohlstedt H.; Pertsev N.A.; Waser R.
Size Effects on polarization in epitaxial ferroelectric thin films
MRS 2001, Boston, USA, 25.11.-29.11.01
23.42.0

IFF-01-22-056
Kohlstedt H.; Pertsev N.A.; Waser R.
Size effects on polarization in epitaxial ferroelectric thin films
MRS 2001, Boston, USA, 25.11.-29.11.01
23.42.0

IFF-01-22-057
Köbler U.
Experimentelle Fakten gegen die Gültigkeit der Bloch-Kubo-Dyson Spinwellentheorie
Karlsruhe, Universität, Seminar des Physikalischen Instituts, 14.05.2001
23.15.0

IFF-01-22-058
Köbler U.
The impact of fourth-order exchange interactions on spin dynamics, order parameters and critical magnetic behaviour
Prag, Tschechische Republik, Karls Universität, 07.05.2001
23.15.0

IFF-01-22-059
Lauter-Pasyuk V.1,2; Lauter H. J.3; Toperverg B.4,5; Nikonov O.2,3; Kravtsov E.6; Ustinov V.6
1TUM, Physik Department, Garching
2Joint Institute for Nuclear Research, Dubna, Russia
3ILL, Grenoble, France
4PNPI, Gatchina, Russia
5FZJ, IFF, Jülich
6Institute of Metal Physics, Ekaterinburg, Russia
Magnetic domains in Fe/Cr multilayers
Jülich, Deutsche Neutronenstreutagung 2001, 19. - 21.02.2001
23.89.1

IFF-01-22-060
Lohse O.; Böttger U. Grossmann M.; Bolten D.; Waser R.
Polarization switching behavior of Nb doped PZT thin films
13th Int. Symp. Integrated Ferroelectrics, Colorado Springs, USA, 11.03.-14.03.01
23.42.0

IFF-01-22-061
Luysberg M.; Kirch D.; Trinkaus H.; Holländer B.1; Lenk St.1; Mantl S.1; Herzog H.-J.2; Hackbarth T.2; Fichtner P.F.P.3
1 ISG, FZ Jülich
2 Daimler Crysler AG, Research and Technology, 89081 Ulm
3 Dept. de Metallurgia, Univ. Fed Do Rio Grande do Sul, 91501-970 Porto
Relaxation of Si1-xGex Buffer Layers on Si(100) through Helium Ion Implantation
MRS Spring Meeting, San Francisco, April 2001
23.42.0

IFF-01-22-062
Luysberg M.; Kirch D.; Trinkaus H.; Holländer B.1; Lenk St.1; Mantl S.1; Herzog H.-J.2; Hackbarth T.2; Fichtner P.F.P.3
1 ISG, FZ Jülich
2 Daimler Crysler AG, Research and Technology, 89081 Ulm
3 Dept. de Metallurgia, Univ. Fed Do Rio Grande do Sul, 91501-970 Porto
Relaxation of Si1-xGex Buffer Layers on Si(100) through Helium Ion Implantation
Proceedings of the XIIth Conference on Microscopy of Semiconducting Materials, 22-25 March 2001, Oxford/UK
23.42.0

IFF-01-22-063
Luysberg M.; Meertens D.; Herfort J.1; Ulrici W.1; Moreno M.1; Ploog K.H.1
1 Paul Drude Institut, Hausvogteiplatz 5-7, 10117 Berlin
Structural Properties of Carbon doped LT-GaAs
3rd Symposium on non-stoichiometric III-V compounds, Erlangen, Oktober 2001
23.42.0

IFF-01-22-064
Luysberg M.; Scholten C.; Houben L.; Carius R.1; Finger F.1; Vetterl O.1
1 IPV, FZ Jülich
Structural Properties of microcrystalline Si solar cells
MRS Spring Meeting, San Francisco, April 2001
23.42.0

IFF-01-22-065
Lüttgens G.; Pontius N.; Bechthold P.S.; Neeb M.; Eberhardt W.
Femtosecond-time-resolved fragmentation of metal-carbonylclusters
The 7th European Conference on Atomic and Molecular Physics (ECAMP) und
DPG-Frühjahrstagung Berlin,
03.04.01
23.20.0

IFF-01-22-066
Massalovitch S.
Neutron image plate detector
Mailand, Italy, TECHNI-Meeting, 03. - 04.05.2001
23.89.1

IFF-01-22-067
Mavropoulos Ph.; Wunnicke O.; Papanikolaou N.*; Zeller R.; Dederichs P.H.
*Martin-Luther-Universität Halle-Wittenberg, FB Physik, Halle
Ballistic spininjection through Fe/ScFe junctions
1st Annual Meeting of the Research Training Network "Computational Magnetoelectronics", 27.-30.09.2001, Budapest, Ungarn
23.20.0

IFF-01-22-068
Monkenbusch M.; Mihailescu M.; Allgaier J.; Richter D.; Jakobs B.1; Sottmann T.1
1Institut für Physikalische Chemie, Universität zu Köln, Luxemburger Str. 116, 50939 Köln
Interface Dynamics in bicontinuous microemulsions investigated by neutron spin echo spectroscopy
75th ACS Conference "Colloids 2001", Pittsburgh, USA, 10.-13.06.01
23.30.0

IFF-01-22-069
Monkenbusch M.; Richter D.; Mezei F.1; Pappas C.1
1Hahn-Meitner-Institut, Glienicker Straße 100, 14109 Berlin
High resolution time-of-flight spin-echo spectrometer
EFAC Meeting, Oak Ridge, USA, 27.03.01
23.30.0

IFF-01-22-070
Monkenbusch M.
Neutron spin echo investigation of the membrane dynamics in bicontinuous microemulsions
Int. Conf. on Neutron Scattering, TU München, 09.-13.09.01
23.30.0

IFF-01-22-071
Neeb M.
Pump-probe Elektronenspektroskopie an Metall und Metall-Carbonylclustern
268. WE-Heraeus Seminar, Cluster 2001, Herzogenhorn
07.10. - 12.10.2001
23.20.0

IFF-01-22-072
Ohly Ch.; Hoffmann-Eifert S.; Szot K.; Waser R.
Alkaline earth titanate thin films - the conduction behavior of doped BST
13th Int. Symp. Integrated Ferroelectrics, Colorado Springs, USA, 11.03.-14.03.01
23.42.0

IFF-01-22-073
Pipich V.; Schwahn D.; Willner L.
Small angle neutron scattering in the vicinity of a double critical point in a ternary polymer blend
Physics of liquid matter: Modern problems, Kiev, Ukraine, 14.-19.09.01
23.30.0

IFF-01-22-074
Pithan Ch.
Synthese von nano-BatiO3 Pulvern über Mikroemulsionen
NANOMAT-Workshop "Trend", Reinstorf, Lüneburger Heide, 21.-23.10.2001
23.42.0

IFF-01-22-075
Rodriguez-Contreras J.; Poppe U.; Szot K.; Jia C.L.; Kohlstedt H.; Waser R.
Structural and ferroelectric properties of PbZr0.52Ti0.48O3/SrRuO3 thin films on SrTiO3 substrates
MRS 2001, Boston, USA, 25.11.-29.11.01
23.42.0

Rodriguez-Contreras J.
Rodriguez-Contreras J.
Experimental Approach to Investigate the Influence of Ferroelectricity on a Tunnel Current
MRS 2001, boston, USA, 25.11.-29.11.01
E223.42.002

IFF-01-22-076
Rodriguez-Contreras J.
Sputtered PbZr0.52Ti0.48O3/SrRuO3 films on SrTiO3-substrates
DPG Tagung, Hamburg, 26.-30.03.01
23.42.0

IFF-01-22-077
Roelofs A.; Pertsev N.A.; Waser R.
Depolarizing-field-induced 180o switching of a-domains in polydomain epitaxial PZT thin films by AFM
MRS 2001, Boston USA, 25.11.-29.11.01
23.42.0

IFF-01-22-078
Rücker U.
Untersuchung lateral strukturierter magnetischer Vielfachschichten
Berlin, Hahn-Meitner-Institut, Workshop Magnetismus und Streumethoden, 22.06.2001
23.89.1

IFF-01-22-079
Sager W., Woudenberg F.C.M.1, Sibelt N.G.M.1, Verweij H.1
1Universität Twente
Characterisation of nanosized oxide particles and ceramic nanocomposite coatings prepared via modified emulsion precipitation
Steinfurter-Keramik-Seminar v. 28.11.-01.12.01
23.30.0

IFF-01-22-080
Schlapp M.
Development of neutron storage phosphors with low (-sensitivity
Mailand, Italy, TECHNI-Meeting, 03. - 04.05.2001
23.89.1

IFF-01-22-081
Schmitz S.; Schroeder H.
Electrical characterization of SrTiO3 thin films
13th Int. Symp. Integrated Ferroelectrics, Colorado Springs, USA, 11.03.-14.03.01
23.42.0

IFF-01-22-082
Schneider St.; Kohlstedt H.; Waser R.
The role of carbonylchemistry to pattern platinum electrodes
MRS 2001, Boston, USA, 25.11.-29.11.01
23.42.0

IFF-01-22-083
Schneider St.
Anisotropic plasma etching of BST thin films for Gigabit-DRAM integration and what to learn for MOCVD reactor cleaning
Aixtron AG, Aachen, 20.09.01
23.42.0

IFF-01-22-084
Schneider St.
High temperature platinum etch processes
Texas Instruments, Dallas, USA 05.11.01
23.42.0

IFF-01-22-085
Schneider St.
SiO2 etch with the ICP sources of OPT's Ionfab300+: Reliability and contamination issues
Characterizing the wafer clamping and heat conduction efficiency in OPT's Ionfab300+ with a SensArray wafertemperature probe
Characterizing of OPT's Ionfab300 + Ionsource by energy dispersive quadrupole mass spectrometry using Hiden's EPQ
Seminar at Oxford Plasmatechnology, Yatton, Great Britain, 07.-08.08.01
23.42.0

IFF-01-22-086
Schober H. R.; Kluge M.
Atomare Hüpfprozesse in Cu33Zr67: Bestimmung von Sprungweiten und Wartezeiten
DPG-Frühjahrstagung, Hamburg, 26.03.2001
23.30.0

IFF-01-22-087
Schwahn D.; Willner L.
Phase Behavior of Binary Polybutadiene Copolymer Mixtures as an Example of Weakly Interacting Polymers
Int. Conf. on Neutron Scattering, TU München, 09.-13.09.01
23.30.0

IFF-01-22-088
Schwahn D.; Willner L.
Phase Behavior of Binary Polybutadiene Copolymer Mixtures as an Example of
Weakly Interacting Polymers
Jülich Soft Matter Days, Kerkrade, The Netherlands, 14.11.01
23.30.0

IFF-01-22-089
Schwahn D.; Willner L.
Phase Behavior of weakly Interacting Binary Polybutadiene Copolymer Mixtures with different Vinyl Content
222nd ACS National Meeting, Chicago, USA, 27.08.01
23.30.0

IFF-01-22-090
Seeck O.
Analysis by Diffraction and Fluorescence Methods
Jülich, 32. Ferienkurs des Instituts für Festkörperforschung, Neue Materialien für die Informationstechnik, 05. - 16.03.2001
23.89.1

IFF-01-22-091
Semmler U.; Simon M.; Ebert Ph.; Urban K.
Stöchiometrieänderungen durch selektive Leerstellenbildung auf (110)-Oberflächen von III-V-Halbleitern: Einfluß elektronischer Effekte
Frühjahrtagung der Deutschen Physikalischen Gesellschaft, Hamburg, Germany, 26.-30.3.2001.
23.42.0

IFF-01-22-092
Shur V.; Nikolaeva E.; Shishkin E.; Baturin I.; Lohse O.; lBolten D.; Waser R.
Fatigue and rejunenation phenomena in PZT thin films
13th Int. Symp. Integrated Ferroelectrics, Colorado Springs, USA, 11.03.-14.03.01
23.42.0

IFF-01-22-093
Spatschek R.; Brener E. A.; Müller-Krumbhaar H.
Theorie der Rißbildung
Arbeitstreffen RWTH Aachen, Altenberg, 26.09.2001
23.15.0

IFF-01-22-094
Spatschek R.; Brener E. A.; Müller-Krumbhaar H.
Vergröberung von Rissen
DPG-Frühjahrstagung, Hamburg, 29.03.2001
23.15.0

IFF-01-22-095
Stein S.; Kohlstedt H.

Influence of spin-polarized injection currents on magnetic tunnelling junctions (O)
JEMS, Grenoble, 28.08.-01.09.01
23.42.0

IFF-01-22-096
Stein S.; Kohlstedt H.
Magneto tunneling injection device
DPG-Tagung, Hamburg, 26.-30.03.01
23.42.0

IFF-01-22-097
Stein S.; Kohlstedt H.
Spin-injection effects in three terminal magnetic tunnelling junctions
MRS 2001, Boston, USA, 25.-30.11.01
23.42.0

IFF-01-22-098
Steinlesberger G.; Reisinger H.; Bachhofer H.; Schroeder H.; Werner W.
Dielectric relaxation and charge carrier transport mechanisms in (Ba,Sr)TiO3 thin films
13th Int. Symp. Integrated Ferroelectrics, Colorado Springs, USA, 11.03.-14.03.01
23.42.0

IFF-01-22-099
Stellbrink J.
Partial Structure Factors in Star polymer/colloid mixtures
Int. Conf. on Neutron Scattering, TU München, 09.-13.09.01
23.30.0

IFF-01-22-100
Stellbrink J.
Partial Structure Factors in Star polymer/colloid mixtures
Jülich Soft Matter Days, Kerkrade, The Netherlands, 14.11.01
23.30.0

IFF-01-22-101
Tillmann K.
Beryllium dopant induced stabilization against intermixing and precipitation upon annealing of LT-GaAs/GaAs:Be multiple quantum wells
3rd Symposium on non-stoichiometric III-V Compounds, Erlangen, Oktober 2001
23.42.0

IFF-01-22-102
Tillmann K.
Mechanisms of Interdiffusion and thermal stability during annealing of AlAs/GaAs:Be quantum wells grown under low temperature conditions
XIIth Conference on Microscopy of Semiconducting Materials, 22-25 March 2001, Oxford
23.42.0

IFF-01-22-103
Waser R.
Oxidkeramische Materialien in der Mikroelektronik und Nanotechnologie
NANOMAT-Meeting 2. Szene, Karlsruhe, 05.04.01
E234

IFF-01-22-104
Willner L.; Poppe A.; Allgaier J.; Monkenbusch M.; Richter D.
Determination of the relaxation kinetics in a PEP-PEO/DMF micellar system by time-resolved SANS
ACS Conf., Colloids and Surface Science Symposium, Pittsburgh, USA, 10.-13.06.01
23.30.0

IFF-01-22-105
Wirth I.
Scanning tunneling spectroscopy of endohedrally doped fullerenes
The 7th European Conference on Atomic and Molecular Physics (ECAMP) und
DPG-Frühjahrstagung Berlin
03.04.01
23.20.0

IFF-01-22-106
Wischnewski A.; Willner L.; Monkenbusch M.; Richter D.; Farago B.1; Ehlers G.1; Schleger P.1
1Institut Laue-Langevin, F-38042 Grenoble Cedex, France
Constraints of motion in polymer melts: coherent and incoherent scattering analyzed by neutron-spin-echo spectroscopy
Int. Conf. on Neutron Scattering, TU München, 09.-13.09.01
23.30.0

IFF-01-22-107
Wortmann D.; Bihlmayer G.; Blügel S.; Ishida H.1
1College of Humanities and Science, Nihon University, Sakura-josui, Tokyo, Japan
A transfer matrix method for ballistic transport: MgO(Fe(001)
1st Annual Meeting of the Research Training Network "Computational Magnetoelectronics", Budapest, Hungary
27. - 30.09.2001
23.20.0

IFF-01-22-108
Wosik J.; Penkalla H.J.; Szot K.; Dubiel B.; Buffat P.A.; Czyrska-Filemonowicz A.
Combination of various microscopical methods for quantitative microstructure analysis of Waspaloy
Conf. on Modern Microscopical Methods, Innsbruck, Austria, 09.-14.09.01
23.42.0

IFF-01-22-109
Wunnicke O.
Ballistic spininjection from Fe(001) into ZnSe and GaAs
1st Annual Meeting of the Research Training Network: Computational Magnetoelectronics, Budapest, Ungarn, 27.-30.09.2001
23.20.0

IFF-01-22-110
Wunnicke O.
Effects of interface states on tunneling
DPG-Frühjahrstagung, Hamburg, 26.-30.03.01
23.20.0

List of references

Allgaier J.	IFF-01-22-068	IFF-01-22-104	
Antons A.	IFF-01-22-001	IFF-01-22-012	
Bechthold P.S.	IFF-01-22-065		
Berger R.	IFF-01-22-001	IFF-01-22-012	
Bihlmayer G.	IFF-01-22-107		
Blügel S.	IFF-01-22-001 IFF-01-22-107	IFF-01-22-003	IFF-01-22-012
Brener E. A.	IFF-01-22-034	IFF-01-22-093	IFF-01-22-094
Brückel Th.	IFF-01-22-004	IFF-01-22-005	IFF-01-22-006
Bürgler D.E.	IFF-01-22-009 IFF-01-22-033	IFF-01-22-010	IFF-01-22-011
Cabria I.	IFF-01-22-018	IFF-01-22-019	
Cao Y.	IFF-01-22-012		
Chen J.	IFF-01-22-013	IFF-01-22-014	IFF-01-22-015
Conrad H.	IFF-01-22-016	IFF-01-22-017	
Dederichs P.H.	IFF-01-22-018 IFF-01-22-029	IFF-01-22-019 IFF-01-22-067	IFF-01-22-020
Divin Y.Y.	IFF-01-22-021	IFF-01-22-022	IFF-01-22-023
Dürr H.A.	IFF-01-22-024		
Eberhardt W.	IFF-01-22-065		
Ebert Ph.	IFF-01-22-025	IFF-01-22-026	IFF-01-22-091
Ehrhart P.	IFF-01-22-028		
Faley M.I.	IFF-01-22-027		
Fitsilis F.	IFF-01-22-028		
Galanakis I.	IFF-01-22-029		
Gareev R.	IFF-01-22-030	IFF-01-22-033	
Goerigk G.	IFF-01-22-031		
Gompper G.	IFF-01-22-032		
Grushko B.	IFF-01-22-025		
Grünberg P.	IFF-01-22-033		
Gutheim F.	IFF-01-22-034		
Hauck J.	IFF-01-22-035	IFF-01-22-036	
Hoffmann-Eifert S.	IFF-01-22-007 IFF-01-22-040	IFF-01-22-038 IFF-01-22-072	IFF-01-22-039
Houben L.	IFF-01-22-041	IFF-01-22-064	
Ioffe A.	IFF-01-22-042	IFF-01-22-043	IFF-01-22-044
Jahnen B.	IFF-01-22-045	IFF-01-22-046	
Jia C.L.	IFF-01-22-021	IFF-01-22-075	
Jung P.	IFF-01-22-013 IFF-01-22-049	IFF-01-22-047	IFF-01-22-048

Kirch D.	IFF-01-22-050	IFF-01-22-061	IFF-01-22-062
Kirstein O.	IFF-01-22-051	IFF-01-22-052	IFF-01-22-053
Klingeler R.	IFF-01-22-054		
Kluge F.	IFF-01-22-025		
Kluge M.	IFF-01-22-086		
Kohlstedt H.	IFF-01-22-055 IFF-01-22-082 IFF-01-22-097	IFF-01-22-056 IFF-01-22-095	IFF-01-22-075 IFF-01-22-096
Kozielewski T.	IFF-01-22-051		
Kromen Wi.	IFF-01-22-003	IFF-01-22-012	
Kuanr B.	IFF-01-22-033		
Köbler U.	IFF-01-22-057	IFF-01-22-058	
Laytti M.	IFF-01-22-022	IFF-01-22-023	
Luysberg M.	IFF-01-22-045 IFF-01-22-063	IFF-01-22-061 IFF-01-22-064	IFF-01-22-062
Lüttgens G.	IFF-01-22-065		
Massalovitch S.	IFF-01-22-066		
Mavropoulos Ph.	IFF-01-22-067		
Meertens D.	IFF-01-22-063		
Mihailescu M.	IFF-01-22-068		
Monkenbusch M.	IFF-01-22-068 IFF-01-22-104	IFF-01-22-069 IFF-01-22-106	IFF-01-22-070
Müller-Krumbhaar H.	IFF-01-22-034	IFF-01-22-093	IFF-01-22-094
Neeb M.	IFF-01-22-065	IFF-01-22-071	
Nonas B.	IFF-01-22-018	IFF-01-22-019	
Ohly Ch.	IFF-01-22-038	IFF-01-22-039	IFF-01-22-072
Pipich V.	IFF-01-22-073		
Pithan Ch.	IFF-01-22-074		
Pontius N.	IFF-01-22-065		
Poppe A.	IFF-01-22-104		
Poppe U.	IFF-01-22-021 IFF-01-22-027	IFF-01-22-022 IFF-01-22-075	IFF-01-22-023
Prager M.	IFF-01-22-051	IFF-01-22-052	IFF-01-22-053
Regnery S.	IFF-01-22-028		
Richter D.	IFF-01-22-068 IFF-01-22-106	IFF-01-22-069	IFF-01-22-104
Ritter S.	IFF-01-22-040		
Rodriguez-Contreras	IFF-01-22-075	IFF-01-22-076	
Rücker U.	IFF-01-22-078		
Sager W.	IFF-01-22-079		
Schlapp M.	IFF-01-22-080		
Schmitz S.	IFF-01-22-081		

Schneider St.	IFF-01-22-082 IFF-01-22-085	IFF-01-22-083	IFF-01-22-084
Schober H. R.	IFF-01-22-086		
Scholten C.	IFF-01-22-064		
Schroeder H.	IFF-01-22-002	IFF-01-22-081	IFF-01-22-098
Schroeder K.	IFF-01-22-001	IFF-01-22-003	IFF-01-22-012
Schwahn D.	IFF-01-22-073 IFF-01-22-089	IFF-01-22-087	IFF-01-22-088
Seeck O.	IFF-01-22-090		
Semmler U.	IFF-01-22-026	IFF-01-22-091	
Shadrin P.M.	IFF-01-22-021	IFF-01-22-022	IFF-01-22-023
Shirotov V.V.	IFF-01-22-022	IFF-01-22-023	
Simon M.	IFF-01-22-026	IFF-01-22-091	
Spatschek R.	IFF-01-22-093	IFF-01-22-094	
Stein S.	IFF-01-22-095	IFF-01-22-096	IFF-01-22-097
Stellbrink J.	IFF-01-22-099	IFF-01-22-100	
Szot K.	IFF-01-22-038 IFF-01-22-108	IFF-01-22-072	IFF-01-22-075
Tillmann K.	IFF-01-22-101	IFF-01-22-102	
Toperverg B.	IFF-01-22-059		
Trinkaus H.	IFF-01-22-061	IFF-01-22-062	
Ullmaier H.	IFF-01-22-013	IFF-01-22-014	
Urban K.	IFF-01-22-021 IFF-01-22-025 IFF-01-22-045	IFF-01-22-022 IFF-01-22-026 IFF-01-22-091	IFF-01-22-023 IFF-01-22-027
Waser R.	IFF-01-22-002 IFF-01-22-037 IFF-01-22-040 IFF-01-22-060 IFF-01-22-077 IFF-01-22-103	IFF-01-22-008 IFF-01-22-038 IFF-01-22-055 IFF-01-22-072 IFF-01-22-082	IFF-01-22-028 IFF-01-22-039 IFF-01-22-056 IFF-01-22-075 IFF-01-22-092
Willner L.	IFF-01-22-073 IFF-01-22-089	IFF-01-22-087 IFF-01-22-104	IFF-01-22-088 IFF-01-22-106
Wirth	IFF-01-22-105		
Wischnewski A.	IFF-01-22-106		
Wortmann D.	IFF-01-22-107		
Wunnicke O.	IFF-01-22-067	IFF-01-22-109	IFF-01-22-110
Zeller R.	IFF-01-22-018	IFF-01-22-019	IFF-01-22-067

Posters

IFF-01-23-001
Allenspach P.1; Andersen K.2; Colognesi D.2; Fak B.2; Kirstein O.; Zoppi M.3
1Laboratory for Neutron Scattering , ETHZ & PSI, CH-5232 Villigen PSI, Schweiz
2ISIS Facility, Rutherford Appleton Laboratory, Chilton Didcot, Oxfordshire, OX11 0QX , UK
3Consiglio Nazionale delle Ricerche, Firenze, Italy
Indirect spectrometers at the European Spallation Source (ESS)
7th General ESS Meeting, Seggau, Austria, 26.-29.09.01
23.89.1

IFF-01-23-002
Antons A.; Berger R.; Blügel S.; Schroeder K.
Structure of steps and small islnads on Si(111): As
Conference on Computational Physics 2001, Aachen, 05.-08. September 2001
23.42.0

IFF-01-23-003
Botti A.; Pyckhout-Hintzen W.; Urban V.1; Richter D.; Straube E.1; Kohlbrecher J.3
1Institut Laue Langevin, F-38042 Grenoble Cedex 9, France
2Martin-Luther-Universität Halle-Wittenberg, Fachbereich Physik, 06099 Halle
3Abt. Spallationsquelle, Paul Scherrer Institut, 5232 Villigen PSI, Schweiz
Silica filled elastomers: polymer chain and filler characterization by a SANS-SAXS approach
Deutsche Neutronenstreutagung, FZ Jülich, 19.-21.02.01
23.30.0

IFF-01-23-004
Botti A.; Pyckhout-Hintzen W.; Urban V.1; Richter D.; Straube E.1; Kohlbrecher J.3
1Institut Laue Langevin, F-38042 Grenoble Cedex 9, France
2Martin-Luther-Universität Halle-Wittenberg, Fachbereich Physik, 06099 Halle
3Abt. Spallationsquelle, Paul Scherrer Institut, 5232 Villigen PSI, Schweiz
Silica filled elastomers: polymer chain and filler characterization by a SANS-SAXS approach
Int. Conf. on Neutron Scattering, TU München, 09.-13.09.01
23.30.0

IFF-01-23-005
Botti A.; Pyckhout-Hintzen W.; Urban V.1; Richter D.; Straube E.1
1Institut Laue Langevin, F-38042 Grenoble Cedex 9, France
2Martin-Luther-Universität Halle-Wittenberg, Fachbereich Physik, 06099 Halle
Composites reinforcement by rods: A SAS study
Int. Conf. on Neutron Scattering, TU München, 09.-13.09.01
23.30.0

IFF-01-23-006
Breuer C.; Blanchard A.; Klingeler R.; Wirth I.; Bürgler D.E.; Bechthold P.S.; Neeb M.; Eberhardt W.
Production and scanning tunneling investigations of deposited endohedrally-doped fullerenes Ce@50, Ce@C44 and Ce@C36
Cluster 2001, 268. WE-Heraeus-Seminar, Herzogenhorn 07. - 12.10.2001
23.20.0

IFF-01-23-007
Byelov D.; Frielinghaus H.; Endo H.; Allgaier J.; Richter D.
Polymer anti boosting. A small angle neutron scattering study of the bicontinuous microemulsion
Int. Summerschool "Fundamental Problems in Statistical Physics X", Odenthal-Altenberg, 25.08.01
23.30.0

IFF-01-23-008
Byelov D.; Frielinghaus H.; Endo H.; Allgaier J.; Richter D.
Polymer anti boosting. A small angle neutron scattering study of the bicontinuous microemulsion.
Jülich Soft Matter Days 2001, Kerkrade, The Netherlands, 15.11.01
23.30.0

IFF-01-23-009
Bürgler D.E.; Gareev R.R.; Buchmeier M.; Olligs D.; Schreiber R.; Grünberg P.
Oscillatory interlayer exchange coupling across epitaxial FeSi spacer layers
Edgar-Lüscher-Seminar, Serneus, Schweiz
06.02.2001-08-06
23.42.0

IFF-01-23-010
Conrad H.; Filges D.1; Hansen G.2; Neef R. D.1; Stelzer H.2; Tietze-Jaensch H.; Ullmaier H.
1FZJ, IKP, Jülich
2FZJ, ZAT, Jülich
Technische und methodische Entwicklungen am Target-Moderator-Reflektor-Komplex der ESS
Jülich, Deutsche Neutronenstreutagung 2001, 19. - 21.02.2001
23.60.0

IFF-01-23-011
Doan T. D.1; Ott F.1; Menelle A.1; Rücker U.; Humbert P.2; Fermon C.2
1LLB, CEA/CNRS, Saclay, France
2SPEC, CEA Saclay, France
New evanescent wave surface diffractometer at the LLB
München, ICNS-Konferenz, 09. - 13.09.2001
23.89.1

IFF-01-23-012
Döbereiner H.G.1, Haluska C.K.1, Godzd W.2 and Gompper G.
1 MPI Golm
2 Academy of Sciences, Warsaw, Poland
Micro-structured Diblock-Copolymer Membranes
Poster auf der Konferenz über "Assembly and Self-Assembly at the
Interface of Biology, Chemistry and Physics", Gioccoi, Italien
20.-25. August 2001
23.30.0

IFF-01-23-013
Eckert S.1; Hoffmann S.; Meier G.; Alig I.1
1DKI Darmstadt
Critical fluctuations in non-critical and critical mixtures of polyethylene glycol and propylene glycol studied by ultrasonic and light scattering experiments
4th IDMRCS, Crete, Greece; 18.06.-26.06.01
23.30.0

IFF-01-23-014
Faley M.I.; Poppe U.; Urban K.; Paulson D. N.1, Starr T. N.1, Fagaly R. L.1
1 Tristan Technologies Inc., CA 92121, USA
Sensitive HTS sensors for magnetic evaluation applications
Tagung Kryoelektronische Bauelemente 2001, 30. Sept. - 2. Okt. 2001, Congrescentrum Rolduc, Kerkrade, Niederlande.
23.42.0

IFF-01-23-015
Faley M.I.; Poppe U.; Urban K.; Paulson D.N.1; Starr T.N.1; Fagaly R.L1.
1 Tristan Technologies Inc., CA 92121, USA
Sensitive HTS gradiometers for magnetic evaluation applications
5th European Conference on Applied Superconductivity, Kopenhagen, Dänemark, 26.-30. August (2001)
23.42.0

IFF-01-23-016

Frielinghaus H.; Batsberg Pedersen W.1; Sommer Larsen P.1; Almdal K.1; Mortensen K.1
1Risø National Laboratory, Dep. of Solid State Physics, DK-4000 Roskilde; Denmark
Endeffekte in Polystyrol/Polyethylenoxid Copolymeren
Deutsche Neutronenstreutagung, FZ Jülich, 19.-21.02.01
23.30.0

IFF-01-23-017
Frielinghaus H.; Endo H.; Allgaier J.; Richter D.; Jakobs B.1; Sottmann T.1; Strey R.1
1Institut für Physikalische Chemie, Universität Köln, 50939 Köln
Polymer boosting effect in der Tröpfchenphase - eine Studie mit Neutronenkleinwinkelstreuung
Würzburger Tagung "Fortschritte für Wasch- und Reinigungsmittel", Würzburg, 02.04.01
23.30.0

IFF-01-23-018
Ganpule C.; Stanishevsky A.; Hill B.K.; Nagarajan V:; Alpay S.P.; Melngailis J.; Williams E.D.; Ramesh R.; Roelofs R.; Waser R.; Tiedke S.; De. Wolf P.; Joshi V.; Paz de Araujo,C.
Scaling of ferroelectric properties in thin films (P)
13th Int. Symp. Integrated Ferroelectrics, Colorado Springs, USA, 11.03.-14.03.01
23.42.0

IFF-01-23-019
Gareev R.R.; Buchmeier M.; Breidbach M.; Schreiber R.; Bürgler D.E.; Grünberg P.
Antiferromagnetic exchange coupling in excess of 8 mJ/m2 in Fe/Si/Fe expitaxial trilayers with thin boundary layers
46th Annual Conference on Magnetism & Magnetic Materials Seattle, Washington
12. - 16.11.2001
23.42.0

IFF-01-23-020
Goerigk G.; Williamson D. L.1
1Colorado School of Mines, Dept. of Physics, Golden, USA
Quantitative ASAXS of Germanium Inhomogeneities in Amorphous Silicon-Germanium Alloys
Hamburg, HASYLAB User meeting, 26.01.2001
23.89.1

IFF-01-23-021
Grimm H.
Relaxational dynamics in drug and humid DNA
Int. Conf. on Neutron Scattering, TU München, 09.-13.09.01
23.30.0

IFF-01-23-022
Grimm H.
Slow relaxation process in DNA at different levels of hydration
Deutsche Neutronenstreutagung, FZ Jülich, 19.-21.02.01
23.30.0

IFF-01-23-023
Hartmann M.
Dewetting Hydrodynamics in 1+1 Dimension
Vorbereitungstreffen zum Gutachterkolloquium des Schwerpunktprogramms
Reisensburg, 18.07.-20.07.2001
23.15.0

IFF-01-23-024
Hartmann M.
Dewetting Hydrodynamics in 2+1 Dimension
Gutachterkolloquium des Schwerpunktprogramms
Bad Honnef, 07.11.-09.11.2001
23.15.0

IFF-01-23-025
Hauck J.; Mika K.
Ground State Structures of Polymers
Europhysics Conference on Computational Physics
Aachen, 05.09.-08.09.2001
23.30.0

IFF-01-23-026
Heinrich M.; Pyckhout-Hintzen W.; Richter D.; Straube W.1; Wiedenmann A.2
1Martin-Luther-Universität Halle-Wittenberg, Fachbereich Physik, 06099 Halle
2Hahn Meitner Institut Berlin, Glienicker Str. 100, 14109 Berlin
Relaxation of entangled model H-shaped polymers: A SANS investigation
Int. Conf. on Neutron Scattering, TU München, 09.-13.09.01
23.30.0

IFF-01-23-027
Hofer C.; Hoffmann-Eifert S.; Waser R.
Dielectric and Raman spectroscopy of SrTiO3 ceramics compared with single crystals
Advanced Electroceramics: Grain Boundary Engineering Kick-off Workshop, Madrid, 24.-28.03.01
23.42.0

IFF-01-23-028
Hoffmann S.; Richter D.; Arbe A.1; Colmenero J.1; Farago B.2
1Departamento de Física de Materiales, Universidad del País Vasco,Apt.1072, E-20080 San Sebastián, Spain
2Institut Laue Langevin, F-38042 Grenoble Cedex 9, France
Component Dynamics in Polymer Blends: A Combined QENS and Dielectric Spectroscopy Investigation
Int. Conf. on Neutron Scattering, TU München, 09.-13.09.01
23.30.0

IFF-01-23-029
Hofmann T.1; Winkler R. G.; Reineker P.1
1 Univ. Ulm, Germany
Structure of Polyelectrolyte Solutions: An Integral Equation Theory
Approach
DPG Frühjahrstagung, Berlin
2.4. - 4.4.2001
23.30.0

IFF-01-23-030
Hupfeld D.; Brückel Th.; Schweika W.; Strempfer J.1; Mattenberger K.2; McIntyre G.3
1Northern Illinois University, de Kalb, USA
2ETH, Zürich, Switzerland
3ILL, Grenoble, France
Investigation of the magnetic properties of GdxEu1-xS with neutrons and x-rays
Jülich, Deutsche Neutronenstreutagung 2001, 19. - 21.02.2001
23.89.1

IFF-01-23-031
Ioffe A.; Conrad H.; Zeiske Th.; Mueller R.; Küssel E.; Massalovitch S.; Schlapp M.; Schmitz B.; Brückel Th.
A New Thermal Neutron Spectrometer/Diffractometer for Polarization Analysis (SV30) at the research reactor FRJ-2
München, ICNS-Konferenz, 09. - 13.09.2001
23.89.1

IFF-01-23-032
Ioffe A.; Conrad H.; Zeiske Th.; Mueller R.; Küssel E.; Massalovitch S.; Schlapp M.; Schmitz B.; Brückel Th.
Spektrometer SV30 für Polarisationsanalyse mit thermischen Neutronen am Forschungsreaktor FRJ-2
Jülich, Deutsche Neutronenstreutagung 2001, 19. - 21.02.2001
23.89.1

IFF-01-23-033
Ioffe A.; Vrana M.1
1CAS, Nuclear Physics Institute, Rez near Prague, Czech
A new neutron interferometry approach to the determination of the neutron-electron interaction amplitude
München, ICNS-Konferenz, 09. - 13.09.2001

23.89.1

IFF-01-23-034
Jahnen B.; Luysberg M.; Urban K.; Bracht H.1; Schmidt R.2; Ungermanns C.2; Bleuel T.3
1 Institut für Materialphysik, Universität Münster
2 ISG, FZ Jülich
3 Fachbereich Physik, Universität Würzburg
Interdiffusion in GaSb/AlxGa1-xSb heterostructures
XIIth Conference on Microscopy of Semiconducting Materials, 22-25 March 2001, Oxford, Microscopy of Seminconducting Materials 2001.
23.42.0

IFF-01-23-035
Kahle S.; Willner L.; Monkenbusch M.; Richter D.; Arbe A.1; Colmenero J.1
1Dep. de Fiscia de Materiales, Universidad del Pais Vasco, Facultad de Quimica, E-20080 San Sebastian, Spain
Dynamic Neutron Scattering on Partially Deuterated Polybutadiene
ILL Millenium Symposium, Grenoble, France, 06.-08.04.01
23.30.0

IFF-01-23-036
Kahle S.; Willner L.; Monkenbusch M.; Richter D.; Arbe A.1; Colmenero J.1
1Dep. de Fiscia de Materiales, Universidad del Pais Vasco, Facultad de Quimica, E-20080 San Sebastian, Spain
Dynamic Neutron Scattering on Partially Deuterated Polybutadiene
Int. Conf. on Neutron Scattering, TU München, 09.-13.09.01
23.30.0

IFF-01-23-037
Kahle S.; Willner L.; Monkenbusch M.; Richter D.; Arbe A.1; Colmenero J.1
1Dep. de Fiscia de Materiales, Universidad del Pais Vasco, Facultad de Quimica, E-20080 San Sebastian, Spain
Dynamische Neutronenstreuung an partiell deuteriertem Polybutadien
Deutsche Neutronenstreutagung, FZ Jülich, 19.-21.02.01
23.30.0

IFF-01-23-038
Kienle D.
Grafted polymers in simple flows
Minerva-Workshop "Frontiers in the physics o complex systems"
Israel, 25.03.-28.03.2001
23.30.0

IFF-01-23-039
Kirstein O.; Kozielewski T.; Prager M.; Andersen K.H.1
1ISIS Department, Rutherford Appleton Laboratory, Chilton, Didcot, Oxon, OX11 0QX, UK
A 0.9 micro eV backscattering spectrometer at the European Spallation Source (ESS)
7th General ESS Meeting, Seggau, Austria, 26.-29.09.01
23.89.1

IFF-01-23-040
Kirstein O.; Kozielewski T.; Prager M.; Richter D.
The high flux backscattering spectrometer (RSSM) for the FRM-II reactor in Munich
Int. Conf. on Neutron Scattering, TU München, 09.-13.09.01
23.89.1

IFF-01-23-041
Kirstein O.; Kozielewski T.; Prager M.
Conceptual analysis for a 1.4 micro eV backscattering spectrometer at the European Spallation Source (ESS)
Int. Conf. on Neutron Scattering, TU München, 09.-13.09.01
23.89.1

IFF-01-23-042
Kirstein O.; Prager M.; Parker S.F.1
1ISIS Facility, Rutherford Appleton Laboratory, Chilton, Didcot, Oxon OX11, 0QX, UK
Gitterdynamik und Methylgruppenrotation von Dimetyhlacetylen (DMA)
Deutsche Neutronenstreutagung, FZ Jülich, 19.-21.02.01
23.89.1

IFF-01-23-043
Kirstein O.; Prager M.
Methyl rotational excitations and lattice dynamics of o-, m-and p-xylene using transferable pair potentials
Int. Conf. on Neutron Scattering, TU München, 09.-13.09.01
23.15.0

IFF-01-23-044
Kirstein o.; Kozielewski T.; Prager M.; Richter D.
Das Rückstreuspektrometer (RSSM) hohen Flusses für den FRM-II Reaktor in München
Deutsche Neutronenstreutagung, FZ Jülich, 19.-21.02.01
23.89.1

IFF-01-23-045
Klingeler R.
La@C60, a metallic endohedral fullerene
15th International Winterschool on Electronic Properties of Novel Materials
3. - 10. März 2001, Kirchberg, Tirol
23.20.0

IFF-01-23-046
Kollmann M.; Nägele G.
Electrokinetic Effects in Charged Colloids: the Role of Hydrodynamic Interactions
Jülich Soft Matter Days 2001 in Kerkrade; 13.11.-16.11.01
23.30.0

IFF-01-23-047
Krause H.-J.1; Wolf W.1; Glaas W.1; Zimmermann E.1; Faley M.I.; Sawade G.2; Mattheus R.2; Neudert G.3; Gampe U.3; Krieger J.4
1 ISG, FZ Jülich
2 Forschungs- und Materialprüfungsanstalt Baden-Württemberg, 70569 Stuttgart
3 Siempelkamp, Prüf- und Gutachtergesellschaft mbH, 01099 Dresden
4 Bundesanstalt für Straßenwesen, 51427 Bergisch-Gladbach
SQUID Array for Magnetic Inspection of Prestressed Concrete Bridges
Conference SQUID2001, Gothenburg, Schweden, 31.08.-03.09. (2001)
23.42.0

IFF-01-23-048
Kronast F.; Dürr H.A.; Eberhardt W.; Bihlmayer G.; Blügel S.; Liebsch A.
Femtosecond spin dynamics of magnetic nanodots
XIII International Conference on Vacuum Ultraviolet Radiation Physics, Trieste, Italy
23. - 27. Juli 2001
23.20.0

IFF-01-23-049
Kronast F.; Dürr H.A.; Eberhardt W.; Landis S.
Non-local pump-probe spectromicroscopy of layered magnetic structures
International Workshop on Ultrafast Surface Dynamics, San Sebastian, Spain
09. - 11. Juli 2001
23.20.0

IFF-01-23-050
Kronast F.; Dürr H.A.; Eberhardt W.
Spin-polarized two-photon photoemission microscopy of magnetic nanostructures
DPG-Frühjahrstagung, Hamburg
März.2001
23.20.0

IFF-01-23-051
Kuanr B.K.; Buchmeier M.; Bürgler D.E.; Grünberg P.
Broadening of the frequency linewidth in exchange-biased or exchange-coupled systems observed by FMR and BLS
4th International Symposium on Metallic Multilayers, Aachen, Deutschland
27.06.2001
23.42.0

IFF-01-23-052
Kuanr B.K.; Buchmeier M.; Bürgler D.E.; Grünberg P.
Exchange coupling of MBE grown Fe/Al/Fe by dynamic techniques
MMM'01, Seattle, USA
16.11.2001
23.42.0

IFF-01-23-053
Köbler U.; Hoser A.1; Kawakami M.2
1RWTH, Institut für Kristallographie, Aachen
2Kagoshima University, Koorimoto, Japan
Beobachtung eines Bloch Exponent von 5/2 am Antiferromagneten MnF2 mit S=5/2 und axialer Austauschanisotropie
Jülich, Deutsche Neutronenstreutagung 2001, 19. - 21.02.2001
23.89.1

IFF-01-23-054
Köbler U.; Hoser A.1; Mueller R.; Fischer K.; Beyss M.
1HMI, Berlin
The impact of fourth-order exchange interactions on spin dynamics, order parameters and critical magnetic behaviour
München, ICNS-Konferenz, 09. - 13.09.2001
23.89.1

IFF-01-23-055
Lauter H. J.1; Lauter-Pasyuk V.2,3,1; Toperverg B.4,5; Nikonov O.1,3; Romashev L.6; Ustinov V.6; Kravtsov E.6; Vorobiev A.7; Major J.7
1ILL, Grenoble, France
2TU, Physik Department, München
3Joint Institute for Nuclear Research, Dubna, Russia
4PNPI, Gatchina, Russia
5FZJ, IFF, Jülich
6Institute of Metal Physics, Ekterinburg, Russia
7MPI Metallforschung, Stuttgart
Spin-resolved unpolarized neutron off-specular scattering for magnetic multilayers studies
München, ICNS-Konferenz, 09. - 13.09.2001
23.89.1

IFF-01-23-056
Lauter-Pasyuk V.1,2,3; Lauter H. J.3; Toperverg B.4,5; Nikonov O.3,2; Petrenko A.2; Schubert D.6; Schreiber J.7; Burcin M.7; Petry W.1; Aksenov V.2
1TUM, Physik Department, Garching
2Joint Institute for Nuclear Research, Dubna, Russia
3ILL, Grenoble, France
4PNPI, Gatchina, Russia
5FZJ, IFF, Jülich
6GKSS Forschungszentrum, Geesthacht
7Fraunhofer Institut für Zerstörungsfreie Prüfverfahren, Dresden
Interface and surface formation in self-assembled polymer multilayers by off-specular neutron scattering
München, ICNS-Konferenz, 09. - 13.09.2001
23.89.1

IFF-01-23-057
Lauter-Pasyuk V.1,2; Lauter H. J.3; Toperverg B.4,5; Nikonov O.2,3
1TUM, Physik Department, Garching
2Joint Institute for Nuclear Research, Dubna, Russia
3ILL, Grenoble, France
4PNPI, Gatchina, Russia
5FZJ, IFF, Jülich
Peculiar off-specular neutron scattering from islands on a lamellar film
Jülich, Deutsche Neutronenstreutagung 2001, 19. - 21.02.2001
23.89.1

IFF-01-23-058
Malagoli M.
Lifetime effects on Gd valence band structure
XIII International Conference on Vacuum Ultraviolet Radiation Physics, Trieste, Italy
23. - 27. Juli 2001
23.20.0

IFF-01-23-059
Massalovitch S.; Ioffe A.; Küssel E.; Schlapp M.; Brückel Th.
Development of Image Plate Based Neutron Detector
Berlin, Hahn-Meitner-Institut, International Workshop on Position-Sensitive Neutron Detectors, 28. - 30.06.2001
23.89.1

IFF-01-23-060
Massalovitch S.; Ioffe A.; Küssel E.; Schlapp M.; Brückel Th.
Development of the large-area 2D neutron detector based on the imaging plate
Jülich, Deutsche Neutronenstreutagung 2001, 19. - 21.02.2001
23.89.1

IFF-01-23-061
Massalovitch S.; Ioffe A.; Küssel E.; Schlapp M.; von Seggern H.1; Brückel Th.
1Universität, Darmstadt
Development of neutron image plate for low flux measurements
München, ICNS-Konferenz, 09. - 13.09.2001
23.89.1

IFF-01-23-062
Mihailescu M.; Monkenbusch M.; Endo H.; Allgaier J.; Richter D.; Jakobs B.1; Sottmann T.1; Farago B.2
1Institut für Physikalische Chemie, Universität zu Köln, 50939 Köln
2Institut Laue Langevin, F-38042 Grenoble Cedex 9, France
Dynamics of bicontinuous phase microemulsions with amphiphilic block-copolymer
Deutsche Neutronenstreutagung, FZ Jülich, 19.-21.02.01
23.30.0

IFF-01-23-063
Monkenbusch M.
Next generation NSE instruments - What are the challenges? - Where are the limits?
Deutsche Neutronenstreutagung, FZ Jülich, 19.-21.02.01
23.30.0

IFF-01-23-064
Mueller R.; Brückel Th.; Horriar-Esser Ch.
Entwicklung einer Anlage zur Herstellung von kernspin-polarisiertem 3He am Forschungszentrum Jülich
Jülich, Deutsche Neutronenstreutagung 2001, 19. - 21.02.2001
23.89.1

IFF-01-23-065
Neumann M.1; Press W.2; Nöldeke C.2; Asmussen B.2; Prager M.; Ibberson R.M.3
1MSI Europ. Headquarters 230/250, The Quorum Barnwell Road, Cambridge CB5 8RE, England
2Institut für Experimentelle und Angewandte Physik, Universität Kiel, Leibnitzstr. 19, 24098 Kiel
3ISIS Rutherford Appleton Laboratory, Chilton Didcot OX11 0QX, UK
The structure of the orientationally ordered phase III of solid methane
Int. Conf. on Neutron Scattering, TU München, 09.-13.09.01

23.15.0

IFF-01-23-066
Nägele G.; Kollmann M.; Pesché R.1; Banchio A.J.2
1University of Delaware, Newark; USA
2CALTECH Institute in Pasadena, USA
Dynamic properties, scaling and related freezing criteria of 2D and 3D dispersions
Jülich Soft Matter Days 2001 in Kerkrade; 13.11.-16.11.01
23.30.0

IFF-01-23-067
Nägele G.
Electrokinetic Effects in Charged Colloids: the Role of Hydrodynamic Interactions
IUAP 21st International Conference on Statistical Physics
Cancum, Mexico; 15.07.-20.07.01
23.30.0

IFF-01-23-068
Ohly Ch.; Hoffmann-Eifert S.; Szot K.; Waser R.
Defects in alkaline earth titanate thin films - structural and morphological aspects
13th Int. Symp. Integrated Ferroelectrics, Colorado Springs, USA, 11.03.-14.03.01
23.42.0

IFF-01-23-069
Ohly Ch.; Hoffmann-Eifert S.; Waser R.
The electrical conductivity of SrTiO3 thin films under changing oxygen ambients
CECAM/PSIK Workshop on Oxide-Metal Interfaces: Theoretical Progress and Challenges, Lyon, 4.10.-6.10.01
23.42.0

IFF-01-23-070
Olligs D.; Bürgler D.E.; Wang Y.G.; Kentzinger E.; Rücker U.; Schreiber R.; Brückel Th.; Grünberg P.
Unambiguous evidence for roughness-induced enhancement of Giant Magnetoresistance in epitaxial Fe/Cr/Fe (001) trilayers
Aachen, MML'01-Tagung, 25.06.2001
23.42.0

IFF-01-23-071
Olligs D.; Bürgler D.E.; Wang Y.G.; Kentzinger E.; Rücker U.; Schreiber R.; Brückel Th.; Grünberg P.
Unambiguous evidence for roughness-induced enhancement of giant magnetoresistance in epitaxial Fe/Cr/Fe(001) trilayers
4th International Symposium on Metallic Multilayers , Aachen, Deutschland
25.06.2001
23.42.0

IFF-01-23-072
Pipich V.; Schwahn D.; Willner L.
Complex phase behavior near the Lifshitz line in a ternary polymer blend
Int. Conf. on Neutron Scattering, TU München, 09.-13.09.01
23.30.0

IFF-01-23-073
Pipich V.; Schwahn D.; Willner L.
Formation of a microemulsion phase in a ternary polymer blend - a SANS study
Deutsche Neutronenstreutagung, FZ Jülich, 19.-21.02.01
23.30.0

IFF-01-23-074
Pipich V.; Schwahn D.; Willner L.
Influence of the reentrance criticality on isotropic Lifshitz critical behavior in a ternary polymer blend near the Lifshitz line
Jülich Soft Matter Days 2001, Kerkrade, NL, 13.-16.11.01
23.30.0

IFF-01-23-075
Pontius N.; Lüttgens G.; Bechthold P.S.; Neeb M.; Eberhardt W.
Hot-electron dynamics in mass-selected transition metal clusters probed by femtosecond pump-probe photoelectron spectroscopy
Cluster 2001, 268. WE-Heraeus-Seminar, Herzogenhorn
07. - 12.10.2001
23.20.0

IFF-01-23-076
Prager M.; Press W.1; Asmussen B.1.; Combet J.2
1Institut für Experimentalphysik, Universität Kiel, Leibnitzstr. 19, 24098 Kiel
2Institut Laue-Langevin, F-38042 Grenoble Cedex 9, France
Phase III of ethane: basing rotational tunnelling on the crystal structure
Conf. on Quantum Atomic and Molecular Tunnelling 2001, Nottingham, UK, 07.09.01
23.15.0

IFF-01-23-077
Prager M.; Press W.1; Asmussen B.2; Combet J.2
1Institut für Experimentelle und Angewandte Physik, Universität Kiel, Leibnitzstr. 19, 24098 Kiel
2Institut Laue-Langevin, F-38042 Grenoble Cedex 9, France
Phase III of methane: crystal structure and rotational tunnelling
Int. Conf. on Neutron Scattering, TU München, 09.-13.09.01
23.15.0

IFF-01-23-078
Prager M.; Schiebel P.1; Grimm H.
1Inst. für Kristallographie, Universität Tübingen, 72070 Tübingen
Dipolar interaction in partially deuterated ammoniumhexachloroplatinate: rotational tunnelling spectroscopy
Int. Conf. on Neutron Scattering, TU München, 09.-13.09.01
23.15.0

IFF-01-23-079
Pyckhout-Hintzen W.
A microscopic model for branched polymers in elongational flow by SANS
GRC New Londen, NH, USA, 05.-12.08.01
23.30.0

IFF-01-23-080
Pyckhout-Hintzen W.
On the length scale dependence of microscopic strain
Deutsche Neutronenstreutagung, FZ Jülich, 19.-21.02.01
23.30.0

IFF-01-23-081
Pyckhout-Hintzen W.
On the length scale dependence of microscopic strain
Int. Conf. on Neutron Scattering, TU München, 09.-13.09.01
23.30.0

IFF-01-23-082
Pyckhout-Hintzen W.
Reinforcement of silica particles by SANS
GRC New Londen, NH, USA, 05.-12.08.01
23.30.0

IFF-01-23-083
Radulescu A.; Schwahn D.; Fetters L.J.; Richter D.
Crystallization of paraffin in decane in the presence of PEB-7 ethylene-butene random copolymers.
Int. Conf. on Neutron Scattering, TU München, 09.-13.09.01
23.30.0

IFF-01-23-084
Regnery S.; Fitsilis F.; Ehrhart P.; Waser R.; Schienle F.; Schumacher M.; Jürgensen H.
Nucleation and growth of ultra thin (Ba,Sr)TiO3 films in a MOCVD reactor
MRS 2001, Boston, USA, 25.11.-29.11.01

23.42.0

IFF-01-23-085
Rhie H.-S.; Link S.; Sievers J.; Dürr H.A.; Eberhardt W.; Smith N.V.1
1NSLS Berkeley, USA
Femtosecond electron dynamics of image potential states on Ni surface
XIII International Conference on Vacuum Ultraviolet Radiation Physics, Trieste, Italy
23. - 27. Juli 2001
23.20.0

IFF-01-23-086
Richter D.; Monkenbusch M.; Schwahn D.; Schweika W.
Scattering Experiments Relevant for Polymer Research at the Neutron Guide Laboratory of the Jülich Research Center
222nd ACS National Meeting Chicago, USA, 27.08.01
23.89.1

IFF-01-23-087
Ritter S.; Hoffmann-Eifert S.; Bolten D.; Waser R.
(Pb1xxBax)TiO3 thin films prepared by liquid delivery MOCVD: influence of the process parameters on film formation and electrical propertie
Int. Meeting on Ferroelectricity, Madrid, 03.-07.09.01
23.42.0

IFF-01-23-088
Ritter S.; Schäfer P.; Hoffmann-Eifert S.; Waser R.
(Pb1-xBax)TiO3 thin films prepared by liquid delivery MOCVD: Influence of process parameters on film formation and electrical properties
13th Int. Symp. Integrated Ferroelectrics, Colorado Springs, USA, 11.03.-14.03.01
23.42.0

IFF-01-23-089
Rodriguez-Contreras J.
Characterization of ferroelectric thin films prepared by High-Pressure Oxygen Sputtering and PLD
MRS 2001, Boston, USA, 25.11.-29.11.01
23.42.0

IFF-01-23-090
Rodriguez-Contreras J.
High-pressure sputtering of PbZr0.52Ti0.48O3/SrRuO3 thin films on SrTiO3 substrates
Int. Meeting on Ferroelectricty, Madrid, 03.-07.09.01
23.42.0

IFF-01-23-091
Rzehak R.; Müller-Krumbhaar H.; Marquardt W. 1
1 Lehrstuhl für Prozesstechnik, RWTH Aachen
Liquid-liquid phase change in systems with flow
253. WE-Heraeus Seminar, Bad Honnef, 22.-24.03.2001
23.15.0

IFF-01-23-092
Rücker U.; Alefeld B.; Bergs W.; Kentzinger E.; Heinen J.; Brückel Th.; Drochner M.1; Ackens A.1; Loevenich H.1; Reinhard P.1; Zwoll K.1
1FZJ, ZEL, Jülich
Das neue Neutronenreflektometer mit Polarisationsanalyse in Jülich
Jülich, Deutsche Neutronenstreutagung 2001, 19. - 21.02.2001
23.89.1

IFF-01-23-093
Rücker U.; Alefeld B.; Bergs W.; Kentzinger E.; Heinen J.; Brückel Th.; Drochner M.1; Ackens A.1; Loevenich H.1; Reinhard P.1; Zwoll K.1
1FZJ, ZEL, Jülich
The new reflectometer with polarization analysis in Jülich
München, ICNS-Konferenz, 09. - 13.09.2001
23.89.1

IFF-01-23-094
Rücker U.; Grünberg P.; Demokritov S.1
1Universität, Kaiserslautern
Magnetic interlayer coupling across semiconducting EuS layers
Aachen, MML'01-Tagung, 25.06.2001
23.42.0

IFF-01-23-095
Rücker U.; Kentzinger E.; Toperverg B.; Brückel Th.; Ott F.1
1LLB, Gif sur Yvette, France
Spinaufgespaltene diffuse Streuung unter streifendem Einfall an polarisierenden Superspiegeln
Jülich, Deutsche Neutronenstreutagung 2001, 19. - 21.02.2001
23.89.1

IFF-01-23-096
Rücker U.; Kentzinger E.; Toperverg B.; Ott F.1; Brückel Th.
1LLB, Gif sur Yvette, France
Layer-by-layer magnetometry on polarizing supermirrors
München, ICNS-Konferenz, 09. - 13.09.2001
23.89.1

IFF-01-23-097
Rücker U.; Kentzinger E.
Characterization of thin layered structures for magnetoelectronic applications
Jülich, ESS-Begutachtung durch den Wissenschaftsrat, 10.12.2001
23.89.1

IFF-01-23-098
Sager W.; Blokhuis E.1; Smeets J.1; Svergun D.I.2,3; Koch M.2; Konarev P.2,3; Volkov V.3
1University of Leiden, The Netherlands
2DESY in Hamburg
3Institute of Crystallography, Moscow
Aggregation and shape transformations in w/o AOT microemulsions
Conference on Assembly and Self Assembly at the Interface of Biology, Chemistry and Physics
Il Ciocco, Italy, 20.08.-25.08.01
23.30.0

IFF-01-23-099
Sager W.; Blokhuis E.1; Smeets J.1; Svergun D.I.2,3; Koch M.2; Konarev P.2,3; Volkov V.3
1University of Leiden, The Netherlands
2DESY in Hamburg
3Institute of Crystallography, Moscow
Aggregation and shape transformations in w/o AOT microemulsions
Jülich Soft Matter Days in Kerkrade v. 13.11.-16.11.01
23.30.0

IFF-01-23-100
Sager W.; Woudenberg F.1; Urban J.2; Weiss K.2; Verweij H.1
1University of Twente; The Netherlands
2MPI in Berlin
Characterisation of nanosized oxide particles and nanocomposite coatings prepared via modified emulsion precipitation
Il Ciocco, Italy, 20.08.-25.08.01
23.30.0

IFF-01-23-101
Sager W.; Woudenberg F.1; Urban J.2; Weiss K.2; Verweij H.1
1University of Twente; The Netherlands
2MPI in Berlin
Characterisation of nanosized oxide particles and nanocomposite coatings prepared via modified emulsion precipitation
Jülich Soft Matter Days in Kerkrade v. 13.11.-16.11.01

23.30.0

IFF-01-23-102
Schilling T.; Gompper G.
Twist Grain Boundaries in Lamellar Phases of Ternary Amphiphilic Systems,
Kurzvortrag und Poster beim 249. WE-Heraeus-Seminar "Wetting of Structured Materials", Bad Honnef
12.-14. Februar 2001
23.30.0

IFF-01-23-103
Schlapp M.1,2, Kolb R.2; von Seggern H.2
1FZJ, IFF, Jülich
2TU, Fachbereich Materialwissenschaften, Darmstadt
Präparative Einflüsse auf die Empfindlichkeit des Speicherleuchtstoffs BaFBr:Eu2+ für Neutronen-Bildplatten
Jülich, Deutsche Neutronenstreutagung 2001, 19. - 21.02.2001
23.89.1

IFF-01-23-104
Schlapp M.; von Seggern H.1; Massalovitch S.; Ioffe A.; Conrad H.; Brückel Th.
1Universität, Darmstadt
Materials for neutron image plates with low (sensitivity
München, ICNS-Konferenz, 09. - 13.09.2001
23.89.1

IFF-01-23-105
Schmidt W.1, Ohl M.1, Buchenau U., Koza M.1
1Institut Laue-Langevin, F-38042 Grenoble Cedex, France
Inelastic Neutron Scattering in Amorphous Systems at Low Momentum Transfer
Deutsche Neutronenstreutagung, FZ Jülich, 19.-21.02.01
23.89.1

IFF-01-23-106
Schneider S.; Kohlstedt H.; Waser R.
High temperature etching characteristics of noble metal electrode
13th Int. Symp. Integrated Ferroelectrics, Colorado Springs, USA, 11.03.-14.03.01
23.42.0

IFF-01-23-107
Schneller T.; Waser R.
Chemical origin of different electrical and morphological qualities in CSD derived PZT thin films
13th Int. Symp. Integrated Ferroelectrics, Colorado Springs, USA, 11.03.-14.03.01
23.42.0

IFF-01-23-108
Schweika W.; Shramchenko N.1; Caudron R.1; Bellissent R.1; Widom M.2, Cousson A.1; Feuerbacher M.; Hennion B.1; Hupfeld D.; Mattauch S.3
Phason disorder in icosahedral AlPdMn quasicrystals
München, ICNS-Konferenz, 09. - 13.09.2001
23.89.1

IFF-01-23-109
Schweika W.; Shramchenko N.1; Caudron R.1; Bellissent R.1; Widom M.2
1LLB, Saclay, France
2Carnegie-Mellon University
Phason disorder in icosahedral AlPdMn quasicrystals
Jülich, Deutsche Neutronenstreutagung 2001, 19. - 21.02.2001
23.89.1

IFF-01-23-110
Schweika W.
Diffuse Neutron Scattering using time-of flight and polarization analysis
Jülich, ESS-Begutachtung durch den Wissenschaftsrat, 10.12.2001
23.89.1

IFF-01-23-111
Seeck O.; Kim H.1; Sinha S. K.1; Basu J. D.2; Kim H.3; Foster M. D.3
1APS/ANL, Argonne, USA
2University of Illinois, USA
3The University of Akron, USA
X-ray experiments on confined liquids
New London, USA, X-Ray Gordon Conference, 22. - 27.07.2001
23.89.1

IFF-01-23-112
Shadrin P. M.; Jia C.L.; Divin Y.Y.
Spread of critical currents in thin-film YBa2Cu3O7-x bicrystal junctions and faceting of grain boundary
5th European Conf. Appl. Supercond., Copenhagen/Dänemark, 26.-30. August (2001)
23.42.0

IFF-01-23-113
Shirotov V. V.; Divin Y.Y.; Urban K.
Far-infrared broadband measurements with Hilbert-transform spectroscopy
5th European Conf. Appl. Supercond., Copenhagen/Dänemark, 26.-30. August (2001)
23.42.0

IFF-01-23-114
Shur W.; Blankov E.; NEgashev S.; Borisova E.; Barannikov A.; Schneller T.; Gerhardt R.; Waser R.
In situ study of crystallization kinetics during rapid thermal annealing of sol-gel PZT and PLZT films
13th Int. Symp. Integrated Ferroelectrics, Colorado Springs, USA, 11.03.-14.03.01
23.42.0

IFF-01-23-115
Sievers J.; Rhie H.-S.; Link S.; Dürr H.A.; Eberhardt W.
Ultrafast electron dynamics of image potential states on Ni surfaces
DPG-Frühjahrstagung, Hamburg
März 2001
23.20.0

IFF-01-23-116
Stellbrink J.; Allgaier J.; Monkenbusch M.; Richter D.
Self and Collective Dynamics of Ordered Star Polymer Solutions
DYPROSO XXVIII, Kerkrade, The Netherlands, 16.-19.09.01
23.30.0

IFF-01-23-117
Stellbrink J.; Allgaier J.; Monkenbusch M.; Richter D.
Self and Collective Dynamics of Ordered Star Polymer Solutions
Deutsche Neutronenstreutagung, FZ Jülich, 19.-21.02.01
23.30.0

IFF-01-23-118
Stellbrink J.; Allgaier J.; Monkenbusch M.; Richter D.
Self and Collective Dynamics of Ordered Star Polymer Solutions
Int. Conf. on Neutron Scattering, TU München, 09.-13.09.01
23.30.0

IFF-01-23-119
Stellbrink J.; Allgaier J.; Richter D.; Schofield A.B.1; Poon W.C.K.1; Pusey P.N.
1Department of Physics and Astronomy, The University of Edinburgh, Mayfield Road, Edinburgh EH9 3JZ, UK
Partial Structure Factors in Star polymer/colloid mixtures
Deutsche Neutronenstreutagung, FZ Jülich, 19.-21.02.01
23.30.0

IFF-01-23-120

Toperverg B.1,2; Kentzinger E.1; Rücker U.1; Brückel Th.1
1FZJ, IFF, Jülich
2Petersburg Nuclear Physics Institute, Gatchina, Russia
Specular reflection and off-specular scattering of polarized neutrons from magnetic multilayers
Jülich, Deutsche Neutronenstreutagung 2001, 19. - 21.02.2001
23.89.1

IFF-01-23-121
Vass S.1; Haimer K.2; Meier G.; Grimm H.; Klapper M.2; Borberly S.1
1KFKI, Budapest
2MPI, Mainz
Sequence-dependent hydration properties of ionic ABA and BAB triblock copolymer micelles for SANS
Deutsche Neutronenstreutagung in Jülich vom 19.02.-21.02.2001
23.30.0

IFF-01-23-122
Voigt J.; Kentzinger E.; Rücker U.; Schweika W.; Brückel Th.; Schmidt W.; Ohl M.; Hupfeld D.
Proximity effects in Er/Tb superlattices: How Neutrons and X-Rays complement each other
München, ICNS-Konferenz, 09. - 13.09.2001
23.89.1

IFF-01-23-123
Voigt J.; Rücker U.; Kentzinger E.; Hupfeld D.; Brückel Th.
Proximity effects in Er/Tb superlattices
Aachen, MML'01-Tagung, 27.06.2001
23.89.1

IFF-01-23-124
Voigt J.; Schmidt W.1; Ohl M.1; Brückel Th.
1Institut Laue-Langevin, F-38042 Grenoble Cedex, France
Magnetische Ordnung in Erbium/Terbium-Schichtsystemen
Deutsche Neutronenstreutagung, FZ Jülich, 19.-21.02.01
23.89.1

IFF-01-23-125
Voigt J.; Schmidt W.; Ohl M.; Brückel Th.
Magnetische Ordnung in Erbium/Terbium-Schichtsystemen
Jülich, Deutsche Neutronenstreutagung 2001, 19. - 21.02.2001
23.89.1

IFF-01-23-126
Vorobiev A.1,2; Gordeev G.2; Major J.1; Toperverg B.2,3; Dosch H.1
1MPI für Metallforschung, Stuttgart
2PNPI, Gatchina, Russia
3FZJ, IFF, Jülich
The structure of ferrofluids in the vicinity of the interface with silicon
München, ICNS-Konferenz, 09. - 13.09.2001
23.89.1

IFF-01-23-127
Willner L.
Bestimmung der Austauschkinetik von PEP-PEO Blockcopolymer-Mizellen mittels zeitaufgelöster NKWS
Deutsche Neutronenstreutagung, FZ Jülich, 19.-21.02.01
23.30.0

IFF-01-23-128
Winkler R.G.; Hofmann T.1 ; Reineker P.1
1 Univ. Ulm, Germany
Structure of Rodlike Polyelectrolytes in Solution
Jülich Soft Matter Days 2001, Kerkrade
13.11. - 16.11.2001
23.30.0

IFF-01-23-129
Winkler R.G.; Hofmann T.1; Reineker P.1
1 Univ. Ulm, Germany
Integral Equation Theory Approach to Polyelectrolyte Solutions
Bridging the Time-Scale Gap, Konstanz
13.11. - 16.11.2001
23.30.0

IFF-01-23-130
Wunnicke O.
Effects of Interface States on Tunneling Magnetoresistance
4th International Symposium on Metallic Multilayers
Aachen, 24.06.-29.06.2001
23.20.0

IFF-01-23-131
Wunnicke O.
Effects of Interface States on Tunneling Magnetoresistance
European Graduate School on Condensed Matter: Physics of Magnetic
Multilayers-Theory and Experiment
Prague, Tschechien, 09.06.-16.06.2001
23.20.0

IFF-01-23-132
Wunnicke O.
Effects of Interface States on Tunneling Magnetoresistance
Summerschool on Density Functional Theory
Caramulo, Portugal, 28.08.-01.09.2001
23.20.0

IFF-01-23-133
Zorn R.; Richter D.; Hartmann L.1; Kremer F.2; Frick B.1
1Institut Laue-Langevin, F-38042 Grenoble Cedex, France
2Fakultät für Physik und Geowissenschaften, Universität Leipzig, Linnéstr. 5, 04103 Leipzig
Inelastische Neutronenstreuungsexperimente zur Glasdynamik in eingeschränkter Geometrie
Deutsche Neutronenstreutagung, FZ Jülich, 20.02.01
23.15.0

IFF-01-23-134
Zorn R.; Richter D.; Hartmann L.1; Kremer F.2; Frick B.1
1Institut Laue-Langevin, F-38042 Grenoble Cedex, France
2Fakultät für Physik und Geowissenschaften, Universität Leipzig, Linnéstr. 5, 04103 Leipzig
Quasielastic neutron scattering experiments on the a relaxation in a confined glass-forming liquid
4th Int. Discussion Meeting on Relaxations in Complex Systems, Cheronissos, Greece, 21.06.01
23.15.0

List of references

Alefeld B.	IFF-01-23-092	IFF-01-23-093	
Allgaier J.	IFF-01-23-007	IFF-01-23-008	IFF-01-23-017
	IFF-01-23-062	IFF-01-23-116	IFF-01-23-117
	IFF-01-23-118	IFF-01-23-119	
Antons A.	IFF-01-23-002		
Bechthold P.S.	IFF-01-23-006	IFF-01-23-075	
Berger R.	IFF-01-23-002		
Bergs W.	IFF-01-23-092	IFF-01-23-093	
Beyss M.	IFF-01-23-054		
Bihlmayer G.	IFF-01-23-048		
Blanchard A.	IFF-01-23-006		
Blügel S.	IFF-01-23-002	IFF-01-23-048	
Bolten D.	IFF-01-23-087		
Botti A.	IFF-01-23-003	IFF-01-23-004	IFF-01-23-005
Breidbach M.	IFF-01-23-019		
Breuer C.	IFF-01-23-006		
Brückel Th.	IFF-01-23-030	IFF-01-23-031	IFF-01-23-032
	IFF-01-23-059	IFF-01-23-060	IFF-01-23-061
	IFF-01-23-064	IFF-01-23-070	IFF-01-23-071
	IFF-01-23-092	IFF-01-23-093	IFF-01-23-095
	IFF-01-23-096	IFF-01-23-104	IFF-01-23-120
	IFF-01-23-122	IFF-01-23-123	IFF-01-23-124
	IFF-01-23-125		
Buchenau U.	IFF-01-23-105		
Buchmeier M.	IFF-01-23-009	IFF-01-23-019	IFF-01-23-051
	IFF-01-23-052		
Byelov D.	IFF-01-23-007	IFF-01-23-008	
Bürgler D.E.	IFF-01-23-006	IFF-01-23-009	IFF-01-23-019
	IFF-01-23-051	IFF-01-23-052	IFF-01-23-070
	IFF-01-23-071		
Conrad H.	IFF-01-23-010	IFF-01-23-031	IFF-01-23-032
	IFF-01-23-104		
Divin Y.Y.	IFF-01-23-112	IFF-01-23-113	
Dürr H.A.	IFF-01-23-048	IFF-01-23-049	IFF-01-23-050
	IFF-01-23-085	IFF-01-23-115	
Eberhardt W.	IFF-01-23-006	IFF-01-23-048	IFF-01-23-049
	IFF-01-23-050	IFF-01-23-075	IFF-01-23-085
	IFF-01-23-115		
Ehrhart P.	IFF-01-23-084		
Endo H.	IFF-01-23-007	IFF-01-23-008	IFF-01-23-017
	IFF-01-23-062		
Faley M.I.	IFF-01-23-014	IFF-01-23-015	IFF-01-23-047
Fetters L.J.	IFF-01-23-083		
Feuerbacher M.	IFF-01-23-108		
Fischer K.	IFF-01-23-054		
Fitsilis F.	IFF-01-23-084		

Frielinghaus H.	IFF-01-23-007 IFF-01-23-017	IFF-01-23-008	IFF-01-23-016
Gareev R.R.	IFF-01-23-009	IFF-01-23-019	
Goerigk G.	IFF-01-23-020		
Gompper G.	IFF-01-23-012	IFF-01-23-102	
Grimm H.	IFF-01-23-021	IFF-01-23-022	IFF-01-23-078
Grünberg P.	IFF-01-23-009 IFF-01-23-052 IFF-01-23-094	IFF-01-23-019 IFF-01-23-070	IFF-01-23-051 IFF-01-23-071
Hartmann M.	IFF-01-23-023	IFF-01-23-024	
Hauck J.	IFF-01-23-025		
Heinen J.	IFF-01-23-092	IFF-01-23-093	
Heinrich M.	IFF-01-23-026		
Hoffmann S.	IFF-01-23-028		
Hoffmann-Eifert S.	IFF-01-23-027 IFF-01-23-087	IFF-01-23-068 IFF-01-23-088	IFF-01-23-069
Horriar-Esser Ch.	IFF-01-23-064		
Hupfeld D.	IFF-01-23-030 IFF-01-23-123	IFF-01-23-108	IFF-01-23-122
Ioffe A.	IFF-01-23-031 IFF-01-23-059 IFF-01-23-104	IFF-01-23-032 IFF-01-23-060	IFF-01-23-033 IFF-01-23-061
Jahnen B.	IFF-01-23-034		
Jia C.L.	IFF-01-23-112		
Kahle S.	IFF-01-23-035	IFF-01-23-036	IFF-01-23-037
Kentzinger E.	IFF-01-23-070 IFF-01-23-093 IFF-01-23-097 IFF-01-23-123	IFF-01-23-071 IFF-01-23-095 IFF-01-23-120	IFF-01-23-092 IFF-01-23-096 IFF-01-23-122
Kienle D.	IFF-01-23-038		
Kirstein O.	IFF-01-23-001 IFF-01-23-041	IFF-01-23-039 IFF-01-23-042	IFF-01-23-040 IFF-01-23-043
Kirstein o.	IFF-01-23-044		
Klingeler R.	IFF-01-23-006	IFF-01-23-045	
Kohlstedt H.	IFF-01-23-106		
Kollmann M.	IFF-01-23-046	IFF-01-23-066	
Kozielewski T.	IFF-01-23-039 IFF-01-23-044	IFF-01-23-040	IFF-01-23-041
Kronast F.	IFF-01-23-048	IFF-01-23-049	IFF-01-23-050
Kuanr B.K.	IFF-01-23-051	IFF-01-23-052	
Köbler U.	IFF-01-23-053	IFF-01-23-054	
Küssel E.	IFF-01-23-031 IFF-01-23-060	IFF-01-23-032 IFF-01-23-061	IFF-01-23-059
Landis S.	IFF-01-23-049		
Liebsch A.	IFF-01-23-048		

Sager W.	IFF-01-23-098	IFF-01-23-099	IFF-01-23-100
	IFF-01-23-101		
Schilling T.	IFF-01-23-102		
Schlapp M.	IFF-01-23-031	IFF-01-23-032	IFF-01-23-059
	IFF-01-23-060	IFF-01-23-061	IFF-01-23-103
	IFF-01-23-104		
Schmidt W.	IFF-01-23-122	IFF-01-23-125	
Schmitz B.	IFF-01-23-031	IFF-01-23-032	
Schneider S.	IFF-01-23-106		
Schreiber R.	IFF-01-23-009	IFF-01-23-019	IFF-01-23-070
	IFF-01-23-071		
Schroeder K.	IFF-01-23-002		
Schwahn D.	IFF-01-23-072	IFF-01-23-073	IFF-01-23-074
	IFF-01-23-083	IFF-01-23-086	
Schweika W.	IFF-01-23-030	IFF-01-23-086	IFF-01-23-108
	IFF-01-23-109	IFF-01-23-110	IFF-01-23-122
Schäfer P.	IFF-01-23-088		
Seeck O.	IFF-01-23-111		
Shadrin P. M.	IFF-01-23-112		
Shirotov V. V.	IFF-01-23-113		
Sievers J.	IFF-01-23-085	IFF-01-23-115	
Stellbrink J.	IFF-01-23-116	IFF-01-23-117	IFF-01-23-118
	IFF-01-23-119		
Szot K.	IFF-01-23-068		
Toperverg B.	IFF-01-23-055	IFF-01-23-056	IFF-01-23-057
	IFF-01-23-095	IFF-01-23-096	IFF-01-23-120
	IFF-01-23-126		
Urban K.	IFF-01-23-014	IFF-01-23-015	IFF-01-23-034
	IFF-01-23-113		
Voigt J.	IFF-01-23-122	IFF-01-23-123	IFF-01-23-124
	IFF-01-23-125		
Wang Y.G.	IFF-01-23-070	IFF-01-23-071	
Waser R.	IFF-01-23-018	IFF-01-23-027	IFF-01-23-068
	IFF-01-23-069	IFF-01-23-084	IFF-01-23-087
	IFF-01-23-088	IFF-01-23-106	IFF-01-23-107
	IFF-01-23-114		
Willner L.	IFF-01-23-035	IFF-01-23-036	IFF-01-23-037
	IFF-01-23-072	IFF-01-23-073	IFF-01-23-074
	IFF-01-23-127		
Winkler R.G.	IFF-01-23-029	IFF-01-23-128	IFF-01-23-129
Wirth I.	IFF-01-23-006		
Wunnicke O.	IFF-01-23-130	IFF-01-23-131	IFF-01-23-132
Zeiske Th.	IFF-01-23-031	IFF-01-23-032	
Zorn R.	IFF-01-23-133	IFF-01-23-134	

Patents granted

IFF-01-31-001
Allgaier J.; Willner L.; Richter D.
Synthese von lipophob-lipophilen polymeren Micellen
US: 6,284,847 (04.09.2001)
PT 1.1375
23.30.0

IFF-01-31-002
Divin Y.Y.; Seo J.W.; Poppe U.
Schichtfolge mit wenigstens einem epitaktischen, nahezu a-Achsen orientierten HTSL-Dünnfilm oder mit einer Schicht aus einem mit HTSL kristallographisch vergleichbarer Struktur, sowie Verfahren zu ihrer Herstellung
US: 6,156,706 (05.12.2000)
PT 1.1333
23.42.0

IFF-01-31-003
Hojczyk R.; Poppe U.; Jia C.L.
Schichtenfolge sowie ein diese enthaltendes Bauelement
US: 6,191,073 (20.02.2001)
PT 1.1385
34.42.0

IFF-01-31-004
Klatt K.H.; Wenzl H.; Chakraborty A.K.1; Rohde J.1; Konrad R.1
1GRS Köln
Katalysator zur Beseitigung von Wasserstoff aus einer Wasserstoff, Sauerstoff und Dampf enthaltenden Atmosphäre
CA: 2,046,820 (02.10.2001)
PT 1.1026
FE 23.42.0

IFF-01-31-005
Kohlstedt H.; Stein S.
Dreitorbauelement, insbesondere Spininjektionstransistor
DE: 100 31 401 (22.11.2001)
PT 1.1810
23.42.0

IFF-01-31-006
Sonnenberg K.; Küssel E.; Bünger T.1; Flade T.1; Weinert B.1
1Fa. Freiberger
Verfahren und Vorrichtung zur Herstellung von Einkristallen sowie Kristallkeim
EP: 1038995 (08.08.2001) (BE,DE,FR,GB,IT,NL)
PT 1.1681
23.42.0

IFF-01-31-007
Wenzl H.; Oates W.
Verfahren zur aktiven Defektsteuerung bei der Züchtung von GaAs-Kristallen
EP: 0931184 (21.03.2001) (CH/LI,DE,FR,GB,IE)
PT 1.1405
23.42.0

IFF-01-31-008
Zhang Y.; Zander W.; Banzet M.; Schubert J.1; Soltner H.
1ISG
Anordnung zur Ankopplung eines rf-SQUID-Magnetometers an einen supraleitenden Tankschwingkreis auf einem Substrat
US: 6,225,800 (01.05.2001)
PT 1.1356
29.85.0

List of references

Allgaier J.	IFF-01-31-001	
Banzet M.	IFF-01-31-008	
Divin Y.Y.	IFF-01-31-002	
Hojczyk R.	IFF-01-31-003	
Jia C.L.	IFF-01-31-003	
Klatt K.H.	IFF-01-31-004	
Kohlstedt H.	IFF-01-31-005	
Küssel E.	IFF-01-31-006	
Oates W.	IFF-01-31-007	
Poppe U.	IFF-01-31-002	IFF-01-31-003
Richter D.	IFF-01-31-001	
Seo J.W.	IFF-01-31-002	
Soltner H.	IFF-01-31-008	
Sonnenberg K.	IFF-01-31-006	
Stein S.	IFF-01-31-005	
Wenzl H.	IFF-01-31-004	IFF-01-31-007
Willner L.	IFF-01-31-001	
Zander W.	IFF-01-31-008	
Zhang Y.	IFF-01-31-008	

Patents applied for

IFF-01-32-001
Kohlstedt H.; Rodriguez Contrearas J.
Verfahren zur Erzeugung eines Tunnelkontaktes sowie Vorrichtung umfassend Mittel zur Erzeugung eines Tunnelkontaktes
PCT: PCT/DE01/04447 (23.11.2001) (EP,US,JP,KR)
PT 1.1859
23.42.0

IFF-01-32-002
Kohlstedt H.; Stein S.
Dreitorbauelement, insbesondere Spininjektionstransistor
PCT: PCT/EP01/07143 (23.06.2001) (EP;US,JP;KR)
PT 1.1810
23.42.0

IFF-01-32-003
Kohlstedt H.
Anordnung zum Messen eines Magnetfeldes und Verfahren zum Herstellen einer Anordnung zum Messen eines Magnetfeldes
PCT: PCT/EP01/01305 (07.02.2001) (EP,US,JP,KR)
PT 1.1782
23.42.0

IFF-01-32-004
Kohlstedt H.
Matrix für einen Magneto-Random-Access Memory (MRAM)
DE: 298 24 631.7 (2001)
PT 1.1583
23.42.0

IFF-01-32-005
Morenzin J.; Eberhardt W.; Schondelmeier D.
Markierungseinrichtung sowie Verfahren zum Auslesen einer solchen Markierungseinrichtung
a) PCT: PCT/EP01/00246 (10.01.2001) (alle Länder)
b) PCT: PCT/EP01/00247 (10.01.2001) (alle Länder)
AR: P0101 00762 (21.02.2001)
CL: 403-01 (21.02.2001)
c) PCT: PCT/EP01/00244 (10.01.2001 (alle Länder)
AR: P0101 00763 (21.02.2001)
CL: 404-01 (21.02.2001)
PT 1.1777
23.55.0

IFF-01-32-006
Morenzin J.; Schondelmeier D.
Markierungseinrichtung sowie Verfahren zum Auslesen der Markierungseinrichtung
DE: 101 30 553.2 (25.06.2001)
PT 1.1922
23.42.0

IFF-01-32-007
Nie X.
Magnetisches Schichtsystem sowie ein solches Schichtsystem aufweisendes Bauelement
PCT: PCT/DE01/03631 (19.09.2001) (EP,US,CA,JP)
PT 1.1832
23.42.0

IFF-01-32-008
Schondelmeier D.; Eberhardt W.
Verfahren zur Behandlung von Oberflächen sowie mit diesen Verfahren hergestellte Gegenstände und Verwendung von Verbindungen als photochemisch spaltbare Reagenzien
PCT: PCT/DE01/02315 (21.06.2001) (EP,US,JP)
PT 1.1798
23.42.0

IFF-01-32-009
Zimmermann E.; Glaas W.; Halling H.1; Faley M.; Soltner H.2
1ZEL
2ESS
SQUID-Mikroskop
EP: 01.125102.2 (23.10.2001)
(AT,BE,CH/Li,CY,DE,DK,ES,FI,FR,GB,GR;IE,IT,LU,MC,NL,PT,SE,TR)
US: (2001)
PT 1.1838
23.42.0

List of references

Eberhardt W.	IFF-01-32-005	IFF-01-32-008	
Faley M.I.	IFF-01-32-009		
Glaas W.	IFF-01-32-009		
Kohlstedt H.	IFF-01-32-001 IFF-01-32-004	IFF-01-32-002	IFF-01-32-003
Morenzin J.	IFF-01-32-005	IFF-01-32-006	
Nie X.	IFF-01-32-007		
Rodriguez-Contrearas	IFF-01-32-001		
Schondelmeier D.	IFF-01-32-005	IFF-01-32-006	IFF-01-32-008
Stein S.	IFF-01-32-002		
Zimmermann E.	IFF-01-32-009		

Lecture courses

IFF-01-41-001
Baumgaertner A.
Einführung in die Bioinformatik
Universität Duisburg, V2
WS 2001/2002
23.30.0

IFF-01-41-002
Baumgaertner A.
Einführung in die theoretische Biophysik II
Universität Duisburg, V2
WS 2000/2001
23.30.0

IFF-01-41-003
Baumgaertner A.
Einführung in die theoretische Biophysik
Universität Duisburg, V2
SS 2001
23.30.0

IFF-01-41-004
Bechthold P.S.
Experimentalphysik für Studierende der Medizin und der Wirtschafts- und Sozialwissenschaften
Vorlesung WS 2001
Universität zu Köln
23.20.0

IFF-01-41-005
Blügel S.; Dederichs P.H.; Müller-Krumbhaar H.; Schroeder K.
Computeranwendungen in der Festkörperphysik
Physikalisches Seminar (6h), WS 2000/2001, RWTH Aachen
23.20.0

IFF-01-41-006
Brückel Th.
Elastic scattering from many-body systems
IFF, 5th Laboratory Course Neutron Scattering, 18.09.2001
23.89.1

IFF-01-41-007
Brückel Th.
Magnetism
IFF, 5th Laboratory Course Neutron Scattering, 21.09.2001
23.89.1

IFF-01-41-008
Bürgler D.E.; Grünberg P.
Magnetoelectronic: Exchange anisotropy, interlayer exchange coupling, GMR, TMR and current induced magnetic switching
Vorlesung während des 32. IFF Ferienkurs 2001 "Neue Materialien für die Informationstechnik"
23.42.0

IFF-01-41-009
Bürgler D.E.
Magnetoelektronik (Teil 2)
IFF-Ferienschule 2001 "Neue Materialien für die Informationstechnik"
05. - 16. March 2001, FZJ
23.42.0

IFF-01-41-010
Conrad H.
Neutron Sources
IFF, 5th Laboratory Course Neutron Scattering, 18.09.2001
23.89.1

IFF-01-41-011
Dederichs P.H.; Schroeder K.
Theoretische Festkörperphysik I
Vorlesung (4h) und Übung (2h), SS 2001, RWTH Aachen
23.20.0

IFF-01-41-012
Dederichs P.H.; Schroeder K.
Theoretische Festkörperphysik II
Vorlesung (4h) und Übung (2h), WS 2001/02, RWTH Aachen
23.20.0

IFF-01-41-013
Dürr H.A.
Magnetic random access memory devices
IFF-Ferienschule 2001 "Neue Materialien für die Informationstechnik"
05. - 16. March 2001, FZJ
23.20.0

IFF-01-41-014
Ehrhart P.
Deposition methods
32. IFF-Ferienkurs, Jülich, 05.03.2001
23.42.0

IFF-01-41-015
Gompper G.
Statistische Mechanik von Grenzflächen und Membranen
Universität Köln
SS 2001
23.30.0

IFF-01-41-016
Grimm H.
Crystal spectrometer: Triple-axis and backscattering spectrometer
WS 01/02, Laboratory Course Neutron Scattering, FZ Jülich, 18.-28.09.01
23.30.0

IFF-01-41-017
Grünberg P.; Bürgler D.E.
Magnetoelektronik in Forschung und Anwendung
Universität zu Köln, SS 2001
23.42.0

IFF-01-41-018
Hoffmann-Eifert S.
Dielectrics and Optics
32. IFF-Ferienkurs, Jülich, 05.03.2001
23.42.0

IFF-01-41-019
Kohlstedt H.
Ferroelectric field-effect transistors
32. IFF-Ferienkurs, Jülich, 05.03.2001
23.42.0

IFF-01-41-020
Kohlstedt H.
Grundlagen und Anwendungen supraleitender Bauelemente (WS 00/01)
Universität zu Köln
23.42.0

IFF-01-41-021
Kohlstedt H.
Halbleiterphysik (SS 01)
Universität zu Köln
23.42.0

IFF-01-41-022
Lang P.
SS: Streuung an fluiden Grenzflächen und biologischen Modellsystemen
TU Berlin, Sommersemester 2001, v. 24.09.-28.09.01
23.30.0

IFF-01-41-023
Lustfeld H.
Methoden der Theoretischen Physik I, Beispiele in C++
Universität Duisburg

WS 2001/2002
23.20.0

IFF-01-41-024
Lustfeld H.
Moderne Probleme der Geophysik
Universität Duisburg
WS 2001/2002
23.20.0

IFF-01-41-025
Lustfeld H.
Wavelets in der Physik I mit Beispielen in C++
Universität Duisburg
WS 2000/2001
23.20.0

IFF-01-41-026
Lustfeld H.
Wavelets in der Physik II mit Beispielen in C++
Universität Duisburg
SS 2001
23.20.0

IFF-01-41-027
Monkenbusch M.
Neutron Spin-Echo Spectrometer (NSE)
WS 01/02, Laboratory Course Neutron Scattering, FZ Jülich, 18.-28.09.01
23.30.0

IFF-01-41-028
Monkenbusch M.
Polymer Dynamics
WS 01/02, Laboratory Course Neutron Scattering, FZ Jülich, 18.-28.09.01
23.30.0

IFF-01-41-029
Monkenbusch M.
Time-of-Flight Spectrometers
WS 01/02, Laboratory Course Neutron Scattering, FZ Jülich, 18.-28.09.01
23.30.0

IFF-01-41-030
Müller-Krumbhaar H.
Einführung zur Theoretischen Physik
WS 2000/2001
23.15.0

IFF-01-41-031
Nägele G.
Kolloide als Modellsysteme weicher Materie: strukturelle und dynamische Eigenschaften
Universität Konstanz, Okt./Nov. 2001
23.30.0

IFF-01-41-032
Prager M.
Translation and Rotation
WS 01/02, Laboratory Course Neutron Scattering, FZ Jülich, 18.-28.09.01
23.15.0

IFF-01-41-033
Richter D.
Ferroelectricity
WS 00/01, IFF Ferienschule: Neue Materialien für die Informationstechnik, FZ Jülich, 05.-16.03.01
23.30.0

IFF-01-41-034
Richter D.
Properties of the neutron, elementary scattering processes
WS 01/02, Laboratory Course Neutron Scattering, FZ Jülich, 18.-28.09.01
23.30.0

IFF-01-41-035
Sager W.
WS: Kolloide und Grenzschichten
Universität in Twente, Wintersemester 2000/2001 v. Nov. 2000 - März 2001
23.30.0

IFF-01-41-036
Schmid D.1; Buchenau U.
1Univ. Düsseldorf, Inst. für Festkörperspektroskopie, Universitätsstraße 1 (Bereich 25), 40225 Düsseldorf
Experimentalphysik IV (Kern- und Elementarteilchenphysik)
Univ. Düsseldorf, SS 2001
23.15.0

IFF-01-41-037
Schroeder H.
Ausgewählte Kapitel der Metallphysik
Vertiefungsfach II: Metallphysik
Fakultät für Bergbau, Hüttenwesen und Geowissenschaften der RWTH Aachen, WS 00/01 und WS 01/02
23.42.0

IFF-01-41-038
Schroeder H.
High-permittivity materials for DRAMs
32. IFF-Ferienkurs, Jülich, 05.03.2001.
23.42.0

IFF-01-41-039
Schwahn D.
Small-angle scattering and reflectometry
WS 01/02, Laboratory Course Neutron Scattering, FZ Jülich, 18.-28.09.2001
23.30.0

IFF-01-41-040
Schwahn D.
Soft Matter: Structure
WS 01/02, Laboratory Course Neutron Scattering, FZ Jülich, 18.-28.09.2001
23.30.0

IFF-01-41-041
Schweika W.
Polarization analysis
IFF, 5th Laboratory Course Neutron Scattering, 19.09.2001
23.89.1

IFF-01-41-042
Schütz G.
Physik der Finanzmärkte
Universität Bonn
SS 2001
23.15.0

IFF-01-41-043
Seeck O.
Analysis by Diffraction and Fluorescence Methods
Jülich, 32. Ferienkurs des Instituts für Festkörperforschung, Neue Materialien für die Informationstechnik, 05. - 16.03.2001
23.89.1

IFF-01-41-044
Seeck O.
Continuum description: Grazing incidence neutron scattering
IFF, 5th Laboratory Course Neutron Scattering, 19.09.2001
23.89.1

IFF-01-41-045
Stellbrink J.
Reaktionskinetik
SS01, Universität Münster
23.30.0

IFF-01-41-046
Urban K.; Ebert Ph.
Neue Materialien: Von der Präparation zur Anwendung
Seminar an der RWTH Aachen, SS 2001.

IFF-01-41-047
Waser R.; Ehrhart P.; Hoffmann S.; Kohlstedt H.; Schroeder H.
Neue Materialien und Bauelemente für die Informationstechnik I (WS 01/02)
Vertiefungsfach II
Fakultät für Elektrotechnik der RWTH Aachen
23.42.0

IFF-01-41-048
Waser R.
Molecular electronics
32. IFF-Ferienkurs, Jülich, 05.03.2001.
23.42.0
Bechthold P.S.
Bechthold P.S.
Symmetrie und Spektroskopie
Vorlesung SS 2001
Universität zu Köln
23.20.0

IFF-01-41-049
Waser R.
Vorlesung Werkstoffe der Elektrotechnik
Sensoren und Sensormeßtechnik I+II
RWTH Aachen
23.42.0

IFF-01-41-050
Winkler R.G.
Einführung in die Theorie der Soft-Matter Systeme
Universität Ulm
SS 2001
23.30.0

IFF-01-41-051
Zorn R.
Correlation functions measured by scattering experiments
WS 01/02, Laboratory Course Neutron Scattering, FZ Jülich,
18.-28.09.2001
23.15.0

IFF-01-41-052
Zorn R.
Liquid Crystal Displays
WS00/01, IFF Ferienschule: Neue Materialien für die Informationstechnik, 05.-16.03.2001
23.15.0

Scientific degrees, further education

Program	Diplomas granted	Doctor. comp.	Habil. comp.	Prof. Pos.off.
1.2 FKF	10	15	2	3
2.1 PGI		4		
Sum	10	19	2	3

List of references

Baumgaertner A.	IFF-01-41-001	IFF-01-41-002	IFF-01-41-003
Bechthold P.S.	IFF-01-41-004		
Blügel S.	IFF-01-41-005		
Brückel Th.	IFF-01-41-006	IFF-01-41-007	
Buchenau U.	IFF-01-41-036		
Bürgler D.E.	IFF-01-41-008	IFF-01-41-009	IFF-01-41-017
Conrad H.	IFF-01-41-010		
Dederichs P.H.	IFF-01-41-005	IFF-01-41-011	IFF-01-41-012
Dürr H.A.	IFF-01-41-013		
Ebert Ph.	IFF-01-41-046		
Ehrhart P.	IFF-01-41-014	IFF-01-41-047	
Gompper G.	IFF-01-41-015		
Grimm H.	IFF-01-41-016		
Grünberg P.	IFF-01-41-008	IFF-01-41-017	
Hoffmann S.	IFF-01-41-047		
Hoffmann-Eifert S.	IFF-01-41-018		
Kohlstedt H.	IFF-01-41-019 IFF-01-41-047	IFF-01-41-020	IFF-01-41-021
Lang P.	IFF-01-41-022		
Lustfeld H.	IFF-01-41-023 IFF-01-41-026	IFF-01-41-024	IFF-01-41-025
Monkenbusch M.	IFF-01-41-027	IFF-01-41-028	IFF-01-41-029
Müller-Krumbhaar H.	IFF-01-41-005	IFF-01-41-030	
Nägele G.	IFF-01-41-031		
Prager M.	IFF-01-41-032		
Richter D.	IFF-01-41-033	IFF-01-41-034	
Sager W.	IFF-01-41-035		
Schroeder H.	IFF-01-41-037	IFF-01-41-038	IFF-01-41-047
Schroeder K.	IFF-01-41-005	IFF-01-41-011	IFF-01-41-012
Schwahn D.	IFF-01-41-039	IFF-01-41-040	
Schweika W.	IFF-01-41-041		
Schütz G.	IFF-01-41-042		
Seeck O.	IFF-01-41-043	IFF-01-41-044	
Stellbrink J.	IFF-01-41-045		
Urban K.	IFF-01-41-046		
Waser R.	IFF-01-41-047	IFF-01-41-048	IFF-01-41-049
Winkler R.G.	IFF-01-41-050		
Zorn R.	IFF-01-41-051	IFF-01-41-052	

Internal reports

IFF-01-51-001
Brückel Th.
Das Institut für Festkörperforschung
IFF, Informationsveranstaltung für den wissenschaftlichen Beirat, 26.04.2001
23.89.1

IFF-01-51-002
Brückel Th.
Elastic scattering from many-body systems
IFF, 5th Laboratory Course Neutron Scattering, 18.09.2001
23.89.1

IFF-01-51-003
Brückel Th.
Magnetism
IFF, 5th Laboratory Course Neutron Scattering, 21.09.2001
23.89.1

IFF-01-51-004
Conrad H.
JESSICA - die Jülicher 10 mW Spallation-Neutronenquelle
IFF, Informationsveranstaltung für den wissenschaftlichen Beirat, 26.04.2001
23.60.0

IFF-01-51-005
Conrad H.
Neutron Sources
IFF, 5th Laboratory Course Neutron Scattering, 18.09.2001
23.89.1

IFF-01-51-006
Ioffe A.
A New Thermal Neutron Spectrometer/Diffractometer for Polarization Analysis (SV30) at the Research Reactor FRJ-2
FZJ, DIDO operators meeting, 01. - 04.10.2001
23.89.1

IFF-01-51-007
Paessens M.
Reptationsdynamik von kurzen verschlauften Polymeren
DMRG Studien für Rubinstein-Duke-Modelle
Diplomarbeit, RWTH Aachen
23.30.0

IFF-01-51-008
Schweika W.
Polarization analysis
IFF, 5th Laboratory Course Neutron Scattering, 19.09.2001
23.89.1

IFF-01-51-009
Seeck O.
Continuum description: Grazing incidence neutron scattering
IFF, 5th Laboratory Course Neutron Scattering, 19.09.2001
23.89.1

IFF-01-51-010
Willmann R.
Lattice gas model for reptation with Disorder
Diplomarbeit, Universität Bonn
23.30.0

List of references

Brückel Th.	IFF-01-51-001	IFF-01-51-002	IFF-01-51-003
Conrad H.	IFF-01-51-004	IFF-01-51-005	
Ioffe A.	IFF-01-51-006		
Paessens M.	IFF-01-51-007		
Schweika W.	IFF-01-51-008		
Seeck O.	IFF-01-51-009		
Willmann R.	IFF-01-51-010		

Internal seminars

IFF-01-61-001
Allakhiarov E.
Multicollisional mesoscopic solvent model and its application to
solvent flow over spherical obstacle
Klausurtagung Theorie der Weichen Materie, Monschau
30.9.-2.10.2001
23.30.0

IFF-01-61-002
Auth T.
Effect of anchored polymers on the elasticity of membranes
Klausurtagung Theorie der Weichen Materie, Monschau
30.9.-2.10.2001
23.30.0

IFF-01-61-003
Baumgaertner A.
Motility of Cells
Klausurtagung Theorie der Weichen Materie, Monschau
30.9.-2.10.2001
23.30.0

IFF-01-61-004
Bürgler D.E.
Magnetische Zwischenschichtkopplung in Fe/FeSi/Fe Systemen
IFF-Beiratssitzung
26.04.2001
23.42.0

IFF-01-61-005
Dhont J.
The Smoluchowski Equation and Spinodal Decomposition
Soft Matter Seminar - Jülich
Heimbach, 18.01.01
23.30.0

IFF-01-61-006
Ehrhart P.
Metal Organic Chemical Vapor Deposition
Klausurtagung des Instituts Elektrokeramische Materialien
Hirschegg, 27.08.01-30.08.01
23.42.0

IFF-01-61-007
Eisenriegler E.
Colloids in polymer solutions: the depletion interaction
Joint Soft Matter Seminar, IFF, FZJ
3. 5. 2001
23.30.0

IFF-01-61-008
Eisenriegler E.
Polymer depletion interaction for anisotropic particles
Klausurtagung Theorie der Weichen Materie, Monschau
30.9.-2.10.2001
23.30.0

IFF-01-61-009
Elsebrock R.
Mikrowellen-Keramiken
Klausurtagung des Instituts Elektrokeramische Materialien
Hirschegg, 27.08.01-30.08.01
23.42.0

IFF-01-61-010
Gompper G.
Forschungsarbeiten auf dem Gebiet der Weichen Materie
Vortrag auf der Informationstagung aus Anlaß der 16. Sitzung des Wissenschaftlichen Beirats des IFF, Forschungszentrum Jülich
26.4.2001
23.30.0

IFF-01-61-011
Gompper G.
Structure and Phase Behavior of Microemulsions
Klausurtagung Theorie der Weichen Materie, Monschau
30.9.-2.10.2001
23.30.0

IFF-01-61-012
Hoffmann-Eifert S.
Defektchemie dünner Schichten
Klausurtagung des Instituts Elektrokeramische Materialien
Hirschegg, 27.08.01-30.08.01
23.42.0

IFF-01-61-013
Kohlstedt H.
TMR&MRAM, Ultradünne FE-Schichten
Klausurtagung des Instituts Elektrokeramische Materialien
Hirschegg, 27.08.01-30.08.01
23.42.0

IFF-01-61-014
Lettinga P.
Microscopic Origin of the non-linear viscoelastic response of colloidal dispersions
IFF, Informationsveranstaltung für den wiss. Beirat, 26.04.01
23.30.0

IFF-01-61-015
Monkenbusch M.; Richter D.; Wischnewski A.
Prototyp eines Neutronenspinecho-Spektrometers für Spallationsquellen
FZJ-HMI ESS HGF Projekt Meeting, FZ Jülich, 16.03.01
23.30.0

IFF-01-61-016
Monkenbusch M.; Wischnewski A.; Willner L.; Richter D.; Pyckhout-Hintzen W.; Farago B.1
1Institut Laue-Langevin, F-38042 Grenoble Cedex, France
Erste direkte Beobachtung des Übergangs von der Rouse- zur Reptationsdynamik in Polyethylen durch inkohärente Neutronenspinechospektroskopie
IFF Beirat, FZ Jülich, 26.04.01
23.30.0

IFF-01-61-017
Monkenbusch M.
Instrumententwicklung für die ESS
ESS Tag, Monschau, 10.05.01
23.30.0

IFF-01-61-018
Paessens M.
Reptation dynamics of short entangled polymers
Klausurtagung Theorie der Weichen Materie, Monschau
30.9.-2.10.2001
23.30.0

IFF-01-61-019
Pithan C.
Pulver- und Keramiksynthese
Klausurtagung des Instituts Elektrokeramische Materialien
Hirschegg, 27.08.01-30.08.01
23.42.0

IFF-01-61-020
Popkov V.
Spontaneous symmetry breaking in 2-component diffusive systems
Klausurtagung Theorie der Weichen Materie, Monschau
30.9.-2.10.2001
23.30.0

IFF-01-61-021
Schroeder H.
Ladungstransport durch dünne Schichten
Klausurtagung des Instituts Elektrokeramische Materialien

Hirschegg, 27.08.01-30.08.01
23.42.0

IFF-01-61-022
Schütz G.
Nonequilibrium relaxation law for entangled polymers,
Klausurtagung Theorie der Weichen Materie, Monschau
30.9.-2.10.2001
23.30.0

IFF-01-61-023
Schütz G.
Vom Mikrokosmos zum Makrokosmos - Strukturbildung und Phasenuebergaenge
in Zufallsprozessen fern vom Gleichgewicht
FZJ-Kolloquium
9.3.2001
23.15.0

IFF-01-61-024
Waser R.
Integration elektrokeramischer Materialien
Klausurtagung des Instituts Elektrokeramische Materialien
Hirschegg, 27.08.01-30.08.01
23.42.0

IFF-01-61-025
Waser R.
Überblick und Ausblick Forschungsarbeiten des Instituts
Klausurtagung des Instituts Elektrokeramische Materialien
Hirschegg, 27.08.01-30.08.01
23.42.0

IFF-01-61-026
Willmann R.
Diffusion coefficient of polymers with kinematic disorder
Klausurtagung Theorie der Weichen Materie, Monschau
30.9.-2.10.2001
23.30.0

IFF-01-61-027
Winkler R.G.
Integral Equation Theory Applied to Polyelectrolyte Systems
Klausurtagung Theorie der Weichen Materie, Monschau
30.9.-2.10.2001
23.30.0

List of references

Allakhiarov E.	IFF-01-61-001		
Auth T.	IFF-01-61-002		
Baumgaertner A.	IFF-01-61-003		
Bürgler D.E.	IFF-01-61-004		
Dhont J.	IFF-01-61-005		
Ehrhart P.	IFF-01-61-006		
Eisenriegler E.	IFF-01-61-007	IFF-01-61-008	
Elsebrock R.	IFF-01-61-009		
Gompper G.	IFF-01-61-010	IFF-01-61-011	
Hoffmann-Eifert S.	IFF-01-61-012		
Kohlstedt H.	IFF-01-61-013		
Lettinga P.	IFF-01-61-014		
Monkenbusch M.	IFF-01-61-015	IFF-01-61-016	IFF-01-61-017
Paessens M.	IFF-01-61-018		
Pithan C.	IFF-01-61-019		
Popkov V.	IFF-01-61-020		
Pyckhout-Hintzen W.	IFF-01-61-016		
Richter D.	IFF-01-61-015	IFF-01-61-016	
Schroeder H.	IFF-01-61-021		
Schütz G.	IFF-01-61-022	IFF-01-61-023	
Waser R.	IFF-01-61-024	IFF-01-61-025	
Willmann R.	IFF-01-61-026		
Willner L.	IFF-01-61-016		
Winkler R.G.	IFF-01-61-027		
Wischnewski A.	IFF-01-61-015	IFF-01-61-016	

Institute for Solid State Research (IFF)

Research Center Jülich GmbH

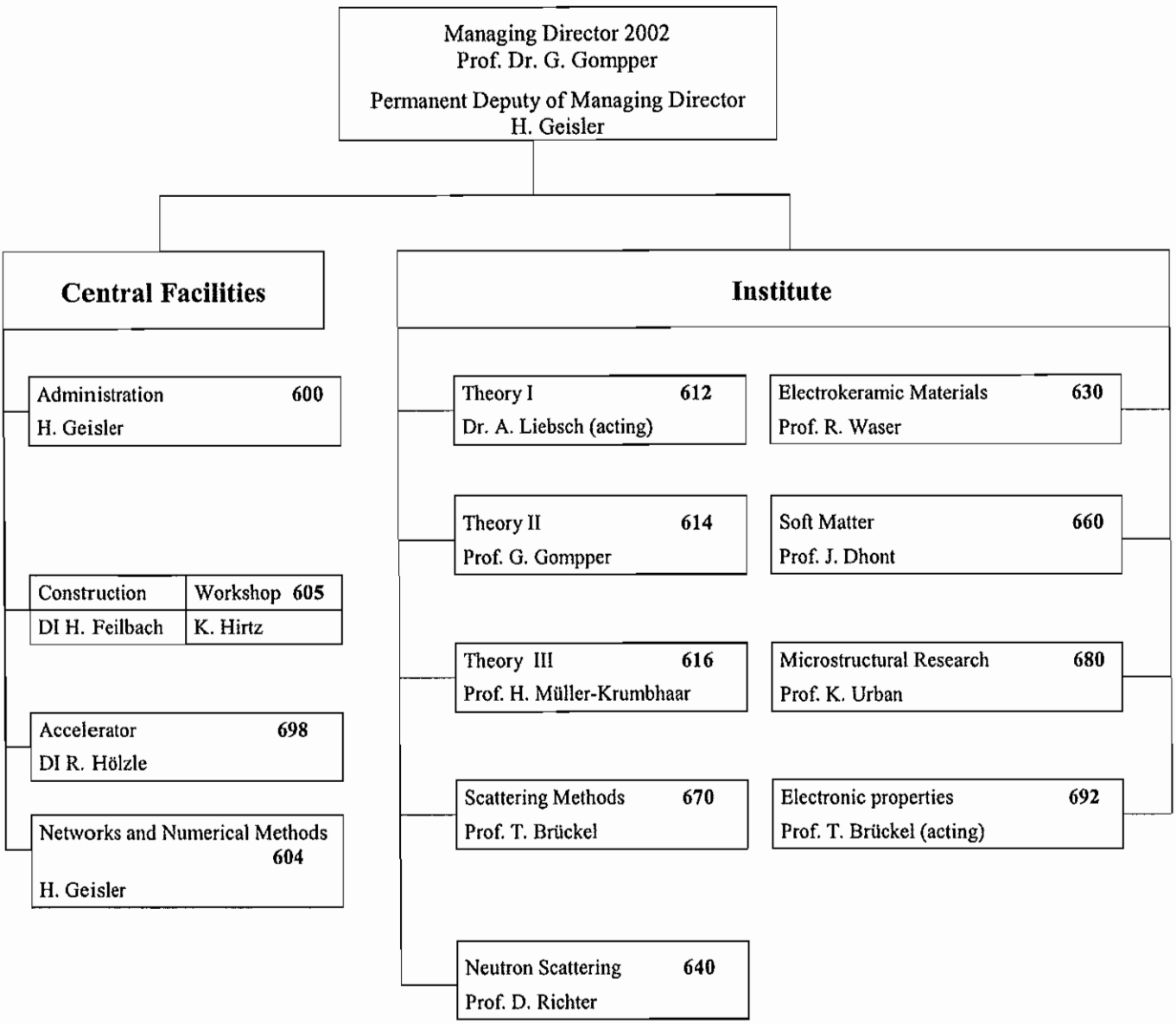

01.01.2002

Scientific Advisory Board 2002

The 2002 meeting of the Scientific Advisory Board will take place on the 21./23. March 2002. Currently, the board consists of the following members:

Dr. C. **Carlile**, Institute Laue-Langevin, Grenoble, France

Prof. R. **Dronskowski**, RWTH Aachen

Prof. K. **Ensslin**, ETH Zürich

Prof. H. **Eschrig**, IFW Dresden **Chairman**

Prof. S. **Hess**, TU Berlin

Prof. H. **Ibach**, ISG-3

Dr. J. **Joosten**, DSM Research, Geleen, NL

Prof. H. **von Löhneysen**, Forschungszentrum Karlsruhe

Prof. M. **Manninen**, University of Jyväskyla, Finland

Prof. T. **Nattermann**, Universität zu Köln

Prof. W. **Press**, Universität Kiel **Vice Chairman**

Dr. J. **Rieger**, BASF, Ludwigshafen

Prof. L. **Singheiser**, Forschungszentrum Jülich, IWV-2

Dr. K. **Sommer**, Bayer AG, Leverkusen

Prof. E. **Umbach**, Universität Würzburg

Prof. M. **Wuttig**, RWTH Aachen

Prof. P. **Wyder**, Centre National de la Recherche Scientifique (MPI), Grenoble, France

Personnel 2001/2002

Staff members (centrally financial)	
- **Scientific Staff**	**104**
including those funded externally	7
- **Technical Staff**	**53**
including those funded externally	1
Post-doc (HGF)	**21**
including those funded externally	3
Staff members of service-groups	**39**
Administrations incl. Secretaries	**22**
Graduate students	**63**
including those funded externally	19
Diploma students	**17**
Trainees	**27**
Guests Scientists staying for two weeks or longer	**56**
Invited lectures	**136**

IFF-Scientists Teaching at Universities

Lecturer:	University:
Dr. A. Baumgärtner	Duisburg
Dr. P.S. Bechthold	Köln
Dr. A. Bringer	Düsseldorf
Prof. Th. Brückel	Aachen
Prof. U. Buchenau	Düsseldorf
Prof. P. Dederichs	Aachen
Prof. J.K.G. Dhont	Düsseldorf
Dr. P. Ebert	Aachen
Dr. P. Ehrhart	Aachen
Prof. E. Eisenriegler	Düsseldorf
Prof. P. Grünberg	Köln
Dr. H. Kohlstedt	Köln
Dr. H. Lustfeld	Duisburg
Prof. H. Müller-Krumbhaar	Aachen
Prof. G. Nägele	Konstanz
Prof. D. Richter	Münster
Prof. T. Schober	Aachen
Dr. H. Schroeder	Aachen
Prof. K. Schroeder	Aachen
Dr. G. Schütz	Bonn
Dr. W. Schweika	Aachen
Prof. K. Urban	Aachen
Prof. R. Waser	Aachen
Prof. R. Winkler	Ulm
Dr. R. Zorn	Münster

IFF Scientists on leave 2001

Dr. St. Eisebitt	University Stanford, USA
Dr. G. Goerigk	HASYLAB at DESY, Hamburg, Germany
Dr. D. Hupfeld	APS Argonne, USA
Dr. R. Lässer	Forschungszentrum Karlsruhe, Germany
Dr. U. Rücker	Laboratoire Leon Brillouin, Saclay, France
Dr. W. Schmidt	ILL Grenoble, France
Dr. O. Seeck	HASYLAB at DESY, Hamburg, Germany
Dr. W. Kockelmann	Rutherford Appleton Laboratory, Chilton, England
Dr. D. Hamann	HASYLAB at DESY, Hamburg, Germany
Dr. G. Kali	ILL Grenoble, France

List of IFF-Scientists

(G: Guests; GS: Graduate students

Abdel-Goad El-, Mahmoud	(Neutron Scattering, G)
Akola, Jaakko	(Theory I, G)
Allakhiarov, Elchad	(Theory II)
Allgaier, Jürgen	(Neutron Scattering)
Arbe, Maria	(Neutron Scattering, G)
Atodiresei, Nicolae	(Theory III, GS)
Auth, Thorsten	(Theory II, GS)
Babik, Waldemar	(Scattering Methods, GS)
Balanetskyy, Sergiy	(Microstructure Research, GS)
Baldus, Oliver	(Electroceramic Materials, GS)
Ballone, Pietro	(Theory I, G)
Baud, Stephanie	(Electronic Properties, G)
Baumgarten, Lutz	(Electronic Properties)
Baumgärtner, Artur	(Theory II)
Bechthold, Paul	(Electronic Properties)
Blanchard, Ariane	(Neutron Scattering, GS)
Blügel, Stefan	(Electronic Properties)
Bombardi, Alessandro	(Neutron Scattering)
Bos, Johanna	(Scattering Methods)
Botti, Alberto	(Neutron Scattering)
Boukhvalov, Danil	(Theory I, GS)
Breidbach, Michael	(Electronic Properties, GS)
Brener, Efim	(Theory III)
Bringer, Andreas	(Theory I)
Buchenau, Ulrich	(Neutron Scattering)
Buchmeier, Matthias	(Electronic Properties, GS)
Buitenhuis, Johan	(Soft Matter)
Bürgler, Daniel Emil	(Electronic Properties)
Byelov, Dmytro	(Neutron Scattering, GS)
Cao, Yigang	(Theory III, GS)
Carletto, Philippe	(Soft Matter, G)
Chen, Xiaosong	(Theory II, G)
Colmenero, Juan	(Neutron Scattering, G)
Conrad, Harald	(Scattering Methods)
Corcoran, Derek	(Electroceramic Materials, G)
Cramm, Stefan	(Electronic Properties)
Damm, Thorsten	(Electronic Properties, GS)

Dederichs, Peter-Heinz	(Theory III)
Demange, Valerie	(Microstructure Research, GS)
Divin, Yuri	(Microstructure Research)
Dorner, Bruno	(Neutron Scattering)
Durcansky, Georg	(Networks and Numerical Methods)
Dürr, Hermann	(Electronic Properties)
Ebert, Philipp	(Microstructure Research)
Ehrhart, Peter	(Electroceramic Materials)
Eisebitt, Stefan	(Electronic Properties)
Eisenriegler, Erich	(Theory II)
Eliashberg, Gerasim	(Electroceramic Materials, G)
Endo, Hitoshi	(Neutron Scattering, GS)
Faley, Mikhail	(Microstructure Research)
Fetters, L.J.	(Neutron Scattering, G)
Feuerbacher, Michael	(Microstructure Research)
Fitsilis, Fotios	(Electroceramic Materials, GS)
Fitsilis, Michael	(Electroceramic Materials, GS)
Fousek, Jan	(Electroceramic Materials, G)
Freiwald, Mirko	(Electronic Properties, GS)
Freyss, Michel	(Theory III, G)
Galanakis, Iosif	(Theory III, G)
Ganster, Ralf	(Electroceramic Materials, GS)
Gareev, Rashid	(Electronic Properties, G)
Goerigk, Günter	(Scattering Methods)
Grimm, Hans	(Neutron Scattering)
Grünberg, Peter	(Electronic Properties)
Grushko, Benjamin	(Microstructure Research)
Gurevich, Vadim	(Theory III, G)
Gutheim, Frank	(Theory III)
Hamann, Dirk	(Scattering Methods)
Harris, John	(Theory I)
Hartmann, Miks Jan	(Theory III, GS)
Haubold, Heinz-Günter	(Scattering Methods)
Hauck, Jürgen	(Soft Matter)
He, Jiaqing	(Microstructure Research, GS)
Heggen, Marc	(Microstructure Research, GS)
Heide, Marcus	(Electronic Properties, GS)
Heil, Marco	(Neutron Scattering)
Heinen, Josef	(Networks and Numerical Methods)
Heinrich, Martine	(Neutron Scattering, G)
Hermes, Helen	(Neutron Scattering)

Höhler, Holger	(Theory III, GS)
Hölzle, Rainer	(Accelerators)
Houben, Lothar	(Microstructure Research)
Ioffe, Alexander	(Scattering Methods)
Istomin, Konstantin	(Scattering Methods, GS)
Jäger, Nikos	(Microstructure Research, GS)
Jahnen, Burkhard	(Microstructure Research, GS)
Jia, Chunlin	(Microstructure Research)
Jin, Hong-Zheng	(Microstructure Research, GS)
Jones, Robert	(Theory I)
Jung, Peter	(Scattering Methods)
Kali, György	(Neutron Scattering)
Kann, Gunther	(Electronic Properties, GS)
Karthäuser, Silvia	(Electroceramic Materials)
Kaufmann, Zoltan	(Theory I, G)
Kaya, Ugur Lehn	(Neutron Scattering, GS)
Kentzinger, Emmanuel	(Scattering Methods)
Kirstein, Oliver	(Neutron Scattering)
Kisielowski, Christian	(Microstructure Research, G)
Kluge, Fanying	(Microstructure Research, GS)
Köbler, Ulrich	(Scattering Methods)
Kockelmann, Winfried	(Scattering Methods)
Kohlstedt, Herbert-Herm	(Electroceramic Materials)
Krasser, Wolfgang	(Electroceramic Materials)
Kuanr, Bijoy Kumar	(Electronic Properties, G)
Lamura, Antonio	(Theory II, G)
Lang, Peter	(Soft Matter)
Lenstra, Tjerk	(Soft Matter, G)
Lentzen, Markus	(Microstructure Research)
Liatti, Matvei	(Microstructure Research, GS)
Liebsch, Ansgar	(Theory I)
Link, Sven	(Electronic Properties, GS)
Lörgen, Markus	(Electronic Properties, GS)
Lund, Reidar	(Neutron Scattering, GS)
Lustfeld, Hans	(Theory I)
Lüttgens, Gunnar	(Electronic Properties)
Luysberg, Martina	(Microstructure Research)
Maassen, Ralph	(Theory I, GS)
Malagoli, Mariachristi	(Electronic Properties, GS)
Masalovitch, Serguei	(Scattering Methods, G)
Maytorena Cord, Jesus Albert	(Theory I, G)

Meier, Gerhard	(Soft Matter)
Meuffels, Paul	(Electroceramic Materials)
Mi, Shaobo	(Microstructure Research, GS)
Mihailescu, Mihaela	(Neutron Scattering, GS)
Mihaylova, Milena	(Scattering Methods, GS)
Mika, Klaus-Peter	(Theory III)
Monkenbusch, Michael	(Neutron Scattering)
Müller, Marcus	(Theory II, G)
Müller, Robert	(Scattering Methods)
Nägele, Gerhard	(Soft Matter)
Neeb, Matthias	(Electronic Properties)
Ohl, Michael	(Neutron Scattering)
Ohly, Christian	(Electroceramic Materials, GS)
Paeßens, Matthias	(Theory II, GS)
Papadopoulos, Georgios	(Theory II, G)
Parshin, Dimitrii	(Theory III, G)
Perny, Sebastien Gilles	(Neutron Scattering, G)
Persson, Bo	(Theory I)
Pipich, Vitaliy	(Neutron Scattering, GS)
Pontius, Nikolaus	(Electronic Properties, GS)
Popkov, Vladislav	(Theory II, G)
Poppe, Ulrich	(Microstructure Research)
Prager, Michael	(Neutron Scattering)
Pyckhout-Hintzen, Wim	(Neutron Scattering)
Qin, Yueling	(Microstructure Research)
Regnery, Stephan	(Electroceramic Materials)
Rhie, Hyoung-Seub	(Electronic Properties, GS)
Rickes, Jürgen	(Electroceramic Materials, GS)
Ritter, Sigrun	(Electroceramic Materials, GS)
Rodriguez Con., Julio	(Electroceramic Materials, GS)
Rücker, Ulrich	(Scattering Methods)
Rzehak, Roland	(Theory III)
Sager, Wiebke	(Soft Matter)
Samoilov, Vladimir N.	(Theory I, G)
Schall, Peter	(Microstructure Research)
Scherer, Ricardo	(Electronic Properties, GS)
Schilling, Tanja	(Theory II)
Schlapp, Michael	(Scattering Methods, GS)
Schmidt, Wolfgang	(Neutron Scattering)
Schmitz, Rolf	(Electroceramic Materials)
Schmitz, Sam	(Electroceramic Materials, GS)

Schober, Herbert	(Theory III)
Schober, Tilmann	(Electroceramic Materials)
Schondelmaier, Daniel	(Electronic Properties, GS)
Schröder, Herbert	(Electroceramic Materials)
Schröder, Kurt	(Theory III)
Schütz, Gunter Markus	(Theory II)
Schwahn, Dietmar	(Neutron Scattering)
Schweika, Werner	(Scattering Methods)
Semmler, Ulrich	(Microstructure Research, GS)
Shadrin, Pavel	(Microstructure Research, G)
Shirotov, Vadim	(Microstructure Research, GS)
Spatschek, Robert	(Theory III, GS)
Stein, Simon	(Electroceramic Materials, GS)
Stellbrink, Jörg	(Neutron Scattering)
Straube, Ekkehard	(Neutron Scattering, G)
Sturm, Kurt	(Theory I)
Swiatek, Piotr	(Electronic Properties)
Szot, Krzysztof	(Electroceramic Materials)
Thust, Andreas	(Microstructure Research)
Tillmann, Karsten	(Microstructure Research)
Toperverg, Boris	(Scattering Methods, G)
Ullmaier, Johann	(Special Group)
Vad, Thomas	(Scattering Methods)
Velikanova, Tamara	(Microstructure Research, G)
Voigt, Jörg	(Scattering Methods, GS)
Volokitin, Alexander	(Theory I, G)
Wang, Hao	(Soft Matter, G)
Wang, Jianbo	(Microstructure Research, GS)
Willmann, Richard	(Theory II, GS)
Willner, Lutz	(Neutron Scattering)
Wingbermuehle, Jörg	(Electronic Properties)
Wingerath, Kurt	(Networks and Numerical Methods)
Winkler, Roland	(Theory II)
Wirth, Ingo	(Electronic Properties, GS)
Wischnewski, Andreas	(Neutron Scattering)
Wortmann, Daniel	(Electronic Properties, GS)
Wu, Jinsong	(Microstructure Research, G)
Wunnicke, Olaf	(Theory III, GS)
Yao, Zhenyu	(Scattering Methods, G)
Yee-Madeira, Hernani Tiago	(Scattering Methods, G)
Yurechko, Mariya	(Microstructure Research, GS)

Zamponi, Michaela	(Neutron Scattering, GS)
Zeiske, Thomas	(Scattering Methods)
Zeller, Rudolf	(Theory III)
Zilkens, Christopher	(Electronic Properties, GS)
Zimina, Anna	(Electronic Properties, GS)
Zorn, Reiner	(Neutron Scattering)

Guest Scientists

Mahmoud Abdel-Goad El-	Minia Univ., Faculty of Engineering, Egypt
Dr. Jaakko Akola	University of Jyväskylä, Finland
Dr. Maria Arbe	University Pais Vasco, Spain
Dr. Pietro Ballone	University Messina, Italy
Stephanie Baud	Labor de Physics Moleculaire, Besancon Cedex, France
Dr. Alexandre Belushkin	Joint Institute for Nuclear Research, Dubna, Russia
Maxim Belushkin	Joint Institute for Nuclear Research, Dubna, Russia
Imants Bucenieks	Institute of Physics, Riga, Latvia
Dr. Vasile Caciuc	University Osnabrück, Germany
Dr. Philippe Carletto	University Nizza-Sophia Antipolis, France
Prof. Xiaosong Chen	Hua-Zhong Normal University, Wuhan, China
Prof. Juan Colmenero	University San Sebastian, Spain
Derek Corcoran	University of St. Andrews, Scotland
Prof. Gesasim Eliashberg	Landau Institute for Teoretical Physics, Russia
Dr. L.J. Fetters	Exxon, Annandale, New Jersey, USA
Dr. Jan Fousek	Acadimy of Sciences, Prag, Czechoslovakia
Dr. Michel Freyss	University Louis Pasteuer, Strasbourgh, France
Iosif Galanakis	University Louis Pasteuer, Strasbourgh, France
Dr. Arturo Garcia Borquez	Instituto Politecnico National, Mexico
Dr. Rashid Gareev	Russian Acadimy of Sciences, Moscow, Russia
Prof. Yuri Gulayev	Russian Acadimy of Sciences, Moscow, Russia
Prof. Vadim Gurevich	IOFFE-Insitut, St. Petersburg, Russia
Dr. Martine Heinrich	University Louis Pasteuer, Strasbourgh, France
Dr. Zoltan Kaufmann	Eötvös University, Hungary
Dr. Christian Kisielowski	Lowrence Berkeley National Labaratory, Berkeley, USA
Prof. Bijoy Kumar Kuanr	University of Delhi, India
Dr. Antonio Lamura	University of Bari, Italy
Dr. Tjerk Lenstra	University Ütrecht, Netherlands

Dr. Georg Madsen	University of Aarhus, Denmark
Prof. S.V. Maleyev	Petersburg Nuclear Physics Insitute, Russia
Prof. V. Marchenko	Russian Acadimy of Sciences, Moscow, Russia
Dr. Serguei Masalovitch	Kurchatov Institut, Moscow, Russia
Dr. Jesus Albert Maytorena Cord	University Cuernavaca, Mexico
Dr. Marcus Müller	University Mainz, Germany
Dr. Georgios Papadopoulos	University of Thessaly, Greece
Prof. Dimitrii Parshin	Technical State University, St. Petersburg, Russia
Dr. Sebastien Gilles Perny	Thomson CSF-LCR, ENS Cachan, France
Dr. Nicholas A. Pertsev	Russian Acadimy of Sciences, St. Petersburg, Russia
Dr. Yuri Petrusenko	Institute of Physics and Technology, Ukraine
Dr. Vladislav Popkov	Russian Acadimy of Sciences, Tomsk, Russia
Dr. Phil Rittenhouse	Los Alamos National Laboratory, USA
Prof. A.I. Ryazanov	Kurchatov Institut, Moscow, Russia
Prof. Vladimir N. Samoilov	State University Moscau, Russia
Dr. Kazunori Sato	University Osaka, Japan
Dr. Pavel Shadrin	Institute of Radioengineering and Electronics, Moscow, Russia
Alexander Smirnov	Joint Institute for Nuclear Research, Dubna, Russia
Prof. Ekkenhard Straube	University Merseburg, Germany
Dr. Boris Toperverg	Petersburg Nuclear Physics Insitute, Russia
Prof. Tamara Velikanova	National Academy of Sciences of Ukraine, Ukraine
Prof. Alexander Volokitin	Polytechnic Institut Kuibyshev, Russia
Dr. Hao Wang	Nankai University, China
Dr. Max Wolff	University of Erlangen, Germany
Dr. Jinsong Wu	Beijing Laboratory of Electron Microscopy, China
Zhenyu Yao	China Institute of Atomic Energy, China
Prof. Hernani Tiago Yee-Madeira	Institute Polytechnique National, Mexico
Dr. Silviu Zilberman	School of Chemistry, Tel Aviv, Israel

Spring Schools of the IFF

Beginning in 1970, our institute has organized an annual two-week Spring School on modern topics in solid state physics.

The topics of the Spring Schools over the past 13 years were:

1990	Solid State research for Information Technology
1991	Physics of Polymers
1992	Synchrotron Radiation for investigating Condensed Matter
1993	Magnetism of Solids and Boundaries
1994	Complex Systems between Atoms and Solids
1995	Electroceramics – Basics and Applications
1996	Scattering Methods for investigating Condensed Matter
1997	Dynamics and Pattern Formation in Condensed Matter
1998	Physics of Nanostructures
1999	Magnetic Layer Structures
2000	Fsec and neV: Dynamics of Condensed Matter
2001	New materials for the information technology
2002	Soft Matter – Complex Materials on Mesoscopic scales

Spring School 2002 on "Soft Matter – Complex Materials on Mesoscopic Scales"

This event was the 33. spring school offered by the IFF. It took place from 04.-15. March 2002 and included the latest developments in the fields of spectroscopic investigations of the dynamics in condensed matter.

The following lectures were presented (in chronological order):

G. Gompper	Introduction
K. Sturm	Statistical Mechanics
J. Allgaier	Polymer Synthesis
K. Kremer	Numerical Methods
S. Hoffmann	Conformations of Single Polymer Chains
G. Nägele	Ornstein-Zernike Theory
T. Brückel	Scattering
M. Gradzielski	Self-assembling Amphiphilic Systems
J. Buitenhuis	Colloid Synthesis
J. Rieger	Nanoparticles in Water
G. Schütz	Dynamics of Many Body Systems
A. Baumgärtner	Scaling Concepts in Polymer Physics
A. Baumgärtner	Homopolymer Mixtures
D. Schwahn	Experiments on Polymers
G. Zaccai	Biopolymers
G. Gompper	Random Surfaces and Membranes
R. Merkel	Biological Membranes
G. Büldt	Biological Nanomachines
E. Eisenriegler	Polymers near Surfaces
W. Zimmermann	Basics of Rheology
D. Richter	Polymer Dynamics
J.K.G. Dhont	Rotational Dynamics of Colloids
H. Löwen	Coarse-Graining Colloids and Polymers
H.-G. Döbereiner	Physics of Membranes and Vesicles
P. Lang	Fluid Interfaces
O. Seeck	Capillary Waves on Polymer Films
S. Kahle	Dielectric Relaxation
G. Meier	Nuclear Magnetic Resonance
P. Lettinga	Phase Separation Kinetics
R. Zorn	Colloidal Glasses
U. Buchenau	Polymer Glasses
K. Sommer	Industry Contribution
W. Sager	Microemulsion Templating
S. Rathgeber	Practical Rheology
M. Monkenbusch	Membrane and Microemulsion Dynamics
R. Winkler	Polyelectrolytes
J.H.G. Joosten	Industry Contributions
C.G. de Kruif	Industry Contribution

Polarised neutron diffraction under grazing incidence from an optical grating covered with a Nickel layer. Data were obtained on the reflectometer "HADAS" in the neutron guide hall ELLA at the DIDO reactor. The graph shows the count rate in the "up-up"-channel (i.e. scattering without change of polarisation) as function of the angle of incidence (abscissa) and exit (ordinate). From the full polarisation dependence, structural and magnetic contributions can be separated and the magnetic roughness and shape anisotropy can be determined.

Forschungszentrum Jülich